NASA
Reference
Publication
1328

January 1994

LSENS—A General Chemical Kinetics and Sensitivity Analysis Code for Homogeneous Gas-Phase Reactions

I. Theory and Numerical Solution Procedures

Krishnan Radhakrishnan

NASA Reference Publication 1328

1994

LSENS—A General Chemical Kinetics and Sensitivity Analysis Code for Homogeneous Gas-Phase Reactions

I. Theory and Numerical Solution Procedures

Krishnan Radhakrishnan
NYMA, Inc.
Lewis Research Center Group
Brook Park, Ohio

National Aeronautics and Space Administration
Office of Management
Scientific and Technical Information Program

Preface

LSENS, the Lewis General Chemical Kinetics and Sensitivity Analysis Code, has been developed for homogeneous, gas-phase chemical kinetics computations and contains sensitivity analysis for a variety of problems, including nonisothermal situations. The code is described in a series of three reference publications, which also provide a detailed guide to its use and many illustrative test problems.

LSENS has been designed for accuracy, efficiency, flexibility, and convenience. A variety of chemical reaction models can be considered: static system; steady, one-dimensional, inviscid flow; reaction behind an incident shock wave, including boundary layer correction; and perfectly stirred (highly backmixed) reactor. In addition, the chemical equilibrium state can be computed for the assigned states of temperature and pressure, enthalpy and pressure, temperature and volume, and internal energy and volume. Any reaction problem can be adiabatic, have an assigned heat transfer profile, or for static and flow problems, have an assigned-temperature profile. For static problems either the density is constant or the pressure-versus-time profile is assigned. For flow problems either the pressure or area can be assigned as a function of time or distance. For a static reaction sensitivity coefficients of the dependent variables and their temporal derivatives with respect to the initial values of the dependent variables and/or the three rate coefficient parameters of the chemical reactions can be obtained.

LSENS checks the legality and sufficiency of all input. At the user's option LSENS checks the reaction mechanism for uniqueness and ensures that each reaction satisfies charge and atom balance requirements.

This volume, part I of the series (chapters 1 to 7), presents the theory and the numerical solution procedures used in LSENS. The ordinary differential equations (ODE's) describing chemical kinetics problems are derived in chapter 2. Chapter 3 describes the numerical integration method and how it is implemented. In chapter 4 the governing ODE's for sensitivity analysis are derived and the solution method and numerical algorithm explained. The governing equations and solution methods for the chemical equilibrium state, equilibrium and frozen thermodynamic states behind an incident shock wave, and perfectly stirred reactor problems are presented in chapters 5 to 7.

Part II of the series (NASA RP–1329), consisting of chapters 8 to 13 and appendixes A to C, describes LSENS, its usage, and how to modify it. Chapter 8

describes the computational capabilities and convenience features built into the code. Chapter 9 presents its structure and description. Chapter 10 lists modifications that may be required to implement LSENS on the user's computer system. Chapter 11 provides a guide to code usage and describes how to prepare the input data files required to execute LSENS. The output information generated by the code is discussed in chapter 12. Example problems illustrating both problem data file construction and code usage are given in chapter 13. These examples supplement chapter 11 by providing additional guidance on preparation of the problem data file.

The partial derivatives required by the numerical solution procedures detailed in chapters 3, 4, and 7 are derived in appendix A. Appendix B shows how to access the system clock for several common computing systems so that execution times can be measured. Appendix C describes the modifications required to change the built-in values for various quantities.

Part III of the series (NASA RP–1330), consisting of appendixes D and E, explains the example problems provided with LSENS and presents sample results. Appendix D describes the kinetics test cases. These problems illustrate the various reaction models that can be solved by, and options built into, LSENS. Appendix E describes the kinetics-plus-sensitivity-analysis test cases supplied with the code. The examples in the two appendixes cover a variety of problem types and so should serve as useful models for the structure of the problem data file required to execute the code. Indeed, it is likely that the desired file can be produced by modifying one of the test cases.

Details regarding code availability and procurement can be obtained from COSMIC, 328 East Broad Street, University of Georgia, Athens, GA 30602 (Telephone: 706–542–3265).

Contents

List of Figures

List of Tables

Symbols

A	flow cross-sectional area
A_j	preexponential factor in forward rate coefficient expression for reaction j
$\underline{\mathrm{A}}$	vector containing the $\{A_j\}$
ATLS	local absolute error tolerance for all sensitivity coefficients
ATOL_i	local absolute error tolerance for ith chemical kinetics dependent variable (see eq. (3.31))
$\mathrm{ATOL}(S_{ij})$	local absolute error tolerance for S_{ij} (see eq. (4.80))
$\mathrm{ATOL}(\underline{S}_j)$	local absolute error tolerance for $\underline{S}_j$ (i.e., for all sensitivity coefficients with respect to η_j)
ATOLSP	local absolute error tolerance for reacting species mole numbers (LSENS) or all dependent variables (SENKIN)
$\mathbf{A}$	prediction matrix used in integrating chemical kinetics and sensitivity analysis ODE's, equation (3.21)
$\mathscr{A}$	iteration matrix for assigned-specific-volume chemical equilibrium calculations, equation (5.54)
a	mass-specific mixture Helmholtz function
a_{ij}	number of atoms of element i in 1 molecule of species j
b_i	total number of atoms of element i per unit mass of mixture
C_i	molar concentration of ith species, moles of species i per unit volume of mixture

Symbols

C_m	molar concentration of general third-body species, equation (2.22)
$\underline{C}$	coefficient vector in local truncation error vector (see eq. (3.5)).
CPU	central processing unit (i.e., execution) time
$\mathbf{C}$	diagonal matrix used in modifying Nordsieck history matrices for chemical kinetics variables and sensitivity coefficients when step size change occurs, equation (3.45)
c	sonic velocity
c_j	rate coefficient parameter in special rate coefficient expression, equation (2.5)
c_m	estimated convergence rate of solution to chemical kinetics ODE's (see eq. (3.33))
c_m'	quantity used in convergence test of solution to chemical kinetics ODE's, equation (3.36)
c_p	constant-pressure, mass-specific heat of mixture
c_Λ	empirical constant used to calculate Λ for incident shock calculations, equation (6.29)
$\mathfrak{c}_{p,i}$	constant-pressure, molar-specific heat of species i
$\mathfrak{c}_{v,i}$	constant-volume, molar-specific heat of species i
D_{ij}	estimated local truncation error in S_{ij}, equation (4.81)
$D_{q'}$	rms norm of weighted estimated local truncation error in solution to chemical kinetics ODE's for integration method order q', equation (3.40)
$\underline{d}$	estimated local truncation error vector in solution to chemical kinetics ODE's
E_j	activation energy in forward rate coefficient expression for reaction j
$\underline{E}$	vector containing the $\{E_j\}$ and/or the $\{c_j\}$
$\underline{E}_j$	vector proportional to local truncation error vector in $\underline{S}_j$ (see eq. (4.81))

EMAX	local relative error tolerance for chemical kinetics dependent variables
EWT_i	ith component of local error weight vector for solution to chemical kinetics ODE's, equation (3.31)
EWT_{ij}	local error weight for S_{ij}, equation (4.80)
$\mathcal{E}(S_{ic})$, $\mathcal{E}(S_{rp})$	average estimated global errors in sensitivity coefficients with respect to initial conditions and rate coefficient parameters, respectively, at all print stations, equation (4.83)
$\mathcal{E}(\underline{Y})$	average estimated global error in solution to chemical kinetics ODE's at all print stations, equation (4.82)
$\underline{\mathcal{E}}_p$	vector arising in assigned-pressure chemical equilibrium state calculation, equations (5.42a) to (5.42c)
$\underline{\mathcal{E}}_p^*$	vector arising in calculation of equilibrium partial derivatives at constant pressure, equations (5.77a) and (5.77b)
$\underline{\mathcal{E}}_T^*$	vector arising in calculation of equilibrium partial derivatives at constant temperature, equations (5.86a) and (5.86b)
$\underline{\mathcal{E}}_v$	vector arising in assigned-specific-volume chemical equilibrium state calculations, equations (5.53a) and (5.53b)
$\underline{e}$	vector proportional to local truncation error vector in solution to chemical kinetics ODE's
$\underline{\mathcal{e}}$	global error in solution to chemical kinetics ODE's
$\underline{F}_j$	first derivative vector of $\underline{S}_j$ with respect to t
$\underline{\mathcal{F}}$	NR functional vector for incident shock calculation, equations (6.19a) and (6.19b)
f_i	net molar rate of formation of species i per unit mass of mixture, equation (2.36), or ith component of $\underline{f}$
$\underline{f}$	first derivative vector of chemical kinetics dependent variables with respect to ξ
$\underline{\mathcal{f}}$	NR functional vector for PSR calculation, equations (7.14a), (7.14b), and (7.15)

Symbols

$\Delta G^{\circ}_{T,j}$	standard-state (1 atm) Gibbs function change at temperature T for reaction j, equation (2.10)
$\underline{G}$	vector function used in advancing sensitivity coefficients by one time step, equation (4.17)
$\mathcal{G}$	iteration matrix for assigned-pressure chemical equilibrium calculations, equation (5.43)
$\mathcal{G}^*$	submatrix of $\mathcal{G}$ used for computing equilibrium first derivatives (see eqs. (5.75) and (5.84))
g	mass-specific Gibbs function of mixture
g_i	molar-specific Gibbs function of species i
$\underline{g}$	vector function used in advancing solution to chemical kinetics ODE's by one integration step, equation (3.15)
h	mass-specific enthalpy of mixture
h^*	mass-specific enthalpy of mixture at PSR inlet
h'	integration step size to be attempted on next step
h_n	integration step size on step $[\xi_{n-1},\xi_n]$
h_o	mixture mass-specific stagnation enthalpy
h_i	molar-specific enthalpy of species i
I_P	number of integration steps between output of results for chemical kinetics problems and sensitivity analysis computations
ITOL	user-supplied integer that indicates if RTOL and ATOL are scalars or arrays
$\mathbf{I}$	identity matrix
$\mathbf{J}$	Jacobian matrix
$K_{c,j}$	concentration equilibrium constant for reaction j, equation (2.8)

K_1, K_2	integers associated with particular linear multistep method (see eq. (3.6))
k_j, k_{-j}	forward (eqs. (2.4) and (2.5)) and reverse (eq. (2.6)) rate coefficients for reaction j
$\underline{k}$	vector containing $\{k_j\}$
L	number of columns of Nordsieck history matrices for chemical kinetics variables and sensitivity coefficients with respect to η_j or number of elements in mixture
$\underline{\ell}$	coefficient vector for linear multistep method in normal form, equation (3.25)
ℓ_q	qth component of $\underline{\ell}$ (see eq. (3.25))
ℓ_0	zeroth component of $\underline{\ell}$ (see eq. (3.25))
M	total number of iterations required for convergence or total number of independent sensitivity parameters for problem
M_w	mixture molar mass
$M_{w,i}$	molar mass of species i
M	general third-body collision partner in third-body reaction
MAXSTP	maximum number of integration steps allowed for solution of ODE's
METH	identifies integration method to be used for solving chemical kinetics ODE's (see eq. (3.53))
MF	method flag that specifies both integration method and corrector iteration technique to be used for solving chemical kinetics ODE's, equation (3.53)
MITER	identifies corrector iteration technique to be used in integrating chemical kinetics ODE's (see eq. (3.53))
$\mathcal{M}$	Mach number

Symbols

m	mass or iteration number
$\dot{m}$	mass flow rate
$\Delta\dot{m}$	mass flow rate increment for successive solutions of assigned-mass-flow-rate PSR problem (see eq. (7.32b))
$\dot{m}_{max}$	mass flow rate for assigned-mass-flow-rate PSR problem
$\dot{m}_0$	mass flow rate to start iteration for first solution of assigned-temperature PSR problem
$\mathfrak{m}_{\ell j}$	relative third-body efficiency of species ℓ in reaction j (see eqs. (2.29) and (2.30))
N	number of chemical kinetics ODE's or number of algebraic equations in PSR problem
N_i	number of moles of species i in mixture
NFE	total number of derivative evaluations required by ODE solver to solve problem
NINERT	number of inert species in mixture
NITER	total number of iterations required for chemical equilibrium state calculation
NJE	total number of Jacobian matrix evaluations required by ODE solver to solve problem
NLM	number of elements in mixture
NR	number of chemical reactions in reaction mechanism
NRS	number of reacting species in mixture
NS	number of (reacting plus inert) species in mixture
$NS_{j,t}$	number of species considered in measuring estimated global error in $\underline{S}_j$ at time t (see eq. (4.83))
NSTEP	total number of integration steps required by ODE solver to solve problem

NTBS	number of third-body species with collisional efficiencies different from unity
n_{ij}	stoichiometric coefficient of species i in reaction j, equation (2.3)
n_j	temperature exponent in forward rate coefficient expression for reaction j
Δn_j	change in number of moles for jth reaction, equation (2.9)
$\underline{\mathrm{n}}$	vector containing $\{n_j\}$
n_i	number density of species i, molecules of species i per unit volume of mixture
P	number of parameters with respect to which sensitivity coefficients are desired
PRNT	user-supplied integer that controls amount of information generated by code PSR
$\mathbf{P}$	iteration matrix, used in solution of ODE's for chemical kinetics and sensitivity coefficients, equation (3.16)
p	pressure
p^*	pressure at PSR inlet
Q_c	heat of combustion
$\dot{Q}$	heat transfer rate
$\delta\dot{Q}$	heat transfer rate from differential element of flow (see fig. 2.1)
$\dot{Q}'$	heat transfer rate per unit length
q	method order used by ODE solver on current integration step
q'	method order to be attempted by ODE solver on next step
$\dot{q}$	heat transfer rate per unit mass of mixture from system
R	universal gas constant

Symbols

R_j, R_{-j}	forward (eqs. (2.17) and (2.31)) and reverse (eqs. (2.18) and (2.32)) molar reaction rates per unit volume of reaction j
RTLS	local relative error tolerance for all sensitivity coefficients
RTOL_i	local relative error tolerance for ith chemical kinetics dependent variable (see eq. (3.31))
$\mathrm{RTOL}(S_{ij})$	local relative error tolerance for S_{ij} (see eq. (4.80))
$\mathrm{RTOL}(\underline{S}_j)$	local relative error tolerance for $\underline{S}_j$ (i.e., for all sensitivity coefficients with respect to η_j)
$\mathcal{R}_j$	total molar rate of reaction j
r	step length ratio
r_j	net molar rate per unit volume of reaction j, equation (2.16)
$r_{q'}$	ratio of step length to be attempted on next step to its current value if method order q' is to be used
rms	root mean square
S_{ij}	sensitivity coefficient of ith dependent variable with respect to jth sensitivity parameter
S_{ij}^*	approximation to exact sensitivity coefficient $\partial y_i/\partial \eta_j$
$\langle S_{ij} \rangle$	normalized sensitivity coefficient of ith dependent variable with respect to jth sensitivity parameter, equation (4.63)
S_m	sum of mass fractions of all species, equations (4.96) and (7.28)
$\underline{S}_j$	sensitivity coefficient vector with respect to jth sensitivity parameter
$\dot{\underline{S}}_j$	approximation to $\underline{E}_j$ produced by BDF method
$\mathcal{S}_i$	chemical symbol for species i
s	mass-specific entropy of mixture
$\mathcal{s}_i$	molar-specific entropy of species i

T	temperature
ΔT	temperature decrement for successive solutions of assigned-temperature PSR problem (see eq. (7.32c))
$\Delta \ln T$	logarithmic correction of temperature for chemical equilibrium calculation
T^*	temperature at PSR inlet
T_{min}	reactor temperature for assigned-temperature PSR problem
TEMP	user-supplied initial estimate of reactor temperature for assigned-mass-flow-rate PSR problem or reactor temperature for assigned-temperature PSR problem, required by code PSR
TRACE	cutoff level for listing mole fractions, used by code CET
t	time
U	unit roundoff of computer
u	mass-specific internal energy of mixture
u_i	molar-specific internal energy of species i
V	flow velocity
$\mathcal{V}$	volume
v	mass-specific volume of mixture
W_i	net molar production rate per unit volume of species i, equation (7.6)
$\dot{w}$	work transfer rate per unit mass of mixture from system
x	distance
x_i	mole fraction of species i
Y_i	ith component of $\underline{Y}$
ΔY_i	ith component of $\Delta\underline{Y}$ or change in ith component of numerical solution vector to chemical kinetics ODE's

Symbols

ΔY_N	correction to temperature for assigned-mass-flow-rate PSR problem or correction to mass flow rate for assigned-temperature PSR problem
Y_i^*	ith component of $\underline{Y}^*$
$\underline{Y}$	numerical solution vector to chemical kinetics ODE's or vector containing $\{\ln y_i\}$ for chemical equilibrium, shock, and PSR problems
$\Delta\underline{Y}$	correction to $\underline{Y}$ obtained on an iteration
$\underline{Y}^*$	numerical solution obtained using exact past values or approximation to exact solution $\underline{y}$
$\dot{\underline{Y}}$	approximation to $\underline{f}$ produced by BDF method
$\underline{Y}_p^*$	vector of equilibrium partial derivatives with respect to temperature at constant pressure, equation (5.76)
$\underline{Y}_T^*$	vector of equilibrium partial derivatives with respect to pressure at constant temperature, equation (5.85)
y_i	ith component of $\underline{y}$ or mass fraction of species i, equation (4.97)
$\underline{y}$	exact solution vector for chemical kinetics problems or vector of dependent variables for chemical equilibrium, shock, and PSR problems
$\dot{\underline{y}}$	first derivative vector of chemical kinetics dependent variables with respect to ξ
$\underline{Z}_j(k)$	kth column of $\mathbf{Z}_j$, equation (4.25)
$\mathbf{Z}_j$	Nordsieck history matrix for sensitivity coefficients with respect to jth sensitivity parameter, equation (4.14)
$\underline{z}(k)$	kth column of **z,** equation (3.49)
$\mathbf{z}$	Nordsieck history matrix for solution to chemical kinetics problem, equation (3.19)
α_j, β_j	method coefficients for linear multistep methods (see eq. (3.6))

α_j^*, β_1^*	method coefficients for predictor formula that produces initial guess for solution to chemical kinetics ODE's (see eq. (3.12))
β_0	integration method coefficient (see eq. (3.6))
γ	frozen specific heat ratio of mixture, equation (2.79)
Δ_{ij}	weighted estimated local truncation errror in S_{ij}, equation (4.85)
$\delta\eta_j$	normalization factor for sensitivity coefficients with respect to η_j
$\delta(\eta_j)$	normalized finite-difference increment $\Delta\eta_j$ (see eqs. (4.75) to (4.78) and (4.103))
$\delta_{c3}(\eta_j)$	value of $\delta(\eta_j)$ needed for sensitivity coefficients (or normalized sensitivity coefficients) with respect to η_j to converge to three significant figures
$\delta_{c4}(\eta_j)$	value of $\delta(\eta_j)$ needed for sensitivity coefficients (or normalized sensitivity coefficients) with respect to η_j to converge to four significant figures
$\varepsilon(\eta_j)$	average rms norm for complete problem of weighted estimated local truncation errors in sensitivity coefficients with respect to η_j, equation (4.84)
ε_m, ε_m'	quantities used to test convergence of solution to chemical kinetics ODE's, equations (3.32) and (3.35)
η_j	jth sensitivity parameter
$\Delta\eta_j$	normalization factor for sensitivity coefficients with respect to η_j or finite-difference increment for η_j (see eqs. (4.73) and (4.74))
$\hat{\eta}_j$	generally accepted nominal value for η_j
Λ	underrelaxation factor used to restrict magnitude of corrections produced by NR iteration method while solving chemical equilibrium, shock, and PSR problems, equations (5.58), (6.28), and (7.26)
Λ_1, Λ_2	quantities used to compute Λ for chemical equilibrium and PSR problems, equations (5.56), (5.57), (7.24), and (7.25)
λ_i	Lagrange multiplier for ith atom conservation equation

Symbols

μ_i	chemical potential of species i
ν'_{ij}, ν''_{ij}	stoichiometric coefficients of reactant and product species i in reaction j (see eq. (2.1))
ξ	independent variable for chemical kinetics ODE's—time or distance
π_i	modified Lagrange multiplier λ_i, equation (5.16)
ρ	mixture mass density
ρ^*	mixture mass density at PSR inlet
σ_i	mole number of species i—moles of species i per unit mass of mixture
$\Delta \ln \sigma_i$	logarithmic correction of mole number of species i for chemical equilibrium calculation
σ_i^*	mole number of species i at PSR inlet
σ_m	sum of mole numbers of species, equation (2.23)
$\Delta \ln \sigma_m$	logarithmic correction of σ_m for chemical equilibrium calculation
$\tau(q)$	test constant used in local truncation error test for BDF method of order q, equation (3.38)
τ_{all}	execution time required for computing concentrations, all initial condition sensitivities, and all rate constant sensititivies
τ_{conc}	execution time required to solve chemical kinetics ODE's alone (i.e., no sensitivity analysis)
τ_{ic}	execution time required for computing concentrations and all initial condition sensitivities
τ_r	average residence time for PSR, equation (7.1)
τ_{rc}	execution time required for computing concentrations and all rate constant sensitivities
χ_j	generalized normalization factor for sensitivities with respect to η_j (see eq. (4.63))

$\underline{\Psi}_j$	previously computed information required by BDF method to advance $\underline{S}_j$, equation (4.10)
$\underline{\Psi}$	previously computed information required by BDF method to advance solution to chemical kinetics ODE's, equation (3.10)

Subscripts:

end	value at end of integration interval
eq	equilibrium state
ic	initial condition
N	index for either temperature or mass flow rate in PSR calculation
n	value at ξ_n or results of (or assigned value for) *n*th PSR solution
out	value at next output station
rp	rate coefficient parameter
st	standard conditions (1 atm)
0	initial condition value or, for chemical equilibrium state calculations, assigned value
1	condition upstream of incident shock wave or results of (or assigned value for) first PSR solution
2	condition downstream of incident shock wave or results of (or assigned value for) second PSR solution

Superscripts:

(j)	*j*th derivative
$[m]$	value at *m*th iteration
T	transpose
[0]	predicted value (i.e., initial guess)
°	standard state (1 atm)

Chapter 1
Introduction

LSENS, the Lewis General Chemical Kinetics and Sensitivity Analysis Code, has been developed for solving complex, homogeneous, gas-phase, chemical kinetics problems and contains sensitivity analysis for a variety of problems, including nonisothermal situations. This report derives the governing equations and describes the numerical solution procedures for the problem types that can be solved by LSENS. Test problems examining the accuracy and efficiency of LSENS, as well as comparisons with other methods and codes, are presented.

There is a continuing interest in developing detailed chemical reaction mechanisms for complex reactions, such as fuel combustion and pollutant formation and destruction. A chemical reaction mechanism is the set of all elementary chemical reactions (i.e., real molecular events) that are required to describe the process of interest (refs. 1 and 2). Mathematical descriptions of chemical kinetics problems constitute sets of coupled, nonlinear, first-order ordinary differential equations (ODE's) (refs. 1 and 3). The number of ODE's can be very large because of the numerous chemical species involved in the reaction mechanism. Further complicating the situation are the many simultaneous reactions needed to describe the chemical kinetics of practical fuels. For example, the mechanism describing the oxidation of the simplest hydrocarbon fuel, methane, involves over 25 species participating in nearly 100 elementary reaction steps (ref. 4).

Validating a chemical reaction mechanism requires repetitive solutions of the governing ODE's for a variety of reaction conditions. Analytical solutions to the systems of ODE's describing chemistry are not possible, except for the simplest cases, which are of little or no practical value. Consequently fast and reliable numerical solution techniques are needed for chemical kinetics problems.

Before fast computers were widely available, numerical results could be obtained only after substantial reduction and approximation of the reaction mechanism, which then bore little resemblance to the true chemistry (refs. 5 to 7). Surprisingly the introduction of digital computers after World War II did not result in significant advances in complex mechanism development, even though numerical integration methods for ODE's had been developed. As discussed in chapter 3, the ODE's describing chemical kinetics exhibit a peculiar behavior (called "stiffness") that makes their solution by classical ODE integration methods prohibitively expensive;

that is, classical methods will require prohibitive amounts of computer time to integrate chemical kinetics equations.[1] It is the development of specialized solution techniques, as well as fast computers, that has made possible economical solution of complex reaction problems.

In addition to solving the ODE's describing chemical kinetics, it is often necessary to know how variations in either initial condition values or chemical reaction mechanism parameters affect the solution. Such a need arises in developing reaction mechanisms from experimental data (ref. 8). The rate coefficients are often not known with great precision, and in general the experimental data are not sufficiently detailed to accurately estimate the rate coefficient parameters. The development of a reaction mechanism is facilitated by a systematic sensitivity analysis, which establishes relationships between the predictions of a kinetics model and the input parameters of the problem (refs. 3, 9, and 10).

LSENS replaces the previous NASA general chemical kinetics codes GCKP (ref. 11) and GCKP84 (ref. 12). The new code is designed for accuracy, efficiency, flexibility, and convenience. A variety of chemical reaction models can be considered. The models include static system; steady, one-dimensional, inviscid flow; incident shock wave; and perfectly stirred (highly backmixed) reactor (PSR). In addition, the chemical equilibrium state can be computed for the following assigned states: temperature and pressure, enthalpy and pressure, temperature and volume, and internal energy and volume. For static problems the code computes sensitivity coefficients with respect to the initial values of the dependent variables and/or the three rate coefficient parameters of the chemical reactions.

To integrate the ODE's describing chemical kinetics problems, LSENS uses the packaged code LSODE—the Livermore Solver for Ordinary Differential Equations (refs. 13 to 15)—because it has been shown to be the most efficient and accurate code for solving such problems (refs. 16 to 20). The sensitivity analysis computations use the decoupled direct method (refs. 20 to 22) as implemented by Dunker (ref. 23) for isothermal problems and extended by Radhakrishnan (ref. 22) to nonisothermal combustion kinetics. This method has shown greater efficiency and stability, with equal or better accuracy, than other sensitivity analysis methods (refs. 20 to 22).

The chemical equilibrium state is obtained by minimizing either the Gibbs or Helmholtz function. The postincident shock equilibrium and frozen thermodynamic states are computed by solving the mass, momentum, and energy conservation equations for steady, one-dimensional, inviscid flow. For the PSR problem the nonlinear algebraic species continuity and energy conservation equations are solved. In all three cases a Newton-Raphson iteration technique that automatically limits the size of the corrections at each iteration to minimize convergence difficulties is used. Also, to avoid negative variables, the equations are cast in terms

[1] In this report the terms "computational expense" (or cost) and "execution time" (i.e., central processing unit (CPU) time) are used synonymously.

of the logarithm of the variables. In order to minimize convergence to a false solution, the calculation procedure for the PSR problem generates a series of solutions, starting with conditions close to the chemical equilibrium state, until the desired state is reached.

The remainder of this report is organized as follows. The ODE's describing static and flow chemically reacting problems are derived in chapter 2. Chapter 3 describes the numerical integration method and how it is implemented. In chapter 4 the governing ODE's for sensitivity analysis are derived and the solution method and numerical algorithm explained. The governing equations and solution methods for the chemical equilibrium state, thermodynamic states behind an incident shock wave, and PSR problems are presented in chapters 5 to 7.

Chapter 2
Governing Ordinary Differential Equations

In order to describe the temporal evolution of homogeneous chemical reaction systems, equations are needed for species concentrations, temperature, density, pressure, and possibly, velocity (ref. 1). In this chapter the governing ordinary differential equations (ODE's) are derived for a variety of problem types. However, for each problem type the ODE's that are actually solved and the forms of these ODE's as used in the code are given in appendix A of part II.

2.1 Chemical Reactions and Rate Coefficients

Consider a chemical reaction mechanism involving NR elementary reactions among NS species. The jth elementary step of the mechanism can be written symbolically in the general form

$$\sum_{i=1}^{NS} \nu'_{ij}\, \mathcal{S}_i \underset{k_{-j}}{\overset{k_j}{\rightleftharpoons}} \sum_{i=1}^{NS} \nu''_{ij}\, \mathcal{S}_i, \quad j = 1,\ldots,NR \tag{2.1}$$

Here ν'_{ij} is the stoichiometric coefficient (i.e., number of moles) of reactant species i in reaction j, ν''_{ij} the stoichiometric coefficient of product species i in reaction j, and $\mathcal{S}_i$ the chemical symbol for species i. For a species i that does not participate in the jth reaction, $\nu'_{ij} = \nu''_{ij} = 0$. The arrows indicate the direction (i.e., forward or reverse) of the chemical reaction. The k_j and k_{-j} are, respectively, the forward and reverse rate coefficients or rate constants for reaction j.

For convenience, the chemical reaction, equation (2.1), is rewritten as

$$0 = \sum_{i=1}^{NS} n_{ij} \mathcal{S}_i \tag{2.2}$$

where

$$n_{ij} = \nu''_{ij} - \nu'_{ij} \tag{2.3}$$

By convention n_{ij} is positive for products and negative for reactants (ref. 24).

Each k_j is a function of temperature and usually given by the empirical expression (ref. 2)

$$k_j = A_j T^{n_j} \exp\left(\frac{-E_j}{RT}\right) \tag{2.4}$$

which is the so-called modified Arrhenius expression. In equation (2.4) the preexponential factor A_j, the temperature exponent n_j, and the activation energy E_j are constants, R is the universal gas constant, and T is the temperature. After Baulch and Drysdale (ref. 25), the present work also considers rate coefficients of the form

$$k_j = A_j T^{n_j} \exp(c_j T) \tag{2.5}$$

where c_j is a constant.

Each reaction may be either irreversible (i.e., in the forward direction only) or reversible (i.e., bidirectional). For a reversible elementary reaction k_{-j} is related to k_j through the principle of detailed balancing or microscopic reversibility (refs. 1 and 24):

$$k_{-j} = k_j / K_{c,j} \tag{2.6}$$

In equation (2.6), $K_{c,j}$ is the concentration equilibrium constant for reaction j and for a fixed temperature is given by

$$K_{c,j} = \frac{\prod_{i=1}^{NS} [\mathcal{S}_i]_{eq}^{\nu''_{ij}}}{\prod_{i=1}^{NS} [\mathcal{S}_i]_{eq}^{\nu'_{ij}}} = \prod_{i=1}^{NS} [\mathcal{S}_i]_{eq}^{n_{ij}} \tag{2.7}$$

where $[\mathcal{S}_i]_{eq}$ represents the concentration of the ith species at equilibrium at the given temperature.

For ideal gases $K_{c,j}$ is a function of temperature only and given by (ref. 24)

$$K_{c,j} = (RT)^{-\Delta n_j} \exp\left(\frac{-\Delta G^\circ_{T,j}}{RT}\right) \tag{2.8}$$

where Δn_j is the change in the total number of moles when reactants are converted to products according to the jth reaction, equation (2.1),

$$\Delta n_j = \sum_{i=1}^{NS} n_{ij} = \sum_{i=1}^{NS} \nu''_{ij} - \sum_{i=1}^{NS} \nu'_{ij} \tag{2.9}$$

and $\Delta G^\circ_{T,j}$ is the standard-state (e.g., 1 atm) Gibbs function change for the jth reaction at temperature T,

$$\Delta G^\circ_{T,j} = \sum_{i=1}^{NS} n_{ij}\, g_i^\circ(T) = \sum_{i=1}^{NS} \nu''_{ij}\, g_i^\circ(T) - \sum_{i=1}^{NS} \nu'_{ij}\, g_i^\circ(T) \tag{2.10}$$

where $g_i^\circ(T)$ is the standard-state Gibbs function of species i at temperature T.

Substituting equation (2.8) into equation (2.6) gives

$$k_{-j} = k_j (RT)^{\Delta n_j} \exp\left(\frac{\Delta G^\circ_{T,j}}{RT}\right) \tag{2.11}$$

2.2 Reaction Rates and Species Production Rates

Consider a closed chemically reacting system (i.e., a fixed mass of reacting gas) of mass m and volume $\mathcal{V}$. Let N_i denote the total number of moles of species i in the system and $(dN_i/dt)_j$ its time rate of change due to reaction j. From the stoichiometric equation (2.2) it is clear that the quantity

$$\mathcal{R}_j = \frac{1}{n_{ij}}\left(\frac{dN_i}{dt}\right)_j \tag{2.12}$$

is the same for all species participating in the reaction and therefore a suitable measure of the total rate of reaction j (ref. 24). The total reaction rate, however, depends on the size of the system. For convenience the dependence is eliminated by dividing the total rate by the volume of the system (ref. 24). The rate of reaction j per unit volume r_j is then given by

$$r_j = \frac{\mathcal{R}_j}{\mathcal{V}} = \frac{1}{\mathcal{V} n_{ij}}\left(\frac{dN_i}{dt}\right)_j \tag{2.13}$$

If σ_i, the mole number of species i, is defined to be the number of moles of species i per unit mass of mixture, that is,

$$\sigma_i = N_i/m \tag{2.14}$$

equation (2.13) can be rewritten as

$$r_j = \frac{1}{\mathcal{V} n_{ij}}\left(\frac{d(m\sigma_i)}{dt}\right)_j = \frac{m}{\mathcal{V} n_{ij}}\left(\frac{d\sigma_i}{dt}\right)_j = \frac{\rho}{n_{ij}}\left(\frac{d\sigma_i}{dt}\right)_j \tag{2.15}$$

where m can be taken outside the derivative because it is constant, $(d\sigma_i/dt)_j$ is the molar formation rate of species i per unit mass of mixture due to the jth reaction, and ρ is the mixture mass density.

Because, in general, a chemical reaction can proceed in both directions, r_j is the difference between the molar forward (R_j) and reverse (R_{-j}) rates of reaction j per unit volume. Hence,

$$r_j = R_j - R_{-j} \tag{2.16}$$

where R_j and R_{-j} are given by the law of mass action (refs. 1 and 24):

$$R_j = k_j \prod_{\ell=1}^{NS} C_\ell^{\nu'_{\ell j}} \tag{2.17}$$

and

$$R_{-j} = k_{-j} \prod_{\ell=1}^{NS} C_\ell^{\nu''_{\ell j}} \tag{2.18}$$

In equations (2.17) and (2.18), C_ℓ ($\equiv [\mathcal{S}_\ell]$) is the molar concentration of species ℓ, that is, moles of species ℓ per unit volume of mixture. The C_ℓ and σ_ℓ are related as follows:

$$C_\ell = \rho \sigma_\ell \tag{2.19}$$

Combining equations (2.15) and (2.16) gives the following equation for the molar rate of formation of species i per unit mass of mixture due to the jth reaction:

$$\left(\frac{d\sigma_i}{dt}\right)_j = \rho^{-1}\left(\nu''_{ij} - \nu'_{ij}\right)\left(R_j - R_{-j}\right) \tag{2.20}$$

where n_{ij} has been replaced by $\nu''_{ij} - \nu'_{ij}$.

For an irreversible reaction $R_{-j} = 0$, which can be obtained simply by setting $k_{-j} = 0$. Hence the preceding formulation can be used without loss in generality.

Because the reaction given by equation (2.1) involves all species, reacting and inert, it includes third-body collisional reactions (ref. 1). An example is

$$O_2 + M \underset{k_{-j}}{\overset{k_j}{\rightleftharpoons}} O + O + M \tag{2.21}$$

where M ($\equiv$ molecule) represents any species that may participate in the reaction. Because M includes all species, its molar concentration C_m is given by

$$C_m = \sum_{\ell=1}^{NS} C_\ell \tag{2.22}$$

The mole number σ_m of M is given by

$$\sigma_m = \sum_{\ell=1}^{NS} \sigma_\ell \tag{2.23}$$

Clearly the concentrations of third-body species are not affected by the third-body reaction. However, the total concentration has an effect on the reaction rates. For the example reaction, equation (2.21),

$$R_j = k_j C_{O_2} C_m = k_j C_{O_2} \sum_{\ell=1}^{NS} C_\ell \tag{2.24}$$

$$R_{-j} = k_{-j} C_O C_O C_m = k_{-j} C_O^2 \sum_{\ell=1}^{NS} C_\ell \tag{2.25}$$

For a general third-body reaction the reaction rates per unit volume are given by

$$R_j = k_j C_m \prod_{\ell=1}^{NS} C_\ell^{\nu'_{\ell j}} \tag{2.26}$$

and

$$R_{-j} = k_{-j} C_m \prod_{\ell=1}^{NS} C_\ell^{\nu''_{\ell j}} \tag{2.27}$$

These two equations can be expressed in the forms given by equations (2.17) and (2.18) if the dependence on the total molar concentration is absorbed into k_j, which is then written as $k_j(T,C_m)$.

Another factor that must be accounted for when evaluating the molar formation rates of third-body reactions is that different third-body species may have different third-body collisional efficiencies in promoting the reaction. For example, the reaction

$$H + O_2 + M \rightleftharpoons HO_2 + M \tag{2.28}$$

has significantly different rates for M = Ar, H_2, O_2, H_2O, and N_2 (approximately in the ratio 1:3:1.3:21.3:1.3). In such a situation the reaction rates per unit volume for the jth reaction are given by

$$R_j = k_j \sum_{\ell=1}^{NS} \mathfrak{m}_{\ell j} C_\ell \prod_{\ell=1}^{NS} C_\ell^{\nu'_{\ell j}} \tag{2.29}$$

and

$$R_{-j} = k_{-j} \sum_{\ell=1}^{NS} \mathfrak{m}_{\ell j} C_\ell \prod_{\ell=1}^{NS} C_\ell^{\nu''_{\ell j}} \tag{2.30}$$

where $\mathfrak{m}_{\ell j}$ is the third-body collisional efficiency of species ℓ in reaction j. Because, in general, only a few species have third-body efficiencies different from unity, for computational efficiency equations (2.29) and (2.30) are rewritten as follows:

$$R_j = k_j \left(C_m + \sum_{\ell=1}^{NTBS} \left(\mathfrak{m}_{\ell j} - 1\right) C_\ell \right) \prod_{\ell=1}^{NS} C_\ell^{\nu'_{\ell j}} \tag{2.31}$$

$$R_{-j} = k_{-j} \left(C_m + \sum_{\ell=1}^{NTBS} \left(\mathfrak{m}_{\ell j} - 1\right) C_\ell \right) \prod_{\ell=1}^{NS} C_\ell^{\nu''_{\ell j}} \tag{2.32}$$

In these equations NTBS is the number of third-body species with efficiencies different from unity in the *j*th reaction.

The net formation rate of species i due to all reactions is given by

$$\frac{d\sigma_i}{dt} = \sum_{j=1}^{NR} \left(\frac{d\sigma_i}{dt} \right)_j = \rho^{-1} \sum_{j=1}^{NR} \left(\nu''_{ij} - \nu'_{ij} \right) \left(R_j - R_{-j} \right) \tag{2.33}$$

As indicated previously, the species can be classified into two types, reacting and inert. For inert species the governing ODE's are given simply by

$$\left.\begin{aligned} \frac{d\sigma_i}{dt} &= 0 \\ \sigma_i\left(t = t_0\right) &= \sigma_{i,0} = \text{Given} \end{aligned}\right\} \; i = 1, \ldots, \text{NINERT} \tag{2.34}$$

where NINERT is the total number of inert species in the mixture and t_0 the time at which the reaction is initiated. Equation (2.34) has the trivial solution

$$\sigma_i(t) = \sigma_{i,0}, \qquad i = 1, \ldots, \text{NINERT} \tag{2.35}$$

for all $t \geq t_0$.

The governing ODE's for reacting species can be written as

$$\left.\begin{aligned} \frac{d\sigma_i}{dt} &= f_i\left(\{\sigma_k\}, T, \rho\right), \qquad k = 1, \ldots, \text{NS} \\ \sigma_i(t = t_0) &= \sigma_{i,0} = \text{Given} \end{aligned}\right\} \quad i = 1, \ldots, \text{NRS} \tag{2.36}$$

where NRS is the total number of reacting species.

For constant-temperature, constant-density problems the set of NRS ODE's given by equation (2.36) completely specifies the temporal evolution of the chemical system. The pressure p is evaluated by using the ideal-gas law

$$p = \rho RT/M_w \tag{2.37}$$

where M_w, the mean molar mass of the mixture, is given by

$$M_w = 1/\sigma_m \tag{2.38}$$

For varying-temperature and varying-density problems equations are needed for temperature and density. In addition, if the reacting gas is in motion, an equation for the velocity is required. The problems examined in this report can be classified conveniently into two categories: static reaction problems, which involve no transport of energy or matter; and one-dimensional, steady reactive-flow problems.

2.3 Static Reaction Problems

For static problems the temperature may be assigned either as a function of time or as a constant. Otherwise its ODE is obtained from the energy equation for a closed system

$$\frac{du}{dt} = -\dot{q} - \dot{w} \tag{2.39}$$

where u is the mixture internal energy per unit mass, $\dot{q}$ the heat transfer rate per unit mass of mixture from the reacting gas to its surroundings, and $\dot{w}$ the work transfer rate per unit mass of mixture from the system. By using the relations

$$h = u + pv \tag{2.40}$$

$$\dot{w} = p(dv/dt) \tag{2.41}$$

and

$$v = 1/\rho \tag{2.42}$$

equation (2.39) can be rewritten as

$$\frac{dh}{dt} = \frac{1}{\rho}\frac{dp}{dt} - \dot{q} \tag{2.43}$$

In equations (2.40) to (2.43), h is the mixture mass-specific enthalpy and v the specific volume of the mixture.

For a mixture of ideal gases

$$h = \sum_{i=1}^{NS} h_i \sigma_i \tag{2.44}$$

where h_i, the molar-specific enthalpy of species i, is a function of temperature only. Differentiating equation (2.44) with respect to t gives

$$\frac{dh}{dt} = \sum_{i=1}^{NRS} h_i \frac{d\sigma_i}{dt} + \sum_{i=1}^{NS} c_{p,i}\,\sigma_i \frac{dT}{dt} \tag{2.45}$$

where $c_{p,i}$ (= dh_i/dT), the molar-specific heat at constant pressure of species i, is also a function of temperature only. The summation in the first term does not include inert species because $d\sigma_i/dt = 0$ for such species. Substituting equation (2.45) into equation (2.43) and rearranging terms give

$$c_p \frac{dT}{dt} = \frac{1}{\rho}\frac{dp}{dt} - \sum_{i=1}^{NRS} h_i \frac{d\sigma_i}{dt} - \dot{q} \tag{2.46}$$

where

$$c_p = \sum_{i=1}^{NS} c_{p,i}\,\sigma_i \tag{2.47}$$

is the frozen mass-specific heat at constant pressure of the gas mixture.

As described in chapter 8 of part II the empirical equations used for the thermodynamic properties produce the nondimensional quantities $c_{p,i}/R$ (i = 1,...,NS) and $h_i/(RT)$ (i = 1,...,NS). In order to avoid repeated conversion to the dimensional quantities $c_{p,i}$ and h_i, both sides of equation (2.46) are divided by the term RT and then equations (2.37) and (2.38) used. The resulting equation is

$$\frac{c_p}{RT}\frac{dT}{dt} = \frac{\sigma_m}{p}\frac{dp}{dt} - \sum_{i=1}^{NRS} \frac{h_i}{RT}\frac{d\sigma_i}{dt} - \frac{\dot{q}}{RT} \tag{2.48}$$

Two types of static problem, constant and varying density, will now be examined.

2.3.1 Constant-Density Static Problem

For a constant-density static problem the ODE for density is simply

$$\left.\begin{aligned} \frac{d\rho}{dt} &= 0 \\ \rho(t = t_0) = \rho_0 &= \text{Given} \end{aligned}\right\} \tag{2.49}$$

which has the trivial solution

$$\rho(t) = \rho_0 \tag{2.50}$$

for all $t \geq t_0$.

When the temperature is not given, its ODE is obtained from the energy equation, equation (2.48). The pressure, which is as yet unknown, is eliminated from equation (2.48) by using the ideal-gas law, equation (2.37), combined with equations (2.38) and (2.23) to give

$$p = \rho RT \sum_{i=1}^{NS} \sigma_i \tag{2.51}$$

Differentiating this equation with respect to t gives for constant density

$$\frac{dp}{dt} = p\left(\frac{1}{T}\frac{dT}{dt} + \frac{\sum_{i=1}^{NRS}\frac{d\sigma_i}{dt}}{\sigma_m}\right) \tag{2.52}$$

Substituting this expression into equation (2.48) and rearranging terms give

$$\frac{dT}{dt} = T\left(\frac{\sum_{i=1}^{NRS}\frac{d\sigma_i}{dt} - \sum_{i=1}^{NRS}\frac{h_i}{RT}\frac{d\sigma_i}{dt} - \frac{\dot{q}}{RT}}{\frac{c_p}{R} - \sigma_m}\right) \tag{2.53}$$

For adiabatic problems $\dot{q} = 0$, but the temperature ODE, equation (2.53), remains unchanged.

An alternative approach to computing the temperature for adiabatic, constant-density problems can be obtained from the first law of thermodynamics

$$u = \sum_{i=1}^{NS} u_i \sigma_i = \text{Constant} \tag{2.54}$$

where u_i is the molar-specific internal energy of species i. The algebraic equation (2.54) can be solved iteratively for the temperature, and there is then no need for a temperature ODE. Use of an algebraic equation for the temperature can be more efficient and accurate than integrating the temperature ODE (refs. 16 to 20). However, use of an ODE is preferred because it is applicable for the general case $\dot{q} \neq 0$. Unless $\dot{q}$ is either a constant or a function of only time, the energy equation ($du/dt = -\dot{q}$) cannot be integrated to give an algebraic equation from which the temperature can be obtained.

2.3.2 Variable-Density Static Problem

In a variable-density static problem the pressure is specified, either as a constant or as a function of time, and the density and the temperature when it is not given are solved for. Because the pressure is known, equation (2.48) can be used to get the following ODE for temperature:

$$\frac{dT}{dt} = T\left(\frac{\frac{\sigma_m}{p}\frac{dp}{dt} - \sum_{i=1}^{NRS}\frac{h_i}{RT}\frac{d\sigma_i}{dt} - \frac{\dot{q}}{RT}}{\frac{c_p}{R}}\right) \tag{2.55}$$

The ODE for density is obtained by differentiating equation (2.51) with respect to time. The result is

$$\frac{d\rho}{dt} = \rho\left(\frac{1}{p}\frac{dp}{dt} - \frac{1}{T}\frac{dT}{dt} - M_w\sum_{i=1}^{NRS}\frac{d\sigma_i}{dt}\right) \tag{2.56}$$

where $1/\sigma_m$ has been replaced by M_w. In equation (2.56), dT/dt is either given by equation (2.55) or evaluated from the assigned temperature profile. For a constant-temperature problem $dT/dt = 0$, but equation (2.56) remains unchanged.

2.4 One-Dimensional, Steady, Reactive-Flow Problems

In many practical devices chemical reactions occur in a flowing gas stream. For such problems the velocity V of the gas stream has to be computed along with the composition, temperature, density, and pressure. The following assumptions were made: steady, inviscid, one-dimensional flow of a chemically reacting ideal-gas mixture in a duct; variables uniform across any cross section but varying with distance along the duct; and negligible diffusion of matter and energy. However, heat transfer between the reacting gas mixture and its surroundings is allowed.

For flow problems the independent variable can be either time t or distance x along the duct. If the independent variable is time, the species ODE's, equation (2.36), remain unchanged. If the independent variable is distance, the ODE's for reacting species are obtained by using the chain rule of differentiation

$$\left.\begin{aligned}\frac{d\sigma_i}{dx} &= \frac{d\sigma_i}{dt}\frac{dt}{dx} = \frac{1}{V}\frac{d\sigma_i}{dt}\\ \sigma_i(x = x_0) &= \sigma_{i,0} = \text{Given}\end{aligned}\right\} \quad i = 1,\ldots,\text{NRS} \tag{2.57}$$

Two different types of flow problem are considered: assigned pressure and assigned area. In the first type of problem the pressure is assigned, either as a constant or as a function of time or distance, and the other thermodynamic variables, species concentrations, velocity, and duct area are solved for. In the second type the duct area is specified, either as a constant or as a function of time or distance, and all thermodynamic variables, species concentrations, and velocity are solved for. For both problem types the temperature may also be assigned, either as a constant or as a function of time or distance.

In order to solve for ρ, T when it is not assigned, and V, appropriate forms of the continuity, momentum, and energy equations are integrated. When the pressure is not assigned, it is obtained from equation (2.51). Because the flow is steady and one-dimensional, mass continuity is expressed by the equation

$$\dot{m} = \rho A V = \text{Constant} \tag{2.58}$$

where $\dot{m}$ is the mass flow rate and ρ, V, and A are, respectively, density, velocity, and duct area at a distance x along the duct (fig. 2.1). Differentiating equation (2.58) and then dividing by ρAV give the result

$$\frac{d\rho}{\rho} + \frac{dA}{A} + \frac{dV}{V} = 0 \tag{2.59}$$

The momentum and energy equations for one-dimensional, steady, frictionless flow are given by (e.g., ref. 26)

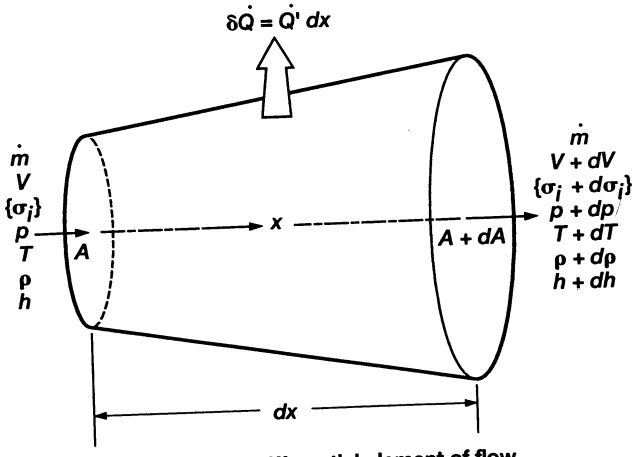

Figure 2.1.—Differential element of flow.

$$dp + \rho V\, dV = 0 \tag{2.60}$$

and

$$dh + V\, dV = -\frac{\delta \dot{Q}}{\dot{m}} = -\frac{\dot{Q}'}{\dot{m}}\, dx \tag{2.61}$$

where $\delta\dot{Q}$ is the heat transfer rate from the differential element of the duct and $\dot{Q}'$ the heat transfer rate per unit length of flow (fig. 2.1). Equation (2.44) gives the following expression for dh:

$$dh = \sum_{i=1}^{NRS} h_i\, d\sigma_i + \sum_{i=1}^{NS} c_{pi}\, \sigma_i\, dT \tag{2.62}$$

Because $d\sigma_i = 0$ for inert species, they are not included in the first term. Substituting equation (2.62) into equation (2.61) and then using equation (2.47) give the result

$$c_p\, dT + \sum_{i=1}^{NRS} h_i\, d\sigma_i + V\, dV + \frac{\dot{Q}'}{\dot{m}}\, dx = 0 \tag{2.63}$$

For reasons discussed in section 2.3, equation (2.63) is divided by RT to non-dimensionalize the $\{c_{p,i}\}$ and $\{h_i\}$. The resulting equation is

$$\frac{c_p}{RT}\, dT + \sum_{i=1}^{NRS} \frac{h_i}{RT}\, d\sigma_i + \frac{V\, dV}{RT} + \frac{\dot{Q}'/\dot{m}}{RT}\, dx = 0 \tag{2.64}$$

Finally the momentum equation, equation (2.60), is used to replace $V\, dV$ by $-dp/\rho$ and then equations (2.51) and (2.23) are used to get

$$\frac{c_p}{RT}\, dT + \sum_{i=1}^{NRS} \frac{h_i}{RT}\, d\sigma_i - \frac{\sigma_m}{p}\, dp + \frac{\dot{Q}'/\dot{m}}{RT}\, dx = 0 \tag{2.65}$$

2.4.1 Assigned-Pressure Flow Problem

For the assigned-pressure flow problem equation (2.60) gives the following velocity differential:

$$dV = -\frac{dp}{\rho V} \tag{2.66}$$

The differential dT, obtained from equation (2.65) by simple rearrangement, is given by

$$dT = T\left(\frac{\frac{\sigma_m}{p}dp - \sum_{i=1}^{NRS}\frac{h_i}{RT}d\sigma_i - \frac{\dot{Q}'/\dot{m}}{RT}dx}{\frac{c_p}{R}}\right) \tag{2.67}$$

The differential $d\rho$ is derived from equations (2.51) and (2.23) and given by

$$d\rho = \rho\left(\frac{dp}{p} - \frac{dT}{T} - \frac{\sum_{i=1}^{NRS}d\sigma_i}{\sigma_m}\right) \tag{2.68}$$

In this equation dT is either given by equation (2.67) or computed from the assigned temperature profile. For a constant-temperature problem, $dT = 0$, but equation (2.68) need not be modified.

It is relatively straightforward to derive the governing ODE's from equations (2.66) to (2.68). If time is the independent variable, the ODE's are

$$\frac{dT}{dt} = T\left(\frac{\frac{\sigma_m}{p}\frac{dp}{dt} - \sum_{i=1}^{NRS}\frac{h_i}{RT}\frac{d\sigma_i}{dt} - \frac{\dot{Q}'/\dot{m}}{RT}V}{\frac{c_p}{R}}\right) \tag{2.69}$$

$$\frac{d\rho}{dt} = \rho\left(\frac{1}{p}\frac{dp}{dt} - \frac{1}{T}\frac{dT}{dt} - M_w \sum_{i=1}^{NRS} \frac{d\sigma_i}{dt}\right) \tag{2.70}$$

$$\frac{dV}{dt} = -\frac{1}{\rho V}\frac{dp}{dt} \tag{2.71}$$

The distance equations are

$$\frac{dT}{dx} = T\left(\frac{\frac{\sigma_m}{p}\frac{dp}{dx} - \sum_{i=1}^{NRS} \frac{h_i}{RT}\frac{d\sigma_i}{dx} - \frac{\dot{Q}'/\dot{m}}{RT}}{\frac{c_p}{R}}\right) \tag{2.72}$$

$$\frac{d\rho}{dx} = \rho\left(\frac{1}{p}\frac{dp}{dx} - \frac{1}{T}\frac{dT}{dx} - M_w \sum_{i=1}^{NRS} \frac{d\sigma_i}{dx}\right) \tag{2.73}$$

$$\frac{dV}{dx} = -\frac{1}{\rho V}\frac{dp}{dx} \tag{2.74}$$

In equations (2.70) and (2.73), $1/\sigma_m$ has been replaced by M_w. Once the ODE's for ρ and V are solved the duct area is obtained from equation (2.58) as

$$A = \frac{\dot{m}}{\rho V} \tag{2.75}$$

2.4.2 Assigned-Area Flow Problem

For the assigned-area flow problem substituting the momentum equation, equation (2.60), into the continuity equation, equation (2.59), gives

$$\frac{d\rho}{\rho} + \frac{dA}{A} - \frac{1}{\rho V^2} dp = 0 \tag{2.76}$$

Introducing the Mach number $\mathcal{M}$, defined for ideal-gas mixtures by

$$\mathcal{M} = \frac{V}{\sqrt{\gamma RT/M_w}} \tag{2.77}$$

allows equation (2.76) to be rewritten as

$$\frac{d\rho}{\rho} + \frac{dA}{A} - \frac{1}{\gamma \mathcal{M}^2}\frac{dp}{p} = 0 \tag{2.78}$$

where the ideal-gas equation of state, equation (2.37), has been used to replace $\rho RT/M_w$ by p. In equations (2.77) and (2.78), γ is the frozen specific-heat ratio of the mixture:

$$\gamma = \frac{c_p}{c_p - R/M_w} \tag{2.79}$$

Combining equations (2.78) and (2.68) eliminates $d\rho$ from equation (2.78) and gives

$$\frac{\gamma \mathcal{M}^2 - 1}{\gamma \mathcal{M}^2}\frac{dp}{p} - \frac{dT}{T} - \frac{\sum_{i=1}^{NRS} d\sigma_i}{\sigma_m} + \frac{dA}{A} = 0 \tag{2.80}$$

If the temperature is assigned, equation (2.80) gives dp. The differential $d\rho$ is then obtained from equation (2.78), which combined with equation (2.80) gives

$$d\rho = \frac{\rho}{\gamma \mathcal{M}^2 - 1}\left(\frac{dT}{T} + \frac{\sum_{i=1}^{NRS} d\sigma_i}{\sigma_m} - \gamma \mathcal{M}^2 \frac{dA}{A} \right) \tag{2.81}$$

Combining equations (2.60) and (2.80) and using equations (2.37) and (2.77) provide the following expression for dV:

$$dV = \frac{-V}{\gamma \mathcal{M}^2 - 1}\left(\frac{dT}{T} + \frac{\sum_{i=1}^{NRS} d\sigma_i}{\sigma_m} - \frac{dA}{A}\right) \tag{2.82}$$

However, if the temperature is not assigned, an expression is needed for dT. Eliminating dp from equation (2.65) by using equation (2.80) produces the following equation for dT:

$$dT = -T\left\{\frac{\gamma - 1}{\mathcal{M}^2 - 1}\left[\mathcal{M}^2\left(\frac{dA}{A} - \frac{\sum_{i=1}^{NRS} d\sigma_i}{\sigma_m}\right) + \frac{\gamma \mathcal{M}^2 - 1}{\gamma \sigma_m}\left(\sum_{i=1}^{NRS} \frac{h_i}{RT} d\sigma_i + \frac{\dot{Q}'/\dot{m}}{RT} dx\right)\right]\right\} \tag{2.83}$$

To derive $d\rho$ and dV, this expression for dT is substituted into equations (2.81) and (2.82), respectively.

If time is the independent variable, equations (2.81) to (2.83) provide the following ODE's for the temperature, density, and velocity:

$$\frac{dT}{dt} = -T\left\{\frac{\gamma - 1}{\mathcal{M}^2 - 1}\left[\mathcal{M}^2\left(\frac{1}{A}\frac{dA}{dt} - M_w \sum_{i=1}^{NRS} \frac{d\sigma_i}{dt}\right)\right.\right.$$

$$\left.\left. + \frac{\gamma \mathcal{M}^2 - 1}{\gamma} M_w \left(\sum_{i=1}^{NRS} \frac{h_i}{RT}\frac{d\sigma_i}{dt} + \frac{\dot{Q}'/\dot{m}}{RT} V\right)\right]\right\} \tag{2.84}$$

$$\frac{d\rho}{dt} = \frac{\rho}{\gamma \mathcal{M}^2 - 1}\left(\frac{1}{T}\frac{dT}{dt} + M_w \sum_{i=1}^{NRS} \frac{d\sigma_i}{dt} - \frac{\gamma \mathcal{M}^2}{A}\frac{dA}{dt}\right) \tag{2.85}$$

$$\frac{dV}{dt} = \frac{-V}{\gamma \mathcal{M}^2 - 1}\left(\frac{1}{T}\frac{dT}{dt} + M_w \sum_{i=1}^{\text{NRS}} \frac{d\sigma_i}{dt} - \frac{1}{A}\frac{dA}{dt}\right) \tag{2.86}$$

The distance equations are

$$\frac{dT}{dx} = -T\left\{\frac{\gamma - 1}{\mathcal{M}^2 - 1}\left[\mathcal{M}^2\left(\frac{1}{A}\frac{dA}{dx} - M_w \sum_{i=1}^{\text{NRS}} \frac{d\sigma_i}{dx}\right)\right.\right.$$

$$\left.\left. + \frac{\gamma \mathcal{M}^2 - 1}{\gamma} M_w \left(\sum_{i=1}^{\text{NRS}} \frac{h_i}{RT}\frac{d\sigma_i}{dx} + \frac{\dot{Q}'/\dot{m}}{RT}\right)\right]\right\} \tag{2.87}$$

$$\frac{d\rho}{dx} = \frac{\rho}{\gamma \mathcal{M}^2 - 1}\left(\frac{1}{T}\frac{dT}{dx} + M_w \sum_{i=1}^{\text{NRS}} \frac{d\sigma_i}{dx} - \frac{\gamma \mathcal{M}^2}{A}\frac{dA}{dx}\right) \tag{2.88}$$

$$\frac{dV}{dx} = \frac{-V}{\gamma \mathcal{M}^2 - 1}\left(\frac{1}{T}\frac{dT}{dx} + M_w \sum_{i=1}^{\text{NRS}} \frac{d\sigma_i}{dx} - \frac{1}{A}\frac{dA}{dx}\right) \tag{2.89}$$

In equations (2.84) to (2.89), $1/\sigma_m$ has been replaced by M_w. In equations (2.85), (2.86), (2.88), and (2.89) the temperature derivative is given by equation (2.84) or (2.87), or evaluated from the assigned temperature profile. After the solutions for T, ρ, and V have been computed, the pressure is given by equation (2.51).

Chapter 3
Numerical Integration

The ordinary differential equations (ODE's) presented in chapter 2 can be generalized as

$$\left.\begin{aligned} \dot{\underline{y}} \equiv \frac{d\underline{y}}{d\xi} &= \underline{f}(\underline{y}) \\ \underline{y}\left(\xi = \xi_0\right) &= \underline{y}_0 = \text{Given} \end{aligned}\right\} \tag{3.1}$$

where an underscore represents a vector quantity. In equation (3.1), $\underline{y}$ is the solution vector with N components,

$$\underline{y} = \left(y_1, \ldots, y_N\right)^T \tag{3.2}$$

where the superscript T indicates transpose; that is, $\underline{y}$ is a column vector. The number of components depends on the problem type, and ξ is the independent variable—time t or distance x. The solution vector contains appropriate species mole numbers, thermodynamic variables, and when necessary, the reacting gas velocity. For clarity in presentation the dependence of $\underline{f}$ on the rate coefficient parameters, the heat transfer rate, etc., has been suppressed. (Also, for the rate coefficient expressions considered in the present work, the $\{f_i\}$ do not have an explicit dependence on ξ.)

The initial value problem is to solve for the species mole numbers, thermodynamic properties and, for a flow problem, velocity at one or more ξ values in a prescribed integration interval $[\xi_0, \xi_{end}]$, given the initial conditions, reaction mechanism, and rate coefficient parameters.

Before the numerical solution of the ODE's arising in combustion chemistry is discussed, the existence and uniqueness of the exact solution to equation (3.1) are addressed. For a first-order, initial value problem a fundamental theorem guarantees solution existence and uniqueness in the region of interest if $\underline{f}$ and $\partial \underline{f}/\partial y_j$ $(j = 1,\ldots,N)$

exist and are continuous in that region (refs. 27 and 28). The quantity $\partial \underline{f}/\partial \underline{y}$ (= **J**) is the Jacobian of $\underline{f}$ with respect to $\underline{y}$. It is an $N \times N$ matrix with element J_{ij} defined as

$$J_{ij} = \partial f_i / \partial y_j, \qquad i, j = 1, \ldots, N \tag{3.3}$$

The expressions given in appendix A of part II for $\{f_i\}$ and $\{J_{ij}\}$ show that both $\underline{f}$ and **J** exist and are bounded except at $\mathcal{M}^2 = 1$ for an assigned-area flow problem and $\gamma\mathcal{M}^2 = 1$ for an assigned-area, assigned-temperature flow problem. Here $\mathcal{M}$ is the Mach number and γ the frozen specific-heat ratio of the mixture. Therefore these two points and small regions around them are excluded from the computational domain. In the code LSENS, if $\mathcal{M}^2$ approaches 1 for an assigned-area flow problem or $\gamma\mathcal{M}^2$ approaches 1 for an assigned-area, assigned-temperature flow problem, an error exit is taken. At all other points the results of the above theorem guarantee solution existence and uniqueness.

Figure 3.1 illustrates the solution to a typical adiabatic, static combustion kinetics problem. This constant-pressure problem, taken from Pratt and Radhakrishnan (ref. 29), describes the ignition and subsequent combustion of a mixture of 33 percent carbon monoxide (CO) and 67 percent hydrogen (H_2) with stoichiometric air at an initial temperature of 1000 K and a pressure of 10 atm. The reaction mechanism consists of 12 reactions among 11 species and is given by Radhakrishnan (refs. 16 and 19).

Three distinct regimes, commonly denoted as induction, heat release, and equilibration, are apparent in figure 3.1. The induction regime is the period of time immediately following some form of reaction initiation, such as the passage of a shock wave through the fuel-air mixture. During the induction regime concentrations of chemically active species (such as O, H, and OH) increase from very small initial values to values sufficiently large to initiate oxidation reactions, with an attendant temperature increase. The induction regime ends and the heat release regime begins when sharply defined changes in temperature and concentration, commonly denoted as ignition, occur. During heat release the temperature and concentrations of combustion products (such as CO_2 and H_2O) and active intermediates increase very rapidly. The heat release regime ends and the equilibration regime begins after the active intermediate species have reached their maximum values and all variables have begun to equilibrate. The equilibration regime is characterized by the monotonic, asymptotic approach of all variables toward their chemical equilibrium values.

3.1 Computational Difficulty—Stiffness

The major difficulty associated with the automatic integration of the ODE's arising in chemical kinetics is that of "stiffness." For reasons discussed by Shampine (ref. 30) stiffness does not have a simple definition involving only the

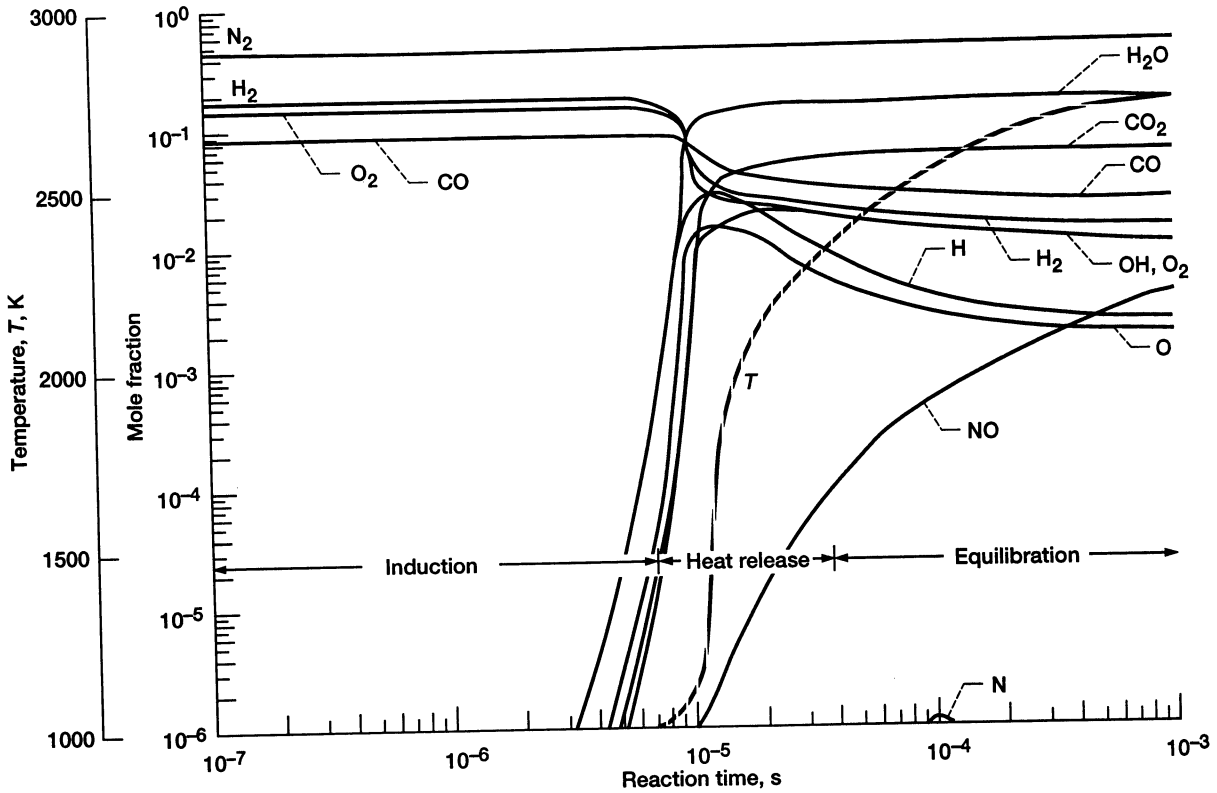

Figure 3.1.—Species mole fractions and temperature profiles for constant-pressure (10 atm) combustion of CO-H_2-air mixture. Initial temperature, 1000 K.

mathematical problem, equation (3.1). However, Shampine and Gear (ref. 31) discuss some fundamental issues related to stiffness and how it arises. Also, Pratt and Radhakrishnan (refs. 32 and 33) give some useful definitions of stiffness, due to others. Stiffness arises in chemical kinetics because of the vastly different relaxation times for the various chemical species. From a practical viewpoint stiffness manifests itself in a readily recognizable way. The use of classical ODE solution methods, such as the popular explicit Runge-Kutta method (e.g., refs. 34 and 35), to solve stiff problems results in prohibitive computational cost (refs. 16, 17, and 36) for reasons discussed here.

In general, numerical integration methods replace the ODE's with difference equations, which are solved step by step. Starting with the initial conditions at ξ_0, approximations $\underline{Y}_n$ (= $Y_{i,n}$, i = 1,...,N) to the exact solution $\underline{y}(\xi_n)$ (= $y_i(\xi_n)$, i = 1,...,N) of the ODE's are generated at discrete points ξ_n (n = 1,2,...), called mesh points, as illustrated in figure 3.2 for a single ODE. The spacing between any two mesh points is called the step size or step length and is denoted by h_n, where

$$h_n = \xi_n - \xi_{n-1} \tag{3.4}$$

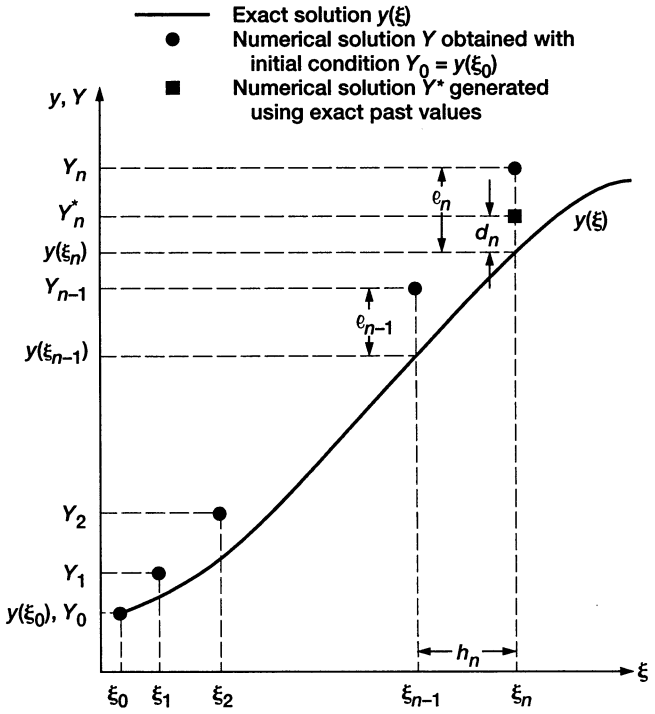

Figure 3.2.—Numerical solution and error types for single ODE $dy/d\xi = f(y)$. The local truncation error is designated by d, the global truncation error by e, and the step length by h.

The step length can vary from one step to the next, or can be constant, and is usually computed by the numerical integration method.

Solution of the relatively small problem illustrated in figure 3.1 was attempted with a classical numerical method, the explicit fourth-order Runge-Kutta method. The variation of the step length successfully used by the method versus reaction time is presented in figure 3.3 (ref. 36). During induction and heat release the step lengths selected by the method are small because the solution changes very rapidly in these regimes. During late heat release and equilibration, however, when the variables change slowly, larger step lengths should be possible. Surprisingly, for reasons discussed here, the step lengths continue to remain small and are of the same magnitude as those used in the earlier regimes. Consequently the number of steps and the computer time (i.e., CPU time) required for the problem are large—approximately 10 700 steps and 1 min, respectively, on an IBM 370/3033 computer (ref. 36). The situation is worse for larger problems. For example, a hydrogen-air combustion problem involving 15 species and 30 reactions required over 80 000 steps and 15 min of CPU time (ref. 36). Such prohibitive computer times required by classical ODE solution methods impeded the development of complex reaction mechanisms.

The difficulty of solving the ODE's describing combustion chemistry by the explicit Runge-Kutta method is related to the stability of the numerical method. Because of the approximate nature of the solutions generated by numerical integration methods, errors are inevitably introduced at every step. For a numerical

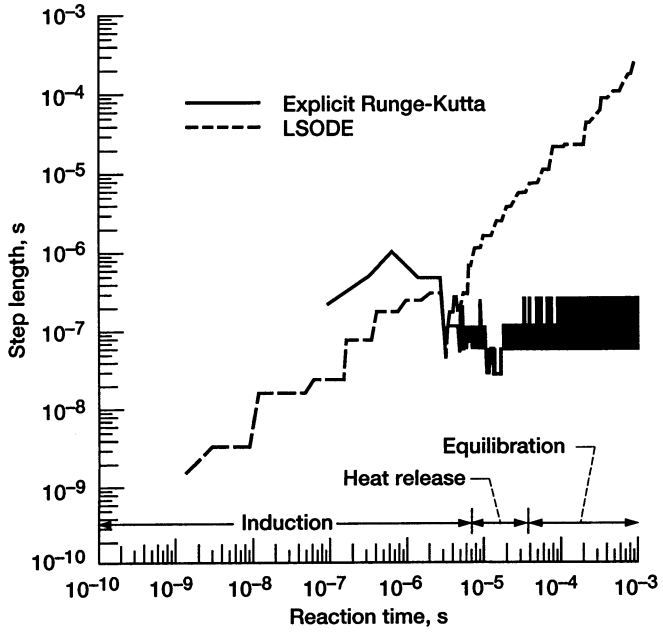

Figure 3.3.—Step length variation with reaction time for problem illustrated in figure 3.1.

method to be stable errors introduced at any one step should not grow unbounded as the calculation proceeds in time. Stiff problems force classical ODE solution methods to use unacceptably small step lengths (fig. 3.3) to maintain numerical stability (ref. 37).

An alternative practical description of a stiff problem is one whose solution by classical ODE methods is significantly more expensive than its solution by stiff methods, that is, methods designed specifically for stiff problems (refs. 38 and 39). For example, figure 3.3 shows the step lengths selected by the stiff ODE solver, LSODE (refs. 13 to 15), through the course of solving the problem illustrated in figure 3.1. Substantially larger step lengths are selected by the stiff ODE solver, especially during late heat release and equilibration. Consequently the computational work required by the stiff ODE solver—approximately 90 steps and 0.35 s (ref. 36)—was significantly less than that required by the explicit Runge-Kutta method.

In addition to being stable the numerical method needs to be accurate. Accuracy of a numerical method refers to the magnitude of the error introduced in a single step or more precisely the local truncation or discretization error. The local truncation error $\underline{d}_n$ at ξ_n is the difference between the computed approximation and the exact solution, with both starting the integration at the previous mesh point ξ_{n-1} and using the exact solution $\underline{y}(\xi_{n-1})$ as the initial value (fig. 3.2). The local truncation error on any step is therefore the error obtained on that step under the assumption of no past errors (e.g., ref. 40). Another commonly used definition is that it is the amount by which the exact solution fails to satisfy the difference equation of the numerical method (refs. 34 and 40 to 42). As discussed by Lambert (ref. 41), the quantities given by the two definitions are not, in general, the same. Although the first definition has been used for illustrative purposes, it is the quantity given by the second definition that is actually estimated and controlled in the program.

The accuracy of a numerical method is usually measured by its order. A method is said to be of order q if the local truncation error varies as h_n^{q+1}. More precisely a numerical method is of order q if there are quantities $\underline{C}$ and h_o (> 0) such that (refs. 28 and 43)

$$\left|\underline{d}_n\right| \leq \underline{C} h_n^{q+1} \qquad \text{for all } 0 < h_n \leq h_o \tag{3.5}$$

where $|\underline{d}_n|$ is an N-dimensional column vector containing the absolute values of the $d_{i,n}$ ($i = 1,...,N$). The coefficient vector $\underline{C}$ may depend on the function defining the ODE and on the total integration interval, but it should be independent of the step size h_n (ref. 43). Accuracy of a numerical method refers to the smallness of the error introduced in a single step; stability refers to whether or not this error grows in subsequent steps (ref. 31).

In addition to the local truncation error, roundoff errors are introduced at every step because computer arithmetic is performed in finite precision (i.e., with a fixed number of significant digits). As discussed by Henrici (ref. 34), for example, the

roundoff error depends on a number of factors. In general, this error increases with the number of calculations (i.e., as the step length is decreased) and can be reduced by using more precision (i.e., increasing the number of significant digits). Detailed discussions and analyses of roundoff errors are given in references 34, 35, and 42.

The phenomenon of stiffness in chemical kinetics was first recognized by Curtiss and Hirschfelder (ref. 44), who developed a simple backward differentiation formula method. Since then many techniques have been developed for stiff ODE's in general (refs. 13, 14, 39 to 42, and 45 to 52) and chemical kinetics equations in particular (refs. 7, 11, 12, 20, 29, 32, 33, 47, 49, and 52 to 56). In several recent publications (refs. 16 to 20 and 36) the efficiency and accuracy of many techniques for solving stiff ODE's arising in combustion chemistry were examined. These studies showed that the packaged code LSODE (refs. 13 to 15) is at present the most efficient and accurate method for combustion chemistry problems. It has therefore been adopted in the present work.

The integration methods used in LSODE and how they are implemented in practice are now described. The material presented here is essentially a summary of reference 15, which may be consulted for details.

3.2 Description of LSODE

3.2.1 Linear Multistep Methods: Backward Differentiation Formula

The numerical methods included in LSODE generate approximate solutions $\underline{Y}_n$ to the ODE's at discrete points ξ_n (n = 1,2,...). Assuming that the approximate solutions $\underline{Y}_{n-j}$ have been obtained at the mesh points ξ_{n-j} (j = 1,2,...), these methods advance the solution to the current value ξ_n of the independent variable by using linear multistep formulas of the type

$$\underline{Y}_n = \sum_{j=1}^{K_1} \alpha_j \underline{Y}_{n-j} + h_n \sum_{j=0}^{K_2} \beta_j \underline{f}_{n-j} \tag{3.6}$$

where the current approximate solution vector $\underline{Y}_n$ consists of N components:

$$\underline{Y}_n = \left(Y_{1,n}, \ldots, Y_{N,n}\right)^T \tag{3.7}$$

In equation (3.6), $\underline{f}_{n-j}$ [= $\underline{f}(\underline{Y}_{n-j})$] is the approximation to the exact derivative vector at ξ_{n-j}, $\dot{\underline{y}}(\xi_{n-j})$ [= $\underline{f}(\underline{y}(\xi_{n-j}))$], and the coefficients $\{\alpha_j\}$ and $\{\beta_j\}$ and integers K_1 and K_2 are associated with a particular method. The method is called linear because the $\underline{Y}_j$ and $\underline{f}_j$ occur linearly. It is called multistep because it uses information from several previous mesh points. The number max(K_1,K_2) gives the number of previous values involved.

The values $K_1 = 1$ and $K_2 = q - 1$ produce the popular implicit Adams, or Adams-Moulton (AM), method of order q:

$$\underline{Y}_n = \underline{Y}_{n-1} + h_n \sum_{j=0}^{q-1} \beta_j \underline{f}_{n-j} \tag{3.8}$$

The method is called implicit because it uses the as yet unknown $\underline{f}_n$ to compute $\underline{Y}_n$.

The choice $K_1 = q$, $K_2 = 0$ results in the backward differentiation formula (BDF) method of order q:

$$\underline{Y}_n = \sum_{j=1}^{q} \alpha_j \underline{Y}_{n-j} + h_n \beta_0 \underline{f}_n = \underline{\psi}_n + h_n \beta_0 \underline{f}(\underline{Y}_n) \tag{3.9}$$

where

$$\underline{\psi}_n = \sum_{j=1}^{q} \alpha_j \underline{Y}_{n-j} \tag{3.10}$$

contains previously computed information. The term "backward differentiation formula" is used to describe the method because equation (3.9), upon division by $h_n\beta_0$ and rearrangement of terms, can be regarded as an approximation for $\dot{\underline{y}}(\xi_n)$ in terms of $\underline{Y}_n, \underline{Y}_{n-1}, \ldots, \underline{Y}_{n-q}$ (refs. 39, 57, and 58).

Because the BDF method has much better stability characteristics than the AM method, it is preferred for stiff problems. In a later section (3.3.3) the use of the AM method for chemical kinetics problems is examined, and its inferiority to the BDF method for such problems is demonstrated. Therefore the discussion here is restricted to the BDF method.

The coefficients $\{\alpha_j\}$ and β_0 are determined such that equation (3.9) will be exact if the solution to equation (3.1) is a polynomial of degree q or less. Stability characteristics limit q in equation (3.9) to 6 (ref. 42). The coefficients $\{\alpha_j\}$ and β_0 for $q \leq 6$ are given by Gear (ref. 42) and reproduced in table 3.1. In LSODE, however, methods of order up to only 5 are used because of additional stability considerations (refs. 31 and 59). In equation (3.6), although the subscript n has been attached to the step length h, indicating that h_n is the step size to be attempted on the current step $[\xi_{n-1}, \xi_n]$, the methods used in LSODE are based on a constant h. When the step length is changed, the data at the new spacing required to continue the integration are obtained by interpolation from the data at the original spacing.

3.2.2 Corrector Iteration Methods

If $\beta_0 = 0$, the methods are called explicit because they involve only the known values $\underline{Y}_{n-j}$ $(j = 1,\ldots,q)$ and equation (3.6) is easy to solve. If, however, $\beta_0 \neq 0$, the

TABLE 3.1.—METHOD COEFFICIENTS FOR BACKWARD DIFFERENTIATION FORMULA METHOD OF ORDERS ONE TO SIX

q	β_0	α_1	α_2	α_3	α_4	α_5	α_6
1	1	1					
2	2/3	4/3	−1/3				
3	6/11	18/11	−9/11	2/11			
4	12/25	48/25	−36/25	16/25	−3/25		
5	60/137	300/137	−300/137	200/137	−75/137	12/137	
6	60/147	360/147	−450/147	400/147	−225/147	72/147	−10/147

methods are implicit and solution of equation (3.6) is generally expensive. For the BDF method of order q, equation (3.9), β_0 is positive for each q (see table 3.1), and because $\underline{f}$ is nonlinear, some type of iterative procedure is needed to solve equation (3.9). Nevertheless, implicit methods are preferred because they are more stable and hence can use much larger step lengths than explicit methods. They are also more accurate for the same order and step size because they have smaller error coefficients, $\underline{C}$ in equation (3.5) (refs. 40 to 42). Explicit methods are used as predictors, which generate an initial guess for $\underline{Y}_n$. The implicit method corrects the initial guess iteratively and provides a reasonable approximation to the solution of equation (3.9).

The predictor-corrector process for advancing the numerical solution to ξ_n therefore consists of first generating a predicted value, denoted by $\underline{Y}_n^{[0]}$, and then correcting this initial estimate by iterating equation (3.9) to convergence. That is, starting with the initial guess $\underline{Y}_n^{[0]}$, approximations $\underline{Y}_n^{[m]}$ ($m = 1,2,\ldots,M$) are generated (by using one of the techniques discussed next) until the magnitude of the difference in two successive approximations approaches zero within a specified accuracy. The quantity $\underline{Y}_n^{[m]}$ is the approximation obtained on the mth iteration, the integer M is the number of iterations required for convergence, and $\underline{Y}_n^{[M]}$ is accepted as an approximation to $\underline{y}(\xi_n)$ and therefore denoted by $\underline{Y}_n$ although in general it does not satisfy equation (3.9) exactly.

At each iteration m the quantity $h_n \dot{\underline{Y}}_n^{[m]}$, which is the mth estimate for $h_n \underline{f}_n$ (ref. 15), is obtained from $\underline{Y}_n^{[m]}$ by using the relation

$$\underline{Y}_n^{[m]} = \underline{\psi}_n + \beta_0 h_n \dot{\underline{Y}}_n^{[m]} \tag{3.11}$$

so that the pair $(\underline{Y}_n^{[m]}, \dot{\underline{Y}}_n^{[m]})$ satisfies the BDF exactly.

The predicted value at ξ_n, $\underline{Y}_n^{[0]}$, is obtained by a qth-order explicit formula similar to equation (3.9) (refs. 60 and 61):

$$\underline{Y}_n^{[0]} = \sum_{j=1}^{q} \alpha_j^* \underline{Y}_{n-j} + h_n \beta_1^* \dot{\underline{Y}}_{n-1} \tag{3.12}$$

where $\dot{\underline{Y}}_{n-1}$ is the approximation to $\underline{f}_{n-1}$ computed on the step $[\xi_{n-2},\xi_{n-1}]$. The coefficients $\{\alpha_j^*\}$ and β_1^* are selected such that equation (3.12) will be exact if the solution to equation (3.1) is a polynomial of degree q or less.

To correct the initial estimate given by equation (3.12), that is, to solve equation (3.9), LSODE includes a variety of iteration techniques—functional, Newton-Raphson, and Jacobi-Newton. All three iteration methods can be generalized by the recursive relations (ref. 15)

$$\underline{Y}_n^{[m+1]} = \underline{Y}_n^{[m]} + \beta_0 \mathbf{P}^{-1} \underline{g}\left(\underline{Y}_n^{[m]}\right) \tag{3.13}$$

and

$$h_n \dot{\underline{Y}}_n^{[m+1]} = h_n \dot{\underline{Y}}_n^{[m]} + \mathbf{P}^{-1} \underline{g}\left(\underline{Y}_n^{[m]}\right) \tag{3.14}$$

where the $N \times N$ iteration matrix $\mathbf{P}$ depends on the iteration technique and

$$\underline{g}\left(\underline{Y}_n^{[m]}\right) \equiv h_n \underline{f}\left(\underline{Y}_n^{[m]}\right) + \frac{\underline{\Psi}_n - \underline{Y}_n^{[m]}}{\beta_0} = h_n \underline{f}\left(\underline{Y}_n^{[m]}\right) - h_n \dot{\underline{Y}}_n^{[m]} \tag{3.15}$$

For functional iteration, also called simple iteration (refs. 38 and 48) and successive substitution (ref. 50), $\mathbf{P} = \mathbf{I}$, the $N \times N$ identity matrix. This method is simple to use, but it converges only linearly (ref. 50). In addition, for successful convergence the step length may be restricted to very small values for stiff problems (refs. 15, 40 to 42, 46, and 48). In fact, the restriction is exactly of the same form as that imposed by stability requirements on classical methods such as the explicit Runge-Kutta methods (refs. 41 and 48). For this reason, when functional iteration is used, the integration method is usually said to be explicit even though it is implicit (ref. 39).

Newton-Raphson (NR) iteration, on the other hand, converges quadratically and can use much larger step lengths than functional iteration (refs. 34, 50, and 62). For this method

$$\mathbf{P} = \mathbf{I} - h_n \beta_0 \mathbf{J} \tag{3.16}$$

where **J** is the Jacobian matrix, equation (3.3). This iteration will converge provided that the predicted value is sufficiently accurate (refs. 40 and 41). However, much computational work is required to form the Jacobian matrix and to perform the linear algebra necessary to solve equation (3.13). In order to reduce the computational work associated with linear algebra, **P** is not updated at every iteration. For additional savings it is updated only when the solution to equation (3.13) does not converge. Hence **P** is only accurate enough for the iteration to converge, and the same matrix may be used over several steps. Inaccuracies in **P** may affect the rate of convergence of the solution but not the solution if it converges (refs. 41 and 63). In any case, LSODE updates the Jacobian matrix at least every twentieth step.

A useful feature of LSODE is that it will estimate the elements of the Jacobian matrix by finite-difference approximations if the user chooses not to provide analytical expressions for them. This method will require $N + 1$ derivative evaluations for a system of N ODE's and, as shown in section 3.3.3, can therefore become much more expensive than the use of an analytical Jacobian, especially for large N.

However **J** is calculated, the linear algebra necessary to solve equation (3.13) is performed by the lower-upper (LU) method (e.g., refs. 64 and 65), rather than by explicitly inverting the iteration matrix, which will require prohibitive amounts of computer time (ref. 43). In the LU method the iteration matrix is factored into the product of two triangular matrices **L** and **U**. Solving equation (3.13) then requires the fairly simple solution of two triangular linear systems in succession.

Jacobi-Newton (JN) iteration (ref. 66), also called Jacobi iteration (ref. 67), is derived from Newton-Raphson iteration by neglecting all off-diagonal elements of the Jacobian matrix. Hence for JN iteration

$$J_{ij} = \begin{cases} 0, & i \neq j \\ \partial f_i / \partial y_j, & i = j \end{cases} \tag{3.17}$$

This technique is as simple to use as functional iteration because it does not require any matrix algebra. It converges faster than functional iteration but not quite as fast as NR iteration. For this iteration technique also either an analytical Jacobian matrix can be used, as explained in table 3.5, or the code will generate finite-difference approximations for the diagonal elements of the matrix.

3.2.3 Matrix Formulation: Nordsieck History Matrix

In order to solve for $\underline{Y}_n$ and $h_n \dot{\underline{Y}}_n$, by using equations (3.13) and (3.14), the $L = q + 1$ column vectors $\underline{Y}_{n-1}, \underline{Y}_{n-2}, \ldots, \underline{Y}_{n-q}$, and $h_n \dot{\underline{Y}}_{n-1}$ are needed and therefore must be saved. However, instead of saving this information, Gear (ref. 60) suggested storing the matrix devised by Nordsieck (ref. 68). If this history matrix is denoted by **z**, then $\mathbf{z}_{n-1}$ at ξ_{n-1} is given by

$$\mathbf{z}_{n-1} = \left(\underline{Y}_{n-1}, h_n \dot{\underline{Y}}_{n-1}, \frac{h_n^2}{2!} \ddot{\underline{Y}}_{n-1}, \ldots, \frac{h_n^q}{q!} \underline{Y}^{(q)}_{n-1} \right) \tag{3.18}$$

that is, the $N \times L$ matrix $\mathbf{z}_{n-1}$ is given by

$$\mathbf{z}_{n-1} = \begin{pmatrix} Y_{1,n-1} & h_n \dot{Y}_{1,n-1} & \cdots & \frac{h_n^q}{q!} Y^{(q)}_{1,n-1} \\ Y_{2,n-1} & h_n \dot{Y}_{2,n-1} & \cdots & \frac{h_n^q}{q!} Y^{(q)}_{2,n-1} \\ \vdots & \vdots & & \vdots \\ Y_{N,n-1} & h_n \dot{Y}_{N,n-1} & \cdots & \frac{h_n^q}{q!} Y^{(q)}_{N,n-1} \end{pmatrix} \tag{3.19}$$

where $Y^{(j)}_{i,n-1}$ is the jth derivative of the approximating polynomial for $Y_{i,n-1}$. The N rows of $\mathbf{z}_{n-1}$ are numbered from 1 to N, so that the ith row ($i = 1,\ldots,N$) contains the $q + 1$ scaled derivatives of the ith component, $Y_{i,n-1}$, of $\underline{Y}_{n-1}$. The $q + 1$ columns are, however, numbered from 0 to q, so that the column number corresponds to the order of the scaled derivative stored in that column. Thus the jth column ($j = 0,1,\ldots,q$) contains the vector $h_n^j \underline{Y}^{(j)}_{n-1}/j!$ The Nordsieck matrix formulation of the method is referred to as "the normal form of the method" (ref. 42).

At each step ξ_n the code constructs the updated matrix $\mathbf{z}_n$, which contains $\underline{Y}_n$ and its q scaled derivatives. The predicted matrix $\mathbf{z}_n^{[0]}$, which contains $\underline{Y}_n^{[0]}$ and its scaled derivatives, is given by (ref. 15)

$$\mathbf{z}_n^{[0]} = \mathbf{z}_{n-1}\mathbf{A} \tag{3.20}$$

where the $L \times L$ prediction matrix $\mathbf{A}$ provides a qth-order approximation to $\mathbf{z}_n^{[0]}$ in terms of $\mathbf{z}_{n-1}$ and is therefore the lower-triangular Pascal triangle matrix (ref. 42), with element A_{ij} given by

$$A_{ij} = \begin{cases} 0, & i < j \\ \binom{i}{j}, & i \geq j \end{cases} \qquad i, j = 0,1,\ldots,q \tag{3.21}$$

where $\binom{i}{j}$ is the binomial coefficient defined as

$$\binom{i}{j} = \frac{i!}{j!(i-j)!} \tag{3.22}$$

The corrector equation is given by (ref. 15)

$$\mathbf{z}_n^{[m+1]} = \mathbf{z}_n^{[0]} + \underline{e}_n^{[m+1]}\,\underline{\ell} \tag{3.23}$$

where $\mathbf{z}_n^{[m]}$ is the Nordsieck history matrix on the mth iteration, $\underline{e}_n^{[m+1]}$ is defined as

$$\underline{e}_n^{[m+1]} = \sum_{j=0}^{m} \mathbf{P}^{-1}\,\underline{g}\left(\underline{Y}_n^{[j]}\right) \tag{3.24}$$

and $\underline{\ell}$ is an L-dimensional vector

$$\underline{\ell} = \left(\ell_0, \ell_1, \ldots, \ell_q\right) \tag{3.25}$$

satisfying $\ell_0 = \beta_0$, $\ell_1 = 1$. For $q \le 6$ the values for $\underline{\ell}$ are given by Gear (ref. 42) and reproduced here in table 3.2. It is clear from the definition of $\underline{e}_n^{[m+1]}$ that

$$\underline{e}_n^{[m+1]} = \underline{e}_n^{[m]} + \mathbf{P}^{-1}\,\underline{g}\left(\underline{Y}_n^{[m]}\right) \tag{3.26}$$

TABLE 3.2.—METHOD COEFFICIENTS FOR BACKWARD DIFFERENTIATION FORMULA METHOD IN NORMAL FORM OF ORDERS ONE TO SIX

q	ℓ_0	ℓ_1	ℓ_2	ℓ_3	ℓ_4	ℓ_5	ℓ_6
1	1	1					
2	2/3	3/3	1/3				
3	6/11	11/11	6/11	1/11			
4	24/50	50/50	35/50	10/50	1/50		
5	120/274	274/274	225/274	85/274	15/274	1/274	
6	720/1764	1764/1764	1624/1764	735/1764	175/1764	21/1764	1/1764

Equation (3.23) can be used to rewrite $\underline{g}(\underline{Y}_n^{[m]})$, equation (3.15), as follows:

$$\underline{g}\left(\underline{Y}_n^{[m]}\right) = h_n \underline{f}\left(\underline{Y}_n^{[m]}\right) - h_n \dot{\underline{Y}}_n^{[0]} - \underline{e}_n^{[m]} \tag{3.27}$$

because $\ell_1 = 1$.

Now only the first two columns of $\mathbf{z}_n$ enter into the solution of equation (3.9) (see eqs. (3.13) and (3.14)). Therefore the successive corrections can be accumulated and applied to the remaining columns of $\mathbf{z}_n$ after convergence. Not updating all columns of the Nordsieck history matrix after each iteration saves computational effort, especially when a high-order method is used and/or N is large. For additional savings of computer time the history matrix is updated only if both the iteration converges and the converged solution satisfies accuracy requirements.

The predictor-corrector formulation utilized in LSODE can be summarized as follows:

Predictor:

$$\left.\begin{aligned} \mathbf{z}_n^{[0]} &= \mathbf{z}_{n-1}\mathbf{A} \\ \underline{e}_n^{[0]} &= 0 \end{aligned}\right\} \tag{3.28}$$

Corrector:

$$\left.\begin{aligned} \underline{g}\left(\underline{Y}_n^{[m]}\right) &= h_n \underline{f}\left(\underline{Y}_n^{[m]}\right) - h_n \dot{\underline{Y}}_n^{[0]} - \underline{e}_n^{[m]} \\ \underline{e}_n^{[m+1]} &= \underline{e}_n^{[m]} + \mathbf{P}^{-1}\underline{g}\left(\underline{Y}_n^{[m]}\right) \\ \underline{Y}_n^{[m+1]} &= \underline{Y}_n^{[0]} + \ell_0 \underline{e}_n^{[m+1]} \end{aligned}\right\} \quad m = 0, 1, \ldots, M-1 \tag{3.29}$$

$$\left.\begin{aligned} \underline{e}_n &= \underline{e}_n^{[M]} \\ \mathbf{z}_n &= \mathbf{z}_n^{[0]} + \underline{e}_n \underline{\ell} \end{aligned}\right\} \tag{3.30}$$

3.2.4 Corrector Convergence and Local Truncation Error Tests

After each iteration m convergence is ascertained by examining the magnitude of the difference $h_n \dot{\underline{Y}}_n^{[m]} - h_n \dot{\underline{Y}}_n^{[m-1]}$. In order to provide for user control of the convergence process, this difference is normalized by an error weight vector $\underline{\mathrm{EWT}}_n$, with element $\mathrm{EWT}_{i,n}$ defined by

$$\mathrm{EWT}_{i,n} = \mathrm{RTOL}_i \left| Y_{i,n-1} \right| + \mathrm{ATOL}_i \tag{3.31}$$

where RTOL_i and ATOL_i are, respectively, the user-supplied local relative and local absolute error tolerances for the ith component. The convergence test is then given by (ref. 15)

$$\varepsilon_m \equiv \sqrt{\frac{1}{N} \sum_{i=1}^{N} \left(\frac{h_n \dot{Y}_{i,n}^{[m]} - h_n \dot{Y}_{i,n}^{[m-1]}}{\mathrm{EWT}_{i,n}} \right)^2} \overset{?}{\leq} \frac{\tau(q)}{2(q+2)} \tag{3.32}$$

where $\tau(q)$ is the test constant used for the local error test (see eqs. (3.37) and (3.38)) and the variable q indicates the method order. If convergence is not achieved after the first iteration, the code anticipates the magnitude of ε_m one iteration in advance by assuming that the approximations converge linearly. Thus, ε_{m+1}, which does not as yet exist, is estimated by

$$\varepsilon_{m+1} = \varepsilon_m c_m \tag{3.33}$$

where c_m ($= \varepsilon_m / \varepsilon_{m-1}$) is the estimated convergence rate. This assumption is used to modify the convergence test as follows:

$$\varepsilon'_m \overset{?}{\leq} \frac{\tau(q)}{2(q+2)} \tag{3.34}$$

where

$$\varepsilon'_m = \varepsilon_m \min(1, 1.5c'_m) \tag{3.35}$$

and

$$c'_m = \max(0.2c_{m-1}, c_m) \tag{3.36}$$

Clearly at least two iterations are required to evaluate c_m. For the first iteration c'_m is set equal to the last value of c_m from the previous step. For the first iteration of the very first step, and for NR or JN iteration after every update of the Jacobian matrix, c'_m is set equal to 0.7.

If the corrector iteration fails to converge in three iterations, h_n is reduced if **P** is current and the step retried; otherwise **P** is updated and the step retried. If the corrector iteration converges after M ($M \leq 3$) iterations, the solution $\underline{Y}_n$ is accepted as sufficiently accurate if the following inequality is satisfied (ref. 15):

$$\sqrt{\frac{1}{N}\sum_{i=1}^{N}\left(\frac{e_{i,n}}{\mathrm{EWT}_{i,n}}\right)^2} \overset{?}{\leq} \tau(q) \tag{3.37}$$

where $\underline{e}_n$ is given by equation (3.30), the error weight vector $\underline{\mathrm{EWT}}_n$ is given by equation (3.31), and

$$\tau(q) = (q+1)/\ell_0 \tag{3.38}$$

is the local error test coefficient for the qth-order BDF method.

If the error test fails, the step is repeated with a reduced step size and/or a lower method order until either the test is passed or the situation considered hopeless. If the test is passed, the step is accepted as successful and the entire Nordsieck array updated by using equation (3.30).

The local error tolerances RTOL and ATOL (see eq. (3.31)) determine the nature of the error control performed by LSODE. Pure relative error control for the ith solution component is obtained by setting $\mathrm{ATOL}_i = 0$, and RTOL_i is then a measure of the number of accurate significant figures in the numerical solution. Setting $\mathrm{RTOL}_i = 0$ gives pure absolute error control, and ATOL_i is then a measure of the largest number that may be neglected. Both RTOL and ATOL can be specified either as scalars, so that the same error tolerances are used for all variables, or as arrays, so that different tolerances are used for different variables. The value of the user-supplied parameter ITOL indicates whether RTOL and ATOL are scalars or arrays. The legal values that can be assigned to ITOL and the corresponding types of RTOL and ATOL are given in table 3.3.

TABLE 3.3.—VALUES OF ITOL USED IN LSODE AND THEIR MEANINGS

ITOL	Description
1	Scalar RTOL and scalar ATOL
2	Scalar RTOL and array ATOL
3	Array RTOL and scalar ATOL
4	Array RTOL and array ATOL

3.2.5 Step Length and Method Order Selection and Change

After every $q + 1$ successful steps with the same method order q and step length h_n, LSODE attempts to change the step length and/or method order to minimize computational work while maintaining prescribed accuracy. In order to minimize the complication associated with method order and step length selection, the new order q' is restricted to the values $q - 1$, q, and $q + 1$. For each method order q' the step size $h'(q')$ that will satisfy exactly the local error bound is obtained by assuming that the highest derivative remains constant, as follows:

$$r_{q'} \equiv \frac{h'(q')}{h_n} = \left(\frac{1}{D_{q'}}\right)^{\frac{1}{q'+1}} \tag{3.39}$$

where r is the ratio of the step length to be attempted on the next step to its current value, the subscript q' denotes the method order to be used on the next step, and

$$D_{q'} = \sqrt{\frac{1}{N}\sum_{i=1}^{N}\left(\frac{d_{i,n}(q')}{\mathrm{EWT}_{i,n}}\right)^2} \tag{3.40}$$

where $d_{i,n}(q')$ is the estimated local truncation error in the ith variable for method order q'.

In computing the three step length ratios certain safety factors are introduced into equation (3.39) to produce smaller h' values to account for inaccuracies in the procedure. The formulas used in LSODE to calculate the step length ratios are as follows (ref. 15):

$$r_{q-1} = \frac{1}{1.3\left[\left(D_{q-1}\right)^{\frac{1}{q}} + 10^{-6}\right]} \tag{3.41}$$

$$r_q = \frac{1}{1.2\left[\left(D_q\right)^{\frac{1}{q+1}} + 10^{-6}\right]} \tag{3.42}$$

$$r_{q+1} = \frac{1}{1.4\left[\left(D_{q+1}\right)^{\frac{1}{q+2}} + 10^{-6}\right]} \tag{3.43}$$

The maximum step length ratio $r = \max(r_{q-1}, r_q, r_{q+1})$ and the corresponding method order are selected to be attempted on the next step if $r \geq 1.1$. Changes in both step length and method order are rejected if the step length increase is less than 10 percent because that is not considered large enough to justify the computational cost required by either change (refs. 42 and 69). Several additional tests, described by Radhakrishnan and Hindmarsh (ref. 15), are performed on r before the step length h' (= rh_n) to be attempted next is selected.

If the step length and/or the method order is changed, the Nordsieck history matrix has to be modified. For $q' = q$ and $h' \neq h_n$, the new $\mathbf{z}_n$ is obtained as follows:

$$\mathbf{z}_n \leftarrow \mathbf{z}_n \mathbf{C} \tag{3.44}$$

where the arrow "←" denotes the replacement operator, which means the overwriting of the contents of a computer storage location, and the $L \times L$ diagonal matrix $\mathbf{C}$ is given by

$$\mathbf{C} = \begin{pmatrix} 1 & & & & 0 \\ & r & & & \\ & & r^2 & & \\ & & & \ddots & \\ 0 & & & & r^q \end{pmatrix} \tag{3.45}$$

For $q' = q - 1$ and $h' \neq h_n$ the same scaling is performed on the first q columns; the last column of the old $\mathbf{z}_n$ is ignored because it is not needed on subsequent steps.

If $q' = q + 1$, $\mathbf{z}_n$ must be augmented by a column containing the vector $(h')^{q+1} \underline{Y}_n^{(q+1)}/(q+1)!$ The column addition is done in two stages. First, a $(q+2)$th column, containing $h_n^{q+1} \underline{Y}_n^{(q+1)}/(q+1)!$, which is given by (ref. 15)

$$\frac{h_n^{q+1}}{(q+1)!}\underline{Y}_n^{(q+1)} \cong \frac{\ell_q \underline{e}_n}{q+1} \tag{3.46}$$

is added to $\mathbf{z}_n$. Second, to account for any change in step length, all $q+2$ columns of the new $\mathbf{z}_n$ are rescaled as before.

Another factor that must be considered if the step length and/or method order is changed is that the iteration matrix $\mathbf{P}$, equation (3.16), may be altered even if the Jacobian matrix is current. In order to minimize convergence failures caused by an inaccurate iteration matrix, the code updates $\mathbf{P}$ and performs its LU-decomposition if the coefficient $h\beta_0$ (= $h\ell_0$) has changed by more than 30 percent since the last evaluation of $\mathbf{P}$.

3.2.6 Interpolation at Output Stations

During the course of solving a problem, solution values may be required at the output stations $\xi_{out,1}, \xi_{out,2}, \ldots$ that may not coincide with the naturally occurring $\{\xi_n\}$. These values are obtained as follows: For each output station ξ_{out}, LSODE continues the integration until the first mesh point n for which $\xi_n \geq \xi_{out}$ and then computes the solution at ξ_{out} by interpolation. Now the solution and its scaled derivatives up to order q'_{n+1} are available at ξ_n, where q'_{n+1} is the order to be attempted on the next step, that is, $[\xi_n, \xi_{n+1}]$. Hence the solution at ξ_{out}, $\underline{Y}(\xi_{out})$, is computed by using a (q'_{n+1})th-order Taylor series expansion about ξ_n:

$$\underline{Y}(\xi_{out}) = \sum_{k=0}^{q'_{n+1}} \frac{(\xi_{out} - \xi_n)^k}{k!}\underline{Y}_n^{(k)} = \sum_{k=0}^{q'_{n+1}} r^k \underline{z}_n(k) \tag{3.47}$$

where

$$r = \frac{\xi_{out} - \xi_n}{h'_{n+1}} \tag{3.48}$$

h'_{n+1} is the step size to be attempted on the next step, and

$$\underline{z}_n(k) = \frac{(h'_{n+1})^k}{k!}\underline{Y}_n^{(k)} \tag{3.49}$$

is the kth column ($k = 0,1,\ldots,q'_{n+1}$) of $\mathbf{z}_n$ (see eq. (3.19)). Because the solution is accurate to order q'_{n+1} at ξ_n and a (q'_{n+1})th-order Taylor series expansion is used to compute $\underline{Y}(\xi_{out})$, the latter is also accurate to order q'_{n+1}.

This method can be used to evaluate the solution derivative of any order (up to q'_{n+1}). For example, the μth derivative at ξ_{out}, $\underline{Y}^{(\mu)}(\xi_{out})$, is given by

$$\underline{Y}^{(\mu)}(\xi_{out}) = \sum_{k=\mu}^{q'_{n+1}} \frac{(\xi_{out} - \xi_n)^{k-\mu}}{(k-\mu)!} \underline{Y}_n^{(k)} = \frac{1}{(h'_{n+1})^{\mu}} \sum_{k=\mu}^{q'_{n+1}} r^{k-\mu} \frac{k!}{(k-\mu)!} \underline{z}_n(k) \qquad (3.50)$$

where r is given by equation (3.48).

3.2.7 Starting Procedure

At the outset of the integration, information is available at only the initial point ξ_0. Hence multistep methods cannot be used on the first step. LSODE resolves the difficulty at the initial point by starting the integration with a single-step, first-order method. The Nordsieck history matrix $\mathbf{z}_0$ at ξ_0 is constructed from the initial conditions $\underline{y}_0$ and the ODE's as follows:

$$\underline{z}_0(0) \equiv \underline{Y}_0 = \underline{y}_0 \qquad (3.51)$$

and

$$\underline{z}_0(1) \equiv h_0 \dot{\underline{Y}}_0 = h_0 \underline{f}(\underline{y}_0) \qquad (3.52)$$

where h_0 is the step length to be attempted on the first step.

As the integration proceeds, the numerical solutions generated at the points ξ_1, ξ_2,... provide necessary values for using multistep methods. Hence, as the numerical solution evolves, LSODE adjusts the method order (and step length) for optimal efficiency by using the procedure described in section 3.2.5.

The step length h_0 is computed by LSODE unless the user has specified a value for it. The calculation procedure for h_0 is based on the initial conditions and the quantity $\max(|\xi_0|, |\xi_{out,1}|)$, where $\xi_{out,1}$ is the first, or only, output station (ref. 15). Now, as explained in chapter 11 of part II, LSENS also includes the option of generating the solution after every I_P ($I_P \geq 1$) integration steps. In this situation $\xi_{out,1}$ is undefined; therefore LSENS sets $\xi_{out,1}$ equal to ξ_{end}, the user-supplied value of the independent variable at which the integration is to be terminated.

LSODE permits integration of the ODE's for either increasing or decreasing value of the independent variable. However, because chemical reaction problems

are irreversible, they are solved in the forward direction only (i.e., increasing ξ).[2] In addition, ξ_0 is usually set equal to zero. Hence $\xi_{out,1} > \xi_0$, and the calculation procedure for h_0 utilizes the user-specified value for $\xi_{out,1}$. Experience with the single-precision version of LSODE showed that the computational work and accuracy can be adversely affected by the choice of $\xi_{out,1}$ (ref. 17). The CPU time required by the double-precision version of LSODE used in LSENS showed less sensitivity to $\xi_{out,1}$. However, some combinations of ATOLSP (= local absolute error tolerance for reacting species mole numbers, see section 3.3.2) and $\xi_{out,1}$ produced inaccurate and unstable solutions. For example, for the problem illustrated in figure 3.1, a value of $\xi_{out,1} = 10^{-6}$ s (with EMAX (= local relative error tolerance for all variables, see section 3.3.2) = 10^{-6}, ATOLSP = 10^{-8}, $\xi_0 = 0$ s, and $\xi_{out,2} = 10^{-3}$ s) produced the correct solution at $\xi = 10^{-3}$ s. However, runs with other values for $\xi_{out,1}$ (between 10^{-3} and 10^{-12} s) failed because they either required excessive computational work[3] ($\xi_{out,1} = 10^{-7}$ s) or predicted little or no change in composition and temperature after an elapsed time of 10^{-3} s (all other $\xi_{out,1}$ values). When the maximum number of steps allowed for the problem was increased to 5000,[3] the run with $\xi_{out,1} = 10^{-7}$ s experienced numerical difficulty, that is, overflow errors. Thus the solutions generated by LSODE can be adversely affected by the value specified for $\xi_{out,1}$.

3.3 Experiments With LSODE

This section examines the use of different integration and corrector iteration methods for solving chemical kinetics problems. All results presented herein were obtained on the NASA Lewis Research Center's Amdahl 5870 computer using the UTS operating system, the Fujitsu 77 compiler (optimization level, 3), and double precision.

LSODE contains the AM method of orders 1 to 12 and the BDF method of orders 1 to 5. In addition, the code includes a variety of corrector iteration techniques. The user selects both the basic integration method and corrector iteration procedure by means of the method flag MF. By definition, MF has the two decimal digits METH and MITER, and

---

[2]For a flow problem with $\xi = x$ the ODE's can be integrated in the backward direction (i.e., decreasing ξ) by specifying a negative velocity. However, because the mass flow rate is by definition a positive quantity, the area should also be negative (see eq. (2.58)). In order to avoid additional testing of the legality of the input, integration is restricted in the direction of increasing ξ. This restriction does not limit the generality of the code because the user can always obtain the desired values for the independent variable by a linear transformation. For example, if the initial value is ξ'_0 and output is required at $\xi'_{out,n}$, $n = 1,2,...$, set $\xi_0 = 0$ and $\xi_{out,n} = |\xi'_{out,n} - \xi'_0|$, $n = 1,2,...$. The velocity V' (= $d\xi'/dt$) is given by $V \text{sign}(\xi'_{end} - \xi'_0)$, where V (= $d\xi/dt$) is computed by LSENS.

[3]As described in chapter 11 of part II, the maximum number of integration steps allowed for the problem is equal to the user-supplied value for the integer variable MAXSTP (default value, 2000). If more than MAXSTP steps are taken without successfully completing the problem, an error exit is taken.

$$MF = 10 \times METH + MITER \tag{3.53}$$

where METH and MITER indicate the integration method and corrector iteration technique to be used on the problem. Table 3.4 summarizes the integration methods included in LSODE, together with the appropriate values for METH. The legal values for MITER and their meanings are given in table 3.5. The iteration procedures corresponding to MITER = 1 to 5 are described as modified Newton iteration techniques because the Jacobian matrix is not updated at every iteration.

In order to identify the optimal integration and corrector iteration methods for chemical kinetics problems, all relevant method flag options (MF = 10 to 13 and 20 to 23) were attempted. The options MITER = 4 and 5 (and hence the methods given by the method flag MF = 14, 15, 24, and 25) were excluded because chemical kinetics problems do not have a Jacobian matrix with a banded structure. For clarity in presentation the integration method and corrector iteration technique corresponding to method flag MF will be designated as method MF. For example, method 21 means the BDF method with modified Newton iteration using an analytical Jacobian.

TABLE 3.4.—SUMMARY OF INTEGRATION METHODS INCLUDED IN LSODE AND CORRESPONDING VALUES OF METH

METH	Integration method
1	Variable-step, variable-order, implicit Adams method of orders 1 to 12
2	Variable-step, variable-order, implicit backward differentiation formula method of orders 1 to 5

TABLE 3.5.—CORRECTOR ITERATION TECHNIQUES AVAILABLE IN LSODE AND CORRESPONDING VALUES OF MITER

MITER	Corrector iteration technique
0	Functional iteration
1	Modified Newton iteration with user-supplied analytical Jacobian
2	Modified Newton iteration with internally generated numerical Jacobian
3	Modified Jacobi-Newton iteration with internally generated numerical Jacobian[a]
[b,c]4	Modified Newton iteration with user-supplied banded Jacobian
[b]5	Modified Newton iteration with internally generated banded Jacobian

[a]Modified Jacobi-Newton iteration with user-supplied analytical Jacobian can be performed by specifying MITER=4 and ML=MU=0,[b] i.e., a banded Jacobian with bandwidth of one.

[b]The user must specify the lower (ML) and upper (MU) half-bandwidths of the Jacobian matrix.

[c]This option should not be used with the present version of LSENS.

3.3.1 Test Problems

The 12 test problems, together with the thermodynamic and transport properties data, supplied with the packaged code GCKP84 (ref. 12), were used to compare the different integration and corrector iteration methods. Table 3.6 briefly describes each test problem. The problem parameters, listed in table 3.7,[4] show that the 12 cases cover a wide range of reaction conditions. Also, the problem size varies from 3 species and 1 reaction to 78 reactions among 33 species. Hence these problems should be useful in assessing solution techniques for chemical kinetics applications.

3.3.2 Selection of Local Error Tolerance Parameters

The accuracy of the solutions generated by LSODE, and hence LSENS, depends on the local error tolerance parameters $\{RTOL_i\}$ and $\{ATOL_i\}$ (see eqs. (3.31) and (3.37)). In a typical combustion kinetics problem the solutions for species concentrations and temperature vary widely (fig. 3.1), and so pure relative error control is appropriate. In addition, the same number of accurate significant figures is acceptable for all components. The option ITOL = 1, with ATOL = 0 (see table 3.3), is therefore appropriate for chemical kinetics problems. However, because

TABLE 3.6.—DESCRIPTION OF TEST PROBLEMS

Test problem	Description
1	Dissociation of bromine in a shock tube
2	Hydrogen-air combustion in supersonic flow with heat transfer
3	Same problem as case 2 but with a larger reaction mechanism
4	Hydrogen-oxygen combustion in subsonic flow with heat transfer
5	Static, rich methane-air combustion at assigned pressure with heat transfer
6	Lean methane-air adiabatic combustion in supersonic flow at constant pressure
7	Same problem as case 6 except that area obtained from case 6 is assigned as input
8	Constant-density, static methanol-air adiabatic combustion
9	Perfectly stirred reactor combustion of a rich propane-air mixture, followed by supersonic expansion of the combustion products with heat loss
10	High-temperature, adiabatic air ionization reaction in constant-area flow
11	High-temperature, high-pressure, static reaction of carbon monoxide–hydrogen mixture at constant density and constant temperature
12	Constant-density, adiabatic, static problem involving photolytic ignition of hydrogen-oxygen mixture at low initial temperature

[4]Since publication of reference 12 the authors reduced the reaction mechanism for test problem 11 from 21 reactions among 11 species to 14 reactions among 10 species. However, see test problem 13 in appendix D of part III.

TABLE 3.7.—PROBLEM PARAMETERS FOR TEST CASES GIVEN IN TABLE 3.6

Test problem	Number of reactions	Number of reacting species	Number of inert species	Number of ODE's	Independent variable	Integration interval[a]	
						ξ_0	ξ_{end}
1	1	2	1	5	x	0	4.0
2	28	13	2	16	x	0	15.24
3	31	13	2	16	x	0	15.24
4	18	8	0	11	x	0	22.845
5	66	25	0	27	t	0	5.85×10^{-4}
6	58	24	0	26	x	0	43
7	58	24	0	27	x	0	42
8	73	28	1	29	t	0	6.2×10^{-4}
9	78	32	1	35	x	0.2	4.0
10	12	12	0	15	x	0	0.7
11	14	10	0	10	t	0	10^9
12	20	8	0	9	t	0	1.147376

[a]Units are centimeters or seconds.

many species are assigned zero initial concentration, pure relative error control cannot be used. A mixed relative/absolute error control must therefore be utilized. Because concentrations of inert species, temperature, density, and velocity can never have zero values, pure relative error control can be used for these quantities. Hence, LSENS uses the option ITOL = 2, that is, a scalar RTOL (= EMAX) and an array ATOL (see table 3.3). For convenience, the same value of ATOL (= ATOLSP) is assigned for all reacting species mole numbers. For inert species mole numbers, temperature, density, and velocity, however, ATOL is set equal to zero.

The procedure for selecting the optimal EMAX and ATOLSP, that is, values that result in the least CPU time while satisfying prescribed accuracy requirements, is not clear. Because LSODE controls only the estimated local error, not much can be said about the actual or global error (e_n in fig. 3.2), which accumulates in a complicated way from the local errors. Because the user wants to control the global error, it must be measured. In the absence of exact solutions some procedure for estimating the global error must be established. One way to estimate the accuracy of the solution obtained with particular values for EMAX and ATOLSP is to compare it with results generated with reduced EMAX and ATOLSP. The solution used as a basis for comparison is referred to as the "standard solution" for the problem. For all test problems standard solutions were generated with method 21 and the local error tolerance values EMAX = 10^{-6} and ATOLSP = 10^{-15}. To provide a measure of the computational work required for a problem, the following parameters were recorded: total number of integration steps, NSTEP; total number of functional (i.e., derivative) evaluations, NFE; total number of Jacobian matrix evaluations and LU-decompositions, NJE; and total execution time (in seconds) to integrate the ODE's, CPU. Table 3.8 presents values of these parameters for the standard solutions.

The optimal values for EMAX and ATOLSP were obtained by a trial-and-error procedure and are given in table 3.9.[5] All experiments related to the optimization procedure were performed with method 21. In selecting the optimal values for the local error tolerances, the prescribed accuracy requirement was that the computed temperature profile agree with the standard solution to within 2 K. However, for

TABLE 3.8.—WORK REQUIRED BY LSENS FOR STANDARD SOLUTIONS
[Method 21, EMAX = 10^{-6}, ATOLSP = 10^{-15}.]

Test problem	NSTEP	NFE	NJE	CPU, s
1	91	114	24	0.040
2	355	484	52	1.0
3	325	448	52	1.0
4	399	511	47	0.63
5	594	741	63	6.0
6	499	642	68	3.0
7	387	511	53	2.5
8	433	522	50	3.1
9	302	397	54	3.1
10	135	172	19	0.23
11	571	737	103	0.53
12	593	841	90	0.94

TABLE 3.9.—OPTIMIZED ERROR TOLERANCES OBTAINED WITH METHOD 21 FOR TEST PROBLEMS

Test problem	EMAX	ATOLSP
1	10^{-2}	10^{-10}
2	5×10^{-3}	10^{-12}
3	5×10^{-3}	10^{-12}
4	10^{-5}	10^{-12}
5	10^{-4}	10^{-13}
6	10^{-4}	10^{-10}
7	5×10^{-5}	10^{-12}
8	5×10^{-4}	10^{-12}
9	10^{-3}	10^{-11}
10	10^{-2}	10^{-11}
11	10^{-2}	10^{-11}
12	10^{-6}	10^{-11}

[5]Although the results presented in this section were generated on the Amdahl 5870 computer, the optimal values for EMAX and ATOLSP were obtained on the NASA Lewis Research Center's IBM 370/3033 computer using an earlier version of LSENS (ref. 70).

problems 1 and 11 the temperature variation was either minimal or none; hence for these two problems the computed concentrations were required to be within 2 percent of the standard solution values. Thus for each test problem the EMAX and ATOLSP values given in table 3.9 minimized the CPU time required by method 21 while generating solutions that satisfied the accuracy criterion.

For each test problem the EMAX given in table 3.9 is not necessarily the maximum value that produced a sufficiently accurate solution. The reason is the dependence of both accuracy and execution time on ATOLSP, as documented in references 17 to 19 for the single-precision version of LSODE. The double-precision version of LSODE used in LSENS showed much less sensitivity to variations in ATOLSP than the single-precision version. However, use of very small ATOLSP to ensure accuracy can result in significantly increased CPU times. For example, for test problem 12 the run with EMAX = 10^{-6} and ATOLSP = 10^{-11} required approximately 0.5 s, which is only about half the CPU time required with ATOLSP = 10^{-15} (table 3.8).

Examination of table 3.9 shows that in several cases the required EMAX values are considerably smaller than the desired accuracy, illustrating the need for the integrator to control the global error. Such a control will also eliminate the trial-and-error procedure needed to optimize the error tolerances—a time-consuming process, especially for large problems.

The computational work required by method 21 to solve the 12 test problems with the optimized local error tolerances is given in table 3.10. Comparing tables 3.10 and 3.8 shows the significant savings in computer time that can be realized by using the optimized EMAX and ATOLSP. In many practical situations the accuracy criterion can be more relaxed than the one used here, resulting in additional savings of CPU time. The development and validation of a chemical reaction mechanism

TABLE 3.10.—WORK REQUIRED BY LSENS WITH METHOD 21 AND OPTIMIZED ERROR TOLERANCES GIVEN IN TABLE 3.9

Test problem	NSTEP	NFE	NJE	CPU, s
1	10	14	5	0.004
2	85	136	23	0.30
3	96	138	24	0.34
4	209	299	37	0.38
5	269	370	40	3.1
6	152	224	28	1.1
7	162	223	30	1.1
8	166	235	32	1.5
9	66	90	21	0.84
10	38	47	12	0.077
11	119	149	37	0.12
12	275	424	51	0.48

require solving the governing ODE's repeatedly. In this situation especially, the use of optimal local error tolerances will substantially shorten both the execution time and, more significantly, the computer turnaround time.

3.3.3 Comparison of Methods

Solutions to the 12 test problems were also attempted with methods 10 to 13 and 20 to 23—the other methods were excluded for reasons given previously. All methods used the optimized error tolerances obtained with method 21 (table 3.9). Using the same local error tolerances ensured that comparisons of computational work and global errors were made among methods that satisfied the same local accuracy requirements. In order to avoid using excessive amounts of CPU time to solve any problem, an error exit was made if more than 2000 integration steps had been taken without successfully completing the problem. Also, to prevent excessive output for problem 12, the output parameters $I_P = 60$ and $\xi_{end} = 1.147376$ s were changed to $\xi_{out,1} = 1.147376$ s.[6]

Methods 10 and 20 successfully completed only test problem 1 and their computational work requirements are given in table 3.11; for all other test problems an error exit occurred because of excessive computational work. Hence functional iteration is inappropriate for chemical kinetics problems. This fact is a consequence of the stiffness exhibited by the ODE's, as discussed in section 3.2.2.

Method 13 also successfully completed only test problem 1, for which the required computational work is given in table 3.11. The method failed on all other test problems because of one of the following three difficulties: excessive computational work (problems 4 and 12); invalid composition, in the sense that mass was not conserved (problems 2, 3, and 5 to 10)[7]; and numerical instability, that is, overflow error (problem 11).

Method 23 successfully completed test problems 1, 7, and 9; the computational work for the three cases is given in table 3.11. It failed on the other problems because of the same three difficulties experienced by method 13: excessive computational work (problems 5 and 12); invalid composition (problems 2 to 4, 6, 8, and 10); and numerical instability (problem 11). Moreover, for problem 7 method 23 was much more expensive and much less accurate than methods 11, 12, 21, and 22. For problem 9 also these four methods were more accurate than method 23, but only methods 11 and 21 were faster.

The results for methods 13 and 23 indicate that the modified Jacobi-Newton iteration technique used in LSODE is also inappropriate for chemical kinetics problems. The difficulties with this iteration method have been reported by others

[6]In reference 12 the values given for I_P and ξ_{end} are, respectively, 90 and 1.147479 s. However, since publication of this report, the output parameters were reset to the values given in the text.

[7]Whenever the solution is printed, LSENS checks the composition to ensure that mass is conserved. If the sum of the species mass fractions is different from unity by more than 5×10^{-5}, an error exit is made (see chapter 12 of part II).

TABLE 3.11.—WORK REQUIRED BY LSENS WITH METHODS 10, 13, 20, AND 23 FOR TEST PROBLEMS SUCCESSFULLY COMPLETED USING OPTIMIZED ERROR TOLERANCES GIVEN IN TABLE 3.9

Test problem	Method	NSTEP	NFE	NJE	CPU, s
1	10	11	15	0	0.004
1	13	12	28	8	0.004
1	20	11	15	0	0.004
1	23	13	30	8	0.004
7	23	1744	4983	1284	15
9	23	215	619	161	2.8

(refs. 71 to 73). When the error tolerances were decreased to EMAX = 10^{-6} and ATOLSP = 10^{-15}, the solutions generated by methods 13 and 23 were significantly more accurate than those obtained with the optimized error tolerances. In addition, several problems (1, 2, 3, 9, and 10) were successfully completed, and the solutions were essentially identical to the standard solutions. However, except for problems 1 and 10 these runs were considerably more expensive than the ones with methods 11 and 21, as shown in table 3.12, which gives the execution times required by the different methods for EMAX = 10^{-6} and ATOLSP=10^{-15}. With the reduced error tolerances methods 13 and 23 failed on all other problems because of excessive computational work.

The computational work required by methods 11, 12, and 22 with the optimized error tolerances is given in tables 3.13 to 3.15. Examination of tables 3.10, 3.11, and 3.13 to 3.15 shows that for test problem 1 there was little difference in the computational work required by the different methods and iteration techniques. However, with the smaller error tolerances the AM method was slightly faster than the BDF method (table 3.12). For almost all other problems method 21 was faster than method 11, and significantly so in several cases. Hence the BDF is the optimal integration method for chemical kinetics problems. The same conclusion was obtained by comparing methods 12 and 22 (tables 3.14 and 3.15) and by examining the CPU times required for the accurate solutions (table 3.12).

Problem 11 required integration of the ODE's over the time interval [0,10^9] s and posed the greatest difficulty for the AM method. Both methods 11 and 12 failed on this problem because of numerical instability. Examination of the solutions generated by the two methods showed that several species concentrations had very large (in magnitude) negative values, indicating that the AM method can be significantly inaccurate for chemical kinetics problems. When the local error tolerances were reduced to EMAX = 10^{-6} and ATOLSP = 10^{-15}, both methods failed because of excessive computational work; they failed on problem 12 also for the same reason but successfully completed all other test problems (table 3.12).

TABLE 3.12.—CPU TIMES REQUIRED WITH LOCAL ERROR TOLERANCES EMAX = 10^{-6} AND ATOLSP = 10^{-15}

Test problem	CPU, s, for method–					
	11	12	13	21	22	23
1	0.032	0.040	0.024	0.040	0.049	0.028
2	1.3	2.3	1.8	1.0	1.3	2.2
3	1.6	2.0	2.3	1.0	1.4	2.3
4	1.6	1.9	(a)	0.63	0.73	(a)
5	16	39	(a)	6.0	14	(a)
6	7.0	14	(a)	3.0	5.7	(a)
7	5.7	13	(a)	2.5	4.4	(a)
8	7.6	18	(a)	3.1	6.1	(a)
9	5.4	14	8.2	3.1	7.1	10
10	0.57	0.83	0.62	0.23	0.32	0.41
11	(a)	(a)	(a)	0.53	0.73	(a)
12	(a)	(a)	(a)	0.94	1.1	(a)

[a]Failed because of excessive computational work.

TABLE 3.13.—WORK REQUIRED BY LSENS WITH METHOD 11 AND OPTIMIZED ERROR TOLERANCES GIVEN IN TABLE 3.9

Test problem	NSTEP	NFE	NJE	CPU, s
1	10	14	5	0.004
2	105	186	26	0.40
3	112	214	33	0.50
4	382	562	77	0.72
5	671	931	72	7.4
6	218	349	50	1.7
7	306	437	50	2.1
8	227	327	38	2.0
9	69	121	24	1.1
10	28	34	9	0.055
11	(a)	(a)	(a)	(a)
12	(b)	(b)	(b)	(b)

[a]Terminated because of overflow error.
[b]Failed because of excessive computational work.

TABLE 3.14.—WORK REQUIRED BY LSENS WITH METHOD 12 AND OPTIMIZED ERROR TOLERANCES GIVEN IN TABLE 3.9

Test problem	NSTEP	NFE	NJE	CPU, s
1	10	39	5	0.003
2	152	762	31	0.79
3	121	741	33	0.79
4	538	1541	72	1.1
5	628	2844	73	17
6	239	1753	53	4.0
7	300	1750	49	4.1
8	243	1312	34	4.0
9	69	961	24	3.3
10	28	169	9	0.089
11	(a)	(a)	(a)	(a)
12	1519	3545	152	2.6

[a]Terminated because of overflow error.

TABLE 3.15.—WORK REQUIRED BY LSENS WITH METHOD 22 AND OPTIMIZED ERROR TOLERANCES GIVEN IN TABLE 3.9

Test problem	NSTEP	NFE	NJE	CPU, s
1	10	39	5	0.004
2	85	504	23	0.49
3	98	582	27	0.60
4	209	706	37	0.49
5	269	1450	40	8.3
6	152	952	28	2.2
7	162	1033	30	2.4
8	166	1163	32	3.4
9	66	825	21	2.8
10	38	227	12	0.12
11	119	519	37	0.19
12	275	894	52	0.59

Comparing the CPU times given in table 3.10 with those given in table 3.15 shows that method 21 was faster than method 22, and by a factor of 2 or more for several problems. Why method 21 was more efficient than method 22 will now be examined in some detail. Tables 3.10 and 3.15 show that for all problems, except cases 3 and 12, the two methods required the same number of steps and Jacobian matrix evaluations and LU-decompositions. Furthermore for these 10 problems the number of derivative evaluations needed by the corrector was the same for both methods. (For method 22 this number equals the total number of derivative evaluations (NFE) minus the additional number (= N×NJE) required for computing

the approximate Jacobians.) The last fact indicates that the number of corrector iterations was, in general, the same for the two methods. Hence the approximate Jacobian generated by the code is sufficiently accurate that the convergence rate was not adversely affected. These observations, together with the fact that the computational work needed for LU-decomposing the iteration matrix and backsolving for the corrections is the same for methods 21 and 22, indicate that the differences in execution times for solving the ODE's were strictly due to differences in the computational work required to form the Jacobian matrix. Careful examination of tables 3.7, 3.10, and 3.15 shows that the difference in CPU times for the two methods increased with both N and NJE. Indeed the CPU time difference per unit Jacobian matrix evaluation was the greatest for problems 5 to 9—the ones with the largest N (see table 3.7). (This CPU time difference was significantly more for problem 5 because the heat transfer model required considerable computational work.) The same behavior was exhibited by the runs with EMAX = 10^{-6} and ATOLSP = 10^{-15}. Now because chemical kinetics problems may involve numerous species, N is large. Hence the optimal corrector iteration technique for these problems is the modified NR iteration using an analytical Jacobian.

The same conclusion was obtained by comparing the CPU times required by methods 11 and 12 (tables 3.13 and 3.14). Except for problem 12 method 11 was faster than method 12, and in several cases by as much as a factor of 2 or more. Test problem 12 was characterized by a very rapid increase in temperature at $t \cong 1.14$ s, figure 3.4. To track this rapid variation accurately required small error tolerances,

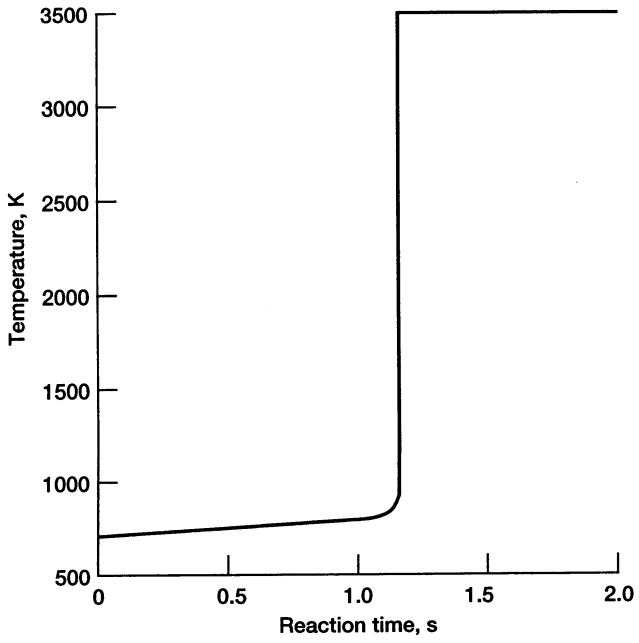

Figure 3.4.—Variation of temperature with reaction time for test problem 12.

which forced the code to use small step lengths and higher order methods. This problem also posed some difficulty for both methods 11 and 12. In particular, the computational work was sensitive to variations in both $\xi_{out,1}$ and ATOLSP. For example, when a print station at 0.1 s was included, the run with method 11 and ATOLSP = 10^{-11} was successfully completed and required about 1.8 s of CPU time. On the other hand, this modification to the input data caused method 12 to fail owing to excessive computational work. Additional experimentation with $\xi_{out,1}$, while keeping ATOLSP fixed at 10^{-11}, showed that either method could be made to fail or to be faster than the other. In light of this discussion, if test problem 12 can be excluded, method 11 was clearly more efficient than method 12. Furthermore examination of the execution times required by the two methods for the accurate runs (table 3.12) showed that method 11 was faster than method 12 for all problems—significantly so in several cases, sometimes by as much as a factor of 2 or more.

Although method 11 was slower than method 21, it was somewhat more accurate on several problems. The AM method was more accurate than the BDF method because it has a smaller local truncation error (ref. 42) and, in general, used smaller step lengths. Comparing the solutions generated by methods 11 and 12 with the optimized error tolerances showed that neither method was consistently more accurate than the other. Similar remarks apply to the solutions produced by methods 21 and 22 with the optimized error tolerances. These observations give credibility to the claim made in section 3.2.2 that inaccuracies in the iteration matrix do not affect the accuracy of the solution, provided of course that the matrix is accurate enough for the iteration to converge. Further confirmation of this beneficial fact was provided by the solutions generated with the reduced error tolerances—all methods produced essentially identical results. Nonetheless for reasons of efficiency an analytical Jacobian is preferred.

The preceding discussion implies that for chemical kinetics problems the best integration method and corrector iteration technique are given by method 21, the BDF method with the modified NR iteration using an analytical Jacobian matrix. The results with the implicit Adams method, together with those presented in section 3.1 for the explicit Runge-Kutta method (e.g., fig. 3.3), illustrate the importance of using implicit solution techniques for the stiff ODE's arising in chemical kinetics.

3.4 Comparisons With GCKP84

This section presents comparisons of the computational work required by the codes LSENS (using method 21) and GCKP84 (ref. 12), which uses the GEAR package (ref. 57) as modified by Zeleznik and McBride (ref. 74), to integrate the ODE's. The results with GCKP84 were also obtained on the NASA Lewis Research Center's Amdahl 5870 computer using the UTS operating system, the Fujitsu 77 compiler (optimization level, 3), and double precision.

The error control used in GCKP84 is different from, and for chemical kinetics problems inferior to, that used in LSODE, as discussed by Radhakrishnan (ref. 19). GCKP84 uses a semirelative local error control and, in contrast to LSODE, requires a single local error tolerance, EMAX. For species with zero initial concentration the error control is purely absolute. For all other variables the error control is purely relative. Hence, for GCKP84, EMAX is a mixed local relative and absolute error tolerance—relative for species with nonzero initial mole number, temperature, density, and velocity and absolute for species with zero initial mole number. Because, in general, most species have zero initial concentration, the error control performed by GCKP84 is mostly absolute. In contrast, the error control used with LSODE is mixed relative and absolute, and EMAX is the local relative error tolerance for all variables. The difference in error control, together with the fact that all $\sigma_i << 1$, implies that GCKP84 should need smaller values of EMAX than LSENS to attain comparable accuracy.

For each test problem the optimal EMAX (i.e., the value that minimized the CPU time while maintaining prescribed accuracy) was obtained with the same trial-and-error procedure and accuracy criterion used for LSENS. However, to prevent bias in favor of LSENS, the selection procedure for the optimal EMAX values for GCKP84 used new standard solutions, which were generated with GCKP84. For each test problem the "standard" EMAX, that is, the value needed for the standard solution, was determined by progressively decreasing EMAX until the solution showed negligible change with further decrease. The standard and optimal values for EMAX are given in table 3.16.[8] The standard solutions produced by GCKP84 were essentially identical to those obtained with LSENS. The computational work required by GCKP84 to generate the standard solutions is given in table 3.17. Examination of tables 3.8 and 3.17 shows that LSENS required substantially less CPU time than GCKP84 to generate standard (i.e., accurate) solutions.

Tables 3.9 and 3.16 show that, as expected, GCKP84 needed significantly smaller EMAX than LSENS to satisfy the same global accuracy requirements. Comparing the execution times given in tables 3.10 and 3.18 shows that for the optimal solutions also GCKP84 was substantially more expensive than LSENS. In fact, for almost all problems LSENS was faster than GCKP84 by a factor of 2 to 8.

The differences in the CPU times required by GCKP84 and LSENS may of course be attributed solely to the smaller standard and optimal EMAX values needed by GCKP84. To investigate this possibility, each code was run with the standard and optimized EMAX for the other code. Tables 3.19 and 3.20 give the computational work required by GCKP84 when run with the standard (10^{-6}) and optimized (table 3.9) EMAX values for LSENS. Test problem 12 required excessive computational work and is therefore excluded from tables 3.19 and 3.20. Comparing

[8]The standard and optimal EMAX values for GCKP84 were also obtained on the NASA Lewis Research Center's IBM 370/3033 computer. For test problem 11 the standard EMAX value ($=10^{-9}$) given in table 3.16 could not be used on the Amdahl 5870 computer because an error exit occurred at $t \cong 5.95\times10^{8}$ s owing to the excessively small step length ($h = 10^{-14}$ s) to be used on the next step. A value of EMAX = 5×10^{-9} was therefore used as the standard for test problem 11.

TABLE 3.16.—STANDARD SOLUTION AND OPTIMAL ERROR TOLERANCES REQUIRED BY GCKP84

Test problem	EMAX	
	Standard	Optimal
1	10^{-8}	10^{-3}
2	10^{-8}	10^{-7}
3	10^{-8}	10^{-7}
4	10^{-9}	10^{-8}
5	10^{-9}	5×10^{-8}
6	10^{-9}	10^{-7}
7	10^{-9}	10^{-8}
8	10^{-9}	10^{-7}
9	10^{-6}	5×10^{-4}
10	10^{-7}	10^{-3}
11	10^{-9}	10^{-6}
12	10^{-10}	5×10^{-9}

TABLE 3.17.—WORK REQUIRED BY GCKP84 FOR STANDARD SOLUTIONS USING EMAX VALUES GIVEN IN TABLE 3.16

Test problem	NSTEP	NFE	NJE	CPU, s
1	233	280	50	0.11
2	3617	3678	671	13
3	3775	3837	669	14
4	368	392	60	0.76
5	2577	5029	394	51
6	1510	1569	235	12
7	1098	1150	157	8.3
8	1504	2544	236	22
9	2368	3396	466	37
10	5183	5534	1341	11
[a]11	1007	1295	194	2.1
12	2556	2677	402	5.1

[a]EMAX = 5×10^{-9}.

TABLE 3.18.—WORK REQUIRED BY GCKP84 WITH OPTIMIZED ERROR TOLERANCES GIVEN IN TABLE 3.16

Test problem	NSTEP	NFE	NJE	CPU, s
1	22	33	8	0.013
2	459	476	73	1.6
3	431	449	79	1.6
4	217	236	39	0.45
5	504	1047	102	11
6	325	352	56	2.6
7	529	571	91	4.2
8	428	811	92	7.2
9	99	205	23	2.1
10	41	84	14	0.14
11	461	611	117	1.0
12	471	515	75	0.98

TABLE 3.19.—WORK REQUIRED BY GCKP84 WITH STANDARD EMAX (= 10^{-6}) USED WITH LSENS

Test problem	NSTEP	NFE	NJE	CPU, s
1	75	92	14	0.031
2	192	200	38	0.71
3	207	219	39	0.82
4	226	285	48	0.55
5	278	562	65	6.0
6	238	257	47	2.0
7	207	225	40	1.7
8	304	559	71	5.1
9	2368	3396	466	37
10	259	322	66	0.60
11	461	611	117	1.0

TABLE 3.20.—WORK REQUIRED BY GCKP84 WITH OPTIMIZED EMAX VALUES OBTAINED FOR LSENS, TABLE 3.9

Test problem	NSTEP	NFE	NJE	CPU, s
1	19	29	7	0.008
2	89	103	33	0.42
3	79	98	27	0.40
4	164	273	40	0.50
5	179	360	54	4.0
6	119	140	32	1.2
7	112	136	33	1.1
8	244	473	76	4.6
9	92	189	22	2.0
10	29	65	14	0.12
11	3406	4028	1331	8.6

the CPU times in tables 3.8 and 3.19 shows that with EMAX = 10^{-6} GCKP84 was faster than LSENS for some problems, especially 6. However, the solutions generated by GCKP84 for this and several other problems were inaccurate, sometimes significantly. For example, for problem 4, at $x = 22.845$ cm the computed temperature was 5444.8 °R, instead of 2193.1 °R. Tables 3.8 and 3.19 show that for most problems LSENS was either as fast as GCKP84 or faster, and significantly so in several instances. The same two conclusions are apparent for the runs with the optimal EMAX (tables 3.10 and 3.20). In this situation also, GCKP84 was quite inaccurate, and severely so for several problems. Hence LSENS was more accurate than GCKP84. Moreover, surprisingly, during equilibration, especially at long times when the ODE's are stiff (refs. 20, 32, 33, and 73), GCKP84 experienced numerical difficulties and sometimes reduced the step length drastically, thereby making the computation both time consuming and expensive. For example, for test problem 12 the run with EMAX = 10^{-6} required over 281 000 steps and a CPU time of approximately 4000 s. (For this problem and EMAX, GCKP84 predicted a shorter reaction time for the end of heat release (and start of equilibration) than that indicated in figure 3.4. Similar behavior has been observed on other problems.)

Final comparisons between the two codes were made by running LSENS with the standard and optimized EMAX values evaluated for GCKP84. For the first set of runs ATOLSP values were obtained by scaling down the standard value (10^{-15}) used with LSENS and are given in table 3.21.[9] For the second set of runs no attempt was made to optimize ATOLSP. Instead, the values obtained earlier (see table 3.9) were simply used. The computational work required by LSENS with these local error tolerances is given in tables 3.21 and 3.22. Examination of tables 3.17, 3.18, 3.21, and 3.22 shows that in these situations also LSENS was, in general, substantially faster than GCKP84.

[9]Although for consistency with GCKP84, EMAX = 5×10^{-9} was used for problem 11, the run with EMAX = 10^{-9} and ATOLSP = 10^{-18} was successfully completed and required about 1.4 s of CPU time.

TABLE 3.21.—WORK REQUIRED BY LSENS FOR ACCURATE EMAX VALUES OBTAINED FOR GCKP84, TABLE 3.16

Test problem	ATOLSP	NSTEP	NFE	NJE	CPU, s
1	10^{-17}	230	287	52	0.10
2	10^{-17}	643	822	67	1.6
3	10^{-17}	595	758	58	1.6
4	10^{-18}	1308	1715	144	2.1
5	10^{-18}	1726	2122	173	17
6	10^{-18}	1237	1512	121	6.8
7	10^{-18}	1400	1796	158	8.4
8	10^{-18}	1473	1870	149	11
9	10^{-15}	302	397	54	3.1
10	10^{-16}	201	254	25	0.33
[a]11	5×10^{-18}	1118	1402	146	0.95
12	10^{-19}	2610	3669	391	4.1

[a]EMAX = 5×10^{-9}.

TABLE 3.22.—WORK REQUIRED BY LSENS WITH OPTIMIZED EMAX VALUES OBTAINED FOR GCKP84, TABLE 3.16, AND ATOLSP VALUES GIVEN IN TABLE 3.9

Test problem	NSTEP	NFE	NJE	CPU, s
1	14	19	6	0.012
2	309	428	42	0.88
3	317	424	39	0.92
4	370	483	43	0.59
5	471	584	50	4.7
6	212	295	26	1.3
7	402	531	65	2.7
8	367	483	54	2.9
9	76	108	24	0.99
10	53	73	13	0.11
11	327	446	73	0.33
12	439	590	57	0.65

Tables 3.8, 3.10, 3.21, and 3.22 show that on average for all problems and local error tolerances less than two derivative evaluations (hence corrector iterations) were required per step by LSODE as pointed out by Byrne and Hindmarsh (ref. 39). In fact, in general, the average number of iterations per step was less than 1.5, in agreement with the findings of Shampine and Gear (ref. 31). The reason for the rapid convergence of the corrector is the accuracy of the predictor. Indeed the predictor is generally more accurate than the corrector, which is nonetheless needed for numerical stability (ref. 31). Rapid improvement in the accuracy of successive estimates is especially important for stiff problems because the corrector must be iterated to convergence; otherwise, its stability property is lost (refs. 40 and 41).

It is clear from tables 3.9 and 3.16 that the local error tolerances were varied widely—by many orders of magnitude. Consequently, the method-order-versus-reaction-time history also varied. Nevertheless tables 3.8, 3.10, 3.21, and 3.22 indicate that the average number of derivative evaluations per step was relatively insensitive to variations in the local error tolerances. Thus the number of iterations per step was essentially independent of the method order, which makes multistep methods particularly attractive when, as in the present application, the derivatives are expensive to evaluate (ref. 40). Careful examination of the four tables does, however, show a slight decrease in the average number of iterations per step when the error tolerances were reduced. The reasons are the generally smaller step lengths and higher method order selected and (the resultant) improvement in accuracy.

For most of the problems the optimized EMAX values evaluated for GCKP84 (table 3.16) were smaller than the standard EMAX (10^{-6}) used with LSENS. Nevertheless tables 3.8 and 3.22 show that the CPU times required by LSENS with these smaller EMAX values were, in general, either the same or less than the CPU times for the standard solutions. The reason is that the standard ATOLSP (10^{-15}) was smaller than the ATOLSP used in the latter runs (see table 3.9). These results illustrate the dependence of the computational work required by LSODE on ATOLSP, as pointed out earlier, and the importance of optimizing it.

Chapter 4
Sensitivity Analysis

The solution of the ordinary differential equations (ODE's) describing chemical kinetics depends on a number of parameters, such as initial conditions, rate coefficient parameters, and thermodynamic properties. The input parameters are often not known exactly, and constructing accurate models for the reaction chemistry (e.g., refs. 2 and 4) and thermodynamic properties (e.g., ref. 75) are active areas of research. The usual procedure for developing a reaction mechanism is to start with all possible reactions involving all relevant species (ref. 76). The mechanism is then fine tuned by discarding unimportant reactions and adjusting rate coefficient parameters to match experimental data.

The development of a reaction mechanism is both facilitated and made more accurate by a systematic sensitivity analysis, which provides the basic methods for studying parameter sensitivities, that is, changes in model behavior due to parameter variation (ref. 77). Sensitivity analysis in chemical kinetics establishes relationships between the predictions of a kinetic model (i.e., reaction mechanism) and the parameters of the problem (i.e., initial conditions, rate coefficient parameters, etc.). It helps to determine the effects of uncertainties in rate coefficient parameters or initial condition values on the model predictions. Parameters that have to be determined accurately because they have a large effect on the solution can thus be identified. At the same time rate coefficient parameters that show little or no effect on the solution need not be known with great precision. In some cases the latter reactions may even be eliminated, thereby simplifying the reaction mechanism. But perhaps the most significant utility of sensitivity analysis is the increased understanding it provides of a complex reaction mechanism. Advantages and applications of sensitivity analysis are discussed by Edelson (ref. 3) and Rabitz et al. (ref. 10).

Sensitivity analysis methods fall into two categories: local methods and global methods. Local methods typically produce the effect of a small change in one parameter about its nominal value by computing the first-order sensitivity coefficient $\partial y_i/\partial \eta_j$ evaluated at the generally accepted nominal values $\{\hat{\eta}_k\}$. Here y_i is a variable of interest (e.g., species concentration or temperature), and η_j a rate

coefficient parameter (eqs. (2.4) and (2.5)) or an initial condition value.[10] The first-order sensitivity coefficient vector $\underline{S}_j$ is defined as

$$\underline{S}_j = \left.\frac{\partial \underline{y}}{\partial \eta_j}\right|_{\text{all other } \eta_k}, \qquad j = 1,\ldots,M \tag{4.1}$$

Here, $\underline{y}$ is the N-dimensional solution vector, equation (3.2), M the total number of independent parameters, and $\underline{S}_j$ a column vector of length N:

$$\underline{S}_j = \left(S_{1,j},\ldots,S_{N,j}\right)^T \tag{4.2}$$

where the superscript T indicates transpose and

$$S_{i,j} = \left.\frac{\partial y_i}{\partial \eta_j}\right|_{\text{all other } \eta_k} \tag{4.3}$$

If sensitivities with respect to P ($P \leq M$) independent parameters are required, the first-order sensitivity matrix $\mathbf{S}$ is of size $N \times P$, with element S_{ij} given by equation (4.3).

The first-order sensitivity coefficient $\partial y_i/\partial \eta_j$ is the gradient of y_i with respect to the parameter η_j at a single point $\{\hat{\eta}_k\}$ in parameter space. The change Δy_i in the solution due to the change $\Delta \eta_j$ in the jth parameter can be approximated by

$$\Delta y_i \approx \left(\frac{\partial y_i}{\partial \eta_j}\right)\Delta \eta_j \tag{4.4}$$

for sufficiently small $\Delta \eta_j$.

The restriction to small changes does not apply to global methods, which can account for simultaneous parameter variations of arbitrary magnitude. These methods provide an average effect of all uncertainties examined. The sensitivities obtained are therefore different from the sensitivity coefficients defined here. However, for small variations in the input parameters there is a simple relationship between the coefficients computed by global methods and the linear sensitivity coefficients, equation (4.1) (ref. 78). Because global methods require repeated solution of the chemical kinetics equations, their computational cost can become

[10]Because, in general, thermodynamic properties are better known than rate coefficient parameters, the present work does not consider sensitivities with respect to thermodynamic properties.

prohibitive as the number of independent parameters increases (refs. 79 to 81). In addition, these methods require statistical information on the uncertainties in the input parameters, and this information is often not well known (ref. 21). Therefore a local sensitivity analysis method has been adopted in the present work. Global methods have been reviewed by Cukier et al. (ref. 9), Tilden et al. (ref. 82), Rabitz et al. (ref. 10), and Oran and Boris (ref. 56).

The simplest method for estimating the effect of an uncertainty in any parameter η_j is to run the simulation program, that is, solve the ODE's describing chemical kinetics, with two different values for η_j, say $\hat{\eta}_j$ and $\hat{\eta}_j + \Delta\eta_j$. The change $\Delta Y_i(t)$ in the numerical solution for the ith component at any time t is then given by

$$\Delta Y_i(t) = Y_i\left(\hat{\eta}_j + \Delta\hat{\eta}_j, t\right) - Y_i\left(\hat{\eta}_j, t\right) \tag{4.5}$$

where $Y_i(\hat{\eta}_j + \Delta\eta_j, t)$ and $Y_i(\hat{\eta}_j, t)$ are the numerical solutions for the ith component at time t obtained with the two different values for η_j. Although such a "brute force" method has been used successfully (refs. 78 and 83 to 85), it can become very expensive when the number of independent parameters is large. For M parameters the simulation program must be run at least $M + 1$ times to generate all first-order sensitivity coefficients. Also $\Delta\eta_j$ must be chosen carefully to ensure accuracy of the sensitivity coefficients (refs. 10, 21, and 81); see section 4.6.

To avoid the expense associated with repeated runs of the simulation program, several methods that solve directly for the sensitivity coefficients have been developed (refs. 20 to 23, 70, 81, and 86 to 102). These methods compute $\underline{S}_j$ by integrating the ODE's describing the temporal evolution of the sensitivity coefficients.

4.1 Governing Ordinary Differential Equations

The ODE's describing chemical kinetics, equation (3.1), are rewritten as[11]

$$\left.\begin{aligned} \frac{d\underline{y}}{dt} &= \underline{f}\left(\underline{y}, \underline{A}, \underline{n}, \underline{E}\right) \\ \underline{y}(t = t_0) &= \underline{y}_0 = \text{Given} \end{aligned}\right\} \tag{4.6}$$

to emphasize the functional dependence of $\underline{y}(t)$ on the rate coefficient parameter vectors $\underline{A}$, $\underline{n}$, and $\underline{E}$, each of which has NR components, where NR is the total number

[11] In the present work sensitivity analysis is limited to static problems. Therefore the independent variable is time t.

of reactions. If any rate coefficients are expressed in the form of equation (2.5), $\underline{E}$ will contain the $\{c_j\}$ in appropriate locations. Thus $\underline{E}$ contains NR parameters, some (or none) of which are the $\{c_j\}$ and the rest activation energies $\{E_j\}$. This notation is used to simplify the presentation. For isothermal reactions the rate coefficients $\{k_j\}$ are time invariant, and there is then no need to consider the individual rate coefficient parameters. For such problems equation (4.6) reduces to

$$\frac{d\underline{y}}{dt} = \underline{f}(\underline{y}, \underline{k}) \tag{4.7}$$

where $\underline{k}$ is the rate constant vector containing the NR rate constants.

The ODE for $\underline{S}_j$ can be obtained by differentiating equation (4.6) with respect to η_j and then interchanging the order of differentiation with respect to t and η_j. The result is

$$\frac{d\underline{S}_j}{dt} \equiv \underline{F}(\underline{S}_j) = \mathbf{J}\underline{S}_j + \left.\frac{\partial \underline{f}}{\partial \eta_j}\right|_{\underline{y}} \tag{4.8}$$

where $\mathbf{J}$ is the Jacobian matrix, equation (3.3), and for clarity in presentation the dependence of $\underline{F}$ on $\underline{y}, \underline{A}$, etc., has been suppressed. In equation (4.8) the first term on the right-hand side accounts for the implicit dependence of $\underline{f}$ on η_j through $\underline{y}$, and the second term takes into account any explicit dependence of $\underline{f}$ on η_j. If η_j is an initial condition value, $\underline{f}$ is not a function of η_j and $\partial \underline{f}/\partial \eta_j|_{\underline{y}} = 0$.

The initial value of $\underline{S}_j$ (i.e., $\underline{S}_j(t_0)$) is equal to the jth column of the $N \times N$ identity matrix if η_j is the jth element of $\underline{y}_0$; if, however, η_j is a rate coefficient parameter, $\underline{S}_j(t_0) = 0$.

Each parameter η_j results in N ODE's given by equation (4.8). Hence, for P independent parameters, NP ODE's have to be solved to produce the required first-order sensitivity coefficients. The ODE's are, however, independent of one another, so they can be solved separately. Also, although the model equation (4.6) can be highly nonlinear, the sensitivity equations (4.8) are linear ODE's with time-dependent coefficients. Therefore the sensitivity equations are easier to solve than the model equations.

4.2 Local Sensitivity Analysis Methods

The methods developed for solving equation (4.8) include the direct method (refs. 86 to 88), the Green's function method (refs. 89 and 90) and its variants (refs. 93 and 94), the analytically integrated Magnus modification of the Green's function

method (refs. 91 and 92), variational methods (refs. 95 to 97), and the decoupled direct method (refs. 21 to 23, 70, and 98 to 102). Local sensitivity analysis methods have been reviewed by Tilden et al. (ref. 82), Rabitz et al. (ref. 10), Kramer et al. (ref. 81), Oran and Boris (ref. 56), and Radhakrishnan (ref. 20).

4.2.1 Direct Method

The direct method (DM) (ref. 87), also called the direct variational method (ref. 88), computes the sensitivity coefficients by simultaneously solving the model and sensitivity equations, (4.6) and (4.8). An alternative implementation of the DM is to decouple the model equations from the sensitivity equations and solve the two sets of equations separately (ref. 86). The coupled DM, that is, solution of the combined system of equations (4.6) and (4.8), has been found to be quite inefficient and unstable or has failed completely on several stiff problems (refs. 90 and 91). Because the ODE's for the sensitivity coefficients are linear, whereas the combined system of ODE's is nonlinear, the decoupled approach to implementing the DM is, in theory, more efficient than the coupled DM. Surprisingly the decoupled procedure has shown no efficiency gains over the coupled DM on some problems (refs. 90 and 91). Furthermore it has proven unstable on some stiff problems (ref. 91); however, see reference 81.

4.2.2 Green's Function Method

The Green's function method (GFM) computes the Green's function for the sensitivity equations and then obtains the sensitivity coefficients from integrals over the Green's function (refs. 89 to 94). For $N < M$, which is generally true in chemical kinetics, the GFM requires the solution of fewer ODE's, and is therefore more efficient, than the DM. However, the GFM can still be expensive (ref. 91). In addition, it can produce significant inaccuracies when the solution changes rapidly. If accurate solutions are desired in rapidly varying regions, the GFM loses its computational advantage over the DM. The computational cost and accuracy of the GFM are also adversely affected by the choice of output stations, that is, the time values at which sensitivities are required.

4.2.3 Green's Function Method With Analytically Integrated Magnus Modification

The Green's function method with the analytically integrated Magnus modification (GFM/AIM) (refs. 91 and 92) was developed to reduce the cost associated with the GFM. The GFM/AIM uses different calculation procedures than the GFM for the Green's function and for the integrals that give the sensitivity coefficients. The GFM/AIM requires the specification of local error tolerances in addition to those required for solving the chemical kinetics equations. Using small values for the error tolerances can make the GFM/AIM much more expensive than the DM (ref. 81). In addition, the GFM/AIM shares with the GFM the disadvantages of the

computational work and accuracy both being adversely affected by the choice of output stations (ref. 21).

4.2.4 Variational Method

The variational method presented by Seigneur et al. (ref. 96) computes the sensitivities of objective functions. The function can be a single variable, such as a species concentration or temperature, or it may involve several variables, such as a class of species like unburnt hydrocarbons or pollutant species. The calculation procedure involves the solution of adjoint equations (ref. 103) and is similar to the GFM (ref. 10). The variational method for computing sensitivity coefficients is described by Koda et al. (ref. 95).

4.2.5 Decoupled Direct Method

The decoupled direct method (DDM) solves the sensitivity equations separately from, but sequentially with, the model equations. The procedure used to decouple the sensitivity equations from the chemical kinetics ODE's is different from, and avoids the instabilities associated with, the decoupled version of the DM.[12] For chemical kinetics applications the DDM has shown greater efficiency and stability, with equal or better accuracy than the DM, GFM, and GFM/AIM (refs. 20 to 22).

The DDM has been incorporated by Dunker (ref. 23) into an efficient computer program, CHEMDDM, which couples this sensitivity analysis method with the code LSODE (refs. 13 to 15) for solving the model equations. However, CHEMDDM is restricted to constant-density, constant-temperature problems. The restriction to constant-temperature problems appears to be characteristic of most sensitivity analysis codes developed to date. However, combustion kinetics is characterized by a narrow region of rapidly varying temperature (see fig. 3.1). Consequently sensitivity analysis of combustion kinetics equations must account for the effects of varying temperature on the rate coefficients (see eqs. (2.4) and (2.5)). However, until recently local sensitivity analysis methods have been successfully applied to constant-temperature problems only. For example, Dougherty and Rabitz (ref. 104) experienced numerical difficulties in attempting nonisothermal calculations of hydrogen-oxygen combustion. When sensitivity analysis of nonisothermal problems has been performed, the temperature has usually been assigned (e.g., refs. 78 and 105) and not computed independently.[13]

Recently Radhakrishnan (ref. 22) extended Dunker's (ref. 23) implementation of the DDM to nonisothermal combustion kinetics. The method can be used to

[12]To avoid confusion between the decoupled version of the direct method and the decoupled direct method, I will refer to the former method as the decoupled version of the DM, and the latter method as the DDM.

[13]Cukier et al. (ref. 9) performed sensitivity analysis of the nonisothermal hydrogen-fluorine reaction with a global method. Because the method involves repeated solution of the model equations for different values of the rate coefficient parameters, the temperature can be computed independently. But their work did not separate the effects of the temperature-independent part (i.e., $\{A_j\}$) from those of the temperature-dependent parts (i.e., $\{n_j\}$ and $\{E_j\}$) of the rate coefficients.

examine the effects of uncertainties in both the temperature-independent part (i.e., $\{A_j\}$) and the temperature-dependent parts (i.e., $\{n_j\}$ and $\{E_j\}$) of the rate coefficients. It has been demonstrated to be accurate and efficient for both constant- and varying-temperature problems (ref. 22) and has therefore been adopted in the present work. Descriptions of the DDM and how it is implemented in CHEMDDM, and hence LSENS, are presented next.

4.3 Decoupled Direct Method

The decoupled direct method solves the ODE's for the sensitivity coefficients separately from, but sequentially with, those describing the chemical kinetics. The same algorithm that solves the ODE's for the reaction chemistry solves the sensitivity equations. The rationale for using the same solver is that the two sets of equations have the same Jacobian.

As discussed in chapter 3, the most efficient and accurate method for solving chemical kinetics problems is the backward differentiation formula (BDF) method included in the packaged code LSODE (refs. 13 to 15). The BDF method, as implemented in LSODE, is therefore used to integrate the sensitivity ODE's. Also the most efficient iteration technique was found to be the modified Newton iteration using an analytical Jacobian. In the following discussion it will therefore be assumed that the BDF method with the modified Newton iteration using an analytical Jacobian, that is, the method flag MF = 21 (see eq. (3.53)), has been selected to solve the model equations.[14]

If the BDF method is used to solve the ODE for $\underline{S}_j$ over the time step $[t_{n-1},t_n]$, the resulting formula, corresponding to equation (3.9), is given by

$$\underline{S}_{j,n} = \sum_{k=1}^{q_n} \alpha_k \underline{S}_{j,n-k} + h_n \beta_0 \underline{F}_{j,n} = \underline{\Psi}_{j,n} + h_n \beta_0 \underline{F}_{j,n} \tag{4.9}$$

where

$$\underline{\Psi}_{j,n} = \sum_{k=1}^{q_n} \alpha_k \underline{S}_{j,n-k} \tag{4.10}$$

contains previously computed information. In equation (4.9), $\underline{S}_{j,n}$ [= $\underline{S}_j(t_n)$] is the sensitivity coefficient vector at the current time t_n; q_n is the order of the numerical approximation for the step $[t_{n-1},t_n]$; the method coefficients $\{\alpha_k\}$ and β_0

[14]Indeed, when sensitivity analysis computation is required, the code LSENS allows only method 21 to be used to solve the chemical kinetics ODE's. For a kinetics-only computation any legal value may be assigned for MF. However, for sensitivity analysis computations, specifiying a value for MF other than 21 will result in an error exit. The default value for MF is 21.

depend on q_n (see table 3.1); $\{\underline{S}_{j,n-k}\ [=\underline{S}_j(t_{n-k})]\}$ are the $\underline{S}_j$ at the previous times t_{n-k}, $k = 1,...,q_n$; h_n $(= t_n - t_{n-1})$ is the step size for this step; and $\underline{F}_{j,n} = \underline{F}(\underline{S}_j(t_n))$. Writing out the expression for $\underline{F}_{j,n}$, equation (4.8), and collecting terms give

$$\mathbf{P}(t_n)\underline{S}_{j,n} = \underline{\Psi}_{j,n} + h_n\beta_0 \frac{\partial \underline{f}}{\partial \eta_j}(t_n) \tag{4.11}$$

where

$$\mathbf{P}(t_n) = \mathbf{I} - h_n\beta_0\mathbf{J}(t_n) \tag{4.12}$$

and $\mathbf{I}$ is the $N \times N$ identity matrix.

Equation (4.11) can also be derived by differentiating equation (3.9) with respect to η_j (ref. 21). Although the model solution vector $\underline{Y}$ is defined only at discrete points in time, it can still be considered as a continuous function of the $\{\eta_j\}$.

Because equation (4.8) is linear, equation (4.11) is also linear. Hence the solution can be obtained explicitly; that is, solution of equation (4.11) does not require an iterative predictor-corrector procedure. Because the original model $\dot{\underline{y}} = \underline{f}(\underline{y})$ has been replaced by the finite-difference model, equation (3.9), the sensitivities $\partial\underline{Y}/\partial\eta_j$ calculated from equation (4.11) are the exact sensitivities of $\underline{Y}$ with respect to η_j, apart from computer roundoff (ref. 21), provided of course that the Jacobian matrix $\mathbf{J}(t_n)$ is accurate. Note, however, that because $\underline{Y}_n$ may be different from $\underline{y}(t_n)$, the solution to equation (4.11) may not give the exact sensitivity coefficient $\partial\underline{y}/\partial\eta_j(t_n)$.

Equations (3.13), (3.15), (3.16), (4.11), and (4.12) show the similarity between the finite-difference equations for the chemical kinetics variables and the sensitivity coefficients. The DDM exploits the similarity by alternating the solution of equation (3.9) with that of equation (4.11) (ref. 21). For any step $[t_{n-1},t_n]$ the solution $\underline{Y}$ to the model equations is advanced by one time step from t_{n-1} to t_n by using LSODE. The solution $\underline{Y}_n$ at t_n is then used in equation (4.11) to update the sensitivity coefficients with respect to all the required (P) parameters. The next step in the calculation procedure is to advance $\underline{Y}$ from t_n to t_{n+1}. Then $\underline{Y}_{n+1}$ is used to advance $\underline{S}_j$ ($j = 1,...,P$) from t_n to t_{n+1}. The process of advancing $\underline{Y}$ and then $\underline{S}_j$ ($j = 1,...,P$) by the same time step, using the same method order, is repeated until the end of the integration interval. This procedure is illustrated schematically in figure 4.1.

During the course of solving the model problem LSODE automatically generates values for q_n, q_{n+1},... and h_n, h_{n+1},... (and hence, t_n, t_{n+1},...), as described in chapter 3 (section 3.2.5). In solving for the sensitivity coefficients the DDM uses exactly the same step length and method order as those used for the model problem, so the error control in the solution of equation (4.11) is determined by the error control in the solution of equation (4.6) (ref. 21). Hence the DDM needs no additional error tolerances beyond those required for the model system, provided that $\mathbf{J}(t)$ is updated before the sensitivities are computed.

To reduce the computational cost associated with matrix algebra, LSODE updates the Jacobian matrix only when the solution to equation (3.9) does not

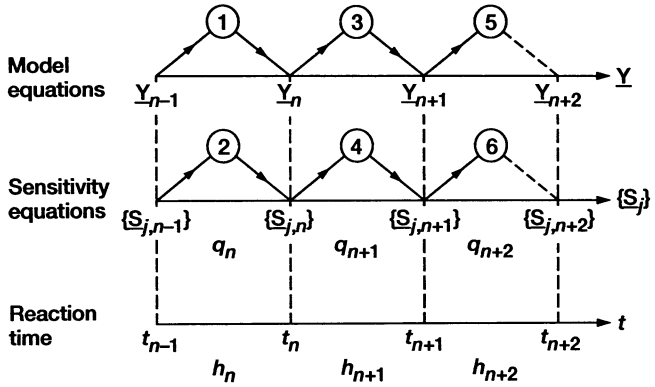

Figure 4.1.—Schematic illustration of decoupled direct method (after ref. 21). The numbers in circles denote the sequence in which the model and sensitivity equations are solved. The step size is designated by *h* and the method order by *q*.

converge. As noted in chapter 3 (section 3.2.2), inaccuracies in **J** may affect the convergence rate but not the accuracy of the solution to equation (3.9) if the iteration converges. However, the ODE's for the sensitivity coefficients, equation (4.8), contain **J** explicitly. To maintain accuracy in the computed $\underline{S}_j$, the matrix **P** in equation (4.11) must therefore be recomputed at every time step unless **J** changes slowly (refs. 21 and 99). For example, during equilibration the solution changes slowly, figure 3.1, and the use of an old Jacobian may be adequate. In the present work use of an old Jacobian is not explored, and **J** and **P** are updated at every step.[15] Note, however, that because the same matrix **P** is required in both equations (3.13) and (4.11), no additional programming is required by the DDM for either the computation of **P** or its LU-decomposition.

At each solution step equation (4.11) must be solved as many times as the number of independent parameters with respect to which the solution sensitivity is required. However, because **P** is independent of the sensitivity parameters, it has to be formed and LU-decomposed only once, irrespective of the number of sensitivity parameters. Hence, although calculating the sensitivities with respect to the first parameter may require considerable work to form **P**, perform its LU-decomposition, and solve equation (4.11), evaluating the sensitivity coefficients with respect to the second and subsequent parameters is significantly less expensive.

The advantage of solving the model and sensitivity equations sequentially step by step is that the computed solution to the model problem does not have to be stored for the entire integration interval, which consists of many steps. In contrast, the decoupled version of the DM, the GFM, the GFM/AIM, and the variational method all have to store the computed solution for the complete integration interval. The

[15]As discussed in appendix C of part II, LSENS includes a switch that can be set so that the Jacobian matrix for sensitivity analysis computations is updated only for steps on which LSODE updates this matrix while solving the model equations.

DDM also avoids the added expense and inherent errors associated with the later approximation of **J** from the stored solution, as done in the other four methods. The decoupled version of the DM, the GFM, the GFM/AIM, and the variational method compute the sensitivity coefficients after the model problem has been solved over the entire integration interval. Hence in solving for the sensitivities these four methods, unlike the DDM, do not necessarily use the same time sequence $t_n, t_{n+1},\cdots$ utilized for the model problem. In order to compute **J** and $\partial \underline{f}/\partial \eta_j$ at the times where the sensitivities are generated, $\underline{Y}$ and $\underline{f}$ must be obtained by interpolation, resulting in additional cost and inaccuracies. The coupled version of the DM avoids the problems associated with interpolation by simultaneously solving the $2N$ model and sensitivity ODE's. However, solving the $2N$ equations requires more computational work than solving the two systems separately. The reason for the increased computational effort is twofold: (1) a larger system of equations has to be solved and (2) the sensitivity equations are linear and therefore do not require iteration, whereas the combined system of equations is nonlinear and therefore requires an iterative procedure.

Finally, as discussed by Dunker (ref. 21), the DDM is easier to program than the GFM/AIM and requires a smaller computer program and less array storage if $M < 7N + C(1 + 1/N)$, where $C \simeq 100$. Hence, in general, the DDM needs less array storage than the GFM/AIM for chemical kinetics problems.

4.3.1 Matrix Formulation

To preserve the similarity between the solution procedures for the model and sensitivity equations, the Nordsieck history matrix formulation of the DDM is constructed. Exactly the same procedures utilized in chapter 3 (section 3.2.3) are followed in developing the matrix formulation of the DDM. The same symbol is also used as before for the history array. However, in order to avoid confusion between the history arrays for the model problem and the sensitivity equations, the upper case letter **Z** is used to denote the history array containing the sensitivity information. Here **Z** is analogous to the **z** array defined in chapter 3 (see eqs. (3.18) and (3.19)). There is, however, one important difference between **Z** and **z**. Whereas **z** is a two-dimensional array of size $N \times L$, **Z** is a three-dimensional array of size $N \times L \times P$, where $L = q_n + 1$. However, because the sensitivity equations for the different parameters are independent of one another, only one parameter, η_j, need be considered. Sensitivities with respect to all other parameters can be computed by following exactly the same procedure developed for η_j. The $N \times L$ Nordsieck history matrix for η_j is denoted by $\mathbf{Z}_j$.

The history matrix for the jth parameter at t_{n-1}, $\mathbf{Z}_{j,n-1}$, which is the analog to $\mathbf{z}_{n-1}$, equation (3.18), is defined as

$$\mathbf{Z}_{j,n-1} = \left(\underline{S}_{j,n-1}, h_n \dot{\underline{S}}_{j,n-1}, \frac{h_n^2}{2!} \ddot{\underline{S}}_{j,n-1}, \ldots, \frac{h_n^{q_n}}{q_n!} \underline{S}^{(q_n)}_{j,n-1} \right) \tag{4.13}$$

that is,

$$\mathbf{Z}_{j,n-1} = \begin{pmatrix} S_{1,j}(t_{n-1}) & h_n \dot{S}_{1,j}(t_{n-1}) & \frac{h_n^2}{2!}\ddot{S}_{1,j}(t_{n-1}) & \cdots & \frac{h_n^{q_n}}{q_n!}S_{1,j}^{(q_n)}(t_{n-1}) \\ S_{2,j}(t_{n-1}) & h_n \dot{S}_{2,j}(t_{n-1}) & \frac{h_n^2}{2!}\ddot{S}_{2,j}(t_{n-1}) & \cdots & \frac{h_n^{q_n}}{q_n!}S_{2,j}^{(q_n)}(t_{n-1}) \\ \vdots & \vdots & \vdots & & \vdots \\ S_{N,j}(t_{n-1}) & h_n \dot{S}_{N,j}(t_{n-1}) & \frac{h_n^2}{2!}\ddot{S}_{N,j}(t_{n-1}) & \cdots & \frac{h_n^{q_n}}{q_n!}S_{N,j}^{(q_n)}(t_{n-1}) \end{pmatrix} \tag{4.14}$$

where $S_{i,j}^{(k)}(t_{n-1})$ is the kth temporal derivative of $S_{i,j}$ at t_{n-1}.

To derive analogs of the prediction and correction procedures utilized on the model equations for the step $[t_{n-1}, t_n]$, the calculation procedure for $\underline{S}_{j,n}$ is split into two stages as follows: An initial estimate $\underline{S}_{j,n}^{[0]}$ is first computed; this step is analogous to the predictor step. The initial estimate is then "corrected" to get the sensitivity coefficient vector at t_n; this step corresponds to a single corrector iteration. Both steps are derived by directly applying equations (3.28) to (3.30) for a single iteration.

The predictor step, obtained from equation (3.28), is given by

$$\mathbf{Z}_{j,n}^{[0]} = \mathbf{Z}_{j,n-1}\mathbf{A} \tag{4.15}$$

where $\mathbf{Z}_{j,n}^{[0]}$ is the "predicted" Nordsieck history matrix at t_n, that is,

$$\mathbf{Z}_{j,n}^{[0]} = \left(\underline{S}_{j,n}^{[0]}, h_n \dot{\underline{S}}_{j,n}^{[0]}, \frac{h_n^2}{2!}\ddot{\underline{S}}_{j,n}^{[0]}, \ldots, \frac{h_n^{q_n}}{q_n!}\underline{S}_{j,n}^{[0](q_n)} \right) \tag{4.16}$$

and the $L \times L$ "prediction" matrix $\mathbf{A}$ is given by equation (3.21).

The corrector step is given by a single application (i.e., with $m = 0$) of equation (3.29). If the analogs of the vector functions $\underline{g}$, equation (3.15), and $\underline{e}_n$, equation (3.24), are denoted by $\underline{G}$ and $\underline{E}_{j,n}$, respectively, the correction process can be summarized as follows:

$$\left.\begin{aligned} \underline{G}\left(\underline{S}_{j,n}^{[0]}\right) &\equiv h_n \underline{F}\left(\underline{S}_{j,n}^{[0]}\right) + \frac{\left(\underline{\Psi}_{j,n} - \underline{S}_{j,n}^{[0]}\right)}{\beta_0} = h_n \underline{F}\left(\underline{S}_{j,n}^{[0]}\right) - h_n \dot{\underline{S}}_{j,n}^{[0]} \\ \underline{E}_{j,n} &= \mathbf{P}^{-1}(t_n)\underline{G}\left(\underline{S}_{j,n}^{[0]}\right) \\ \mathbf{Z}_{j,n} &= \mathbf{Z}_{j,n}^{[0]} + \underline{E}_{j,n}\underline{\ell} \end{aligned}\right\} j = 1,\ldots,P \quad (4.17)$$

where the method coefficient vector $\underline{\ell}$ is given in table 3.2; $\underline{E}_{j,n}$ is proportional to the local error in $\underline{S}_{j,n}$ (see eq. (3.37)); and $\mathbf{Z}_{j,n}$ is the Nordsieck history matrix for the jth parameter at t_n:

$$\mathbf{Z}_{j,n} = \left(\underline{S}_{j,n}, h_n \dot{\underline{S}}_{j,n}, \frac{h_n^2}{2!}\ddot{\underline{S}}_{j,n}, \ldots, \frac{h_n^{q_n}}{q_n!}\underline{S}_{j,n}^{(q_n)}\right) \quad (4.18)$$

Equation (4.8) gives the following expression for $\underline{F}(\underline{S}_{j,n}^{[0]})$:

$$\underline{F}\left(\underline{S}_{j,n}^{[0]}\right) = \mathbf{J}(t_n)\underline{S}_{j,n}^{[0]} + \frac{\partial \underline{f}}{\partial \eta_j}(t_n) \quad (4.19)$$

so that $\underline{G}(\underline{S}_{j,n}^{[0]})$ becomes

$$\underline{G}\left(\underline{S}_{j,n}^{[0]}\right) = h_n\left(\mathbf{J}(t_n)\underline{S}_{j,n}^{[0]} + \frac{\partial \underline{f}}{\partial \eta_j}(t_n)\right) - h_n \dot{\underline{S}}_{j,n}^{[0]} \quad (4.20)$$

Hence at each step the formulation given by equation (4.17) requires one matrix-vector multiplication $\mathbf{J}(t_n)\underline{S}_{j,n}^{[0]}$ for each sensitivity parameter η_j. To avoid the

computational cost associated with this multiplication, the method is reformulated as follows (ref. 23): Equation (4.17) gives

$$\underline{S}_{j,n} = \underline{S}_{j,n}^{[0]} + \ell_0 \mathbf{P}^{-1}(t_n)\underline{G}\left(\underline{S}_{j,n}^{[0]}\right) \tag{4.21}$$

where the expression for $\underline{E}_{j,n}$ has been written out. Substituting equation (4.20) into equation (4.21) gives

$$\underline{S}_{j,n} = \underline{S}_{j,n}^{[0]} + \ell_0 \mathbf{P}^{-1}(t_n)\left[h_n \mathbf{J}(t_n)\underline{S}_{j,n}^{[0]} + h_n \frac{\partial \underline{f}}{\partial \eta_j}(t_n) - h_n \dot{\underline{S}}_{j,n}^{[0]}\right] \tag{4.22}$$

Both sides of equation (4.22) are now premultiplied by $\mathbf{P}(t_n)$, the expression for $\mathbf{P}(t_n)$ $[=\mathbf{I}-h_n\beta_0\mathbf{J}(t_n)=\mathbf{I}-h_n\ell_0\mathbf{J}(t_n)$ because $\ell_0=\beta_0]$ is written out, and the resulting equation is simplified to give

$$\underline{S}_{j,n} = \mathbf{P}^{-1}(t_n)\left[\underline{S}_{j,n}^{[0]} + \ell_0\left(h_n \frac{\partial \underline{f}}{\partial \eta_j}(t_n) - h_n \dot{\underline{S}}_{j,n}^{[0]}\right)\right] \tag{4.23}$$

Note that this formulation does not require the matrix-vector multiplication $\mathbf{J}(t_n)\underline{S}_{j,n}^{[0]}$ required by equation (4.17).

Finally equation (4.17) gives

$$\underline{E}_{j,n} = \frac{\underline{S}_{j,n} - \underline{S}_{j,n}^{[0]}}{\ell_0} \tag{4.24}$$

which can be used to compute the remaining columns of $\mathbf{Z}_{j,n}$ (see eq. (4.17)).

If the kth column ($k = 0,1,...,q_n$) of $\mathbf{Z}_{j,n}$ is defined as the vector $\underline{Z}_{j,n}(k)$, that is,

$$\underline{Z}_{j,n}(k) = \frac{h_n^k}{k!}\underline{S}_{j,n}^{(k)}, \qquad k = 0,1,...,q_n \tag{4.25}$$

the Nordsieck history matrix formulation of the DDM can be summarized as follows:

$$\left.\begin{aligned}
&\mathbf{Z}_{j,n}^{[0]} = \mathbf{Z}_{j,n-1}\mathbf{A} \\
&\underline{Z}_{j,n}(0) \equiv \underline{S}_{j,n} = \mathbf{P}^{-1}(t_n)\left[\underline{S}_{j,n}^{[0]} + \ell_0\left(h_n \frac{\partial \underline{f}}{\partial \eta_j}(t_n) - h_n \dot{\underline{S}}_{j,n}^{[0]}\right)\right] \\
&\underline{E}_{j,n} = \frac{\underline{S}_{j,n} - \underline{S}_{j,n}^{[0]}}{\ell_0} \\
&\underline{Z}_{j,n}(k) = \underline{Z}_{j,n}^{[0]}(k) + \ell_k \underline{E}_{j,n}, \qquad k = 1,\ldots,q_n
\end{aligned}\right\} \; j = 1,\ldots,P \qquad (4.26)$$

where $\underline{Z}_{j,n}^{[0]}(k)$ is the kth column of $\mathbf{Z}_{j,n}^{[0]}$.

Because the sensitivity ODE's are linear and $\mathbf{P}$ is updated on every time step, the $\mathbf{Z}_{j,n}$ given by equation (4.26) need not be tested for either convergence or accuracy and is accepted as the sensitivity history matrix at the new time t_n. Although the subscript j has been attached to the quantity $\underline{E}_n$, only N storage locations are required because the sensitivity equations are independent of one another and are (therefore) solved sequentially.

4.3.2 Step Length and Method Order Changes

At each step $[t_{n-1},t_n]$ the DDM uses exactly the same step length and method order as those used for that step by LSODE. As discussed in chapter 3 (section 3.2.5), both h_n and q_n vary as the integration proceeds. Because the sensitivity history array $\mathbf{Z}$ depends on both h_n and q_n, it has to be modified whenever there is a change in either quantity.

The sensitivity history array is modified by using exactly the same procedure utilized for the history array of the model problem. The two history arrays are, however, updated at different times. The history matrix for the model problem at t_n, $\mathbf{z}_n$, is modified after the step $[t_{n-1},t_n]$ in anticipation of using a different step length and/or method order on the next step. It may also be altered during a step because of a failed convergence or error test. In contrast, $\mathbf{Z}_{n-1}$, the sensitivity history array at t_{n-1}, is updated only after the model problem has been solved over the step $[t_{n-1},t_n]$. The reason is that the step length and method order to be used for the sensitivity computations on any step are known only after the model problem has been solved over that step. Not updating $\mathbf{Z}_n$ at t_n by using h'_{n+1} and q'_{n+1}, the step length and method order, respectively, to be attempted for the model problem on the next step (i.e., $[t_n,t_{n+1}]$), avoids the expense associated with the later modification

of $\mathbf{Z}_n$ in the event of a failed step by LSODE. However, for reasons discussed later, for the case $q'_{n+1} = q_n + 1$, $\mathbf{Z}_n$ is updated at t_n to reflect the new order to be attempted on the next step. Any modification to $\mathbf{Z}_n$ due to h'_{n+1} being different from h_n is, however, postponed until after the model problem has been solved over the step $[t_n, t_{n+1}]$.

The actions taken in advancing the sensitivity history array by one step from t_{n-1} to t_n are now described. At the start, if h_n is different from the step length h_{n-1} for the previous step, $[t_{n-2}, t_{n-1}]$, the new sensitivity history matrices $\mathbf{Z}_{j,n-1}$ $(j = 1,...,P)$ are rescaled as follows:

$$\mathbf{Z}_{j,n-1} \leftarrow \mathbf{Z}_{j,n-1}\mathbf{C}, \qquad j = 1,..., P \tag{4.27}$$

where the $L \times L$ diagonal matrix $\mathbf{C}$ is given by equation (3.45), with the step length ratio $r = h_n/h_{n-1}$.

The rescaling given by equation (4.27) is performed on all $q_n + 1$ columns of $\mathbf{Z}_{j,n-1}$ $(j = 1,...,P)$. If $q_n = q_{n-1} - 1$, the last column of the old $\mathbf{Z}_{j,n-1}$ $(j = 1,...,P)$ is ignored because it is not needed. After the rescaling new history matrices $\{\mathbf{Z}_{j,n}\}$ are generated, as described in section 4.3.1.

After all the $\mathbf{Z}_{j,n}$ $(j = 1,...,P)$ have been computed, q'_{n+1} is examined. If $q'_{n+1} \leq q_n$, the solution of the model problem over the time step $[t_n, t_{n+1}]$ is proceeded with. If, however, $q'_{n+1} = q_n + 1$, each $\mathbf{Z}_{j,n}$ is augmented by a column containing the vector $h_n^{q_n+1} \underline{S}_{j,n}^{(q_n+1)}/(q_n+1)!$, the scaled (q_n+1)th derivative of $\underline{S}_{j,n}$. By employing exactly the same procedure used to calculate $h_n^{q_n+1}\underline{Y}_n^{(q_n+1)}/(q_n+1)!$ when there is an order increase (see eq. (3.46)), the following expression for $h_n^{q_n+1} \underline{S}_{j,n}^{(q_n+1)}/(q_n+1)!$ is derived:

$$\frac{h_n^{q_n+1}}{(q_n+1)!}\underline{S}_{j,n}^{(q_n+1)} \cong \frac{\ell_{q_n}\underline{E}_{j,n}}{q_n+1}, \qquad j = 1,..., P \tag{4.28}$$

This equation is the analog to equation (3.46).

The column augmentation could also be performed at the start of the next step. It would, however, require storing the P vectors $\underline{E}_{j,n}$ $(j = 1,...,P)$, each of length N. Performing the column addition at the end of the step minimizes storage requirement. In the event that the order increase is unsuccessful, the new column is simply ignored on the next step.

The method order may also be reduced because of a failed error test. If, on the step $[t_{n-1}, t_n]$ the method order is reduced to $q_n = q_{n-1} - k$ $(k \geq 1)$, the following actions are taken before the $\{\mathbf{Z}_{j,n}\}$ are computed: If $q_n > 1$, any necessary rescaling is performed on the first $(q_n + 1)$ columns of the old $\{\mathbf{Z}_{j,n-1}\}$; the last k columns are ignored because they are not needed. If, however, $q_n = 1$, new matrices $\{\mathbf{Z}_{j,n-1}\}$ are constructed as described next.

After three and more error test failures on any step $[t_{n-1},t_n]$ LSODE assumes that the derivatives that have accumulated in the history matrix have errors of the wrong order. Therefore the first derivative $\dot{\underline{Y}}_{n-1}[=\underline{f}(\underline{Y}_{n-1})]$ is recomputed and the method order set equal to 1 (ref. 15). A new history matrix $\mathbf{z}_{n-1}$ is then constructed from $\underline{Y}_{n-1}$ and $\dot{\underline{Y}}_{n-1}$. Analogously new history matrices $\{\mathbf{Z}_{j,n-1}\}$ should be constructed from the $\{\underline{S}_{j,n-1}\}$ and $\{\dot{\underline{S}}_{j,n-1}\}$, which are given by equation (4.8):

$$\dot{\underline{S}}_{j,n-1} = \mathbf{J}(t_{n-1})\underline{S}_{j,n-1} + \frac{\partial \underline{f}}{\partial \eta_j}(t_{n-1}), \qquad j = 1,\ldots,P \tag{4.29}$$

This equation requires the evaluation of the Jacobian matrix $\mathbf{J}(t_{n-1})$ and one matrix-vector multiplication $\mathbf{J}(t_{n-1})\underline{S}_{j,n-1}$ for each parameter. For rate coefficient parameters the $\{\partial \underline{f}/\partial \eta_j(t_{n-1})\}$ also need to be computed. However, as pointed out by Dunker (ref. 23) and shown here, because the first-order BDF method will be used on the step, $h_n \dot{\underline{S}}_{j,n-1}$ will cancel with itself during the calculation procedures for both $\underline{S}_{j,n}$ and $h_n \dot{\underline{S}}_{j,n}$, the two columns of $\mathbf{Z}_{j,n}$, and so $\dot{\underline{S}}_{j,n-1}$ is obtained trivially.

Consider a step $[t_{n-1},t_n]$ on which the first-order BDF method is used. Because $q_n = 1$, (1) each $\mathbf{Z}_{j,n}$ will consist of the two columns $\underline{Z}_{j,n}(0)$ $(= \underline{S}_{j,n})$ and $\underline{Z}_{j,n}(1)$ $(= h_n \dot{\underline{S}}_{j,n})$, (2) $\ell_0 = \ell_1 = 1$ (see table 3.2), and (3) the "predicted" values $\underline{S}_{j,n}^{[0]}$ and $h_n \dot{\underline{S}}_{j,n}^{[0]}$ at t_n are

$$\underline{S}_{j,n}^{[0]} = \underline{S}_{j,n-1} + h_n \dot{\underline{S}}_{j,n-1} \tag{4.30}$$

$$h_n \dot{\underline{S}}_{j,n}^{[0]} = h_n \dot{\underline{S}}_{j,n-1} \tag{4.31}$$

For $q_n = 1$, equation (4.23) provides the following expression for $\underline{S}_{j,n}$:

$$\underline{S}_{j,n} = \mathbf{P}^{-1}(t_n)\left(\underline{S}_{j,n}^{[0]} + h_n \frac{\partial \underline{f}}{\partial \eta_j}(t_n) - h_n \dot{\underline{S}}_{j,n}^{[0]}\right) \tag{4.32}$$

because $\ell_0 = 1$. Substituting equations (4.30) and (4.31) into equation (4.32) and simplifying the resulting equation produce

$$\underline{S}_{j,n} = \mathbf{P}^{-1}(t_n)\left(\underline{S}_{j,n-1} + h_n \frac{\partial \underline{f}}{\partial \eta_j}(t_n)\right) \tag{4.33}$$

which is independent of $\dot{\underline{S}}_{j,n-1}$.

For the first-order BDF method equation (4.26) gives the following result for $h_n \dot{\underline{S}}_{j,n}$:

$$h_n \dot{\underline{S}}_{j,n} = h_n \dot{\underline{S}}^{[0]}_{j,n} + \underline{S}_{j,n} - \underline{S}^{[0]}_{j,n} \tag{4.34}$$

because $\ell_0 = \ell_1 (= 1)$. Substituting equations (4.30) and (4.31) into equation (4.34) and simplifying give

$$h_n \dot{\underline{S}}_{j,n} = \underline{S}_{j,n} - \underline{S}_{j,n-1} \tag{4.35}$$

which is also independent of $\dot{\underline{S}}_{j,n-1}$.[16]

Because all columns of $\mathbf{Z}_{j,n}$ can be computed without knowledge of $\dot{\underline{S}}_{j,n-1}$, the latter can be set equal to any value. The $\{\underline{Z}_{j,n-1}(1)\}$ are set equal to zero to minimize roundoff errors. Now, because $\mathbf{Z}_{j,n}$ is independent of $\dot{\underline{S}}_{j,n-1}$, the first two columns of the old $\mathbf{Z}_{j,n-1}$ could be elected to be used and the remaining columns ignored. Not constructing the new history matrix reduces the computational work. However, to ensure accuracy in the $\{\mathbf{Z}_{j,n}\}$, all $\underline{Z}_{j,n-1}(1)$ $(j = 1,...,P)$ are set equal to zero. The computational work required for this operation is not significant.

The method order may also be reduced to unity because it is the optimal order for the step. In this situation also the $\{\mathbf{Z}_{j,n-1}\}$ are updated by setting all $\underline{Z}_{j,n-1}(1)$ $(j = 1,...,P)$ equal to zero. Although the reconstruction is not necessary, it will result in more accurate $\{\mathbf{Z}_{j,n}\}$. However, note that it will produce inaccurate $\{\underline{S}^{[0]}_{j,n}\}$ (see eq. (4.30)) and hence inaccurate $\{\underline{E}_{j,n}\}$ (see eq. (4.24)). Now, if the method order is increased (from 1 to 2), each $\mathbf{Z}_{j,n}$ is augmented by a column containing the vector $h_n^2 \underline{S}^{(2)}_{j,n}/2!$, which is computed by using $\underline{E}_{j,n}$ (see eq. (4.28)). Hence, although the first two columns of the $\{\mathbf{Z}_{j,n}\}$ may be made more accurate by the above reconstruction, the remaining column may be significantly inaccurate. As the calculation proceeds, inaccuracies will be introduced into the first two columns as well. For this reason the $\{\underline{Z}_{j,n}(1)\}$ are not altered on steps for which a first-order method is used if the method order to be attempted on the next step has been increased (to 2).

4.3.3 Interpolation at Output Stations

The sensitivity coefficients at the output times $t_{\text{out},1}, t_{\text{out},2}, \ldots$ are computed by using the interpolation procedure described in chapter 3 (section 3.2.6) for the model problem. For each output station t_{out} the $\{\underline{S}_j(t_{\text{out}})\}$ are given by a (q'_{n+1})th-order Taylor series expansion about t_n, the first mesh point at or beyond t_{out}. Here

[16] Equations (4.33) and (4.35) can be derived by an alternative, easier procedure as follows: For $q_n = 1$, $\alpha_1 = \beta_0 = 1$ (see table 3.1), and so $\underline{\Psi}_{j,n}$, equation (4.10), reduces to $\underline{S}_{j,n-1}$. Substituting this expression into equation (4.11) gives equation (4.33). By definition $\dot{\underline{S}}_{j,n}$ satisfies the BDF method (see section 3.2.2 and eq. (3.11)), and so the result for $h_n \dot{\underline{S}}_{j,n}$, equation (4.35), follows directly from equation (4.9).

q'_{n+1} is the order to be attempted by LSODE on the next step (i.e., $[t_n,t_{n+1}]$). The expression for $\underline{S}_j(t_{out})$, corresponding to equation (3.47), is

$$\underline{S}_j(t_{out}) = \sum_{k=0}^{q'_{n+1}} r^k \underline{Z}_{j,n}(k), \qquad j = 1,\ldots,P \tag{4.36}$$

where r is now defined as

$$r = \frac{t_{out} - t_n}{h_n} \tag{4.37}$$

because the $\{\mathbf{Z}_{j,n}\}$ are based on h_n.

Sensitivity coefficient derivatives of any order (up to q'_{n+1}) can also be obtained at t_{out} by a (q'_{n+1})th-order Taylor series expansion about t_n. The equation for $\underline{S}_j^{(\mu)}(t_{out})$, the μth temporal derivative of $\underline{S}_j$ at t_{out}, corresponding to equation (3.50), is

$$\underline{S}_j^{(\mu)}(t_{out}) = \frac{1}{h_n^{\mu}} \sum_{k=\mu}^{q'_{n+1}} r^{k-\mu} \frac{k!}{(k-\mu)!} \underline{Z}_{j,n}(k), \qquad j = 1,\ldots,P \tag{4.38}$$

where r is given by equation (4.37). Because t and η_j are independent of one another, $\underline{S}_j^{(\mu)} = \partial \underline{Y}^{(\mu)}/\partial \eta_j$. Hence $\underline{S}_j^{(\mu)}(t_{out})$ can also be interpreted as the sensitivity coefficient of the μth temporal derivative of $\underline{Y}$ with respect to η_j at t_{out}.

4.3.4 Starting Procedure

The integration of the model problem is started with a single-step, first-order method. Hence the history matrix $\mathbf{Z}_{j,0}$ $(j = 1,\ldots,P)$ at t_0 consists of the two columns $\underline{Z}_{j,0}(0)$ and $\underline{Z}_{j,0}(1)$:

$$\left.\begin{aligned} \underline{Z}_{j,0}(0) &= \underline{S}_{j,0} \\ \underline{Z}_{j,0}(1) &= h_1 \dot{\underline{S}}_{j,0} \end{aligned}\right\} j = 1,\ldots,P \tag{4.39}$$

where h_1 is the step length used by LSODE on the first step, that is, $[t_0,t_1]$. The initial value $\underline{S}_{j,0}$ is equal to the jth column of the $N \times N$ identity matrix if η_j is the jth element of $\underline{y}_0$; if, however, η_j is a rate coefficient parameter, $\underline{S}_{j,0}$ is equal to the null vector. Because the first-order BDF method is used on the first step, the sensitivity history

matrix $\mathbf{Z}_{j,1}$ at t_1 is independent of $\dot{\underline{S}}_{j,0}$, as shown in section 4.3.2. Also LSODE does not attempt to increase the method order after the first step. Hence, for reasons presented in section 4.3.2, the $\{\underline{Z}_{j,0}(1)\}$ are set equal to zero, rather than computing $\dot{\underline{S}}_{j,0}$ from the ODE, equation (4.8).

4.4 Pressure Sensitivity Coefficients

If sensitivity coefficients of the pressure p are required, they have to be computed separately from the other variables because a pressure ODE is not solved. In order to derive an expression for the first-order sensitivity coefficient $\partial p/\partial \eta_j$ with respect to the jth parameter ($j = 1,...,P$), the ideal-gas equation of state is used:

$$p = \rho RT\sigma_m = \rho RT\sum_{i=1}^{NS}\sigma_i \tag{4.40}$$

where ρ is the mixture mass density; R is the universal gas constant; T is the temperature; σ_m (= inverse of the mixture mean molar mass) is equal to the sum of the species mole numbers $\{\sigma_i\}$; and NS is the total number of (reacting and inert) species. Differentiating equation (4.40) with respect to η_j and simplifying the resulting expression give

$$\frac{\partial p}{\partial \eta_j} = p\left(\frac{1}{\rho}\frac{\partial \rho}{\partial \eta_j} + \frac{1}{T}\frac{\partial T}{\partial \eta_j} + \frac{1}{\sigma_m}\sum_{i=1}^{NS}\frac{\partial \sigma_i}{\partial \eta_j}\right), \qquad j = 1,...,P \tag{4.41}$$

As discussed in chapter 11 of part II, sensitivity coefficients of the temporal derivatives of variables are also computed, if required. In order to derive an expression for $\partial\dot{p}/\partial\eta_j$ (j = 1,...,P), where $\dot{p} = dp/dt$, equation (4.40) is first differentiated with respect to t to get

$$\dot{p} = p\left(\frac{\dot{\rho}}{\rho} + \frac{\dot{T}}{T} + \frac{\sum_{i=1}^{NRS}\dot{\sigma}_i}{\sigma_m}\right) \tag{4.42}$$

where NRS is the number of reacting species. (The summation excludes inert species mole numbers because their temporal derivatives are equal to zero.)

Equation (4.42) is then differentiated with respect to η_j and the resulting equation simplified to obtain the following expression for $\partial\dot{p}/\partial\eta_j$:

$$\frac{\partial\dot{p}}{\partial\eta_j} = \frac{\dot{p}}{p}\frac{\partial p}{\partial\eta_j} - p\left(\frac{\dot{\rho}}{\rho^2}\frac{\partial\rho}{\partial\eta_j} + \frac{\dot{T}}{T^2}\frac{\partial T}{\partial\eta_j} + \frac{\sum_{i=1}^{NRS}\dot{\sigma}_i}{\sigma_m^2}\sum_{i=1}^{NS}\frac{\partial\sigma_i}{\partial\eta_j}\right)$$

$$+ p\left(\frac{1}{\rho}\frac{\partial\dot{\rho}}{\partial\eta_j} + \frac{1}{T}\frac{\partial\dot{T}}{\partial\eta_j} + \frac{1}{\sigma_m}\sum_{i=1}^{NRS}\frac{\partial\dot{\sigma}_i}{\partial\eta_j}\right), \qquad j = 1,\ldots,P \tag{4.43}$$

This result can also be obtained by differentiating equation (4.41) with respect to t and then interchanging the order of differentiation with respect to η_j and t.

4.5 Normalization of Sensitivity Coefficients

The sensitivity coefficients $\{S_{ij} = \partial Y_i/\partial\eta_j\}$ may display artificial variation because of the differences in the magnitudes of the $\{Y_i\}$ and $\{\eta_j\}$. In order to remove this variation and enable meaningful comparisons with respect to different η_j, the $\{S_{ij}\}$ are usually presented in normalized form. A simple way of accomplishing the normalization is to use the relation

$$\langle S_{ij}\rangle = \frac{\eta_j}{Y_i}\frac{\partial Y_i}{\partial\eta_j} \tag{4.44}$$

where $\langle S_{ij}\rangle$ is the normalized sensitivity coefficient S_{ij}. This procedure can be used only if η_j is nonzero. For example, for isothermal problems the rate coefficients $\{k_j\}$, equations (2.4) and (2.5), are time invariant, and setting $\eta_j = k_j$ presents no difficulty with using equation (4.44); $\langle S_{ij}\rangle$ can then be interpreted as the percent change in Y_i due to a change or uncertainty of 1 percent in k_j. In evaluating the partial derivative $\partial Y_i/\partial k_j$, all other rate coefficients are assumed to be held constant at their nominal values. However, for nonconstant-temperature problems the $\{k_j\}$ vary with time, and $\partial Y_i/\partial k_j$ is thus undefined. A change in any one rate coefficient will produce a change in the temperature, which, in turn, will affect all other rate coefficients. Hence for varying-temperature problems sensitivities with respect to the individual rate coefficient parameters $\{A_j\}$, $\{n_j\}$, $\{E_j\}$, and $\{c_j\}$ must be

computed. Also the temperature exponents $\{n_j\}$, the activation energies $\{E_j\}$, the rate coefficient parameters $\{c_j\}$, and the initial conditions $\{Y_{j,0}\}$ can have zero values. Therefore equation (4.44) cannot be used to normalize the sensitivity coefficients with respect to these quantities. For $\eta_j = 0$ equation (4.44) will give the correct result (= 0.0), because a change of 1 percent in η_j will indeed have no effect on the solution (any percent change in η_j leaves η_j unchanged). This fact is, however, without any physical value and (therefore) of little consolation to the chemist, who wants to use the sensitivity analysis information to improve (or deduce) values for the rate coefficient parameters. Therefore more appropriate normalization factors for rate coefficient parameters and initial condition values are derived next.

4.5.1 Rate Coefficient Parameter Sensitivities

Because the preexponential factors $\{A_j\}$ are nonzero, equation (4.44) can be used to normalize the sensitivity coefficients with respect to A_j. Hence for $\eta_j = A_j$, $\langle S_{ij} \rangle$ is given by

$$\langle S_{ij} \rangle = \frac{A_j}{Y_i} \frac{\partial Y_i}{\partial A_j} \tag{4.45}$$

The $\langle S_{ij} \rangle$ is then the percent change in Y_i due to a change or uncertainty of 1 percent in A_j, with all other rate coefficient parameters held constant at their nominal values.

For constant-temperature problems $\partial Y_i / \partial A_j$ can be related to $\partial Y_i / \partial k_j$ by using the chain rule of differentiation:

$$\frac{\partial Y_i}{\partial A_j} = \frac{\partial Y_i}{\partial k_j} \frac{\partial k_j}{\partial A_j} \tag{4.46}$$

The rate coefficient expression, equation (2.4) or (2.5), gives for constant temperature

$$\frac{\partial k_j}{\partial A_j} = \frac{k_j}{A_j} \tag{4.47}$$

which implies that for a small change ΔA_j in A_j

$$\frac{\Delta k_j}{k_j} = \frac{\Delta A_j}{A_j} \tag{4.48}$$

Hence for a constant-temperature problem the percent change in k_j is equal to the percent change in A_j. Of course, this result follows directly from the fact that $k_j \propto A_j$ for constant temperature (see eqs. (2.4) and (2.5)), and so equation (4.48) is valid even for finite changes in A_j.

Substituting equation (4.47) into equation (4.46), rearranging terms, and dividing both sides by Y_i give

$$\frac{A_j}{Y_i}\frac{\partial Y_i}{\partial A_j} = \frac{k_j}{Y_i}\frac{\partial Y_i}{\partial k_j} \tag{4.49}$$

which shows that for constant-temperature problems the normalized sensitivity coefficients with respect to A_j are identically equal to the normalized sensitivity coefficients with respect to k_j.

For nonconstant-temperature problems the relationship between $\Delta k_j/k_j$ and $\Delta A_j/A_j$ is not as straightforward as equation (4.48) because the temperature is affected by a change in A_j. For k_j given by equation (2.4) $(\partial k_j/\partial A_j)_{n_j,E_j}$ is as follows:

$$\left(\frac{\partial k_j}{\partial A_j}\right)_{n_j,E_j} = \left(\frac{\partial k_j}{\partial T}\right)_{A_j,n_j,E_j}\left(\frac{\partial T}{\partial A_j}\right)_{n_j,E_j} + \left(\frac{\partial k_j}{\partial A_j}\right)_{T,n_j,E_j} \tag{4.50}$$

The first term on the right-hand side accounts for the implicit dependence of k_j on A_j through T, and the second term takes into account the explicit dependence of k_j on A_j. From equation (2.4) expressions are derived for $\partial k_j/\partial T$ and $\partial k_j/\partial A_j$ and substituted into equation (4.50). The resulting equation is simplified to get

$$\frac{1}{k_j}\left(\frac{\partial k_j}{\partial A_j}\right)_{n_j,E_j} = \left(n_j + \frac{E_j}{RT}\right)\frac{1}{T}\frac{\partial T}{\partial A_j} + \frac{1}{A_j} \tag{4.51}$$

Hence a small change ΔA_j in A_j produces the following change $\Delta k_j(A_j)$ in k_j:

$$\frac{\Delta k_j(A_j)}{k_j} \cong \left(n_j + \frac{E_j}{RT}\right)\frac{\Delta T(A_j)}{T} + \frac{\Delta A_j}{A_j} \tag{4.52}$$

where $\Delta T(A_j)$ $(= (\partial T/\partial A_j)\Delta A_j)$ is the temperature change caused by ΔA_j. In equation (4.52) the first term on the right-hand side gives the implicit dependence of Δk_j on ΔA_j (through T), and the second term the explicit dependence. This equation shows that the explicit dependence of $\Delta k_j(A_j)$ on ΔA_j is linear. While the implicit dependence of $\Delta k_j(A_j)$ on ΔA_j varies with time as the solution evolves, the explicit

dependence on ΔA_j is constant (and this change in k_j is equal to 1 percent for a change of 1 percent in A_j).

Normalization factors for n_j, E_j, and c_j are derived by analogy to the normalization procedure for A_j, equation (4.45), which gives the percent change in Y_i due to a change or uncertainty of 1 percent in A_j. For this change in A_j (i.e., $\Delta A_j = 0.01A_j$) equation (4.52) gives the following change in k_j:

$$\frac{\Delta k_j}{k_j} \cong \left[\left(n_j + \frac{E_j}{RT}\right)\frac{1}{T}\left(\frac{\partial T}{\partial A_j}\right)_{n_j, E_j} + \frac{1}{A_j}\right] 0.01A_j \tag{4.53}$$

This equation shows that 1 percent change in A_j produces 1 percent change in k_j at the initial time t_0. The normalization factor for n_j is obtained simply by requiring that it produces the same change in k_j at t_0. Consider a rate coefficient expression of the form given by equation (2.4). Now the change $\Delta k_j(n_j)$ in k_j produced by the change or uncertainty Δn_j in n_j is

$$\Delta k_j(n_j) \cong \left(\frac{\partial k_j}{\partial T}\right)_{A_j, n_j, E_j} \left(\frac{\partial T}{\partial n_j}\right)_{A_j, E_j} \Delta n_j + \left(\frac{\partial k_j}{\partial n_j}\right)_{T, A_j, E_j} \Delta n_j \tag{4.54}$$

where the first term on the right-hand side takes into account the implicit dependence of k_j on n_j through T and the second term gives the explicit dependence of k_j on n_j. Performing the differentiations $\partial k_j/\partial T$ and $\partial k_j/\partial n_j$, substituting them into equation (4.54), and simplifying the result produce

$$\frac{\Delta k_j(n_j)}{k_j} \cong \left(n_j + \frac{E_j}{RT}\right)\frac{\Delta T(n_j)}{T} + \Delta n_j \ln T \tag{4.55}$$

where $\Delta T(n_j)$ (= $(\partial T/\partial n_j)\Delta n_j$) is the temperature change produced by Δn_j. This equation gives the following expression for the change δn_j that produces a change of 1 percent in k_j at t_0:

$$\delta n_j = \frac{0.01}{\ln T_0} \tag{4.56}$$

where T_0 is the initial temperature. The normalized sensitivity coefficient with respect to n_j is then given by

$$\langle S_{ij} \rangle = \frac{\delta n_j}{Y_i} \frac{\partial Y_i}{\partial n_j} \tag{4.57}$$

Equations (4.56) and (4.57) use a different symbol for the change in n_j than equations (4.54) and (4.55) to emphasize that it is not independent. The normalized sensitivities $(100\,\Delta A_j/Y_i)(\partial Y_i/\partial A_j)$ and $(100\,\delta n_j/Y_i)(\partial Y_i/\partial n_j)$ give the percent changes in Y_i due to the changes in A_j and n_j, respectively, that produce the same fractional change (i.e., an increase of 1 percent) in k_j at the initial time; therefore comparing the two quantities is meaningful. Also for a constant-temperature problem both normalized sensitivities are identically equal to the normalized sensitivities with respect to the rate constants.

By using the same procedure the following normalization factors δE_j and δc_j for E_j and c_j, respectively, are derived:

$$\delta E_j = -0.01 R T_0 \tag{4.58}$$

and

$$\delta c_j = \frac{0.01}{T_0} \tag{4.59}$$

The normalized sensitivity coefficients with respect to E_j and c_j have the same meaning as those with respect to A_j and n_j. They are also identical to the normalized sensitivities with respect to the rate constants for a constant-temperature problem.

Use of the above normalization procedures has two important advantages. First, for a given reaction the relative importance of the three rate coefficient parameters can be gauged because all three normalization factors cause the same change in the rate coefficient at the initial time, when the rate coefficient parameters are set; that is, they are generally time invariant. Second, for a given rate coefficient parameter the relative importance of different reactions can be studied because the percent change in rate coefficient at t_0 is the same for all reactions. The two facts imply of course that one can compare the importance of any two rate coefficient parameters for any two reactions.

Normalization factors for the rate coefficient parameters may also be obtained by using other arguments. For example, in the author's previous work (ref. 22) they were derived as follows: Equation (4.53) shows that at any temperature a change of 1 percent in A_j produces 1 percent change in k_j at that temperature (i.e., the explicit dependence of k_j on A_j). Hence for a given temperature the normalization factor δn_j was defined as the change in n_j which produces a change of 1 percent in k_j at that temperature. Equation (4.55) shows that the required δn_j is

$$\delta n_j = \frac{0.01}{\ln T} \tag{4.60}$$

The normalized sensitivity coefficient $(100\ \delta n_j/Y_i)(\partial Y_i/\partial n_j)$ is then the percent change in Y_i due to the change δn_j that produces the same percent change in the explicit dependence of k_j as a change of 1 percent in A_j. Equation (4.56) is preferred because it requires only one evaluation of the normalization factor, which can be set at the beginning of the problem. (On the other hand, equation (4.60) will require that the normalization factor be calculated whenever the normalized sensitivity coefficients are needed.) More significantly equation (4.60) shows that for a nonconstant-temperature problem the normalization factor varies with time; therefore normalized sensitivity coefficients with respect to a given rate coefficient parameter at different reaction times cannot be compared. Also (except at t_0) for a given reaction j, the relative importance of the rate coefficient parameters cannot be studied because their normalization factors will cause different changes in k_j at t_0. (However, for a given rate coefficient parameter the relative importance of different reactions can be examined.)

Finally consider finite (i.e., nonzero) $\{E_j\}$ (or $\{n_j\}$). In this case the normalization factor could be defined as, say, $\Delta E_j = 0.01 E_j$ (or $\Delta n_j = 0.01 n_j$). Then the normalized sensitivity coefficient gives the percent change in the dependent variable due to a change or uncertainty of 1 percent in E_j (or n_j). There are several difficulties with this approach. First, this change in E_j may produce a significantly larger change in k_j, so that nonlinear effects become important. Second, the relative importance of the rate coefficient parameters cannot be studied because, in general, a change of 1 percent in each parameter will produce different changes in k_j at t_0. Similarly a change of 1 percent in different E_j (or n_j) will, in general, manifest disparate percent changes in the $\{k_j\}$. Therefore the effects of different E_j (or n_j), that is, the relative importance of different reactions, cannot be compared.

4.5.2 Initial Condition Sensitivities

The normalization procedure given by equation (4.44) can be used for the sensitivity coefficients with respect to the initial density, temperature, and inert species mole numbers because these variables cannot have zero values. The procedure also works for species whose initial concentrations are assigned nonzero values. Hence, for $\eta_j = Y_{j,0}$, the initial value of one of these variables, the normalized sensitivity coefficient of the ith variable, is defined as

$$\langle S_{ij} \rangle = \frac{Y_{j,0}}{Y_i} \frac{\partial Y_i}{\partial Y_{j,0}} \tag{4.61}$$

The $\langle S_{ij} \rangle$ gives the percent change in Y_i due to a change of 1 percent in $Y_{j,0}$ with all other initial conditions and all rate coefficient parameters held constant. The

quantity $(\rho_0/Y_i)(\partial Y_i/\partial \rho_0)$ is identically equal to the normalized sensitivity with respect to the initial pressure, $(p_0/Y_i)(\partial Y_i/\partial p_0)$. The effect of changing the initial pressure can therefore be studied by generating sensitivities with respect to the initial density.

Caution must be exercised in interpreting and using the sensitivity information with respect to the initial temperature. Because of the highly nonlinear dependence of the solution on temperature, even modest changes in T_0 may have a drastic effect on the solution. It is therefore unlikely that a change of 1 percent in T_0 will produce the normalized sensitivities given by equation (4.61). A more appropriate normalization factor could be the change δT_0 that produces a change of 1 percent in the initial rate coefficient of the most important reaction. But this procedure will require that sensitivities be computed with respect to the rate coefficient parameters. It is also complicated by the fact that different reactions may be important in different regions. Another alternative is to use a fixed temperature change, say $\Delta T_0 = 1$ K. The effects of different temperature changes have not been examined in detail. It is likely that the required value for ΔT_0 (which would produce a measurable change but not so large that nonlinear effects must be accounted for) will depend on both the problem and initial conditions. In any case the quantity given by equation (4.61) can be divided by a suitable factor to obtain the effect of the desired (small) change in T_0.

The sensitivities with respect to initial mole numbers must also be interpreted with caution for the following reason: Consider, for example, the sensitivity coefficient $\partial Y_i/\partial \sigma_{j,0}$, where $\sigma_{j,0}$ is the initial mole number of species j. By definition, $\partial Y_i/\partial \sigma_{j,0}$ is the gradient of Y_i with respect to $\sigma_{j,0}$ with all other variables held constant. Now, $\sigma_{j,0}$ can be changed while keeping the density and temperature constant. However, it is physcially impossible to perturb $\sigma_{j,0}$ without causing a change in the initial mole number of other reactants. For example, $\sigma_{j,0}$ can be increased by adding a small amount of species j to the initial mixture. This addition will not change the number of moles of any other species. However, the total mass of the initial mixture is increased, and so the mole numbers of all other reactants are marginally reduced. (The temperature and density can be held constant by isothermally increasing the mixture volume by the required amount.) For this reason it is preferred to interpret the sensitivity coefficients with respect to initial concentration of reactants as the effects of errors in measurements rather than a change in these quantities.

For a species with zero initial concentration the normalization procedure given by equation (4.61) cannot be used. Such species usually include intermediate active radicals and stable products. Now even trace amounts of radical species can have significant effects on the solution. It is therefore important that the normalization factor used for such a species be equivalent to changing its initial concentration by only a very small amount. The normalization factor used here for the sensitivities with respect to the initial concentration of an active intermediate is equivalent to adding 1 ppm of the radical to the initial mixture. Hence the normalized sensitivitity coefficient is given by

$$\langle S_{ij} \rangle = \frac{10^{-6} \sigma_{m,0}}{Y_i} \frac{\partial Y_i}{\partial \sigma_{j,0}} \tag{4.62}$$

where $\sigma_{m,0} = \sigma_m$ at t_0. The quantity $100 \langle S_{ij} \rangle$ is then the percent change in Y_i due to the introduction of 1 ppm of species j at time t_0. For convenience this procedure is used for all species with zero initial concentration.

For stable products other definitions of the normalization factor can be used. However, use of a different factor than equation (4.62) will require lists of species for each species type so that the correct factor is used in all cases. Also, for reasons given above, the allowed change in stable products must be small. Finally use of equation (4.62) minimizes the required input and reduces both the testing for, and possibility of introducing, errors.

4.5.3 Summary

All of the normalization procedures discussed in sections 4.5.1 and 4.5.2 can be generalized by a single equation as follows:

$$\langle S_{ij} \rangle = \left(\frac{\chi_j}{Y_i} \frac{\partial Y_i}{\partial \eta_j} \right) \times 100\% \tag{4.63}$$

where the normalization factor χ_j depends on the sensitivity parameter. Table 4.1 lists the appropriate normalization factor for each sensitivity parameter type considered in the present work. Equation (4.63) can be interpreted as the percent change in Y_i due to a change or uncertainty of χ_j in η_j.

TABLE 4.1.—NORMALIZATION FACTORS FOR SENSITIVITY PARAMETERS

Sensitivity parameter, η_j	Normalization factor, χ_j
A_j	$0.01A_j$
n_j	$0.01/\ln T_0$
E_j	$-0.01RT_0$
c_j	$0.01/T_0$
$Y_{j,0}$	$0.01Y_{j,0}$ for $Y_{j,0} \neq 0$ $10^{-6}\sigma_{m,0}$ for $Y_{j,0} = 0$

4.6 Test Problems

In this section the accuracy and efficiency of the decoupled direct method and, in particular, LSENS are examined by applying it to nine test problems. The first six problems describe constant-temperature, constant-density chemical reactions. They have been studied by several researchers, and so results obtained with other methods and codes are available, permitting comparisons with LSENS. The last three test problems demonstrate the accuracy and efficiency of the decoupled direct method for sensitivity analysis of nonisothermal combustion kinetics problems. Except where indicated, all calculations with LSENS were performed on the NASA Lewis Research Center's Amdahl 5870 computer using the UTS operating system, the Fujitsu 77 compiler (optimization level, 3), and double-precision arithmetic. Also, for reasons given in section 4.6.5, some solutions of the nonisothermal problems were generated on the NASA Lewis Research Center's VAX 8800 and 9410 computers, using the VAX FORTRAN compiler, double-precision arithmetic, and VAX G_floating data type (i.e., the code was compiled with the G_FLOATING option); see also sections 4.6.2 and 4.6.4.

4.6.1 Three Simple Isothermal Problems

Test problem 1, taken from Hwang (ref. 93), describes a simple, isothermal, first-order reversible reaction

$$\left.\begin{array}{c} \mathcal{A} \underset{k_{-1}}{\overset{k_1}{\rightleftharpoons}} \mathcal{B} \\ \\ k_1 = 1000, \quad k_{-1} = 1 \\ \\ \sigma_{\mathcal{A},0} = 1000, \quad \sigma_{\mathcal{B},0} = 1 \end{array}\right\} \tag{4.64}$$

which describes a rapidly varying system. The solution, given by

$$\left.\begin{aligned} \sigma_{\mathcal{A}}(t) &= \frac{k_{-1}\left(\sigma_{\mathcal{A},0}+\sigma_{\mathcal{B},0}\right)+\left(k_1\sigma_{\mathcal{A},0}-k_{-1}\sigma_{\mathcal{B},0}\right)e^{-\left(k_1+k_{-1}\right)t}}{k_1+k_{-1}} \\ \sigma_{\mathcal{B}}(t) &= \sigma_{\mathcal{A},0}+\sigma_{\mathcal{B},0}-\sigma_{\mathcal{A}}(t) \end{aligned}\right\} \tag{4.65}$$

is illustrated graphically in figure 4.2.

The chemical composition and sensitivity coefficients were generated at the same five output stations, $t = 1.5\times10^{-4}$, 10^{-3}, 10^{-2}, 1.5×10^{-2}, and 2×10^{-2} s, as in Hwang (ref. 93). These reaction times encompassed all regimes of reactedness, including when the system had essentially equilibrated (see fig. 4.2). This problem was also attempted with the code CHEMDDM (ref. 23) to check the modifications made to the routines adapted from it; that is, to ensure that LSENS duplicates the results produced by CHEMDDM. All calculations with CHEMDDM for this and two subsequent problems on which it was used were also executed on the NASA Lewis Research Center's Amdahl 5870 computer using the UTS operating system, the Fujitsu 77 compiler (optimization level, 3), and double-precision arithmetic.

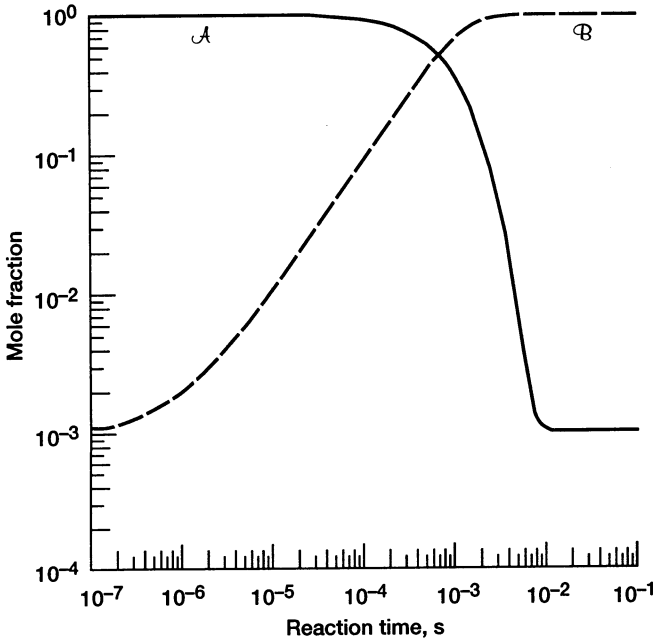

Figure 4.2.—Variation of species mole fractions with reaction time for test problem 1.

Table 4.2 gives the chemical composition predicted by LSENS and CHEMDDM and the analytical results. The numerical solutions were generated with the local tolerance EMAX = 10^{-6} to be consistent with Hwang (ref. 93); ATOLSP was set equal to 0.0. Normalized sensitivities with respect to initial mole numbers are listed in tables 4.3 and 4.4. The normalization procedure given by equation (4.61) was used for both species because both initial concentrations are nonzero (eq. (4.64)). Normalized sensitivity coefficients

$$\langle S_{ij} \rangle = \frac{k_j}{Y_i} \frac{\partial Y_i}{\partial k_j} \tag{4.66}$$

with respect to the two rate constants are given in tables 4.5 and 4.6, together with the results reported for $\sigma_{\mathcal{A}}$ by Hwang (ref. 93), who used a scaled Green's function

TABLE 4.2.—VARIATION OF CHEMICAL COMPOSITION WITH TIME FOR TEST PROBLEM 1

Time, s	Species mole numbers, mole species i per gram of mixture					
	$\sigma_{\mathcal{A}}$			$\sigma_{\mathcal{B}}$		
	Exact	LSENS	CHEMDDM	Exact	LSENS	CHEMDDM
1.5×10^{-4}	860.7	860.7	860.8	140.3	140.3	140.2
1.0×10^{-3}	368.1	368.1	368.2	632.9	632.9	632.9
1.0×10^{-2}	1.045	1.045	1.045	1000	1000	1000
1.5×10^{-2}	1.000	1.000	1.000	1000	1000	1000
2.0×10^{-2}	1.000	1.000	1.000	1000	1000	1000

TABLE 4.3.—NORMALIZED SENSITIVITY COEFFICIENTS WITH RESPECT TO INITIAL CONDITION $\sigma_{\mathcal{A},0}$ FOR TEST PROBLEM 1

Time, s	Normalized sensitivities with respect to $\sigma_{\mathcal{A},0}$					
	$\langle \partial\sigma_{\mathcal{A}} / \partial\sigma_{\mathcal{A},0} \rangle$			$\langle \partial\sigma_{\mathcal{B}} / \partial\sigma_{\mathcal{A},0} \rangle$		
	Exact	LSENS	CHEMDDM	Exact	LSENS	CHEMDDM
1.5×10^{-4}	1.000	1.000	0.9999	0.9929	0.9929	0.9933
1.0×10^{-3}	1.000	1.000	0.9998	0.9984	0.9984	0.9985
1.0×10^{-2}	0.9990	0.9990	0.9990	0.9990	0.9990	0.9990
1.5×10^{-2}	0.9990	0.9990	0.9990	0.9990	0.9990	0.9990
2.0×10^{-2}	0.9990	0.9990	0.9990	0.9990	0.9990	0.9990

TABLE 4.4.—NORMALIZED SENSITIVITY COEFFICIENTS WITH RESPECT TO INITIAL CONDITION $\sigma_{\Phi,0}$ FOR TEST PROBLEM 1

Time, s	Normalized sensitivities with respect to $\sigma_{\Phi,0}$[a]					
	$\langle \partial \sigma_{\mathcal{A}} / \partial \sigma_{\Phi,0} \rangle$			$\langle \partial \sigma_{\Phi} / \partial \sigma_{\Phi,0} \rangle$		
	Exact	LSENS	CHEMDDM	Exact	LSENS	CHEMDDM
1.5×10^{-4}	1.618(−7)	1.618(−7)	1.618(−7)	7.128(−3)	7.128(−3)	7.130(−3)
1.0×10^{-3}	1.716(−6)	1.716(−6)	1.716(−6)	1.579(−3)	1.579(−3)	1.579(−3)
1.0×10^{-2}	9.560(−4)	9.560(−4)	9.559(−4)	9.990(−4)	9.990(−4)	9.990(−4)
1.5×10^{-2}	9.987(−4)	9.987(−4)	9.987(−4)	9.990(−4)	9.990(−4)	9.990(−4)
2.0×10^{-2}	9.990(−4)	9.990(−4)	9.990(−4)	9.990(−4)	9.990(−4)	9.990(−4)

[a]Numbers in parentheses denote powers of 10.

TABLE 4.5.—NORMALIZED SENSITIVITY COEFFFICIENTS WITH RESPECT TO RATE CONSTANT k_1 FOR TEST PROBLEM 1

Time, s	Normalized sensitivities with respect to k_1[a]						
	$\langle \partial \sigma_{\mathcal{A}} / \partial k_1 \rangle$				$\langle \partial \sigma_{\Phi} / \partial k_1 \rangle$[c]		
	Exact	LSENS	CHEMDDM	SGFM[b]	Exact	LSENS	CHEMDDM
1.5×10^{-4}	−1.500(−1)	−1.500(−1)	−1.500(−1)	−1.48(−1)	9.203(−1)	9.203(−1)	9.203(−1)
1.0×10^{-3}	−9.990(−1)	−9.990(−1)	−9.990(−1)	−1.03	5.811(−1)	5.811(−1)	5 .811(−1)
1.0×10^{-2}	−1.386	−1.386	−1.386	−1.37	1.448(−3)	1.448(−3)	1.448(−3)
1.5×10^{-2}	−1.003	−1.003	−1.003	−1.00	1.004(−3)	1.004(−3)	1.004(−3)
2.0×10^{-2}	−9.990(−1)	−9.990(−1)	−9.990(−1)	−9.99(−1)	9.990(−4)	9.990(−4)	9.990(−4)

[a]Numbers in parentheses denote powers of 10.
[b]From reference 93.
[c]SGFM results not given.

TABLE 4.6.—NORMALIZED SENSITIVITY COEFFFICIENTS WITH RESPECT TO RATE CONSTANT k_{-1} FOR TEST PROBLEM 1

Time, s	Normalized sensitivities with respect to k_{-1}[a]						
	$\langle \partial \sigma_{\mathcal{A}} / \partial k_{-1} \rangle$				$\langle \partial \sigma_{\Phi} / \partial k_{-1} \rangle$[c]		
	Exact	LSENS	CHEMDDM	SGFM[b]	Exact	LSENS	CHEMDDM
1.5×10^{-4}	1.199(−5)	1.199(−5)	1.199(−5)	1.35(−5)	−7.360(−5)	−7.360(−5)	**−7.360(−5)**
1.0×10^{-3}	7.190(−4)	7.190(−4)	7.190(−4)	8.10(−4)	−4.183(−4)	−4.183(−4)	**−4.183(−4)**
1.0×10^{-2}	9.556(−1)	9.556(−1)	9.556(−1)	9.58(−1)	−9.986(−4)	−9.986(−4)	**−9.986(−4)**
1.5×10^{-2}	9.987(−1)	9.987(−1)	9.987(−1)	9.99(−1)	−9.990(−4)	−9.990(−4)	**−9.990(−4)**
2.0×10^{-2}	9.990(−1)	9.990(−1)	9.990(−1)	9.99(−1)	−9.990(−4)	−9.990(−4)	**−9.990(−4)**

[a]Numbers in parentheses denote powers of 10.
[b]From reference 93.
[c]SGFM results not given.

method (SGFM). To compute these coefficients with LSENS, the preexponential factors $\{A_j\}$ were specified as sensitivity parameters. As discussed in section 4.5.1, for isothermal problems the normalized sensitivity coefficients with respect to k_j and A_j are identically equal (see eq. (4.49)).

Tables 4.2 to 4.6 show the excellent agreement between LSENS and CHEMDDM at all levels of reactedness. In addition, both codes compared very favorably with the exact solutions. In contrast, although the SGFM results agreed well with the exact solutions, there were some discrepancies at early times. In particular, the sensitivity coefficients with respect to k_{-1} at $t = 1.5\times10^{-4}$ and 10^{-3} s were noticeably inaccurate; however, their magnitudes are not significant. Hwang (ref. 93) attempted this problem with the coupled version of the DM also. He states that the DM was more accurate than the SGFM. However, because the DM results are not given in reference 93, an accuracy comparison with the DDM was precluded.

To solve for the chemical composition, both LSENS and CHEMDDM required 135 steps, 153 derivative evaluations, and 15 Jacobian matrix evaluations and LU-decompositions. The execution times were, however, different: 0.016 and 0.027 s, respectively, for LSENS and CHEMDDM. The sensitivity analysis calculations required additional computational work of 135 derivative evaluations and 135 Jacobian matrix evaluations and LU-decompositions. The execution times for the composition and sensitivities with respect to (1) the two initial concentrations, (2) the two rate constants, and (3) the two initial conditions and the two rate constants were, respectively, 0.049, 0.053, and 0.061 s for LSENS and 0.063, 0.074, and 0.090 s for CHEMDDM. These times show that, excluding the cost of forming **J** and LU-decomposing **P**, LSENS required approximately 4 and 6 ms, respectively, to compute sensitivity coefficients for one initial condition and one rate constant. These times were confirmed by the execution times required to generate sensitivity coefficients with respect to one initial condition and one rate constant: 0.045 and 0.047 s, respectively. The execution times required by CHEMDDM were approximately 8 and 13.5 ms, respectively, for one initial condition and one rate constant. The rate constant sensitivities are more expensive to evaluate because of the added cost of computing the partial derivatives $\{\partial f_i/\partial \eta_j\}$. Hwang (ref. 93) states that the DM and SGFM required approximately 7 and 8 s, respectively, on a CDC–CYBER–172 computer using single precision. The efficiencies of the DM and SGFM could not be compared with that of the DDM because the former two methods were used to compute both first- and second-order sensitivity coefficients of $\sigma_{\mathcal{A}}$ with respect to the rate constants. In any case the test problem is so small that it was difficult to draw definitive conclusions regarding computational efficiency.

Tables 4.3 to 4.6 show that the normalized sensitivity coefficients approached constant values with increasing reaction time. This behavior, more apparent for the initial condition sensitivities, was to be expected because of the equilibration of the chemical system. Indeed, equation (4.65) shows that as $t \to \infty$

$$\left.\begin{aligned}
&\left\langle \frac{\partial \sigma_{\mathcal{A}}}{\partial \sigma_{\mathcal{A},0}} \right\rangle = \left\langle \frac{\partial \sigma_{\mathcal{B}}}{\partial \sigma_{\mathcal{A},0}} \right\rangle = 0.9990 \\
&\left\langle \frac{\partial \sigma_{\mathcal{A}}}{\partial \sigma_{\mathcal{B},0}} \right\rangle = \left\langle \frac{\partial \sigma_{\mathcal{B}}}{\partial \sigma_{\mathcal{B},0}} \right\rangle = 9.990 \times 10^{-4} \\
&\left\langle \frac{\partial \sigma_{\mathcal{A}}}{\partial k_1} \right\rangle = -0.9990, \left\langle \frac{\partial \sigma_{\mathcal{B}}}{\partial k_1} \right\rangle = 9.990 \times 10^{-4} \\
&\left\langle \frac{\partial \sigma_{\mathcal{A}}}{\partial k_{-1}} \right\rangle = 0.9990, \left\langle \frac{\partial \sigma_{\mathcal{B}}}{\partial k_{-1}} \right\rangle = -9.990 \times 10^{-4}
\end{aligned}\right\} \qquad (4.67)$$

To verify that the DDM reproduced the correct long-time behavior, LSENS was run up to t = 1 s and output generated at the following additional times: 5×10^{-2}, 0.1, 0.5, and 1 s. For $t \geq 2\times10^{-2}$ s the normalized sensitivities were identically equal to the theoretical values at $t = \infty$. Thus the DDM was accurate in all regimes of the problem.

The chemical equilibrium composition is a function of the initial state, as discussed in chapter 5. Changing rate constants may affect the rate at which the system approaches the equilibrium state, but not the final state. However, the sensitivities with respect to the rate constants were not zero at equilibrium. The reason for this behavior is now examined. As described in chapter 2, for a reversible elementary reaction j the backward rate coefficient k_{-j} is related to the forward rate coefficient k_j through the concentration equilibrium constant $K_{c,j}$ (see eq. (2.6)). For test problem 1, $K_{c,1}$ is given by (see eq. (2.7))

$$K_{c,1} = \sigma_{\mathcal{B},\mathrm{eq}} / \sigma_{\mathcal{A},\mathrm{eq}} \qquad (4.68)$$

where $\sigma_{i,\mathrm{eq}}$ is the mole number of species i at equilibrium. Because k_1 and k_{-1} are treated as independent parameters, a change in either one, while keeping the other fixed, is equivalent to changing $K_{c,1}$. Now equation (4.68) shows that a perturbation in $K_{c,1}$ will produce a change in the chemical equilibrium composition. Hence the sensitivity coefficients with respect to rate constants were nonzero at equilibrium.

If the two rate constants are not independent of one another, $\langle(\partial\sigma_i/\partial k_1)\,\underline{y}_0\rangle$ can be related to the two sensitivities $\langle(\partial\sigma_i/\partial k_1)_{k_{-1}},\underline{y}_0\rangle$ and $\langle(\partial\sigma_i/\partial k_{-1})_{k_1},\underline{y}_0\rangle$ as follows:

$$\left\langle\left(\frac{\partial\sigma_i}{\partial k_1}\right)_{\underline{y}_0}\right\rangle=\left\langle\left(\frac{\partial\sigma_i}{\partial k_1}\right)_{k_{-1},\underline{y}_0}\right\rangle+\left\langle\left(\frac{\partial\sigma_i}{\partial k_{-1}}\right)_{k_1,\underline{y}_0}\right\rangle \tag{4.69}$$

The results given previously (eq. (4.67)) show that, as expected, $\langle(\partial\sigma_{\mathcal{A}}/\partial k_1)\,\underline{y}_0\rangle$ and $\langle(\partial\sigma_{\mathcal{B}}/\partial k_1)\,\underline{y}_0\rangle$ are both identically equal to zero at equilibrium.

As discussed in chapter 11 of part II, LSENS can be used to compute the sensitivity coefficients of the temporal derivatives of the dependent variables. To illustrate this capability, the species derivatives and their normalized sensitivity coefficients are listed in tables 4.7 to 4.9. The agreement between the analytical results and LSENS was, in general, very good. LSENS predicted a sharper decrease

TABLE 4.7.—SPECIES DERIVATIVES FOR TEST PROBLEM 1

Time, s	Species derivatives	
	$\dot{\sigma}_{\mathcal{A}}\ (=-\dot{\sigma}_{\mathcal{B}})$	
	Exact	LSENS
1.5×10^{-4}	-8.606×10^{5}	-8.606×10^{5}
1.0×10^{-3}	-3.675×10^{5}	-3.675×10^{5}
1.0×10^{-2}	−44.95	−44.95
1.5×10^{-2}	−0.3013	−0.3024
2.0×10^{-2}	-2.020×10^{-3}	-2.564×10^{-3}

TABLE 4.8.—NORMALIZED SENSITIVITIES OF SPECIES DERIVATIVES WITH RESPECT TO INITIAL CONDITIONS FOR TEST PROBLEM 1

Time, s	Normalized sensitivities of species derivatives with respect to initial conditions[a]					
	$\langle\partial\dot{\sigma}_i/\partial\sigma_{\mathcal{A},0}\rangle$[b]		$\langle\partial\dot{\sigma}_{\mathcal{A}}/\partial\sigma_{\mathcal{B},0}\rangle$		$\langle\partial\dot{\sigma}_{\mathcal{B}}/\partial\sigma_{\mathcal{B},0}\rangle$	
	Exact	LSENS	Exact	LSENS	Exact	LSENS
1.5×10^{-4}	1.000	1.000	−1.000(−6)	−1.000(−6)	−1.000(−6)	−1.000(−6)
1.0×10^{-3}	1.000	1.000	−1.000(−6)	−1.000(−6)	−1.000(−6)	−1.000(−6)
1.0×10^{-2}	1.000	1.000	−1.000(−6)	−1.000(−6)	−1.000(−6)	−1.000(−6)
1.5×10^{-2}	1.000	1.000	−1.000(−6)	−1.000(−6)	−1.000(−6)	−1.000(−6)
2.0×10^{-2}	1.000	9.972(−1)	−1.000(−6)	−9.972(−7)	−1.000(−6)	−9.970(−7)

[a]Numbers in parentheses denote powers of 10.
[b]$\langle\partial\dot{\sigma}_{\mathcal{A}}/\partial\sigma_{\mathcal{A},0}\rangle = \langle\partial\dot{\sigma}_{\mathcal{B}}/\partial\sigma_{\mathcal{A},0}\rangle$ for both analytical results and LSENS.

TABLE 4.9.—NORMALIZED SENSITIVITIES OF SPECIES DERIVATIVES WITH RESPECT TO RATE CONSTANTS FOR TEST PROBLEM 1

Time, s	Normalized sensitivities of species derivatives with respect to rate constants[a]			
	$\langle \partial \dot{\sigma}_i / \partial k_1 \rangle$[b]		$\langle \partial \dot{\sigma}_i / \partial k_{-1} \rangle$[b]	
	Exact	LSENS	Exact	LSENS
1.5×10^{-4}	8.500(−1)	8.500(−1)	−1.510(−4)	−1.510(−4)
1.0×10^{-3}	1.000(−6)	−7.587(−6)	−1.001(−3)	−1.001(−3)
1.0×10^{-2}	−9.000	−9.000	−1.000(−2)	−1.000(−2)
1.5×10^{-2}	−1.400(1)	−1.399(1)	−1.500(−2)	−1.500(−2)
2.0×10^{-2}	−1.900(1)	−1.808(1)	−2.000(−2)	−1.908(−2)

[a]Numbers in parentheses denote powers of 10.
[b]For each rate constant η (= k_1 and k_{-1}), $\langle \partial \dot{\sigma}_{\mathcal{A}} / \partial \eta \rangle = \langle \partial \dot{\sigma}_{\mathcal{B}} / \partial \eta \rangle$.

with time of the sensitivity coefficients with respect to k_1 than the analytical results; hence the discrepancy at $t = 10^{-3}$ s. EMAX $\leq 10^{-8}$ produced much better agreement with the exact solution.

Test problem 2, taken from Hwang et al. (ref. 89), is also a simple isothermal problem for which the analytical solution is known:

$$\left.\begin{array}{c} \mathcal{A} \underset{k_{-1}}{\overset{k_1}{\rightleftharpoons}} \mathcal{B} \underset{k_{-2}}{\overset{k_2}{\rightleftharpoons}} \mathcal{C} \\ k_1 = 1, \quad K_{c,1} = 0.01, \quad k_2 = 100, \quad K_{c,2} = 100 \\ \sigma_{\mathcal{A},0} = 1, \quad \sigma_{\mathcal{B},0} = \sigma_{\mathcal{C},0} = 0 \end{array}\right\} \tag{4.70}$$

Figure 4.3 shows the variation of species mole fractions with reaction time. This figure shows that the chemical system had essentially equilibrated at $t \simeq 5$ s.

To solve this problem with LSENS, the code had to be modified because there is no provision for supplying the equilibrium constants. For each reaction the forward and reverse rate constants were assumed to be independent of each other, and sensitivities with respect to both were generated. Equation (4.69) was then used to compute the normalized sensitivity coefficients $\{\langle (\partial \sigma_i / \partial k_j)\, \underline{y}_0 \rangle\}$. Finally, to be consistent with Hwang et al. (ref. 89), the results were unnormalized by using equation (4.66). Because each rate constant k_j was expressed as $k_j = A_j$ (i.e., $n_j = E_j = 0.0$), $\partial \sigma_i / \partial k_j = \partial \sigma_i / \partial A_j$.

Sensitivity coefficients with respect to k_1 and k_2 were generated at the same six output stations, t=0.1, 1.45, 1.5, 2.5, 3.5, and 4.5 s, as in Hwang et al. (ref. 89). These

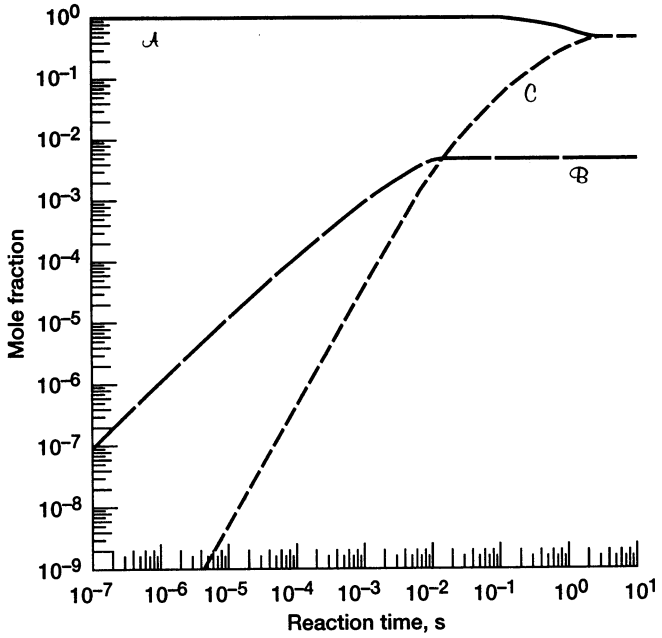

Figure 4.3.—Variation of species mole fractions with reaction time for test problem 2.

reaction times restricted study of the behavior of the sensitivities during equilibration (see fig. 4.3). The results, along with the exact solution and those obtained with the GFM by Hwang et al. (ref. 89), are given in table 4.10. The LSENS results were generated with EMAX = 10^{-6}. Now the molar mass of each species was arbitrarily set equal to 1. In order to ensure relative error control for species with mole fractions ≥ 0.1 ppm, an ATOLSP value of 10^{-13} was assigned (see ref. 19 for rationale).

Table 4.10 shows the excellent agreement between the analytical solution and the numerical results produced by LSENS. The GFM was less accurate than the DDM, and significantly so at $t = 0.1$ s. Although the sensitivities appear to be small in magnitude, the normalized sensitivity coefficients, especially for σ_B and σ_C, were significant. Hwang et al. (ref. 89) attribute this inaccuracy in the GFM to an insufficient number of grid points. They attempted the problem with the DM, and the predicted results were essentially the same as the exact solution. Thus for this problem the DM and DDM were both better than the GFM.

To solve test problem 2, LSENS required 150 steps, 182 derivative evaluations, and 23 Jacobian matrix computations and LU-decompositions. The execution times for the composition alone and for the composition and rate constant sensitivities were 0.034 and 0.11 s, respectively. Comparisons with the DM and GFM were not possible because the corresponding execution times are not given in reference 89. The authors state that to achieve comparable accuracy both methods required a few seconds on an IBM 360/91 computer.

TABLE 4.10.—SENSITIVITY COEFFICIENTS WITH RESPECT TO RATE CONSTANTS FOR TEST PROBLEM 2

Time, s	Species	Sensitivities with respect to rate constants[a]					
		$\partial\sigma_i/\partial k_1$			$\partial\sigma_i/\partial k_2$		
		Exact[b]	GFM[b]	LSENS	Exact[b]	GFM[b]	LSENS
0.10	$\mathcal{A}$	−2.49(−2)	−3.71(−2)	−2.488(−2)	−2.04(−4)	−8.16(−5)	−2.036(−4)
	$\mathcal{B}$	2.26(−3)	3.38(−3)	2.262(−3)	−2.26(−5)	−3.83(−5)	−2.262(−5)
	$\mathcal{C}$	2.26(−2)	7.63(−3)	2.262(−2)	2.26(−4)	2.77(−4)	2.262(−4)
1.45	$\mathcal{A}$	−8.56(−2)	−8.69(−2)	−8.562(−2)	−8.45(−4)	−8.31(−4)	−8.445(−4)
	$\mathcal{B}$	5.86(−4)	5.80(−4)	5.864(−4)	−5.86(−6)	−5.80(−6)	−5.864(−6)
	$\mathcal{C}$	8.50(−2)	8.56(−2)	8.503(−2)	8.50(−4)	8.45(−4)	8.503(−4)
1.50	$\mathcal{A}$	−8.42(−2)	−8.61(−2)	−8.423(−2)	−8.31(−4)	−8.13(−4)	−8.312(−4)
	$\mathcal{B}$	5.58(−4)	5.63(−4)	5.578(−4)	−5.58(−6)	−5.63(−6)	−5.578(−6)
	$\mathcal{C}$	8.37(−2)	8.36(−2)	8.367(−2)	8.37(−4)	8.38(−4)	8.367(−4)
2.50	$\mathcal{A}$	−5.15(−2)	−5.22(−2)	−5.151(−2)	−5.11(−4)	−5.04(−4)	−5.110(−4)
	$\mathcal{B}$	2.05(−4)	2.07(−4)	2.052(−4)	−2.05(−6)	−2.07(−6)	−2.052(−6)
	$\mathcal{C}$	5.13(−2)	5.13(−2)	5.130(−2)	5.13(−4)	5.14(−4)	5.130(−4)
3.50	$\mathcal{A}$	−2.65(−2)	−2.68(−2)	−2.650(−2)	−2.64(−4)	−2.61(−4)	−2.635(−4)
	$\mathcal{B}$	7.55(−5)	7.62(−5)	7.550(−5)	−7.55(−7)	−7.62(−7)	−7.550(−7)
	$\mathcal{C}$	2.64(−2)	2.64(−2)	2.642(−2)	2.64(−4)	2.64(−4)	2.642(−4)
4.50	$\mathcal{A}$	−1.25(−2)	−1.26(−2)	−1.252(−2)	−1.25(−4)	−1.24(−4)	−1.247(−4)
	$\mathcal{B}$	2.78(−5)	2.80(−5)	2.778(−5)	−2.78(−7)	−2.80(−7)	−2.778(−7)
	$\mathcal{C}$	1.25(−2)	1.25(−2)	1.250(−2)	1.25(−4)	1.25(−4)	1.250(−4)

[a]Numbers in parentheses denote powers of 10.
[b]From reference 89.

Test problem 3 was used by Kramer et al. (ref. 92) to illustrate their code, which employs the GFM/AIM. It is a simple isothermal problem involving two reversible reactions and four species:

$$\left.\begin{array}{c} \mathcal{A} + \mathcal{B} \underset{k_{-1}}{\overset{k_1}{\rightleftharpoons}} \mathcal{D} \\ \\ \mathcal{B} + \mathcal{B} \underset{k_{-2}}{\overset{k_2}{\rightleftharpoons}} \mathcal{E} \\ \\ k_1 = 100,\ k_{-1} = 1,\ k_2 = 10^4,\ k_{-2} = 1 \\ \\ C_{\mathcal{A},0} = C_{\mathcal{B},0} = 1,\ C_{\mathcal{D},0} = C_{\mathcal{E},0} = 0 \end{array}\right\} \tag{4.71}$$

where C_i is the molar concentration of species i, that is, moles of species i per unit volume. The variation of species mole fractions with reaction time is presented in figure 4.4.

The chemical composition and sensitivity coefficients with respect to all four initial conditions and all four rate constants were produced at $t = 10^{-3}$, 10^{-2}, 0.1, 1, and 10 s, after Kramer et al. (ref. 92). However, they give results at only $t = 10$ s, when the system had essentially equilibrated (fig. 4.4). The local error tolerances were also taken from reference 92: EMAX = 10^{-6} and ATOLSP = 10^{-8}. The composition and sensitivity coefficients are listed in tables 4.11 and 4.12. To be consistent with Kramer et al. (ref. 92), table 4.12 gives the unnormalized sensitivity coefficients of the molar concentrations. The $\{\partial C_i/\partial k_j\}$ were computed from the $\{\partial \sigma_i/\partial k_j\}$ by means of the relation (see eq. (2.19))

$$\frac{\partial C_i}{\partial k_j} = \rho \frac{\partial \sigma_i}{\partial k_j} \tag{4.72}$$

which is valid because the density is constant. For the same reason $\partial \sigma_i/\partial \sigma_{j,0}$ and $\partial C_i/\partial C_{j,0}$ are identically equal. Finally, for reasons given for the previous test problem $\partial \sigma_i/\partial k_j = \partial \sigma_i/\partial A_j$.

To check the accuracy of the two methods, results were generated with the brute force method (BFM) because the analytical solution is not known. For a rate

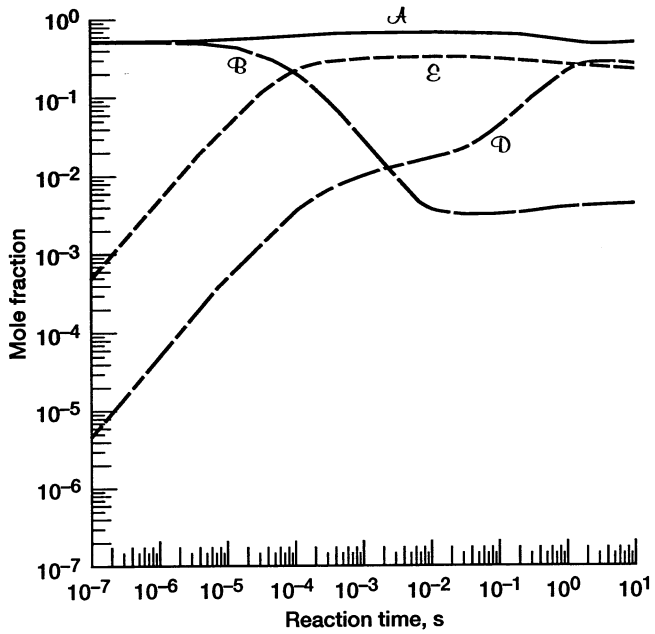

Figure 4.4.—Variation of species mole fractions with reaction time for test problem 3.

TABLE 4.11.—CHEMICAL COMPOSITION AT t = 10 s FOR TEST PROBLEM 3

Method	Concentration of species, mol/cm^3			
	𝒜	ℬ	𝒟	ℰ
LSENS	0.6398	5.631×10^{-3}	0.3602	0.3171
GFM/AIM[a]	0.6398	5.631×10^{-3}	0.3602	0.3171

[a]From reference 92.

coefficient parameter η_j the sensitivity coefficient $S_{ij}(t)$ at time t was computed by the central-difference formula (e.g., ref. 35)

$$S_{ij}(t) = \frac{Y_i\left(\eta_j + \Delta\eta_j, t\right) - Y_i\left(\eta_j - \Delta\eta_j, t\right)}{2\Delta\eta_j} \tag{4.73}$$

where $Y_i(\eta_j + \Delta\eta_j,t)$ and $Y_i(\eta_j - \Delta\eta_j,t)$ are the numerical solutions for the ith component at time t obtained with parameter values of $\eta_j + \Delta\eta_j$ and $\eta_j - \Delta\eta_j$,

TABLE 4.12.—SENSITIVITY COEFFICIENTS OF SPECIES CONCENTRATIONS AT t = 10 s FOR TEST PROBLEM 3

Sensitivity parameter, η_j	Sensitivity coefficients of species[a,b]											
	$\mathcal{A}$			$\mathcal{B}$			$\mathcal{D}$			$\mathcal{E}$		
	BFM	LSENS	GFM/AIM[c]	BFM	LSENS	GFM/AIM[c]	BFM	LSENS	GFM/AIM[c]	BFM	LSENS	GFM/AIM[c]
$C_{\mathcal{A},0}$	6.949(−1)	6.949(−1)	6.951(−1)	−1.348(−3)	−1.348(−3)	−1.348(−3)	3.051(−1)	3.051(−1)	3.049(−1)	−1.519(−1)	−1.519(−1)	−1.518(−1)
$C_{\mathcal{B},0}$	−1.532(−1)	−1.532(−1)	−1.534(−1)	3.743(−3)	3.743(−3)	3.743(−3)	1.532(−1)	1.532(−1)	1.534(−1)	4.215(−1)	4.215(−1)	4.214(−1)
$C_{\mathcal{D},0}$	5.417(−1)	5.417(−1)	5.417(−1)	2.395(−3)	2.395(−3)	2.395(−3)	4.583(−1)	4.583(−1)	4.538(−1)	2.697(−1)	2.697(−1)	2.696(−1)
$C_{\mathcal{E},0}$	−3.064(−1)	−3.064(−1)	−3.068(−1)	7.486(−3)	7.486(−3)	7.486(−3)	3.064(−1)	3.064(−1)	3.068(−1)	8.431(−1)	8.431(−1)	8.429(−1)
k_1	−1.952(−3)	−1.952(−3)	−1.951(−3)	−8.626(−6)	−8.626(−6)	−8.628(−6)	1.952(−3)	1.952(−3)	1.951(−3)	−9.714(−4)	−9.714(−4)	−9.714(−4)
k_{-1}	1.952(−1)	1.952(−1)	1.951(−1)	8.626(−4)	8.626(−4)	8.627(−4)	−1.952(−1)	−1.952(−1)	−1.951(−1)	9.714(−2)	9.714(−2)	9.712(−2)
k_2	9.714(−6)	9.714(−6)	9.730(−6)	−2.374(−7)	−2.374(−7)	−2.374(−7)	−9.714(−6)	−9.714(−6)	−9.730(−6)	4.976(−6)	4.976(−6)	4.975(−6)
k_{-2}	−9.714(−2)	−9.714(−2)	−9.728(−2)	2.374(−3)	2.374(−3)	2.374(−3)	9.714(−2)	9.714(−2)	9.728(−2)	−4.976(−2)	−4.976(−2)	−4.983(−2)

[a]Sensitivity coefficients are defined as $\partial C_i/\partial \eta_j$ for this problem.
[b]Numbers in parentheses denote powers of 10.
[c]From reference 92.

respectively. This method has a leading error of order $(\Delta\eta_j)^2$. It requires two solutions of the ODE's describing chemical kinetics (i.e., eq. (4.6)) for a given $\Delta\eta_j$. Now LSENS was modified to generate BFM results in one computer run. Hence, if normalized sensitivities were required, an additional solution of equation (4.6) with the rate coefficient parameter value of η_j had to be generated.

Equation (4.73) can also be used to compute sensitivities with respect to initial condition values of species with nonzero initial concentration, temperature, density, and pressure. However, it cannot be used for species with zero initial concentration because none of the dependent variables can be less than zero. For such species $S_{ij}(t)$ was computed by the forward-difference formula (ref. 35)

$$S_{ij}(t) = \frac{Y_i\left(\eta_j + \Delta\eta_j, t\right) - Y_i\left(\eta_j, t\right)}{\Delta\eta_j} \tag{4.74}$$

which has a leading error of order $\Delta\eta_j$. This formula requires two solutions of equation (4.6), irrespective of whether or not the sensitivities are normalized.

As discussed previously, $\Delta\eta_j$ has to be chosen carefully to ensure accuracy of the $\{S_{ij}\}$. The $\Delta\eta_j$ must be sufficiently small that the finite-difference approximations are accurate. However, it must not be so small that roundoff errors become significant.

To gain insight into the selection of $\Delta\eta_j$, the BFM was used on test problems 1 and 2. Because analytical solutions are known for the two problems, an objective study of the effects of $\Delta\eta_j$ on the $\{S_{ij}\}$ could be made. The following procedure was adopted for the preexponential factor sensitivities: Starting with a value of $5\times10^{-2}A_j$, $\Delta\eta_j$ was progressively decreased, generating sensitivities with $\Delta\eta_j = 5\times10^{-n}A_j$ and $10^{-n}A_j$ (n = 2,3,...,6). At each print station the sensitivities (or normalized sensitivities) were considered to have converged if two or more consecutive $\Delta\eta_j$ values produced the same results to a specified number (3 or 4) of significant figures. In the rest of this chapter it will be assumed that (1) results which do not agree to three significant figures with the converged solution are incorrect and (2) solutions which agree with one another to four significant figures are identical.

The same procedure was used to judge convergence of the sensitivities with respect to initial condition values. For species with nonzero initial concentration, temperature, density, and pressure, sensitivities were generated with $\Delta\eta_j = 5\times10^{-n}Y_{j,0}$ and $10^{-n}Y_{j,0}$ (n = 2,3,...,6). The $\Delta\eta_j$ values attempted for species with zero initial concentration were $5\times10^{-n}\sigma_{m,0}$ and $10^{-n}\sigma_{m,0}$ (n = 2,3,...). For presentational convenience the quantity $\delta(\eta_j)$ for the three parameter types is defined as follows:

(1) Preexponential factor

$$\delta\left(A_j\right)=\frac{\Delta A_j}{A_j} \tag{4.75}$$

(2) Initial condition value of variable with nonzero initial value

$$\delta\left(Y_{j,0}\right)=\frac{\Delta Y_{j,0}}{Y_{j,0}} \tag{4.76}$$

(3) Initial condition value of species with zero initial concentration

$$\delta\left(Y_{j,0}\right)=\frac{\Delta Y_{j,0}}{\sigma_{m,0}} \tag{4.77}$$

Then for all parameter types sensitivities were generated with $\delta(\eta_j) = 5\times10^{-n}$ and 10^{-n} (n = 2,3,...). The $\delta(\eta_j)$ values required for convergence of the sensitivity coefficients (or normalized ones) to three and four significant figures at all print stations will be referred to as $\delta_{c3}(\eta_j)$ and $\delta_{c4}(\eta_j)$, respectively.

For test problem 1 and local error tolerances EMAX = 10^{-6} and ATOLSP = 0.0, $\delta(A_1) = 10^{-2}$ to 10^{-6} produced the same results to three significant figures at all print stations. Hence $\delta_{c3}(A_1) = 10^{-2}$. The $\delta(A_1)$ required for convergence to four significant figures, that is, $\delta_{c4}(A_1)$, was 10^{-3}. For both A_2 and $\sigma_{\mathcal{A},0}$, $\delta_{c4}(\eta_j)$ was equal to 5×10^{-2}. All $\delta(\sigma_{\mathcal{A},0})$ values produced identical results. However, $\delta(A_2) = 10^{-6}$ gave incorrect sensitivities at $t = 1.5\times10^{-4}$ and 10^{-3} s; also at these two times results with $\delta(A_2) = 5\times10^{-5}$ and 10^{-5} were correct to only three significant figures. The sensitivities with $\delta(\sigma_{\mathcal{B},0}) = 5\times10^{-2}$ to 10^{-4} agreed with one another to three significant figures, as did those with $\delta(\sigma_{\mathcal{B},0}) = 10^{-5}$ and 5×10^{-6}. The two "converged" solutions showed different $\langle\partial\sigma_{\mathcal{A}}/\partial\sigma_{\mathcal{B},0}\rangle$ values at $t = 1.5\times10^{-4}$ and 10^{-3} s. The results with $\delta(\sigma_{\mathcal{B},0}) = 5\times10^{-5}$ and 10^{-6} were incorrect. Agreement to four significant figures was displayed by the results obtained with $\delta(\sigma_{\mathcal{B},0}) = 5\times10^{-2}$ to 5×10^{-3} and with $\delta(\sigma_{\mathcal{B},0}) = 10^{-3}$ to 10^{-4}. The two solutions gave different $\langle\partial\sigma_{\mathcal{A}}/\partial\sigma_{\mathcal{B},0}\rangle$ at $t = 10^{-3}$ s: 1.562×10^{-6} and 1.560×10^{-6}. Neither result agreed with the exact solution (table 4.4). This sensitivity coefficient varied from the analytical result at $t = 1.5\times10^{-4}$ s also. However, the converged results for the other three parameters agreed with the exact solutions.

To examine the effects of EMAX on the BFM results, sensitivities were generated with EMAX = 10^{-2} to 10^{-12}. For all parameters $\delta(\eta_j)$ was held constant at 10^{-3}. This study was performed on the NASA Lewis Research Center's Cray-XM/P computer using double-precision arithmetic to minimize roundoff errors. The EMAX values required for convergence to three and four significant figures, respectively, were 10^{-5} and 10^{-6} for A_1 and A_2, 10^{-5} and 10^{-5} for $\sigma_{\mathcal{A},0}$, and 10^{-8} and

10^{-9} for $\sigma_{\mathcal{B},0}$. The converged results were identical to the exact solutions for all parameters. On the Amdahl 5870 computer, the same EMAX values were needed for convergence to three significant figures for all parameters and to four significant figures for A_1, A_2, and $\sigma_{\mathcal{A},0}$. For $\sigma_{\mathcal{B},0}$, however, although EMAX = 10^{-8} reproduced the exact solution, no two consecutive EMAX values gave identical $\langle \partial\sigma_{\mathcal{A}}/\partial\sigma_{\mathcal{B},0} \rangle$ at $t = 1.5\times10^{-4}$ s. In fact, EMAX = 10^{-10} and 10^{-11} produced incorrect values for this sensitivity coefficient. However, the results with EMAX = 10^{-12} agreed with the exact solution at all output stations. Finally EMAX = 10^{-2} to 10^{-4} gave many significantly inaccurate sensitivity coefficients; in several instances the sign was wrong.

The same study was made with $\delta(\eta_j) = 10^{-2}$ on the Cray-XM/P computer using double precision. The EMAX values required for convergence to three and four significant figures were the same as with $\delta(\eta_j) = 10^{-3}$. However, EMAX = 10^{-10} produced incorrect $\langle \partial\sigma_{\mathcal{A}}/\partial\sigma_{\mathcal{B},0} \rangle$ at $t = 10^{-3}$ s. Also, as expected, the $\{\langle \partial\sigma_i/\partial A_1 \rangle\}$ agreed to only three significant figures with the exact solutions. The effects of $\{\delta(\eta_j)\}$ on the sensitivities were studied with EMAX = 10^{-12} and ATOLSP = 0.0. For A_1, A_2, and $\sigma_{\mathcal{A},0}$, the $\delta_{c3}(\eta_j)$ and $\delta_{c4}(\eta_j)$ were the same as those obtained on the Amdahl 5870 computer with EMAX = 10^{-6} and ATOLSP = 0.0; the required $\delta_{c4}(\sigma_{\mathcal{B},0})$ was 5×10^{-2}. The converged results were identical to the exact solutions for all parameters. In addition, for each parameter the sensitivities produced with $\delta(\eta_j)$ in the range $[\delta_{c4}(\eta_j), 10^{-6}]$ were identical to one another.

The preceding discussion indicates that EMAX = 10^{-9} was required to guarantee accuracy of the BFM results. For this EMAX the effects of $\{\delta(\eta_j)\}$ on the sensitivities were examined on the Amdahl 5870 computer. The $\delta_{c3}(\eta_j)$ values were the same for all parameters as with EMAX = 10^{-6}. The same was true of $\delta_{c4}(A_1)$ and $\delta_{c4}(A_2)$. For the other two parameters, $\delta_{c4}(\sigma_{\mathcal{A},0}) = 10^{-3}$ and $\delta_{c4}(\sigma_{\mathcal{B},0}) = 10^{-2}$. For both A_1 and $\sigma_{\mathcal{A},0}$, results with $\delta(\eta_j) = \delta_{c4}(\eta_j)$ to 10^{-6} were identical. The runs with $\delta(A_2) = 10^{-5}$ and 5×10^{-6} produced incorrect solutions at $t = 1.5\times10^{-4}$ s; however, $\delta(A_2) = 10^{-6}$ gave the correct sensitivities. At this time $\delta(\sigma_{\mathcal{B},0}) = 5\times10^{-4}$ and 5×10^{-5} gave incorrect $\langle \partial\sigma_{\mathcal{A}}/\partial\sigma_{\mathcal{B},0} \rangle$. Also, $\langle \partial\sigma_{\mathcal{A}}/\partial A_2 \rangle$ with $\delta(A_2) = 10^{-3}$ was correct to three significant figures only, as was $\langle \partial\sigma_{\mathcal{A}}/\partial\sigma_{\mathcal{B},0} \rangle$ for $\delta(\sigma_{\mathcal{B},0}) = 10^{-6}$. However, $\delta(\sigma_{\mathcal{B},0}) = 10^{-6}$ reproduced the exact solution; the same was true of the result produced with $\delta(\sigma_{\mathcal{B},0}) = 5\times10^{-2}$. In other words, although the results with $\delta(\sigma_{\mathcal{B},0}) = 10^{-2}$ to 10^{-3}, 10^{-4}, 10^{-5}, and 5×10^{-6} agreed with one another to four significant figures, $\langle \partial\sigma_{\mathcal{A}}/\partial\sigma_{\mathcal{B},0} \rangle$ was not identical to the exact solution at $t = 1.5\times10^{-4}$ s.

To examine if roundoff errors were causing the above problems in the sensitivities with respect to A_2 and $\sigma_{\mathcal{B},0}$, BFM results were generated on the Cray-XM/P computer with EMAX = 10^{-9}, ATOLSP = 0.0, and double-precision arithmetic. The $\{\delta_{c3}(\eta_j)\}$ and $\{\delta_{c4}(\eta_j)\}$ values were the same as those obtained with EMAX = 10^{-12} and ATOLSP = 0.0. For each parameter the results for all $\delta(\eta_j)$ in the range $[\delta_{c4}(\eta_j), 10^{-6}]$ were identical to both one another and the analytical solutions.

To verify that roundoff errors were causing the difficulties on the Amdahl computer, the preceding experiment was repeated on the Cray-XM/P computer using single-precision arithmetic. The results were noticeably worse than on the Amdahl

computer. Indeed the sensitivities with respect to $\sigma_{\Phi,0}$ did not converge at $t = 1.5\times10^{-4}$ and 10^{-3} s. Now the machine unit roundoff (U) values for double-precision arithmetic are 2.2×10^{-16} and 2.5×10^{-29}, respectively, on the Amdahl 5870 and Cray-XM/P. For single-precision arithmetic, however, $U = 7.1\times10^{-15}$ on the Cray-XM/P. (U is the smallest positive number such that $(1 + U) > 1$ on the computer.)

The final experiment performed to verify that roundoff errors were responsible for the difficulties in generating the sensitivities was the study of the effects of $\{\delta(\eta_j)\}$ on the Cray-XM/P using single-precision arithmetic and the local error tolerances EMAX = 10^{-12} and ATOLSP = 0.0. Although the exact solutions were reproduced for all parameters, the variation of the sensitivities with $\delta(\eta_j)$ was not as consistent as when double-precision arithmetic was used.

The above discussion indicates that care must be exercised in specifying not only the value of $\Delta\eta_j$ but also that of EMAX. In addition, it is very important to control roundoff errors.

For test problem 2 the BFM runs on the Amdahl 5870 computer with EMAX = 10^{-6} and ATOLSP = 10^{-13} did not converge at $t = 3.5$ s for A_1. Also, $\delta_{c3}(A_2)$ and $\delta_{c4}(A_2)$ could not be identified; that is, a single value of $\delta(A_2)$ that produced converged results to three significant figures at all print stations could not be obtained. When ATOLSP was increased to 10^{-8}, significant improvements were noticed. In particular, $\delta_{c3}(A_1) = 5\times10^{-3}$, $\delta_{c4}(A_1) = 10^{-3}$, $\delta_{c3}(A_2) = 10^{-2}$ or 10^{-3}, and $\delta_{c4}(A_2) = 10^{-3}$. The $\delta(A_2)$ values of 10^{-2} and 10^{-3} produced different $\partial\sigma_{\mathcal{A}}/\partial A_2$ at 1.45 s, with the former agreeing with the exact solution. Because the convergence criterion previously given frequently caused difficulty in identifying the $\delta_{c3}(\eta_j)$ and $\delta_{c4}(\eta_j)$, it was modified to require that at least three consecutive $\delta(\eta_j)$ values produce the same results before convergence is declared. Using the new criterion gave $\delta_{c3}(A_2) = 10^{-3}$. All sensitivities were in essential (but not exact) agreement with the analytical solutions. Also $\delta(\eta_j)$ in the range $[10^{-3},10^{-6}]$ gave identical results for both parameters.

The preceding experiment was repeated with EMAX = 10^{-9} and ATOLSP = 10^{-16} to produce more accurate results. The values $\delta_{c3}(A_1) = 10^{-2}$ and $\delta_{c3}(A_2) = 5\times10^{-3}$ were obtained. Convergence difficulties for both parameters at $t = 4.5$ s prevented identification of the $\{\delta_{c4}(\eta_j)\}$. Also at this time $\delta(A_1) = 10^{-5}$ to 10^{-6} and $\delta(A_2) = 10^{-5}$ and 10^{-6} produced inaccurate results. However, the converged values agreed with the analytical solutions. The local error tolerance EMAX was varied from 10^{-2} to 10^{-12} to study its effect on accuracy. For this study both $\delta(\eta_j)$ were set equal to 10^{-3}, and two different ATOLSP, 10^{-2}EMAX and 10^{-7}EMAX, were attempted. For both ATOLSP and both parameters the EMAX values required for convergence to three and four significant figures were 10^{-8} and 10^{-9}, respectively.

To examine if the inaccuracies for small $\{\delta(\eta_j)\}$ were caused by roundoff errors, sensitivities were produced on the Cray-XM/P computer using double-precision arithmetic. The local error tolerances EMAX = 10^{-12} and ATOLSP = 10^{-19} were used to ensure accuracy. The resulting $\delta(\eta_j)$ values for convergence were $\delta_{c3}(A_1) = 10^{-2}$, $\delta_{c4}(A_1) = 5\times10^{-3}$, $\delta_{c3}(A_2) = 5\times10^{-3}$, and $\delta_{c4}(A_2) = 10^{-3}$. For both parameters

and at all times, $\delta(\eta_j)$ in the range $[\delta_{c4}(\eta_j), 10^{-6}]$ produced identical results, which agreed with the exact solutions. For $\delta(\eta_j) = 10^{-3}$ and ATOLSP = 10^{-7}EMAX, an EMAX of 10^{-8} was required by both parameters for the sensitivities to become tolerance independent. Finally the variations of the sensitivities with $\delta(\eta_j)$ were examined with EMAX = 10^{-9} and ATOLSP = 10^{-16}. The results were identical to those obtained with EMAX = 10^{-12} and ATOLSP = 10^{-19}.

The BFM experiments on test problem 2 also illustrated the importance of generating accurate solutions by both using small error tolerances and increasing the precision of the arithmetic. Hence, except where indicated, BFM results for all isothermal problems were evaluated on the Cray-XM/P computer using double-precision arithmetic.

Table 4.12 gives the BFM results obtained for test problem 3 with EMAX = 10^{-12} and ATOLSP = 10^{-19} and verified with EMAX = 10^{-15} and ATOLSP = 10^{-22}. The $\delta(\eta_j)$ values required for convergence were $\delta_{c3}(\sigma_{\mathcal{A},0}) = 5\times10^{-2}$, $\delta_{c4}(\sigma_{\mathcal{A},0}) = 10^{-2}$, $\delta_{c3}(\sigma_{\mathcal{B},0}) = 10^{-2}$, $\delta_{c4}(\sigma_{\mathcal{B},0}) = 5\times10^{-3}$, $\delta_{c3}(\sigma_{\mathcal{D},0}) = 5\times10^{-5}$, $\delta_{c4}(\sigma_{\mathcal{D},0}) = 10^{-5}$, $\delta_{c3}(\sigma_{\mathcal{E},0}) = 10^{-4}$, $\delta_{c4}(\sigma_{\mathcal{E},0}) = 10^{-5}$, $\delta_{c3}(\eta_j) = 10^{-2}$ for all four rate constants, $\delta_{c4}(A_1) = \delta_{c4}(A_2) = 5\times10^{-3}$, $\delta_{c4}(A_3) = 5\times10^{-4}$, and $\delta_{c4}(A_4) = 10^{-3}$. Table 4.12 shows the excellent agreement between the BFM and LSENS at $t = 10$ s. The same level of agreement was obtained at all other print stations. The GFM/AIM also compared well with the BFM. Thus for this problem neither method was significantly more accurate than the other at $t = 10$ s.

LSENS required 289 steps, 339 derivative evaluations, 44 Jacobian matrix evaluations, and 0.077 s of CPU time to solve for the chemical composition. The execution time for the chemical composition and sensitivities with respect to all eight parameters was 0.36 s. When only one parameter was specified, the CPU time was 0.18 s for both initial condition and rate constant sensitivities. Therefore the CPU times required for the first parameter and then for each subsequent parameter were approximately 0.1 and 0.026 s. The latter time was significantly less than the at least 0.15 s required by the BFM. The computational cost for the second and subsequent parameters was verified by generating sensitivities with respect to all initial conditions and all rate constants. The two runs took up approximately 0.25 and 0.26 s, respectively. The GFM/AIM required two steps to generate the sensitivities. However, the execution time is not given in reference 92; therefore an efficiency comparison with LSENS could not be made.

4.6.2 Pyrolysis of Ethane

Test problem 4, taken from Kramer et al. (ref. 91), describes the pyrolysis of ethane at a temperature of 923 K. This constant-temperature, constant-density problem consists of five irreversible reactions among seven species. The reaction mechanism, rate coefficient parameters, and rate constants at 923 K are given in table 4.13. The initial concentration of ethane was 3.584×10^{18} molecules/cm^3 (5.951×10^{-6} mol/cm^3); the initial concentration of all other species was zero. The variation of species mole fractions with reaction time is shown in figure 4.5.

TABLE 4.13.—REACTION MECHANISM FOR TEST PROBLEM 4

Reaction number, j	Reaction	Rate coefficient parameters[a,b]			Rate constant, k_j, at 923 K[a,c]
		A_j	n_j	E_j	
1	$C_2H_6 \rightarrow CH_3 + CH_3$	1.20(12)	0.0	5.92(4)	1.14(–2)
2	$CH_3 + C_2H_6 \rightarrow CH_4 + C_2H_5$	8.01(8)	0.0	1.19(4)	1.19(6)
3	$C_2H_5 \rightarrow C_2H_4 + H$	3.00(11)	0.0	3.50(4)	1.57(3)
4	$H + C_2H_6 \rightarrow H_2 + C_2H_5$	1.30(11)	0.0	8.98(3)	9.72(8)
5	$H + H \rightarrow H_2$	6.99(13)	0.0	0.0	6.99(13)

[a]Units are moles, centimeters, seconds, and calories. Numbers in parentheses denote powers of 10.
[b]From reference 91.
[c]From reference 21.

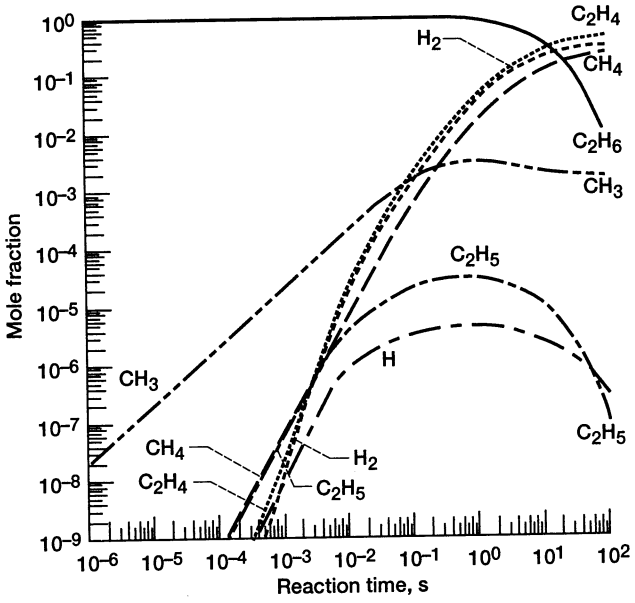

Figure 4.5.—Variation of species mole fractions with reaction time for test problem 4.

Although the mechanism is quite small, the problem is very stiff with the ratio of the largest to smallest nonzero eigenvalues being ~10^5 (ref. 91). These authors attempted the problem with the DM, GFM, and GFM/AIM. The decoupled version of the DM was unstable. The coupled version of the DM produced accurate results, but sensitivity coefficients with respect to the rate coefficient parameter A_2 could not be obtained because of numerical difficulty. For this parameter they experienced no such difficulty with the decoupled version of the DM; however, the accuracy was very poor.

Sensitivity coefficients with respect to the $\{\sigma_{j,0}\}$, T_0, $\{A_j\}$, and $\{E_j\}$ (18 parameters in all) were generated with LSENS at the two output stations $t = 1$ and 20 s. (The code had to be modified to generate sensitivities with respect to the activation energies because the problem was at constant temperature.) No difficulty was experienced and all coefficients were successfully computed. To be consistent with Kramer et al. (ref. 91), the sensitivity coefficients were of the species concentrations in molecules per cubic centimeter $\{n_i\}$. The $\{\partial n_i/\partial \eta_j\}$ were obtained from the $\{\partial C_i/\partial \eta_j\}$ by multiplying them with appropriate powers of the Avogadro number ($= 6.023 \times 10^{23}$ molecules/mol). Of course, because the density is constant, $\partial n_i/\partial n_{j,0} = \partial \sigma_i/\partial \sigma_{j,0}$. Finally for the activation energies the sensitivities were with respect to the activation temperatures, that is, $\{E_j/R\}$, where R (= 1.987) is the universal gas constant in calories per mole-Kelvin.

The numerical solutions produced by LSENS at 1 s are given in tables 4.14 to 4.19 for the parameters $n_{C_2H_6,0}$, T_0, A_1, A_2, E_1/R, and E_4/R. EMAX was set equal to 10^{-4}, after Kramer et al. (ref. 91), who used this value with the GFM. In order to ensure relative error control for species with mole fractions ≥ 0.1 ppm, ATOLSP was set equal to 10^{-13}. Also listed in tables 4.14 to 4.19 are the results from reference 91 for the GFM, GFM/AIM, and coupled version of DM. The EMAX used with the DM and GFM were 10^{-3} and 10^{-4}, respectively. (EMAX values used to generate the kinetics solution for the GFM and GFM/AIM are not given in reference 91.)

To check the accuracy of the methods, BFM results were generated with EMAX = 10^{-12} and ATOLSP = 10^{-21} and verified with EMAX = 10^{-15} and ATOLSP = 10^{-24}. For the activation energies $\{\Delta E_j\}$ were set equal to $-5 \times 10^{-n} RT_0$ and $-10^{-n} RT_0$ ($n = 2,3,...,6$), and $\delta(E_j)$ was defined as

TABLE 4.14.—SENSITIVITY COEFFICIENTS WITH RESPECT TO INITIAL CONDITION $n_{C_2H_6,0}$ AT $t = 1$ s

FOR TEST PROBLEM 4

Species	Sensitivities with respect to $n_{C_2H_6,0}$ at 1 s[a]				
	BFM	LSENS	DM[b]	GFM[b]	GFM/AIM[b]
C_2H_6	9.253(−1)	9.253(−1)	9.25(−1)	9.25(−1)	9.25(−1)
CH_3	2.223(−5)	2.201(−5)	(c)	(c)	(c)
C_2H_5	3.958(−5)	3.958(−5)	3.96(−5)	3.90(−5)	3.98(−5)
CH_4	2.197(−2)	2.197(−2)	2.20(−2)	2.20(−2)	2.19(−2)
C_2H_4	6.365(−2)	6.365(−2)	(c)	(c)	(c)
H	2.512(−6)	2.512(−6)	2.51(−6)	2.43(−6)	2.50(−6)
H2	5.269(−2)	5.269(−2)	(c)	(c)	(c)

[a]Sensitivity coefficients are defined here as $\partial n_i/\partial n_{C_2H_6,0}$. Numbers in parentheses denote powers of 10.

[b]From reference 91.

[c]Not given.

TABLE 4.15.—SENSITIVITY COEFFICIENTS WITH RESPECT TO INITIAL TEMPERATURE AT t = 1 s FOR TEST PROBLEM 4

Species	Sensitivities with respect to T_0 at 1 s[a]				
	BFM	LSENS	DM[b]	GFM[b]	GFM/AIM[b]
C_2H_6	−5.863(15)	−5.863(15)	−5.87(15)	−5.88(15)	−5.86(15)
CH_3	3.227(14)	3.227(14)	3.23(14)	3.23(14)	3.19(14)
C_2H_5	5.924(11)	5.924(11)	5.93(11)	5.80(11)	6.02(11)
CH_4	2.399(15)	2.399(15)	2.40(15)	2.40(15)	2.40(15)
C_2H_4	4.502(15)	4.502(15)	(c)	(c)	(c)
H	3.034(11)	3.034(11)	3.03(11)	3.78(11)	3.05(11)
H_2	3.302(15)	3.302(15)	(c)	(c)	(c)

[a]Sensitivity coefficients are defined here as $\partial n_i/\partial T_0$. Numbers in parentheses denote powers of 10.
[b]From reference 91.
[c]Not given.

TABLE 4.16.—SENSITIVITY COEFFICIENTS WITH RESPECT TO RATE COEFFICIENT PARAMETER A_1 AT t = 1 s FOR TEST PROBLEM 4

Species	Sensitivities with respect to A_1 at 1 s[a]				
	BFM	LSENS	DM[b]	GFM[b]	GFM/AIM[b]
C_2H_6	−1.248(5)	−1.248(5)	−1.25(5)	−1.25(5)	−1.27(5)
CH_3	9.612(3)	9.613(3)	9.62(3)	9.62(3)	9.50(3)
C_2H_5	6.198(1)	6.199(1)	6.20(1)	6.17(1)	6.23(1)
CH_4	5.542(4)	5.542(4)	5.54(4)	5.54(4)	5.50(4)
C_2H_4	9.222(4)	9.222(4)	(c)	(c)	(c)
H	7.259	7.259	7.26	9.42	7.26
H_2	6.455(4)	6.453(4)	(c)	(c)	(c)

[a]Sensitivity coefficients are defined here as $\partial n_i/\partial A_1$. Numbers in parentheses denote powers of 10.
[b]From reference 91.
[c]Not given.

TABLE 4.17.—SENSITIVITY COEFFICIENTS WITH RESPECT TO RATE COEFFICIENT PARAMETER A_2 AT t = 1 s FOR TEST PROBLEM 4

Species	Sensitivities with respect to A_2 at 1 s[a]			
	BFM	LSENS	GFM[b]	GFM/AIM[b]
C_2H_6	−1.474(31)	−1.474(31)	−1.49(31)	−1.65(31)
CH_3	−8.614(30)	−8.614(30)	−8.62(30)	−8.47(30)
C_2H_5	−2.030(26)	−2.073(26)	(c)	(c)
CH_4	8.361(30)	8.361(30)	8.34(30)	8.21(30)
C_2H_4	1.486(31)	1.486(31)	(d)	(d)
H	8.224(24)	7.744(24)	−1.79(27)	−4.77(25)
H_2	1.068(31)	1.068(31)	(d)	(d)

[a]Sensitivity coefficients are defined here as $\partial n_i/\partial A_2$. Numbers in parentheses denote powers of 10.

[b]From reference 91. DM results could not be computed for A_2 because of numerical difficulty.

[c]Not given because the scaled sensitivity ($\partial \ln n_{C_2H_5}/\partial \ln A_2$) was less than 10^{-4}.

[d]Not given.

TABLE 4.18.—SENSITIVITY COEFFICIENTS WITH RESPECT TO PARAMETER E_1/R AT t = 1 s FOR TEST PROBLEM 4

Species	Sensitivities with respect to E_1/R at 1 s[a]				
	BFM	LSENS	DM[b]	GFM[b]	GFM/AIM[b]
C_2H_6	1.623(14)	1.623(14)	1.62(14)	1.63(14)	1.65(14)
CH_3	−1.250(13)	−1.250(13)	−1.20(13)	−1.25(13)	−1.23(13)
C_2H_5	−8.059(10)	−8.059(10)	−8.06(10)	−8.00(10)	−8.11(10)
CH_4	−7.204(13)	−7.204(13)	−7.21(13)	−7.20(13)	−7.15(13)
C_2H_4	−1.199(14)	−1.199(14)	(c)	(c)	(c)
H	−9.436(9)	−9.436(9)	−9.44(9)	−1.19(10)	−9.44(9)
H_2	−8.391(13)	−8.391(13)	(c)	(c)	(c)

[a]Sensitivity coefficients are defined here as $(\partial n_i/\partial(E_1/R))$. Numbers in parentheses denote powers of 10.

[b]From reference 91.

[c]Not given.

TABLE 4.19.—SENSITIVITY COEFFICIENTS WITH RESPECT TO PARAMETER E_4/R AT t = 1 s FOR TEST PROBLEM 4

Species	Sensitivities with respect to E_4/R at 1 s[a]				
	BFM	LSENS	DM[b]	GFM[b]	GFM/AIM[b]
C_2H_6	9.869(13)	9.869(13)	9.88(13)	9.81(13)	9.84(13)
CH_3	1.082(9)	1.071(9)	(c)	(c)	(c)
C_2H_5	–6.438(10)	–6.438(10)	–6.44(10)	–6.46(10)	–6.44(10)
CH_4	1.069(12)	1.069(12)	1.07(12)	1.05(12)	1.06(12)
C_2H_4	–9.916(13)	–9.916(13)	(d)	(d)	(d)
H	2.656(8)	2.656(8)	2.66(8)	2.74(8)	2.63(8)
H_2	–9.971(13)	–9.971(13)	(d)	(d)	(d)

[a]Sensitivity coefficients are defined here as $(\partial n_i/\partial(E_4/R))$. Numbers in parentheses denote powers of 10.

[b]From reference 91.

[c]Not given because the scaled sensitivity $(\partial \ln n_{CH_3}/\partial \ln E_4)$ was less than 10^{-4}.

[d]Not given.

$$\delta(E_j) = -\frac{\Delta E_j}{RT_0} \tag{4.78}$$

The $\delta_{c3}(\eta_j)$ and $\delta_{c4}(\eta_j)$ were as follows: $\delta_{c3}(\sigma_{C_2H_6,0}) = \delta_{c3}(A_1) = \delta_{c3}(E_1) = \delta_{c3}(E_4) = 10^{-2}$, $\delta_{c3}(T_0) = 5\times10^{-4}$, $\delta_{c3}(A_2) = 5\times10^{-3}$, $\delta_{c4}(\sigma_{C_2H_6,0}) = \delta_{c4}(A_1) = 5\times10^{-3}$, $\delta_{c4}(T_0) = 10^{-4}$, $\delta_{c4}(A_2) = \delta_{c4}(E_1) = 10^{-3}$, and $\delta_{c4}(E_4) = 5\times10^{-3}$. (However, as discussed later, several sensitivity coefficients could not be obtained at t = 20 s.)

Tables 4.14 to 4.19 show the excellent agreement between the BFM and LSENS. The DM produced accurate results, confirming Kramer et al.'s observations (ref. 91). In contrast, the GFM had difficulty tracking rapidly varying species. In particular, the sensitivities of H with respect to T_0, A_1, A_2, and E_1/R were all significantly incorrect, with $\partial n_H/\partial A_2$ having the wrong sign. The GFM/AIM was significantly more accurate than the GFM. However, it too produced the wrong sign for $\partial n_H/\partial A_2$, and $\partial n_{C_2H_6}/\partial A_2$ was incorrect (table 4.17). Kramer et al. (ref. 91) do not give results for $\partial n_{C_2H_5}/\partial A_2$ and $\partial n_{CH_3}/\partial(E_4/R)$ because their methods predicted scaled sensitivities $(\partial \ln n_i/\partial \ln \eta_j) < 10^{-4}$ in magnitude for both quantities. Although not explicitly stated in reference 91, it was assumed that the same reason applied to $\partial n_{CH_3}/\partial n_{C_2H_6,0}$ also. The BFM results, however, showed that $\partial \ln n_{CH_3}/\partial \ln n_{C_2H_6,0} = 6.91\times10^{-3}$, $\partial \ln n_{C_2H_5}/\partial \ln A_2 = -2.40\times10^{-3}$, and $\partial \ln n_{CH_3}/\partial \ln E_4 = 4.24\times10^{-4}$. Note the excellent agreement between LSENS and the BFM for all three sensitivities (tables 4.14, 4.17, and 4.19). The results for this problem indicate that the DDM was more accurate than the DM, GFM, and GFM/AIM.

Kramer et al. (ref. 91) state that the GFM experienced difficulty tracking the rapidly varying species H and C_2H_5, as observed previously, and therefore EMAX had to be reduced to 10^{-4}. To illustrate the effect of EMAX, they present the

variation of the C_2H_5 sensitivities with EMAX. Table 4.20 reproduces their results together with those obtained with LSENS and the BFM. For the LSENS runs ATOLSP was set equal to 10^{-9}EMAX. Note that in all cases the DDM was superior to the GFM, and for several parameters significantly so. Indeed, except for A_2, even with EMAX as large as 10^{-2} LSENS produced accurate solutions, with errors less than 1 percent.

For completeness the sensitivity coefficients $\{\partial n_i/\partial \eta_j\}$ with respect to the six parameters $n_{C_2H_6,0}$, T_0, A_1, A_2, E_1/R, and E_4/R at $t = 20$ s are presented in table 4.21. The LSENS results were generated with the local error tolerances EMAX = 10^{-4} and ATOLSP = 10^{-13}. Again the agreement between the BFM and LSENS was excellent for all variables and all parameters. The sensitivity coefficients $\partial\sigma_{CH_3}/\partial\sigma_{C_2H_6,0}$ and $\partial\sigma_{CH_3}/\partial E_4$ could not be obtained with the BFM. For several values of $\delta(\eta_j)$ sensitivities equal to zero were produced. LSENS predicted the normalized sensitivities $\langle\partial\sigma_{CH_3}/\partial\sigma_{C_2H_6,0}\rangle = -4.03\times10^{-6}$ and $\langle\partial\sigma_{CH_3}/\partial E_4\rangle = 2.05\times10^{-6}$, indicating that these sensitivities are unimportant.

Examination of the normalized results showed that $\langle\partial\sigma_i/\partial E_j\rangle = \langle\partial\sigma_i/\partial A_j\rangle$ at both times for all seven species and all five reactions. This result is additional evidence of the accuracy of the DDM. Numerical solutions at 20 s are not given in reference 91, and so accuracy comparisons of the DDM with the DM, GFM, and GFM/AIM at this print station were not possible.

The computational work requirements for the integration intervals [0,1] s and [0,20] s are given in table 4.22. In this table NSTEP is the number of integration steps, NFE the number of functional (i.e., derivative) evaluations, NJE the number of Jacobian matrix evaluations and LU-decompositions, and CPU the execution

TABLE 4.20.—EFFECTS OF LOCAL ERROR TOLERANCE ON SENSITIVITY COEFFICIENTS OF $n_{C_2H_5}$ AT $t = 1$ s FOR TEST PROBLEM 4

Sensitivity parameter, η_j	Sensitivities of $n_{C_2H_5}$ at 1 s[a]						
	BFM	LSENS[b]			GFM[c]		
		EMAX = 10^{-2}	EMAX = 10^{-3}	EMAX = 10^{-4}	EMAX = 10^{-2}	EMAX = 10^{-3}	EMAX = 10^{-4}
$n_{C_2H_6,0}$	3.958(−5)	3.951(−5)	3.958(−5)	3.958(−5)	3.54(−5)	3.99(−5)	3.90(−5)
T_0	5.924(11)	5.912(11)	5.926(11)	5.924(11)	2.00(13)	1.20(12)	5.80(11)
A_1	6.198(1)	6.210(1)	6.197(1)	6.199(1)	9.92(1)	7.92(1)	6.17(1)
A_2	−2.030(26)	−5.334(26)	−1.605(26)	−2.073(26)	(d)	(d)	(d)
E_1/R	−8.059(10)	−8.074(10)	−8.057(10)	−8.059(10)	−1.11(11)	−1.03(11)	−8.00(10)
E_4/R	−6.438(10)	−6.444(10)	−6.436(10)	−6.438(10)	−6.18(10)	−5.93(10)	−6.46(10)

[a]Sensitivity coefficients are defined here as $(\partial n_{C_2H_5}/\partial\eta_j)$. Numbers in parentheses denote powers of 10.
[b]ATOLSP = 10^{-9} EMAX.
[c]From reference 91.
[d]Not given.

TABLE 4.21.—SENSITIVITY COEFFICIENTS AT t = 20 s FOR TEST PROBLEM 4

Species	Sensitivity coefficients at t = 20 s with respect to parameter[a]					
	$n_{C_2H_6,0}$	T_0	A_1	A_2	E_1/R	E_4/R
C_2H_6	2.542(−1)	−3.550(16)	−7.858(5)	−4.079(30)	1.022(15)	5.069(14)
	2.542(−1)	−3.551(16)	−7.858(5)	−4.079(30)	1.022(15)	5.071(14)
CH_3	(b)	3.225(14)	9.624(3)	−8.685(30)	−1.251(13)	(b)
	−1.297(−8)	3.225(14)	9.624(3)	−8.685(30)	−1.251(13)	−2.564(7)
C_2H_5	7.860(−6)	−8.315(11)	−5.122	−1.261(26)	6.661(9)	2.065(9)
	7.860(−6)	−8.316(11)	−5.124	−1.259(26)	6.663(9)	2.066(9)
CH_4	2.410(−1)	2.042(16)	5.086(5)	4.915(30)	−6.611(14)	1.984(14)
	2.410(−1)	2.042(16)	5.086(5)	4.915(30)	−6.611(14)	1.984(14)
C_2H_4	6.253(−1)	2.513(16)	5.267(5)	5.963(30)	−6.847(14)	−6.063(14)
	6.253(−1)	2.513(16)	5.267(5)	5.964(30)	−6.847(14)	−6.063(14)
H	1.175(−6)	2.190(10)	7.996(−1)	−1.886(25)	−1.040(9)	2.343(9)
	1.175(−6)	2.189(10)	7.994(−1)	−1.881(25)	−1.039(9)	2.343(9)
H_2	5.048(−1)	1.493(16)	2.723(5)	3.506(30)	−3.542(14)	−7.055(14)
	5.048(−1)	1.493(16)	2.723(5)	3.507(30)	−3.542(14)	−7.055(14)

[a]Sensitivity coefficients are defined here as $\partial n_i/\partial \eta_j$. For each species the top row gives the BFM results and the bottom row the LSENS results. Numbers in parentheses denote powers of 10.

[b]See text.

TABLE 4.22.—EFFECTS OF LOCAL ERROR TOLERANCE ON COMPUTATIONAL WORK FOR TEST PROBLEM 4

Local relative error tolerance, EMAX	Computational work requirements								
	For the interval [0,1] s					For the interval [0,20] s			
	LSENS[a]				GFM[c]	LSENS[a]			
	NSTEP	NFE[b]	NJE[b]	CPU, s	NSTEP	NSTEP	NFE[b]	NJE[b]	CPU, s
10^{-2}	46	59	14	0.17	35	55	70	17	0.20
10^{-3}	67	81	15	0.26	68	84	102	20	0.33
10^{-4}	93	117	18	0.38	83	117	149	22	0.48

[a]ATOLSP = 10^{-9} EMAX.

[b]Sensitivity analysis calculations require additional NSTEP derivative evaluations and NSTEP Jacobian matrix evaluations.

[c]From reference 91: NSTEP is not given for the interval [0,20] s.

time (in seconds) required to compute the dependent variables (i.e., the seven species mole numbers and temperature) and sensitivities with respect to the 18 parameters. Of course, when sensitivity analysis is performed, additional NSTEP functional and NSTEP Jacobian matrix evaluations and LU-decompositions are required. Now, because this is a constant-temperature problem, temperature was not a dependent variable when solving for the composition alone, as described in chapter 9 of part II. However, because T_0 was a sensitivity parameter, temperature had to be included as a dependent variable for the sensitivity computations (see eq. (4.8)). (For the BFM calculations, however, T was not a dependent variable.) In order to ensure that the correct composition calculation cost incurred during the sensitivity run was measured, a kinetics-only run was made with the code modified to include the temperature as a dependent variable. For the interval [0,1] s the execution times for computing the dependent variables were 0.02, 0.03, and 0.04 s, respectively, for EMAX = 10^{-2}, 10^{-3}, and 10^{-4}. For the interval [0,20] s the corresponding execution times were 0.03, 0.04, and 0.06 s.

Table 4.22 also presents the variation of NSTEP with EMAX for the GFM and the interval [0,1] s. The GFM/AIM required 28 steps to solve for the sensitivities in the same time interval. The execution times required by the GFM to generate sensitivities at five output times in the interval [0,20] s were 9.7, 14.3, and 79.2 s, respectively, for EMAX = 10^{-2}, 10^{-3}, and 10^{-4} (ref. 91). The DM and GFM/AIM required 12.5 and 1.8 s, respectively, for the same calculations. Efficiency comparisons with LSENS were not possible because the authors do not identify the computer on which the execution times were measured.

However, solution to this problem with the DDM and GFM/AIM was attempted on an IBM 370 computer by Dunker (ref. 21) using the rate constants listed in table 4.13. To enable accuracy and efficiency comparisons with LSENS, the code CHEMDDM (ref. 23) was run on the Amdahl 5870 computer, as discussed in section 4.6.1.

Normalized sensitivity coefficients $\{\langle S_{ij} \rangle\}$ computed at $t = 1$ and 20 s with LSENS and CHEMDDM are given in tables 4.23 and 4.24. All sensitivity coefficients are with respect to the rate constant k_1. Both LSENS and CHEMDDM were run with the same local error tolerances: the values used by Dunker (ref. 21), EMAX = 10^{-6} and ATOLSP = 10^{-8}. Also presented in tables 4.23 and 4.24 are results produced with the BFM (EMAX = 10^{-12} and ATOLSP = 10^{-21}) and those obtained by Dunker (ref. 21) with the DDM and GFM/AIM.

Tables 4.23 and 4.24 show the excellent agreement between LSENS and CHEMDDM at both 1 and 20 s. In addition, both codes agreed well with the DDM results of Dunker (ref. 21) and the BFM. The GFM/AIM was accurate at 1 s. But at t = 20 s it produced inaccurate results, especially for CH_3. Even by decreasing the error tolerances required for the sensitivity calculations by the GFM/AIM, Dunker (ref. 21) was unable to obtain better agreement for sensitivities with respect to k_1. Instead the reduction significantly worsened the accuracy of the other rate constant sensitivities. Better agreement could be obtained by increasing the number of output stations at which sensitivities were computed. The increase in the number of output stations had no effect on the DDM results. Both the lack of

TABLE 4.23.—NORMALIZED SENSITIVITY COEFFICIENTS WITH RESPECT TO RATE CONSTANT k_1 AT t = 1 s FOR TEST PROBLEM 4

Species	Normalized sensitivities with respect to k_1 at t = 1 s				
	BFM	LSENS	CHEMDDM	DDM[a]	GFM/AIM[a]
C_2H_6	–0.0443	–0.0443	–0.0443	–0.044	–0.044
CH_3	1.000	1.000	1.000	1.000	0.999
C_2H_5	0.662	0.662	0.662	0.662	0.688
CH_4	0.976	0.976	0.976	0.976	0.977
C_2H_4	0.680	0.680	0.680	0.681	0.682
H	0.478	0.478	0.478	0.478	0.493
H_2	0.602	0.602	0.602	0.602	0.604

[a]From reference 21.

TABLE 4.24.—NORMALIZED SENSITIVITY COEFFICIENTS WITH RESPECT TO RATE CONSTANT k_1 AT t = 20 s FOR TEST PROBLEM 4

Species	Normalized sensitivities with respect to k_1 at t = 20 s				
	BFM	LSENS	CHEMDDM	DDM[a]	GFM/AIM[a]
C_2H_6	–0.819	–0.819	–0.819	–0.820	–0.824
CH_3	1.000	1.000	1.000	1.000	0.692
C_2H_5	–0.210	–0.210	–0.210	–0.210	–0.266
CH_4	0.644	0.644	0.644	0.643	0.652
C_2H_4	0.324	0.324	0.324	0.323	0.325
H	0.0905	0.0905	0.0905	0.090	0.080
H_2	0.221	0.221	0.221	0.221	0.220

[a]From reference 21.

improvement in the accuracy of the GFM/AIM results with error tolerance reduction and the dependence of the solutions on the number of output stations have been attributed to difficulties in computing the Green's function (ref. 21).

For the two output stations, t = 1 and 20 s, LSENS required 86 steps, 112 derivative evaluations, and 20 Jacobian matrix evaluations and LU-decompositions to complete the problem, whereas CHEMDDM required 140 steps, 193 derivative evaluations, and 28 Jacobian matrix evaluations and LU-decompositions. To solve for the composition and sensitivity coefficients of all seven species with respect to all seven initial species mole numbers and all five rate constants, LSENS required approximately 0.22 s of CPU time, whereas CHEMDDM required approximately 0.51 s. For four output stations between 0 and 20 s Dunker (ref. 21) obtained execution times of 1.25 and 1.55 s, respectively, for the DDM and the GFM/AIM on an IBM 370 computer. On the NASA Lewis Research Center's IBM 370/3033 computer CHEMDDM and a previous version of LSENS required approximately

1.4 and 0.6 s, respectively. These observations indicate that LSENS was significantly more efficient than both CHEMDDM and the GFM/AIM. In particular, these execution times and the CPU times given by Kramer et al. (ref. 91) for the DM, GFM, and GFM/AIM (see above) show that LSENS was faster than CHEMDDM, GFM/AIM, GFM, and DM by factors of approximately 2.3, 3, 127, and 20, respectively.

This test problem was also studied by Leis and Kramer (ref. 100) with their code ODESSA (ref. 101), which uses the DDM, but implemented differently than in CHEMDDM and LSENS. In particular, the estimated local truncation errors in the sensitivity coefficients are controlled by requiring that they satisfy an inequality similar to equation (3.37) for the model problem:

$$\sqrt{\frac{1}{N}\sum_{i=1}^{N}\left(\frac{D_{ij,n}}{\mathrm{EWT}_{ij,n}}\right)^2} \leq 1, \qquad j = 1,\ldots,M \tag{4.79}$$

Here $D_{ij,n}$ is the estimated local truncation error in $S_{ij}(t_n)$ and

$$\mathrm{EWT}_{ij,n} = \mathrm{RTOL}\left(S_{ij}\right)\left|S_{ij}\left(t_{n-1}\right)\right| + \mathrm{ATOL}\left(S_{ij}\right) \tag{4.80}$$

where $\mathrm{RTOL}(S_{ij})$ and $\mathrm{ATOL}(S_{ij})$ are, respectively, the local relative and absolute error tolerances for S_{ij}. For the BDF method of order q, $D_{ij,n}$ is given by (see eqs. (3.37) and (4.79) and ref. 15)

$$D_{ij,n} = \frac{E_{ij,n}}{\tau(q)} \tag{4.81}$$

where $E_{ij,n}$ and $\tau(q)$, the local error test coefficient for the method of order q, are defined by equations (4.24) and (3.38), respectively.

Therefore in ODESSA the inequalities given by equations (3.37) and (4.79) are satisfied at every step $[t_{n-1},t_n]$. Leis and Kramer (ref. 100) refer to this implementation as "the mutually dependent error control strategy." If equation (4.79) is satisfied, the $\{\underline{S}_{j,n}\}$ are considered to be sufficiently accurate and the integration is continued. However, if the error test fails for any parameter, both $\{\underline{S}_{j,n}\}$ and $\underline{Y}_n$ are rejected. The step size and/or the method order is then reduced and the calculation sequence, that is, advance $\underline{Y}$ and then the $\{\underline{S}_j\}$ over the step $[t_{n-1},t_n]$, is repeated.

CHEMDDM and LSENS do not attempt to control the local errors in the $\{\underline{S}_j\}$. The argument made is that the formula for $\underline{S}_j$, equation (4.9), can be obtained by directly differentiating that for $\underline{Y}$, equation (3.9), with respect to η_j. Therefore the sensitivities $\{\partial Y_i/\partial\eta_j\}$ are the exact sensitivities of $\{Y_i\}$ (but not necessarily those

of $\{y_i\}$) with respect to η_j. This implementation of the DDM is referred to as "fully-dependent error control" because the error in $\underline{S}_j$ depends on the error control of $\underline{Y}$ (ref. 100). Note that the accuracy of $\underline{Y}$ has a direct effect on the accuracy of the $\{\underline{S}_j\}$ because the ODE for $\underline{S}_j$ is a function of the Jacobian matrix and, for a rate coefficient parameter, of $\partial \underline{f}/\partial \eta_j$ (see eq. (4.8)).

Leis and Kramer (ref. 100) examined the differences between the two approaches by computing an average error, $\mathcal{E}(\underline{Y})$, in the kinetics solution. Here $\mathcal{E}(\underline{Y})$ is the average of the errors in the kinetics solutions at the two print stations $t = 1$ and 20 s. For given values of EMAX and ATOLSP they estimated $\mathcal{E}(\underline{Y})$ by using the relation

$$\mathcal{E}(\underline{Y}) = \left[\frac{1}{2\mathrm{NS}} \sum_{i=1}^{\mathrm{NS}} \left(\left| \frac{Y_i(t=1) - Y_i^*(t=1)}{Y_i^*(t=1)} \right| + \left| \frac{Y_i(t=20) - Y_i^*(t=20)}{Y_i^*(t=20)} \right| \right) \right] \times 100\% \tag{4.82}$$

In this equation the bars | | denote absolute value, and $\underline{Y}^*(t)$, the approximation to the exact solution at time t, was computed with the local error tolerances EMAX = 10^{-10} and ATOLSP = 10^{-12}. For both error control types Leis and Kramer (ref. 100) examined the variation of $\mathcal{E}(\underline{Y})$ with EMAX, using ATOLSP = 10^{-2}EMAX. Their results are reproduced in table 4.25. The errors with fully dependent error control were measured by performing kinetics-only calculations, that is, without sensitivity analysis. For the mutually dependent error control calculations sensitivity coefficients with respect to the $\{k_j\}$ were generated. The sensitivity coefficient error tolerances were set equal to the error tolerances used for the model problem, that is, RTOL(S_{ij}) = EMAX and ATOL(S_{ij}) = ATOLSP for all i and all j.

In order to compare the accuracy of LSENS and ODESSA, the above procedure (i.e., eq. (4.82)) was used to measure the average error incurred by LSENS with EMAX = 10^{-2} to 10^{-8} (ATOLSP = 10^{-2}EMAX). The rate coefficient parameter values given by Kramer et al. (ref. 91) (see table 4.13) were used for this study. The resulting average errors are given in table 4.25.

This table shows that LSENS was significantly more accurate than ODESSA, irrespective of the error control used by the latter. Indeed for EMAX $\leq 10^{-3}$ the average error incurred by LSENS was less than 1 percent. ODESSA, on the other hand, required EMAX $\leq 10^{-6}$ for the same accuracy. In addition, LSENS showed monotonically decreasing error as EMAX was reduced. In contrast, for the kinetics-only calculation ODESSA displayed significant nonmonotonicity in the $\mathcal{E}(\underline{Y})$-versus-EMAX variation. This difference is surprising inasmuch as for a kinetics-only problem both codes use the same solver (LSODE; refs. 13 to 15) and error control.

The effects of the local error tolerances on the accuracy of the sensitivity coefficients produced by LSENS were studied as follows: Average errors $\mathcal{E}(S_{ic})$ and $\mathcal{E}(S_{rp})$ for the initial mole number and preexponential factor sensitivities, respectively,

TABLE 4.25.—VARIATION OF AVERAGE ERROR IN KINETICS SOLUTION WITH LOCAL ERROR TOLERANCE FOR TEST PROBLEM 4

Local relative error tolerance, EMAX[a]	Average error in species mole numbers, $\mathcal{E}(Y)$, percent[b]		
	ODESSA[c,d]	ODESSA[c,e]	LSENS
10^{-2}	(f)	(f)	4.39
10^{-3}	405.6	154.5	0.391
10^{-4}	1112.8	122.6	5.40×10^{-2}
10^{-5}	155.4	9.5	1.23×10^{-2}
10^{-6}	0.5	0.1	6.10×10^{-4}
10^{-7}	223.4	< 0.1	1.85×10^{-4}
10^{-8}	0.1	< 0.1	2.79×10^{-5}

[a]ATOLSP = 10^{-2}EMAX.
[b]See equation (4.82).
[c]From reference 100.
[d]Independent kinetic solution. The results will be the same as with fully dependent error control.
[e]Mutually dependent error control. Sensitivity analysis performed with respect to the $\{k_j\}$ with all RTOL_{ij} = EMAX and all ATOL_{ij} = ATOLSP.
[f]Not given.

defined by

$$\mathcal{E}\left(S_{ic} \text{ or } S_{rp}\right)=\left[\frac{1}{2\left(M_{ic} \text{ or } M_{rp}\right)}\sum_{j=1}^{M_{ic} \text{ or } M_{rp}}\left(\frac{1}{\mathrm{NS}_{j,1}}\sum_{i=1}^{\mathrm{NS}_{j,1}}\left|\frac{S_{ij}(t=1)-S^{*}_{ij}(t=1)}{S^{*}_{ij}(t=1)}\right|\right.\right.$$

$$\left.\left.+\frac{1}{\mathrm{NS}_{j,20}}\sum_{i=1}^{\mathrm{NS}_{j,20}}\left|\frac{S_{ij}(t=20)-S^{*}_{ij}(t=20)}{S^{*}_{ij}(t=20)}\right|\right)\right]\times 100\% \qquad (4.83)$$

were generated with the same tolerances used for the kinetics-only calculations. In equation (4.83) M_{ic} (= 7) and M_{rp} (= 5) are the total number of initial concentrations and preexponential factors, respectively; $S^{*}_{ij}(t)$ is the approximation to the exact sensitivity coefficient, $(\partial y_i/\partial \eta_j)$, at time t; and $\mathrm{NS}_{j,1}$ and $\mathrm{NS}_{j,20}$ are the total number of species with $|\langle S^{*}_{ij}\rangle| \geq 10^{-6}$ at t = 1 and 20 s, respectively. As with the kinetics-only computations the $\{S^{*}_{ij}(t)\}$ were generated with EMAX = 10^{-10} and ATOLSP = 10^{-12}. In order to avoid both division by zero (e.g., all S_{ij} $(i \neq j)$ are zero for $\sigma_{CH_4,0}$, $\sigma_{C_2H_4,0}$, and $\sigma_{H_2,0}$) and measuring errors in sensitivities with very small magnitude, each summation in equation (4.83) excluded any species with $|\langle S^{*}_{ij}\rangle| < 10^{-6}$; the average at that print station was taken over only species with

$|\langle S^*_{ij}\rangle| \geq 10^{-6}$. In addition to the $(\partial\sigma_i/\partial\sigma_{j,0})$ $(i \neq j, j = CH_4, C_2H_4, \text{and } H_2)$ at both print stations, the sensitivities of σ_{CH_3} with respect to A_3 at 1 s and with respect to all $\sigma_{j,0}$, A_3, A_4, and A_5 at 20 s were not included in the summations.

Table 4.26 presents the variations of the average errors for the two parameter types. Also given is the average error, $\mathcal{E}(\partial\underline{Y}/\partial A_1)$, in the sensitivity coefficients with respect to A_1. The error $\mathcal{E}(\partial\underline{Y}/\partial A_1)$ was included because Leis and Kramer (ref. 100) observed that during the joint calculations of kinetics and sensitivity with respect to rate constants the local sensitivity error test failures were always caused by k_1. Table 4.26 shows that all errors displayed monotonic decreases with EMAX. Also the average error for A_1 was always less than the average error for all preexponential factors, indicating that the coefficients with respect to A_1 were not the least accurate. Furthermore, examination of the $\{\mathcal{E}(\partial\underline{Y}/\partial A_j)\}$ showed that $\mathcal{E}(\partial\underline{Y}/\partial A_1)$ was less than all other $\mathcal{E}(\partial\underline{Y}/\partial A_j)$ for all EMAX. These observations suggest that the local error estimate for $\{S_{ij}\}$ was not reliable, in that it was not a good measure of the global, or actual, error, which is the quantity that is usually of interest. Finally table 4.26 shows that average errors < 5 percent can be achieved with EMAX $\leq 10^{-5}$. For EMAX $\leq 10^{-4}$ the rate coefficient parameter sensitivities were significantly more accurate than the initial condition results. Thus for this problem if very accurate solutions are required, the initial condition sensitivities will require a smaller EMAX and therefore more computational effort than the rate coefficient parameter sensitivities. Leis and Kramer (ref. 100) reached the same conclusion.

The variation of the average sensitivity errors with EMAX is not given in reference 100, and so detailed comparisons of LSENS with ODESSA were not possible. However, the average errors, $\mathcal{E}(\partial\underline{Y}/\partial k_1)$, in the sensitivity coefficients with respect to k_1 are given for several combinations of the local error tolerances. Their results, including computational work requirements, are reproduced in

TABLE 4.26.—EFFECTS OF LOCAL ERROR TOLERANCE ON AVERAGE ERRORS IN SENSITIVITY COEFFICIENTS PRODUCED BY LSENS FOR TEST PROBLEM 4

Local relative error tolerance, EMAX[a]	Average error in initial condition sensitivities, $\mathcal{E}(S_{ic})$, percent[b]	Average error in sensitivities with respect to A_1, $\mathcal{E}(\partial\underline{Y}/\partial A_1)$, percent[c]	Average error in preexponential factor sensitivities, $\mathcal{E}(S_{rp})$, percent[b]
10^{-2}	72.8	3.42	131.9
10^{-3}	39.6	1.69	63.3
10^{-4}	14.4	0.136	8.41
10^{-5}	4.89	2.32×10^{-2}	2.26
10^{-6}	1.47	2.59×10^{-3}	0.309
10^{-7}	0.264	1.11×10^{-3}	8.07×10^{-2}
10^{-8}	2.26×10^{-2}	6.26×10^{-5}	3.51×10^{-3}

[a]ATOLSP = 10^{-2}EMAX.
[b]See equation (4.83).
[c]See text.

table 4.27. Here RTOL($\partial \underline{Y}/\partial k_j$) and ATOL($\partial \underline{Y}/\partial k_j$) are the local relative and absolute error tolerances, respectively, for the sensitivity coefficients of all variables with respect to k_j. Comparing table 4.27 with tables 4.25 and 4.26 shows that for the same value of EMAX LSENS produced more accurate $\underline{Y}$ and $\partial \underline{Y}/\partial A_1$ than ODESSA, irrespective of the local error tolerances used in the latter code for the sensitivity coefficients.

The computational work required for the interval [0,20] s is given in table 4.28. For kinetics-only calculations ODESSA consistently required fewer steps than LSENS and, except for EMAX = 10^{-4}, either comparable or smaller execution times when differences between the two computing systems were factored in. When sensitivity analysis was included, the number of integration steps used by ODESSA increased quite dramatically, and LSENS was significantly faster for all EMAX. In general, it was twice as fast; for EMAX = 10^{-4}, however, the CPU time for ODESSA was more than five times that for LSENS. For the rate constant sensitivity runs with EMAX = 10^{-6} and RTOL($\partial \underline{Y}/\partial k_1$) = 10^{-5} and with EMAX = 10^{-8} and RTOL($\partial \underline{Y}/\partial k_1$) = 10^{-6}, ODESSA required 5.37 and 8.83 s, respectively, on the VAX 11/750 computer (table 4.27). These times compare favorably with the computational cost of LSENS with EMAX = 10^{-6} and 10^{-8}. For the initial condition sensitivities ODESSA required 88 steps and 14.81 s of CPU time to produce solutions with errors $\leq$ 1 percent in $\{S_{ij}\}$ with magnitude greater than 10^{-6}; when only $\{S_{ij}\}$ with absolute value greater than 10^{-3} were considered, the computational work requirement for the same accuracy was 75 steps and 12.70 s of CPU time (ref. 100). Examination of the results given for EMAX = 10^{-7} in tables 4.26 and 4.28 shows that both execution times were considerably larger than that required by LSENS for comparable accuracy. Leis and Kramer (ref. 100) also state that with

TABLE 4.27.—EFFECTS OF LOCAL ERROR TOLERANCE ON AVERAGE ERRORS IN KINETICS SOLUTION AND SENSITIVITY COEFFICIENTS WITH RESPECT TO RATE CONSTANT k_1 PRODUCED BY ODESSA AND COMPUTATIONAL WORK REQUIREMENT FOR TEST PROBLEM 4[a]

Local relative error tolerance for model problem, EMAX[b]	Local relative error tolerance for sensitivities with respect to k_1, RTOL($\partial \underline{Y}/\partial k_1$)[c]	Average error in kinetic solution, $\mathcal{E}(\underline{Y})$, percent[d]	Average error in sensitivities with respect to k_1, $\mathcal{E}(\partial \underline{Y}/\partial k_1)$, percent[e]	Computational work requirement	
				NSTEP	CPU,[f] s
10^{-8}	10^{-8}	< 0.1	< 0.1	90	16.47
10^{-8}	10^{-6}	0.1	0.1	51	8.83
10^{-6}	10^{-6}	0.1	0.1	44	7.66
10^{-6}	10^{-5}	0.2	0.3	30	5.37

[a]From reference 100: results from joint solution of composition and sensitivities with respect to rate constants.
[b]ATOLSP = 10^{-2} EMAX.
[c]RTOL($\partial \underline{Y}/\partial k_j$) = EMAX, j = 2,...,5; ATOL($\partial \underline{Y}/\partial k_j$) = 10^{-2} RTOL($\partial \underline{Y}/\partial k_j$), j = 1,...,5.
[d]See equation (4.82).
[e]See text.
[f]On a VAX 11/750 computer.

TABLE 4.28.—VARIATION OF COMPUTATIONAL WORK WITH LOCAL ERROR TOLERANCE FOR TEST PROBLEM 4

Local relative error tolerance, EMAX[a]	Computational work requirements									
	LSENS						ODESSA[e,f]		ODESSA[e,i]	
	NSTEP	NFE[b]	NJE[b]	CPU, s[c]			NSTEP	CPU for concentrations alone, s[g]	NSTEP	CPU for rate constant sensitivities, s[d,g]
				For concentrations alone	For initial condition sensitivities[d]	For preexponential factor sensitivities[d]				
10^{-2}	17	27	9	0.010	0.031	0.029	(h)	(h)	(h)	(h)
10^{-3}	22	35	11	0.012	0.041	0.037	5	0.26	20	3.33
10^{-4}	50	75	18	0.026	0.090	0.083	25	1.47	102	17.51
10^{-5}	58	82	13	0.028	0.10	0.095	16	0.72	57	10.10
10^{-6}	86	112	20	0.040	0.16	0.14	15	0.65	44	7.66
10^{-7}	135	179	23	0.060	0.24	0.22	19	0.87	63	11.14
10^{-8}	178	233	25	0.077	0.33	0.30	51	2.02	90	16.47

[a]ATOLSP = 10^{-2}EMAX.
[b]Sensitivity analysis calculations require additional NSTEP derivative evaluations and NSTEP Jacobian matrix evaluations.
[c]On an Amdahl 5870 computer using the UTS operating system.
[d]Includes execution time for concentrations.
[e]From reference 100.
[f]For kinetics-only calculation.
[g]On a VAX 11/750 computer.
[h]Not given.
[i]For joint solution of concentrations and sensitivities with respect to rate constants; RTOL($\underline{S}_j$) = EMAX, ATOL($\underline{S}_j$) = ATOLSP.

fully dependent error control the initial condition sensitivity calculation with EMAX = 10^{-6} and ATOLSP = 10^{-8} required 2.60 s of CPU time and that the average error in the normalized sensitivity coefficients with respect to $\sigma_{C_2H_6,0}$ (i.e., $\mathcal{E}(\langle \partial \underline{Y}/\partial \sigma_{C_2H_6,0} \rangle)$) was 1.8 percent. Tables 4.26 and 4.28 would seem to indicate that for this run ODESSA compared favorably with LSENS in terms of both accuracy and computational cost. However, the LSENS results showed that for this EMAX, $\mathcal{E}(\langle \partial \underline{Y}/\partial \sigma_{C_2H_6,0} \rangle) = 0.044$ percent. In fact, even for EMAX = 10^{-5}, $\mathcal{E}(\langle \partial \underline{Y}/\partial \sigma_{C_2H_6,0} \rangle)$ (= 0.082 percent) was less than 1 percent. Thus LSENS was more accurate than ODESSA.

In order to examine if the differences in the results produced by the two codes were due to the different computers used, the runs with LSENS were repeated on the NASA Lewis Research Center's VAX 6320 computer. Essentially the same results were obtained for the average errors and for NSTEP, NFE, and NJE, thus eliminating this possibility.

The effects of ATOLSP on solution accuracy were studied by generating average errors with LSENS, using ATOLSP = 10^{-9}EMAX, which value ensures relative error control for species with mole fraction ≥ 0.1 ppm. For this study $\underline{Y}^*$ and $\{\underline{S}_j^*\}$ were computed with EMAX = 10^{-10} and ATOLSP = 10^{-19}. The results for EMAX = 10^{-2} to 10^{-8} are given in table 4.29; again errors were measured for only $|\langle S_{ij}^* \rangle| \geq 10^{-6}$. Comparing this table with tables 4.25 and 4.26 shows the significant accuracy improvements produced by decreasing ATOLSP. In particular, all average errors in the ATOLSP = 10^{-9}EMAX results were less than 1 percent for EMAX $\leq 10^{-3}$. In contrast, EMAX had to be reduced to 10^{-7} to achieve the same accuracy in the ATOLSP = 10^{-2}EMAX solutions. These observations give credibility to the arguments that accuracy improvements in $\underline{Y}$ lead to more accurate $\{S_{ij}\}$ and that ATOLSP must be selected with care. For the local tolerances

TABLE 4.29.—EFFECTS OF LOCAL ERROR TOLERANCE (WITH ATOLSP = 10^{-9} EMAX) ON AVERAGE ERRORS FOR TEST PROBLEM 4

Local relative error tolerance, EMAX[a]	Average error in species mole numbers, $\mathcal{E}(\underline{Y})$, percent[b]	Average error in initial condition sensitivities, $\mathcal{E}(S_{ic})$, percent[c]	Average error in preexponential factor sensitivities, $\mathcal{E}(S_{rp})$, percent[c]
10^{-2}	8.76×10^{-2}	8.57	20.4
10^{-3}	3.58×10^{-2}	0.302	0.569
10^{-4}	2.52×10^{-3}	3.81×10^{-2}	6.22×10^{-2}
10^{-5}	4.02×10^{-4}	2.07×10^{-2}	3.14×10^{-2}
10^{-6}	5.88×10^{-5}	1.53×10^{-3}	1.62×10^{-3}
10^{-7}	9.57×10^{-6}	3.28×10^{-4}	2.93×10^{-4}
10^{-8}	5.87×10^{-7}	4.10×10^{-5}	1.15×10^{-4}

[a]ATOLSP = 10^{-9}EMAX.
[b]See equation (4.82).
[c]See equation (4.83).

EMAX = 10^{-3} and ATOLSP = 10^{-12}, LSENS required 83 steps, 101 derivative evaluations, 18 Jacobian matrix evaluations, and 0.040 s of CPU time to solve for the composition. The CPU times for the composition and initial condition sensitivities and for the composition and preexponential factor sensitivities were 0.15 and 0.14 s, respectively. All execution times were significantly less than those with EMAX = 10^{-7} and ATOLSP = 10^{-9} (table 4.28). Thus judicious selection of ATOLSP is indicated.

The average errors in tables 4.26 and 4.29 were measured by using solutions produced by LSENS. Because such a comparison is not adequate proof of accuracy, BFM results were generated. These calculations were attempted with EMAX = 10^{-12} and ATOLSP = 10^{-21}. Even with such small values for the local error tolerances $\delta_{c3}(\eta_j)$ could not be identified for $\sigma_{CH_3,0}$, $\sigma_{C_2H_5,0}$, $\sigma_{H,0}$, and A_3; convergence difficulties were caused by the species C_2H_6, CH_3, C_2H_5, and H. BFM solutions were therefore attempted with progressively smaller tolerances, keeping ATOLSP = 10^{-9}EMAX. The EMAX values necessary for convergence of the results to three significant figures were 10^{-13}, 10^{-15}, 10^{-16}, and 10^{-14}, respectively, for $\sigma_{CH_3,0}$, $\sigma_{C_2H_5,0}$, $\sigma_{H,0}$, and A_3. This finding further illustrates the difficulty of using the BFM to compute sensitivity coefficients.

The BFM could not produce reliable sensitivity coefficients for several parameters. In particular, the $\{\partial\sigma_i/\partial\sigma_{j,0}\}$ ($i \neq j$, j = CH_4, C_2H_4, and H_2) could not be obtained at either print station. Now the three species do not appear as reactants in the reaction mechanism (see table 4.13). Because all reactions are irreversible, the reaction rates and hence net species production rates are independent of the concentrations of CH_4, C_2H_4, and H_2. Therefore the ODE's for the sensitivity coefficients with respect to the initial concentrations of these three species are given by $d\underline{S}_j/dt = 0$ for all t (see eq. (4.8)). Hence for all t the $\{\partial\sigma_i/\partial\sigma_{j,0}\}$ (j = CH_4, C_2H_4, and H_2) must be equal to their initial values (= 0.0 for $i \neq j$ and 1.0 for $i=j$). Now, the BFM produces initial concentration sensitivities by perturbing the $\{\sigma_{j,0}\}$. However, perturbation of the initial mole numbers of CH_4, C_2H_4, and H_2 should affect neither the reaction rates nor the Jacobian matrix. Nonetheless for reasons that are not clear the BFM could not reproduce $S_{ij} = 0.0$ for initial condition values. The magnitudes of the $\{\langle S_{ij}\rangle\}$ were usually small, but $\langle S_{ij}\rangle$ of order 10^{-4} were sometimes produced. Thus $|\langle S_{ij}\rangle|$ less than 10^{-3} may be considered insignificant.

The BFM could not also produce reliable sensitivity coefficients of σ_{CH_3} with respect to $\sigma_{C_2H_6,0}$, $\sigma_{CH_3,0}$, $\sigma_{C_2H_5,0}$, $\sigma_{H,0}$, A_3, A_4, and A_5 at $t = 20$ s. In order to check if the difficulties were caused by essentially zero values, solutions were generated with LSENS on the Cray-XM/P computer using EMAX = 10^{-12}, ATOLSP = 10^{-21}, and double-precision arithmetic. At $t = 20$ s the normalized sensitivity coefficients of σ_{CH_3} with respect to $\sigma_{C_2H_6,0}$, $\sigma_{CH_3,0}$, $\sigma_{C_2H_5,0}$, $\sigma_{H,0}$, and A_3 to A_5 were equal to 2.8×10^{-30}, -6.5×10^{-34}, -2.6×10^{-33}, -2.8×10^{-33}, -8.2×10^{-35}, -1.4×10^{-30}, and 7.2×10^{-31}, respectively. Thus these sensitivities are unimportant and need not be considered in judging accuracy.

The BFM results are given in tables 4.30 to 4.33, along with the solutions computed by LSENS with EMAX = 10^{-4} and ATOLSP = 10^{-13}. The agreement between LSENS and BFM was excellent for all parameters at both print stations.

TABLE 4.30.—SENSITIVITY COEFFICIENTS WITH RESPECT TO INITIAL CONDITION VALUES AT t = 1 s FOR TEST PROBLEM 4

Species	Sensitivity coefficients at t = 1 s with respect to[a]						
	$\sigma_{C_2H_6,0}$	$\sigma_{CH_3,0}$	$\sigma_{C_2H_5,0}$	$\sigma_{CH_4,0}$	$\sigma_{C_2H_4,0}$	$\sigma_{H,0}$	$\sigma_{H_2,0}$
C_2H_6	9.25(–1)	–2.17	–8.53	(b)	(b)	–9.26	(b)
	9.25(–1)	–2.17	–8.53	0.00	0.00	–9.26	0.00
CH_3	2.22(–5)	9.65(–4)	–2.04(–4)	(b)	(b)	–2.21(–4)	(b)
	2.23(–5)	9.86(–4)	–2.04(–4)	0.00	0.00	–2.22(–4)	0.00
C_2H_5	3.96(–5)	–8.55(–5)	–3.65(–4)	(b)	(b)	–3.96(–4)	(b)
	3.96(–5)	–8.53(–5)	–3.65(–4)	0.00	0.00	–3.96(–4)	0.00
CH_4	2.20(–2)	9.54(–1)	–2.02(–1)	1.00	(b)	–2.19(–1)	(b)
	2.20(–2)	9.54(–1)	–2.02(–1)	1.00	0.00	–2.19(–1)	0.00
C_2H_4	6.37(–2)	2.19	9.63	(b)	1.00	9.37	(b)
	6.37(–2)	2.19	9.64	0.00	1.00	9.37	0.00
H	2.51(–6)	–5.07(–6)	–2.32(–5)	(b)	(b)	–2.51(–5)	(b)
	2.51(–6)	–5.05(–6)	–2.32(–5)	0.00	0.00	–2.51(–5)	0.00
H_2	5.27(–2)	1.71	9.23	(b)	(b)	9.98	1.00
	5.27(–2)	1.71	9.24	0.00	0.00	9.98	1.00

[a]For each species the top row lists BFM results and the bottom row, LSENS results. Numbers in parentheses are powers of 10.

[b]See text.

TABLE 4.31.—SENSITIVITY COEFFICIENTS WITH RESPECT TO PREEXPONENTIAL FACTORS AT t = 1 s FOR TEST PROBLEM 4

Species	Sensitivity coefficients at t = 1 s with respect to[a]				
	A_1	A_2	A_3	A_4	A_5
C_2H_6	–1.16(–15)	–2.27(–13)	–5.31(–18)	–6.50(–15)	6.04(–18)
	–1.16(–15)	–2.27(–13)	–5.32(–18)	–6.50(–15)	6.04(–18)
CH_3	8.92(–17)	–1.33(–13)	–1.21(–22)	–7.13(–20)	6.62(–23)
	8.92(–17)	–1.33(–13)	–1.21(–22)	–7.18(–20)	6.67(–23)
C_2H_5	5.75(–19)	–3.13(–18)	–3.48(–18)	4.24(–18)	–3.94(–21)
	5.75(–19)	–3.12(–18)	–3.48(–18)	4.24(–18)	–3.94(–21)
CH_4	5.14(–16)	1.29(–13)	–1.20(–19)	–7.04(–17)	6.55(–20)
	5.14(–16)	1.29(–13)	–1.20(–19)	–7.04(–17)	6.55(–20)
C_2H_4	8.56(–16)	2.29(–13)	8.85(–18)	6.53(–15)	–6.07(–18)
	8.56(–16)	2.29(–13)	8.85(–18)	6.53(–15)	–6.07(–18)
H	6.74(–20)	1.27(–19)	–4.59(–23)	–1.75(–20)	–1.19(–21)
	6.74(–20)	1.28(–19)	–4.59(–23)	–1.75(–20)	–1.19(–21)
H_2	5.99(–16)	1.65(–13)	7.17(–18)	6.57(–15)	–6.11(–18)
	5.99(–16)	1.65(–13)	7.17(–18)	6.57(–15)	–6.11(–18)

[a]For each species the top row lists BFM results and the bottom row, LSENS results. Numbers in parentheses are powers of 10.

TABLE 4.32.—SENSITIVITY COEFFICIENTS WITH RESPECT TO INITIAL CONDITION VALUES AT t = 20 s FOR TEST PROBLEM 4

Species	Sensitivity coefficients at t = 20 s with respect to[a]						
	$\sigma_{C_2H_6,0}$	$\sigma_{CH_3,0}$	$\sigma_{C_2H_5,0}$	$\sigma_{CH_4,0}$	$\sigma_{C_2H_4,0}$	$\sigma_{H,0}$	$\sigma_{H_2,0}$
C_2H_6	2.54(−1)	−5.96(−1)	−2.34	(b)	(b)	−2.54	(b)
	2.54(−1)	−5.95(−1)	−2.34	0.00	0.00	−2.54	0.00
CH_3	(b)	(b)	(b)	(b)	(b)	(b)	(b)
	6.89(−9)	−2.50(−7)	−6.38(−8)	0.00	0.00	−6.92(−8)	0.00
C_2H_5	7.86(−6)	−1.84(−5)	−7.25(−5)	(b)	(b)	−7.86(−5)	(b)
	7.86(−6)	−1.84(−5)	−7.25(−5)	0.00	0.00	−7.87(−5)	0.00
CH_4	2.41(−1)	4.42(−1)	−2.22	1.00	(b)	−2.41	(b)
	2.41(−1)	4.41(−1)	−2.22	1.00	0.00	−2.41	0.00
C_2H_4	6.25(−1)	8.75(−1)	4.45	(b)	1.00	3.75	(b)
	6.25(−1)	8.75(−1)	4.46	0.00	1.00	3.75	0.00
H	1.18(−6)	−2.75(−6)	−1.08(−5)	(b)	(b)	−1.18(−5)	(b)
	1.18(−6)	−2.75(−6)	−1.08(−5)	0.00	0.00	−1.18(−5)	0.00
H_2	5.05(−1)	6.54(−1)	5.06	(b)	(b)	5.45	1.00
	5.05(−1)	6.54(−1)	5.07	0.00	0.00	5.45	1.00

[a]For each species the top row lists BFM results and the bottom row, LSENS results. Numbers in parentheses are powers of 10.
[b]See text.

TABLE 4.33.—SENSITIVITY COEFFICIENTS WITH RESPECT TO PREEXPONENTIAL FACTORS AT t = 20 s FOR TEST PROBLEM 4

Species	Sensitivity coefficients at t = 20 s with respect to[a]				
	A_1	A_2	A_3	A_4	A_5
C_2H_6	−7.29(−15)	−6.28(−14)	−8.34(−19)	−3.34(−14)	3.11(−17)
	−7.29(−15)	−6.28(−14)	−8.34(−19)	−3.34(−14)	3.11(−17)
CH_3	8.93(−17)	−1.34(−13)	(b)	(b)	(b)
	8.93(−17)	−1.34(−13)	−9.32(−27)	−1.74(−21)	1.62(−24)
C_2H_5	−4.75(−20)	−1.94(−18)	−9.06(−19)	−1.36(−19)	1.27(−22)
	−4.76(−20)	−1.95(−18)	−9.06(−19)	−1.36(−19)	1.27(−22)
CH_4	4.72(−15)	7.57(−14)	−1.13(−18)	−1.31(−14)	1.22(−17)
	4.72(−15)	7.57(−14)	−1.13(−18)	−1.31(−14)	1.22(−17)
C_2H_4	4.89(−15)	9.19(−14)	2.30(−18)	3.99(−14)	−3.71(−17)
	4.89(−15)	9.19(−14)	2.30(−18)	4.00(−14)	−3.72(−17)
H	7.42(−21)	−2.91(−19)	−1.53(−23)	−1.54(−19)	−5.62(−22)
	7.41(−21)	−2.91(−19)	−1.53(−23)	−1.55(−19)	−5.62(−22)
H_2	2.53(−15)	5.40(−14)	2.41(−18)	4.65(−14)	−4.32(−17)
	2.53(−15)	5.40(−14)	2.41(−18)	4.65(−14)	−4.32(−17)

[a]For each species the top row lists BFM results and the bottom row, LSENS results. Numbers in parentheses are powers of 10.
[b]See text.

In addition, for $\sigma_{CH_4,0}$, $\sigma_{C_2H_4,0}$, and $\sigma_{H_2,0}$ LSENS reproduced the exact sensitivity coefficients (= 0.0 or 1.0, as discussed previously), illustrating the accuracy of the DDM. At $t = 20$ s the normalized sensitivity coefficients of σ_{CH_3} with respect to $\sigma_{C_2H_6,0}$, $\sigma_{CH_3,0}$, $\sigma_{C_2H_5,0}$, $\sigma_{H,0}$, and A_3 to A_5 were equal to 2.1×10^{-6}, -7.7×10^{-9}, -2.0×10^{-9}, -2.1×10^{-9}, -2.6×10^{-11}, -2.1×10^{-6}, and 1.1×10^{-6}. Not surprisingly the magnitudes of these quantities were larger than the values obtained on the Cray-XM/P computer. These results suggest that normalized sensitivity coefficients with absolute values less than, say, 10^{-5}, may be ignored. That is, if $|\langle S_{ij}(t)\rangle|$ is less than 10^{-5}, η_j has essentially no effect on y_i at time t.

Comparing the magnitudes of the normalized sensitivities with the results in tables 4.30 to 4.33 shows the importance of normalizing the sensitivity coefficients. For example, table 4.30 gives $\partial\sigma_{C_2H_5}/\partial\sigma_{C_2H_6,0} = 4.0\times10^{-5}$ and $\partial\sigma_{CH_4}/\partial\sigma_{C_2H_6,0} = 2.2\times10^{-2}$ at $t = 1$ s, indicating that $\sigma_{C_2H_6,0}$ has a much larger effect on σ_{CH_4} than on $\sigma_{C_2H_5}$ at this time. However, the normalized sensitivity coefficients of $\sigma_{C_2H_5}$ and σ_{CH_4} with respect to $\sigma_{C_2H_6,0}$ were 1.3 and 1.2, respectively. Thus a given change in $\sigma_{C_2H_6,0}$ will produce about the same percent change in the two species at 1 s. Because normalized sensitivity coefficients are more meaningful than the unnormalized quantities, if species are to be excluded from the summations in equation (4.83) to avoid measuring errors in unimportant sensitivities, the test for exclusion should be based on the magnitude of the $\langle S^*_{ij}\rangle$ and not that of S^*_{ij}. For example, if errors in initial condition sensitivities were not measured for species with $|S^*_{ij}| < 10^{-3}$, several species that would show significant changes due to a perturbation in $\sigma_{j,0}$ would be excluded from equation (4.83) (e.g., $\sigma_{C_2H_5}$ from the error calculation for the $\sigma_{C_2H_6,0}$ results—see above.)

In order to understand why LSENS, which uses indirect error control for the sensitivity coefficients, produced more accurate solutions than ODESSA using direct error control, the following study was made with LSENS. For each parameter η_j the quantity $\varepsilon(\eta_j)$ was computed, where $\varepsilon(\eta_j)$ is defined as

$$\varepsilon(\eta_j) = \frac{1}{\text{NSTEP}} \sum_{i=1}^{\text{NSTEP}} \sqrt{\frac{1}{\text{NS}} \sum_{i=1}^{\text{NS}} \left(\Delta_{ij,n}\right)^2} \tag{4.84}$$

and

$$\Delta_{ij,n} = \frac{D_{ij,n}}{\text{RTOL}\left(\underline{S}_j\right)\left|S_{ij,n}\right| + \text{ATOL}\left(\underline{S}_j\right)} \tag{4.85}$$

In equation (4.85) RTOL($\underline{S}_j$) and ATOL($\underline{S}_j$) are, respectively, the local relative and absolute error tolerances for the sensitivity coefficients of all species with respect to η_j. The quantity $\varepsilon(\eta_j)$ is the average root-mean-square (rms) norm of the weighted local truncation errors in the sensitivity coefficients with respect to η_j for the complete problem. All results discussed herein were obtained with scalar RTOL($\underline{S}_j$)

(= RTOL) and ATOL(S_j) (= ATOL). For all runs RTOL was set equal to EMAX and, unless otherwise stated, ATOL was equal to ATOLSP.

For the initial conditions $\sigma_{CH_4,0}$, $\sigma_{C_2H_4,0}$, and $\sigma_{H_2,0}$ the $\{\varepsilon(\eta_j)\}$ were equal to zero for all EMAX and both ATOLSP (10^{-2}EMAX and 10^{-9}EMAX). The reason is that all sensitivity coefficients with respect to these parameters are constant, as discussed previously. Discussion will therefore be restricted to the other initial mole numbers, for all of which $\varepsilon(\sigma_{j,0})$ was greater than 1 for all EMAX and both ATOLSP. Now a necessary (but not sufficient) condition for equation (4.79), the local error test for the sensitivity coefficients in ODESSA, to be satisfied on every step is

$$\varepsilon\left(\eta_j\right) \leq 1 \tag{4.86}$$

Therefore the sensitivity coefficients with respect to $\sigma_{C_2H_6,0}$, $\sigma_{CH_3,0}$, $\sigma_{C_2H_5,0}$, and $\sigma_{H,0}$ did not satisfy equation (4.79) at one or more steps.

In contrast to the $\{\varepsilon(\sigma_{j,0})\}$ all $\{\varepsilon(A_j)\}$ were much less than unity for all EMAX, with ATOLSP = 10^{-2}EMAX. Indeed,

$$\max_j \varepsilon\left(A_j\right) = 5.3 \times 10^{-10}$$

Now NSTEP ≤ 178 (see table 4.28), which implies that equation (4.79) was satisfied at all steps for all A_j. It was also observed that for all EMAX $\varepsilon(A_2) > \varepsilon(A_4) > \varepsilon(A_1) > \varepsilon(A_3)$ and $\varepsilon(A_5)$. The same two conclusions could be made for the runs with ATOLSP = 10^{-9}EMAX, for which

$$\max_j \varepsilon\left(A_j\right) = 4.5 \times 10^{-5}$$

and NSTEP ≤ 491. However, the $\{\varepsilon(A_j)\}$ were significantly greater than the values produced with ATOLSP = 10^{-2}EMAX. The same was true of the $\varepsilon(\sigma_{j,0})$ for almost all EMAX. Nevertheless ATOLSP = 10^{-9}EMAX produced significantly more accurate results than the larger ATOLSP, as observed earlier (see tables 4.25, 4.26, and 4.29). These observations indicate that the estimate for the local truncation error (which is proportional to the difference between the "corrected" and "predicted" values, see eqs. (4.81) and (4.24)) overestimated the true error. Therefore, equation (4.79) is not a reliable local error test.

To confirm that reducing ATOLSP does indeed improve accuracy, average global errors were measured for EMAX = 10^{-2} to 10^{-4} (ATOLSP = 10^{-9}EMAX) by comparing the results with the solution obtained with EMAX = 10^{-10} and ATOLSP = 10^{-12}. They were essentially the same as the values given in table 4.29.

Both conclusions regarding the $\{\varepsilon(A_j)\}$ contradict the findings of Leis and Kramer (ref. 100), who observed that the local sensitivity error test failed on several

steps. Also, as discussed previously, each such failure was caused by k_1; that is, $\varepsilon(k_1) > \varepsilon(k_j), j = 2,...,5$.

In order to examine if the differences in the local errors incurred by LSENS and ODESSA were caused by the different sensitivity parameters ($\{A_j\}$ and $\{k_j\}$, respectively) specified in the two calculations, the runs with LSENS were repeated with the rate constants (given in table 4.13) as sensitivity parameters. That is, each A_j was set equal to k_j and all n_j and E_j were set equal to zero. For both ATOLSP and all EMAX (including 10^{-10}), $\varepsilon(k_1)$ was greater than unity. It was also significantly greater than the other $\{\varepsilon(k_j)\}$, which were all less than unity. Thus for the rate constant sensitivities LSENS agreed with ODESSA. However, the average error $\mathcal{E}(S_{rp})$ displayed a monotonic decrease with EMAX. Also for most values of EMAX the average errors were essentially the same as those obtained with the original rate coefficient parameters. Finally, $\mathcal{E}(S_{rp})$ was less than 1 percent for EMAX $\leq 10^{-6}$ and 10^{-3}, respectively, for ATOLSP = 10^{-2}EMAX and 10^{-9}EMAX. Both EMAX values were exactly the same as for the original rate coefficient parameters (see tables 4.26 and 4.29).

Why the local errors increased with a reduction in ATOLSP and displayed significant differences when different rate constant parameters were used is now examined. Tables 4.30 to 4.33 show that the $\{S_{ij}\}$ displayed widely varying magnitudes. Hence pure relative error control, which is obtained by setting ATOL = 0.0, is appropriate. However, it is undefined if any $S_{ij} = 0.0$ (e.g., sensitivities with respect to certain initial conditions, see tables 4.30 and 4.32). Therefore the mixed relative/absolute error control given by equation (4.80) was used. The ATOL must, however, be selected such that the error control is mostly relative, for reasons given previously. Such error control is achieved if RTOL$|S_{ij}|$ >> ATOL for all $|S_{ij}|$ (greater than some minimum value to avoid incurring excessive computational cost in attempting to control errors in insignificant sensitivities).

Consider now the $\{A_j\}$. Tables 4.31 and 4.33 show that for all A_j and both ATOL, ATOL >> RTOL$|S_{ij}|$ for all i. (To obtain relative error control with ATOL=10^{-2}RTOL and 10^{-9}RTOL, $|S_{ij}|$ must be much greater than 10^{-2} and 10^{-9}, respectively.) Therefore $\Delta_{ij,n}$, equation (4.85), effectively reduces to

$$\Delta_{ij,n} \approx D_{ij,n}/\text{ATOL} \tag{4.87}$$

The average D_{ij} for the complete problem was only approximately two orders of magnitude smaller for ATOLSP = 10^{-9}EMAX than for ATOLSP=10^{-2}EMAX—hence the significant increase in $\varepsilon(A_j)$ when ATOL was reduced.

The rate constant sensitivities $\{\partial Y_i/\partial k_j\}$ are related to the $\{\partial Y_i/\partial A_j\}$ by (see eq. (4.49))

$$\frac{\partial Y_i}{\partial k_j} = \frac{A_j}{k_j}\frac{\partial Y_i}{\partial A_j} \tag{4.88}$$

Table 4.13 shows that $A_j >> k_j$ for $j = 1$ to 4 ($A_5 = k_5$). Nevertheless only the $\{|\partial Y_i/\partial k_1|\}$ were sufficiently large to satisfy the requirement for relative error control. This fact explains Leis and Kramer's (ref. 100) observation that the local error test failures were always caused by k_1. Now the local truncation errors for the $\{k_j\}$ must be equal to (A_j/k_j) times the local errors for the $\{A_j\}$. This relationship was confirmed by the results with EMAX = 10^{-4} and both ATOLSP. Hence, if the error control was indeed mostly absolute for k_j, $j = 2$ to 5, $\varepsilon(k_j)$ ($j \neq 1$) must be equal to $(A_j/k_j)\varepsilon(A_j)$. The estimated local errors for both ATOLSP satisfied this requirement. Therefore, if equation (4.81) did indeed give the true error, the $\{S_{ij}\}$ obtained by Leis and Kramer (ref. 100) (and those produced by LSENS) would not be accurate to EMAX significant figures. In fact, the errors in the $\{\underline{S}_j\}$ could then be guaranteed to be only less than ATOL for k_j, $j = 2$ to 5. For each of these k_j, ATOL > $|S_{ij}|$ for almost all i; so the local error may actually be greater than the sensitivity coefficient for several variables.

In contrast to the $\{A_j\}$ and $\{k_j\}$ the initial condition sensitivities with respect to $\sigma_{C_2H_6,0}$, $\sigma_{CH_3,0}$, $\sigma_{C_2H_5,0}$, and $\sigma_{H,0}$ were sufficiently large to ensure mostly relative error control, especially for ATOLSP = 10^{-9}EMAX (see tables 4.30 and 4.32)—hence the difficulties encountered by Leis and Kramer (ref. 100) in solving for the initial condition sensitivities.

The effects of ATOL on $\varepsilon(\eta_j)$ were further examined as follows: For the local tolerances EMAX = 10^{-4} and ATOLSP = 10^{-13}, $\{\varepsilon(\eta_j)\}$ were measured for ATOL = 10^{-16} and 10^{-19}. The $\{\varepsilon(\sigma_{j,0})\}$ showed little change from the values obtained for ATOL = 10^{-13}. However, the $\{\varepsilon(A_j)\}$ for ATOL = 10^{-13} and 10^{-16} were essentially inversely proportional to ATOL. (The same behavior was observed with ATOL = 10^{-10}.) For ATOL = 10^{-19} some of the sensitivities with respect to A_1, A_2, and A_4 were large enough for the error control to become relative, and the errors did not scale with ATOL. When ATOL was set equal to zero, it was observed that all $\varepsilon(A_j)$ were significantly greater than unity, with $\varepsilon(A_5) > \varepsilon(A_4) > \varepsilon(A_3) > \varepsilon(A_2) > \varepsilon(A_1)$. Also $\varepsilon(A_j)$ and $\varepsilon(k_j)$ were essentially equal to one another for all j. The $\{\varepsilon(\sigma_{j,0})\}$ were essentially unchanged from the values obtained with ATOL = 10^{-13}. For EMAX = 10^{-4}, ATOLSP = 10^{-6}, and ATOL = 0.0 all $\varepsilon(\eta_j)$, except for A_5 and k_5, were significantly greater than those obtained with ATOLSP = 10^{-13}. This fact and the fact that the average $\{D_{ij}\}$ were much less for the smaller ATOLSP indicate that the error control of $\underline{Y}$ does indeed determine the error control of the $\{\underline{S}_j\}$.

In summary, if local error control of the sensitivity solutions is to be performed, it must be purely (or mostly) relative. However, in order to avoid difficulty when $S_{ij} = 0.0$ and in controlling errors in insignificantly small $|\langle S_{ij}\rangle|$, the error test must be applied only to species with $|\langle S_{ij}\rangle|$ greater than a minimum value (say, 10^{-5} or 10^{-4}) that would indicate an insignificant sensitivity. The results presented for the $\varepsilon(\eta_j)$ and the $\varepsilon(\underline{S}_j)$ showed that the average global errors were very small (less than 1 percent) despite the significantly large average local errors. Thus it is not clear that local error control, by means of equations (4.79), (4.81), and (4.24), for the sensitivities is either meaningful or necessary. Note also that when the local error test fails, ODESSA first recomputes the kinetics solution with a reduced step size and/or method order before generating new sensitivities. The improvement in the

sensitivity coefficients may arise simply because of the more accurate $\underline{Y}$. The same result can be accomplished by simply reducing EMAX and ATOLSP. However the improvement is obtained, the only way to judge the accuracy of the results is by comparing them with solutions generated using reduced EMAX and ATOLSP. Alternatively solutions can be produced with progressively smaller EMAX (and ATOLSP) until they show little or no change with a further decrease. Both methods require several solutions of the sensitivity coefficients. Not performing the local error test on the sensitivities reduces the computational work. It also reduces the complexity of the code. Finally, in any case, the implementation of the DDM in CHEMDDM, and hence LSENS, did produce sufficiently accurate results.

4.6.3 Oxidation of Methane

The fifth test problem was studied by Boni and Penner (ref. 106) with a global method, the Fourier amplitude sensitivity test (FAST), and then by Dougherty et al. (ref. 90) with the coupled version of the DM and the GFM. The problem describes the kinetics of a CH_4-O_2-Ar system at a temperature of 2000 K. The reaction mechanism consists of 22 reversible reactions among 14 species (13 reacting species and the inert species Ar) and is given in table 4.34, along with the rate constants at 2000 K. Boni and Penner (ref. 106) write reaction 19 as two reactions

$$H + OH + Ar \rightleftharpoons H_2O + Ar \tag{4.89}$$

and

$$H + OH + H_2O \rightleftharpoons H_2O + H_2O \tag{4.90}$$

The mechanism given in their paper therefore consists of 23 reversible reactions. The initial concentrations (in moles per cubic centimeter) were $[CH_4] = 3.761\times10^{-6}$, $[O_2] = 7.521\times10^{-6}$, $[H_2] = [CO_2] = 1.660\times10^{-24}$, and $[Ar] = 2.972\times10^{-5}$; all other species had zero initial concentration. The variation of species molar concentrations with reaction time is shown in figure 4.6. Comparing these concentration profiles with figures 1 and 2 in reference 106 verified that LSENS reproduced their results.

Boni and Penner (ref. 106) tabulate sensitivity coefficients with respect to the rate constants at $t = 2.5\times10^{-5}$ s, when the concentrations of the species CH_3, CH_2O, and HCO attain their maximum values (see fig. 4.6). This reaction time corresponds to conditions immediately preceding ignition (ref. 90).

Sensitivity coefficients with respect to the rate constants were generated with LSENS at one print station, $t = 2.5\times10^{-5}$ s, using the local error tolerances EMAX $= 10^{-3}$, after Dougherty et al. (ref. 90), and ATOLSP $= 10^{-12}$ to ensure relative error control for species with mole fraction ≥ 0.1 ppm. Because the forward and reverse rate constants were both specified, the mechanism was actually written as 44

TABLE 4.34.—REACTION MECHANISM FOR TEST PROBLEM 5[a]

Reaction number, j	Reaction	Forward rate constant, k_j[b]	Reverse rate constant, k_{-j}[b]
1	$CH_4 + M \rightleftharpoons CH_3 + H + M$	4.337(7)	1.106(17)
2	$CH_4 + OH \rightleftharpoons CH_3 + H_2O$	2.590(13)	1.048(11)
3	$CH_4 + H \rightleftharpoons CH_3 + H_2$	1.988(13)	8.071(11)
4	$CH_4 + O \rightleftharpoons CH_3 + OH$	2.168(12)	6.625(10)
5	$CH_3 + O \rightleftharpoons CH_2O + H$	1.000(14)	5.300(7)
6	$CH_3 + O_2 \rightleftharpoons CH_2O + OH$	2.000(10)	4.337(4)
7	$CH_2O + O \rightleftharpoons HCO + OH$	1.584(13)	9.035(9)
8	$CH_2O + OH \rightleftharpoons HCO + H_2O$	1.108(14)	8.553(9)
9	$CH_2O + H \rightleftharpoons HCO + H_2$	5.240(12)	4.216(9)
10	$CH_2O + M \rightleftharpoons HCO + H + M$	3.843(8)	1.959(16)
11	$HCO + O \rightleftharpoons CO + OH$	1.000(14)	1.144(5)
12	$HCO + OH \rightleftharpoons CO + H_2O$	1.000(14)	1.265(4)
13	$HCO + H \rightleftharpoons CO + H_2$	2.000(14)	2.771(5)
14	$HCO + M \rightleftharpoons CO + H + M$	4.216(10)	3.628(12)
15	$CO + OH \rightleftharpoons CO_2 + H$	5.360(11)	2.289(11)
16	$H_2 + OH \rightleftharpoons H + H_2O$	1.807(13)	1.807(12)
17	$H_2 + O \rightleftharpoons H + OH$	7.228(12)	6.625(12)
18	$H + O_2 \rightleftharpoons O + OH$	3.216(12)	1.385(13)
[c]19	$H + OH + M \rightleftharpoons H_2O + M$	2.104(15)	3.096(3)
20	$H + HO_2 \rightleftharpoons OH + OH$	1.554(14)	6.023(8)
21	$H + O_2 + M \rightleftharpoons HO_2 + M$	1.930(15)	2.168(10)
22	$OH + OH \rightleftharpoons H_2O + O$	9.456(12)	1.205(12)

[a]From reference 106.

[b]Units are moles, centimeters, and seconds and the temperature is 2000 K. Numbers in parentheses denote powers of 10.

[c]Third-body collisional efficiency for H_2O = 16.7.

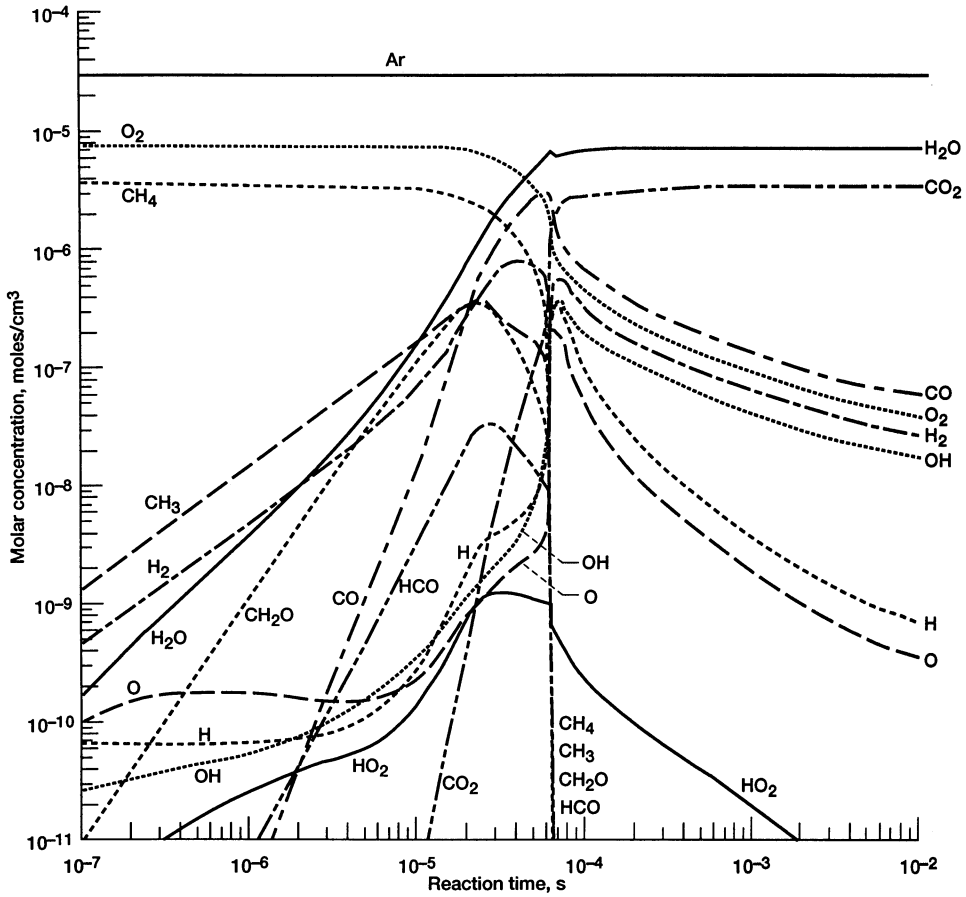

Figure 4.6.—Variation of species molar concentrations with reaction time for test problem 5.

TABLE 4.35.—REACTION IMPORTANCE LISTS AND NORMALIZED SENSITIVITY COEFFICIENTS AT $t = 2.5\times10^{-5}$ s FOR TEST PROBLEM 5

Species	Method	Reaction numbers in order of decreasing importance and normalized sensitivities at $t = 2.5\times10^{-5}$ s[a]												
CH_4	BFM	1	6	18	14	10	13							
		−0.294	−0.263	−0.220	−0.130	−0.0896	0.0800							
	LSENS	1	6	18	14	10	13							
		−0.295	−0.263	−0.220	−0.130	−0.0896	0.0800							
	FAST[b]	1	6	18	10	14	3							
	DM[c]	1	6	18	14	10	3							
	GFM[c]	1	6	18	14	10	3							
CH_3	BFM	6	5	8	1	14	13	2	4	3	7			
		−0.473	−0.235	−0.193	−0.189	0.179	−0.158	0.126	0.0964	0.0654	0.0651			
	LSENS	6	5	8	1	14	13	2	4	3	7			
		−0.473	−0.235	−0.194	−0.189	0.179	−0.159	0.127	0.0965	0.0656	0.0650			
	FAST[b]	1	18	5	14	10	8	6	2	13	4			
	DM[c]	1	6	14	5	18	8	13	10	2	4			
	GFM[c]	6	1	14	5	8	2	13	4	18	10			
H	BFM	14	1	13	6	10	18	3	12					
		0.680	0.635	−0.449	0.411	0.327	0.305	−0.110	−0.105					
	LSENS	14	1	13	6	10	18	3	12					
		0.680	0.636	−0.449	0.412	0.327	0.305	−0.110	−0.105					
	FAST[b]	1	6	14	10	18	3	13						
	DM[c]	1	6	14	10	18	13	3	12					
	GFM[c]	1	6	14	10	18	13	3	12					
OH	BFM	18	1	14	6	13	5	8	10	2	4	7	12	3
		0.877	0.551	0.526	0.431	−0.351	−0.331	−0.298	0.289	−0.270	0.125	0.120	−0.118	−0.104
	LSENS	18	1	14	6	13	5	8	10	2	4	7	12	3
		0.878	0.551	0.526	0.431	−0.351	−0.331	−0.298	0.289	−0.270	0.126	0.120	−0.118	−0.104
	FAST[b]	1	18	6	2	14	10	8	5	3				
	DM[c]	1	18	6	14	2	10	8	5	13	3			
	GFM[c]	1	18	6	14	2	8	10	13	5	7			
H_2O	BFM	1	6	18	14	10	3	13	5					
		0.805	0.761	0.671	0.249	0.217	−0.171	−0.146	−0.130					
	LSENS	1	6	18	14	10	3	13	5					
		0.806	0.761	0.671	0.249	0.217	−0.171	−0.145	−0.130					
	FAST[b]	1	6	18	3	10								
	DM[c]	1	6	18	3	10	14	5	13					
	GFM[c]	1	6	18	3	10	14	4	5					

H_2	BFM	1	6	14	10	8	18	13	5				
		0.717	0.666	0.333	0.259	0.186	0.169	−0.150	0.148				
	LSENS	1	6	14	10	8	18	13	5				
		0.719	0.666	0.333	0.259	0.186	0.169	−0.150	0.148				
	FAST[b]	1	6	10	14	8	18						
	DM[c]	1	6	14	10	8	18	2	5				
	GFM[c]	1	6	14	10	8	18	2	5				
O	BFM	18	1	5	14	6	13	10	8	3	11	7	4
		1.16	0.558	−0.552	0.524	0.484	−0.288	0.255	0.139	−0.124	−0.118	−0.116	−0.111
	LSENS	18	1	5	14	6	13	10	8	3	11	7	4
		1.16	0.559	−0.552	0.524	0.484	−0.288	0.255	0.139	−0.124	−0.118	−0.116	−0.111
	FAST[b]	18	1	6	5	14	10	3					
	DM[c]	18	1	6	5	14	10	3	13	8	7		
	GFM[c]	18	1	6	5	14	10	8	3	4	2		
CH_2O	BFM	8	2	5	7	1	6	10					
		−0.541	0.296	0.206	−0.118	−0.117	0.114	−0.107					
	LSENS	8	2	5	7	1	6	10					
		−0.541	0.296	0.206	−0.118	−0.116	0.115	−0.107					
	FAST[b]	6	1	8	2	18	5						
	DM[c]	8	6	1	2	5	18	7					
	GFM[c]	6	8	1	2	5	18	7					
O_2	BFM	1	6	18	14	10							
		−0.154	−0.151	−0.119	−0.0483	−0.0411							
	LSENS	1	6	18	14	10							
		−0.154	−0.151	−0.119	−0.0482	−0.0411							
	FAST[b]	1	6	18	3	10							
	DM[c]	1	6	18	10	3							
	GFM[c]	1	6	18	10	3							

[a]For each species the top row for BFM and LSENS gives the reaction numbers and the bottom row, the normalized sensitivity coefficients of that species with respect to the rate constants of the reactions corresponding to these reaction numbers. For DM and GFM each row gives the reaction numbers.

[b]From reference 106.

[c]From reference 90.

TABLE 4.35.—Concluded.

Species	Method	Reaction numbers in order of decreasing importance and normalized sensitivities at $t = 2.5\times10^{-5}$ s[a]												
HCO	BFM	18	13	6	14	1	10	12						
		0.545	−0.418	0.401	−0.372	0.228	0.126	−0.115						
	LSENS	18	13	6	14	1	10	12						
		0.546	−0.418	0.402	−0.371	0.229	0.126	−0.115						
	FAST[b]	1	6	18	14	10	13	8						
	DM[c]	6	1	18	14	13	10	8						
	GFM[c]	6	1	18	14	13	8	10						
CO	BFM	1	6	18	14	10	8	3	13	2	5			
		1.19	1.09	0.799	0.388	0.353	0.263	−0.221	−0.178	−0.123	−0.114			
	LSENS	1	6	18	14	10	8	3	13	2	5			
		1.19	1.09	0.798	0.387	0.353	0.264	−0.221	−0.178	−0.124	−0.114			
	FAST[b]	1	6	18	8	10	3	14	2					
	DM[c]	1	6	18	8	10	14	3	2	5	13			
	GFM[c]	1	6	18	8	10	14	3	2	5	13			
CO_2	BFM	1	6	18	15	14	10	2	3	5	13	4	7	12
		2.23	1.86	1.59	0.995	0.730	0.680	−0.591	−0.440	−0.375	−0.359	0.169	0.163	−0.132
	LSENS	1	6	18	15	14	10	2	3	5	13	4	7	12
		2.23	1.86	1.59	0.995	0.730	0.679	−0.591	−0.439	−0.375	−0.360	0.169	0.163	−0.133
	FAST[b]	1	6	18	15	2	10	14	3					
	DM[c]	1	6	18	15	2	10	14	3	5	8			
	GFM[c]	1	6	18	15	2	10	14	3	8	5			
HO_2[d]	BFM	14	21	20	1	13	10	6	18					
		0.391	0.372	−0.350	0.336	−0.256	0.189	0.167	0.106					
	LSENS	14	21	20	1	13	10	6	18					
		0.391	0.372	−0.350	0.336	−0.256	0.189	0.167	0.107					
	DM[c]	1	6	14	21	20	10	18	13					
	GFM[c]	1	6	14	21	10	20	13	3					

[a]For each species the top row for BFM and LSENS gives the reaction numbers and the bottom row, the normalized sensitivity coefficients of that species with respect to the rate constants of the reactions corresponding to these reaction numbers. For DM and GFM each row gives the reaction numbers.

[b]From reference 106.

[c]From reference 90.

[d]FAST results not given in reference 106.

irreversible reactions. However, the two rate constants were assumed to be related to one other through the concentration equilibrium constant. Therefore the procedure described for test problem 2 was used to compute the sensitivity coefficients with respect to the forward rate constants. That is, normalized sensitivities with respect to the 44 rate constants were first generated. The solutions for each forward and reverse rate constant were then combined by using equation (4.69).

Table 4.35 lists reaction numbers in order of decreasing importance, that is, decreasing normalized sensitivity coefficients, at $t = 2.5\times10^{-5}$ s for all reacting species. Also given are the normalized sensitivity coefficients produced by LSENS and the BFM, which used EMAX = 10^{-12} and ATOLSP = 10^{-21}. The reaction importance lists given in reference 106 for the FAST and reference 90 for the GFM and coupled version of DM are reproduced in table 4.35. The $\{\langle S_{ij}\rangle\}$ are not reported by Dougherty et al. (ref. 90). The FAST results are not included in table 4.35 because they represent average effects of all uncertainties and are therefore different from the coefficients produced by local methods. For each species i either all reactions for which $|\langle S_{ij}\rangle| \geq 0.1$ or the same number of reactions as in Boni and Penner (ref. 106) have been included.

Table 4.35 shows that for all species the agreement between LSENS and the BFM was excellent for both order of importance and sensitivity coefficients. All methods showed that the five most important reactions at $t = 2.5\times10^{-5}$ s were 1, 6, 10, 14, and 18. Other important reactions were 2, 3, 5, 8, and 13, in agreement with Dougherty et al. (ref. 90). However, for several species the actual order of the reaction importance lists produced by the DM and GFM were different from the BFM results. In several cases the differences were significant. For example, for CH_3 the DM predicted reaction 18 to be the fifth most important reaction, whereas the BFM (and LSENS) showed it to be only 17th most important, with $\langle \partial\sigma_{CH_3}/\partial k_{18}\rangle = -0.012$. Similarly reaction 8 for HCO was ranked 6th by the GFM but only 12th by the BFM (and LSENS), with $\langle \partial\sigma_{HCO}/\partial k_8\rangle = 0.046$. Because the $\{\langle S_{ij}\rangle\}$ are not given in reference 90, more detailed accuracy comparisons of the DDM with the DM and GFM could not be made.

In addition to the above inaccuracies in the DM solutions, Dougherty et al. (ref. 90) experienced a number of numerical problems with this method. In particular, at long times near equilibrium they encountered overflow errors while computing sensitivities with respect to k_6. The computations with LSENS were therefore performed up to a reaction time (= 0.1 s) when the system had essentially equilibrated. Solutions were successfully generated with no numerical difficulty.

To solve for the composition in the interval $[0,2.5\times10^{-5}]$ s, LSENS required 92 steps, 123 functional evaluations, 21 Jacobian matrix evaluations, and 0.18 s. The computational cost for the composition and sensitivities with respect to all rate constants was 1.7 s. Dougherty et al. (ref. 90) report execution times of about 2.8 min and 24 s, respectively, for the DM and GFM on an IBM 360/91 computer. They also estimated that the FAST would require approximately an hour of computing time. A previous version of LSENS (ref. 70) required 4.6 s on the NASA

Lewis Research Center's IBM 370/3033 computer. Thus for this problem the DDM was both faster and more accurate than the DM and GFM.

4.6.4 Oxidation of Formaldehyde

Test problem 6 has also been studied extensively; so detailed comparisons of methods and codes are possible. This constant-temperature, constant-density problem describes the oxidation of formaldehyde in the presence of carbon monoxide. Dougherty et al. (ref. 90) examined the behavior of this system at a temperature of 952 K with the DM and GFM. They calculated sensitivity coefficients with respect to the rate constants in the interval $[0,5\times10^{-3}]$ s and report the results at $t = 5\times10^{-3}$ s. This problem was subsequently studied by Dunker (ref. 21).

The reaction mechanism and rate constants at 952 K are given in table 4.36. The initial concentrations (in moles per cubic centimeter) were $[CH_2O] = 1.124\times10^{-7}$, $[O_2] = 2.109\times10^{-6}$, $[CO] = 4.699\times10^{-6}$, and $[N_2] = 4.832\times10^{-6}$; all other initial concentrations were zero. The variation of species mole fractions with reaction time is shown in figure 4.7.

The reaction mechanism is only of moderate size, involving 25 irreversible reactions among 15 species (including the artificial HO_2 and H_2O_2 wall species and the inert species N_2). Nonetheless Dougherty et al. (ref. 90) could not compute all sensitivities with the DM because of numerical problems (overflow errors) at $t \gtrsim 10^{-3}$ s. No such difficulty was experienced by LSENS. For each reacting species (except the wall species) table 4.37 lists reaction numbers in order of decreasing importance and normalized sensitivity coefficients at $t = 5\times10^{-3}$ s. For each species the reaction importance list includes only reactions for which $|\langle S_{ij}\rangle| \geq 0.1$. Table 4.37 does not contain CO, O_2, and CH_2O because all their normalized sensitivity coefficients were less than 0.1 in magnitude. Dougherty et al. (ref. 90) arrived at the same conclusion for the DM and GFM results. The LSENS results were generated at the four output stations $t = 10^{-6}$, 10^{-4}, 10^{-3}, and 5×10^{-3} s, with the local error tolerances EMAX = 10^{-6} and ATOLSP = 10^{-8}, after Dunker (ref. 21). For reasons discussed later two sets of BFM results are presented in table 4.37. One was produced on the Cray-XM/P computer using EMAX= 10^{-12} and ATOLSP = 10^{-21} and the other on the Amdahl 5870 computer using the UTS operating system and tolerances EMAX = 10^{-6} and ATOLSP = 10^{-8}. Finally, the GFM solutions of Dougherty et al. (ref. 90) are reproduced in table 4.37. (Reference 90 does not list the DM results, although the authors state that, with few exceptions, the DM and GFM results agreed reasonably well.)

Table 4.37 shows that all methods predicted reactions 2, 3, 4, 9, 10, and 22 as being the most important at $t = 5\times10^{-3}$ s. The agreement between the LSENS and accurate BFM results (i.e., the calulations with EMAX = 10^{-12} and ATOLSP = 10^{-21}) was, in general, good. However, for HO_2 the reaction importance list obtained with LSENS showed that reactions 2 and 22 were the second and third most important reactions, whereas the accurate BFM results gave the opposite order.

TABLE 4.36.—REACTION MECHANISM FOR TEST PROBLEM 6[a]

Reaction number, j	Reaction	Rate constant, k_j[b]
1	$HCO + O_2 \rightarrow HO_2 + CO$	6.02(10)
2	$HO_2 + CH_2O \rightarrow H_2O_2 + HCO$	3.43(10)
3	$H_2O_2 + M \rightarrow OH + OH + M$	4.01(6)
4	$OH + CH_2O \rightarrow H_2O + HCO$	9.64(13)
5	$OH + H_2O_2 \rightarrow H_2O + HO_2$	3.07(12)
6	$H_2O_2 \rightarrow H_2O_2$ (wall)	1.05(2)
7	$HO_2 \rightarrow HO_2$ (wall)	1.05(1)
8	$HO_2 + HO_2 \rightarrow H_2O_2 + O_2$	1.81(12)
9	$OH + CO \rightarrow CO_2 + H$	1.99(11)
10	$HO_2 + CO \rightarrow CO_2 + OH$	7.23(8)
11	$H + CH_2O \rightarrow H_2 + HCO$	1.63(12)
12	$H + O_2 \rightarrow OH + O$	3.32(10)
13	$H + O_2 + M \rightarrow HO_2 + M$	3.63(15)
14	$HO_2 + M \rightarrow H + O_2 + M$	2.83(5)
15	$O + H_2 \rightarrow OH + H$	1.82(11)
16	$O + CH_2O \rightarrow OH + HCO$	6.02(13)
17	$H + H_2O_2 \rightarrow HO_2 + H_2$	7.83(11)
18	$H + H_2O_2 \rightarrow H_2O + OH$	3.55(12)
19	$O + H_2O_2 \rightarrow OH + HO_2$	6.02(10)
20	$HCO \rightarrow H + CO$	4.60(−12)
21	$OH + H_2 \rightarrow H_2O + H$	6.02(12)
22	$CH_2O + O_2 \rightarrow HCO + HO_2$	1.75(4)
23	$H + HO_2 \rightarrow OH + OH$	3.01(12)
24	$H + HO_2 \rightarrow H_2O + O$	3.01(13)
25	$H + HO_2 \rightarrow H_2 + O_2$	2.71(13)

[a]From reference 90.

[b]Units are moles, centimeters, and seconds and the temperature is 952 K. Numbers in parentheses denote powers of 10.

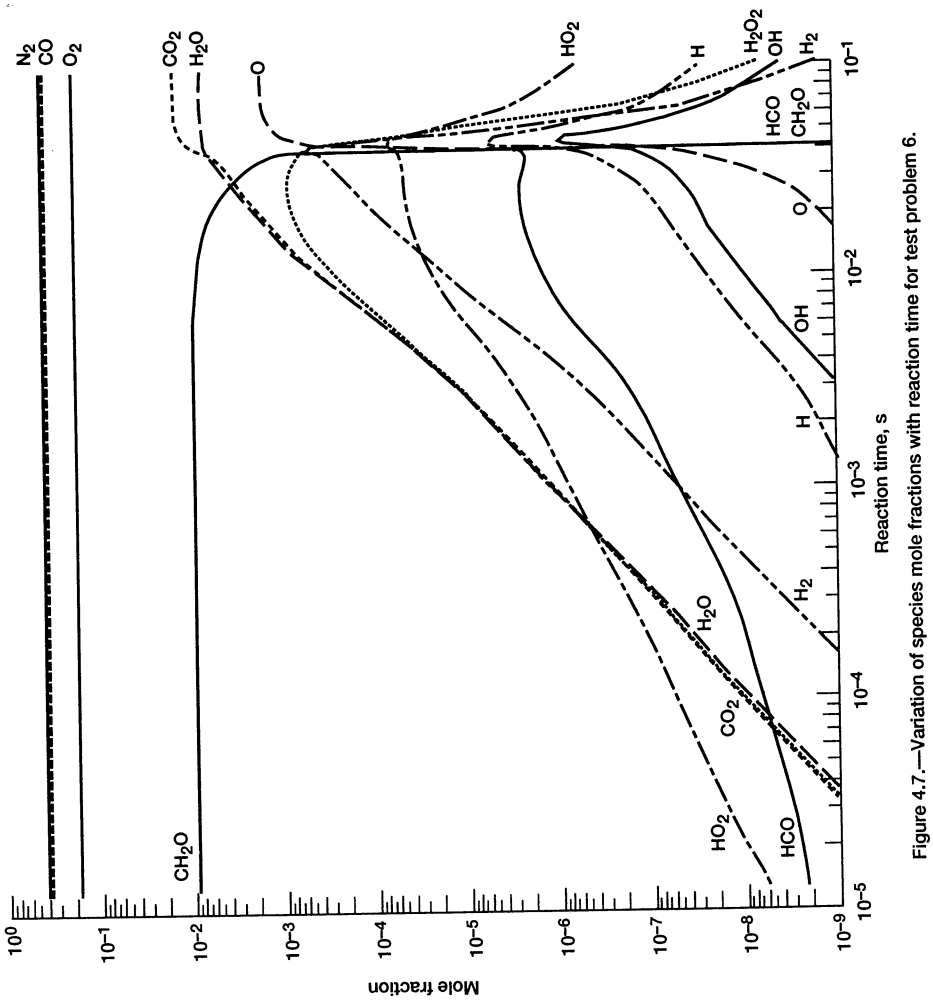

Figure 4.7.—Variation of species mole fractions with reaction time for test problem 6.

TABLE 4.37.—REACTION IMPORTANCE LISTS AND NORMALIZED SENSITIVITY COEFFICIENTS AT $t = 5\times10^{-3}$ s FOR TEST PROBLEM 6

[LSENS solution generated with EMAX = 10^{-6} and ATOLSP = 10^{-8}.]

Species	Method	Reaction numbers in order of decreasing importance and normalized sensitivities at $t = 5\times10^{-3}$ s[a]									
HCO	BFM[b]	2	1	3	22	10	8	9	4	12	11
		1.21	−0.923	0.746	0.694	0.596	−0.292	0.211	−0.211	0.201	−0.122
	BFM[c]	2	1	3	22	10	8	9	4	12	11
		1.24	−0.916	0.767	0.671	0.600	−0.310	0.213	−0.213	0.203	−0.123
	LSENS	2	1	3	22	10	8	9	4	12	11
		1.24	−0.923	0.770	0.684	0.598	−0.306	0.214	−0.214	0.203	−0.124
	GFM[d]	2	1	3	22	10	8	9	4	12	11
		1.25	−1.06	0.80	0.72	0.66	−0.32	−0.22	−0.21	0.21	−0.12
HO_2	BFM[b]	3	22	2	8	9	4	12	10	11	
		0.699	0.686	0.682	−0.306	0.210	−0.209	0.189	0.164	−0.121	
	BFM[c]	3	2	22	8	9	4	12	10	11	
		0.719	0.706	0.663	−0.325	0.212	−0.211	0.191	0.169	−0.122	
	LSENS	3	2	22	8	9	4	12	10	11	
		0.722	0.705	0.676	−0.320	0.213	−0.212	0.192	0.166	−0.123	
	GFM[d]	3	22	2	8	9	4	12	10	11	
		0.73	0.71	0.65	0.33	0.21	0.21	0.19	0.16	−0.12	
H_2O_2	BFM[b]	2	22	3	9	4	6	12	8	10	11
		1.47	0.829	0.464	0.180	−0.180	−0.175	0.161	−0.159	0.135	−0.104
	BFM[c]	2	22	3	9	4	6	8	12	10	11
		1.49	0.797	0.489	0.183	−0.183	−0.182	−0.177	0.164	0.138	−0.106
	LSENS	2	22	3	9	4	6	8	12	10	11
		1.49	0.810	0.492	0.184	−0.184	−0.183	−0.177	0.165	0.138	−0.107
	GFM[d]	2	22	3	6	9	4	12	8	10	11
		1.48	0.85	0.44	−0.18	0.17	0.17	0.15	−0.15	0.13	−0.10

[a]For each species and method the top row gives the reaction numbers and the bottom row, the normalized sensitivity coefficients of that species with respect to the rate constants of the reactions corresponding to these reaction numbers.

[b]Generated on the Cray-XM/P computer with the local error tolerances EMAX = 10^{-12} and ATOLSP = 10^{-21}.

[c]Generated on the Amdahl 5870 computer using the UTS operating system and the local error tolerances EMAX = 10^{-6} and ATOLSP = 10^{-8}.

[d]From reference 90.

TABLE 4.37.—Concluded.

Species	Method	Reaction numbers in order of decreasing importance and normalized sensitivities at $t = 5\times10^{-3}$ s[a]									
OH	BFM[b]	4	10	3	2	22	8	12	9	11	
		−1.16	1.03	0.813	0.804	0.716	−0.287	0.213	0.159	−0.138	
	BFM[c]	4	10	3	2	22	8	12	9	11	
		−1.16	1.03	0.835	0.830	0.692	−0.306	0.216	0.161	−0.139	
	LSENS	4	10	3	2	22	8	12	9	11	
		−1.16	1.03	0.838	0.830	0.705	−0.302	0.216	0.162	−0.140	
	GFM[d]	4	10	3	22	2	1	8	12	11	9
		−1.40	1.10	0.88	0.77	0.64	0.39	−0.32	0.22	−0.13	0.12
H_2O	BFM[b]	10	22	3	2	12	8	9	4	11	
		1.01	0.837	0.574	0.553	0.175	−0.159	0.119	−0.118	−0.115	
	BFM[c]	10	22	3	2	12	8	9	4	11	
		1.01	0.802	0.603	0.583	0.179	−0.177	0.123	−0.122	−0.117	
	LSENS	10	22	3	2	12	8	9	4	11	
		1.01	0.818	0.608	0.588	0.180	−0.178	0.124	−0.123	−0.118	
	GFM[d]	10	22	3	2	12	8	11	9	4	
		1.02	0.87	0.55	0.53	0.17	−0.15	−0.11	0.11	0.11	
CO_2	BFM[b]	10	22	3	2	9	4	8	12	11	
		1.12	0.829	0.487	0.463	0.251	−0.250	−0.167	0.153	−0.0997	
	BFM[c]	10	22	3	2	9	4	8	12	11	
		1.12	0.795	0.514	0.491	0.254	−0.254	−0.185	0.157	−0.102	
	LSENS	10	22	3	2	9	4	8	12	11	
		1.12	0.811	0.518	0.495	0.255	−0.255	−0.186	0.158	−0.102	
	GFM[d]	10	22	3	2	9	4	8	12	11	
		1.13	0.86	0.46	0.44	0.24	−0.24	−0.16	0.15	−0.10	

H	BFM[b]	9	4	10	3	2	22	11	13	8		
		1.15	−1.15	1.02	0.800	0.788	0.705	−0.653	−0.324	−0.282		
	BFM[c]	9	4	10	3	2	22	11	13	8		
		1.15	−1.15	1.02	0.821	0.812	0.680	−0.654	−0.324	−0.300		
	LSENS	9	4	10	3	2	22	11	13	8		
		1.15	−1.15	1.02	0.826	0.813	0.694	−0.655	−0.325	−0.296		
	GFM[d]	9	4	10	3	11	22	2	13	8	1	
		1.42	−1.41	1.23	0.88	−0.81	0.76	0.75	−0.40	−0.31	0.14	
H_2	BFM[b]	9	4	10	22	3	2	11	13	8		
		1.11	−1.11	1.00	0.836	0.572	0.549	0.352	−0.315	−0.159		
	BFM[c]	9	4	10	22	3	2	11	13	8		
		1.11	−1.11	1.01	0.801	0.601	0.580	0.350	−0.316	−0.177		
	LSENS	9	4	10	22	3	2	11	13	8		
		1.11	−1.11	1.01	0.818	0.606	0.585	0.349	−0.316	−0.178		
	GFM[d]	9	4	10	22	3	2	11	13	8		
		1.13	−1.13	1.02	0.88	0.55	0.54	0.37	−0.32	−0.14		
O	BFM[b]	9	4	10	16	12	3	2	22	11	13	8
		1.16	−1.16	1.03	−1.00	0.979	0.834	0.826	0.742	−0.659	−0.327	−0.296
	BFM[c]	9	4	10	16	12	3	2	22	11	13	8
		1.16	−1.16	1.04	−1.00	0.981	0.858	0.854	0.719	−0.660	−0.327	−0.316
	LSENS	9	4	10	16	12	3	2	22	11	13	8
		1.16	−1.16	1.03	−1.00	0.981	0.860	0.853	0.730	−0.660	−0.327	−0.311
	GFM[d]	4	9	10	11	3	13	16	22	1	12	8
		4.78	4.68	4.02	−2.67	1.38	−1.32	−1.31	0.83	0.74	0.63	−0.33

[a]For each species and method the top row gives the reaction numbers and the bottom row, the normalized sensitivity coefficients of that species with respect to the rate constants of the reactions corresponding to these reaction numbers.

[b]Generated on the Cray-XM/P computer with the local error tolerances EMAX = 10^{-12} and ATOLSP = 10^{-21}.

[c]Generated on the Amdahl 5870 computer using the UTS operating system and the local error tolerances EMAX = 10^{-6} and ATOLSP = 10^{-8}.

[d]From reference 90.

Similar remarks apply to reactions 8 and 12 for H_2O_2. The solutions with CHEMDDM also experienced these problems with HO_2 and H_2O_2, and the reaction importance lists were identical to those produced by LSENS. In order to examine if the inaccuracies in the DDM were caused by an insufficiently accurate kinetic solution, BFM results were generated on the Amdahl 5870 computer using the UTS operating system and the same error tolerances as for the sensitivity calculations. The agreement of the new BFM and LSENS results was much better: both calculations gave the same reaction importance lists for all species (table 4.37).

The GFM did not exhibit the inaccuracies observed in the DDM results for HO_2 and H_2O_2, but reaction 6 was predicted to be more important for H_2O_2 than the BFM indicated (see table 4.37). In fact, reaction importance lists that were different from the BFM lists were produced by the GFM for several species. In addition, several sensitivity coefficients were substantially inaccurate. For example, the GFM predicted reaction 1 to be the sixth most important reaction for OH and $\langle \partial\sigma_{OH}/\partial k_1 \rangle = 0.39$. In contrast, the BFM ranked this reaction as the 11th most important with $\langle \partial\sigma_{OH}/\partial k_1 \rangle = 0.0759$. More significantly the GFM results for several important sensitivities had the wrong sign, as for example, $\langle \partial\sigma_O/\partial k_4 \rangle$.

Dunker (ref. 21) solved this test problem with the DDM and GFM/AIM and gives normalized sensitivity coefficients of magnitude ≥ 0.10 for the species O and HO_2 at $t = 5\times10^{-3}$ s. His results are reproduced in tables 4.38 and 4.39, together with the solutions obtained with the BFM, LSENS, and CHEMDDM. The tables also list the GFM results of Dougherty et al. (ref. 90).

The agreement between LSENS and both CHEMDDM and Dunker's (ref. 21) results was, in general, excellent. All three calculations were in close agreement with the BFM. The GFM was, in contrast, significantly incorrect, with several sensitivity coefficients having the wrong sign, as already observed. The GFM/AIM was much more accurate, and essentially agreed with the DDM. However, the GFM/AIM was found to be unstable to variations in the local error tolerances required for the sensitivity calculations, and the results were affected by the choice of print stations, indicating difficulties in selecting step lengths during the calculation of the Green's function matrix (ref. 21).

Tables 4.38 and 4.39 show that for some reactions the agreement of CHEMDDM with the BFM was slightly better than that of LSENS with the BFM. However, more significantly, both codes produced the wrong reaction importance list for HO_2 (and H_2O_2, as previously observed). This inaccuracy in the HO_2 results was exhibited by the GFM/AIM also (see table 4.39). Now the GFM/AIM computes the sensitivity coefficients after the kinetics solution is generated for the entire integration interval. The method also uses local error tolerances to test the accuracy of the Green's function matrix. The results given in tables 4.38 and 4.39 were generated with very small values for these tolerances (ref. 21). Nevertheless the method incurred the error described previously. Therefore it would appear that EMAX = 10^{-6} and ATOLSP = 10^{-8} did not produce a sufficiently accurate kinetics solution: ATOLSP was much larger than that required to ensure relative error control, the importance of which is discussed in chapter 3 and reference 19. Equations (3.31) and (3.37) show that the requirement for relative error control for σ_i is σ_iEMAX >>

TABLE 4.38.—NORMALIZED SENSITIVITY COEFFICIENTS OF SPECIES O AT $t = 5\times10^{-3}$ s FOR TEST PROBLEM 6

Reaction number, j	Normalized sensitivities $\langle \partial\sigma_O/\partial k_j \rangle$ at $t = 5\times10^{-3}$ s					
	BFM[a]	LSENS	CHEMDDM	DDM[b]	GFM/AIM[b]	GFM[c]
9	1.156	1.159	1.158	1.158	1.150	4.68
4	−1.156	−1.158	−1.157	−1.157	−1.145	4.78
10	1.031	1.031	1.032	1.031	1.017	4.02
16	−1.000	−1.000	−1.000	−1.000	−0.996	−1.31
12	0.979	0.981	0.980	0.980	0.978	0.63
3	0.834	0.860	0.842	0.843	0.844	1.38
2	0.826	0.853	0.835	0.836	0.831	<0.10
22	0.742	0.730	0.737	0.737	0.726	0.83
11	−0.659	−0.660	−0.660	−0.660	−0.655	−2.67
13	−0.327	−0.327	−0.327	−0.327	−0.325	−1.32
8	−0.296	−0.311	−0.301	−0.300	−0.302	−0.33

[a]Generated on the Cray-XM/P computer with the local error tolerances EMAX = 10^{-12} and ATOLSP = 10^{-21}.
[b]From reference 21.
[c]From reference 90.

TABLE 4.39.—NORMALIZED SENSITIVITY COEFFICIENTS OF SPECIES HO_2 AT $t = 5\times10^{-3}$ s FOR TEST PROBLEM 6

Reaction number, j	Normalized sensitivities $\langle \partial\sigma_{HO_2}/\partial k_j \rangle$ at $t = 5\times10^{-3}$ s					
	BFM[a]	LSENS	CHEMDDM	DDM[b]	GFM/AIM[b]	GFM[c]
3	0.699	0.722	0.706	0.707	0.730	0.73
22	0.686	0.676	0.681	0.682	0.693	0.71
2	0.682	0.705	0.689	0.690	0.709	0.65
8	−0.306	−0.320	−0.310	−0.309	−0.320	0.33
9	0.210	0.213	0.211	0.211	0.217	0.21
4	−0.209	−0.212	−0.210	−0.210	−0.217	0.21
12	0.189	0.192	0.189	0.190	0.195	0.19
10	0.164	0.166	0.165	0.165	0.170	0.16
11	−0.121	−0.123	−0.122	−0.122	−0.125	−0.12

[a]Generated on the Cray-XM/P computer with the local error tolerances EMAX = 10^{-12} and ATOLSP = 10^{-21}.
[b]From reference 21.
[c]From reference 90.

ATOLSP. For EMAX = 10^{-6} and ATOLSP = 10^{-8} this requirement means that σ_i has to be much greater than 0.01 to achieve relative error control for species i. This σ_i corresponds to a mole fraction x_i of approximately 0.3. Examination of the BFM solutions at the four print stations showed that only CO ($x_{CO} \sim 0.40$), O_2 ($x_{O_2} \sim 0.18$), and N_2 ($x_{N_2} \sim 0.41$) had mole fractions greater than 0.1.

To confirm that ATOLSP was indeed too large, the runs with LSENS and CHEMDDM were repeated with the local error tolerances EMAX = 10^{-3} and ATOLSP = 10^{-12}. The new solutions and the accurate BFM results are given in table 4.40. Note the excellent agreement among LSENS, CHEMDDM, and the BFM. Note also the significant improvements over the results given in table 4.37, despite using a much larger EMAX.

The above observations support the arguments made earlier that the error control in the solution of the sensitivity equations is determined by the error control in the solution of the kinetics equations and that inaccuracies in the sensitivity coefficients result from insufficiently accurate composition calculations. Further confirmation of these hypotheses was provided by the GFM/AIM results, which produced an inaccurate reaction importance list despite independent error control of the Green's function matrix and use of very small tolerances for this calculation. Thus the need for local truncation error test and control during the sensitivity computations remains in doubt.

For the four output stations $t = 10^{-6}$, 10^{-4}, 10^{-3}, and 5×10^{-3} s and local error tolerances EMAX = 10^{-6} and ATOLSP = 10^{-8}, LSENS required 13 steps, 15 derivative evaluations, and 4 Jacobian matrix evaluations and LU-decompositions. In contrast, CHEMDDM required 20 steps, 27 derivative evaluations, and 6 Jacobian matrix evaluations and LU-decompositions. To solve for the composition and sensitivity coefficients of all species with respect to all 15 initial concentrations and all 25 rate constants, LSENS required 0.22 s, whereas CHEMDDM required 0.57 s. For the same four output stations and local error tolerances Dunker (ref. 21) reports execution times of 1.25 and 8.28 s, respectively, for the DDM and the GFM/AIM on an IBM 370 computer. On the NASA Lewis Research Center's IBM 370/3033 computer the cost of CHEMMDM and a previous version of LSENS (ref. 70) were 1.54 and 0.6 s, respectively. Dougherty et al. (ref. 90) give an execution time of about 15 s per parameter for the coupled version of the DM on an IBM 360/91 computer. Depending on how the integrals that give the Green's function matrix were evaluated, the GFM was about a factor of 2 or 5 faster than the DM (ref. 90). Thus LSENS was more efficient than the other methods and codes examined. For this problem LSENS was faster than CHEMDDM and the GFM/AIM by factors of 2.6 and 17, respectively.

For the local error tolerances EMAX = 10^{-3} and ATOLSP = 10^{-12}, LSENS required 34 steps, 43 derivative evaluations, 10 Jacobian matrix evaluations, and 0.39 s to solve for the composition and sensitivities with respect to the 25 rate constants. The computational cost of CHEMDDM was 46 steps, 55 derivative evaluations, 12 Jacobian matrix evaluations, and 1.1 s of CPU time. These runs were more expensive than the ones with EMAX = 10^{-6} and ATOLSP = 10^{-8} because of

the smaller ATOLSP, further confirming the dependence, discussed in chapter 3, of the computational work on ATOLSP.

Efficiency differences among the methods and codes were further explored as follows: After Dunker (ref. 21), execution times were measured for computing (1) the concentrations alone (τ_{conc}), (2) the concentrations and all initial condition sensitivities (τ_{ic}), (3) the concentrations and all rate constant sensitivities (τ_{rc}), and (4) the concentrations, all initial condition sensitivities, and all rate constant sensitivities (τ_{all}). The execution times required by LSENS and CHEMDDM for the four calculations are given in table 4.41 for test problems 4 and 6. For both problems the computational costs were measured with EMAX = 10^{-6} and ATOLSP = 10^{-8} to be consistent with Dunker (ref.21), who used these error tolerances in his work with the DDM and GFM/AIM. The execution times reported by this author are also listed in table 4.41. Finally to facilitate efficiency comparisons, the costs incurred on the NASA Lewis Research Center's IBM 370/3033 computer by CHEMDDM and an earlier version of LSENS (ref. 70) are included in this table.

Table 4.41 shows that all execution times were much smaller for LSENS. More specifically, for problem 6 τ_{all} was smaller for LSENS than for CHEMDDM by a factor of about 2.6 and CHEMDDM was more efficient than the GFM/AIM by a factor of about 6.7. Hence LSENS was more efficient than the GFM/AIM by a factor of about 17. One important difference between LSENS and CHEMDDM deserves mention. LSENS can be used to generate any number of sensitivity coefficients from just one initial condition or one rate coefficient parameter to the full set of all initial conditions and all rate coefficient parameters. CHEMDDM does not have this feature, and all initial concentration sensitivities and/or all rate constant sensitivities are computed. This difference can result in even smaller execution times for LSENS if not all sensitivity coefficients are required. For example, for test problem 4 LSENS required only about 0.085 s to generate one initial concentration sensitivity instead of the 0.15 s for all initial concentration sensitivities. For one rate constant sensitivity the CPU time was about 0.086 s. Thus each additional sensitivity costs less than 0.014 s. The BFM requires at least one additional calculation of the concentrations for each sensitivity coefficient. Table 4.41 shows the cost to be about 0.038 s, which is significantly more. (Of course, as discussed previously, if accurate BFM results are desired, the concentration profiles have to be produced with significantly smaller error tolerances. Therefore the BFM cost would be much larger than the estimate given here.)

As discussed in section 4.3 much of the computational work required by the DDM is associated with calculating the first sensitivity coefficient because it requires evaluation and LU-decomposition of the matrix **P**. Subsequent sensitivity coefficient computations cost much less. Similarly calculating the Green's function matrix, which is related to the initial condition sensitivities, takes up much of the computational work required by the GFM and GFM/AIM (refs. 20, 21, and 89 to 91). The rate constant sensitivities require much less work. A useful measure for comparing efficiencies of the DDM and GFM/AIM is therefore the difference $\tau_{all} - \tau_{ic}$, the additional time needed to calculate the rate constant sensitivities (ref. 21).

TABLE 4.40.—REACTION IMPORTANCE LISTS AND NORMALIZED SENSITIVITY COEFFICIENTS AT $t = 5\times10^{-3}$ s FOR TEST PROBLEM 6

[LSENS and CHEMDDM solutions generated with EMAX = 10^{-3} and ATOLSP = 10^{-12}.]

Species	Method or code	Reaction numbers in order of decreasing importance and normalized sensitivities at $t = 5\times10^{-3}$ s[a]									
HCO		2	1	3	22	10	8	9	4	12	11
	BFM[b]	1.21	–0.923	0.746	0.694	0.596	–0.292	0.211	–0.211	0.201	–0.122
	LSENS	1.21	–0.923	0.745	0.695	0.596	–0.291	0.211	–0.210	0.200	–0.122
	CHEMDDM	1.21	–0.923	0.745	0.695	0.596	–0.291	0.211	–0.210	0.200	–0.122
HO_2		3	22	2	8	9	4	12	10	11	
	BFM[b]	0.699	0.686	0.682	–0.306	0.210	–0.209	0.189	0.164	–0.121	
	LSENS	0.698	0.686	0.681	–0.305	0.210	–0.209	0.188	0.164	–0.121	
	CHEMDDM	0.698	0.686	0.681	–0.305	0.210	–0.209	0.188	0.164	–0.121	
H_2O_2		2	22	3	9	4	6	12	8	10	11
	BFM[b]	1.47	0.829	0.464	0.180	–0.180	–0.175	0.161	–0.159	0.135	–0.104
	LSENS	1.46	0.829	0.463	0.180	–0.179	–0.175	0.161	–0.159	0.135	–0.104
	CHEMDDM	1.46	0.829	0.462	0.180	–0.179	–0.175	0.161	–0.159	0.135	–0.104
OH		4	10	3	2	22	8	12	9	11	
	BFM[b]	–1.16	1.03	0.813	0.804	0.716	–0.287	0.213	0.159	–0.138	
	LSENS	–1.16	1.03	0.812	0.803	0.717	–0.286	0.213	0.159	–0.138	
	CHEMDDM	–1.16	1.03	0.812	0.803	0.717	–0.286	0.213	0.159	–0.138	
H_2O		10	22	3	2	12	8	9	4	11	
	BFM[b]	1.01	0.837	0.574	0.553	0.175	–0.159	0.119	–0.118	–0.115	
	LSENS	1.01	0.837	0.573	0.552	0.175	–0.159	0.119	–0.118	–0.115	
	CHEMDDM	1.01	0.837	0.573	0.551	0.175	–0.159	0.119	–0.118	–0.115	

CO_2		10	22	3	2	9	4	8	12	11		
	BFM[b]	1.12	0.829	0.487	0.463	0.251	–0.250	–0.167	0.153	–0.0997		
	LSENS	1.12	0.829	0.486	0.462	0.250	–0.250	–0.167	0.153	–0.0995		
	CHEMDDM	1.12	0.829	0.486	0.462	0.250	–0.250	–0.167	0.153	–0.0995		
H		9	4	10	3	2	22	11	13	8		
	BFM[b]	1.15	–1.15	1.02	0.800	0.788	0.705	–0.653	–0.324	–0.282		
	LSENS	1.15	–1.15	1.02	0.799	0.787	0.705	–0.653	–0.324	–0.281		
	CHEMDDM	1.15	–1.15	1.02	0.799	0.786	0.705	–0.653	–0.324	–0.281		
H_2		9	4	10	22	3	2	11	13	8		
	BFM[b]	1.11	–1.11	1.00	0.836	0.572	0.549	0.352	–0.315	–0.159		
	LSENS	1.11	–1.11	1.00	0.836	0.571	0.548	0.352	–0.315	–0.159		
	CHEMDDM	1.11	–1.11	1.00	0.836	0.571	0.548	0.352	–0.315	–0.159		
O		9	4	10	16	12	3	2	22	11	13	8
	BFM[b]	1.16	–1.16	1.03	–1.00	0.979	0.834	0.826	0.742	–0.659	–0.327	–0.296
	LSENS	1.16	–1.16	1.03	–1.00	0.979	0.833	0.825	0.742	–0.659	–0.327	–0.295
	CHEMDDM	1.16	–1.16	1.03	–1.00	0.979	0.833	0.825	0.743	–0.659	–0.327	–0.295

[a]For each species the top row gives the reaction numbers. The next three rows give the normalized sensitivity coefficients produced by the BFM, LSENS, and CHEMDDM, respectively. For each species and method or code the $\{\langle S_{ij} \rangle\}$ are those of that species with respect to the rate constants of the reactions corresponding to the numbers listed in the first row.
[b]Generated on the Cray-XM/P computer with the local error tolerances EMAX = 10^{-12} and ATOLSP = 10^{-21}.

TABLE 4.41.—EXECUTION TIMES FOR TEST PROBLEMS 4 AND 6

Test problem	Method/code	Execution time, s			
		Concentrations alone	Initial condition sensitivities[a]	Rate constant sensitivities[a]	Initial condition and rate constant sensitivities[a]
4	LSENS[b]	0.038	0.15	0.14	0.22
	CHEMDDM[b]	0.088	0.37	0.37	0.51
	LSENS[c,d]	0.13	0.44	0.41	0.62
	CHEMDDM[c]	0.26	1.01	1.02	1.38
	DDM[e]	0.21	0.90	(f)	1.25
	GFM/AIM[e]	0.21	1.10	(f)	1.55
6	LSENS[b]	0.020	0.11	0.15	0.22
	CHEMDDM[b]	0.084	0.38	0.48	0.57
	LSENS[c,d]	0.064	0.32	0.42	0.60
	CHEMDDM[c]	0.24	1.05	1.27	1.54
	DDM[e]	0.18	0.82	(f)	1.25
	GFM/AIM[e]	0.18	4.18	(f)	8.28

[a]Includes execution time for concentrations.
[b]Execution times on the Amdahl 5870 computer using the UTS operating system.
[c]Execution times on the IBM 370/3033 computer.
[d]Execution times for a previous version of LSENS (ref. 70).
[e]From reference 21: execution times on an IBM 370 computer.
[f]Not given.

Table 4.41 shows that by this measure also the decoupled direct method is more efficient than the GFM/AIM and LSENS is the most efficient code. For both problems $\tau_{all} - \tau_{ic}$ was smaller for LSENS than for CHEMDDM by a factor of about 2. For problem 6 $\tau_{all} - \tau_{ic}$ was smaller for CHEMDDM than for the GFM/AIM by a factor of 9.5. Hence it was smaller for LSENS than for the GFM/AIM by a factor of almost 17. In addition, if only rate constant sensitivities are required, the decoupled direct method is even more efficient than the GFM and GFM/AIM because it does not then have to calculate the initial condition sensitivities and its execution time is only τ_{rc}. The GFM and GFM/AIM, however, still require approximately τ_{all} because they must compute the Green's function matrix before they can calculate the rate constant sensitivities.

Efficiency comparisons of local sensitivity analysis methods have also been made by Kramer et al. (ref. 81), who studied the dependence of the execution time on the number of sensitivity parameters. They present the execution times required by the BFM, GFM, GFM/AIM, and decoupled version of DM for a constant-density, constant-temperature problem describing the oxidation of CO in the presence of H_2O. These results were adapted by Leis and Kramer (ref. 100), who solved the problem with their code ODESSA (ref. 101), described in section 4.6.2. To provide a convenient measure for comparing efficiency, Leis and Kramer (ref. 100) express the computational cost in terms of the execution time required for the kinetics-only calculation. This execution time is termed "simulation time equiv-

alent" (STE), and all computational costs are given in units of STE's. Leis and Kramer's (ref. 100) results are reproduced in figure 4.8, which gives the variation of relative execution time with number of rate constants. The integration interval is not given in reference 100 but was presumably the same as in reference 81: [0,0.1] s.

The different methods included in figure 4.8 use different error control strategies. To ensure that efficiency comparisons were made for comparably accurate solutions, the local error tolerances for each method were selected such that an average error of about 2 percent in normalized sensitivity coefficients $\{\langle \partial Y_i/\partial k_j \rangle\}$ with magnitude greater than 10^{-3} was incurred at $t = 0.1$ s (ref. 100).

Sensitivity coefficients with respect to different numbers of rate constants were generated with LSENS at the one print station, $t = 0.1$ s, using the same reaction mechanism as used by Leis and Kramer (ref. 100). The mechanism consisted of 52 irreversible reactions among 11 reacting species and the inert species N_2. The initial temperature and pressure were 1100 K and 1 atm, respectively, and the initial mole fractions were $x_{CO} = 0.002$, $x_{H_2O} = 0.01$, $x_{O_2} = 0.028$, and $x_{N_2} = 0.96$. The relative execution times required by LSENS on the NASA Lewis Research Center's VAX 6320 computer (using VAX G_floating data type) are shown in figure 4.8. This study used the local error tolerances EMAX = 10^{-3} and ATOLSP = 10^{-12}, for which an average global error of 0.69 percent in $\{\langle \partial Y_i/\partial k_j \rangle\}$ was obtained at $t = 0.1$ s. Errors were measured only for species i and rate constants k_j for which $|\langle S_{ij}^* \rangle| \geq 10^{-3}$, where S_{ij}^*, the approximation to $\partial y_i/\partial k_j$, was generated with EMAX = 10^{-10} and ATOLSP

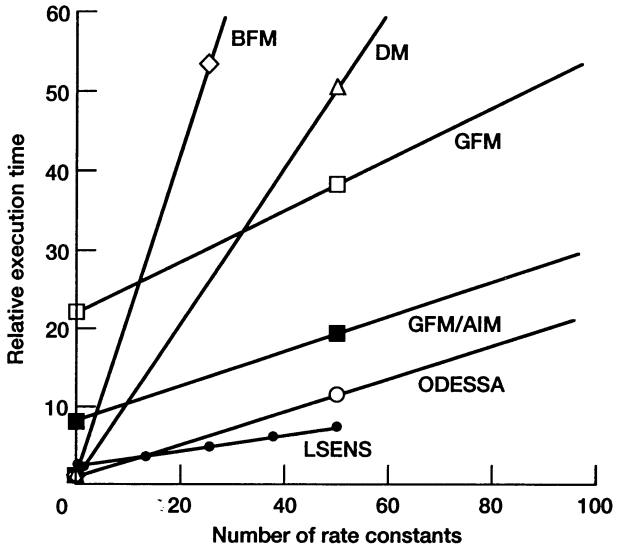

Figure 4.8.—Relative execution times for rate constant sensitivities versus number of rate constants for problem describing constant-density, constant-temperature oxidation of CO in presence of H_2O (adapted from ref. 100).

$= 10^{-19}$. When the cutoff value of $|\langle S_{ij}^{*}\rangle|$ for measuring global error was decreased to 10^{-6}, the average error in $\{\langle \partial Y_i/\partial k_j\rangle\}$ at $t = 0.1$ s was 1.3 percent. Thus the relative execution times reported for LSENS in figure 4.8 were for results that were more accurate than those produced by the other methods and codes. In this figure, 1 STE equals 0.28 s of CPU time on the VAX 6320 for LSENS and 22.6 s of CPU time on the VAX 11/750 for ODESSA (ref. 100).

Figure 4.8 shows that by this measure of efficiency comparison also the DDM is the most efficient method and LSENS the most efficient code. For P (= number of sensitivity parameters) ≥ 1 the relative execution time required by LSENS varies linearly with P, and the slope of this line is significantly smaller than that of the line that would connect the relative execution times for $P = 0$ and $P = 1$. These observations indicate that the computational cost of each rate constant after the first is the same, and that this cost is much less than that of the first rate constant.

As discussed previously, if sensitivities with respect to only rate constants are needed, the GFM and GFM/AIM incur an overhead related to calculating the initial condition sensitivities, whereas the DDM does not, as is clear from figure 4.8. This overhead can be significant. For example, the execution time required by the GFM to construct the Green's function matrix was more than twice that required by the DDM to calculate sensitivity coefficients with respect to all 52 rate constants (see fig. 4.8).

4.6.5 Simple Nonisothermal Problem

Test problem 7 describes a simple, nonisothermal problem for which the analytical solution is known. It involves a first-order irreversible reaction

$$\left.\begin{array}{l} \mathcal{R} \xrightarrow{k_1} \mathcal{P} \\ \\ k_1 = A_1 T^{n_1} \exp\left(\dfrac{-E_1}{RT}\right) \\ \\ A_1 = 1.0,\ n_1 = 1.0,\ E_1 = 0.0 \\ \\ \sigma_{\mathcal{R},0} = 1,\ \sigma_{\mathcal{P},0} = 0,\ T_0 = 1000\ \text{K} \end{array}\right\} \tag{4.91}$$

In order to solve this problem analytically, the following simplifying assumptions were made: (1) constant-pressure, adiabatic reaction and (2) constant and equal

specific heats c_p for species $\mathcal{R}$ and $\mathcal{P}$. The solution is

$$\left.\begin{aligned} \sigma_{\mathcal{R}}(t) &= \frac{C\sigma_{\mathcal{R},0}e^{-A_1Ct}}{C-\lambda\sigma_{\mathcal{R},0}\left(1-e^{-A_1Ct}\right)} \\ \sigma_{\mathcal{P}}(t) &= \sigma_{\mathcal{R},0}+\sigma_{\mathcal{P},0}-\sigma_{\mathcal{R}}(t) \\ T(t) &= T_0+\lambda\left(\sigma_{\mathcal{R},0}-\sigma_{\mathcal{R}}(t)\right) \end{aligned}\right\} \tag{4.92}$$

where

$$C = T_0 + \lambda\sigma_{\mathcal{R},0} \tag{4.93}$$

and

$$\lambda = \frac{Q_c}{c_p\left(\sigma_{\mathcal{R},0}+\sigma_{\mathcal{P},0}\right)} \tag{4.94}$$

where Q_c is the heat of combustion, which dictates the temperature rise due to the reaction. The variations of species mole fractions and temperature with reaction time are shown in figure 4.9. The solution was generated with Q_c = 5000 cal/mol and c_p = 5 cal/mol-K, which together give a 1000 K temperature rise when reactant $\mathcal{R}$ is completely converted to product $\mathcal{P}$.

The solution to the model problem and sensitivity coefficients with respect to the initial conditions $\{\sigma_{j,0}\}$ and T_0 and the three rate coefficient parameters A_1, n_1, and E_1 were computed at the five output stations t = 10^{-6}, 10^{-5}, 10^{-4}, 10^{-3}, and 10^{-2} s. The analytical results for the composition and temperature are given in table 4.42, together with the numerical solutions generated with LSENS using the local error tolerances EMAX = 10^{-6} and ATOLSP = 10^{-13}. The agreement between the analytical and numerical results was excellent at all levels of reactedness.

Since publication of a preliminary version of LSENS, called GCKP86 (ref. 70), the first code that could be used for sensitivity analysis of nonisothermal combustion kinetics problems, Lutz et al. (ref. 102) developed the code SENKIN, which also works for such problems. The chemical kinetics and sensitivity analysis solutions are executed with the code DASAC developed by Caracotsios and Stewart (ref. 99), who, in turn, modified the differential/algebraic system solver DASSL (ref. 107).

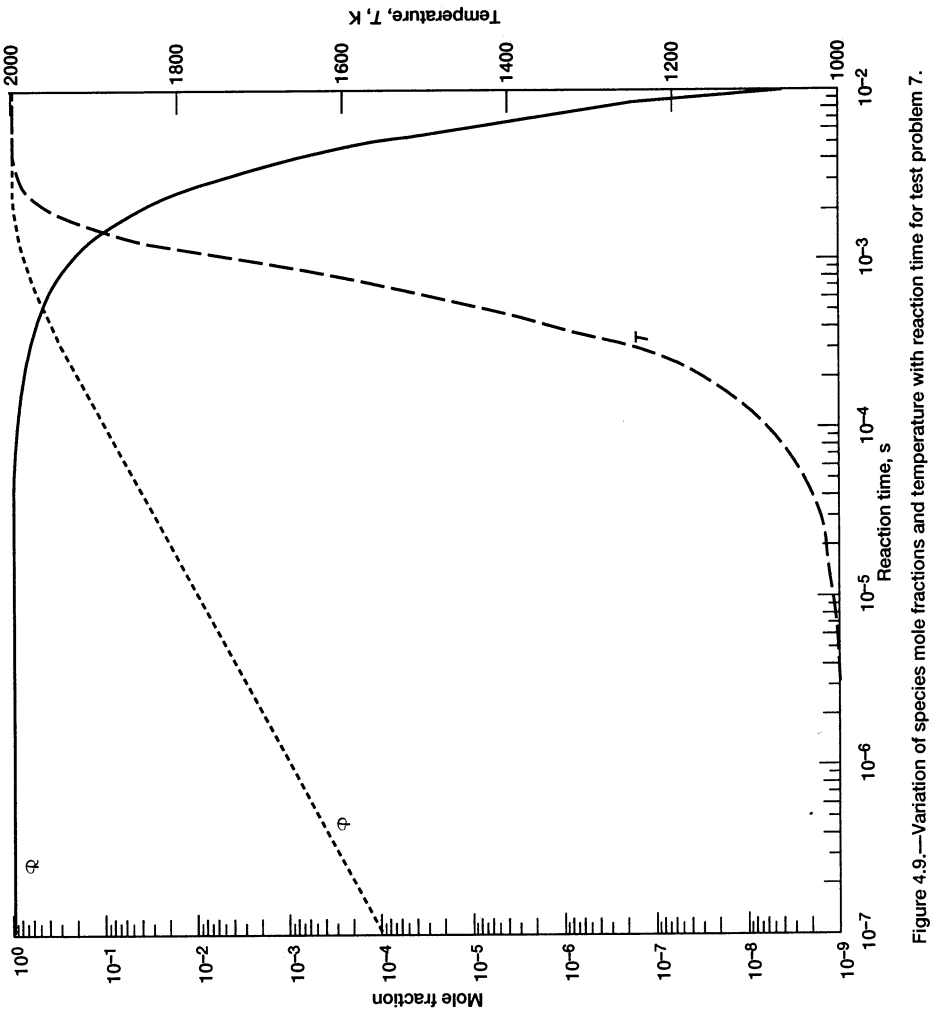

Figure 4.9.—Variation of species mole fractions and temperature with reaction time for test problem 7.

TABLE 4.42.—VARIATION OF CHEMICAL COMPOSITION AND TEMPERATURE WITH REACTION TIME FOR TEST PROBLEM 7

Time, s	σ_{Φ}			σ_{Φ}			T, K		
	Exact	LSENS	SENKIN	Exact	LSENS	SENKIN	Exact	LSENS	SENKIN
10^{-6}	0.9990	0.9990	0.9990	1.000×10^{-3}	1.000×10^{-3}	1.000×10^{-3}	1001.0	1001.0	1001.0
10^{-5}	0.9900	0.9900	0.9900	1.000×10^{-2}	1.000×10^{-2}	1.000×10^{-2}	1010.0	1010.0	1010.0
10^{-4}	0.9003	0.9003	0.9003	9.967×10^{-2}	9.967×10^{-2}	9.967×10^{-2}	1099.7	1099.7	1099.7
10^{-3}	0.2384	0.2384	0.2384	0.7616	0.7616	0.7616	1761.6	1761.6	1761.6
10^{-2}	4.122×10^{-9}	4.123×10^{-9}	4.123×10^{-9}	1.000	1.000	1.000	2000.0	2000.0	2000.0

Both the chemical kinetics and sensitivity analysis ODE's are solved by using the BDF method.

SENKIN solves a variety of problem types, but it calculates sensitivities for the preexponential factors $\{A_j\}$ only. That is, sensitivity coefficients with respect to the other two rate coefficient parameters or initial condition values cannot be computed. When the sensitivity analysis option is selected, sensitivity coefficients with respect to all (NR) reactions are generated; there is no provision to specify a subset of the reaction list. Another difference between LSENS and SENKIN concerns the number (N) of chemical kinetics ODE's solved. The number of species ODE's is equal to the number of reacting species (NRS) in LSENS, whereas it is equal to the total number of species (NS) in SENKIN. Also for a nonconstant-density problem LSENS includes a density ODE, whereas SENKIN does not. Thus, while the number of ODE's solved by LSENS depends on the problem (and the sensitivity parameters), it is always equal to NS + 1 in SENKIN for a nonconstant-temperature problem. Finally SENKIN uses finite-difference approximations, generated within DASSL, for the elements $\{\partial f_i/\partial y_j\}$ of the Jacobian matrix and the partial derivatives $\{\partial f_i/\partial \eta_j\}$, whereas LSENS uses analytical expressions for these quantities.

DASAC also uses the mutually dependent error control described for ODESSA (ref. 101) in section 4.6.2. However, unlike ODESSA, which performs the local error tests on the model problem and sensitivity coefficients separately, DASAC executes the two tests simultaneously. Thus at each step $[t_{n-1},t_n]$ the solutions to the model problem and sensitivity ODE's must satisfy the inequality

$$\sqrt{\frac{1}{N(\mathrm{NR}+1)}\left(\sum_{i=1}^{N}\left(\frac{d_{i,n}}{\mathrm{EWT}_{i,n}}\right)^2+\sum_{j=1}^{\mathrm{NR}}\sum_{i=1}^{N}\left(\frac{D_{ij,n}}{\mathrm{EWT}_{ij,n}}\right)^2\right)} \le 1 \qquad (4.95)$$

where the $\{d_{i,n}\}$ and $\{D_{ij,n}\}$ are the local truncation errors in the model and sensitivity solutions, respectively, and the error weights $\mathrm{EWT}_{i,n}$ and $\mathrm{EWT}_{ij,n}$ are given by equations (3.31) and (4.80), except that SENKIN uses scalar RTOL (= EMAX), ATOL (= ATOLSP), RTOL(S_{ij}) (= RTLS), and ATOL(S_{ij}) (= ATLS).

In order to compare the accuracy and efficiency of SENKIN and LSENS, the former code had to be modified. SENKIN produces the kinetics solution at the times $t \ge t_0 + i\,\Delta t$, $i = 1,2,...$ in the interval $[t_0,t_{\mathrm{end}}]$, where Δt and t_{end} are both set by the user. Also the kinetics solution and unnormalized sensitivity coefficients are written in binary form after every successful integration step. The program was changed to produce output at the user-specified times $t_{\mathrm{out},1},t_{\mathrm{out},2},....$ Subprograms to measure computational work and normalize and print the sensitivity coefficients were also added. The required coding was taken from LSENS to ensure that both programs used the same procedures. Finally the user-set variable MAXSTP (= maximum number of integration steps allowed for the problem) was included.

Solution to test problem 7 was attempted with SENKIN (version 1.8, dated December 1991) on the Amdahl 5870 computer using the UTS operating system, the Fujitsu 77 compiler (optimization level, 3), and double precision. However,

compilation errors prevented its use on this computer. Execution on the NASA Lewis Research Center's VAX 9410 computer, using the VAX/VMS operating system (version 5.5–2), the VAX FORTRAN compiler (version 6.1–6.8), double precision, and VAX G_floating arithmetic, was therefore attempted. No difficulty was encountered and the kinetics-only solution generated with EMAX = 10^{-6} and ATOLSP = 10^{-13} is given in table 4.42. The thermodynamic properties, species formation rates, and temporal derivatives of the dependent variables were computed with the chemical kinetics library CKLIB (version 3.9, dated April 1992) supplied with the chemical kinetics package CHEMKIN–II (ref. 108). The agreement between LSENS and SENKIN was excellent. (LSENS gave exactly the same results on both computers.)

To solve for the composition and temperature, SENKIN required 231 steps, 438 derivative evaluations, 43 Jacobian matrix evaluations, and 0.14 s of CPU time. (Here and in all subsequent computational costs reported for SENKIN the number of derivative evaluations does not include that required for either the numerical Jacobian or, when sensitivity analysis was performed, the numerical $\{\partial f_i/\partial \eta_j\}$). In contrast, the computational cost of LSENS was 176 steps, 196 derivative evaluations, 16 Jacobian matrix evaluations, and about 0.04 s of CPU time. In order to examine whether the difference in execution times was due to the different solvers (DASSL and LSODE) or the different calculation procedures for the Jacobian matrix used in SENKIN and LSENS, the kinetics-only calculation with LSENS was repeated with the method flag MF = 22, which tells LSODE to use the internally generated finite-difference approximations for the elements of the Jacobian matrix (see chapter 3). The computational cost was the same as with MF = 21 (i.e., analytical Jacobian). Thus LSODE is more efficient than DASSL. Because the execution times were quite small, the calculations were repeated on the NASA Lewis Research Center's VAX 8800 computer, which is much slower than the VAX 9410 computer. The execution times for SENKIN, LSENS with MF = 21, and LSENS with MF = 22 were 0.77, 0.20, and 0.21 s, respectively. For this calculation LSENS was therefore faster than SENKIN by a factor of about 4.

Normalized sensitivity coefficients with respect to the initial conditions are given in tables 4.43 to 4.45. The agreement between the analytical and numerical solutions was in general excellent. For very small and therefore unimportant normalized sensitivities, LSENS produced inaccurate values. The BFM also had difficulties with these sensitivities: for example, for EMAX = 10^{-6} and ATOLSP = 10^{-13} convergence could not be ascertained on the Amdahl 5870 computer using the UTS operating system. Thus the DDM was more accurate than the BFM. On the Cray-XM/P computer using double-precision arithmetic EMAX had to be reduced to 10^{-10} before the BFM results agreed with the exact solution to three significant figures. To achieve agreement to four significant figures required an EMAX value of 10^{-11}. For this EMAX, LSENS also reproduced the exact results.

The temperature did not display any sensitivity to $\sigma_{\mathcal{R},0}$ (table 4.43). The reason is that the initial mixture was composed of only the reactant. However, because of roundoff errors $(\partial \dot{T}/\partial \sigma_{\mathcal{R}})(\partial \sigma_{\mathcal{R}}/\partial \sigma_{\mathcal{R},0})$ and $(\partial \dot{T}/\partial \sigma_{\mathcal{P}})(\partial \sigma_{\mathcal{P}}/\partial \sigma_{\mathcal{R},0})$ did not sum to zero at some time $t > 0$, producing a finite $d/dt(\partial T/\partial \sigma_{\mathcal{R},0})$. Hence LSENS produced

TABLE 4.43.—NORMALIZED SENSITIVITY COEFFICIENTS WITH RESPECT TO INITIAL CONDITION $\sigma_{\Phi,0}$ FOR TEST PROBLEM 7

Time, s	Normalized sensitivities with respect to $\sigma_{\Phi,0}$					
	$\langle \partial\sigma_{\Phi}/\partial\sigma_{\Phi,0} \rangle$		$\langle \partial\sigma_{\Psi}/\partial\sigma_{\Phi,0} \rangle$		$\langle \partial T/\partial\sigma_{\Phi,0} \rangle$	
	Exact	LSENS	Exact	LSENS	Exact	LSENS
10^{-6}	1.000	1.000	1.000	1.000	0.0	-4.512×10^{-20}
10^{-5}	1.000	1.000	1.000	1.000	0.0	-3.083×10^{-16}
10^{-4}	1.000	1.000	1.000	1.000	0.0	1.663×10^{-12}
10^{-3}	1.000	1.000	1.000	1.000	0.0	-4.740×10^{-8}
10^{-2}	1.000	1.000	1.000	1.000	0.0	2.120×10^{-7}

TABLE 4.44.—NORMALIZED SENSITIVITY COEFFICIENTS WITH RESPECT TO INITIAL CONDITION $\sigma_{\Psi,0}$ FOR TEST PROBLEM 7

Time, s	Normalized sensitivities with respect to $\sigma_{\Psi,0}$[a]					
	$\langle \partial\sigma_{\Phi}/\partial\sigma_{\Psi,0} \rangle$		$\langle \partial\sigma_{\Psi}/\partial\sigma_{\Psi,0} \rangle$		$\langle \partial T/\partial\sigma_{\Psi,0} \rangle$	
	Exact	LSENS	Exact	LSENS	Exact	LSENS
10^{-6}	5.002(−11)	8.842(−11)	1.000(−1)	1.000(−1)	−9.995(−8)	−9.999(−8)
10^{-5}	5.016(−9)	5.101(−9)	1.000(−2)	1.000(−2)	−9.950(−7)	−9.951(−7)
10^{-4}	5.149(−7)	5.150(−7)	9.987(−4)	9.987(−4)	−9.485(−6)	−9.485(−6)
10^{-3}	5.000(−5)	5.000(−5)	1.157(−4)	1.157(−4)	−5.000(−5)	−5.000(−5)
10^{-2}	9.500(−4)	9.499(−4)	1.000(−4)	1.000(−4)	−5.000(−5)	−5.000(−5)

[a]Numbers in parentheses are powers of 10.

TABLE 4.45.—NORMALIZED SENSITIVITY COEFFICIENTS WITH RESPECT TO INITIAL CONDITION T_0 FOR TEST PROBLEM 7

Time, s	Normalized sensitivities with respect to T_0					
	$\langle \partial\sigma_{\Phi}/\partial T_0 \rangle$		$\langle \partial\sigma_{\Psi}/\partial T_0 \rangle$		$\langle \partial T/\partial T_0 \rangle$	
	Exact	LSENS	Exact	LSENS	Exact	LSENS
10^{-6}	-1.000×10^{-3}	-1.000×10^{-3}	0.9995	0.9991	1.000	1.000
10^{-5}	-1.005×10^{-2}	-1.005×10^{-2}	0.9950	0.9949	1.000	0.9999
10^{-4}	−0.1048	−0.1048	0.9468	0.9468	0.9952	0.9952
10^{-3}	−1.262	−1.262	0.3949	0.3949	0.7384	0.7384
10^{-2}	−10.50	−10.50	4.328×10^{-8}	4.330×10^{-8}	0.5000	0.5000

a nonzero $\partial T/\partial\sigma_{\Phi,0}$. The values given in table 4.43 show that $\{|\langle S_{ij}\rangle|\}$ less than 10^{-6} can be discarded as unimportant. Again the BFM could not reproduce zero sensitivities with respect to initial mole numbers. Indeed, no two EMAX values (between 10^{-2} and 10^{-15}) produced the same $\langle\partial T/\partial\sigma_{\Phi,0}\rangle$ at any output station. Adding some product to the initial mixture should, however, produce a nonzero $\langle\partial T/\partial\sigma_{\Phi,0}\rangle$. To verify that the DDM produces the correct $\langle\partial T/\partial\sigma_{\Phi,0}\rangle$, the calculation was repeated with $\sigma_{\Phi,0}=0.9$, $\sigma_{\Phi,0}=0.1$, and $Q_c=7500$ cal/mol. The analytical and LSENS results for $\langle\partial T/\partial\sigma_{\Phi,0}\rangle$ and $\langle\partial\dot{T}/\partial\sigma_{\Phi,0}\rangle$ are given in table 4.46. The agreement between the two calculations was excellent for both quantities.

The chemical reaction, equation (4.91), is irreversible and therefore the reaction rate is independent of σ_Φ. Nonetheless the sensitivity coefficients of σ_Φ with respect to $\sigma_{\Phi,0}$ were nonzero (see table 4.44). The reason is that increasing $\sigma_{\Phi,0}$ causes a decrease in the temperature, which, in turn, results in a slower reaction rate. Thus $\sigma_{\Phi,0}$ has an indirect effect on σ_Φ through T, and $\langle\partial\sigma_\Phi/\partial\sigma_{\Phi,0}\rangle$ was greater than 0.

The analytical and computed sensitivity coefficients with respect to the rate coefficient parameter A_1 are given in table 4.47. The solution with SENKIN was obtained with default values for the local tolerances RTLS (= 10^{-5}) and ATLS (= 10^{-5}). For these sensitivity tolerances EMAX had to be reduced to 10^{-6} (ATOLSP = 10^{-7}EMAX) to achieve agreement to four significant figures with the exact solution for the larger sensitivities. The same was true of the LSENS results. Table 4.47 shows that the agreement among the LSENS, SENKIN, and analytical results was in general excellent. The computational cost of SENKIN was 215 steps, 618 derivative evaluations, 216 Jacobian matrix evaluations, 0.29 s on the VAX 9410, and 1.7 s on the VAX 8800. LSENS required about 0.07 and 0.40 s on the two computers and was therefore faster than SENKIN by a factor of about 4.

TABLE 4.46.—NORMALIZED SENSITIVITY COEFFICIENTS OF TEMPERATURE AND ITS TEMPORAL DERIVATIVE WITH RESPECT TO INITIAL CONDITION $\sigma_{\Phi,0}$ FOR TEST PROBLEM 7 WITH MODIFIED INITIAL CONDITIONS AND HEAT OF COMBUSTION

Time, s	Normalized sensitivity coefficients of T and $\dot{T}$ with respect to $\sigma_{\Phi,0}$[a]			
	$\langle\partial T/\partial\sigma_{\Phi,0}\rangle$		$\langle\partial\dot{T}/\partial\sigma_{\Phi,0}\rangle$	
	Exact	LSENS	Exact	LSENS
10^{-6}	1.349(−4)	1.349(−4)	1.001(−1)	1.001(−1)
10^{-5}	1.343(−3)	1.343(−3)	1.013(−1)	1.013(−1)
10^{-4}	1.279(−2)	1.279(−2)	1.121(−1)	1.121(−1)
10^{-3}	6.144(−2)	6.144(−2)	8.788(−2)	8.788(−2)
10^{-2}	5.745(−2)	5.745(−2)	−1.135	−1.135

[a]Numbers in parentheses are powers of 10.

TABLE 4.47.—NORMALIZED SENSITIVITY COEFFICIENTS WITH RESPECT TO RATE COEFFICIENT PARAMETER A_1 FOR TEST PROBLEM 7

Time, s	Normalized sensitivities with respect to A_1								
	$\langle \partial \sigma_{\Phi} / \partial A_1 \rangle$			$\langle \partial \sigma_{\Phi} / \partial A_1 \rangle$			$\langle \partial T / \partial A_1 \rangle$		
	Exact	LSENS	SENKIN	Exact	LSENS	SENKIN	Exact	LSENS	SENKIN
10^{-6}	-1.001×10^{-3}	-1.001×10^{-3}	-1.001×10^{-3}	1.000	1.000	1.000	9.990×10^{-4}	9.990×10^{-4}	9.990×10^{-4}
10^{-5}	-1.010×10^{-2}	-1.010×10^{-2}	-1.010×10^{-2}	0.9999	0.9999	0.9999	9.900×10^{-3}	9.900×10^{-3}	9.900×10^{-3}
10^{-4}	−0.1100	−0.1100	−0.1100	0.9934	0.9934	0.9934	9.003×10^{-2}	9.003×10^{-2}	9.003×10^{-2}
10^{-3}	−1.762	−1.762	−1.762	0.5514	0.5514	0.5514	0.2384	0.2384	0.2384
10^{-2}	−20.00	−20.00	−20.00	8.245×10^{-8}	8.245×10^{-8}	8.207×10^{-8}	4.122×10^{-8}	4.123×10^{-8}	4.336×10^{-8}

Table 4.47 shows that at $t = 10^{-2}$ s the normalized sensitivities $\langle \partial\sigma_\Phi/\partial A_1 \rangle$ and $\langle \partial T/\partial A_1 \rangle$ computed by SENKIN were somewhat inaccurate. LSENS, on the other hand, essentially reproduced the exact solutions. Of course, these sensitivities are very small in magnitude and therefore unimportant. Nevertheless, the results provide an opportunity to explore the effects of RTLS and ATLS on solution accuracy and computational cost and to acquire an understanding of the relationship between these tolerances and the error tolerances for the kinetics solution. Such experimentation may help identify the optimal combination of error tolerances for the two calculations. In any case, it is fairly inexpensive and not very time consuming because of the (small) size of the problem.

Now SENKIN required fewer integration steps for the sensitivity analysis computation than for the kinetics-only calculation. The number of failed steps due to local truncation error test failure was also less. Therefore smaller weighted errors were incurred by the sensitivity coefficients than by the dependent variables for the model problem. This result may of course be due to the smaller error tolerances specified for the kinetics solution than for the sensitivity coefficients. This hypothesis was verified by repeating the sensitivity calculation with RTLS = EMAX (= 10^{-6}) and ATLS = ATOLSP (= 10^{-13}). The computational cost increased to 287 steps, 822 derivative evaluations, 287 Jacobian matrix evaluations, and 2.3 s of CPU time on the VAX 8800 computer, but the accuracy was worse: $\langle \partial\sigma_\Phi/\partial A_1 \rangle = 8.132\times10^{-8}$ and $\langle \partial T/\partial A_1 \rangle = 4.718\times10^{-8}$ at $t = 10^{-2}$ s. Because ATLS = 10^{-13} was not small enough to guarantee relative error control for these sensitivity coefficients, it was decreased to 10^{-15}. The computational cost was essentially the same as with ATLS = 10^{-13}, but the accuracy improvement was mixed: $\langle \partial\sigma_\Phi/\partial A_1 \rangle = 8.376\times10^{-8}$ and $\langle \partial T/\partial A_1 \rangle = 3.954\times10^{-8}$ at $t = 10^{-2}$ s. When RTLS and ATLS were both increased to 10^{-2}, the computational cost was 220 steps, 654 functional evaluations, 226 Jacobian matrix evaluations, 1.8 s of CPU time on the VAX 8800 computer, and $\langle \partial\sigma_\Phi/\partial A_1 \rangle = 8.153\times10^{-8}$ and $\langle \partial T/\partial A_1 \rangle = 3.884\times10^{-8}$ at $t = 10^{-2}$ s. Surprisingly, this run was marginally more expensive than the one with RTLS = 10^{-5} and ATLS = 10^{-5} but not as accurate. It was, however, more accurate than the RTLS = 10^{-6} and ATLS = 10^{-13} run and about as accurate as that with RTLS = 10^{-6} and ATLS = 10^{-15}, despite using much larger tolerances. Therefore the selection procedure for the optimal values of RTLS and ATLS is not clear.

The effects of all error tolerances on solution accuracy and computational cost were further examined as follows: (To minimize execution time, all calculations were performed on the VAX 9410 computer.) RTLS was varied from 10^{-2} to 10^{-12}, with ATLS = 10^{-9}RTLS. For each RTLS, starting with a value of 10^{-2}, EMAX was progressively decreased, with ATOLSP = 10^{-7}EMAX, until the larger normalized sensitivity coefficients agreed with the exact solutions to four significant figures. The computational work required for each such combination of RTLS and EMAX is given in table 4.48, together with the error tolerances and the computed solutions for $\langle \partial\sigma_\Phi/\partial A_1 \rangle$ and $\langle \partial T/\partial A_1 \rangle$ at $t = 10^{-2}$ s. In this table NEF is the number of steps on which the local error test failed (and so had to be repeated). Several conclusions are apparent from table 4.48. Decreasing RTLS generally increases computational cost, without an attendant improvement in accuracy.

TABLE 4.48.—EFFECTS OF LOCAL ERROR TOLERANCES FOR MODEL PROBLEM AND SENSITIVITY COEFFICIENTS ON COMPUTATIONAL WORK REQUIRED BY SENKIN FOR TEST PROBLEM 7 AND SELECTED NORMALIZED SENSITIVITY COEFFICIENTS AT $t = 10^{-2}$ s

Local relative error tolerance for sensitivity coefficients, RTLS[a]	Local relative error tolerance for model problem, EMAX[b]	Computational work					Normalized sensitivity coefficients of σ_Φ and T with respect to A_1 at 10^{-2} s	
		NSTEP	NFE[c]	NJE	NEF	CPU, s	$\langle \partial\sigma_\Phi/\partial A_1 \rangle$	$\langle \partial T/\partial A_1 \rangle$
10^{-2}	10^{-6}	222	659	228	6	0.29	8.302×10^{-8}	4.061×10^{-8}
10^{-3}	10^{-6}	221	635	224	3	0.30	8.534×10^{-8}	3.909×10^{-8}
10^{-4}	10^{-6}	226	642	227	1	0.29	8.234×10^{-8}	4.213×10^{-8}
10^{-5}	10^{-2}	185	415	188	3	0.21	8.401×10^{-8}	3.639×10^{-8}
10^{-6}	10^{-2}	252	548	259	7	0.32	8.086×10^{-8}	4.129×10^{-8}
10^{-7}	10^{-2}	386	788	391	5	0.46	8.282×10^{-8}	4.441×10^{-8}
10^{-8}	10^{-2}	538	1 084	542	4	0.64	8.187×10^{-8}	3.995×10^{-8}
10^{-9}	10^{-2}	2 001	4 068	2 034	33	2.4	8.234×10^{-8}	4.110×10^{-8}
10^{-10}	10^{-2}	10 416	21 572	10 786	370	12	8.262×10^{-8}	4.133×10^{-8}
10^{-11}	10^{-2}	87 738	182 468	91 234	3 496	103	8.251×10^{-8}	4.115×10^{-8}
10^{-12}	10^{-2}	776 985	1 624 056	812 028	35 043	905	8.245×10^{-8}	4.138×10^{-8}

[a]ATLS = 10^{-9}RTLS.
[b]ATOLSP = 10^{-7}EMAX.
[c]Does not include number of derivatives required for numerical $\{\partial f_i/\partial y_j\}$ and $\{\partial f_i/\partial \eta_j\}$.

In fact, no RTLS reproduced the exact solution. In addition, the solutions did not converge as RTLS was decreased; that is, the solutions did not become tolerance independent. For RTLS $\leq 10^{-5}$ even EMAX $= 10^{-2}$ satisfied the accuracy requirement. Contrast this value to the 10^{-6} needed with RTLS $= 10^{-5}$ and ATLS $= 10^{-5}$. The accuracy improvement gained by using relative error control is obvious. The run with EMAX $= 10^{-6}$ and RTLS $= 10^{-2}$ was a little faster and somewhat more accurate and experienced fewer failed steps than that with EMAX $= 10^{-2}$ and RTLS $= 10^{-6}$. Also for EMAX $= 10^{-6}$ the number of failed steps decreased as RTLS was reduced, but not so for EMAX $= 10^{-2}$. However, for the former EMAX the RTLS values were much larger than for the latter and not varied as extensively (table 4.48). Therefore, to better understand the relationship between EMAX and RTLS, the effects of RTLS on the EMAX $= 10^{-6}$ and ATOLSP $= 10^{-13}$ results were studied: RTLS was varied between 10^{-2} and 10^{-12}, with ATLS $= 10^{-9}$RTLS. RTLS values less than 10^{-12} were not attempted because of excessive computational work. For example, the run with RTLS $= 10^{-13}$ exceeded 1 million steps at $t \approx 8.6\times10^{-11}$ s and required an execution time of well over 1000 s to advance the solution to this reaction time. The computational work requirement and normalized sensitivities $\langle \partial\sigma_\Phi/\partial A_1 \rangle$ and $\langle \partial T/\partial A_1 \rangle$ at $t = 10^{-2}$ s are given in table 4.49. Again the exact solutions were not reproduced although in general these results were more accurate than those produced with EMAX $= 10^{-2}$. Also, except for RTLS $= 10^{-12}$, the number of error test failures with EMAX $= 10^{-6}$ was either comparable to, or less than, that with EMAX $= 10^{-2}$. These factors indicate that the accuracy of the kinetics solution controls the accuracy of the sensitivity coefficients. The computational cost of the smaller EMAX was not significantly different from that required by EMAX $= 10^{-2}$. Thus the general conclusion is to generate an accurate kinetics solution and use somewhat loose error tolerances for the sensitivity coefficients, as recommended by Lutz et al. (ref. 102).

The next experiment examined the effects of local error tolerance for the kinetics solution. For RTLS $= 10^{-6}$ and ATLS $= 10^{-15}$, EMAX was varied from 10^{-2} to the smallest value, 10^{-14}, allowed by the code, keeping ATOLSP $= 10^{-7}$EMAX. The computational work requirement and normalized sensitivities $\langle \partial\sigma_\Phi/\partial A_1 \rangle$ and $\langle \partial T/\partial A_1 \rangle$ at $t = 10^{-2}$ s are given in table 4.50. This table shows that while the computational cost generally increased with a reduction in EMAX, the results did not get progressively more accurate. Indeed no EMAX value reproduced the exact solution. What is more disconcerting is that the numerical solutions did not converge as EMAX was reduced. The reason for failure to reproduce the exact solutions may be the use of finite-difference approximations for $\mathbf{J}$ and $\{\partial f_i/\partial \eta_j\}$. As observed with the BFM, $\Delta\eta_j$ must be selected with care to ensure accurate results. Comparing tables 4.49 and 4.50 shows that the computational cost increased much more rapidly with decreasing RTLS than with decreasing EMAX. This behavior was much more pronounced for RTLS $\leq$ EMAX. Thus the need to exercise caution in selecting RTLS is clear. If accuracy improvement is desired, it is accomplished much more economically by reducing EMAX than by reducing RTLS.

Finally solution was attempted with EMAX $= 10^{-12}$, ATOLSP $= 10^{-19}$, RTLS $= 10^{-12}$, and ATLS $= 10^{-21}$. The computational cost was 782 770 steps, 1 931 409

TABLE 4.49.—EFFECTS OF LOCAL ERROR TOLERANCE FOR SENSITIVITY COEFFICIENTS ON COMPUTATIONAL WORK REQUIRED BY SENKIN FOR TEST PROBLEM 7 AND SELECTED NORMALIZED SENSITIVITY COEFFICIENTS AT $t = 10^{-2}$ s (EMAX = 10^{-6}, ATOLSP = 10^{-13})

Local relative error tolerance for sensitivity coefficients, RTLS[a]	Computational work					Normalized sensitivity coefficients of σ_Φ and T with respect to A_1 at 10^{-2} s	
	NSTEP	NFE[b]	NJE	NEF	CPU, s	$\langle \partial\sigma_\Phi/\partial A_1 \rangle$	$\langle \partial T/\partial A_1 \rangle$
10^{-2}	222	659	228	6	0.29	8.302×10^{-8}	4.061×10^{-8}
10^{-3}	221	635	224	3	0.30	8.534×10^{-8}	3.909×10^{-8}
10^{-4}	226	642	227	1	0.29	8.234×10^{-8}	4.213×10^{-8}
10^{-5}	278	804	282	4	0.36	8.262×10^{-8}	4.397×10^{-8}
10^{-6}	289	825	291	2	0.38	8.376×10^{-8}	3.954×10^{-8}
10^{-7}	347	946	347	0	0.45	8.339×10^{-8}	4.071×10^{-8}
10^{-8}	543	1 374	549	6	0.68	8.202×10^{-8}	4.014×10^{-8}
10^{-9}	1 984	4 106	2 016	32	2.3	8.233×10^{-8}	4.149×10^{-8}
10^{-10}	10 436	21 524	10 762	326	12	8.256×10^{-8}	4.151×10^{-8}
10^{-11}	87 171	181 018	90 509	3 338	102	8.246×10^{-8}	4.123×10^{-8}
10^{-12}	780 157	1 631 287	815 643	35 486	915	8.244×10^{-8}	4.119×10^{-8}

[a]ATLS = 10^{-9}RTLS.

[b]Does not include number of derivatives required for numerical $\{\partial f_i/\partial y_j\}$ and $\{\partial f_i/\partial \eta_j\}$.

TABLE 4.50.—EFFECTS OF LOCAL ERROR TOLERANCE FOR MODEL PROBLEM ON COMPUTATIONAL WORK REQUIRED BY SENKIN FOR TEST PROBLEM 7 AND SELECTED NORMALIZED SENSITIVITY COEFFICIENTS AT $t = 10^{-2}$ s (RTLS = 10^{-6}, ATLS = 10^{-15})

Local relative error tolerance for model problem, EMAX[a]	Computational work					Normalized sensitivity coefficients of σ_Φ and T with respect to A_1 at 10^{-2} s	
	NSTEP	NFE[b]	NJE	NEF	CPU, s	$\langle \partial \sigma_\Phi / \partial A_1 \rangle$	$\langle \partial T / \partial A_1 \rangle$
10^{-2}	252	548	259	7	0.32	8.086×10^{-8}	4.129×10^{-8}
10^{-3}	239	522	242	3	0.30	7.972×10^{-8}	3.961×10^{-8}
10^{-4}	239	622	243	4	0.32	8.333×10^{-8}	3.782×10^{-8}
10^{-5}	253	716	257	4	0.34	8.151×10^{-8}	4.496×10^{-8}
10^{-6}	289	825	291	2	0.38	8.376×10^{-8}	3.954×10^{-8}
10^{-7}	310	888	311	1	0.41	8.191×10^{-8}	4.441×10^{-8}
10^{-8}	424	1234	425	1	0.56	8.236×10^{-8}	4.363×10^{-8}
10^{-9}	561	1647	563	2	0.76	8.196×10^{-8}	4.223×10^{-8}
10^{-10}	793	2340	793	0	1.1	8.237×10^{-8}	3.897×10^{-8}
10^{-11}	1120	3325	1120	0	1.5	8.244×10^{-8}	4.157×10^{-8}
10^{-12}	1642	4897	1646	4	2.3	8.271×10^{-8}	4.059×10^{-8}
10^{-13}	2423	7169	2425	2	3.2	8.253×10^{-8}	3.900×10^{-8}
10^{-14}	3369	9369	3373	4	4.4	8.291×10^{-8}	4.131×10^{-8}

[a]ATOLSP = 10^{-7}EMAX.

[b]Does not include number of derivatives required for numerical $\{\partial f_i / \partial y_j\}$ and $\{\partial f_i / \partial \eta_j\}$.

derivative evaluations, 817 289 Jacobian matrix evaluations, 973 s of CPU time, and $\langle \partial \sigma_\Phi / \partial A_1 \rangle = 8.242 \times 10^{-8}$ and $\langle \partial T / \partial A_1 \rangle = 4.133 \times 10^{-8}$ at $t = 10^{-2}$ s. Despite such stringent accuracy requirements (34 519 steps failed because the local error test was not satisfied) SENKIN did not reproduce the exact solution. These results reinforce the doubts raised previously about the need for local error test and control during the sensitivity computations. Note that LSENS essentially reproduced the exact solution, despite using fully dependent error control: EMAX = 10^{-7} gave the exact solution and the execution times were 0.10 and 0.59 s on the VAX 9410 and 8800 computers. The results presented here also show that reducing the local error tolerances for sensitivity coefficients does not necessarily effect better accuracy, and more significantly that specifying very small values for these tolerances can result in prohibitive computational cost.

Sensitivities with respect to n_1 and E_1 could not be obtained analytically. Therefore BFM results were generated for these quantities on the Cray-XM/P computer using EMAX = 10^{-12}, ATOLSP = 10^{-19}, and double-precision arithmetic. The normalized sensitivities with respect to n_1 and E_1 obtained with the BFM and LSENS are listed in tables 4.51 and 4.52. These tables show that the accuracy of the DDM for this nonisothermal problem was excellent at all reaction conditions.

In tables 4.53 and 4.54 the sensitivity coefficients of the temporal derivatives of the dependent variables are presented to illustrate the capability of LSENS to compute these quantities. The analytical solutions were evaluated by differentiating the ODE's with respect to the appropriate parameter. The solutions with respect to all initial conditions and A_1 are exact, but those with respect to n_1 and E_1 were computed by using the BFM results for $\{\partial Y_i / \partial n_1\}$ and $\{\partial Y_i / \partial E_1\}$. Again the agreement between the analytical and LSENS results was excellent for the important sensitivities, illustrating the accuracy of the DDM for nonisothermal problems. For reasons given previously the code had difficulty tracking sensitivities that are zero in magnitude.

On the Amdahl 5870 computer LSENS required 176 steps, 196 derivative evaluations, 16 Jacobian matrix evaluations and LU-decompositions, and 0.048 s of execution time to solve for the dependent variables (species mole numbers, temperature, and density). The computational cost for the dependent variables and sensitivities with respect to all four initial conditions and all three rate coefficient parameters was 0.21 s. The BFM would require at least 0.38 s. Thus the DDM was more efficient and, as discussed previously, also more accurate than the BFM for this nonisothermal problem.

This test problem was selected because the analytical solution is known, thereby permitting an objective evaluation of the accuracy of the DDM in general and LSENS in particular for nonisothermal problems. However, it is recognized that the (small) size of the problem precludes drawing definitive conclusions regarding efficiency. Two additional, and more realistic, nonisothermal problems were therefore studied.

TABLE 4.51.—NORMALIZED SENSITIVITY COEFFICIENTS WITH RESPECT TO RATE COEFFICIENT PARAMETER n_1 FOR TEST PROBLEM 7

Time, s	Normalized sensitivities with respect to n_1					
	$\langle \partial \sigma_R / \partial n_1 \rangle$		$\langle \partial \sigma_\Phi / \partial n_1 \rangle$		$\langle \partial T / \partial n_1 \rangle$	
	BFM	LSENS	BFM	LSENS	BFM	LSENS
10^{-6}	-1.001×10^{-3}	-1.001×10^{-3}	1.000	1.000	9.991×10^{-4}	9.991×10^{-4}
10^{-5}	-1.011×10^{-2}	-1.011×10^{-2}	1.001	1.001	9.907×10^{-3}	9.907×10^{-3}
10^{-4}	−0.1107	−0.1107	1.000	1.000	9.066×10^{-2}	9.066×10^{-2}
10^{-3}	−1.850	−1.850	0.5792	0.5792	0.2504	0.2504
10^{-2}	−21.89	−21.89	9.023×10^{-8}	9.024×10^{-8}	4.511×10^{-8}	4.512×10^{-8}

TABLE 4.52.—NORMALIZED SENSITIVITY COEFFICIENTS WITH RESPECT TO RATE COEFFICIENT PARAMETER E_1 FOR TEST PROBLEM 7

Time, s	Normalized sensitivities with respect to E_1					
	$\langle \partial \sigma_R / \partial E_1 \rangle$		$\langle \partial \sigma_\Phi / \partial E_1 \rangle$		$\langle \partial T / \partial E_1 \rangle$	
	BFM	LSENS	BFM	LSENS	BFM	LSENS
10^{-6}	-1.000×10^{-3}	-1.000×10^{-3}	0.9995	0.9991	9.985×10^{-4}	9.981×10^{-4}
10^{-5}	-1.005×10^{-2}	-1.005×10^{-2}	0.9950	0.9949	9.851×10^{-3}	9.850×10^{-3}
10^{-4}	−0.1048	−0.1048	0.9468	0.9468	8.582×10^{-2}	8.582×10^{-2}
10^{-3}	−1.262	−1.262	0.3949	0.3949	0.1707	0.1707
10^{-2}	−10.50	−10.50	4.328×10^{-8}	4.329×10^{-8}	2.164×10^{-8}	2.164×10^{-8}

TABLE 4.53.—NORMALIZED SENSITIVITY COEFFICIENTS OF TEMPORAL DERIVATIVES OF DEPENDENT VARIABLES WITH RESPECT TO INITIAL CONDITION VALUES FOR TEST PROBLEM 7

Time, s	Normalized sensitivities of temporal derivatives with respect to initial condition values									
	$\langle \partial \dot{\sigma}_i / \partial \sigma_{\Phi,0} \rangle$[a]		$\langle \partial \dot{T} / \partial \sigma_{\Phi,0} \rangle$		$\langle \partial \dot{\sigma}_i / \partial \sigma_{\Phi,0} \rangle$[a]		$\langle \partial \dot{T} / \partial \sigma_{\Phi,0} \rangle$		$\langle \partial \dot{y}_i / \partial T_0 \rangle$[b]	
	Exact	LSENS	Exact	LSENS	Exact	LSENS	Exact	LSENS	Exact	LSENS
10^{-6}	1.000	1.000	0.0	1.999×10^{-17}	-9.990×10^{-8}	-1.339×10^{-7}	-1.001×10^{-4}	-1.001×10^{-4}	0.9990	0.9987
10^{-5}	1.000	1.000	0.0	-5.948×10^{-14}	-9.900×10^{-7}	-9.900×10^{-7}	-1.010×10^{-4}	-1.010×10^{-4}	0.9899	0.9899
10^{-4}	1.000	1.000	0.0	1.589×10^{-10}	-8.970×10^{-6}	-8.971×10^{-6}	-1.090×10^{-4}	-1.090×10^{-4}	0.8904	0.8904
10^{-3}	1.000	1.000	0.0	-5.371×10^{-7}	0.0	-3.652×10^{-9}	-1.000×10^{-4}	-1.000×10^{-4}	–0.5232	–0.5231
10^{-2}	1.000	1.000	0.0	-4.586×10^{-6}	9.000×10^{-4}	9.000×10^{-4}	8.000×10^{-4}	8.000×10^{-4}	–10.00	–10.00

[a]For each initial condition value η (= $\sigma_{\Phi,0}$ and $\sigma_{\Phi,0}$), $\langle \partial \dot{\sigma}_\Phi / \partial \eta \rangle = \langle \partial \dot{\sigma}_\Phi / \partial \eta \rangle$.
[b]For T_0, $\langle \partial \dot{\sigma}_\Phi / \partial T_0 \rangle = \langle \partial \dot{\sigma}_\Phi / \partial T_0 \rangle = \langle \partial \dot{T} / \partial T_0 \rangle$.

TABLE 4.54.—NORMALIZED SENSITIVITY COEFFICIENTS OF TEMPORAL DERIVATIVES OF DEPENDENT VARIABLES WITH RESPECT TO RATE COEFFICIENT PARAMETERS FOR TEST PROBLEM 7

Time, s	Normalized sensitivities of $\dot{y}_i$ with respect to parameter–[a]					
	A_1		n_1		E_1	
	Exact	LSENS	Exact	LSENS	Exact	LSENS
10^{-6}	1.000	1.000	1.000	1.000	0.9990	0.9987
10^{-5}	0.9998	0.9998	1.001	1.001	0.9899	0.9899
10^{-4}	0.9801	0.9801	0.9937	0.9937	0.8904	0.8904
10^{-3}	–0.5232	–0.5230	–0.5176	–0.5177	–0.5236	–0.5231
10^{-2}	–19.00	–19.00	–20.79	–20.79	–10.00	–10.00

[a]For each rate coefficient parameter η (= A_1, n_1, and E_1), $\langle \partial \dot{\sigma}_\Phi / \partial \eta \rangle = \langle \partial \dot{\sigma}_\Phi / \partial \eta \rangle = \langle \partial \dot{T} / \partial \eta \rangle$.

4.6.6 Combustion of Hydrogen-Oxygen-Nitrogen

The constant-pressure, adiabatic reaction of a stoichiometric hydrogen-oxygen-nitrogen mixture at 2 atm and 1500 K initial temperature was considered. The nitrogen-to-oxygen molar ratio was the standard value (3.72735) built into the code (see chapter 8 of part II). The fuel-air stoichiometry and air composition correspond to the following initial mixture composition: 29.73 percent hydrogen, 14.86 percent oxygen, and 55.41 percent nitrogen.

The reaction mechanism for test problem 8 consisted of 30 reversible reactions among 13 reacting species (H_2, O_2, N_2, O, H, OH, HO_2, H_2O_2, N, NO, NO_2, N_2O, and H_2O). The kinetic mechanism and forward rate coefficient parameters are listed in table 4.55. The hydrogen-oxygen mechanism is the most recent version of the scheme developed by Brabbs and Musiak (ref. 109) and is given by Bittker (ref. 110). The nitrogen-oxygen reactions were taken from Brabbs et al. (ref. 111). For each reaction the backward rate coefficient was computed by using the law of microscopic reversibility, equation (2.6), and the concentration equilibrium constant. In using this procedure Brabbs and Musiak (ref. 109) discovered that the heat of formation of HO_2 was an important factor when calculating k_{-4} for the initiation reaction (–4). Following their recommendation a heat of formation of 500 cal/mole was used for this species.

The variations of the species mole fractions and temperature with reaction time are illustrated in figure 4.10. The three regimes described in the previous chapter, induction, heat release, and equilibration, are apparent. In order to check the accuracy of the DDM in all combustion regimes, sensitivity coefficients were generated at the output stations t = 10^{-6}, 3×10^{-6}, 5×10^{-6}, 7.5×10^{-6}, 1.5×10^{-5}, 10^{-4}, 10^{-3}, 10^{-2}, 0.1, and 1 s. The mixture temperatures obtained with LSENS and SENKIN at these reaction times are given in table 4.56, which shows that these times encompassed all reaction conditions from preignition to when the system had essentially equilibrated. In order to confirm that a reaction time of 1 s was indeed long enough for the system to equilibrate, the composition and temperature at chemical equilibrium were computed by using the procedure described in chapter 5. These results were essentially identical to the kinetics solution at 1 s, indicating that the system had equilibrated at this reaction time and the reaction mechanism gave the correct final state.

To ensure that comparison of codes was meaningful, the numerical results with both LSENS and SENKIN were generated with the same thermodynamic data and local error tolerances: EMAX = 10^{-7} and ATOLSP = 10^{-16}, for reasons given later. Table 4.56 shows that at each reaction time the two codes gave essentially the same temperature. For the kinetics-only calculation SENKIN required 707 steps, 1441 derivative evaluations, 62 Jacobian matrix evaluations, and 3.1 s of CPU time on the VAX 9410 computer. The computational cost of LSENS was 735 steps, 996 derivative evaluations, 94 Jacobian matrix evaluations, and 1.2 s of CPU time. When the method given by MF = 22 was used, LSENS required 711 steps, 2188 derivative evaluations, 83 Jacobian matrix evaluations, and 1.5 s of CPU time. Therefore for this problem LSENS was faster than SENKIN by a factor of between

TABLE 4.55.—REACTION MECHANISM AND FORWARD RATE COEFFICIENT PARAMETERS FOR TEST PROBLEM 8

Reaction number, j	Reaction	Forward rate coefficient parameters[a]		
		A_j	n_j	E_j
1	$O + H_2O \rightleftharpoons OH + OH$	6.80(13)	0.0	18 365
2	$H + O_2 \rightleftharpoons OH + O$	1.89(14)	0.0	16 400
3	$O + H_2 \rightleftharpoons OH + H$	4.20(14)	0.0	13 750
4	$H + HO_2 \rightleftharpoons H_2 + O_2$	7.28(13)	0.0	2 126
5	$O + HO_2 \rightleftharpoons OH + O_2$	5.00(13)	0.0	1 000
6	$HO_2 + OH \rightleftharpoons H_2O + O_2$	8.00(12)	0.0	0
7	$H + HO_2 \rightleftharpoons OH + OH$	1.34(14)	0.0	1 070
8	$H_2 + HO_2 \rightleftharpoons H_2O_2 + H$	7.91(13)	0.0	25 000
9	$OH + H_2O_2 \rightleftharpoons H_2O + HO_2$	6.10(12)	0.0	1 430
10	$HO_2 + HO_2 \rightleftharpoons H_2O_2 + O_2$	1.80(12)	0.0	0
11	$H + H_2O_2 \rightleftharpoons OH + H_2O$	7.80(11)	0.0	0
[b]12	$H_2O_2 + M \rightleftharpoons OH + OH + M$	1.44(17)	0.0	45 510
13	$H_2 + OH \rightleftharpoons H_2O + H$	4.74(13)	0.0	6 098
[b]14	$H + O_2 + M \rightleftharpoons HO_2 + M$	1.46(15)	0.0	–1 000
[b]15	$H_2O + M \rightleftharpoons H + OH + M$	1.30(15)	0.0	105 140
16	$H + O + M \rightleftharpoons OH + M$	7.10(18)	–1.0	0
[b]17	$H_2 + M \rightleftharpoons H + H + M$	2.20(14)	0.0	96 000
18	$O_2 + M \rightleftharpoons O + O + M$	1.80(18)	–1.0	118 020
19	$HO_2 + NO \rightleftharpoons NO_2 + OH$	2.09(12)	0.0	–477
20	$O + NO_2 \rightleftharpoons NO + O_2$	1.00(13)	0.0	596
21	$NO + O + M \rightleftharpoons NO_2 + M$	5.62(15)	0.0	–1 160
22	$NO_2 + H \rightleftharpoons NO + OH$	3.47(14)	0.0	1 470
23	$NO + O \rightleftharpoons N + O_2$	3.80(9)	1.0	41 370
24	$O + N_2 \rightleftharpoons NO + N$	1.80(14)	0.0	76 250
25	$NO + H \rightleftharpoons N + OH$	2.63(14)	0.0	50 410
26	$N_2O + M \rightleftharpoons N_2 + O + M$	6.92(23)	–2.5	65 000
27	$O + N_2O \rightleftharpoons N_2 + O_2$	1.00(14)	0.0	28 020
28	$O + N_2O \rightleftharpoons NO + NO$	6.92(13)	0.0	26 630
29	$N + NO_2 \rightleftharpoons NO + NO$	4.00(12)	0.0	0
30	$N_2O + H \rightleftharpoons N_2 + OH$	7.59(13)	0.0	15 100

[a]Rate coefficient $k_j = A_j T^{n_j} \exp(-E_j/RT)$; units are moles, centimeters, seconds, and calories; numbers in parentheses are powers of 10.

[b]Third-body collisional efficiencies:

Reaction 12: $H_2 = 2.3$, $O_2 = 0.78$, $H_2O = 6.0$, $H_2O_2 = 6.6$

Reaction 14: $H_2 = 3.0$, $O_2 = 1.3$, $H_2O = 21.3$, $N_2 = 1.3$

Reaction 15: $H_2 = 4.0$, $O_2 = 1.5$, $H_2O = 20.0$, $N_2 = 1.5$

Reaction 17: $H_2 = 4.1$, $O_2 = 2.0$, $H_2O = 15.0$, $N_2 = 2.0$.

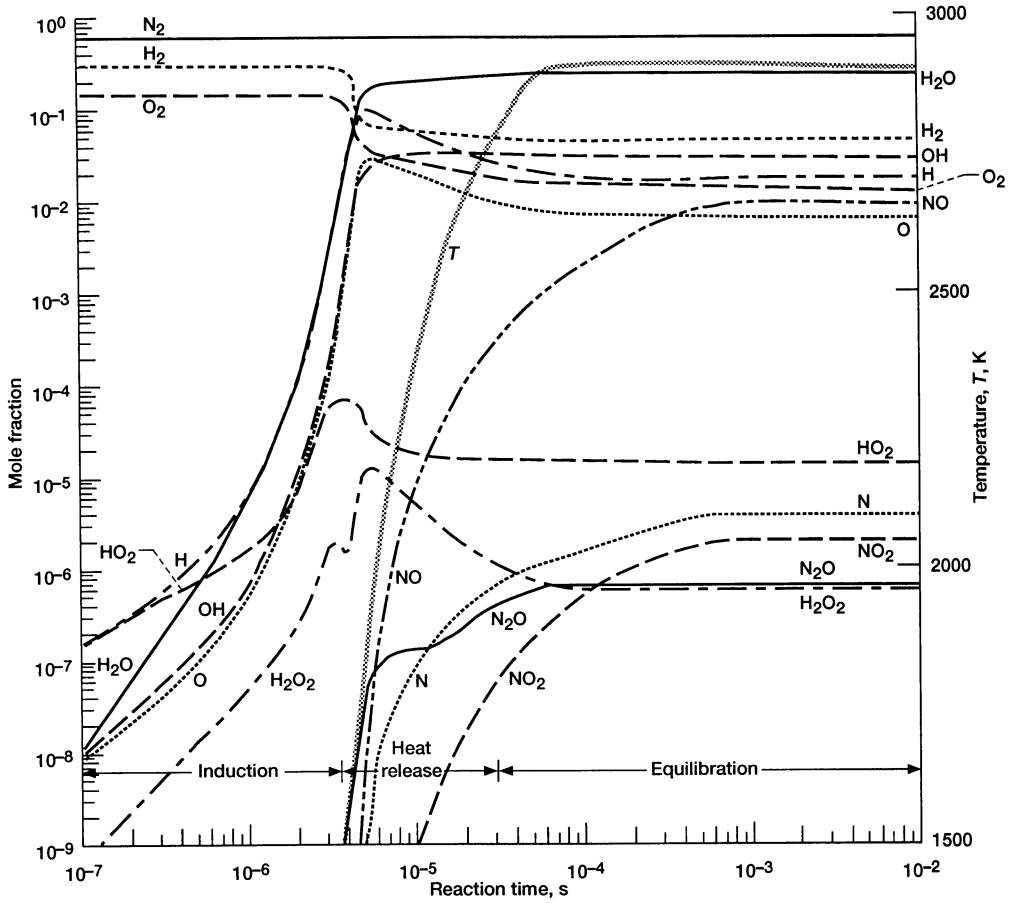

Figure 4.10.—Variation of species mole fractions and temperature with reaction time for test problem 8.

TABLE 4.56.—VARIATION OF TEMPERATURE WITH REACTION TIME FOR TEST PROBLEM 8

Reaction time, s	Temperature, K	
	LSENS	SENKIN
10^{-6}	1500.0	1500.0
3×10^{-6}	1502.5	1502.5
5×10^{-6}	1829.4	1828.8
7.5×10^{-6}	2203.9	2203.5
1.5×10^{-5}	2562.3	2562.0
10^{-4}	2920.4	2920.4
10^{-3}	2911.6	2911.6
10^{-2}	2911.4	2911.4
0.1	2911.4	2911.4
1.0	2911.4	2911.4

about 2 and 2.5. Note also that the average number of derivative evaluations per step was less for LSENS than for SENKIN. This fact means that on average LSODE required fewer corrector iterations per step than DASSL to achieve solution convergence.

Normalized sensitivity coefficients of the dependent variables (species mole numbers, temperature, and density) with respect to all initial conditions at the eight output stations, $t = 10^{-6}$, 3×10^{-6}, 5×10^{-6}, 7.5×10^{-6}, 1.5×10^{-5}, 10^{-4}, 10^{-3}, and 1 s, are given in tables 4.57 to 4.64. (The results at 0.01 and 0.1 s were identical to those at 1 s and are therefore not reported.) Also given in these tables are the BFM results, which were generated on the NASA Lewis Research Center's Cray-XM/P and Cray-YM/P computers and NASA Ames Research Center's Cray-2 computer; in all cases, double-precision arithmetic was used. The BFM solutions were generated with EMAX $\leq 10^{-12}$ (ATOLSP = 10^{-9}EMAX). For EMAX = 10^{-12} and ATOLSP = 10^{-21}, $\delta_{c3}(\sigma_{j,0})$ could not be determined at $t = 10^{-4}$ and 10^{-3} s for several initial conditions, especially those of the active intermediates such as H and O. For example, for $\sigma_{H,0}$, EMAX had to be reduced to 10^{-16} to produce reliable results. Even by using such small EMAX values, $\delta_{c4}(\sigma_{j,0})$ could not be determined for several species. The results are therefore given to three significant figures only. With LSENS, EMAX had to be decreased to 10^{-7} (ATOLSP = 10^{-9}EMAX) to obtain essentially tolerance-independent sensitivities during equilibration. (To achieve the same result for the kinetics solution during heat release required an EMAX value of 10^{-5}. The same was true of the kinetics-only calculation with SENKIN.) Therefore, if accurate sensitivity coefficients are required, especially during equilibration when they are small in magnitude, the EMAX needed to produce accurate kinetics solutions must first be determined, and

then sensitivity analysis performed with a somewhat smaller EMAX. Tables 4.57 to 4.64 show the excellent agreement between the BFM and LSENS solutions in all regimes of the combustion problem. This agreement is especially noteworthy because the results given in these tables span over 30 orders of magnitude.

Normalized sensitivity coefficients with respect to the preexponential factors $\{A_j\}$ at reaction times $t = 10^{-6}$, 3×10^{-6}, 5×10^{-6}, 7.5×10^{-6}, 1.5×10^{-5}, 10^{-4}, and 10^{-3} s are listed in tables 4.65 to 4.71. For each dependent variable i the 10 most important reactions in order of decreasing $|\langle\partial Y_i/\partial A_j\rangle|$ are listed. All methods produced the same reaction importance lists for all variables at all output times. Therefore, for clarity in presentation, only one reaction importance list appears for each dependent variable in tables 4.65 to 4.71. These tables also give the normalized sensitivity coefficients $\{\langle\partial Y_i/\partial A_j\rangle\}$ produced by LSENS, SENKIN, and the BFM, which used EMAX = 10^{-12} and ATOLSP = 10^{-21}, except for A_3, which required EMAX = 10^{-14} and ATOLSP = 10^{-23}. The magnitudes of the $\{\langle S_{ij}\rangle\}$ were not considered in constructing the tables. The reason is that it is just as important to verify that reactions predicted to be unimportant are indeed so, as it is to validate the accuracy of sensitivity coefficients with large magnitude.

It was difficult to judge convergence of the BFM results at $t = 10^{-3}$ s for several A_j (none of which appears in table 4.71). At longer times virtually none of the sensitivity coefficients converged. The reason is that at long reaction time, when the system is equilibrating, the sensitivity coefficients become very small in magnitude. Indeed at equilibrium they must vanish, for reasons discussed in section 4.6.1. However, because of roundoff errors, the BFM did not reproduce this result. For the same reason LSENS predicted nonzero sensitivities at long times. Note, however, that a requirement for the code to be accurate is that the sensitivity coefficients at long times must reach steady-state values, which must be small in magnitude. The LSENS results at 1 s showed that all $\{|\langle S_{ij}\rangle|\} \leq 1.1\times10^{-8}$. In addition, for H_2O, sensitivities with respect to A_2 and A_{29} (the two reactions were ranked first and thirtieth, respectively, at $t = 1$ s) were generated at various times up to $t = 10$ s. For $t \geq 0.15$ s the normalized sensitivities agreed with one another to three significant figures at all print stations. The same level of agreement was displayed at all $t \geq 0.1$ s by the results generated on the VAX 9410 computer. In fact, for $t \geq 0.1$ s the reaction importance lists were identical for all dependent variables at all print stations. All $\{\langle S_{ij}\rangle\}$ were also identical, except $\langle\partial\sigma_{N_2}/\partial A_{14}\rangle$, which was constant for $t \geq 0.25$ s. This sensitivity coefficient was, however, essentially the same at the two times: 2.234×10^{-12} and 2.235×10^{-12}, respectively, at $t = 0.1$ and 0.25 s. Finally the complete reaction importance lists containing all 30 preexponential factors were identical for all dependent variables at all $t \geq 0.3$ s.

To check further the consistency of the preexponential factor sensitivities computed by LSENS, the following tests, after Dougherty et al. (ref. 90), were made. Mass conservation provided the basis for the first test. Because mass is conserved during the chemical reaction, the composition must satisfy the following constraint:

TABLE 4.57.—NORMALIZED SENSITIVITY COEFFICIENTS WITH RESPECT

Sensitivity parameter	Normalized sensitivity						
	σ_O	σ_{H_2O}	σ_{OH}	σ_H	σ_{O_2}	σ_{H_2}	σ_{HO_2}
$\sigma_{H_2,0}$	6.31(−1)	1.57	6.55(−1)	1.52	−5.04(−5)	1.00	1.11
	6.31(−1)	1.57	6.55(−1)	1.52	−5.04(−5)	1.00	1.11
$\sigma_{O_2,0}$	3.36	2.91	3.34	2.44	1.00	−1.00(−4)	1.35
	3.36	2.91	3.34	2.44	1.00	−1.00(−4)	1.35
$\sigma_{N_2,0}$	−2.84(−2)	−1.87(−2)	−2.67(−2)	−3.00(−2)	−1.91(−7)	6.21(−7)	6.30(−2)
	−2.84(−2)	−1.87(−2)	−2.67(−2)	−3.00(−2)	−1.91(−7)	6.21(−7)	6.30(−2)
$\sigma_{O,0}$	3.24(2)	3.87(2)	3.24(2)	3.21(2)	−1.02(−2)	−1.28(−2)	6.00(1)
	3.24(2)	3.87(2)	3.24(2)	3.21(2)	−1.02(−2)	−1.28(−2)	6.00(1)
$\sigma_{H,0}$	1.93(2)	2.25(2)	1.93(2)	1.92(2)	−6.13(−3)	−7.31(−3)	3.62(1)
	1.93(2)	2.25(2)	1.93(2)	1.92(2)	−6.13(−3)	−7.31(−3)	3.62(1)
$\sigma_{OH,0}$	1.77(2)	2.19(2)	1.76(2)	1.75(2)	−5.56(−3)	−6.96(−3)	3.28(1)
	1.77(2)	2.19(2)	1.76(2)	1.75(2)	−5.56(−3)	−6.97(−3)	3.28(1)
$\sigma_{HO_2,0}$	7.36	7.93	7.79	7.39	−1.98(−4)	−2.77(−4)	5.36(1)
	7.36	7.93	7.79	7.39	−1.98(−4)	−2.77(−4)	5.36(1)
$\sigma_{H_2O_2,0}$	7.07(1)	8.80(1)	7.38(1)	7.05(1)	−2.01(−3)	−2.69(−3)	1.19(1)
	7.07(1)	8.80(1)	7.38(1)	7.05(1)	−2.01(−3)	−2.69(−3)	1.19(1)
$\sigma_{N,0}$	1.56(2)	1.77(2)	1.55(2)	1.53(2)	−5.14(−3)	−5.92(−3)	2.67(1)
	1.56(2)	1.77(2)	1.55(2)	1.53(2)	−5.14(−3)	−5.92(−3)	2.67(1)
$\sigma_{NO,0}$	1.07(−3)	1.37(−3)	1.36(−3)	1.10(−3)	−2.66(−8)	−3.92(−8)	−1.63(−3)
	1.07(−3)	1.37(−3)	1.36(−3)	1.10(−3)	−2.66(−8)	−3.92(−8)	−1.63(−3)
$\sigma_{NO_2,0}$	1.68(−2)	1.22(−1)	1.13(−1)	1.33(−2)	−4.77(−7)	−2.95(−6)	3.41(−3)
	1.68(−2)	1.22(−1)	1.13(−1)	1.33(−2)	−4.77(−7)	−2.95(−6)	3.41(−3)
$\sigma_{N_2O,0}$	4.94(−3)	5.30(−3)	4.97(−3)	4.57(−3)	−1.25(−7)	−1.77(−7)	7.49(−4)
	4.94(−3)	5.30(−3)	4.97(−3)	4.57(−3)	−1.25(−7)	−1.77(−7)	7.49(−4)
$\sigma_{H_2O,0}$	−1.15(−4)	1.56(1)	−1.22(−5)	−1.11(−4)	−1.12(−10)	2.60(−9)	1.85(−4)
	−1.15(−4)	1.56(1)	−1.22(−5)	−1.11(−4)	−1.12(−10)	2.60(−9)	1.85(−4)
T_0	3.02(1)	3.17(1)	3.26(1)	2.93(1)	−1.06(−3)	−1.14(−3)	1.94(1)
	3.02(1)	3.17(1)	3.26(1)	2.93(1)	−1.06(−3)	−1.14(−3)	1.94(1)
ρ_0	2.96	3.47	2.97	2.93	−1.06(−4)	−1.18(−4)	1.52
	2.96	3.47	2.97	2.93	−1.06(−4)	−1.18(−4)	1.52

[a]For each sensitivity parameter the top row gives the BFM results and the bottom row gives the

TO INITIAL CONDITION VALUES FOR TEST PROBLEM 8 AT $t = 10^{-6}$ s

coefficients at $t = 10^{-6}$ s of[a]							
$\sigma_{H_2O_2}$	σ_{NO}	σ_{NO_2}	σ_N	σ_{N_2}	σ_{N_2O}	T	ρ
1.94	5.34(−1)	1.54	5.69(−1)	−6.24(−13)	8.23(−1)	9.37(−7)	−4.91(−7)
1.94	5.34(−1)	1.54	5.69(−1)	−6.24(−13)	8.23(−1)	9.37(−7)	−4.91(−7)
1.16	3.05	4.10	2.64	−2.30(−12)	3.03	4.17(−6)	−3.30(−6)
1.16	3.05	4.10	2.64	−2.30(−12)	3.03	4.17(−6)	−3.30(−6)
−5.00(−2)	9.81(−1)	1.04	9.77(−1)	1.00	1.52	2.18(−6)	−2.23(−6)
−5.00(−2)	9.81(−1)	1.04	9.77(−1)	1.00	1.52	2.18(−6)	−2.23(−6)
3.92(1)	4.24(2)	5.76(2)	3.52(2)	−2.99(−10)	3.93(2)	1.48(−3)	−1.37(−3)
3.92(1)	4.24(2)	5.76(2)	3.52(2)	−2.99(−10)	3.93(2)	1.48(−3)	−1.37(−3)
2.41(1)	2.32(2)	2.94(2)	2.08(2)	−1.67(−10)	2.20(2)	8.31(−4)	−7.66(−4)
2.41(1)	2.32(2)	2.94(2)	2.08(2)	−1.67(−10)	2.20(2)	8.31(−4)	−7.66(−4)
2.17(1)	2.10(2)	2.64(2)	1.89(2)	−1.51(−10)	1.99(2)	8.75(−4)	−8.16(−4)
2.17(1)	2.10(2)	2.64(2)	1.89(2)	−1.51(−10)	1.99(2)	8.75(−4)	−8.16(−4)
1.05(2)	7.11	7.51(1)	7.23	−5.31(−12)	6.99	8.20(−6)	−8.78(−6)
1.05(2)	7.11	7.51(1)	7.23	−5.31(−12)	6.99	8.20(−6)	−8.78(−6)
8.57(2)	7.24(1)	8.24(1)	7.18(1)	−5.36(−11)	7.06(1)	1.65(−4)	−1.96(−4)
8.57(2)	7.24(1)	8.24(1)	7.18(1)	−5.36(−11)	7.06(1)	1.65(−4)	−1.96(−4)
1.59(1)	3.23(10)	7.18(10)	6.05(9)	−1.42(−10)	1.87(2)	9.30(−4)	−8.82(−4)
1.59(1)	3.23(10)	7.18(10)	6.05(9)	−1.42(−10)	1.87(2)	9.30(−4)	−8.82(−4)
−1.27(−3)	3.49(10)	9.14(10)	2.00(1)	−7.27(−16)	9.96(−4)	8.36(−9)	−8.04(−9)
−1.27(−3)	3.49(10)	9.14(10)	2.00(1)	−7.27(−16)	9.96(−4)	8.36(−9)	−8.04(−9)
2.14(−3)	2.61(8)	2.73(15)	1.17(−1)	−2.12(−14)	2.80(−2)	2.45(−6)	−2.49(−6)
2.14(−3)	2.61(8)	2.73(15)	1.17(−1)	−2.12(−14)	2.80(−2)	2.45(−6)	−2.49(−6)
4.04(−4)	1.68(3)	1.72(3)	5.31(−3)	1.08(−8)	2.39(8)	1.69(−8)	−1.99(−8)
4.04(−4)	1.68(3)	1.72(3)	5.31(−3)	1.08(−8)	2.39(8)	1.69(−8)	−1.99(−8)
1.64(−5)	−8.31(−5)	6.48(−5)	−9.57(−5)	−9.37(−18)	1.28(−5)	1.60(−9)	−1.31(−9)
1.64(−5)	−8.31(−5)	6.48(−5)	−9.58(−5)	−9.37(−18)	1.28(−5)	1.60(−9)	−1.31(−9)
2.39(1)	5.33(1)	7.07(1)	5.20(1)	−2.60(−11)	3.42(1)	1.00	2.30(−5)
2.39(1)	5.33(1)	7.07(1)	5.20(1)	−2.60(−11)	3.42(1)	1.00	2.30(−5)
2.05	3.57	5.68	3.19	−3.32(−12)	4.38	7.28(−6)	1.00
2.05	3.57	5.68	3.19	−3.32(−12)	4.38	7.28(−6)	1.00

LSENS results; numbers in parentheses are powers of 10.

TABLE 4.58.—NORMALIZED SENSITIVITY COEFFICIENTS WITH RESPECT

Sensitivity parameter	Normalized sensitivity						
	σ_O	σ_{H_2O}	σ_{OH}	σ_H	σ_{O_2}	σ_{H_2}	σ_{HO_2}
$\sigma_{H_2,0}$	1.59	2.47	1.67	2.48	−2.38(−2)	9.82(−1)	1.38
	1.59	2.47	1.67	2.48	−2.38(−2)	9.82(−1)	1.38
$\sigma_{O_2,0}$	7.76	6.98	7.83	6.79	9.39(−1)	−8.78(−2)	3.40
	7.76	6.98	7.83	6.79	9.39(−1)	−8.78(−2)	3.40
$\sigma_{N_2,0}$	−1.14(−1)	−8.78(−2)	−9.87(−2)	−1.14(−1)	7.62(−4)	1.17(−3)	3.48(−1)
	−1.14(−1)	−8.78(−2)	−9.87(−2)	−1.14(−1)	7.62(−4)	1.17(−3)	3.48(−1)
$\sigma_{O,0}$	3.02(2)	3.04(2)	3.06(2)	2.99(2)	−3.05	−3.82	1.14(2)
	3.02(2)	3.04(2)	3.06(2)	2.99(2)	−3.05	−3.82	1.14(2)
$\sigma_{H,0}$	1.80(2)	1.81(2)	1.83(2)	1.78(2)	−1.82	−2.28	6.82(1)
	1.80(2)	1.81(2)	1.83(2)	1.78(2)	−1.82	−2.28	6.82(1)
$\sigma_{OH,0}$	1.64(2)	1.66(2)	1.67(2)	1.63(2)	−1.66	−2.08	6.23(1)
	1.64(2)	1.66(2)	1.67(2)	1.63(2)	−1.66	−2.08	6.23(1)
$\sigma_{HO_2,0}$	7.64	7.73	7.78	7.58	−7.70(−2)	−9.68(−2)	3.18
	7.64	7.73	7.78	7.58	−7.70(−2)	−9.68(−2)	3.18
$\sigma_{H_2O_2,0}$	6.82(1)	6.88(1)	6.93(1)	6.76(1)	−6.90(−1)	−8.63(−1)	2.59(1)
	6.82(1)	6.88(1)	6.93(1)	6.76(1)	−6.90(−1)	−8.63(−1)	2.59(1)
$\sigma_{N,0}$	1.45(2)	1.46(2)	1.47(2)	1.43(2)	−1.47	−1.83	5.48(1)
	1.45(2)	1.46(2)	1.47(2)	1.43(2)	−1.47	−1.83	5.48(1)
$\sigma_{NO,0}$	1.41(−3)	1.45(−3)	1.47(−3)	1.41(−3)	−1.44(−5)	−1.81(−5)	−3.54(−4)
	1.41(−3)	1.45(−3)	1.47(−3)	1.41(−3)	−1.44(−5)	−1.81(−5)	−3.54(−4)
$\sigma_{NO_2,0}$	−1.31(−2)	2.36(−2)	−3.95(−3)	−1.34(−2)	1.28(−4)	−1.49(−4)	−4.86(−3)
	−1.31(−2)	2.36(−2)	−3.95(−3)	−1.34(−2)	1.28(−4)	−1.49(−4)	−4.86(−3)
$\sigma_{N_2O,0}$	4.50(−3)	4.77(−3)	4.79(−3)	4.45(−3)	−4.56(−5)	−5.90(−5)	1.76(−3)
	4.50(−3)	4.77(−3)	4.79(−3)	4.45(−3)	−4.56(−5)	−5.90(−5)	1.76(−3)
$\sigma_{H_2O,0}$	−3.95(−4)	3.98(−2)	−2.50(−4)	−3.87(−4)	2.71(−6)	4.08(−6)	1.01(−3)
	−3.95(−4)	3.98(−2)	−2.50(−4)	−3.87(−4)	2.71(−6)	4.08(−6)	1.01(−3)
T_0	5.96(1)	5.89(1)	6.25(1)	5.83(1)	−5.94(−1)	−7.41(−1)	1.99(1)
	5.96(1)	5.89(1)	6.25(1)	5.83(1)	−5.94(−1)	−7.41(−1)	1.99(1)
ρ_0	8.23	8.36	8.40	8.16	−8.43(−2)	−1.05(−1)	4.12
	8.23	8.36	8.40	8.16	−8.43(−2)	−1.05(−1)	4.12

[a]For each sensitivity parameter the top row gives the BFM results and the bottom row gives the

TO INITIAL CONDITION VALUES FOR TEST PROBLEM 8 AT $t = 3\times10^{-6}$ s

coefficients at $t = 3\times10^{-6}$ s of[a]							
$\sigma_{H_2O_2}$	σ_{NO}	σ_{NO_2}	σ_N	σ_{N_2}	σ_{N_2O}	T	ρ
2.14	1.44	1.44	1.54	−4.84(−10)	1.71	4.50(−3)	−4.22(−3)
2.14	1.44	1.44	1.54	−4.84(−10)	1.71	4.50(−3)	−4.22(−3)
2.91	7.16	7.04	6.93	−2.01(−9)	7.11	1.23(−2)	−1.16(−2)
2.91	7.16	7.04	6.93	−2.01(−9)	7.11	1.23(−2)	−1.16(−2)
2.29(−1)	8.96(−1)	1.32	8.84(−1)	1.00	1.46	−8.20(−4)	7.91(−4)
2.29(−1)	8.96(−1)	1.32	8.84(−1)	1.00	1.46	−8.20(−4)	7.91(−4)
1.17(2)	3.10(2)	2.84(2)	3.05(2)	−8.56(−8)	3.02(2)	5.57(−1)	−5.23(−1)
1.17(2)	3.10(2)	2.84(2)	3.05(2)	−8.56(−8)	3.02(2)	5.57(−1)	−5.23(−1)
6.97(1)	1.85(2)	1.69(2)	1.82(2)	−5.10(−8)	1.80(2)	3.32(−1)	−3.12(−1)
6.97(1)	1.85(2)	1.69(2)	1.82(2)	−5.10(−8)	1.80(2)	3.32(−1)	−3.12(−1)
6.36(1)	1.69(2)	1.54(2)	1.66(2)	−4.65(−8)	1.64(2)	3.03(−1)	−2.85(−1)
6.36(1)	1.69(2)	1.54(2)	1.66(2)	−4.65(−8)	1.64(2)	3.03(−1)	−2.85(−1)
5.82	7.81	7.67	7.73	−2.16(−9)	7.62	1.43(−2)	−1.35(−2)
5.82	7.81	7.67	7.73	−2.16(−9)	7.62	1.43(−2)	−1.35(−2)
3.08(1)	6.99(1)	6.40(1)	6.90(1)	−1.93(−8)	6.82(1)	1.26(−1)	−1.18(−1)
3.08(1)	6.99(1)	6.40(1)	6.90(1)	−1.93(−8)	6.82(1)	1.26(−1)	−1.18(−1)
5.59(1)	8.46(7)	1.33(8)	9.51(4)	−4.10(−8)	1.45(2)	2.67(−1)	−2.51(−1)
5.59(1)	8.46(7)	1.33(8)	9.51(4)	−4.10(−8)	1.45(2)	2.67(−1)	−2.51(−1)
−7.83(−4)	8.46(7)	1.34(8)	1.93(1)	−4.10(−13)	1.49(−3)	2.73(−6)	−2.56(−6)
−7.83(−4)	8.46(7)	1.34(8)	1.93(1)	−4.10(−13)	1.49(−3)	2.73(−6)	−2.56(−6)
−1.65(−3)	7.86(7)	2.42(10)	1.51(1)	3.35(−12)	−1.18(−2)	3.20(−4)	−3.22(−4)
−1.65(−3)	7.86(7)	2.42(10)	1.51(1)	3.35(−12)	−1.18(−2)	3.20(−4)	−3.22(−4)
1.78(−3)	1.56(3)	1.57(3)	4.84(−3)	1.10(−6)	6.37(5)	1.18(−5)	−1.14(−5)
1.78(−3)	1.56(3)	1.57(3)	4.84(−3)	1.10(−6)	6.37(5)	1.18(−5)	−1.14(−5)
8.57(−4)	−3.41(−4)	7.17(−4)	−3.67(−4)	6.97(−14)	−2.46(−4)	1.13(−8)	6.78(−8)
8.57(−4)	−3.41(−4)	7.17(−4)	−3.67(−4)	6.97(−14)	−2.46(−4)	1.13(−8)	6.78(−8)
2.22(1)	8.11(1)	7.14(1)	8.09(1)	−1.73(−8)	6.11(1)	1.10	−9.45(−2)
2.22(1)	8.11(1)	7.14(1)	8.09(1)	−1.73(−8)	6.11(1)	1.10	−9.45(−2)
4.28	8.50	8.81	8.35	−2.63(−9)	9.27	1.60(−2)	9.85(−1)
4.28	8.50	8.81	8.35	−2.63(−9)	9.27	1.60(−2)	9.85(−1)

LSENS results; numbers in parentheses are powers of 10.

TABLE 4.59.—NORMALIZED SENSITIVITY COEFFICIENTS WITH RESPECT

Sensitivity parameter	Normalized sensitivity						
	σ_O	σ_{H_2O}	σ_{OH}	σ_H	σ_{O_2}	σ_{H_2}	σ_{HO_2}
$\sigma_{H_2,0}$	2.02(−1)	1.08	7.68(−1)	9.39(−1)	−2.33	9.02(−1)	−1.68
	2.02(−1)	1.08	7.68(−1)	9.39(−1)	−2.33	9.02(−1)	−1.68
$\sigma_{O_2,0}$	3.69	1.38	2.70	−4.59(−1)	−9.47(−1)	−3.32	−9.05(−1)
	3.69	1.38	2.70	−4.59(−1)	−9.47(−1)	−3.32	−9.05(−1)
$\sigma_{N_2,0}$	−2.24(−1)	−1.36(−2)	−2.01(−1)	−4.88(−2)	1.42(−1)	9.72(−2)	3.83(−1)
	−2.24(−1)	−1.36(−2)	−2.01(−1)	−4.88(−2)	1.42(−1)	9.72(−2)	3.83(−1)
$\sigma_{O,0}$	5.82(1)	3.00(1)	4.48(1)	−8.54	−8.61(1)	−7.09(1)	−8.57(1)
	5.82(1)	3.00(1)	4.48(1)	−8.54	−8.61(1)	−7.09(1)	−8.57(1)
$\sigma_{H,0}$	3.47(1)	1.79(1)	2.67(1)	−5.09	−5.14(1)	−4.23(1)	−5.11(1)
	3.47(1)	1.79(1)	2.67(1)	−5.09	−5.14(1)	−4.23(1)	−5.11(1)
$\sigma_{OH,0}$	3.17(1)	1.63(1)	2.44(1)	−4.65	−4.69(1)	−3.86(1)	−4.67(1)
	3.17(1)	1.63(1)	2.44(1)	−4.65	−4.69(1)	−3.86(1)	−4.67(1)
$\sigma_{HO_2,0}$	1.48	7.61(−1)	1.14	−2.17(−1)	−2.18	−1.80	−2.17
	1.48	7.61(−1)	1.14	−2.17(−1)	−2.18	−1.80	−2.17
$\sigma_{H_2O_2,0}$	1.32(1)	6.78	1.01(1)	−1.93	−1.95(1)	−1.60(1)	−1.94(1)
	1.32(1)	6.78	1.01(1)	−1.93	−1.95(1)	−1.60(1)	−1.94(1)
$\sigma_{N,0}$	2.79(1)	1.44(1)	2.15(1)	−4.10	−4.13(1)	−3.40(1)	−4.11(1)
	2.79(1)	1.44(1)	2.15(1)	−4.10	−4.13(1)	−3.40(1)	−4.11(1)
$\sigma_{NO,0}$	2.28(−4)	1.46(−4)	2.02(−4)	−6.91(−5)	−4.00(−4)	−3.24(−4)	−3.84(−4)
	2.28(−4)	1.46(−4)	2.02(−4)	−6.91(−5)	−4.00(−4)	−3.24(−4)	−3.84(−4)
$\sigma_{NO_2,0}$	−9.38(−4)	−4.54(−4)	−5.11(−4)	−1.50(−4)	2.45(−3)	1.25(−3)	2.39(−3)
	−9.38(−4)	−4.54(−4)	−5.11(−4)	−1.50(−4)	2.45(−3)	1.25(−3)	2.39(−3)
$\sigma_{N_2O,0}$	1.45(−3)	6.74(−4)	1.53(−3)	−4.44(−4)	−1.34(−3)	−1.49(−3)	−1.53(−3)
	1.45(−3)	6.74(−4)	1.53(−3)	−4.44(−4)	−1.34(−3)	−1.49(−3)	−1.53(−3)
$\sigma_{H_2O,0}$	−2.20(−4)	5.35(−4)	1.46(−4)	−1.52(−4)	1.62(−4)	2.50(−4)	5.80(−4)
	−2.20(−4)	5.35(−4)	1.46(−4)	−1.52(−4)	1.62(−4)	2.50(−4)	5.80(−4)
T_0	1.69(1)	7.91	1.34(1)	−1.97	−2.36(1)	−1.92(1)	−2.33(1)
	1.69(1)	7.91	1.34(1)	−1.97	−2.36(1)	−1.92(1)	−2.33(1)
ρ_0	2.67	1.44	2.27	−5.68(−1)	−4.14	−3.32	−3.21
	2.67	1.44	2.27	−5.68(−1)	−4.14	−3.32	−3.21

[a]For each sensitivity parameter the top row gives the BFM results and the bottom row gives the

TO INITIAL CONDITION VALUES FOR TEST PROBLEM 8 AT $t = 5\times10^{-6}$ s

coefficients at $t = 5\times10^{-6}$ s of[a]							
$\sigma_{H_2O_2}$	σ_{NO}	σ_{NO_2}	σ_N	σ_{N_2}	σ_{N_2O}	T	ρ
–4.61(–2)	6.77	5.86	5.69	–1.87(–7)	1.57	2.79(–1)	–2.46(–1)
–4.62(–2)	6.77	5.86	5.69	–1.87(–7)	1.57	2.79(–1)	–2.46(–1)
3.09	2.07(1)	2.38(1)	1.54(1)	–8.19(–7)	8.08	6.25(–1)	–5.35(–1)
3.09	2.07(1)	2.38(1)	1.54(1)	–8.19(–7)	8.08	6.25(–1)	–5.35(–1)
2.04(–1)	–5.57(–1)	–7.45(–2)	–4.35(–1)	1.00	1.16	–6.65(–2)	5.97(–2)
2.04(–1)	–5.57(–1)	–7.45(–2)	–4.35(–1)	1.00	1.16	–6.65(–2)	5.97(–2)
2.55(1)	5.22(2)	5.60(2)	3.87(2)	–1.93(–5)	1.86(2)	1.60(1)	–1.38(1)
2.55(1)	5.22(2)	5.60(2)	3.87(2)	–1.93(–5)	1.86(2)	1.60(1)	–1.38(1)
1.52(1)	3.11(2)	3.34(2)	2.31(2)	–1.15(–5)	1.11(2)	9.54	–8.21
1.52(1)	3.11(2)	3.34(2)	2.31(2)	–1.15(–5)	1.11(2)	9.54	–8.21
1.39(1)	2.84(2)	3.05(2)	2.11(2)	–1.05(–5)	1.01(2)	8.71	–7.50
1.39(1)	2.84(2)	3.05(2)	2.11(2)	–1.05(–5)	1.01(2)	8.71	–7.50
6.49(–1)	1.32(1)	1.42(1)	9.83	–4.89(–7)	4.71	4.06(–1)	–3.50(–1)
6.49(–1)	1.32(1)	1.42(1)	9.83	–4.89(–7)	4.71	4.06(–1)	–3.50(–1)
5.77	1.18(2)	1.27(2)	8.76(1)	–4.36(–6)	4.19(1)	3.62	–3.12
5.77	1.18(2)	1.27(2)	8.76(1)	–4.36(–6)	4.19(1)	3.62	–3.12
1.22(1)	1.04(4)	1.05(4)	1.87(2)	–9.24(–6)	8.89(1)	7.67	–6.61
1.22(1)	1.04(4)	1.05(4)	1.87(2)	–9.24(–6)	8.89(1)	7.67	–6.61
1.71(–4)	1.01(4)	1.03(4)	1.57	–6.90(–11)	9.33(–4)	7.53(–5)	–6.42(–5)
1.71(–4)	1.01(4)	1.03(4)	1.57	–6.90(–11)	9.33(–4)	7.53(–5)	–6.42(–5)
2.53(–4)	1.01(4)	1.03(4)	1.56	3.75(–10)	–3.44(–3)	–2.56(–4)	1.84(–4)
2.53(–4)	1.01(4)	1.03(4)	1.56	3.75(–10)	–3.44(–3)	–2.56(–4)	1.84(–4)
1.20(–3)	6.12(1)	6.18(1)	1.93(–2)	1.19(–4)	8.05(2)	4.87(–4)	–4.62(–4)
1.20(–3)	6.12(1)	6.18(1)	1.93(–2)	1.19(–4)	8.05(2)	4.87(–4)	–4.62(–4)
6.31(–4)	–2.65(–4)	–2.18(–4)	–2.79(–4)	1.31(–11)	–1.36(–4)	4.05(–6)	–1.28(–6)
6.31(–4)	–2.65(–4)	–2.18(–4)	–2.79(–4)	1.31(–11)	–1.36(–4)	4.05(–6)	–1.28(–6)
8.00	1.51(2)	1.62(2)	1.14(2)	–5.51(–6)	5.27(1)	4.75	–3.19
8.00	1.51(2)	1.62(2)	1.14(2)	–5.51(–6)	5.27(1)	4.75	–3.19
2.25	2.59(1)	2.86(1)	1.97(1)	–1.00(–6)	9.81	8.37(–1)	2.80(–1)
2.25	2.59(1)	2.86(1)	1.97(1)	–1.00(–6)	9.81	8.37(–1)	2.80(–1)

LSENS results; numbers in parentheses are powers of 10.

TABLE 4.60.—NORMALIZED SENSITIVITY COEFFICIENTS WITH RESPECT

Sensitivity parameter	Normalized sensitivity						
	σ_O	σ_{H_2O}	σ_{OH}	σ_H	σ_{O_2}	σ_{H_2}	σ_{HO_2}
$\sigma_{H_2,0}$	−8.24(−1)	7.23(−1)	3.33(−1)	9.67(−1)	−2.18	2.02	−1.55
	−8.24(−1)	7.23(−1)	3.33(−1)	9.67(−1)	−2.18	2.02	−1.55
$\sigma_{O_2,0}$	1.19	4.26(−1)	1.40	−1.09	2.57	−1.03	2.10
	1.19	4.26(−1)	1.40	−1.09	2.57	−1.03	2.10
$\sigma_{N_2,0}$	−2.28(−1)	7.43(−2)	−2.37(−1)	−1.30(−1)	−3.02(−2)	−9.70(−2)	2.76(−1)
	−2.28(−1)	7.43(−2)	−2.37(−1)	−1.30(−1)	−3.02(−2)	−9.70(−2)	2.76(−1)
$\sigma_{O,0}$	−8.64	2.25	4.98	−1.26(1)	−6.44	−1.09	−1.16(1)
	−8.64	2.25	4.98	−1.26(1)	−6.44	−1.09	−1.16(1)
$\sigma_{H,0}$	−5.15	1.34	2.97	−7.52	−3.84	−6.47(−1)	−6.94
	−5.15	1.34	2.97	−7.52	−3.84	−6.47(−1)	−6.94
$\sigma_{OH,0}$	−4.70	1.23	2.71	−6.87	−3.51	−5.91(−1)	−6.33
	−4.70	1.23	2.71	−6.87	−3.51	−5.91(−1)	−6.33
$\sigma_{HO_2,0}$	−2.18(−1)	5.74(−2)	1.27(−1)	−3.21(−1)	−1.62(−1)	−2.79(−2)	−2.94(−1)
	−2.18(−1)	5.74(−2)	1.27(−1)	−3.21(−1)	−1.62(−1)	−2.79(−2)	−2.94(−1)
$\sigma_{H_2O_2,0}$	−1.95	5.09(−1)	1.13	−2.85	−1.46	−2.46(−1)	−2.63
	−1.95	5.09(−1)	1.13	−2.85	−1.46	−2.46(−1)	−2.63
$\sigma_{N,0}$	−4.14	1.08	2.39	−6.05	−3.09	−5.20(−1)	−5.58
	−4.14	1.08	2.39	−6.05	−3.09	−5.20(−1)	−5.58
$\sigma_{NO,0}$	−1.42(−4)	3.83(−5)	1.27(−5)	−1.65(−4)	−7.46(−5)	−2.83(−5)	−9.66(−5)
	−1.42(−4)	3.83(−5)	1.27(−5)	−1.65(−4)	−7.46(−5)	−2.83(−5)	−9.66(−5)
$\sigma_{NO_2,0}$	4.40(−4)	1.41(−4)	2.27(−4)	−1.85(−4)	9.82(−4)	−3.81(−4)	9.99(−4)
	4.40(−4)	1.41(−4)	2.27(−4)	−1.85(−4)	9.82(−4)	−3.81(−4)	9.99(−4)
$\sigma_{N_2O,0}$	2.93(−4)	1.60(−4)	6.78(−4)	−5.95(−4)	7.15(−4)	−3.24(−4)	3.25(−4)
	2.93(−4)	1.60(−4)	6.78(−4)	−5.95(−4)	7.15(−4)	−3.24(−4)	3.25(−4)
$\sigma_{H_2O,0}$	−2.71(−4)	5.17(−4)	1.45(−4)	−2.53(−4)	8.80(−5)	1.59(−4)	4.63(−4)
	−2.71(−4)	5.17(−4)	1.45(−4)	−2.53(−4)	8.80(−5)	1.59(−4)	4.63(−4)
T_0	−1.78	4.06(−1)	2.40	−3.36	−1.84	3.71(−2)	−3.19
	−1.78	4.06(−1)	2.40	−3.36	−1.84	3.71(−2)	−3.19
ρ_0	−8.60(−1)	2.23(−1)	4.94(−1)	−1.26	−6.37(−1)	−1.04(−1)	−1.75(−1)
	−8.60(−1)	2.23(−1)	4.94(−1)	−1.26	−6.37(−1)	−1.04(−1)	−1.75(−1)

[a]For each sensitivity parameter the top row gives the BFM results and the bottom row gives

TO INITIAL CONDITION VALUES FOR TEST PROBLEM 8 AT $t = 7.5\times10^{-6}$ s

coefficients at $t = 7.5\times10^{-6}$ s of[a]							
$\sigma_{H_2O_2}$	σ_{NO}	σ_{NO_2}	σ_N	σ_{N_2}	σ_{N_2O}	T	ρ
−1.28	3.05	1.46	2.49	−3.93(−6)	−1.23	2.07(−1)	−1.76(−1)
−1.28	3.05	1.46	2.49	−3.93(−6)	−1.23	2.07(−1)	−1.76(−1)
4.21(−1)	7.52	9.67	4.91	−1.08(−5)	2.39	3.10(−1)	−2.51(−1)
4.21(−1)	7.52	9.67	4.91	−1.08(−5)	2.39	3.10(−1)	−2.51(−1)
4.16(−1)	−5.72(−1)	−8.99(−2)	−4.35(−1)	1.00	1.42	−8.61(−2)	7.25(−2)
4.16(−1)	−5.72(−1)	−8.99(−2)	−4.35(−1)	1.00	1.42	−8.61(−2)	7.25(−2)
−2.46(1)	1.01(2)	1.02(2)	6.04(1)	−1.39(−4)	6.58	4.33	−3.56
−2.46(1)	1.01(2)	1.02(2)	6.04(1)	−1.39(−4)	6.58	4.33	−3.56
−1.46(1)	6.02(1)	6.09(1)	3.60(1)	−8.29(−5)	3.92	2.58	−2.12
−1.46(1)	6.02(1)	6.09(1)	3.60(1)	−8.30(−5)	3.92	2.58	−2.12
−1.34(1)	5.49(1)	5.56(1)	3.29(1)	−7.57(−5)	3.58	2.36	−1.94
−1.34(1)	5.49(1)	5.56(1)	3.29(1)	−7.57(−5)	3.58	2.36	−1.94
−6.23(−1)	2.56	2.60	1.54	−3.53(−6)	1.68(−1)	1.10(−1)	−9.05(−2)
−6.23(−1)	2.56	2.60	1.54	−3.53(−6)	1.68(−1)	1.10(−1)	−9.05(−2)
−5.55	2.28(1)	2.31(1)	1.37(1)	−3.15(−5)	1.49	9.80(−1)	−8.05(−1)
−5.55	2.28(1)	2.31(1)	1.37(1)	−3.15(−5)	1.49	9.80(−1)	−8.05(−1)
−1.18(1)	1.16(2)	1.16(2)	2.93(1)	−6.67(−5)	3.15	2.08	−1.71
−1.18(1)	1.16(2)	1.16(2)	2.93(1)	−6.67(−5)	3.15	2.08	−1.71
−1.96(−4)	6.71(1)	6.74(1)	3.17(−1)	2.06(−9)	1.31(−4)	3.25(−5)	−2.63(−5)
−1.96(−4)	6.71(1)	6.74(1)	3.17(−1)	2.06(−9)	1.31(−4)	3.25(−5)	−2.63(−5)
8.22(−4)	6.71(1)	6.74(1)	3.16(−1)	3.90(−9)	6.19(−4)	−3.61(−5)	−6.32(−6)
8.22(−4)	6.71(1)	6.74(1)	3.16(−1)	3.90(−9)	6.19(−4)	−3.61(−5)	−6.32(−6)
−6.12(−4)	9.86(−1)	9.92(−1)	8.41(−3)	1.79(−4)	2.38	2.38(−4)	−2.62(−4)
−6.12(−4)	9.86(−1)	9.92(−1)	8.41(−3)	1.79(−4)	2.38	2.38(−4)	−2.62(−4)
3.48(−4)	−3.03(−5)	7.98(−5)	−2.11(−4)	3.13(−11)	7.94(−5)	1.18(−5)	−6.40(−6)
3.48(−4)	−3.03(−5)	7.98(−5)	−2.11(−4)	3.13(−11)	7.94(−5)	1.18(−5)	−6.40(−6)
−7.79	3.67(1)	3.81(1)	2.37(1)	−5.09(−5)	3.43	1.63	−4.54(−1)
−7.79	3.67(1)	3.81(1)	2.37(1)	−5.09(−5)	3.43	1.63	−4.54(−1)
−1.44	9.00	1.00(1)	5.97	−1.26(−5)	1.58	4.30(−1)	6.46(−1)
−1.44	9.00	1.00(1)	5.97	−1.26(−5)	1.58	4.30(−1)	6.46(−1)

the LSENS results; numbers in parentheses are powers of 10.

TABLE 4.61.—NORMALIZED SENSITIVITY COEFFICIENTS WITH RESPECT

Sensitivity parameter	Normalized sensitivity						
	σ_O	σ_{H_2O}	σ_{OH}	σ_H	σ_{O_2}	σ_{H_2}	σ_{HO_2}
$\sigma_{H_2,0}$	−1.06	6.68(−1)	7.40(−2)	1.32	−2.80	2.38	−1.74
	−1.06	6.68(−1)	7.40(−2)	1.32	−2.80	2.38	−1.74
$\sigma_{O_2,0}$	1.41	4.30(−1)	1.28	−1.29	3.29	−1.50	3.16
	1.41	4.30(−1)	1.28	−1.29	3.29	−1.50	3.16
$\sigma_{N_2,0}$	−4.04(−1)	1.04(−1)	−3.41(−1)	−2.92(−1)	−9.52(−2)	−1.80(−1)	1.49(−2)
	−4.04(−1)	1.04(−1)	−3.41(−1)	−2.92(−1)	−9.52(−2)	−1.80(−1)	1.49(−2)
$\sigma_{O,0}$	−4.38	8.40(−1)	4.45(−2)	−5.23	−2.49	−1.27	−1.53
	−4.38	8.40(−1)	4.45(−2)	−5.23	−2.49	−1.27	−1.53
$\sigma_{H,0}$	−2.61	5.01(−1)	2.64(−2)	−3.12	−1.49	−7.55(−1)	−9.14(−1)
	−2.61	5.01(−1)	2.64(−2)	−3.12	−1.49	−7.55(−1)	−9.14(−1)
$\sigma_{OH,0}$	−2.38	4.57(−1)	2.43(−2)	−2.84	−1.35	−6.89(−1)	−8.33(−1)
	−2.38	4.57(−1)	2.43(−2)	−2.84	−1.35	−6.90(−1)	−8.33(−1)
$\sigma_{HO_2,0}$	−1.10(−1)	2.17(−2)	1.98(−3)	−1.33(−1)	−6.14(−2)	−3.27(−2)	−3.70(−2)
	−1.10(−1)	2.17(−2)	1.98(−3)	−1.33(−1)	−6.14(−2)	−3.27(−2)	−3.70(−2)
$\sigma_{H_2O_2,0}$	−9.89(−1)	1.90(−1)	1.05(−2)	−1.18	−5.62(−1)	−2.87(−1)	−3.45(−1)
	−9.89(−1)	1.90(−1)	1.05(−2)	−1.18	−5.62(−1)	−2.87(−1)	−3.45(−1)
$\sigma_{N,0}$	−2.10	4.02(−1)	2.11(−2)	−2.51	−1.20	−6.07(−1)	−7.36(−1)
	−2.10	4.02(−1)	2.11(−2)	−2.51	−1.20	−6.07(−1)	−7.36(−1)
$\sigma_{NO,0}$	−2.45(−4)	5.13(−5)	−6.03(−5)	−2.56(−4)	−1.10(−4)	−8.13(−5)	−7.01(−5)
	−2.45(−4)	5.13(−5)	−6.03(−5)	−2.56(−4)	−1.10(−4)	−8.13(−5)	−7.01(−5)
$\sigma_{NO_2,0}$	2.76(−4)	1.94(−4)	2.76(−4)	−5.80(−4)	1.06(−3)	−5.90(−4)	9.95(−4)
	2.76(−4)	1.94(−4)	2.76(−4)	−5.80(−4)	1.06(−3)	−5.90(−4)	9.95(−4)
$\sigma_{N_2O,0}$	5.02(−4)	1.30(−4)	4.98(−4)	−4.24(−4)	1.08(−3)	−4.74(−4)	1.01(−3)
	5.02(−4)	1.30(−4)	4.98(−4)	−4.24(−4)	1.08(−3)	−4.74(−4)	1.01(−3)
$\sigma_{H_2O,0}$	−3.81(−4)	4.97(−4)	5.20(−5)	−3.60(−4)	4.31(−5)	7.53(−5)	3.81(−4)
	−3.81(−4)	4.97(−4)	5.20(−5)	−3.60(−4)	4.31(−5)	7.53(−5)	3.81(−4)
T_0	−8.44(−1)	9.69(−2)	8.47(−1)	−1.47	−8.07(−1)	−8.87(−2)	2.62(−1)
	−8.44(−1)	9.69(−2)	8.47(−1)	−1.47	−8.07(−1)	−8.87(−2)	2.62(−1)
ρ_0	−1.05	2.02(−1)	1.06(−2)	−1.26	−5.98(−1)	−3.04(−1)	4.33(−1)
	−1.05	2.02(−1)	1.06(−2)	−1.26	−5.98(−1)	−3.04(−1)	4.33(−1)

[a]For each sensitivity parameter the top row gives the BFM results and the bottom row gives the

TO INITIAL CONDITION VALUES FOR TEST PROBLEM 8 AT $t = 1.5\times10^{-5}$ s

coefficients at $t = 1.5\times10^{-5}$ s of[a]							
$\sigma_{H_2O_2}$	σ_{NO}	σ_{NO_2}	σ_N	σ_{N_2}	σ_{N_2O}	T	ρ
−1.48	1.71	1.32(−1)	1.63	−6.40(−5)	−9.43(−1)	1.69(−1)	−1.39(−1)
−1.48	1.71	1.32(−1)	1.63	−6.40(−5)	−9.43(−1)	1.69(−1)	−1.39(−1)
5.40(−1)	5.04	7.94	3.23	−1.91(−4)	3.36	2.24(−1)	−1.72(−1)
5.40(−1)	5.04	7.94	3.23	−1.91(−4)	3.36	2.24(−1)	−1.72(−1)
4.76(−1)	−9.49(−1)	−8.22(−1)	−8.38(−1)	1.00	8.13(−1)	−1.20(−1)	9.52(−2)
4.76(−1)	−9.49(−1)	−8.22(−1)	−8.38(−1)	1.00	8.13(−1)	−1.20(−1)	9.52(−2)
−1.02(1)	2.41(1)	2.75(1)	1.28(1)	−9.10(−4)	6.56	1.14	−8.97(−1)
−1.02(1)	2.41(1)	2.75(1)	1.28(1)	−9.10(−4)	6.56	1.14	−8.97(−1)
−6.10	1.44(1)	1.64(1)	7.62	−5.42(−4)	3.91	6.77(−1)	−5.35(−1)
−6.10	1.44(1)	1.64(1)	7.62	−5.42(−4)	3.91	6.77(−1)	−5.35(−1)
−5.57	1.31(1)	1.50(1)	6.95	−4.95(−4)	3.57	6.18(−1)	−4.88(−1)
−5.57	1.31(1)	1.50(1)	6.95	−4.95(−4)	3.57	6.18(−1)	−4.88(−1)
−2.59(−1)	6.15(−1)	7.01(−1)	3.26(−1)	−2.32(−5)	1.68(−1)	2.90(−2)	−2.29(−2)
−2.59(−1)	6.15(−1)	7.01(−1)	3.26(−1)	−2.32(−5)	1.68(−1)	2.90(−2)	−2.29(−2)
−2.31	5.46	6.21	2.89	−2.06(−4)	1.48	2.57(−1)	−2.03(−1)
−2.31	5.46	6.21	2.89	−2.06(−4)	1.48	2.57(−1)	−2.03(−1)
−4.91	1.40(1)	1.56(1)	6.24	−4.36(−4)	3.14	5.45(−1)	−4.30(−1)
−4.91	1.40(1)	1.56(1)	6.24	−4.36(−4)	3.14	5.45(−1)	−4.30(−1)
−3.05(−4)	2.40	2.41	1.15(−1)	6.31(−8)	2.03(−4)	2.17(−5)	−1.69(−5)
−3.05(−4)	2.40	2.41	1.15(−1)	6.31(−8)	2.03(−4)	2.17(−5)	−1.69(−5)
3.28(−4)	2.41	2.41	1.15(−1)	5.31(−8)	9.16(−4)	2.44(−5)	−5.50(−5)
3.28(−4)	2.41	2.41	1.15(−1)	5.31(−8)	9.16(−4)	2.44(−5)	−5.50(−5)
−1.06(−4)	3.82(−2)	3.93(−2)	3.49(−3)	1.79(−4)	1.53(−3)	1.14(−4)	−1.56(−4)
−1.06(−4)	3.82(−2)	3.93(−2)	3.49(−3)	1.79(−4)	1.53(−3)	1.14(−4)	−1.56(−4)
1.80(−4)	−3.05(−4)	−1.16(−4)	−4.94(−4)	1.15(−8)	1.51(−4)	−3.58(−6)	7.09(−6)
1.80(−4)	−3.05(−4)	−1.16(−4)	−4.94(−4)	1.15(−8)	1.51(−4)	−3.58(−6)	7.09(−6)
−4.50	1.47(1)	1.72(1)	9.79	−5.55(−4)	4.74	7.65(−1)	2.84(−1)
−4.50	1.47(1)	1.72(1)	9.79	−5.55(−4)	4.74	7.65(−1)	2.84(−1)
−1.47	4.80	6.24	3.02	−1.81(−4)	2.23	2.74(−1)	7.84(−1)
−1.47	4.80	6.24	3.02	−1.81(−4)	2.23	2.74(−1)	7.84(−1)

[a] LSENS results; numbers in parentheses are powers of 10.

TABLE 4.62.—NORMALIZED SENSITIVITY COEFFICIENTS WITH RESPECT

Sensitivity parameter	Normalized sensitivity						
	σ_O	σ_{H_2O}	σ_{OH}	σ_H	σ_{O_2}	σ_{H_2}	σ_{HO_2}
$\sigma_{H_2,0}$	−1.10	5.54(−1)	−1.47(−1)	2.50	−3.97	3.42	−2.25
	−1.10	5.54(−1)	−1.47(−1)	2.50	−3.97	3.42	−2.25
$\sigma_{O_2,0}$	2.94	2.98(−1)	1.68	−6.96(−1)	5.21	−1.98	4.26
	2.94	2.98(−1)	1.68	−6.96(−1)	5.21	−1.98	4.26
$\sigma_{N_2,0}$	−1.18	1.83(−1)	−6.30(−1)	−1.11	−4.47(−1)	−5.31(−1)	−7.34(−1)
	−1.18	1.83(−1)	−6.30(−1)	−1.11	−4.47(−1)	−5.31(−1)	−7.34(−1)
$\sigma_{O,0}$	−6.45(−2)	2.95(−3)	−2.76(−2)	−3.53(−2)	−6.28(−2)	6.38(−4)	−4.38(−2)
	−6.45(−2)	2.94(−3)	−2.76(−2)	−3.53(−2)	−6.28(−2)	6.39(−4)	−4.38(−2)
$\sigma_{H,0}$	−3.89(−2)	1.74(−3)	−1.67(−2)	−2.02(−2)	−3.90(−2)	1.49(−3)	−2.71(−2)
	−3.89(−2)	1.74(−3)	−1.67(−2)	−2.02(−2)	−3.90(−2)	1.49(−3)	−2.71(−2)
$\sigma_{OH,0}$	−3.52(−2)	1.81(−3)	−1.50(−2)	−1.93(−2)	−3.42(−2)	4.27(−4)	−2.38(−2)
	−3.52(−2)	1.81(−3)	−1.50(−2)	−1.93(−2)	−3.42(−2)	4.28(−4)	−2.38(−2)
$\sigma_{HO_2,0}$	1.19(−4)	3.70(−4)	3.77(−4)	−9.56(−4)	1.20(−3)	−7.34(−4)	1.31(−3)
	1.19(−4)	3.70(−4)	3.77(−4)	−9.56(−4)	1.20(−3)	−7.34(−4)	1.31(−3)
$\sigma_{H_2O_2,0}$	−1.40(−2)	1.16(−3)	−5.71(−3)	−8.32(−3)	−1.27(−2)	−2.61(−4)	−8.62(−3)
	−1.40(−2)	1.16(−3)	−5.71(−3)	−8.32(−3)	−1.27(−2)	−2.61(−4)	−8.62(−3)
$\sigma_{N,0}$	−3.14(−2)	1.13(−3)	−1.36(−2)	−1.58(−2)	−3.23(−2)	1.66(−3)	−2.25(−2)
	−3.14(−2)	1.13(−3)	−1.36(−2)	−1.58(−2)	−3.23(−2)	1.66(−3)	−2.25(−2)
$\sigma_{NO,0}$	−1.22(−4)	3.77(−5)	−5.78(−5)	−2.06(−4)	5.47(−5)	−1.38(−4)	−5.46(−6)
	−1.22(−4)	3.77(−5)	−5.78(−5)	−2.06(−4)	5.47(−5)	−1.38(−4)	−5.46(−6)
$\sigma_{NO_2,0}$	6.53(−4)	1.73(−4)	3.88(−4)	−6.49(−4)	1.74(−3)	−9.07(−4)	1.28(−3)
	6.53(−4)	1.73(−4)	3.88(−4)	−6.49(−4)	1.74(−3)	−9.07(−4)	1.28(−3)
$\sigma_{N_2O,0}$	1.12(−3)	7.53(−5)	6.30(−4)	−8.34(−5)	1.78(−3)	−5.85(−4)	1.47(−3)
	1.12(−3)	7.53(−5)	6.30(−4)	−8.34(−5)	1.78(−3)	−5.85(−4)	1.47(−3)
$\sigma_{H_2O,0}$	−3.89(−4)	4.49(−4)	−2.44(−5)	−3.71(−4)	5.78(−5)	7.61(−6)	6.51(−5)
	−3.89(−4)	4.49(−4)	−2.44(−5)	−3.71(−4)	5.78(−5)	7.61(−6)	6.51(−5)
T_0	1.77	−3.00(−1)	1.02	1.72	5.43(−1)	8.97(−1)	1.50
	1.77	−3.00(−1)	1.02	1.72	5.43(−1)	8.97(−1)	1.50
ρ_0	−3.28(−1)	3.56(−2)	−9.89(−2)	−3.10(−1)	−2.05(−1)	−9.25(−2)	2.80(−1)
	−3.28(−1)	3.56(−2)	−9.89(−2)	−3.10(−1)	−2.05(−1)	−9.25(−2)	2.80(−1)

[a]For each sensitivity parameter the top row gives the BFM results and the bottom row gives the

TO INITIAL CONDITION VALUES FOR TEST PROBLEM 8 AT $t = 10^{-4}$ s

coefficients at $t = 10^{-4}$ s of[a]							
$\sigma_{H_2O_2}$	σ_{NO}	σ_{NO_2}	σ_N	σ_{N_2}	σ_{N_2O}	T	ρ
−1.07	2.12(−1)	−1.94	2.13	−3.73(−4)	−1.48	8.97(−2)	−7.25(−2)
−1.07	2.12(−1)	−1.94	2.13	−3.73(−4)	−1.48	8.97(−2)	−7.25(−2)
3.01	3.65	6.22	1.51	−6.41(−3)	2.71	4.10(−2)	−2.45(−2)
3.01	3.65	6.22	1.51	−6.41(−3)	2.71	4.10(−2)	−2.45(−2)
−4.36(−1)	−1.34	−1.39	−1.73	1.00	3.67(−1)	−9.63(−2)	7.15(−2)
−4.36(−1)	−1.34	−1.39	−1.73	1.00	3.67(−1)	−9.63(−2)	7.15(−2)
−7.37(−2)	1.29	1.29	6.59(−1)	−2.27(−3)	2.35(−2)	2.30(−3)	−1.29(−3)
−7.37(−2)	1.29	1.29	6.59(−1)	−2.27(−3)	2.35(−2)	2.30(−3)	−1.29(−3)
−4.46(−2)	7.71(−1)	7.65(−1)	3.94(−1)	−1.35(−3)	1.34(−2)	1.40(−3)	−7.91(−4)
−4.46(−2)	7.71(−1)	7.65(−1)	3.94(−1)	−1.35(−3)	1.34(−2)	1.40(−3)	−7.91(−4)
−4.00(−2)	7.03(−1)	6.99(−1)	3.58(−1)	−1.23(−3)	1.27(−2)	1.24(−3)	−6.98(−4)
−4.00(−2)	7.03(−1)	6.99(−1)	3.58(−1)	−1.23(−3)	1.27(−2)	1.24(−3)	−6.98(−4)
−8.39(−5)	3.51(−2)	3.62(−2)	1.79(−2)	−6.15(−5)	2.10(−3)	9.62(−5)	−1.07(−4)
−8.38(−5)	3.51(−2)	3.62(−2)	1.79(−2)	−6.15(−5)	2.10(−3)	9.62(−5)	−1.07(−4)
−1.55(−2)	2.93(−1)	2.92(−1)	1.49(−1)	−5.13(−4)	5.97(−3)	5.06(−4)	−3.46(−4)
−1.55(−2)	2.93(−1)	2.92(−1)	1.49(−1)	−5.13(−4)	5.97(−3)	5.06(−4)	−3.46(−4)
−3.65(−2)	6.68(−1)	6.63(−1)	3.42(−1)	−1.08(−3)	1.06(−2)	1.16(−3)	−6.97(−4)
−3.65(−2)	6.68(−1)	6.63(−1)	3.42(−1)	−1.08(−3)	1.06(−2)	1.16(−3)	−6.97(−4)
−1.76(−5)	4.76(−2)	4.76(−2)	2.40(−2)	7.01(−6)	1.62(−4)	−1.16(−5)	7.38(−6)
−1.76(−5)	4.76(−2)	4.76(−2)	2.40(−2)	7.01(−6)	1.62(−4)	−1.16(−5)	7.38(−6)
8.95(−4)	4.82(−2)	4.91(−2)	2.39(−2)	5.85(−6)	9.29(−4)	−1.81(−5)	−2.32(−5)
8.95(−4)	4.82(−2)	4.91(−2)	2.39(−2)	5.85(−6)	9.29(−4)	−1.81(−5)	−2.32(−5)
1.01(−3)	2.31(−3)	3.14(−3)	1.30(−3)	1.77(−4)	1.11(−3)	2.20(−5)	−8.31(−5)
1.01(−3)	2.31(−3)	3.14(−3)	1.30(−3)	1.77(−4)	1.11(−3)	2.20(−5)	−8.31(−5)
2.92(−4)	−7.77(−4)	−6.62(−4)	−1.15(−3)	1.36(−6)	−1.18(−4)	−3.92(−5)	3.46(−5)
2.92(−4)	−7.77(−4)	−6.62(−4)	−1.15(−3)	1.36(−6)	−1.18(−4)	−3.92(−5)	3.46(−5)
1.19	5.91	6.30	5.83	−1.04(−2)	1.64	2.02(−1)	7.36(−1)
1.19	5.91	6.30	5.83	−1.04(−2)	1.64	2.02(−1)	7.36(−1)
5.10(−1)	1.53	1.90	9.03(−1)	−2.68(−3)	6.02(−1)	3.43(−2)	9.75(−1)
5.10(−1)	1.53	1.90	9.03(−1)	−2.68(−3)	6.02(−1)	3.43(−2)	9.75(−1)

LSENS results; numbers in parentheses are powers of 10.

TABLE 4.63.—NORMALIZED SENSITIVITY COEFFICIENTS WITH RESPECT

Sensitivity parameter	Normalized sensitivity						
	σ_O	σ_{H_2O}	σ_{OH}	σ_H	σ_{O_2}	σ_{H_2}	σ_{HO_2}
$\sigma_{H_2,0}$	−1.04	5.34(−1)	−1.32(−1)	2.54	−3.94	3.42	−2.23
	−1.04	5.34(−1)	−1.32(−1)	2.54	−3.94	3.42	−2.23
$\sigma_{O_2,0}$	3.04	3.12(−1)	1.73	−6.54(−1)	5.33	−1.98	4.35
	3.04	3.12(−1)	1.73	−6.54(−1)	5.33	−1.98	4.35
$\sigma_{N_2,0}$	−1.27	1.84(−1)	−6.76(−1)	−1.15	−5.56(−1)	−5.18(−1)	−8.22(−1)
	−1.27	1.84(−1)	−6.76(−1)	−1.15	−5.56(−1)	−5.18(−1)	−8.22(−1)
$\sigma_{O,0}$	9.96(−4)	−8.02(−5)	5.41(−4)	6.06(−4)	7.73(−4)	1.31(−4)	8.54(−4)
	9.97(−4)	−8.03(−5)	5.41(−4)	6.07(−4)	7.73(−4)	1.31(−4)	8.54(−4)
$\sigma_{H,0}$	1.19(−4)	−6.86(−5)	1.18(−4)	1.21(−3)	−1.15(−3)	1.19(−3)	−5.45(−4)
	1.19(−4)	−6.86(−5)	1.18(−4)	1.21(−3)	−1.15(−3)	1.19(−3)	−5.45(−4)
$\sigma_{OH,0}$	4.06(−4)	1.60(−4)	3.11(−4)	2.53(−4)	4.11(−4)	1.51(−4)	4.91(−4)
	4.06(−4)	1.60(−4)	3.11(−4)	2.53(−4)	4.11(−4)	1.51(−4)	4.91(−4)
$\sigma_{HO_2,0}$	1.85(−3)	2.99(−4)	1.12(−3)	−1.32(−5)	2.89(−3)	−7.50(−4)	2.50(−3)
	1.85(−3)	2.99(−4)	1.12(−3)	−1.32(−5)	2.89(−3)	−7.50(−4)	2.50(−3)
$\sigma_{H_2O_2,0}$	8.58(−4)	4.77(−4)	6.64(−4)	−1.86(−4)	1.71(−3)	−3.79(−4)	1.50(−3)
	8.58(−4)	4.77(−4)	6.64(−4)	−1.86(−4)	1.71(−3)	−3.79(−4)	1.50(−3)
$\sigma_{N,0}$	1.36(−3)	−3.08(−4)	7.04(−4)	1.73(−3)	1.67(−6)	1.03(−3)	5.05(−4)
	1.36(−3)	−3.08(−4)	7.04(−4)	1.73(−3)	1.78(−6)	1.03(−3)	5.05(−4)
$\sigma_{NO,0}$	1.26(−3)	6.04(−5)	7.06(−4)	4.22(−5)	1.85(−3)	−5.27(−4)	1.58(−3)
	1.26(−3)	6.04(−5)	7.06(−4)	4.22(−5)	1.85(−3)	−5.27(−4)	1.58(−3)
$\sigma_{NO_2,0}$	2.06(−3)	2.02(−4)	1.16(−3)	−3.97(−4)	3.55(−3)	−1.30(−3)	2.88(−3)
	2.06(−3)	2.02(−4)	1.16(−3)	−3.97(−4)	3.55(−3)	−1.30(−3)	2.88(−3)
$\sigma_{N_2O,0}$	1.18(−3)	7.99(−5)	6.58(−4)	−6.46(−5)	1.84(−3)	−5.91(−4)	1.52(−3)
	1.18(−3)	7.99(−5)	6.58(−4)	−6.46(−5)	1.84(−3)	−5.91(−4)	1.52(−3)
$\sigma_{H_2O,0}$	−3.91(−4)	4.49(−4)	−2.61(−5)	−3.72(−4)	5.77(−5)	6.39(−6)	6.07(−5)
	−3.91(−4)	4.49(−4)	−2.61(−5)	−3.72(−4)	5.77(−5)	6.40(−6)	6.07(−5)
T_0	1.95	−3.11(−1)	1.09	1.84	6.97(−1)	9.09(−1)	1.61
	1.95	−3.11(−1)	1.09	1.84	6.97(−1)	9.09(−1)	1.61
ρ_0	−2.71(−1)	3.04(−2)	−7.92(−2)	−2.63(−1)	−1.64(−1)	−8.13(−2)	2.98(−1)
	−2.71(−1)	3.04(−2)	−7.92(−2)	−2.63(−1)	−1.64(−1)	−8.13(−2)	2.98(−1)

[a]For each sensitivity parameter the top row gives the BFM results and the bottom row gives the

TO INITIAL CONDITION VALUES FOR TEST PROBLEM 8 AT $t = 10^{-3}$ s

coefficients at $t = 10^{-3}$ s of[a]							
$\sigma_{H_2O_2}$	σ_{NO}	σ_{NO_2}	σ_N	σ_{N_2}	σ_{N_2O}	T	ρ
−1.03	−1.49	−3.65	1.85	1.17(−2)	−1.59	8.83(−2)	−7.45(−2)
−1.03	−1.49	−3.65	1.85	1.17(−2)	−1.59	8.83(−2)	−7.45(−2)
3.15	2.84	5.44	7.43(−1)	−2.23(−2)	2.80	3.65(−2)	−1.79(−2)
3.15	2.84	5.44	7.43(−1)	−2.23(−2)	2.80	3.65(−2)	−1.79(−2)
−5.37(−1)	−2.34(−1)	−3.16(−1)	−1.45	1.01	3.41(−1)	−9.51(−2)	7.00(−2)
−5.37(−1)	−2.34(−1)	−3.16(−1)	−1.45	1.01	3.41(−1)	−9.51(−2)	7.00(−2)
5.76(−4)	9.03(−3)	9.31(−3)	7.15(−3)	−7.09(−5)	1.16(−3)	6.02(−5)	−3.54(−5)
5.76(−4)	9.03(−3)	9.31(−3)	7.15(−3)	−7.09(−5)	1.15(−3)	6.02(−5)	−3.58(−5)
−3.36(−4)	4.75(−3)	4.04(−3)	4.93(−3)	−3.73(−5)	1.99(−5)	6.75(−5)	−4.39(−5)
−3.36(−4)	4.75(−3)	4.04(−3)	4.93(−3)	−3.73(−5)	1.98(−5)	6.75(−5)	−4.42(−5)
4.50(−4)	4.84(−3)	5.01(−3)	3.63(−3)	−3.80(−5)	5.69(−4)	2.00(−5)	−1.48(−5)
4.50(−4)	4.84(−3)	5.01(−3)	3.63(−3)	−3.80(−5)	5.69(−4)	2.00(−5)	−1.50(−5)
1.89(−3)	1.84(−3)	3.19(−3)	9.21(−4)	−1.44(−5)	1.57(−3)	3.64(−5)	−7.15(−5)
1.89(−3)	1.84(−3)	3.19(−3)	9.21(−4)	−1.44(−5)	1.57(−3)	3.64(−5)	−7.16(−5)
1.29(−3)	2.72(−3)	3.55(−3)	1.31(−3)	−2.14(−5)	9.25(−4)	−2.54(−6)	−6.06(−5)
1.29(−3)	2.72(−3)	3.55(−3)	1.31(−3)	−2.14(−5)	9.25(−4)	−2.54(−6)	−6.07(−5)
2.58(−4)	5.01(−3)	4.73(−3)	5.79(−3)	5.16(−5)	8.61(−4)	1.28(−4)	−1.45(−4)
2.58(−4)	5.01(−3)	4.73(−3)	5.79(−3)	5.16(−5)	8.61(−4)	1.28(−4)	−1.45(−4)
1.12(−3)	1.43(−3)	2.28(−3)	9.23(−4)	7.98(−5)	1.15(−3)	3.18(−5)	−4.04(−5)
1.12(−3)	1.43(−3)	2.28(−3)	9.23(−4)	7.98(−5)	1.15(−3)	3.18(−5)	−4.04(−5)
2.07(−3)	2.23(−3)	3.93(−3)	7.79(−4)	7.34(−5)	1.94(−3)	2.43(−5)	−6.91(−5)
2.07(−3)	2.23(−3)	3.93(−3)	7.79(−4)	7.34(−5)	1.94(−3)	2.43(−5)	−6.91(−5)
1.07(−3)	1.13(−3)	1.97(−3)	5.66(−4)	1.73(−4)	1.15(−3)	2.12(−5)	−8.17(−5)
1.07(−3)	1.13(−3)	1.97(−3)	5.66(−4)	1.73(−4)	1.15(−3)	2.12(−5)	−8.17(−5)
2.95(−4)	−1.78(−4)	−6.45(−5)	−8.32(−4)	1.40(−6)	−1.32(−4)	−3.98(−5)	3.50(−5)
2.95(−4)	−1.78(−4)	−6.45(−5)	−8.32(−4)	1.40(−6)	−1.32(−4)	−3.98(−5)	3.50(−5)
1.39	1.40	1.80	3.64	−1.10(−2)	1.59	1.95(−1)	7.41(−1)
1.39	1.40	1.80	3.64	−1.10(−2)	1.59	1.95(−1)	7.41(−1)
5.87(−1)	1.15(−1)	4.72(−1)	1.49(−1)	−9.03(−4)	5.43(−1)	2.97(−2)	9.78(−1)
5.87(−1)	1.15(−1)	4.72(−1)	1.49(−1)	−9.03(−4)	5.43(−1)	2.97(−2)	9.78(−1)

LSENS results; numbers in parentheses are powers of 10.

TABLE 4.64.—NORMALIZED SENSITIVITY COEFFICIENTS WITH RESPECT

Sensitivity parameter	Normalized sensitivity						
	σ_O	σ_{H_2O}	σ_{OH}	σ_H	σ_{O_2}	σ_{H_2}	σ_{HO_2}
$\sigma_{H_2,0}$	−1.02 −1.02	5.34(−1) 5.34(−1)	−1.22(−1) −1.22(−1)	2.54 2.54	−3.92 −3.92	3.41 3.41	−2.21 −2.21
$\sigma_{O_2,0}$	3.05 3.05	3.13(−1) 3.13(−1)	1.73 1.73	−6.53(−1) −6.53(−1)	5.34 5.34	−1.98 −1.98	4.36 4.36
$\sigma_{N_2,0}$	−1.29 −1.29	1.84(−1) 1.84(−1)	−6.84(−1) −6.84(−1)	−1.15 −1.15	−5.75(−1) −5.75(−1)	−5.14(−1) −5.14(−1)	−8.39(−1) −8.39(−1)
$\sigma_{O,0}$	2.12(−3) 2.12(−3)	−6.15(−5) −6.16(−5)	1.16(−3) 1.16(−3)	8.06(−4) 8.06(−4)	2.24(−3) 2.24(−3)	−1.88(−4) −1.87(−4)	2.15(−3) 2.15(−3)
$\sigma_{H,0}$	7.98(−4) 7.98(−4)	−5.75(−5) −5.75(−5)	4.93(−4) 4.93(−4)	1.33(−3) 1.33(−3)	−2.72(−4) −2.72(−4)	9.98(−4) 9.98(−4)	2.33(−4) 2.33(−4)
$\sigma_{OH,0}$	1.02(−3) 1.02(−3)	1.70(−4) 1.70(−4)	6.48(−4) 6.48(−4)	3.61(−4) 3.61(−4)	1.20(−3) 1.20(−3)	−2.20(−5) −2.19(−5)	1.19(−3) 1.19(−3)
$\sigma_{HO_2,0}$	1.88(−3) 1.88(−3)	3.00(−4) 3.00(−4)	1.14(−3) 1.14(−3)	−7.16(−6) −7.15(−6)	2.94(−3) 2.94(−3)	−7.60(−4) −7.60(−4)	2.54(−3) 2.54(−3)
$\sigma_{H_2O_2,0}$	1.11(−3) 1.11(−3)	4.81(−4) 4.81(−4)	8.03(−4) 8.03(−4)	−1.42(−4) −1.42(−4)	2.04(−3) 2.04(−3)	−4.50(−4) −4.50(−4)	1.78(−3) 1.78(−3)
$\sigma_{N,0}$	1.96(−3) 1.96(−3)	−2.99(−4) −2.99(−4)	1.04(−3) 1.04(−3)	1.84(−3) 1.84(−3)	7.80(−4) 7.80(−4)	8.61(−4) 8.61(−4)	1.19(−3) 1.19(−3)
$\sigma_{NO,0}$	1.31(−3) 1.31(−3)	6.13(−5) 6.13(−5)	7.32(−4) 7.32(−4)	5.02(−5) 5.02(−5)	1.91(−3) 1.91(−3)	−5.40(−4) −5.40(−4)	1.63(−3) 1.63(−3)
$\sigma_{NO_2,0}$	2.10(−3) 2.10(−3)	2.03(−4) 2.03(−4)	1.19(−3) 1.19(−3)	−3.89(−4) −3.89(−4)	3.61(−3) 3.61(−3)	−1.31(−3) −1.31(−3)	2.93(−3) 2.93(−3)
$\sigma_{N_2O,0}$	1.18(−3) 1.18(−3)	8.01(−5) 8.01(−5)	6.60(−4) 6.60(−4)	−6.38(−5) −6.38(−5)	1.85(−3) 1.85(−3)	−5.93(−4) −5.93(−4)	1.52(−3) 1.52(−3)
$\sigma_{H_2O,0}$	−3.99(−4) −3.99(−4)	4.49(−4) 4.49(−4)	−3.03(−5) −3.03(−5)	−3.74(−4) −3.74(−4)	4.80(−5) 4.80(−5)	8.48(−6) 8.48(−6)	5.21(−5) 5.21(−5)
T_0	1.99 1.99	−3.10(−1) −3.10(−1)	1.11 1.11	1.84 1.84	7.54(−1) 7.54(−1)	8.96(−1) 8.96(−1)	1.66 1.66
ρ_0	−2.60(−1) −2.60(−1)	3.06(−2) 3.06(−2)	−7.31(−2) −7.31(−2)	−2.61(−1) −2.61(−1)	−1.50(−1) −1.50(−1)	−8.44(−2) −8.44(−2)	3.10(−1) 3.10(−1)

[a]For each sensitivity parameter the top row gives the BFM results and the bottom row gives the

TO INITIAL CONDITION VALUES FOR TEST PROBLEM 8 AT t = 1 s

coefficients at t = 1 s of[a]							
$\sigma_{H_2O_2}$	σ_{NO}	σ_{NO_2}	σ_N	σ_{N_2}	σ_{N_2O}	T	ρ
−1.02	−1.62	−3.76	1.77	1.29(−2)	−1.59	8.89(−2)	−7.52(−2)
−1.02	−1.62	−3.76	1.77	1.29(−2)	−1.59	8.89(−2)	−7.52(−2)
3.16	2.80	5.40	7.11(−1)	−2.23(−2)	2.80	3.67(−2)	−1.81(−2)
3.16	2.80	5.40	7.11(−1)	−2.23(−2)	2.80	3.67(−2)	−1.81(−2)
−5.49(−1)	−1.42(−1)	−2.33(−1)	−1.39	1.01	3.36(−1)	−9.55(−2)	7.05(−2)
−5.49(−1)	−1.42(−1)	−2.33(−1)	−1.39	1.01	3.36(−1)	−9.55(−2)	7.05(−2)
1.50(−3)	1.47(−3)	2.39(−3)	1.90(−3)	−1.17(−5)	1.49(−3)	9.59(−5)	−7.45(−5)
1.50(−3)	1.47(−3)	2.39(−3)	1.90(−3)	−1.17(−5)	1.49(−3)	9.60(−5)	−7.50(−5)
2.21(−4)	1.98(−4)	−1.22(−4)	1.76(−3)	−1.58(−6)	2.22(−4)	8.91(−5)	−6.75(−5)
2.21(−4)	1.98(−4)	−1.22(−4)	1.76(−3)	−1.59(−6)	2.22(−4)	8.91(−5)	−6.78(−5)
9.52(−4)	7.47(−4)	1.26(−3)	7.80(−4)	−5.96(−6)	7.52(−4)	3.94(−5)	−3.60(−5)
9.52(−4)	7.47(−4)	1.26(−3)	7.80(−4)	−5.96(−6)	7.52(−4)	3.94(−5)	−3.62(−5)
1.92(−3)	1.60(−3)	2.97(−3)	7.58(−4)	−1.28(−5)	1.59(−3)	3.75(−5)	−7.27(−5)
1.92(−3)	1.60(−3)	2.97(−3)	7.58(−4)	−1.28(−5)	1.59(−3)	3.75(−5)	−7.27(−5)
1.49(−3)	1.04(−3)	2.01(−3)	1.36(−4)	−8.26(−6)	1.00(−3)	5.44(−6)	−6.93(−5)
1.49(−3)	1.04(−3)	2.01(−3)	1.36(−4)	−8.26(−6)	1.00(−3)	5.44(−6)	−6.94(−5)
7.51(−4)	9.86(−4)	1.04(−3)	2.99(−3)	8.31(−5)	1.04(−3)	1.47(−4)	−1.66(−4)
7.51(−4)	9.86(−4)	1.04(−3)	2.99(−3)	8.31(−5)	1.04(−3)	1.47(−4)	−1.66(−4)
1.16(−3)	1.12(−3)	1.99(−3)	7.08(−4)	8.20(−5)	1.16(−3)	3.33(−5)	−4.19(−5)
1.16(−3)	1.12(−3)	1.99(−3)	7.08(−4)	8.20(−5)	1.16(−3)	3.33(−5)	−4.19(−5)
2.10(−3)	1.94(−3)	3.67(−3)	5.73(−4)	7.55(−5)	1.96(−3)	2.57(−5)	−7.06(−5)
2.10(−3)	1.94(−3)	3.67(−3)	5.73(−4)	7.55(−5)	1.96(−3)	2.57(−5)	−7.06(−5)
1.07(−3)	1.09(−3)	1.94(−3)	5.42(−4)	1.73(−4)	1.15(−3)	2.13(−5)	−8.18(−5)
1.07(−3)	1.09(−3)	1.94(−3)	5.42(−4)	1.73(−4)	1.15(−3)	2.13(−5)	−8.18(−5)
2.89(−4)	−1.26(−4)	−1.69(−5)	−7.96(−4)	1.01(−6)	−1.34(−4)	−4.01(−5)	3.52(−5)
2.89(−4)	−1.26(−4)	−1.69(−5)	−7.96(−4)	1.01(−6)	−1.34(−4)	−4.01(−5)	3.52(−5)
1.43	1.11	1.53	3.44	−8.86(−3)	1.60	1.96(−1)	7.40(−1)
1.43	1.11	1.53	3.44	−8.86(−3)	1.60	1.96(−1)	7.40(−1)
5.96(−1)	3.81(−2)	4.01(−1)	9.49(−2)	−3.05(−4)	5.46(−1)	3.01(−2)	9.77(−1)
5.96(−1)	3.81(−2)	4.01(−1)	9.49(−2)	−3.05(−4)	5.46(−1)	3.01(−2)	9.77(−1)

LSENS results; numbers in parentheses are powers of 10.

TABLE 4.65.—REACTION IMPORTANCE LISTS AND NORMALIZED SENSITIVITY COEFFICIENTS WITH RESPECT TO PREEXPONENTIAL FACTORS FOR TEST PROBLEM 8 AT $t = 10^{-6}$ s

Dependent variable	Method or code	Reaction numbers in order of decreasing importance and normalized sensitivity coefficients at $t = 10^{-6}$ s[a]									
σ_O		2	4	3	13	14	8	12	7	5	17
	BFM	2.45	1.00	−5.80(−1)	2.14(−1)	−7.74(−2)	3.11(−2)	5.83(−3)	5.30(−4)	−5.52(−5)	3.51(−5)
	LSENS	2.45	1.00	−5.80(−1)	2.14(−1)	−7.74(−2)	3.11(−2)	5.83(−3)	5.30(−4)	−5.52(−5)	3.51(−5)
	SENKIN	2.45	1.00	−5.80(−1)	2.14(−1)	−7.74(−2)	3.11(−2)	5.83(−3)	5.30(−4)	−5.52(−5)	3.50(−5)
σ_{H_2O}		2	4	3	13	14	8	12	7	17	5
	BFM	1.97	1.00	2.93(−1)	2.75(−1)	−5.47(−2)	2.88(−2)	7.50(−3)	1.34(−3)	3.60(−5)	−4.50(−6)
	LSENS	1.97	1.00	2.93(−1)	2.75(−1)	−5.47(−2)	2.88(−2)	7.50(−3)	1.34(−3)	3.60(−5)	−4.50(−6)
	SENKIN	1.97	1.00	2.92(−1)	2.75(−1)	−5.47(−2)	2.88(−2)	7.49(−3)	1.34(−3)	3.59(−5)	−4.50(−6)
σ_{OH}		2	4	13	3	14	8	12	7	17	6
	BFM	2.42	1.00	−6.94(−1)	3.47(−1)	−7.59(−2)	3.41(−2)	8.51(−3)	1.96(−3)	3.50(−5)	−1.26(−5)
	LSENS	2.42	1.00	−6.94(−1)	3.47(−1)	−7.59(−2)	3.41(−2)	8.51(−3)	1.96(−3)	3.50(−5)	−1.26(−5)
	SENKIN	2.42	1.00	−6.94(−1)	3.47(−1)	−7.59(−2)	3.41(−2)	8.50(−3)	1.96(−3)	3.49(−5)	−1.26(−5)
σ_H		2	4	3	13	14	8	12	7	17	5
	BFM	1.53	1.00	3.00(−1)	2.23(−1)	−8.15(−2)	3.19(−2)	6.10(−3)	5.89(−4)	3.48(−5)	−1.61(−5)
	LSENS	1.53	1.00	3.00(−1)	2.23(−1)	−8.15(−2)	3.19(−2)	6.10(−3)	5.89(−4)	3.48(−5)	−1.61(−5)
	SENKIN	1.53	1.00	3.00(−1)	2.23(−1)	−8.15(−2)	3.19(−2)	6.09(−3)	5.88(−4)	3.47(−5)	−1.61(−5)
σ_{O_2}		2	4	3	13	8	14	12	7	5	17
	BFM	−5.54(−5)	−3.80(−5)	−6.52(−6)	−4.89(−6)	−7.26(−7)	−3.49(−7)	−1.23(−7)	−9.25(−9)	1.04(−9)	−1.00(−9)
	LSENS	−5.54(−5)	−3.80(−5)	−6.52(−6)	−4.89(−6)	−7.26(−7)	−3.49(−7)	−1.23(−7)	−9.25(−9)	1.04(−9)	−1.00(−9)
	SENKIN	−5.53(−5)	−3.80(−5)	−6.52(−6)	−4.88(−6)	−7.25(−7)	−3.50(−7)	−1.23(−7)	−9.24(−9)	1.04(−9)	−9.99(−10)

σ_{H_2}		2	4	3	13	14	8	12	7	17	5
	BFM	−6.44(−5)	−3.79(−5)	−1.04(−5)	−7.77(−6)	1.77(−6)	−1.13(−6)	−2.07(−7)	−3.18(−8)	−1.25(−9)	5.06(−10)
	LSENS	−6.44(−5)	−3.79(−5)	−1.04(−5)	−7.77(−6)	1.77(−6)	−1.13(−6)	−2.07(−7)	−3.18(−8)	−1.25(−9)	5.06(−10)
	SENKIN	−6.43(−5)	−3.78(−5)	−1.04(−5)	−7.76(−6)	1.77(−6)	−1.13(−6)	−2.07(−7)	−3.18(−8)	−1.25(−9)	5.06(−10)
σ_{HO_2}		4	2	14	3	8	13	7	12	5	6
	BFM	9.96(−1)	1.76(−1)	1.57(−1)	3.88(−2)	−3.48(−2)	2.91(−2)	−2.16(−3)	7.27(−4)	−6.81(−5)	−2.06(−5)
	LSENS	9.96(−1)	1.76(−1)	1.57(−1)	3.88(−2)	−3.48(−2)	2.91(−2)	−2.16(−3)	7.27(−4)	−6.81(−5)	−2.06(−5)
	SENKIN	9.96(−1)	1.75(−1)	1.57(−1)	3.88(−2)	−3.48(−2)	2.90(−2)	−2.16(−3)	7.26(−4)	−6.81(−5)	−2.06(−5)
$\sigma_{H_2O_2}$		4	8	12	14	2	3	13	7	10	5
	BFM	9.98(−1)	9.72(−1)	−2.12(−1)	9.17(−2)	7.41(−2)	1.84(−2)	1.39(−2)	−9.70(−4)	2.58(−4)	−2.99(−5)
	LSENS	9.98(−1)	9.72(−1)	−2.12(−1)	9.17(−2)	7.41(−2)	1.84(−2)	1.39(−2)	−9.70(−4)	2.58(−4)	−2.99(−5)
	SENKIN	9.98(−1)	9.72(−1)	−2.11(−1)	9.16(−2)	7.40(−2)	1.84(−2)	1.39(−2)	−9.69(−4)	2.58(−4)	−2.99(−5)
σ_{NO}		2	24	4	3	23	13	14	8	12	7
	BFM	1.93	1.00	1.00	−6.28(−1)	1.80(−1)	1.62(−1)	−5.30(−2)	2.42(−2)	3.93(−3)	2.70(−4)
	LSENS	1.93	1.00	1.00	−6.28(−1)	1.80(−1)	1.62(−1)	−5.30(−2)	2.42(−2)	3.93(−3)	2.70(−4)
	SENKIN	1.93	1.00	1.00	−6.29(−1)	1.80(−1)	1.62(−1)	−5.30(−2)	2.42(−2)	3.93(−3)	2.70(−4)
σ_{NO_2}		4	2	24	19	3	23	13	14	20	21
	BFM	1.98	1.84	1.00	9.69(−1)	−6.27(−1)	1.78(−1)	1.60(−1)	6.97(−2)	1.71(−2)	1.37(−2)
	LSENS	1.98	1.84	1.00	9.69(−1)	−6.27(−1)	1.78(−1)	1.60(−1)	6.97(−2)	1.71(−2)	1.37(−2)
	SENKIN	1.98	1.84	1.00	9.69(−1)	−6.27(−1)	1.78(−1)	1.60(−1)	6.97(−2)	1.71(−2)	1.37(−2)

[a]For each dependent variable the top row lists the reaction numbers. The next three rows give the normalized sensitivity coefficients produced by BFM, LSENS, and SENKIN, respectively. For each dependent variable and method or code the $\{\langle S_{ij} \rangle\}$ are those of that variable with respect to the preexponential factors of the reactions corresponding to the numbers listed in the first row. Numbers in parentheses designate powers of 10.

TABLE 4.65.—Concluded.

Dependent variable	Method or code	Reaction numbers in order of decreasing importance and normalized sensitivity coefficients at $t = 10^{-6}$ s[a]									
σ_N		2	24	4	3	23	13	14	8	12	7
	BFM	2.13	1.00	1.00	−6.13(−1)	−4.19(−1)	1.84(−1)	−6.25(−2)	2.73(−2)	4.73(−3)	3.58(−4)
	LSENS	2.13	1.00	1.00	−6.13(−1)	−4.19(−1)	1.84(−1)	−6.25(−2)	2.73(−2)	4.73(−3)	3.58(−4)
	SENKIN	2.13	1.00	1.00	−6.13(−1)	−4.19(−1)	1.83(−1)	−6.25(−2)	2.73(−2)	4.73(−3)	3.58(−4)
σ_{N_2}		2	4	26	3	13	14	8	27	24	12
	BFM	−1.48(−12)	−7.42(−13)	−7.39(−13)	4.63(−13)	−1.25(−13)	4.15(−14)	−1.87(−14)	−1.69(−14)	−3.70(−15)	−3.10(−15)
	LSENS	−1.48(−12)	−7.42(−13)	−7.39(−13)	4.63(−13)	−1.25(−13)	4.15(−14)	−1.87(−14)	−1.69(−14)	−3.70(−15)	−3.10(−15)
	SENKIN	−1.48(−12)	−7.40(−13)	−7.37(−13)	4.62(−13)	−1.25(−13)	4.14(−14)	−1.86(−14)	−1.69(−14)	−3.68(−15)	−3.09(−15)
σ_{N_2O}		2	26	4	3	13	14	8	27	12	7
	BFM	1.95	9.78(−1)	9.78(−1)	−6.10(−1)	1.65(−1)	−5.46(−2)	2.46(−2)	2.23(−2)	4.08(−3)	2.90(−4)
	LSENS	1.95	9.78(−1)	9.78(−1)	−6.10(−1)	1.65(−1)	−5.46(−2)	2.46(−2)	2.23(−2)	4.08(−3)	2.90(−4)
	SENKIN	1.95	9.78(−1)	9.77(−1)	−6.10(−1)	1.65(−1)	−5.46(−2)	2.46(−2)	2.24(−2)	4.07(−3)	2.90(−4)
T		2	4	13	3	14	8	7	12	5	6
	BFM	5.51(−6)	−3.06(−6)	1.42(−6)	1.23(−6)	1.11(−6)	−5.36(−8)	2.04(−8)	−9.95(−9)	5.10(−10)	1.50(−10)
	LSENS	5.51(−6)	−3.06(−6)	1.42(−6)	1.23(−6)	1.11(−6)	−5.36(−8)	2.04(−8)	−9.95(−9)	5.10(−10)	1.50(−10)
	SENKIN	5.50(−6)	−3.07(−6)	1.41(−6)	1.23(−6)	1.11(−6)	−5.36(−8)	2.04(−8)	−9.94(−9)	5.10(−10)	1.49(−10)
ρ[b]		2	4	13	3	14	8	7	12	5	6
	BFM	−5.19(−6)	3.35(−6)	−1.36(−6)	−1.16(−6)	−8.34(−7)	4.75(−8)	−2.03(−8)	−6.03(−10)	−5.13(−10)	−1.51(−10)
	LSENS	−5.19(−6)	3.35(−6)	−1.36(−6)	−1.16(−6)	−8.34(−7)	4.75(−8)	−2.03(−8)	−6.03(−10)	−5.13(−10)	−1.51(−10)

[a]For each dependent variable the top row lists the reaction numbers. The next three rows give the normalized sensitivity coefficients produced by BFM, LSENS, and SENKIN, respectively. For each dependent variable and method or code the $\{\langle S_{ij} \rangle\}$ are those of that variable with respect to the preexponential factors of the reactions corresponding to the numbers listed in the first row. Numbers in parentheses designate powers of 10.

[b]Sensitivity coefficients of density are not calculated by SENKIN.

TABLE 4.66.—REACTION IMPORTANCE LISTS AND NORMALIZED SENSITIVITY COEFFICIENTS WITH RESPECT TO PREEXPONENTIAL FACTORS FOR TEST PROBLEM 8 AT $t = 3\times10^{-6}$ s

Dependent variable	Method or code	Reaction numbers in order of decreasing importance and normalized sensitivity coefficients at $t = 3\times10^{-6}$ s[a]									
σ_O		2	4	13	14	8	3	7	12	5	17
	BFM	7.05	9.92(−1)	6.58(−1)	−2.85(−1)	4.63(−2)	2.69(−2)	2.55(−2)	1.06(−2)	−2.08(−3)	−6.61(−4)
	LSENS	7.05	9.92(−1)	6.58(−1)	−2.85(−1)	4.63(−2)	2.69(−2)	2.55(−2)	1.06(−2)	−2.08(−3)	−6.61(−4)
	SENKIN	7.05	9.92(−1)	6.57(−1)	−2.85(−1)	4.63(−2)	2.65(−2)	2.54(−2)	1.06(−2)	−2.07(−3)	−6.57(−4)
σ_{H_2O}		2	4	3	13	14	8	7	12	5	17
	BFM	6.20	1.00	8.42(−1)	6.71(−1)	−2.22(−1)	4.54(−2)	3.55(−2)	1.06(−2)	−6.14(−4)	−3.04(−4)
	LSENS	6.20	1.00	8.42(−1)	6.71(−1)	−2.22(−1)	4.54(−2)	3.55(−2)	1.06(−2)	−6.14(−4)	−3.04(−4)
	SENKIN	6.20	1.00	8.42(−1)	6.71(−1)	−2.22(−1)	4.54(−2)	3.55(−2)	1.06(−2)	−6.13(−4)	−3.03(−4)
σ_{OH}		2	4	3	14	13	7	8	12	5	15
	BFM	7.06	1.00	9.58(−1)	−2.43(−1)	−2.34(−1)	5.09(−2)	4.66(−2)	1.09(−2)	−1.20(−3)	−8.65(−4)
	LSENS	7.06	1.00	9.58(−1)	−2.43(−1)	−2.34(−1)	5.09(−2)	4.66(−2)	1.09(−2)	−1.20(−3)	−8.65(−4)
	SENKIN	7.06	1.00	9.58(−1)	−2.43(−1)	−2.35(−1)	5.09(−2)	4.66(−2)	1.09(−2)	−1.20(−3)	−8.60(−4)
σ_H		2	4	3	13	14	8	7	12	5	17
	BFM	6.10	9.82(−1)	8.98(−1)	6.68(−1)	−2.86(−1)	4.60(−2)	2.62(−2)	1.06(−2)	−8.45(−4)	−7.46(−4)
	LSENS	6.10	9.82(−1)	8.98(−1)	6.68(−1)	−2.86(−1)	4.60(−2)	2.62(−2)	1.06(−2)	−8.45(−4)	−7.46(−4)
	SENKIN	6.10	9.82(−1)	8.98(−1)	6.68(−1)	−2.86(−1)	4.60(−2)	2.62(−2)	1.05(−2)	−8.44(−4)	−7.42(−4)
σ_{O_2}		2	4	3	13	14	8	7	12	5	6
	BFM	−6.34(−2)	−1.00(−2)	−8.07(−3)	−5.97(−3)	1.92(−3)	−4.61(−4)	−1.99(−4)	−1.04(−4)	1.25(−5)	4.32(−6)
	LSENS	−6.34(−2)	−1.00(−2)	−8.07(−3)	−5.97(−3)	1.92(−3)	−4.62(−4)	−1.99(−4)	−1.04(−4)	1.25(−5)	4.32(−6)
	SENKIN	−6.32(−2)	−9.98(−3)	−8.04(−3)	−5.95(−3)	1.91(−3)	−4.60(−4)	−1.98(−4)	−1.03(−4)	1.25(−5)	4.30(−6)

[a]For each dependent variable the top row lists the reaction numbers. The next three rows give the normalized sensitivity coefficients produced by BFM, LSENS, and SENKIN, respectively. For each dependent variable and method or code the $\{\langle S_{ij}\rangle\}$ are those of that variable with respect to the preexponential factors of the reactions corresponding to the numbers listed in the first row. Numbers in parentheses designate powers of 10.

TABLE 4.66.—Concluded.

Dependent variable	Method or code	Reaction numbers in order of decreasing importance and normalized sensitivity coefficients at $t = 3\times10^{-6}$ s[a]									
σ_{H_2}		2	4	3	13	14	8	7	12	5	17
	BFM	−7.82(−2)	−1.26(−2)	−1.09(−2)	−8.07(−3)	2.95(−3)	−5.78(−4)	−3.78(−4)	−1.32(−4)	1.01(−5)	5.60(−6)
	LSENS	−7.82(−2)	−1.26(−2)	−1.09(−2)	−8.07(−3)	2.95(−3)	−5.78(−4)	−3.78(−4)	−1.32(−4)	1.01(−5)	5.60(−6)
	SENKIN	−7.79(−2)	−1.25(−2)	−1.08(−2)	−8.04(−3)	2.94(−3)	−5.76(−4)	−3.77(−4)	−1.32(−4)	1.01(−5)	5.55(−6)
σ_{HO_2}		2	14	7	3	4	13	5	8	6	12
	BFM	2.02	8.82(−1)	−4.22(−1)	3.15(−1)	2.34(−1)	2.29(−1)	−1.35(−2)	4.55(−3)	−4.18(−3)	2.80(−3)
	LSENS	2.02	8.82(−1)	−4.22(−1)	3.15(−1)	2.34(−1)	2.29(−1)	−1.35(−2)	4.55(−3)	−4.18(−3)	2.80(−3)
	SENKIN	2.02	8.81(−1)	−4.21(−1)	3.15(−1)	2.35(−1)	2.29(−1)	−1.35(−2)	4.54(−3)	−4.18(−3)	2.81(−3)
$\sigma_{H_2O_2}$		2	14	8	4	7	3	12	13	10	5
	BFM	1.53	8.34(−1)	7.84(−1)	3.82(−1)	−2.46(−1)	2.44(−1)	−2.44(−1)	1.59(−1)	1.13(−2)	−7.77(−3)
	LSENS	1.53	8.34(−1)	7.84(−1)	3.82(−1)	−2.46(−1)	2.44(−1)	−2.44(−1)	1.59(−1)	1.13(−2)	−7.77(−3)
	SENKIN	1.53	8.34(−1)	7.84(−1)	3.84(−1)	−2.46(−1)	2.45(−1)	−2.44(−1)	1.59(−1)	1.13(−2)	−7.75(−3)
σ_{NO}		2	4	24	13	14	23	3	8	7	12
	BFM	6.23	1.02	9.99(−1)	5.75(−1)	−2.43(−1)	1.63(−1)	−8.59(−2)	4.61(−2)	1.59(−2)	1.04(−2)
	LSENS	6.23	1.02	9.99(−1)	5.75(−1)	−2.43(−1)	1.63(−1)	−8.59(−2)	4.61(−2)	1.59(−2)	1.04(−2)
	SENKIN	6.23	1.02	9.99(−1)	5.74(−1)	−2.43(−1)	1.63(−1)	−8.64(−2)	4.60(−2)	1.58(−2)	1.04(−2)
σ_{NO_2}		2	24	19	4	14	22	13	3	7	23
	BFM	5.17	9.99(−1)	8.67(−1)	8.53(−1)	6.44(−1)	−6.25(−1)	4.55(−1)	−3.55(−1)	−2.95(−1)	1.64(−1)
	LSENS	5.17	9.99(−1)	8.67(−1)	8.53(−1)	6.44(−1)	−6.25(−1)	4.55(−1)	−3.55(−1)	−2.95(−1)	1.64(−1)
	SENKIN	5.17	9.99(−1)	8.67(−1)	8.55(−1)	6.43(−1)	−6.24(−1)	4.56(−1)	−3.54(−1)	−2.95(−1)	1.64(−1)

σ_N		2	4	24	13	23	14	8	3	7	25
	BFM	6.66	1.01	1.00	6.40(−1)	−4.67(−1)	−2.60(−1)	4.63(−2)	−2.61(−2)	2.04(−2)	−1.78(−2)
	LSENS	6.66	1.01	1.00	6.40(−1)	−4.67(−1)	−2.60(−1)	4.63(−2)	−2.61(−2)	2.04(−2)	−1.78(−2)
	SENKIN	6.66	1.01	1.00	6.39(−1)	−4.67(−1)	−2.60(−1)	4.63(−2)	−2.65(−2)	2.03(−2)	−1.77(−2)
σ_{N_2}		2	4	26	13	14	3	8	7	12	24
	BFM	−1.76(−9)	−2.82(−10)	−2.82(−10)	−1.63(−10)	7.04(−11)	2.48(−11)	−1.28(−11)	−4.41(−12)	−2.89(−12)	−1.44(−12)
	LSENS	−1.76(−9)	−2.82(−10)	−2.82(−10)	−1.63(−10)	7.04(−11)	2.48(−11)	−1.28(−11)	−4.41(−12)	−2.89(−12)	−1.44(−12)
	SENKIN	−1.75(−9)	−2.81(−10)	−2.81(−10)	−1.62(−10)	7.01(−11)	2.48(−11)	−1.28(−11)	−4.38(−12)	−2.88(−12)	−1.43(−12)
σ_{N_2O}		2	26	4	13	14	3	8	7	12	30
	BFM	6.22	1.00	9.96(−1)	5.76(−1)	−2.49(−1)	−8.77(−2)	4.53(−2)	1.56(−2)	1.02(−2)	−2.93(−3)
	LSENS	6.22	1.00	9.96(−1)	5.76(−1)	−2.49(−1)	−8.77(−2)	4.53(−2)	1.56(−2)	1.02(−2)	−2.93(−3)
	SENKIN	6.22	1.00	9.96(−1)	5.76(−1)	−2.49(−1)	−8.81(−2)	4.52(−2)	1.55(−2)	1.02(−2)	−2.93(−3)
T		2	4	3	13	14	7	8	12	17	15
	BFM	1.04(−2)	1.87(−3)	1.57(−3)	1.32(−3)	2.92(−4)	1.51(−4)	7.31(−5)	1.74(−5)	4.01(−6)	3.69(−6)
	LSENS	1.04(−2)	1.87(−3)	1.57(−3)	1.32(−3)	2.92(−4)	1.51(−4)	7.31(−5)	1.74(−5)	4.01(−6)	3.69(−6)
	SENKIN	1.04(−2)	1.87(−3)	1.56(−3)	1.32(−3)	2.91(−4)	1.50(−4)	7.28(−5)	1.73(−5)	3.97(−6)	3.66(−6)
ρ^b		2	4	3	13	14	7	8	12	17	15
	BFM	−9.81(−3)	−1.76(−3)	−1.48(−3)	−1.25(−3)	−2.10(−4)	−1.49(−4)	−6.86(−5)	−1.67(−5)	−3.53(−6)	−3.26(−6)
	LSENS	−9.81(−3)	−1.76(−3)	−1.48(−3)	−1.25(−3)	−2.10(−4)	−1.49(−4)	−6.86(−5)	−1.67(−5)	−3.53(−6)	−3.26(−6)

[a]For each dependent variable the top row lists the reaction numbers. The next three rows give the normalized sensitivity coefficients produced by BFM, LSENS, and SENKIN, respectively. For each dependent variable and method or code the $\{\langle S_{ij'}\rangle\}$ are those of that variable with respect to the preexponential factors of the reactions corresponding to the numbers listed in the first row. Numbers in parentheses designate powers of 10.

[b]Sensitivity coefficients of density are not calculated by SENKIN.

TABLE 4.67.—REACTION IMPORTANCE LISTS AND NORMALIZED SENSITIVITY COEFFICIENTS WITH RESPECT TO PREEXPONENTIAL FACTORS FOR TEST PROBLEM 8 AT $t = 5\times10^{-6}$ s

Dependent variable	Method or code	Reaction numbers in order of decreasing importance and normalized sensitivity coefficients at $t = 5\times10^{-6}$ s[a]									
σ_O		2	13	3	4	14	7	17	15	8	1
	BFM	2.02	3.17(−1)	2.50(−1)	1.75(−1)	−3.60(−2)	2.64(−2)	−1.26(−2)	−1.11(−2)	8.63(−3)	8.61(−3)
	LSENS	2.02	3.17(−1)	2.50(−1)	1.75(−1)	−3.60(−2)	2.64(−2)	−1.26(−2)	−1.11(−2)	8.63(−3)	8.61(−3)
	SENKIN	2.04	3.19(−1)	2.52(−1)	1.76(−1)	−3.61(−2)	2.66(−2)	−1.25(−2)	−1.10(−2)	8.71(−3)	8.64(−3)
σ_{H_2O}		2	13	3	4	15	7	14	17	8	16
	BFM	9.62(−1)	1.61(−1)	1.45(−1)	9.12(−2)	1.30(−2)	1.16(−2)	1.11(−2)	5.90(−3)	4.67(−3)	2.20(−3)
	LSENS	9.62(−1)	1.61(−1)	1.45(−1)	9.12(−2)	1.30(−2)	1.16(−2)	1.11(−2)	5.90(−3)	4.67(−3)	2.20(−3)
	SENKIN	9.69(−1)	1.62(−1)	1.46(−1)	9.19(−2)	1.30(−2)	1.17(−2)	1.11(−2)	5.89(−3)	4.70(−3)	2.21(−3)
σ_{OH}		2	3	4	13	14	15	17	7	1	16
	BFM	1.45	2.32(−1)	1.34(−1)	1.19(−1)	8.37(−2)	3.38(−2)	3.03(−2)	2.07(−2)	−1.19(−2)	1.18(−2)
	LSENS	1.45	2.32(−1)	1.34(−1)	1.19(−1)	8.37(−2)	3.38(−2)	3.03(−2)	2.07(−2)	−1.19(−2)	1.18(−2)
	SENKIN	1.45	2.33(−1)	1.34(−1)	1.19(−1)	8.37(−2)	3.37(−2)	3.02(−2)	2.08(−2)	−1.20(−2)	1.18(−2)
σ_H		2	14	15	17	13	4	3	16	12	1
	BFM	−2.13(−1)	−7.82(−2)	−4.13(−2)	−3.32(−2)	2.89(−2)	−2.82(−2)	−2.31(−2)	−9.64(−3)	−3.73(−3)	2.08(−3)
	LSENS	−2.13(−1)	−7.82(−2)	−4.13(−2)	−3.32(−2)	2.89(−2)	−2.82(−2)	−2.31(−2)	−9.64(−3)	−3.73(−3)	2.08(−3)
	SENKIN	−2.07(−1)	−7.82(−2)	−4.11(−2)	−3.31(−2)	2.99(−2)	−2.77(−2)	−2.22(−2)	−9.61(−3)	−3.71(−3)	2.07(−3)
σ_{O_2}		2	13	3	4	7	14	15	17	8	16
	BFM	−2.81	−4.34(−1)	−4.10(−1)	−2.61(−1)	−3.48(−2)	−3.28(−2)	−3.04(−2)	−1.53(−2)	−1.32(−2)	−5.50(−3)
	LSENS	−2.81	−4.34(−1)	−4.10(−1)	−2.61(−1)	−3.48(−2)	−3.28(−2)	−3.04(−2)	−1.53(−2)	−1.32(−2)	−5.50(−3)
	SENKIN	−2.83	−4.36(−1)	−4.12(−1)	−2.62(−1)	−3.49(−2)	−3.26(−2)	−3.03(−2)	−1.53(−2)	−1.32(−2)	−5.49(−3)

σ_{H_2}		2	13	3	4	7	14	8	15	17	1
	BFM	−2.32	−4.17(−1)	−3.57(−1)	−2.14(−1)	−2.95(−2)	1.71(−2)	−1.06(−2)	−5.96(−3)	5.40(−3)	−3.45(−3)
	LSENS	−2.32	−4.17(−1)	−3.57(−1)	−2.14(−1)	−2.95(−2)	1.71(−2)	−1.06(−2)	−5.96(−3)	5.40(−3)	−3.45(−3)
	SENKIN	−2.34	−4.19(−1)	−3.60(−1)	−2.15(−1)	−2.97(−2)	1.73(−2)	−1.07(−2)	−5.97(−3)	5.38(−3)	−3.44(−3)
σ_{HO_2}		2	14	7	4	13	3	12	5	15	17
	BFM	−2.74	8.44(−1)	−6.93(−1)	−5.30(−1)	−4.11(−1)	−3.98(−1)	6.29(−2)	−5.97(−2)	−5.39(−2)	−3.26(−2)
	LSENS	−2.74	8.44(−1)	−6.93(−1)	−5.30(−1)	−4.11(−1)	−3.98(−1)	6.29(−2)	−5.97(−2)	−5.39(−2)	−3.26(−2)
	SENKIN	−2.75	8.44(−1)	−6.93(−1)	−5.31(−1)	−4.13(−1)	−4.00(−1)	6.27(−2)	−5.96(−2)	−5.37(−2)	−3.25(−2)
$\sigma_{H_2O_2}$		2	12	8	3	4	13	14	1	7	9
	BFM	9.75(−1)	8.14(−1)	−7.75(−1)	1.59(−1)	6.79(−2)	−5.25(−2)	5.17(−2)	−2.41(−2)	1.84(−2)	−1.65(−2)
	LSENS	9.75(−1)	8.14(−1)	−7.75(−1)	1.59(−1)	6.79(−2)	−5.25(−2)	5.17(−2)	−2.41(−2)	1.84(−2)	−1.65(−2)
	SENKIN	9.85(−1)	8.15(−1)	−7.75(−1)	1.61(−1)	6.87(−2)	−5.27(−2)	5.20(−2)	−2.43(−2)	1.85(−2)	−1.65(−2)
σ_{NO}		2	3	13	4	24	14	15	17	7	25
	BFM	1.59(1)	2.26	2.05	1.62	9.71(−1)	5.87(−1)	3.62(−1)	2.56(−1)	1.68(−1)	1.03(−1)
	LSENS	1.59(1)	2.26	2.05	1.62	9.71(−1)	5.87(−1)	3.62(−1)	2.56(−1)	1.68(−1)	1.03(−1)
	SENKIN	1.60(1)	2.26	2.05	1.62	9.71(−1)	5.86(−1)	3.61(−1)	2.55(−1)	1.69(−1)	1.03(−1)
σ_{NO_2}		2	3	13	4	24	22	21	14	15	17
	BFM	1.73(1)	2.40	2.22	1.72	9.71(−1)	−9.63(−1)	9.57(−1)	5.96(−1)	3.51(−1)	2.49(−1)
	LSENS	1.73(1)	2.40	2.22	1.72	9.71(−1)	−9.63(−1)	9.57(−1)	5.96(−1)	3.51(−1)	2.49(−1)
	SENKIN	1.73(1)	2.40	2.22	1.73	9.71(−1)	−9.63(−1)	9.57(−1)	5.96(−1)	3.50(−1)	2.48(−1)

[a]For each dependent variable the top row lists the reaction numbers. The next three rows give the normalized sensitivity coefficients produced by BFM, LSENS, and SENKIN, respectively. For each dependent variable and method or code the $\{\langle S_{ij}\rangle\}$ are those of that variable with respect to the preexponential factors of the reactions corresponding to the numbers listed in the first row. Numbers in parentheses designate powers of 10.

TABLE 4.67.—Concluded.

Dependent Variable	Method or code	Reaction numbers in order of decreasing importance and normalized sensitivity coefficients at $t = 5\times10^{-6}$ s[a]									
σ_N		2	3	13	4	24	25	14	15	17	7
	BFM	1.18(1)	1.73	1.63	1.20	1.00	−7.03(−1)	6.34(−1)	4.18(−1)	2.83(−1)	1.24(−1)
	LSENS	1.18(1)	1.73	1.63	1.20	1.00	−7.03(−1)	6.34(−1)	4.18(−1)	2.83(−1)	1.24(−1)
	SENKIN	1.18(1)	1.73	1.64	1.21	1.00	−7.02(−1)	6.34(−1)	4.17(−1)	2.82(−1)	1.25(−1)
σ_{N_2}		2	26	13	3	4	30	24	15	14	7
	BFM	−6.10(−7)	−7.63(−8)	−7.51(−8)	−7.35(−8)	−5.97(−8)	2.72(−8)	−9.99(−9)	−6.88(−9)	−6.60(−9)	−6.45(−9)
	LSENS	−6.10(−7)	−7.63(−8)	−7.51(−8)	−7.35(−8)	−5.97(−8)	2.72(−8)	−9.99(−9)	−6.88(−9)	−6.60(−9)	−6.45(−9)
	SENKIN	−6.08(−7)	−7.59(−8)	−7.48(−8)	−7.32(−8)	−5.95(−8)	2.70(−8)	−9.88(−9)	−6.81(−9)	−6.51(−9)	−6.43(−9)
σ_{N_2O}		2	26	13	3	4	30	7	15	8	17
	BFM	5.94	9.99(−1)	7.19(−1)	6.71(−1)	5.74(−1)	−3.56(−1)	6.29(−2)	4.07(−2)	2.87(−2)	2.67(−2)
	LSENS	5.94	9.99(−1)	7.19(−1)	6.71(−1)	5.74(−1)	−3.56(−1)	6.29(−2)	4.07(−2)	2.87(−2)	2.67(−2)
	SENKIN	5.96	9.99(−1)	7.21(−1)	6.73(−1)	5.76(−1)	−3.55(−1)	6.31(−2)	4.06(−2)	2.88(−2)	2.67(−2)
T		2	3	13	4	14	15	17	16	7	8
	BFM	4.77(−1)	7.36(−2)	6.07(−2)	4.98(−2)	3.74(−2)	2.37(−2)	1.64(−2)	5.27(−3)	4.98(−3)	2.70(−3)
	LSENS	4.77(−1)	7.36(−2)	6.07(−2)	4.98(−2)	3.74(−2)	2.37(−2)	1.64(−2)	5.27(−3)	4.98(−3)	2.70(−3)
	SENKIN	4.78(−1)	7.37(−2)	6.08(−2)	4.98(−2)	3.74(−2)	2.36(−2)	1.64(−2)	5.26(−3)	4.99(−3)	2.70(−3)
ρ[b]		2	3	13	4	14	15	17	16	7	8
	BFM	−4.11(−1)	−6.34(−2)	−5.26(−2)	−4.29(−2)	−3.19(−2)	−2.03(−2)	−1.40(−2)	−4.51(−3)	−4.29(−3)	−2.33(−3)
	LSENS	−4.11(−1)	−6.34(−2)	−5.26(−2)	−4.29(−2)	−3.19(−2)	−2.03(−2)	−1.40(−2)	−4.51(−3)	−4.29(−3)	−2.33(−3)

[a]For each dependent variable the top row lists the reaction numbers. The next three rows give the normalized sensitivity coefficients produced by BFM, LSENS, and SENKIN, respectively. For each dependent variable and method or code the $\{\langle S_{ij}\rangle\}$ are those of that variable with respect to the preexponential factors of the reactions corresponding to the numbers listed in the first row. Numbers in parentheses designate powers of 10.

[b]Sensitivity coefficients of density are not calculated by SENKIN.

TABLE 4.68.—REACTION IMPORTANCE LISTS AND NORMALIZED SENSITIVITY COEFFICIENTS WITH RESPECT TO PREEXPONENTIAL FACTORS FOR TEST PROBLEM 8 AT $t = 7.5\times10^{-6}$ s

Dependent variable	Method or code	Reaction numbers in order of decreasing importance and normalized sensitivity coefficients at $t = 7.5\times10^{-6}$ s[a]									
σ_O		2	14	15	17	3	13	4	16	8	12
	BFM	−2.57(−1)	−8.68(−2)	−8.46(−2)	−4.40(−2)	−4.13(−2)	−3.10(−2)	−2.81(−2)	−2.32(−2)	−6.25(−3)	−5.86(−3)
	LSENS	−2.57(−1)	−8.68(−2)	−8.46(−2)	−4.40(−2)	−4.13(−2)	−3.10(−2)	−2.81(−2)	−2.32(−2)	−6.25(−3)	−5.86(−3)
	SENKIN	−2.57(−1)	−8.69(−2)	−8.45(−2)	−4.40(−2)	−4.13(−2)	−3.10(−2)	−2.81(−2)	−2.32(−2)	−6.25(−3)	−5.86(−3)
σ_{H_2O}		2	14	15	17	3	13	4	16	12	8
	BFM	6.75(−2)	2.30(−2)	2.19(−2)	1.08(−2)	1.06(−2)	8.82(−3)	6.71(−3)	5.56(−3)	1.40(−3)	1.39(−3)
	LSENS	6.75(−2)	2.30(−2)	2.19(−2)	1.08(−2)	1.06(−2)	8.82(−3)	6.71(−3)	5.56(−3)	1.40(−3)	1.39(−3)
	SENKIN	6.76(−2)	2.30(−2)	2.19(−2)	1.08(−2)	1.06(−2)	8.82(−3)	6.71(−3)	5.57(−3)	1.40(−3)	1.39(−3)
σ_{OH}		2	14	15	3	17	13	4	16	7	12
	BFM	1.50(−1)	5.44(−2)	4.51(−2)	2.44(−2)	2.43(−2)	1.73(−2)	1.41(−2)	1.30(−2)	3.72(−3)	3.07(−3)
	LSENS	1.50(−1)	5.44(−2)	4.51(−2)	2.44(−2)	2.43(−2)	1.73(−2)	1.41(−2)	1.30(−2)	3.72(−3)	3.07(−3)
	SENKIN	1.50(−1)	5.46(−2)	4.50(−2)	2.45(−2)	2.43(−2)	1.73(−2)	1.41(−2)	1.30(−2)	3.73(−3)	3.08(−3)
σ_H		2	14	15	17	3	13	4	16	8	12
	BFM	−3.78(−1)	−1.30(−1)	−1.23(−1)	−6.35(−2)	−5.81(−2)	−4.57(−2)	−3.93(−2)	−3.23(−2)	−8.64(−3)	−8.29(−3)
	LSENS	−3.78(−1)	−1.30(−1)	−1.23(−1)	−6.35(−2)	−5.81(−2)	−4.57(−2)	−3.93(−2)	−3.23(−2)	−8.64(−3)	−8.29(−3)
	SENKIN	−3.78(−1)	−1.31(−1)	−1.22(−1)	−6.35(−2)	−5.81(−2)	−4.57(−2)	−3.93(−2)	−3.24(−2)	−8.63(−3)	−8.30(−3)
σ_{O_2}		2	14	15	3	17	13	4	16	7	12
	BFM	−1.94(−1)	−6.89(−2)	−6.07(−2)	−3.06(−2)	−3.02(−2)	−2.52(−2)	−1.77(−2)	−1.56(−2)	−4.86(−3)	−3.90(−3)
	LSENS	−1.94(−1)	−6.89(−2)	−6.07(−2)	−3.06(−2)	−3.02(−2)	−2.52(−2)	−1.77(−2)	−1.56(−2)	−4.86(−3)	−3.90(−3)
	SENKIN	−1.95(−1)	−6.89(−2)	−6.06(−2)	−3.06(−2)	−3.02(−2)	−2.53(−2)	−1.77(−2)	−1.56(−2)	−4.86(−3)	−3.90(−3)

[a]For each dependent variable the top row lists the reaction numbers. The next three rows give the normalized sensitivity coefficients produced by BFM, LSENS, and SENKIN, respectively. For each dependent variable and method or code the $\{\langle S_{ij}\rangle\}$ are those of that variable with respect to the preexponential factors of the reactions corresponding to the numbers listed in the first row. Numbers in parentheses designate powers of 10.

TABLE 4.68.—Concluded.

Dependent variable	Method or code	Reaction numbers in order of decreasing importance and normalized sensitivity coefficients at $t = 7.5\times10^{-6}$ s[a]									
σ_{H_2}		2	14	15	3	13	17	16	4	7	12
	BFM	−3.32(−2)	−1.13(−2)	−9.84(−3)	−6.13(−3)	−5.80(−3)	−3.72(−3)	−2.22(−3)	−2.07(−3)	−1.96(−3)	−4.57(−4)
	LSENS	−3.32(−2)	−1.13(−2)	−9.84(−3)	−6.13(−3)	−5.80(−3)	−3.72(−3)	−2.22(−3)	−2.07(−3)	−1.96(−3)	−4.57(−4)
	SENKIN	−3.31(−2)	−1.13(−2)	−9.79(−3)	−6.12(−3)	−5.80(−3)	−3.70(−3)	−2.21(−3)	−2.06(−3)	−1.96(−3)	−4.55(−4)
σ_{HO_2}		14	7	2	4	15	5	8	17	3	13
	BFM	7.38(−1)	−6.18(−1)	−3.50(−1)	−2.96(−1)	−1.12(−1)	−7.61(−2)	6.82(−2)	−5.64(−2)	−5.43(−2)	−4.44(−2)
	LSENS	7.38(−1)	−6.18(−1)	−3.50(−1)	−2.96(−1)	−1.12(−1)	−7.61(−2)	6.82(−2)	−5.64(−2)	−5.43(−2)	−4.44(−2)
	SENKIN	7.38(−1)	−6.18(−1)	−3.50(−1)	−2.96(−1)	−1.12(−1)	−7.61(−2)	6.81(−2)	−5.63(−2)	−5.43(−2)	−4.44(−2)
$\sigma_{H_2O_2}$		2	8	12	15	14	17	3	13	4	16
	BFM	−7.34(−1)	−2.93(−1)	2.73(−1)	−2.46(−1)	−2.41(−1)	−1.23(−1)	−1.12(−1)	−9.38(−2)	−7.98(−2)	−6.20(−2)
	LSENS	−7.34(−1)	−2.93(−1)	2.73(−1)	−2.46(−1)	−2.41(−1)	−1.23(−1)	−1.12(−1)	−9.38(−2)	−7.98(−2)	−6.20(−2)
	SENKIN	−7.34(−1)	−2.94(−1)	2.74(−1)	−2.45(−1)	−2.41(−1)	−1.23(−1)	−1.12(−1)	−9.37(−2)	−7.98(−2)	−6.20(−2)
σ_{NO}		2	24	14	15	3	13	17	4	16	12
	BFM	3.03	9.90(−1)	6.82(−1)	6.13(−1)	4.66(−1)	3.79(−1)	3.38(−1)	3.11(−1)	1.59(−1)	4.58(−2)
	LSENS	3.03	9.90(−1)	6.82(−1)	6.13(−1)	4.66(−1)	3.79(−1)	3.38(−1)	3.11(−1)	1.59(−1)	4.58(−2)
	SENKIN	3.04	9.90(−1)	6.83(−1)	6.13(−1)	4.67(−1)	3.79(−1)	3.38(−1)	3.11(−1)	1.60(−1)	4.59(−2)
σ_{NO_2}		2	24	22	21	14	15	3	13	17	4
	BFM	3.07	9.90(−1)	−8.93(−1)	8.90(−1)	7.17(−1)	6.23(−1)	4.71(−1)	3.84(−1)	3.43(−1)	3.08(−1)
	LSENS	3.07	9.90(−1)	−8.93(−1)	8.90(−1)	7.17(−1)	6.23(−1)	4.71(−1)	3.84(−1)	3.43(−1)	3.08(−1)
	SENKIN	3.07	9.90(−1)	−8.93(−1)	8.90(−1)	7.18(−1)	6.22(−1)	4.71(−1)	3.84(−1)	3.43(−1)	3.08(−1)

σ_N		2	24	25	14	15	17	3	13	4	16
	BFM	1.81	1.00	−8.92(−1)	6.07(−1)	5.79(−1)	2.95(−1)	2.79(−1)	2.26(−1)	1.87(−1)	1.50(−1)
	LSENS	1.81	1.00	−8.92(−1)	6.07(−1)	5.79(−1)	2.95(−1)	2.79(−1)	2.26(−1)	1.87(−1)	1.50(−1)
	SENKIN	1.81	1.00	−8.92(−1)	6.08(−1)	5.78(−1)	2.95(−1)	2.80(−1)	2.27(−1)	1.87(−1)	1.50(−1)
σ_{N_2}		2	24	14	15	3	13	17	4	16	26
	BFM	−4.18(−6)	−1.36(−6)	−9.48(−7)	−8.53(−7)	−6.42(−7)	−5.23(−7)	−4.69(−7)	−4.29(−7)	−2.22(−7)	−2.13(−7)
	LSENS	−4.18(−6)	−1.36(−6)	−9.48(−7)	−8.53(−7)	−6.42(−7)	−5.23(−7)	−4.69(−7)	−4.29(−7)	−2.22(−7)	−2.13(−7)
	SENKIN	−4.16(−6)	−1.36(−6)	−9.45(−7)	−8.48(−7)	−6.40(−7)	−5.20(−7)	−4.67(−7)	−4.27(−7)	−2.21(−7)	−2.12(−7)
σ_{N_2O}		26	30	2	14	15	3	13	17	4	27
	BFM	9.72(−1)	−8.84(−1)	2.01(−1)	5.15(−2)	4.43(−2)	2.81(−2)	2.49(−2)	2.37(−2)	1.92(−2)	−1.86(−2)
	LSENS	9.72(−1)	−8.84(−1)	2.01(−1)	5.15(−2)	4.43(−2)	2.81(−2)	2.49(−2)	2.37(−2)	1.92(−2)	−1.86(−2)
	SENKIN	9.72(−1)	−8.84(−1)	2.01(−1)	5.17(−2)	4.43(−2)	2.82(−2)	2.50(−2)	2.37(−2)	1.92(−2)	−1.85(−2)
T		2	14	15	17	3	13	4	16	8	12
	BFM	1.30(−1)	4.44(−2)	4.22(−2)	2.16(−2)	2.02(−2)	1.61(−2)	1.34(−2)	1.11(−2)	2.90(−3)	2.82(−3)
	LSENS	1.30(−1)	4.44(−2)	4.22(−2)	2.16(−2)	2.02(−2)	1.61(−2)	1.34(−2)	1.11(−2)	2.90(−3)	2.82(−3)
	SENKIN	1.30(−1)	4.45(−2)	4.22(−2)	2.15(−2)	2.02(−2)	1.61(−2)	1.34(−2)	1.11(−2)	2.90(−3)	2.82(−3)
ρ^b		2	14	15	17	3	13	4	16	8	12
	BFM	−1.07(−1)	−3.65(−2)	−3.47(−2)	−1.77(−2)	−1.66(−2)	−1.32(−2)	−1.10(−2)	−9.09(−3)	−2.39(−3)	−2.31(−3)
	LSENS	−1.07(−1)	−3.65(−2)	−3.47(−2)	−1.77(−2)	−1.66(−2)	−1.32(−2)	−1.10(−2)	−9.09(−3)	−2.39(−3)	−2.31(−3)

[a]For each dependent variable the top row lists the reaction numbers. The next three rows give the normalized sensitivity coefficients produced by BFM, LSENS, and SENKIN, respectively. For each dependent variable and method or code the $\{\langle S_{ij}\rangle\}$ are those of that variable with respect to the preexponential factors of the reactions corresponding to the numbers listed in the first row. Numbers in parentheses designate powers of 10.

[b]Sensitivity coefficients of density are not calculated by SENKIN.

TABLE 4.69.—REACTION IMPORTANCE LISTS AND NORMALIZED SENSITIVITY COEFFFICIENTS WITH RESPECT TO PREEXPONENTIAL FACTORS FOR TEST PROBLEM 8 AT $t = 1.5\times10^{-5}$ s

Dependent variable	Method or code	Reaction numbers in order of decreasing importance and normalized sensitivity coefficients at $t = 1.5\times10^{-5}$ s[a]									
σ_O		15	14	2	17	16	3	13	4	8	12
	BFM	−1.64(−1)	−1.56(−1)	−1.31(−1)	−5.75(−2)	−3.66(−2)	−2.10(−2)	−1.57(−2)	−1.53(−2)	−1.16(−2)	−4.31(−3)
	LSENS	−1.64(−1)	−1.56(−1)	−1.31(−1)	−5.75(−2)	−3.66(−2)	−2.10(−2)	−1.57(−2)	−1.53(−2)	−1.16(−2)	−4.31(−3)
	SENKIN	−1.64(−1)	−1.56(−1)	−1.31(−1)	−5.74(−2)	−3.67(−2)	−2.10(−2)	−1.57(−2)	−1.53(−2)	−1.16(−2)	−4.31(−3)
σ_{H_2O}		15	14	2	17	16	3	13	4	8	7
	BFM	3.13(−2)	3.01(−2)	2.52(−2)	1.09(−2)	6.92(−3)	3.98(−3)	3.31(−3)	2.75(−3)	2.16(−3)	9.67(−4)
	LSENS	3.13(−2)	3.01(−2)	2.52(−2)	1.09(−2)	6.92(−3)	3.98(−3)	3.31(−3)	2.75(−3)	2.16(−3)	9.67(−4)
	SENKIN	3.13(−2)	3.01(−2)	2.52(−2)	1.09(−2)	6.93(−3)	3.98(−3)	3.32(−3)	2.75(−3)	2.16(−3)	9.67(−4)
σ_{OH}		14	2	7	3	15	17	16	4	13	24
	BFM	2.89(−3)	1.47(−3)	9.57(−4)	6.58(−4)	5.07(−4)	4.47(−4)	4.19(−4)	−3.78(−4)	−3.20(−4)	−2.60(−4)
	LSENS	2.89(−3)	1.47(−3)	9.57(−4)	6.58(−4)	5.06(−4)	4.47(−4)	4.19(−4)	−3.78(−4)	−3.20(−4)	−2.60(−4)
	SENKIN	2.94(−3)	1.51(−3)	9.59(−4)	6.64(−4)	5.56(−4)	4.64(−4)	4.31(−4)	−3.74(−4)	−3.15(−4)	−2.59(−4)
σ_H		15	14	2	17	16	3	13	4	8	7
	BFM	−1.96(−1)	−1.88(−1)	−1.57(−1)	−6.85(−2)	−4.34(−2)	−2.42(−2)	−1.88(−2)	−1.77(−2)	−1.37(−2)	−5.20(−3)
	LSENS	−1.96(−1)	−1.88(−1)	−1.57(−1)	−6.85(−2)	−4.34(−2)	−2.42(−2)	−1.88(−2)	−1.77(−2)	−1.37(−2)	−5.20(−3)
	SENKIN	−1.95(−1)	−1.88(−1)	−1.57(−1)	−6.85(−2)	−4.34(−2)	−2.43(−2)	−1.88(−2)	−1.77(−2)	−1.37(−2)	−5.20(−3)
σ_{O_2}		15	14	2	17	16	3	13	4	8	7
	BFM	−9.14(−2)	−9.05(−2)	−7.49(−2)	−3.19(−2)	−2.03(−2)	−1.21(−2)	−9.97(−3)	−7.31(−3)	−6.21(−3)	−3.79(−3)
	LSENS	−9.14(−2)	−9.05(−2)	−7.49(−2)	−3.19(−2)	−2.03(−2)	−1.21(−2)	−9.97(−3)	−7.31(−3)	−6.21(−3)	−3.79(−3)
	SENKIN	−9.13(−2)	−9.06(−2)	−7.49(−2)	−3.19(−2)	−2.03(−2)	−1.21(−2)	−9.97(−3)	−7.31(−3)	−6.22(−3)	−3.79(−3)

σ_{H_2}		15	14	2	17	16	3	13	4	8	7
	BFM	−4.67(−2)	−4.56(−2)	−3.81(−2)	−1.62(−2)	−1.03(−2)	−6.33(−3)	−5.51(−3)	−3.76(−3)	−3.14(−3)	−1.95(−3)
	LSENS	−4.67(−2)	−4.56(−2)	−3.81(−2)	−1.62(−2)	−1.03(−2)	−6.33(−3)	−5.51(−3)	−3.76(−3)	−3.14(−3)	−1.95(−3)
	SENKIN	−4.66(−2)	−4.56(−2)	−3.81(−2)	−1.62(−2)	−1.03(−2)	−6.33(−3)	−5.50(−3)	−3.76(−3)	−3.14(−3)	−1.95(−3)
σ_{HO_2}		14	7	4	5	15	2	8	6	17	16
	BFM	6.30(−1)	−4.48(−1)	−2.01(−1)	−6.32(−2)	−5.61(−2)	−4.61(−2)	3.82(−2)	−2.74(−2)	−1.95(−2)	−1.24(−2)
	LSENS	6.30(−1)	−4.48(−1)	−2.01(−1)	−6.32(−2)	−5.61(−2)	−4.61(−2)	3.82(−2)	−2.74(−2)	−1.95(−2)	−1.24(−2)
	SENKIN	6.30(−1)	−4.49(−1)	−2.01(−1)	−6.32(−2)	−5.62(−2)	−4.62(−2)	3.83(−2)	−2.74(−2)	−1.96(−2)	−1.24(−2)
$\sigma_{H_2O_2}$		15	14	2	17	16	8	3	12	13	4
	BFM	−3.85(−1)	−3.60(−1)	−3.06(−1)	−1.34(−1)	−8.47(−2)	−7.74(−2)	−4.73(−2)	4.45(−2)	−3.93(−2)	−3.65(−2)
	LSENS	−3.85(−1)	−3.60(−1)	−3.06(−1)	−1.34(−1)	−8.47(−2)	−7.74(−2)	−4.73(−2)	4.45(−2)	−3.93(−2)	−3.65(−2)
	SENKIN	−3.85(−1)	−3.61(−1)	−3.06(−1)	−1.34(−1)	−8.48(−2)	−7.75(−2)	−4.73(−2)	4.46(−2)	−3.93(−2)	−3.65(−2)
σ_{NO}		24	2	15	14	17	16	3	13	4	8
	BFM	9.96(−1)	7.23(−1)	5.03(−1)	5.01(−1)	2.03(−1)	1.19(−1)	1.12(−1)	9.07(−2)	7.58(−2)	3.63(−2)
	LSENS	9.96(−1)	7.23(−1)	5.03(−1)	5.01(−1)	2.03(−1)	1.19(−1)	1.12(−1)	9.07(−2)	7.58(−2)	3.63(−2)
	SENKIN	9.96(−1)	7.24(−1)	5.03(−1)	5.01(−1)	2.03(−1)	1.20(−1)	1.12(−1)	9.08(−2)	7.59(−2)	3.64(−2)
σ_{NO_2}		24	2	14	15	21	22	17	16	3	13
	BFM	9.95(−1)	8.24(−1)	6.36(−1)	6.27(−1)	5.94(−1)	−5.93(−1)	2.47(−1)	1.47(−1)	1.28(−1)	1.03(−1)
	LSENS	9.95(−1)	8.24(−1)	6.36(−1)	6.27(−1)	5.94(−1)	−5.93(−1)	2.47(−1)	1.47(−1)	1.28(−1)	1.03(−1)
	SENKIN	9.95(−1)	8.24(−1)	6.37(−1)	6.27(−1)	5.94(−1)	−5.94(−1)	2.47(−1)	1.47(−1)	1.28(−1)	1.03(−1)

[a]For each dependent variable the top row lists the reaction numbers. The next three rows give the normalized sensitivity coefficients produced by BFM, LSENS, and SENKIN, respectively. For each dependent variable and method or code the $\{\langle S_{ij}\rangle\}$ are those of that variable with respect to the preexponential factors of the reactions corresponding to the numbers listed in the first row. Numbers in parentheses designate powers of 10.

TABLE 4.69.—Concluded.

Dependent variable	Method or code	Reaction numbers in order of decreasing importance and normalized sensitivity coefficients at $t = 1.5\times10^{-5}$ s[a]									
σ_N		24	25	15	14	2	17	16	23	3	13
	BFM	9.98(−1)	−8.74(−1)	4.57(−1)	4.38(−1)	3.83(−1)	1.61(−1)	1.01(−1)	−7.17(−2)	5.92(−2)	4.90(−2)
	LSENS	9.98(−1)	−8.74(−1)	4.57(−1)	4.38(−1)	3.83(−1)	1.61(−1)	1.01(−1)	−7.17(−2)	5.92(−2)	4.90(−2)
	SENKIN	9.98(−1)	−8.74(−1)	4.57(−1)	4.39(−1)	3.83(−1)	1.61(−1)	1.01(−1)	−7.17(−2)	5.92(−2)	4.90(−2)
σ_{N_2}		24	2	15	14	17	16	3	13	4	8
	BFM	−3.76(−5)	−2.73(−5)	−1.90(−5)	−1.89(−5)	−7.67(−6)	−4.51(−6)	−4.23(−6)	−3.42(−6)	−2.86(−6)	−1.37(−6)
	LSENS	−3.76(−5)	−2.73(−5)	−1.90(−5)	−1.89(−5)	−7.67(−6)	−4.51(−6)	−4.23(−6)	−3.42(−6)	−2.86(−6)	−1.37(−6)
	SENKIN	−3.74(−5)	−2.72(−5)	−1.90(−5)	−1.89(−5)	−7.65(−6)	−4.51(−6)	−4.22(−6)	−3.41(−6)	−2.85(−6)	−1.37(−6)
σ_{N_2O}		26	30	15	14	2	17	16	28	3	13
	BFM	6.53(−1)	−5.67(−1)	2.31(−1)	2.24(−1)	1.97(−1)	8.23(−2)	5.17(−2)	−3.05(−2)	3.04(−2)	2.41(−2)
	LSENS	6.53(−1)	−5.67(−1)	2.31(−1)	2.24(−1)	1.97(−1)	8.23(−2)	5.17(−2)	−3.05(−2)	3.04(−2)	2.41(−2)
	SENKIN	6.53(−1)	−5.68(−1)	2.31(−1)	2.24(−1)	1.97(−1)	8.23(−2)	5.17(−2)	−3.04(−2)	3.04(−2)	2.41(−2)
T		15	14	2	17	16	3	13	4	8	7
	BFM	4.25(−2)	4.07(−2)	3.40(−2)	1.48(−2)	9.42(−3)	5.34(−3)	4.25(−3)	3.82(−3)	2.96(−3)	1.15(−3)
	LSENS	4.25(−2)	4.07(−2)	3.40(−2)	1.48(−2)	9.42(−3)	5.34(−3)	4.25(−3)	3.82(−3)	2.96(−3)	1.15(−3)
	SENKIN	4.24(−2)	4.08(−2)	3.40(−2)	1.48(−2)	9.43(−3)	5.35(−3)	4.25(−3)	3.82(−3)	2.96(−3)	1.15(−3)
ρ[b]		15	14	2	17	16	3	13	4	8	7
	BFM	−3.36(−2)	−3.21(−2)	−2.69(−2)	−1.17(−2)	−7.44(−3)	−4.22(−3)	−3.36(−3)	−3.02(−3)	−2.34(−3)	−9.09(−4)
	LSENS	−3.36(−2)	−3.21(−2)	−2.69(−2)	−1.17(−2)	−7.44(−3)	−4.22(−3)	−3.36(−3)	−3.02(−3)	−2.34(−3)	−9.09(−4)

[a]For each dependent variable the top row lists the reaction numbers. The next three rows give the normalized sensitivity coefficients produced by BFM, LSENS, and SENKIN, respectively. For each dependent variable and method or code the $\{\langle S_{ij}\rangle\}$ are those of that variable with respect to the preexponential factors of the reactions corresponding to the numbers listed in the first row. Numbers in parentheses designate powers of 10.

[b]Sensitivity coefficients of density are not calculated by SENKIN.

TABLE 4.70.—REACTION IMPORTANCE LISTS AND NORMALIZED SENSITIVITY COEFFICIENTS WITH RESPECT TO PREEXPONENTIAL FACTORS FOR TEST PROBLEM 8 AT $t = 10^{-4}$ s

Dependent variable	Method or code	Reaction numbers in order of decreasing importance and normalized sensitivity coefficients at $t = 10^{-4}$ s[a]									
σ_O		24	15	14	17	16	2	7	4	25	8
	BFM	−2.72(−2)	−1.49(−2)	−9.19(−3)	−2.72(−3)	−2.01(−3)	−1.90(−3)	−1.56(−3)	−8.88(−4)	−4.39(−4)	−4.04(−4)
	LSENS	−2.72(−2)	−1.49(−2)	−9.19(−3)	−2.72(−3)	−2.01(−3)	−1.90(−3)	−1.56(−3)	−8.88(−4)	−4.39(−4)	−4.04(−4)
	SENKIN	−2.72(−2)	−1.50(−2)	−9.23(−3)	−2.72(−3)	−2.02(−3)	−1.91(−3)	−1.56(−3)	−8.91(−4)	−4.38(−4)	−4.06(−4)
σ_{H_2O}		15	14	24	17	16	7	2	4	8	5
	BFM	1.53(−3)	8.60(−4)	−4.68(−4)	2.46(−4)	1.88(−4)	1.77(−4)	9.44(−5)	8.69(−5)	3.29(−5)	2.63(−5)
	LSENS	1.53(−3)	8.60(−4)	−4.68(−4)	2.46(−4)	1.88(−4)	1.77(−4)	9.44(−5)	8.69(−5)	3.29(−5)	2.63(−5)
	SENKIN	1.53(−3)	8.65(−4)	−4.68(−4)	2.47(−4)	1.89(−4)	1.78(−4)	9.49(−5)	8.73(−5)	3.30(−5)	2.64(−5)
σ_{OH}		24	15	14	17	2	16	7	4	25	8
	BFM	−1.52(−2)	−4.71(−3)	−3.05(−3)	−9.20(−4)	−8.14(−4)	−6.68(−4)	−4.52(−4)	−2.88(−4)	−2.48(−4)	−1.45(−4)
	LSENS	−1.52(−2)	−4.71(−3)	−3.05(−3)	−9.20(−4)	−8.14(−4)	−6.68(−4)	−4.52(−4)	−2.88(−4)	−2.48(−4)	−1.45(−4)
	SENKIN	−1.52(−2)	−4.72(−3)	−3.06(−3)	−9.21(−4)	−8.15(−4)	−6.70(−4)	−4.53(−4)	−2.89(−4)	−2.47(−4)	−1.45(−4)
σ_H		15	14	24	17	16	7	2	4	8	5
	BFM	−1.35(−2)	−7.80(−3)	−4.04(−3)	−2.26(−3)	−1.71(−3)	−1.52(−3)	−1.08(−3)	−7.79(−4)	−3.12(−4)	−2.25(−4)
	LSENS	−1.35(−2)	−7.80(−3)	−4.04(−3)	−2.26(−3)	−1.71(−3)	−1.52(−3)	−1.08(−3)	−7.79(−4)	−3.12(−4)	−2.25(−4)
	SENKIN	−1.35(−2)	−7.84(−3)	−4.03(−3)	−2.26(−3)	−1.72(−3)	−1.53(−3)	−1.08(−3)	−7.83(−4)	−3.13(−4)	−2.26(−4)
σ_{O_2}		24	15	14	2	17	16	7	4	25	8
	BFM	−3.56(−2)	−9.92(−3)	−6.58(−3)	−2.06(−3)	−1.98(−3)	−1.43(−3)	−9.72(−4)	−5.98(−4)	−5.59(−4)	−3.13(−4)
	LSENS	−3.56(−2)	−9.92(−3)	−6.58(−3)	−2.06(−3)	−1.98(−3)	−1.43(−3)	−9.72(−4)	−5.97(−4)	−5.59(−4)	−3.13(−4)
	SENKIN	−3.55(−2)	−9.94(−3)	−6.60(−3)	−2.06(−3)	−1.98(−3)	−1.44(−3)	−9.75(−4)	−5.99(−4)	−5.58(−4)	−3.14(−4)

[a]For each dependent variable the top row lists the reaction numbers. The next three rows give the normalized sensitivity coefficients produced by BFM, LSENS, and SENKIN, respectively. For each dependent variable and method or code the $\{\langle S_{ij} \rangle\}$ are those of that variable with respect to the preexponential factors of the reactions corresponding to the numbers listed in the first row. Numbers in parentheses designate powers of 10.

TABLE 4.70.—Concluded.

Dependent variable	Method or code	Reaction numbers in order of decreasing importance and normalized sensitivity coefficients at $t = 10^{-4}$ s[a]									
σ_{H_2}		24	15	14	17	7	16	4	25	5	8
	BFM	8.26(−3)	−3.78(−3)	−1.96(−3)	−5.42(−4)	−4.80(−4)	−4.30(−4)	−2.07(−4)	1.48(−4)	−7.12(−5)	−6.30(−5)
	LSENS	8.26(−3)	−3.78(−3)	−1.96(−3)	−5.42(−4)	−4.80(−4)	−4.30(−4)	−2.07(−4)	1.48(−4)	−7.12(−5)	−6.30(−5)
	SENKIN	8.25(−3)	−3.79(−3)	−1.97(−3)	−5.45(−4)	−4.83(−4)	−4.33(−4)	−2.08(−4)	1.48(−4)	−7.16(−5)	−6.35(−5)
σ_{HO_2}		24	15	7	14	2	4	17	16	25	5
	BFM	−3.19(−2)	−3.62(−3)	−2.88(−3)	1.45(−3)	−1.42(−3)	−1.38(−3)	−9.02(−4)	−6.21(−4)	−5.08(−4)	−4.15(−4)
	LSENS	−3.19(−2)	−3.62(−3)	−2.88(−3)	1.45(−3)	−1.42(−3)	−1.38(−3)	−9.02(−4)	−6.21(−4)	−5.08(−4)	−4.15(−4)
	SENKIN	−3.18(−2)	−3.62(−3)	−2.89(−3)	1.46(−3)	−1.41(−3)	−1.39(−3)	−9.01(−4)	−6.22(−4)	−5.07(−4)	−4.17(−4)
$\sigma_{H_2O_2}$		15	24	14	17	16	7	2	4	8	3
	BFM	−2.15(−2)	−2.15(−2)	−1.27(−2)	−3.74(−3)	−2.80(−3)	−2.36(−3)	−2.16(−3)	−1.27(−3)	−6.51(−4)	−3.61(−4)
	LSENS	−2.15(−2)	−2.15(−2)	−1.27(−2)	−3.74(−3)	−2.80(−3)	−2.36(−3)	−2.16(−3)	−1.27(−3)	−6.51(−4)	−3.61(−4)
	SENKIN	−2.16(−2)	−2.14(−2)	−1.28(−2)	−3.75(−3)	−2.81(−3)	−2.37(−3)	−2.16(−3)	−1.28(−3)	−6.54(−4)	−3.61(−4)
σ_{NO}		24	15	14	2	17	16	25	4	3	7
	BFM	9.17(−1)	9.25(−2)	7.57(−2)	3.88(−2)	2.40(−2)	1.64(−2)	1.50(−2)	6.19(−3)	6.00(−3)	5.97(−3)
	LSENS	9.17(−1)	9.25(−2)	7.57(−2)	3.88(−2)	2.40(−2)	1.64(−2)	1.50(−2)	6.19(−3)	6.00(−3)	5.97(−3)
	SENKIN	9.17(−1)	9.25(−2)	7.58(−2)	3.88(−2)	2.41(−2)	1.64(−2)	1.50(−2)	6.20(−3)	6.01(−3)	5.98(−3)
σ_{NO_2}		24	15	14	2	17	16	25	7	4	3
	BFM	9.01(−1)	9.68(−2)	7.78(−2)	3.86(−2)	2.46(−2)	1.69(−2)	1.47(−2)	6.50(−3)	6.40(−3)	5.96(−3)
	LSENS	9.01(−1)	9.68(−2)	7.78(−2)	3.86(−2)	2.46(−2)	1.69(−2)	1.47(−2)	6.50(−3)	6.40(−3)	5.96(−3)
	SENKIN	9.01(−1)	9.68(−2)	7.80(−2)	3.86(−2)	2.46(−2)	1.69(−2)	1.47(−2)	6.51(−3)	6.41(−3)	5.97(−3)

σ_N		24	25	15	14	23	2	17	16	7	4
	BFM	8.81(−1)	−3.85(−1)	5.23(−2)	4.12(−2)	−3.10(−2)	1.98(−2)	1.30(−2)	8.94(−3)	3.68(−3)	3.44(−3)
	LSENS	8.81(−1)	−3.85(−1)	5.23(−2)	4.12(−2)	−3.10(−2)	1.98(−2)	1.30(−2)	8.94(−3)	3.68(−3)	3.44(−3)
	SENKIN	8.81(−1)	−3.86(−1)	5.23(−2)	4.13(−2)	−3.10(−2)	1.98(−2)	1.30(−2)	8.96(−3)	3.69(−3)	3.44(−3)
σ_{N_2}		24	15	14	2	17	16	25	4	3	7
	BFM	−1.61(−3)	−1.62(−4)	−1.33(−4)	−6.81(−5)	−4.22(−5)	−2.88(−5)	−2.58(−5)	−1.09(−5)	−1.05(−5)	−1.05(−5)
	LSENS	−1.61(−3)	−1.62(−4)	−1.33(−4)	−6.81(−5)	−4.22(−5)	−2.88(−5)	−2.58(−5)	−1.09(−5)	−1.05(−5)	−1.05(−5)
	SENKIN	−1.61(−3)	−1.62(−4)	−1.33(−4)	−6.80(−5)	−4.21(−5)	−2.88(−5)	−2.57(−5)	−1.09(−5)	−1.05(−5)	−1.05(−5)
σ_{N_2O}		28	30	24	15	14	26	17	16	7	27
	BFM	−3.72(−2)	2.74(−2)	−2.03(−2)	1.95(−2)	1.07(−2)	8.33(−3)	3.02(−3)	2.34(−3)	2.34(−3)	1.58(−3)
	LSENS	−3.72(−2)	2.74(−2)	−2.03(−2)	1.95(−2)	1.07(−2)	8.33(−3)	3.02(−3)	2.34(−3)	2.34(−3)	1.58(−3)
	SENKIN	−3.72(−2)	2.74(−2)	−2.03(−2)	1.96(−2)	1.08(−2)	8.34(−3)	3.04(−3)	2.36(−3)	2.35(−3)	1.58(−3)
T		15	24	14	17	16	7	4	2	8	5
	BFM	1.45(−3)	−1.01(−3)	8.06(−4)	2.30(−4)	1.77(−4)	1.71(−4)	8.26(−5)	6.61(−5)	2.99(−5)	2.56(−5)
	LSENS	1.45(−3)	−1.01(−3)	8.06(−4)	2.30(−4)	1.77(−4)	1.71(−4)	8.26(−5)	6.61(−5)	2.99(−5)	2.56(−5)
	SENKIN	1.46(−3)	−1.01(−3)	8.10(−4)	2.31(−4)	1.78(−4)	1.72(−4)	8.30(−5)	6.66(−5)	3.01(−5)	2.58(−5)
ρ^b		24	15	14	17	16	7	4	2	8	5
	BFM	1.10(−3)	−1.07(−3)	−5.85(−4)	−1.66(−4)	−1.28(−4)	−1.28(−4)	−6.05(−5)	−3.62(−5)	−2.11(−5)	−1.92(−5)
	LSENS	1.10(−3)	−1.07(−3)	−5.85(−4)	−1.66(−4)	−1.28(−4)	−1.28(−4)	−6.05(−5)	−3.62(−5)	−2.11(−5)	−1.92(−5)

[a]For each dependent variable the top row lists the reaction numbers. The next three rows give the normalized sensitivity coefficients produced by BFM, LSENS, and SENKIN, respectively. For each dependent variable and method or code the $\{\langle S_{ij}\rangle\}$ are those of that variable with respect to the preexponential factors of the reactions corresponding to the numbers listed in the first row. Numbers in parentheses designate powers of 10.

[b]Sensitivity coefficients of density are not calculated by SENKIN.

TABLE 4.71.—REACTION IMPORTANCE LISTS AND NORMALIZED SENSITIVITY COEFFICIENTS WITH RESPECT TO PREEXPONENTIAL FACTORS FOR TEST PROBLEM 8 AT $t = 10^{-3}$ s

Dependent variable	Method or code	Reaction numbers in order of decreasing importance and normalized sensitivity coefficients at $t = 10^{-3}$ s[a]									
σ_O		24	25	15	23	14	2	28	17	16	7
	BFM	−9.06(−3)	−1.01(−3)	−9.15(−5)	−7.59(−5)	−7.03(−5)	−3.19(−5)	−2.48(−5)	−2.23(−5)	−1.53(−5)	−6.85(−6)
	LSENS	−9.06(−3)	−1.01(−3)	−9.15(−5)	−7.59(−5)	−7.03(−5)	−3.19(−5)	−2.48(−5)	−2.23(−5)	−1.53(−5)	−6.85(−6)
	SENKIN	−9.10(−3)	−1.02(−3)	−9.19(−5)	−7.61(−5)	−7.07(−5)	−3.18(−5)	−2.49(−5)	−2.24(−5)	−1.54(−5)	−6.88(−6)
σ_{H_2O}		24	25	23	14	2	28	15	17	16	3
	BFM	−1.51(−4)	−1.71(−5)	−1.27(−6)	−5.98(−7)	−4.50(−7)	−4.04(−7)	−1.94(−7)	−1.87(−7)	−1.24(−7)	−9.51(−8)
	LSENS	−1.51(−4)	−1.71(−5)	−1.27(−6)	−5.98(−7)	−4.51(−7)	−4.04(−7)	−1.94(−7)	−1.87(−7)	−1.24(−7)	−9.53(−8)
	SENKIN	−1.52(−4)	−1.72(−5)	−1.27(−6)	−6.03(−7)	−5.07(−7)	−4.05(−7)	−1.94(−7)	−1.88(−7)	−1.24(−7)	−1.04(−7)
σ_{OH}		24	25	15	23	14	2	28	17	16	7
	BFM	−5.01(−3)	−5.60(−4)	−4.79(−5)	−4.19(−5)	−3.77(−5)	−1.77(−5)	−1.37(−5)	−1.20(−5)	−8.19(−6)	−3.38(−6)
	LSENS	−5.01(−3)	−5.60(−4)	−4.79(−5)	−4.19(−5)	−3.77(−5)	−1.77(−5)	−1.37(−5)	−1.20(−5)	−8.19(−6)	−3.38(−6)
	SENKIN	−5.03(−3)	−5.62(−4)	−4.81(−5)	−4.21(−5)	−3.79(−5)	−1.76(−5)	−1.38(−5)	−1.20(−5)	−8.23(−6)	−3.40(−6)
σ_H		24	25	15	14	23	2	17	28	16	7
	BFM	−1.59(−3)	−1.77(−4)	−2.42(−5)	−1.59(−5)	−1.33(−5)	−5.91(−6)	−5.06(−6)	−4.40(−6)	−3.49(−6)	−2.40(−6)
	LSENS	−1.59(−3)	−1.77(−4)	−2.42(−5)	−1.59(−5)	−1.33(−5)	−5.90(−6)	−5.06(−6)	−4.40(−6)	−3.50(−6)	−2.40(−6)
	SENKIN	−1.59(−3)	−1.77(−4)	−2.43(−5)	−1.59(−5)	−1.33(−5)	−5.76(−6)	−5.08(−6)	−4.43(−6)	−3.52(−6)	−2.42(−6)
σ_{O_2}		24	25	15	23	14	2	28	17	16	7
	BFM	−1.18(−2)	−1.32(−3)	−1.12(−4)	−9.93(−5)	−8.82(−5)	−4.74(−5)	−3.21(−5)	−2.80(−5)	−1.92(−5)	−7.97(−6)
	LSENS	−1.18(−2)	−1.32(−3)	−1.12(−4)	−9.93(−5)	−8.82(−5)	−4.74(−5)	−3.21(−5)	−2.80(−5)	−1.92(−5)	−7.97(−6)
	SENKIN	−1.18(−2)	−1.32(−3)	−1.12(−4)	−9.96(−5)	−8.87(−5)	−4.75(−5)	−3.23(−5)	−2.81(−5)	−1.93(−5)	−8.01(−6)

σ_{H_2}		24	25	23	15	14	2	28	17	16	3
	BFM	2.57(−3)	2.88(−4)	2.15(−5)	1.99(−5)	1.73(−5)	8.69(−6)	6.99(−6)	5.49(−6)	3.74(−6)	1.57(−6)
	LSENS	2.57(−3)	2.88(−4)	2.15(−5)	1.99(−5)	1.73(−5)	8.69(−6)	6.99(−6)	5.49(−6)	3.74(−6)	1.57(−6)
	SENKIN	2.58(−3)	2.89(−4)	2.16(−5)	2.00(−5)	1.74(−5)	8.78(−6)	7.01(−6)	5.51(−6)	3.76(−6)	1.59(−6)
σ_{HO_2}		24	25	15	23	14	2	28	17	7	16
	BFM	−1.04(−2)	−1.16(−3)	−9.48(−5)	−8.76(−5)	−6.07(−5)	−4.04(−5)	−2.84(−5)	−2.42(−5)	−1.69(−5)	−1.66(−5)
	LSENS	−1.04(−2)	−1.16(−3)	−9.48(−5)	−8.76(−5)	−6.07(−5)	−4.03(−5)	−2.84(−5)	−2.42(−5)	−1.69(−5)	−1.66(−5)
	SENKIN	−1.04(−2)	−1.17(−3)	−9.51(−5)	−8.79(−5)	−6.11(−5)	−4.04(−5)	−2.85(−5)	−2.43(−5)	−1.70(−5)	−1.66(−5)
$\sigma_{H_2O_2}$		24	25	15	23	14	2	28	17	16	7
	BFM	−7.43(−3)	−8.31(−4)	−8.21(−5)	−6.21(−5)	−6.04(−5)	−2.57(−5)	−2.04(−5)	−1.93(−5)	−1.32(−5)	−6.72(−6)
	LSENS	−7.43(−3)	−8.31(−4)	−8.21(−5)	−6.21(−5)	−6.04(−5)	−2.57(−5)	−2.04(−5)	−1.93(−5)	−1.32(−5)	−6.72(−6)
	SENKIN	−7.46(−3)	−8.33(−4)	−8.24(−5)	−6.23(−5)	−6.08(−5)	−2.58(−5)	−2.05(−5)	−1.94(−5)	−1.33(−5)	−6.75(−6)
σ_{NO}		24	25	15	23	14	2	28	17	16	7
	BFM	6.08(−2)	6.81(−3)	5.49(−4)	5.12(−4)	4.44(−4)	2.30(−4)	1.66(−4)	1.41(−4)	9.63(−5)	3.68(−5)
	LSENS	6.08(−2)	6.81(−3)	5.49(−4)	5.12(−4)	4.44(−4)	2.30(−4)	1.66(−4)	1.41(−4)	9.63(−5)	3.68(−5)
	SENKIN	6.11(−2)	6.83(−3)	5.51(−4)	5.14(−4)	4.46(−4)	2.31(−4)	1.67(−4)	1.41(−4)	9.68(−5)	3.70(−5)
σ_{NO_2}		24	25	15	23	14	2	28	17	16	7
	BFM	5.57(−2)	6.23(−3)	5.07(−4)	4.69(−4)	4.08(−4)	2.12(−4)	1.52(−4)	1.30(−4)	8.86(−5)	3.41(−5)
	LSENS	5.57(−2)	6.23(−3)	5.07(−4)	4.69(−4)	4.08(−4)	2.12(−4)	1.52(−4)	1.30(−4)	8.86(−5)	3.41(−5)
	SENKIN	5.59(−2)	6.25(−3)	5.09(−4)	4.70(−4)	4.11(−4)	2.13(−4)	1.53(−4)	1.30(−4)	8.91(−5)	3.43(−5)

[a]For each dependent variable the top row lists the reaction numbers. The next three rows give the normalized sensitivity coefficients produced by BFM, LSENS, and SENKIN, respectively. For each dependent variable and method or code the $\{\langle S_{ij}\rangle\}$ are those of that variable with respect to the preexponential factors of the reactions corresponding to the numbers listed in the first row. Numbers in parentheses designate powers of 10.

TABLE 4.71.—Concluded.

Dependent variable	Method or code	Reaction numbers in order of decreasing importance and normalized sensitivity coefficients at $t = 10^{-3}$ s[a]									
σ_N		24	25	15	14	2	28	17	23	16	7
	BFM	4.64(−2)	9.50(−4)	3.85(−4)	3.10(−4)	1.60(−4)	1.16(−4)	9.83(−5)	7.69(−5)	6.72(−5)	2.60(−5)
	LSENS	4.64(−2)	9.50(−4)	3.85(−4)	3.10(−4)	1.60(−4)	1.16(−4)	9.83(−5)	7.69(−5)	6.72(−5)	2.60(−5)
	SENKIN	4.65(−2)	9.48(−4)	3.86(−4)	3.12(−4)	1.61(−4)	1.16(−4)	9.87(−5)	7.68(−5)	6.76(−5)	2.61(−5)
σ_{N_2}		24	25	15	23	14	2	28	17	16	7
	BFM	−4.78(−4)	−5.35(−5)	−4.31(−6)	−4.02(−6)	−3.49(−6)	−1.80(−6)	−1.30(−6)	−1.11(−6)	−7.56(−7)	−2.89(−7)
	LSENS	−4.78(−4)	−5.35(−5)	−4.31(−6)	−4.02(−6)	−3.49(−6)	−1.80(−6)	−1.30(−6)	−1.11(−6)	−7.56(−7)	−2.89(−7)
	SENKIN	−4.79(−4)	−5.36(−5)	−4.33(−6)	−4.03(−6)	−3.50(−6)	−1.81(−6)	−1.31(−6)	−1.11(−6)	−7.60(−7)	−2.91(−7)
σ_{N_2O}		24	28	30	25	26	27	23	14	15	2
	BFM	−2.72(−3)	−1.12(−3)	8.86(−4)	−3.06(−4)	1.78(−4)	4.61(−5)	−2.28(−5)	−1.32(−5)	−9.26(−6)	−9.17(−6)
	LSENS	−2.72(−3)	−1.12(−3)	8.86(−4)	−3.06(−4)	1.78(−4)	4.61(−5)	−2.28(−5)	−1.32(−5)	−9.25(−6)	−9.17(−6)
	SENKIN	−2.73(−3)	−1.13(−3)	8.90(−4)	−3.07(−4)	1.79(−4)	4.64(−5)	−2.29(−5)	−1.33(−5)	−9.29(−6)	−9.10(−6)
T		24	25	23	14	15	2	28	17	16	3
	BFM	−2.90(−4)	−3.25(−5)	−2.44(−6)	−1.62(−6)	−1.46(−6)	−1.08(−6)	−7.82(−7)	−5.09(−7)	−3.44(−7)	−1.69(−7)
	LSENS	−2.90(−4)	−3.25(−5)	−2.44(−6)	−1.62(−6)	−1.46(−6)	−1.08(−6)	−7.82(−7)	−5.09(−7)	−3.44(−7)	−1.69(−7)
	SENKIN	−2.91(−4)	−3.26(−5)	−2.45(−6)	−1.63(−6)	−1.47(−6)	−1.07(−6)	−7.86(−7)	−5.11(−7)	−3.46(−7)	−1.68(−7)
ρ[b]		24	25	23	15	14	2	28	17	16	3
	BFM	3.17(−4)	3.55(−5)	2.67(−6)	1.98(−6)	1.93(−6)	1.19(−6)	8.56(−7)	6.10(−7)	4.14(−7)	1.84(−7)
	LSENS	3.17(−4)	3.55(−5)	2.67(−6)	1.99(−6)	1.94(−6)	1.18(−6)	8.56(−7)	6.19(−7)	4.16(−7)	1.83(−7)

[a]For each dependent variable the top row lists the reaction numbers. The next three rows give the normalized sensitivity coefficients produced by BFM, LSENS, and SENKIN, respectively. For each dependent variable and method or code the $\{\langle S_{ij} \rangle\}$ are those of that variable with respect to the preexponential factors of the reactions corresponding to the numbers listed in the first row. Numbers in parentheses designate powers of 10.

[b]Sensitivity coefficients of density are not calculated by SENKIN.

$$S_m = \sum_{k=1}^{NS} y_k = 1 \tag{4.96}$$

In this equation y_k is the mass fraction of species k and S_m the sum of the mass fractions of all NS species. Because

$$y_k = M_{w,k}\sigma_k \tag{4.97}$$

where $M_{w,k}$ is the molar mass of species k, mass conservation can be expressed as

$$S_m = \sum_{k=1}^{NS} M_{w,k}\sigma_k = 1 \tag{4.98}$$

Differentiating equation (4.98) with respect to A_j gives the following condition that must be satisfied by the $\{\partial\sigma_k/\partial A_j\}$:

$$\frac{\partial S_m}{\partial A_j} = \sum_{k=1}^{NRS} M_{w,k}\frac{\partial\sigma_k}{\partial A_j} = 0 \tag{4.99}$$

The summation excludes inert species because their sensitivity coefficients with respect to rate coefficient parameters are equal to zero. The values of all NR $\partial S_m/\partial A_j$ were examined at each print station. Although, presumably because of roundoff, the magnitudes were not all equal to zero, they were very small, and $\max(\partial S_m/\partial A_j) = 3.1\times10^{-19}$.

Atoms are also conserved during chemical reactions. Conservation of the ith atomic species can be expressed as

$$b_i = \sum_{k=1}^{NS} a_{ik}\sigma_k = b_{i,0}, \qquad i = 1,\ldots,\text{NLM} \tag{4.100}$$

where b_i is the total number of atoms of element i per unit mass of mixture, $b_{i,0}$ the value of b_i for the initial mixture, a_{ik} the number of atoms of element i in one molecule of species k, and NLM the total number of elements. Differentiating equation (4.100) with respect to A_j gives

$$\frac{\partial b_i}{\partial A_j} = \sum_{k=1}^{NRS} a_{ik}\frac{\partial\sigma_k}{\partial A_j} = 0, \qquad i = 1,\ldots,\text{NLM} \tag{4.101}$$

This conservation condition was also checked at each print station for all 30 reactions and all 3 elements (H, O, and N). Again the magnitudes of $\{\partial b_i/\partial A_j\}$ were very small, but usually nonzero. The value of the $\partial b_i/\partial A_j$ with largest magnitude was 1.9×10^{-20}.

The SENKIN results given in tables 4.65 to 4.71 were generated on the VAX 9410 computer, using the local tolerances EMAX = 10^{-7}, ATOLSP = 10^{-16}, RTLS = 10^{-5}, and ATLS = 10^{-5}. For these values of RTLS and ATLS, EMAX had to be decreased to 10^{-6} (ATOLSP= 10^{-9}EMAX) to reproduce the BFM reaction importance lists at all reaction times. On the VAX 9410 computer the LSENS results with EMAX = 10^{-6} and ATOLSP = 10^{-15} showed that A_2 was more important than A_{15} for the species N_2O at $t = 10^{-3}$ s. In particular, $\langle\partial\sigma_{N_2O}/\partial A_2\rangle = -9.28\times10^{-6}$ and $\langle\partial\sigma_{N_2O}/\partial A_{15}\rangle = -9.26\times10^{-6}$. For all other dependent variables at this time and for all variables at all other times the correct reaction importance lists were reproduced. Because the two sensitivities are negligibly small in magnitude, the inaccuracy in the reaction importance list for N_2O at $t = 10^{-3}$ s is of little consequence. Also, the normalized sensitivity coefficients were more accurate than the SENKIN results. And, when a print station was included at $t = 10^{-7}$ s, the inaccuracy in the σ_{N_2O} sensitivities disappeared, and the correct reaction importance lists were obtained for all variables at all times. This result is due to the dependence of the numerical solution produced by LSODE on the first output station, as discussed in chapter 3 (section 3.2.7).

Examination of the LSENS (and SENKIN) results generated on the VAX 9410 computer showed that the requirement for small EMAX was caused by difficulties in reproducing the correct reaction importance lists during equilibration. In the earlier regimes larger EMAX values could be used successfully. For example, in the interval $[0,10^{-4}]$ s LSENS with EMAX = 10^{-4} produced the correct reaction importance lists at all print stations, except at $t = 5\times10^{-6}$ s, when A_1 was predicted to be more important than A_8 for σ_O (cf. table 4.67). The differences in the normalized sensitivity coefficients were, however, negligible: $\langle\partial\sigma_O/\partial A_1\rangle = \langle\partial\sigma_O/\partial A_8\rangle = 8.60\times10^{-3}$, instead of 8.61×10^{-3} and 8.63×10^{-3}, respectively. In addition, the two reactions were only the ninth and tenth most important. For this EMAX at each print station the average global error in all $\{\langle\partial Y_i/\partial A_j\rangle\}$ with magnitude $\geq 10^{-3}$ was less than 1 percent; the maximum error was 0.22 percent at $t = 10^{-4}$ s. At every print station for each A_j the average global error in the $\{\langle\partial Y_i/\partial A_j\rangle\}$ with magnitude $\geq 10^{-3}$ was also less than 1 percent, except for A_2 and A_{22} at $t = 10^{-4}$ s, when the average errors in the normalized sensitivities with respect to these two parameters were 1.1 and 1.3 percent, respectively.

The finding that a much smaller EMAX was required to track accurately the sensitivities during equilibration than during induction and heat release is very surprising inasmuch as in the equilibration regime the ODE's are stiff (refs. 20, 29, 32, 33, and 73) and the BDF method is especially well suited for such problems (ref. 15). Experience has shown that while use of a large EMAX may produce an inaccurate kinetics solution during heat release, it has little impact on the solution during equilibration (ref. 19). Note also the contrast with constant-temperature

problems, for which much looser error tolerances were adequate, even at long reaction time.

Comparisons of the results generated with EMAX = 10^{-7} on the Amdahl 5870 and VAX 9410 computers showed some differences, especially during equilibration; in virtually every instance the latter results were more accurate. When EMAX was increased to 10^{-6}, the reaction importance lists produced on the Amdahl 5870 computer displayed the same inaccuracy at $t = 10^{-3}$ s in the σ_{N_2O} results as described above; in addition, at this time the reaction importance list for ρ was also inaccurate and A_{28} was predicted to be more important than A_2 (see table 4.71). The unit roundoff U values on the Amdahl 5870 and VAX 9410 computers are 2.2×10^{-16} and 1.1×10^{-16}, respectively. To examine if roundoff errors were causing the difficulties described above during equilibration, the calculation with EMAX = 10^{-6} was performed on the Cray-XM/P computer using double precision, for which $U = 2.5\times10^{-29}$. Exactly the same reaction importance lists as on the VAX 9410 computer, including the inaccuracy in the σ_{N_2O} results at 10^{-3} s, were obtained. When single-precision arithmetic ($U = 7.1\times10^{-15}$) was used, the same inaccuracies as on the Amdahl 5870 computer (i.e., in the σ_{N_2O} and ρ results at $t = 10^{-3}$ s) were incurred. The complete reaction importance lists containing all 30 reactions produced with EMAX = 10^{-7} on the Amdahl 5870, the VAX 9410, and the Cray-XM/P using double precision were identical for all dependent variables at all reaction times in the interval $[0,10^{-3}]$ s. The same was true of the lists obtained with EMAX = 10^{-7} on the Cray-XM/P computer using single precision, except for ρ at $t = 10^{-3}$ s.

Solutions were also generated on the VAX 9410 computer using the default D_floating data type, which has a smaller unit roundoff ($U = 1.4\times10^{-17}$) than the G_floating data type, but a smaller exponent range: approximately 2.94×10^{-39} through approximately $1.70\times10^{+38}$, versus the approximate range 5.57×10^{-309} through $8.98\times10^{+307}$. The run with EMAX = 10^{-7} did not give the correct reaction importance lists for σ_{NO_2}, σ_{N_2}, and σ_{N_2O} at $t = 10^{-6}$ s and for σ_{N_2O} at $t = 3\times10^{-6}$ s. For all other variables at these two times and for all variables at all $t \geq 5\times10^{-6}$ s the correct lists were obtained. At $t \leq 5\times10^{-6}$ s normalized sensitivities equal to zero were computed for several variables. Although, in general, the magnitude of the correct $\langle S_{ij} \rangle$ was negligible, it was significant in some cases: for example, at $t = 10^{-6}$ s, $\langle \partial\sigma_{N_2O}/\partial A_{26} \rangle = 0$, instead of 0.978 (see table 4.65). The run with EMAX = 10^{-6} gave the same reaction importance lists as EMAX = 10^{-7} for all variables at all reaction times, except for σ_{N_2O} at $t = 10^{-3}$ s, when A_2 was incorrectly listed before A_{15}.

The above discussion indicates that reducing roundoff errors produced some improvement in accuracy in the equilibration regime. However, the inaccuracy at $t = 10^{-3}$ s in the σ_{N_2O} results produced with EMAX = 10^{-6} persisted even when double-precision arithmetic was used on the Cray-XM/P computer. This finding suggests that roundoff is not the primary reason for the small EMAX values required to track accurately the sensitivity coefficients during equilibration; further study is required to elucidate its cause.

Tables 4.65 to 4.71 show that the agreement between the BFM and LSENS was excellent at all reaction times. Note again the large variation (of 16 orders of magnitude) in the solutions. SENKIN was also very accurate; however, for small and therefore relatively unimportant sensitivities, it experienced some difficulty tracking the BFM solutions. The discrepancies were most pronounced at $t = 10^{-3}$ s, when the system was equilibrating. For example, at this reaction time, $\langle \partial \sigma_{H_2O} / \partial A_2 \rangle = -5.07 \times 10^{-7}$, instead of -4.50×10^{-7}. Note that the magnitude of this sensitivity coefficient is significantly larger than those of σ_{N_2} at $t = 10^{-6}$ s (see table 4.65). Nonetheless the latter quantities were much more accurate and essentially agreed with the BFM solutions. This observation suggests that it is not the small magnitude of the sensitivity coefficients that poses problems for SENKIN, but rather the code's difficulty in tracking the solution in the equilibration regime. Now the BFM also experienced this difficulty, as discussed previously. The problem could be cured by either using smaller local error tolerances or increasing the magnitude of the finite-difference increment $\Delta\eta_j$.

Solution with SENKIN was therefore attempted with the tolerances EMAX $= 10^{-7}$, ATOLSP $= 10^{-16}$, RTLS $= 10^{-7}$, and ATLS $= 10^{-16}$. However, an error exit occurred at $t \approx 1.5 \times 10^{-7}$ s because of excessive computational work: to advance the solution to this reaction time required 50 000 integration steps and an execution time of over 3000 s on the VAX 9410 computer. The other "cure," namely increasing the finite-difference increments $\{\Delta\eta_j\}$ during equilibration, was attempted by increasing both RTLS and ATLS to 10^{-2}. Up to $t = 10^{-4}$ s the normalized sensitivity coefficients were the same as the SENKIN results given in tables 4.65 to 4.70 (i.e., those produced with the smaller RTLS and ATLS). At $t = 10^{-3}$ s, however, the larger tolerances produced different, and, in general, more accurate, results for several variables. For example, $\langle \partial \sigma_{H_2O} / \partial A_2 \rangle$ was equal to -4.34×10^{-7}; the accuracy improvement is readily observed (see table 4.71).

For the local tolerances EMAX $= 10^{-7}$, ATOLSP $= 10^{-16}$, RTLS $= 10^{-5}$, and ATLS $= 10^{-5}$, SENKIN required 542 steps, 1602 derivative evaluations, 542 Jacobian matrix evaluations, and 35 s on the VAX 9410 computer. The cost of the RTLS = ATLS $= 10^{-2}$ run was comparable: 531 steps, 1572 derivative evaluations, 532 Jacobian matrix evaluations, and 34 s of CPU time. Note again that the kinetics-plus-sensitivity calculation required fewer steps than the kinetics-only run. (The number of failed steps also decreased: from four to zero for RTLS $= 10^{-5}$, and to one for RTLS $= 10^{-2}$.) Therefore the larger tolerances for the sensitivity coefficients produced smaller weighted errors in these quantities than in the kinetics solution.

The quantity $\varepsilon(\eta_j)$, the average rms norm of the weighted estimated local truncation errors in the sensitivity coefficients, was measured with LSENS, using RTOL$(\underline{S}_j) = 10^{-7}$ and ATOL$(\underline{S}_j) = 10^{-16}$ (see eqs. (4.84) and (4.85)). The $\{\varepsilon(A_j)\}$ were all much less than unity and

$$\max_j \varepsilon(A_j) = \varepsilon(A_{23}) = 1.7 \times 10^{-3}$$

Since NSTEP = 762, it is clear that equation (4.79) was satisfied at all steps for all A_j. (For the initial conditions, however, all $\{\varepsilon(Y_{j,0})\}$ were significantly larger than unity.) Examination of the $\{\partial Y_i/\partial A_j\}$ at all output times showed that $\max(|\partial Y_i/\partial A_j|) = 4.6\times10^{-12}$. Therefore the local error tolerances $\text{RTOL}(\underline{S}_j) = 10^{-7}$ and $\text{ATOL}(\underline{S}_j) = 10^{-16}$ would have provided only absolute error control. This conclusion was confirmed by measuring $\varepsilon(\eta_j)$ with parameter values $\text{RTOL}(\underline{S}_j) = \text{ATOL}(\underline{S}_j) = 10^{-5}$ and $\text{RTOL}(\underline{S}_j) = \text{ATOL}(\underline{S}_j) = 10^{-2}$; all $\{\varepsilon(A_j)\}$ were inversely proportional to $\text{ATOL}(\underline{S}_j)$ (see eq. (4.87)). Therefore, if equation (4.81) were to give the true local error, the local errors in the $\{\partial Y_i/\partial A_j\}$ computed by SENKIN could be guaranteed to be only less than approximately ATLS, which was significantly greater than all $\{\partial Y_i/\partial A_j\}$. However, even with $\text{ATLS} = 10^{-2}$ (which is many orders of magnitude greater than the largest $|\partial Y_i/\partial A_j|$), SENKIN produced accurate results. These observations further reinforce the doubts raised in sections 4.6.2 and 4.6.4 about measuring and controlling local truncation errors in sensitivity coefficients through equations (4.79) (or (4.95)), (4.81), and (4.24).

The computational cost of LSENS was 7.4 s on the VAX 9410. For this problem LSENS was over a factor of 4 faster than SENKIN. To further explore the efficiency differences between the two codes, the execution time required by LSENS for computing the dependent variables and sensitivities with respect to all 15 initial condition values and all 90 rate coefficient parameters was measured and found to be 18 s. Note that the cost of this calculation is significantly less than that of SENKIN for the $\{A_j\}$ sensitivities alone.

Sensitivity coefficients were also computed with respect to temperature exponents and activation energies. However, to minimize the computational work required by the BFM, these results were generated for only the five most important reactions: 2, 4, 14, 15, and 24. The LSENS and BFM solutions, which were obtained with $\text{EMAX} = 10^{-12}$ and $\text{ATOLSP} = 10^{-21}$, are given in tables 4.72 to 4.78. In all cases the agreement between the two sets of results was excellent at all times. Examination of the sensitivities with respect to the three rate coefficient parameters showed that, as expected, at early times in the essentially isothermal induction regime, $\langle\partial Y_i/\partial A_j\rangle = \langle\partial Y_i/\partial n_j\rangle = \langle\partial Y_i/\partial E_j\rangle$ for all i and all j. At longer times, however, the three parameters generally displayed different sensitivity coefficients, sometimes even different signs (e.g., see table 4.77).

On the Amdahl 5870 computer LSENS required 762 steps, 1010 derivative evaluations, 94 Jacobian matrix evaluations and LU-decompositions, and 2.0 s of execution time to solve for the dependent variables (species mole numbers, temperature, and density). The computational cost of the dependent variables and sensitivity coefficients with respect to all 15 initial conditions and all 90 rate coefficient parameters was approximately 37 s, which is considerably less than the estimated BFM cost of about 212 s. To compute the dependent variables and sensitivities with respect to one initial condition and one preexponential factor required execution times of 5.8 and 5.9 s, respectively. For all 15 initial conditions, all 30 preexponential factors, and all 90 rate coefficient parameters, the CPU times

TABLE 4.72.—NORMALIZED SENSITIVITY COEFFICIENTS WITH RESPECT TO SELECTED TEMPERATURE EXPONENTS AND ACTIVATION ENERGIES FOR TEST PROBLEM 8 AT $t = 10^{-6}$ s

Dependent variable	Normalized sensitivity coefficients at $t = 10^{-6}$ s with respect to[a]									
	n_2	n_4	n_{14}	n_{15}	n_{24}	E_2	E_4	E_{14}	E_{15}	E_{24}
σ_O	2.45	1.00	−7.74(−2)	−1.30(−6)	−8.32(−10)	2.45	1.00	−7.74(−2)	−1.30(−6)	−8.32(−10)
	2.45	1.00	−7.74(−2)	−1.30(−6)	−8.32(−10)	2.45	1.00	−7.74(−2)	−1.30(−6)	−8.32(−10)
σ_{H_2O}	1.97	1.00	−5.47(−2)	−4.86(−7)	−5.19(−10)	1.97	1.00	−5.47(−2)	−4.86(−7)	−5.19(−10)
	1.97	1.00	−5.47(−2)	−4.86(−7)	−5.19(−10)	1.97	1.00	−5.47(−2)	−4.86(−7)	−5.19(−10)
σ_{OH}	2.42	1.00	−7.59(−2)	−2.27(−6)	−6.63(−10)	2.42	1.00	−7.59(−2)	−2.27(−6)	−6.63(−10)
	2.42	1.00	−7.59(−2)	−2.27(−6)	−6.63(−10)	2.42	1.00	−7.59(−2)	−2.27(−6)	−6.63(−10)
σ_H	1.53	1.00	−8.15(−2)	−1.51(−6)	−5.56(−10)	1.53	1.00	−8.15(−2)	−1.51(−6)	−5.56(−10)
	1.53	1.00	−8.15(−2)	−1.51(−6)	−5.56(−10)	1.53	1.00	−8.15(−2)	−1.51(−6)	−5.56(−10)
σ_{O_2}	−5.54(−5)	−3.80(−5)	−3.49(−7)	2.02(−11)	5.59(−15)	−5.54(−5)	−3.80(−5)	−3.49(−7)	2.02(−11)	5.59(−15)
	−5.54(−5)	−3.80(−5)	−3.49(−7)	2.02(−11)	5.59(−15)	−5.54(−5)	−3.80(−5)	−3.49(−7)	2.02(−11)	5.59(−15)
σ_{H_2}	−6.44(−5)	−3.79(−5)	1.77(−6)	3.18(−11)	1.88(−14)	−6.44(−5)	−3.79(−5)	1.77(−6)	3.18(−11)	1.88(−14)
	−6.44(−5)	−3.79(−5)	1.77(−6)	3.18(−11)	1.88(−14)	−6.44(−5)	−3.79(−5)	1.77(−6)	3.18(−11)	1.88(−14)
σ_{HO_2}	1.76(−1)	9.96(−1)	1.57(−1)	−1.20(−7)	−6.60(−11)	1.76(−1)	9.96(−1)	1.57(−1)	−1.20(−7)	−6.60(−11)
	1.76(−1)	9.96(−1)	1.57(−1)	−1.20(−7)	−6.60(−11)	1.76(−1)	9.96(−1)	1.57(−1)	−1.20(−7)	−6.60(−11)

$\sigma_{H_2O_2}$	7.41(−2)	9.98(−1)	9.17(−2)	−3.81(−8)	−2.87(−11)	7.41(−2)	9.98(−1)	9.17(−2)	−3.81(−8)	−2.87(−11)
	7.41(−2)	9.98(−1)	9.17(−2)	−3.81(−8)	−2.87(−11)	7.41(−2)	9.98(−1)	9.17(−2)	−3.81(−8)	−2.87(−11)
σ_{NO}	1.93	1.00	−5.30(−2)	−5.58(−7)	1.00	1.93	1.00	−5.30(−2)	−5.58(−7)	1.00
	1.93	1.00	−5.30(−2)	−5.58(−7)	1.00	1.93	1.00	−5.30(−2)	−5.58(−7)	1.00
σ_{NO_2}	1.84	1.98	6.97(−2)	−4.01(−7)	1.00	1.84	1.98	6.97(−2)	−4.01(−7)	1.00
	1.84	1.98	6.97(−2)	−4.01(−7)	1.00	1.84	1.98	6.97(−2)	−4.01(−7)	1.00
σ_N	2.13	1.00	−6.25(−2)	−7.79(−7)	1.00	2.13	1.00	−6.25(−2)	−7.79(−7)	1.00
	2.13	1.00	−6.25(−2)	−7.79(−7)	1.00	2.13	1.00	−6.25(−2)	−7.79(−7)	1.00
σ_{N_2}	−1.48(−12)	−7.42(−13)	4.15(−14)	4.63(−19)	−3.70(−15)	−1.48(−12)	−7.42(−13)	4.15(−14)	4.64(−19)	−3.70(−15)
	−1.48(−12)	−7.42(−13)	4.15(−14)	4.64(−19)	−3.70(−15)	−1.48(−12)	−7.42(−13)	4.15(−14)	4.64(−19)	−3.70(−15)
σ_{N_2O}	1.95	9.78(−1)	−5.46(−2)	−6.10(−7)	−6.82(−10)	1.95	9.78(−1)	−5.46(−2)	−6.10(−7)	−6.82(−10)
	1.95	9.78(−1)	−5.46(−2)	−6.10(−7)	−6.82(−10)	1.95	9.78(−1)	−5.46(−2)	−6.10(−7)	−6.82(−10)
T	5.51(−6)	−3.06(−6)	1.11(−6)	3.67(−11)	−1.27(−14)	5.51(−6)	−3.06(−6)	1.11(−6)	3.67(−11)	−1.27(−14)
	5.51(−6)	−3.06(−6)	1.11(−6)	3.67(−11)	−1.27(−14)	5.51(−6)	−3.06(−6)	1.11(−6)	3.67(−11)	−1.27(−14)
ρ	−5.19(−6)	3.35(−6)	−8.34(−7)	−3.26(−11)	1.26(−14)	−5.19(−6)	3.35(−6)	−8.34(−7)	−3.26(−11)	1.26(−14)
	−5.19(−6)	3.35(−6)	−8.34(−7)	−3.26(−11)	1.26(−14)	−5.19(−6)	3.35(−6)	−8.34(−7)	−3.26(−11)	1.26(−14)

[a]For each dependent variable the top row gives the BFM results and the bottom row gives the LSENS results; numbers in parentheses denote powers of 10.

TABLE 4.73.— NORMALIZED SENSITIVITY COEFFICIENTS WITH RESPECT TO SELECTED TEMPERATURE EXPONENTS AND ACTIVATION ENERGIES FOR TEST PROBLEM 8 AT $t = 3\times10^{-6}$ s

Dependent variable	Normalized sensitivity coefficients at $t = 3\times10^{-6}$ s with respect to[a]									
	n_2	n_4	n_{14}	n_{15}	n_{24}	E_2	E_4	E_{14}	E_{15}	E_{24}
σ_O	7.05	9.92(−1)	−2.85(−1)	−5.71(−4)	−2.28(−9)	7.05	9.92(−1)	−2.85(−1)	−5.71(−4)	−2.28(−9)
	7.05	9.92(−1)	−2.85(−1)	−5.71(−4)	−2.28(−9)	7.05	9.92(−1)	−2.85(−1)	−5.71(−4)	−2.28(−9)
σ_{H_2O}	6.20	1.00	−2.22(−1)	−2.45(−4)	−1.85(−9)	6.20	1.00	−2.22(−1)	−2.45(−4)	−1.85(−9)
	6.20	1.00	−2.22(−1)	−2.45(−4)	−1.85(−9)	6.20	1.00	−2.22(−1)	−2.45(−4)	−1.85(−9)
σ_{OH}	7.06	1.00	−2.43(−1)	−8.65(−4)	−2.14(−9)	7.06	1.00	−2.43(−1)	−8.64(−4)	−2.14(−9)
	7.06	1.00	−2.43(−1)	−8.65(−4)	−2.14(−9)	7.06	1.00	−2.43(−1)	−8.64(−4)	−2.14(−9)
σ_H	6.10	9.82(−1)	−2.86(−1)	−6.41(−4)	−1.98(−9)	6.10	9.82(−1)	−2.86(−1)	−6.40(−4)	−1.98(−9)
	6.10	9.82(−1)	−2.86(−1)	−6.41(−4)	−1.98(−9)	6.10	9.82(−1)	−2.86(−1)	−6.40(−4)	−1.98(−9)
σ_{O_2}	−6.34(−2)	−1.00(−2)	1.92(−3)	3.18(−6)	1.50(−11)	−6.34(−2)	−1.00(−2)	1.92(−3)	3.18(−6)	1.50(−11)
	−6.34(−2)	−1.00(−2)	1.92(−3)	3.18(−6)	1.50(−11)	−6.34(−2)	−1.00(−2)	1.92(−3)	3.18(−6)	1.50(−11)
σ_{H_2}	−7.82(−2)	−1.26(−2)	2.95(−3)	4.80(−6)	2.39(−11)	−7.82(−2)	−1.26(−2)	2.95(−3)	4.80(−6)	2.39(−11)
	−7.82(−2)	−1.26(−2)	2.95(−3)	4.80(−6)	2.39(−11)	−7.82(−2)	−1.26(−2)	2.95(−3)	4.80(−6)	2.39(−11)
σ_{HO_2}	2.02	2.34(−1)	8.82(−1)	−1.27(−4)	−6.58(−10)	2.02	2.34(−1)	8.81(−1)	−1.27(−4)	−6.58(−10)
	2.02	2.34(−1)	8.82(−1)	−1.27(−4)	−6.58(−10)	2.02	2.34(−1)	8.81(−1)	−1.27(−4)	−6.58(−10)

$\sigma_{H_2O_2}$	1.53	3.82(−1)	8.34(−1)	−1.05(−5)	−5.07(−10)	1.53	3.82(−1)	8.34(−1)	−1.05(−5)	−5.07(−10)
	1.53	3.82(−1)	8.34(−1)	−1.05(−5)	−5.07(−10)	1.53	3.82(−1)	8.34(−1)	−1.05(−5)	−5.07(−10)
σ_{NO}	6.23	1.02	−2.43(−1)	−2.33(−4)	9.99(−1)	6.23	1.02	−2.43(−1)	−2.33(−4)	9.98(−1)
	6.23	1.02	−2.43(−1)	−2.33(−4)	9.99(−1)	6.23	1.02	−2.43(−1)	−2.33(−4)	9.98(−1)
σ_{NO_2}	5.17	8.53(−1)	6.44(−1)	−1.88(−5)	9.99(−1)	5.17	8.53(−1)	6.43(−1)	−1.89(−5)	9.99(−1)
	5.17	8.53(−1)	6.44(−1)	−1.88(−5)	9.99(−1)	5.17	8.53(−1)	6.43(−1)	−1.89(−5)	9.99(−1)
σ_N	6.66	1.01	−2.60(−1)	−3.24(−4)	1.00	6.66	1.01	−2.60(−1)	−3.24(−4)	9.99(−1)
	6.66	1.01	−2.60(−1)	−3.24(−4)	1.00	6.66	1.01	−2.60(−1)	−3.24(−4)	9.99(−1)
σ_{N_2}	−1.76(−9)	−2.82(−10)	7.04(−11)	7.87(−14)	−1.44(−12)	−1.76(−9)	−2.82(−10)	7.04(−11)	7.87(−14)	−1.44(−12)
	−1.76(−9)	−2.82(−10)	7.04(−11)	7.87(−14)	−1.44(−12)	−1.76(−9)	−2.82(−10)	7.04(−11)	7.87(−14)	−1.44(−12)
σ_{N_2O}	6.22	9.96(−1)	−2.49(−1)	−2.78(−4)	−2.01(−9)	6.22	9.96(−1)	−2.49(−1)	−2.78(−4)	−2.01(−9)
	6.22	9.96(−1)	−2.49(−1)	−2.78(−4)	−2.01(−9)	6.22	9.96(−1)	−2.49(−1)	−2.78(−4)	−2.01(−9)
T	1.04(−2)	1.87(−3)	2.92(−4)	3.69(−6)	−7.31(−12)	1.04(−2)	1.87(−3)	2.91(−4)	3.69(−6)	−7.31(−12)
	1.04(−2)	1.87(−3)	2.92(−4)	3.69(−6)	−7.31(−12)	1.04(−2)	1.87(−3)	2.91(−4)	3.69(−6)	−7.31(−12)
ρ	−9.81(−3)	−1.76(−3)	−2.10(−4)	−3.26(−6)	7.12(−12)	−9.81(−3)	−1.76(−3)	−2.10(−4)	−3.26(−6)	7.12(−12)
	−9.81(−3)	−1.76(−3)	−2.10(−4)	−3.26(−6)	7.12(−12)	−9.81(−3)	−1.76(−3)	−2.10(−4)	−3.26(−6)	7.12(−12)

[a]For each dependent variable the top row gives the BFM results and the bottom row gives the LSENS results; numbers in parentheses denote powers of 10.

TABLE 4.74.—NORMALIZED SENITIVITY COEFFICIENTS WITH RESPECT TO SELECTED TEMPERATURE EXPONENTS AND ACTIVATION ENERGIES FOR TEST PROBLEM 8 AT $t = 5\times10^{-6}$ s

Dependent variable	Normalized sensitivity coefficients at $t = 5\times10^{-6}$ s with respect to[a]									
	n_2	n_4	n_{14}	n_{15}	n_{24}	E_2	E_4	E_{14}	E_{15}	E_{24}
σ_O	2.03	1.75(−1)	−3.60(−2)	−1.13(−2)	−1.28(−7)	1.97	1.76(−1)	−3.63(−2)	−9.35(−3)	−1.05(−7)
	2.03	1.75(−1)	−3.60(−2)	−1.13(−2)	−1.28(−7)	1.97	1.76(−1)	−3.63(−2)	−9.35(−3)	−1.05(−7)
σ_{H_2O}	9.64(−1)	9.12(−2)	1.16(−2)	1.33(−2)	−8.04(−9)	9.49(−1)	9.17(−2)	7.97(−3)	1.13(−2)	−6.89(−9)
	9.64(−1)	9.12(−2)	1.16(−2)	1.33(−2)	−8.04(−9)	9.49(−1)	9.17(−2)	7.97(−3)	1.13(−2)	−6.89(−9)
σ_{OH}	1.45	1.34(−1)	8.56(−2)	3.44(−2)	−1.05(−7)	1.42	1.35(−1)	7.08(−2)	3.00(−2)	−8.63(−8)
	1.45	1.34(−1)	8.56(−2)	3.44(−2)	−1.05(−7)	1.42	1.35(−1)	7.08(−2)	3.00(−2)	−8.63(−8)
σ_H	−2.13(−1)	−2.82(−2)	−7.95(−2)	−4.21(−2)	3.10(−9)	−2.14(−1)	−2.80(−2)	−6.91(−2)	−3.59(−2)	2.52(−9)
	−2.13(−1)	−2.82(−2)	−7.95(−2)	−4.21(−2)	3.10(−9)	−2.14(−1)	−2.80(−2)	−6.91(−2)	−3.59(−2)	2.52(−9)
σ_{O_2}	−2.82	−2.61(−1)	−3.42(−2)	−3.09(−2)	−3.60(−8)	−2.77	−2.62(−1)	−2.32(−2)	−2.67(−2)	−2.98(−8)
	−2.82	−2.61(−1)	−3.42(−2)	−3.09(−2)	−3.60(−8)	−2.77	−2.62(−1)	−2.32(−2)	−2.67(−2)	−2.98(−8)
σ_{H_2}	−2.33	−2.14(−1)	1.67(−2)	−6.04(−3)	3.25(−8)	−2.29	−2.15(−1)	1.99(−2)	−5.37(−3)	2.75(−8)
	−2.33	−2.14(−1)	1.67(−2)	−6.04(−3)	3.25(−8)	−2.29	−2.15(−1)	1.99(−2)	−5.37(−3)	2.75(−8)
σ_{HO_2}	−2.75	−5.37(−1)	8.67(−1)	−5.49(−2)	−1.44(−8)	−2.70	−4.83(−1)	6.93(−1)	−4.70(−2)	−1.21(−8)
	−2.75	−5.37(−1)	8.67(−1)	−5.49(−2)	−1.44(−8)	−2.70	−4.83(−1)	6.93(−1)	−4.70(−2)	−1.21(−8)

$\sigma_{H_2O_2}$	9.81(−1)	6.76(−2)	5.31(−2)	−1.35(−2)	−1.17(−7)	9.36(−1)	6.99(−2)	4.24(−2)	−1.00(−2)	−9.64(−8)
	9.81(−1)	6.76(−2)	5.31(−2)	−1.35(−2)	−1.17(−7)	9.36(−1)	6.99(−2)	4.24(−2)	−1.00(−2)	−9.64(−8)
σ_{NO}	1.60(1)	1.62	5.99(−1)	3.68(−1)	9.93(−1)	1.58(1)	1.62	5.01(−1)	3.21(−1)	8.25(−1)
	1.60(1)	1.62	5.99(−1)	3.68(−1)	9.93(−1)	1.58(1)	1.62	5.01(−1)	3.21(−1)	8.25(−1)
σ_{NO_2}	1.73(1)	1.72	6.09(−1)	3.57(−1)	9.93(−1)	1.71(1)	1.73	5.05(−1)	3.12(−1)	8.25(−1)
	1.73(1)	1.72	6.09(−1)	3.57(−1)	9.93(−1)	1.71(1)	1.73	5.05(−1)	3.12(−1)	8.25(−1)
σ_N	1.18(1)	1.20	6.47(−1)	4.26(−1)	1.03	1.17(1)	1.20	5.44(−1)	3.65(−1)	8.27(−1)
	1.18(1)	1.20	6.47(−1)	4.26(−1)	1.03	1.17(1)	1.20	5.44(−1)	3.65(−1)	8.27(−1)
σ_{N_2}	−6.11(−7)	−5.97(−8)	−6.87(−9)	−7.00(−9)	−1.02(−8)	−6.02(−7)	−5.98(−8)	−4.76(−9)	−6.10(−9)	−8.45(−9)
	−6.11(−7)	−5.97(−8)	−6.87(−9)	−7.00(−9)	−1.02(−8)	−6.02(−7)	−5.98(−8)	−4.76(−9)	−6.10(−9)	−8.45(−9)
σ_{N_2O}	5.95	5.74(−1)	8.79(−3)	4.14(−2)	−7.96(−8)	5.86	5.75(−1)	−5.65(−3)	3.62(−2)	−6.75(−8)
	5.95	5.74(−1)	8.79(−3)	4.14(−2)	−7.96(−8)	5.86	5.75(−1)	−5.65(−3)	3.62(−2)	−6.75(−8)
T	4.78(−1)	4.98(−2)	3.81(−2)	2.41(−2)	−1.74(−8)	4.74(−1)	4.99(−2)	3.23(−2)	2.05(−2)	−1.44(−8)
	4.78(−1)	4.98(−2)	3.81(−2)	2.41(−2)	−1.74(−8)	4.74(−1)	4.99(−2)	3.23(−2)	2.05(−2)	−1.44(−8)
ρ	−4.11(−1)	−4.28(−2)	−3.26(−2)	−2.07(−2)	1.74(−8)	−4.08(−1)	−4.29(−2)	−2.76(−2)	−1.76(−2)	1.44(−8)
	−4.11(−1)	−4.28(−2)	−3.26(−2)	−2.07(−2)	1.74(−8)	−4.08(−1)	−4.29(−2)	−2.76(−2)	−1.76(−2)	1.44(−8)

[a]For each dependent variable the top row gives the BFM results and the bottom row gives the LSENS results; numbers in parentheses denote powers of 10.

TABLE 4.75.—NORMALIZED SENSITIVITY COEFFICIENTS WITH RESPECT TO SELECTED TEMPERATURE EXPONENTS AND ACTIVATION ENERGIES FOR TEST PROBLEM 8 AT $t = 7.5\times10^{-6}$ s

Dependent variable	Normalized sensitivity coefficients at $t = 7.5\times10^{-6}$ s with respect to[a]									
	n_2	n_4	n_{14}	n_{15}	n_{24}	E_2	E_4	E_{14}	E_{15}	E_{24}
σ_O	−2.58(−1)	−2.81(−2)	−9.00(−2)	−8.80(−2)	−1.26(−5)	−2.56(−1)	−2.77(−2)	−6.64(−2)	−6.37(−2)	−8.49(−6)
	−2.58(−1)	−2.81(−2)	−9.00(−2)	−8.80(−2)	−1.26(−5)	−2.56(−1)	−2.77(−2)	−6.64(−2)	−6.37(−2)	−8.49(−6)
σ_{H_2O}	6.76(−2)	6.70(−3)	2.39(−2)	2.28(−2)	−7.89(−7)	6.70(−2)	6.81(−3)	1.76(−2)	1.65(−2)	−5.36(−7)
	6.76(−2)	6.70(−3)	2.39(−2)	2.28(−2)	−7.89(−7)	6.70(−2)	6.81(−3)	1.76(−2)	1.65(−2)	−5.36(−7)
σ_{OH}	1.50(−1)	1.40(−2)	5.65(−2)	4.68(−2)	−9.85(−6)	1.49(−1)	1.45(−2)	4.13(−2)	3.42(−2)	−6.65(−6)
	1.50(−1)	1.40(−2)	5.65(−2)	4.68(−2)	−9.85(−6)	1.49(−1)	1.45(−2)	4.13(−2)	3.42(−2)	−6.65(−6)
σ_H	−3.78(−1)	−3.93(−2)	−1.35(−1)	−1.27(−1)	1.09(−6)	−3.75(−1)	−3.93(−2)	−9.94(−2)	−9.23(−2)	7.33(−7)
	−3.78(−1)	−3.93(−2)	−1.35(−1)	−1.27(−1)	1.09(−6)	−3.75(−1)	−3.93(−2)	−9.94(−2)	−9.23(−2)	7.33(−7)
σ_{O_2}	−1.95(−1)	−1.76(−2)	−7.15(−2)	−6.31(−2)	−1.42(−5)	−1.93(−1)	−1.85(−2)	−5.23(−2)	−4.58(−2)	−9.64(−6)
	−1.95(−1)	−1.76(−2)	−7.15(−2)	−6.31(−2)	−1.42(−5)	−1.93(−1)	−1.85(−2)	−5.23(−2)	−4.58(−2)	−9.64(−6)
σ_{H_2}	−3.32(−2)	−2.00(−3)	−1.17(−2)	−1.02(−2)	4.18(−6)	−3.27(−2)	−2.48(−3)	−8.62(−3)	−7.45(−3)	2.83(−6)
	−3.32(−2)	−2.00(−3)	−1.17(−2)	−1.02(−2)	4.18(−6)	−3.27(−2)	−2.48(−3)	−8.62(−3)	−7.45(−3)	2.83(−6)
σ_{HO_2}	−3.50(−1)	−3.09(−1)	7.78(−1)	−1.16(−1)	−1.07(−5)	−3.47(−1)	−2.13(−1)	4.92(−1)	−8.43(−2)	−7.33(−6)
	−3.50(−1)	−3.09(−1)	7.78(−1)	−1.16(−1)	−1.07(−5)	−3.47(−1)	−2.13(−1)	4.92(−1)	−8.43(−2)	−7.33(−6)

$\sigma_{H_2O_2}$	−7.35(−1)	−8.00(−2)	−2.50(−1)	−2.55(−1)	−5.11(−6)	−7.29(−1)	−7.88(−2)	−1.85(−1)	−1.84(−1)	−3.44(−6)
	−7.35(−1)	−8.00(−2)	−2.50(−1)	−2.55(−1)	−5.11(−6)	−7.29(−1)	−7.88(−2)	−1.85(−1)	−1.84(−1)	−3.44(−6)
σ_{NO}	3.04	3.11(−1)	7.04(−1)	6.35(−1)	1.04	3.01	3.12(−1)	5.38(−1)	4.77(−1)	7.03(−1)
	3.04	3.11(−1)	7.04(−1)	6.35(−1)	1.04	3.01	3.12(−1)	5.38(−1)	4.77(−1)	7.03(−1)
σ_{NO_2}	3.08	3.07(−1)	7.41(−1)	6.45(−1)	1.04	3.05	3.11(−1)	5.63(−1)	4.85(−1)	7.03(−1)
	3.08	3.07(−1)	7.41(−1)	6.45(−1)	1.04	3.05	3.11(−1)	5.63(−1)	4.85(−1)	7.03(−1)
σ_N	1.81	1.87(−1)	6.29(−1)	6.01(−1)	1.05	1.80	1.87(−1)	4.64(−1)	4.36(−1)	6.82(−1)
	1.81	1.87(−1)	6.29(−1)	6.01(−1)	1.05	1.80	1.87(−1)	4.64(−1)	4.36(−1)	6.82(−1)
σ_{N_2}	−4.19(−6)	−4.28(−7)	−9.79(−7)	−8.83(−7)	−1.43(−6)	−4.15(−6)	−4.30(−7)	−7.47(−7)	−6.63(−7)	−9.68(−7)
	−4.19(−6)	−4.28(−7)	−9.79(−7)	−8.83(−7)	−1.43(−6)	−4.15(−6)	−4.30(−7)	−7.47(−7)	−6.63(−7)	−9.68(−7)
σ_{N_2O}	2.01(−1)	1.91(−2)	5.34(−2)	4.59(−2)	−9.79(−6)	1.99(−1)	1.96(−2)	3.98(−2)	3.40(−2)	−6.71(−6)
	2.01(−1)	1.91(−2)	5.34(−2)	4.59(−2)	−9.79(−6)	1.99(−1)	1.96(−2)	3.98(−2)	3.40(−2)	−6.71(−6)
T	1.30(−1)	1.34(−2)	4.61(−2)	4.39(−2)	−1.64(−6)	1.29(−1)	1.35(−2)	3.39(−2)	3.18(−2)	−1.11(−6)
	1.30(−1)	1.34(−2)	4.61(−2)	4.39(−2)	−1.64(−6)	1.29(−1)	1.35(−2)	3.39(−2)	3.18(−2)	−1.11(−6)
ρ	−1.07(−1)	−1.10(−2)	−3.79(−2)	−3.61(−2)	1.65(−6)	−1.06(−1)	−1.11(−2)	−2.78(−2)	−2.61(−2)	1.12(−6)
	−1.07(−1)	−1.10(−2)	−3.79(−2)	−3.61(−2)	1.65(−6)	−1.06(−1)	−1.11(−2)	−2.78(−2)	−2.61(−2)	1.12(−6)

[a]For each dependent variable the top row gives the BFM results and the bottom row gives the LSENS results; numbers in parentheses denote powers of 10.

TABLE 4.76.—NORMALIZED SENSITIVITY COEFFICIENTS WITH RESPECT TO SELECTED TEMPERATURE EXPONENTS AND ACTIVATION ENERGIES FOR TEST PROBLEM 8 AT $t = 1.5\times10^{-5}$ s

Dependent variable	Normalized sensitivity coefficients at $t = 1.5\times10^{-5}$ s with respect to[a]									
	n_2	n_4	n_{14}	n_{15}	n_{24}	E_2	E_4	E_{14}	E_{15}	E_{24}
σ_O	−1.31(−1)	−1.54(−2)	−1.65(−1)	−1.74(−1)	−4.07(−4)	−1.30(−1)	−1.46(−2)	−1.03(−1)	−1.07(−1)	−2.34(−4)
	−1.31(−1)	−1.54(−2)	−1.65(−1)	−1.74(−1)	−4.07(−4)	−1.30(−1)	−1.46(−2)	−1.03(−1)	−1.07(−1)	−2.34(−4)
σ_{H_2O}	2.52(−2)	2.76(−3)	3.18(−2)	3.31(−2)	−2.33(−5)	2.50(−2)	2.70(−3)	1.99(−2)	2.05(−2)	−1.34(−5)
	2.52(−2)	2.76(−3)	3.18(−2)	3.31(−2)	−2.33(−5)	2.50(−2)	2.70(−3)	1.99(−2)	2.05(−2)	−1.34(−5)
σ_{OH}	1.48(−3)	−4.16(−4)	3.08(−3)	5.19(−4)	−2.77(−4)	1.39(−3)	−1.65(−4)	1.82(−3)	4.12(−4)	−1.59(−4)
	1.48(−3)	−4.16(−4)	3.08(−3)	5.19(−4)	−2.77(−4)	1.39(−3)	−1.65(−4)	1.82(−3)	4.12(−4)	−1.59(−4)
σ_H	−1.57(−1)	−1.78(−2)	−1.99(−1)	−2.07(−1)	1.92(−5)	−1.55(−1)	−1.71(−2)	−1.24(−1)	−1.28(−1)	1.10(−5)
	−1.57(−1)	−1.78(−2)	−1.99(−1)	−2.07(−1)	1.92(−5)	−1.55(−1)	−1.71(−2)	−1.24(−1)	−1.28(−1)	1.10(−5)
σ_{O_2}	−7.50(−2)	−7.27(−3)	−9.57(−2)	−9.67(−2)	−5.48(−4)	−7.42(−2)	−7.51(−3)	−5.98(−2)	−6.00(−2)	−3.15(−4)
	−7.50(−2)	−7.27(−3)	−9.57(−2)	−9.67(−2)	−5.48(−4)	−7.42(−2)	−7.51(−3)	−5.98(−2)	−6.00(−2)	−3.15(−4)
σ_{H_2}	−3.81(−2)	−3.75(−3)	−4.82(−2)	−4.94(−2)	1.60(−4)	−3.77(−2)	−3.84(−3)	−3.02(−2)	−3.06(−2)	9.19(−5)
	−3.81(−2)	−3.75(−3)	−4.82(−2)	−4.94(−2)	1.60(−4)	−3.77(−2)	−3.84(−3)	−3.02(−2)	−3.06(−2)	9.19(−5)
σ_{HO_2}	−4.62(−2)	−2.16(−1)	6.77(−1)	−5.94(−2)	−5.03(−4)	−4.57(−2)	−1.20(−1)	3.65(−1)	−3.68(−2)	−2.90(−4)
	−4.62(−2)	−2.16(−1)	6.77(−1)	−5.94(−2)	−5.03(−4)	−4.57(−2)	−1.20(−1)	3.65(−1)	−3.68(−2)	−2.90(−4)

$\sigma_{H_2O_2}$	−3.07(−1)	−3.68(−2)	−3.81(−1)	−4.08(−1)	−1.79(−4)	−3.04(−1)	−3.46(−2)	−2.39(−1)	−2.52(−1)	−1.03(−4)
	−3.07(−1)	−3.68(−2)	−3.81(−1)	−4.08(−1)	−1.79(−4)	−3.04(−1)	−3.46(−2)	−2.39(−1)	−2.52(−1)	−1.03(−4)
σ_{NO}	7.24(−1)	7.59(−2)	5.26(−1)	5.29(−1)	1.06	7.18(−1)	7.56(−2)	3.49(−1)	3.47(−1)	6.11(−1)
	7.24(−1)	7.59(−2)	5.26(−1)	5.29(−1)	1.06	7.18(−1)	7.56(−2)	3.49(−1)	3.47(−1)	6.11(−1)
σ_{NO_2}	8.25(−1)	8.21(−2)	6.69(−1)	6.60(−1)	1.06	8.17(−1)	8.37(−2)	4.37(−1)	4.28(−1)	6.11(−1)
	8.25(−1)	8.21(−2)	6.69(−1)	6.60(−1)	1.06	8.17(−1)	8.37(−2)	4.37(−1)	4.28(−1)	6.11(−1)
σ_N	3.83(−1)	4.27(−2)	4.63(−1)	4.84(−1)	1.07	3.80(−1)	4.14(−2)	2.91(−1)	3.00(−1)	5.86(−1)
	3.83(−1)	4.27(−2)	4.63(−1)	4.84(−1)	1.07	3.80(−1)	4.14(−2)	2.91(−1)	3.00(−1)	5.86(−1)
σ_{N_2}	−2.73(−5)	−2.86(−6)	−1.99(−5)	−2.00(−5)	−4.01(−5)	−2.71(−5)	−2.85(−6)	−1.32(−5)	−1.31(−5)	−2.31(−5)
	−2.73(−5)	−2.86(−6)	−1.99(−5)	−2.00(−5)	−4.01(−5)	−2.71(−5)	−2.85(−6)	−1.32(−5)	−1.31(−5)	−2.31(−5)
σ_{N_2O}	1.97(−1)	2.15(−2)	2.37(−1)	2.44(−1)	−4.83(−4)	1.95(−1)	2.10(−2)	1.49(−1)	1.52(−1)	−2.79(−4)
	1.97(−1)	2.15(−2)	2.37(−1)	2.44(−1)	−4.83(−4)	1.95(−1)	2.10(−2)	1.49(−1)	1.52(−1)	−2.79(−4)
T	3.41(−2)	3.84(−3)	4.30(−2)	4.50(−2)	−3.91(−5)	3.38(−2)	3.71(−3)	2.69(−2)	2.78(−2)	−2.25(−5)
	3.41(−2)	3.84(−3)	4.30(−2)	4.50(−2)	−3.91(−5)	3.38(−2)	3.71(−3)	2.69(−2)	2.78(−2)	−2.25(−5)
ρ	−2.69(−2)	−3.03(−3)	−3.40(−2)	−3.55(−2)	3.92(−5)	−2.67(−2)	−2.93(−3)	−2.13(−2)	−2.20(−2)	2.26(−5)
	−2.69(−2)	−3.03(−3)	−3.40(−2)	−3.55(−2)	3.92(−5)	−2.67(−2)	−2.93(−3)	−2.13(−2)	−2.20(−2)	2.26(−5)

[a]For each dependent variable the top row gives the BFM results and the bottom row gives the LSENS results; numbers in parentheses denote powers of 10.

TABLE 4.77.—NORMALIZED SENSITIVITY COEFFICIENTS WITH RESPECT TO SELECTED TEMPERATURE EXPONENTS AND ACTIVATION ENERGIES FOR TEST PROBLEM 8 AT $t = 10^{-4}$ s

Dependent variable	Normalized sensitivity coefficients at $t = 10^{-4}$ s with respect to[a]									
	n_2	n_4	n_{14}	n_{15}	n_{24}	E_2	E_4	E_{14}	E_{15}	E_{24}
σ_O	−1.90(−3)	−9.48(−4)	−9.92(−3)	−1.62(−2)	−2.96(−2)	−1.93(−3)	−5.64(−4)	−5.17(−3)	−8.16(−3)	−1.43(−2)
	−1.90(−3)	−9.48(−4)	−9.92(−3)	−1.62(−2)	−2.96(−2)	−1.93(−3)	−5.64(−4)	−5.17(−3)	−8.16(−3)	−1.43(−2)
σ_{H_2O}	9.49(−5)	9.38(−5)	9.32(−4)	1.66(−3)	−5.10(−4)	9.16(−5)	4.98(−5)	4.68(−4)	8.13(−4)	−2.45(−4)
	9.49(−5)	9.38(−5)	9.32(−4)	1.66(−3)	−5.10(−4)	9.16(−5)	4.98(−5)	4.68(−4)	8.13(−4)	−2.45(−4)
σ_{OH}	−8.11(−4)	−3.05(−4)	−3.29(−3)	−5.09(−3)	−1.66(−2)	−8.30(−4)	−1.94(−4)	−1.75(−3)	−2.62(−3)	−7.98(−3)
	−8.11(−4)	−3.05(−4)	−3.29(−3)	−5.09(−3)	−1.66(−2)	−8.30(−4)	−1.94(−4)	−1.75(−3)	−2.62(−3)	−7.98(−3)
σ_H	−1.08(−3)	−8.39(−4)	−8.44(−3)	−1.46(−2)	−4.40(−3)	−1.07(−3)	−4.61(−4)	−4.28(−3)	−7.24(−3)	−2.12(−3)
	−1.08(−3)	−8.38(−4)	−8.44(−3)	−1.46(−2)	−4.40(−3)	−1.07(−3)	−4.61(−4)	−4.28(−3)	−7.24(−3)	−2.12(−3)
σ_{O_2}	−2.07(−3)	−6.32(−4)	−7.08(−3)	−1.07(−2)	−3.87(−2)	−1.99(−3)	−4.11(−4)	−3.79(−3)	−5.53(−3)	−1.87(−2)
	−2.07(−3)	−6.32(−4)	−7.08(−3)	−1.07(−2)	−3.87(−2)	−1.99(−3)	−4.11(−4)	−3.79(−3)	−5.53(−3)	−1.87(−2)
σ_{H_2}	−1.72(−5)	−2.25(−4)	−2.13(−3)	−4.11(−3)	8.99(−3)	4.73(−6)	−1.06(−4)	−1.03(−3)	−1.97(−3)	4.33(−3)
	−1.72(−5)	−2.25(−4)	−2.13(−3)	−4.11(−3)	8.99(−3)	4.75(−6)	−1.06(−4)	−1.03(−3)	−1.97(−3)	4.33(−3)
σ_{HO_2}	−1.42(−3)	−1.50(−3)	1.64(−3)	−3.89(−3)	−3.47(−2)	−1.38(−3)	−7.82(−4)	4.76(−4)	−2.14(−3)	−1.67(−2)
	−1.42(−3)	−1.50(−3)	1.64(−3)	−3.89(−3)	−3.47(−2)	−1.38(−3)	−7.82(−4)	4.76(−4)	−2.14(−3)	−1.67(−2)

$\sigma_{H_2O_2}$	−2.15(−3)	−1.36(−3)	−1.38(−2)	−2.33(−2)	−2.34(−2)	−2.19(−3)	−7.77(−4)	−7.08(−3)	−1.16(−2)	−1.13(−2)
	−2.15(−3)	−1.36(−3)	−1.38(−2)	−2.33(−2)	−2.34(−2)	−2.19(−3)	−7.77(−4)	−7.08(−3)	−1.16(−2)	−1.13(−2)
σ_{NO}	3.89(−2)	6.37(−3)	8.08(−2)	9.91(−2)	9.98(−1)	3.84(−2)	5.21(−3)	4.63(−2)	5.53(−2)	4.81(−1)
	3.89(−2)	6.37(−3)	8.08(−2)	9.91(−2)	9.98(−1)	3.84(−2)	5.21(−3)	4.63(−2)	5.53(−2)	4.81(−1)
σ_{NO_2}	3.87(−2)	6.60(−3)	8.32(−2)	1.04(−1)	9.81(−1)	3.82(−2)	5.30(−3)	4.74(−2)	5.75(−2)	4.72(−1)
	3.87(−2)	6.60(−3)	8.32(−2)	1.04(−1)	9.81(−1)	3.82(−2)	5.30(−3)	4.74(−2)	5.75(−2)	4.72(−1)
σ_N	1.98(−2)	3.56(−3)	4.41(−2)	5.61(−2)	9.60(−1)	1.96(−2)	2.80(−3)	2.50(−2)	3.08(−2)	4.57(−1)
	1.98(−2)	3.56(−3)	4.41(−2)	5.61(−2)	9.60(−1)	1.96(−2)	2.80(−3)	2.50(−2)	3.08(−2)	4.57(−1)
σ_{N_2}	−6.82(−5)	−1.12(−5)	−1.42(−4)	−1.74(−4)	−1.75(−3)	−6.74(−5)	−9.13(−6)	−8.13(−5)	−9.69(−5)	−8.43(−4)
	−6.82(−5)	−1.12(−5)	−1.42(−4)	−1.74(−4)	−1.75(−3)	−6.74(−5)	−9.13(−6)	−8.13(−5)	−9.69(−5)	−8.43(−4)
σ_{N_2O}	7.01(−4)	1.19(−3)	1.16(−2)	2.12(−2)	−2.21(−2)	6.74(−4)	6.06(−4)	5.73(−3)	1.03(−2)	−1.06(−2)
	7.01(−4)	1.19(−3)	1.16(−2)	2.12(−2)	−2.21(−2)	6.74(−4)	6.06(−4)	5.73(−3)	1.03(−2)	−1.06(−2)
T	6.62(−5)	8.94(−5)	8.74(−4)	1.58(−3)	−1.10(−3)	6.56(−5)	4.63(−5)	4.35(−4)	7.72(−4)	−5.30(−4)
	6.61(−5)	8.94(−5)	8.74(−4)	1.58(−3)	−1.10(−3)	6.55(−5)	4.63(−5)	4.35(−4)	7.72(−4)	−5.30(−4)
ρ	−3.62(−5)	−6.56(−5)	−6.35(−4)	−1.16(−3)	1.19(−3)	−3.60(−5)	−3.33(−5)	−3.14(−4)	−5.66(−4)	5.74(−4)
	−3.62(−5)	−6.56(−5)	−6.35(−4)	−1.16(−3)	1.19(−3)	−3.60(−5)	−3.33(−5)	−3.14(−4)	−5.66(−4)	5.74(−4)

[a]For each dependent variable the top row gives the BFM results and the bottom row gives the LSENS results; numbers in parentheses denote powers of 10.

TABLE 4.78.—NORMALIZED SENSITIVITY COEFFICIENTS WITH RESPECT TO SELECTED TEMPERATURE EXPONENTS AND ACTIVATION ENERGIES FOR TEST PROBLEM 8 AT $t = 10^{-3}$ s

Dependent variable	Normalized sensitivity coefficients at $t = 10^{-3}$ s with respect to[a]									
	n_2	n_4	n_{14}	n_{15}	n_{24}	E_2	E_4	E_{14}	E_{15}	E_{24}
σ_O	-3.18(-5)	-6.18(-6)	-7.52(-5)	-9.83(-5)	-9.88(-3)	-3.23(-5)	-4.81(-6)	-4.25(-5)	-5.37(-5)	-4.67(-3)
	-3.18(-5)	-6.18(-6)	-7.52(-5)	-9.83(-5)	-9.88(-3)	-3.23(-5)	-4.81(-6)	-4.25(-5)	-5.37(-5)	-4.67(-3)
σ_{H_2O}	-4.41(-7)	-2.79(-8)	-6.28(-7)	-1.87(-7)	-1.65(-4)	-4.93(-7)	-4.43(-8)	-4.13(-7)	-2.08(-7)	-7.80(-5)
	-4.43(-7)	-2.81(-8)	-6.28(-7)	-1.87(-7)	-1.65(-4)	-4.94(-7)	-4.45(-8)	-4.12(-7)	-2.08(-7)	-7.80(-5)
σ_{OH}	-1.76(-5)	-3.26(-6)	-4.03(-5)	-5.14(-5)	-5.46(-3)	-1.79(-5)	-2.58(-6)	-2.29(-5)	-2.83(-5)	-2.58(-3)
	-1.76(-5)	-3.26(-6)	-4.03(-5)	-5.14(-5)	-5.46(-3)	-1.78(-5)	-2.58(-6)	-2.29(-5)	-2.83(-5)	-2.58(-3)
σ_H	-5.92(-6)	-1.55(-6)	-1.70(-5)	-2.62(-5)	-1.73(-3)	-5.84(-6)	-1.07(-6)	-9.28(-6)	-1.37(-5)	-8.18(-4)
	-5.91(-6)	-1.55(-6)	-1.70(-5)	-2.62(-5)	-1.73(-3)	-5.83(-6)	-1.07(-6)	-9.29(-6)	-1.37(-5)	-8.18(-4)
σ_{O_2}	-4.79(-5)	-7.56(-6)	-9.43(-5)	-1.20(-4)	-1.28(-2)	-4.50(-5)	-6.02(-6)	-5.37(-5)	-6.60(-5)	-6.06(-3)
	-4.79(-5)	-7.56(-6)	-9.43(-5)	-1.20(-4)	-1.28(-2)	-4.50(-5)	-6.02(-6)	-5.37(-5)	-6.60(-5)	-6.06(-3)
σ_{H_2}	8.64(-6)	1.41(-6)	1.85(-5)	2.13(-5)	2.80(-3)	8.96(-6)	1.20(-6)	1.07(-5)	1.21(-5)	1.33(-3)
	8.64(-6)	1.41(-6)	1.85(-5)	2.13(-5)	2.80(-3)	8.96(-6)	1.20(-6)	1.07(-5)	1.21(-5)	1.33(-3)
σ_{HO_2}	-4.06(-5)	-1.06(-5)	-6.45(-5)	-1.02(-4)	-1.13(-2)	-3.90(-5)	-7.15(-6)	-3.85(-5)	-5.64(-5)	-5.36(-3)
	-4.06(-5)	-1.06(-5)	-6.45(-5)	-1.02(-4)	-1.13(-2)	-3.90(-5)	-7.15(-6)	-3.85(-5)	-5.63(-5)	-5.36(-3)

$\sigma_{H_2O_2}$	−2.56(−5)	−5.52(−6)	−6.47(−5)	−8.83(−5)	−8.10(−3)	−2.63(−5)	−4.16(−6)	−3.63(−5)	−4.77(−5)	−3.83(−3)
	−2.56(−5)	−5.52(−6)	−6.47(−5)	−8.83(−5)	−8.10(−3)	−2.63(−5)	−4.16(−6)	−3.63(−5)	−4.77(−5)	−3.83(−3)
σ_{NO}	2.31(−4)	3.77(−5)	4.74(−4)	5.89(−4)	6.64(−2)	2.25(−4)	3.05(−5)	2.71(−4)	3.27(−4)	3.14(−2)
	2.31(−4)	3.77(−5)	4.74(−4)	5.89(−4)	6.64(−2)	2.25(−4)	3.05(−5)	2.71(−4)	3.27(−4)	3.14(−2)
σ_{NO_2}	2.13(−4)	3.46(−5)	4.37(−4)	5.44(−4)	6.07(−2)	2.06(−4)	2.80(−5)	2.49(−4)	3.01(−4)	2.87(−2)
	2.13(−4)	3.46(−5)	4.37(−4)	5.44(−4)	6.07(−2)	2.06(−4)	2.80(−5)	2.49(−4)	3.01(−4)	2.87(−2)
σ_N	1.60(−4)	2.64(−5)	3.31(−4)	4.12(−4)	5.06(−2)	1.56(−4)	2.13(−5)	1.89(−4)	2.29(−4)	2.39(−2)
	1.60(−4)	2.64(−5)	3.31(−4)	4.12(−4)	5.06(−2)	1.56(−4)	2.13(−5)	1.89(−4)	2.29(−4)	2.39(−2)
σ_{N_2}	−1.81(−6)	−2.96(−7)	−3.72(−6)	−4.62(−6)	−5.21(−4)	−1.76(−6)	−2.39(−7)	−2.13(−6)	−2.57(−6)	−2.46(−4)
	−1.81(−6)	−2.96(−7)	−3.72(−6)	−4.62(−6)	−5.21(−4)	−1.76(−6)	−2.39(−7)	−2.13(−6)	−2.57(−6)	−2.46(−4)
σ_{N_2O}	−9.12(−6)	−8.18(−7)	−1.40(−5)	−9.64(−6)	−2.97(−3)	−9.44(−6)	−9.48(−7)	−8.71(−6)	−6.72(−6)	−1.40(−3)
	−9.12(−6)	−8.18(−7)	−1.40(−5)	−9.64(−6)	−2.97(−3)	−9.44(−6)	−9.48(−7)	−8.70(−6)	−6.72(−6)	−1.40(−3)
T	−1.08(−6)	−1.14(−7)	−1.72(−6)	−1.54(−6)	−3.16(−4)	−1.06(−6)	−1.14(−7)	−1.03(−6)	−9.60(−7)	−1.49(−4)
	−1.08(−6)	−1.14(−7)	−1.72(−6)	−1.54(−6)	−3.16(−4)	−1.06(−6)	−1.14(−7)	−1.03(−6)	−9.60(−7)	−1.49(−4)
ρ	1.19(−6)	1.46(−7)	2.06(−6)	2.11(−6)	3.45(−4)	1.16(−6)	1.35(−7)	1.22(−6)	1.25(−6)	1.63(−4)
	1.18(−6)	1.44(−7)	2.06(−6)	2.11(−6)	3.45(−4)	1.15(−6)	1.33(−7)	1.23(−6)	1.26(−6)	1.63(−4)

[a]For each dependent variable the top row gives the BFM results and the bottom row gives the LSENS results; numbers in parentheses denote powers of 10.

were 9.8, 14.5, and 32 s, respectively. Thus each additional initial condition after the first costs approximately 0.29 s. For rate coefficient parameters the figure is approximately 0.30 s. Both execution times are significantly less than the approximately 2.0 s that the BFM would need.

4.6.7 Benzene-Oxygen-Argon Ignition and Combustion

The ninth, and last, test problem, which is the largest studied to date, describes the ignition and subsequent combustion of a near-stoichiometric (fuel-air equivalence ratio, 1.007) benzene-oxygen-argon mixture (with 85.728 percent argon in the mixture). The initial temperature and pressure were 1405 K and 2.3868 atm, respectively. This constant-density, adiabatic problem consisted of 120 reversible reactions among 39 reacting species (C_6H_6, O_2, C_6H_5O, OH, C_6H_5, $C_{12}H_{10}$, H, H_2, O, H_2O, C_4H_3, C_4H_2, C_5H_5, CO, HO_2, C_2H_2, C_6H_5OH, C_5H_6, C_5H_5O, H_2O_2, C_4H_5, C_5H_4OH, C_4H_4, HCO, C_2H_3, C_2HO, C_2H, C_3H_2, C_2H_4, CH_3, CH_2O, CH_2, C_2H_2O, CH, CO_2, C_3H_3, C_3H_4, CH_4, and CH_3O) and the inert species Ar. The reaction mechanism, forward rate coefficient parameters, and initial conditions were taken from Bittker (ref. 110) (see also example problem 3 in chapter 13 of part II). The reverse rate coefficients were computed from the forward rate coefficients and concentration equilibrium constants (see eq. (2.6)).

Because of the size of this problem attention was restricted to the species C_6H_6, O_2, OH, H, H_2, O, H_2O, CO, C_2H_2, and CO_2 and to the temperature and pressure. This species list includes several species from each species type: reactant, active intermediate, and product. The reactions that were found to be important, as defined later, for the 12 variables are given in table 4.79, together with the forward rate coefficient parameters. The variations of these variables with reaction time are shown in figure 4.11.

For reaction times $t \geq 3.2\times10^{-4}$ s several species displayed negative concentrations. (The same behavior was noticed in the SENKIN results.) It was also observed that the kinetics solution at long reaction time (10 s) did not agree with the equilibrium results. For example, the reaction mechanism given in reference 110 produced a temperature of 2899 K at t = 10 s, whereas the equilibrium temperature was 3090 K. At this time for several Y_i and A_j both LSENS and SENKIN produced $\{\langle \partial Y_i / \partial A_j \rangle\}$ with magnitude very much greater than unity, instead of vanishingly small. The same was true of the $\{n_j\}$ and $\{E_j\}$ sensitivities computed with LSENS. Finally, at $t \geq 3.2\times10^{-4}$ s the BFM results did not converge for several species with respect to any parameter examined. These observations indicate that some important reactions are missing from the mechanism, as acknowledged by Bittker (ref. 110). Indeed the maximum temperature at which the mechanism was validated by comparisons with experimental data was 1600 K. Therefore attention was restricted to the interval $[0,3\times10^{-4}]$ s, in which the temperature rise was only about 500 K (fig. 4.11).

The kinetics solution and sensitivity coefficients were computed at the output stations t = 10^{-6}, 10^{-5}, 6×10^{-5}, 2.8×10^{-4}, and 3×10^{-4} s. LSENS gave the temperatures 1405, 1407, 1417, 1652, and 1910 K, respectively, at these reaction

TABLE 4.79.—IMPORTANT REACTIONS FOR VARIABLES CONSIDERED IN TEST PROBLEM 9 AND FORWARD RATE COEFFICIENT PARAMETERS

Reaction number, j	Reaction	Forward rate coefficient parameters[a]		
		A_j	n_j	E_j
1	$C_6H_6 + O_2 \rightleftharpoons C_6H_5O + OH$	4.00(13)	0.0	34 000
4	$C_6H_6 + H \rightleftharpoons C_6H_5 + H_2$	2.50(14)	0.0	16 000
5	$C_6H_6 + O \rightleftharpoons C_6H_5O + H$	2.78(13)	0.0	4910
6	$C_6H_6 + OH \rightleftharpoons C_6H_5 + H_2O$	2.13(13)	0.0	4 580
8	$C_6H_5O \rightleftharpoons C_5H_5 + CO$	2.51(11)	0.0	43 900
9	$C_6H_5 + O_2 \rightleftharpoons C_6H_5O + O$	2.10(12)	0.0	7 470
11	$C_6H_5 \rightleftharpoons C_4H_3 + C_2H_2$	4.50(13)	0.0	72 530
12	$C_6H_5OH \rightleftharpoons C_6H_5O + H$	2.00(16)	0.0	88 000
13	$C_6H_5OH + H \rightleftharpoons C_6H_6 + OH$	2.20(13)	0.0	7 910
16	$C_5H_6 \rightleftharpoons C_5H_5 + H$	8.13(24)	−2.981	78 682
17	$C_5H_6 + O_2 \rightleftharpoons C_5H_5O + OH$	1.00(13)	0.0	20 712
18	$C_6H_5OH + OH \rightleftharpoons C_6H_5O + H_2O$	3.00(13)	0.0	0
21	$C_5H_5 + O \rightleftharpoons C_5H_5O$	1.00(13)	0.0	0
22	$C_5H_5 + OH \rightleftharpoons C_5H_4OH + H$	1.00(13)	0.0	0
24	$C_5H_5 + HO_2 \rightleftharpoons C_5H_5O + OH$	2.00(13)	0.0	0
49	$C_2H_2 + O \rightleftharpoons CH_2 + CO$	1.60(14)	0.0	9 890
50	$C_2H_2 + O \rightleftharpoons C_2HO + H$	4.00(14)	0.0	10 660
92	$HCO + HO_2 \rightleftharpoons CH_2O + O_2$	1.00(14)	0.0	3 000
101	$CO + OH \rightleftharpoons CO_2 + H$	4.17(11)	0.0	1 000
104	$H + O_2 \rightleftharpoons OH + O$	1.89(14)	0.0	16 400
[b]116	$H + O_2 + M \rightleftharpoons HO_2 + M$	1.46(15)	0.0	−1 000

[a]Rate coefficient $k_j = A_j T^{n}j \exp(-E_j/RT)$; units are moles, centimeters, seconds, and calories; numbers in parentheses are powers of 10.

[b]Third-body collisional efficiencies for reaction 116:
$C_6H_6 = 20.0$, $O_2 = 1.3$, $H_2 = 3.0$, $H_2O = 21.3$, $CO_2 = 7.0$, $CH_4 = 5.0$.

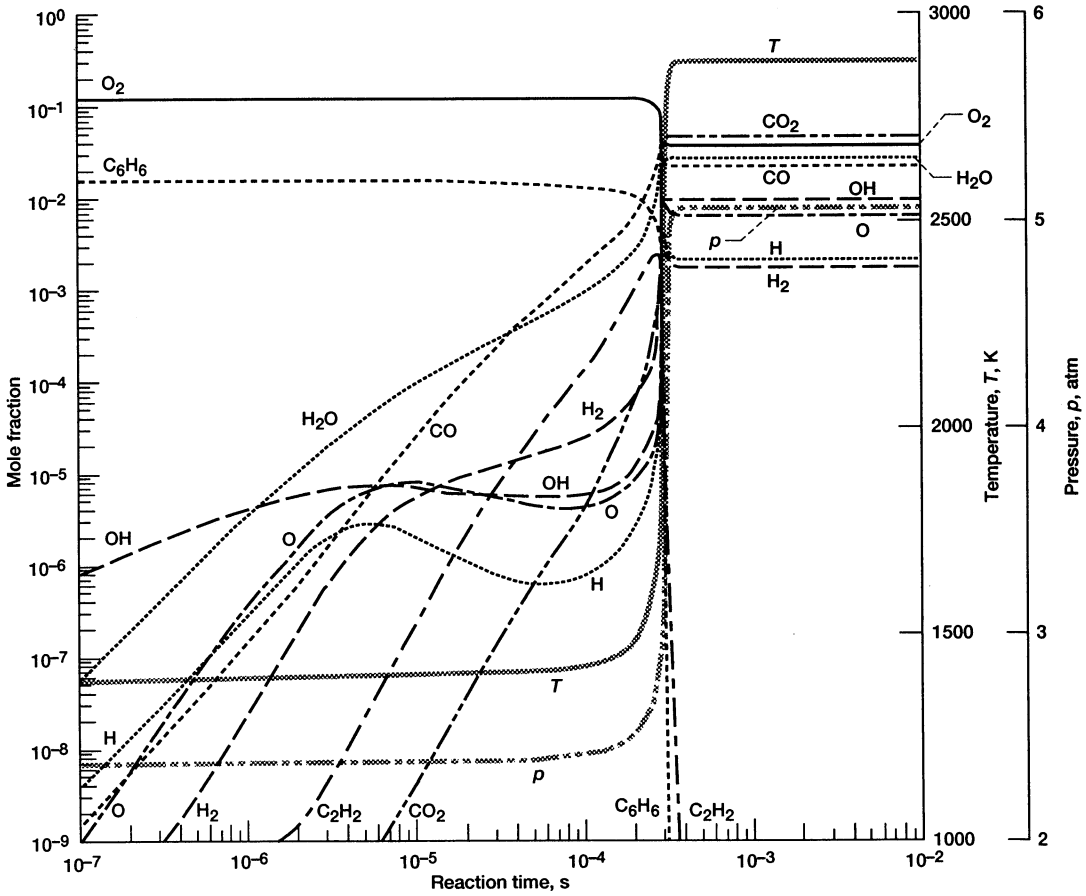

Figure 4.11.—Variation of species mole fractions, temperature, and pressure with reaction time for test problem 9.

times. The temperatures obtained with SENKIN were 1405, 1407, 1417, 1651, and 1904 K. Thus the five output stations encompassed reaction conditions from preignition to early heat release. Again the calculations with both codes used the same thermodynamic data and local error tolerances: EMAX = 10^{-6} and ATOLSP = 10^{-15}. The discrepancy in the temperatures produced by the two codes at 3×10^{-4} s may be attributed to the reaction mechanism not containing reactions that become important at this temperature. Both LSENS and SENKIN required an EMAX value of 10^{-5} (ATOLSP = 10^{-9}EMAX) for the temperature-time profile to stabilize to within 0.1 K (see table 13.7 in chapter 13 of part II). To ensure accuracy of the sensitivity coefficients, a smaller EMAX was used. (The effects of EMAX and ATOLSP on the accuracy of both the kinetics solution and sensitivity coefficients are examined in detail in chapter 13 of part II.) The kinetics-only calculation with SENKIN required 357 steps, 707 derivative evaluations, 39 Jacobian matrix evaluations, and 12 s of CPU time on the VAX 9410 computer. Now, as described in chapter 9 of part II, LSENS solves the ODE's only for variables that both are required for a given problem and vary during the course of the integration. Therefore, for a kinetics-only run, the mole number of the inert species Ar and the density (which are both constant) are not treated as dependent variables. However, when sensitivity analysis with respect to the initial value of either variable is required, that variable must be regarded as a dependent variable and its ODE included in the ODE set. In order to ensure that the computational cost of solving for the dependent variables was not a function of the problem type, the code was modified so that σ_{Ar} and ρ were always included in the dependent variable list. All solutions and execution times given for test problem 9 were obtained with this modified version of the code. (However, the BFM results were generated with the unmodified version of the code, which solved only 40 ODE's—for the 39 reacting species and temperature.) LSENS required 376 steps, 547 derivative evaluations, 43 Jacobian matrix evaluations, and 3.9 s of CPU time on the VAX 9410 computer for the kinetics-only calculation. Again LSENS required fewer corrector iterations per integration step and was significantly faster than SENKIN. The cost of the MF = 22 run was, however, comparable to that of SENKIN: 399 steps, 2830 derivative evaluations, 54 Jacobian matrix evaluations, and 11 s of CPU time. This result reinforces the desirability of using an analytical Jacobian matrix: note that MF = 21 was a factor of 2.8 faster than MF = 22.

Normalized sensitivity coefficients of the 12 variables considered in this work with respect to their initial values and $\sigma_{Ar,0}$ at the above five output stations are given in tables 4.80 to 4.84. The BFM results were generated using EMAX $\leq 10^{-12}$ (ATOLSP = 10^{-9}EMAX) and double-precision arithmetic on the same three Cray computers as for the previous problem. Again EMAX had to be reduced to small values (10^{-15}) for several species, especially the active intermediates such as OH, before satisfactory results could be produced. In order to obtain sensitivities with respect to the initial pressure with LSENS, the initial density was specified as a parameter. As discussed in section 4.5.2, $\langle \partial Y_i/\partial p_0 \rangle$ is identically equal to $\langle \partial Y_i/\partial \rho_0 \rangle$. (That this assertion is indeed correct was verified by generating BFM sensitivity coefficients with respect to both initial density and initial pressure for this problem

TABLE 4.80.—NORMALIZED SENSITIVITY COEFFICIENTS WITH RESPECT TO INITIAL CONDITION VALUES FOR TEST PROBLEM 9 AT $t = 10^{-6}$ s

Sensitivity parameter	Normalized sensitivity coefficients at $t = 10^{-6}$ s of[a]											
	$\sigma_{C_6H_6}$	σ_{O_2}	σ_{OH}	σ_{H}	σ_{H_2}	σ_{O}	σ_{H_2O}	σ_{CO}	$\sigma_{C_2H_2}$	σ_{CO_2}	T	p
$\sigma_{C_6H_6,0}$	1.00	−8.18(−5)	4.47(−1)	1.93	2.94	1.38	1.61	1.04	1.70	1.56	7.97(−6)	1.69(−2)
	1.00	−8.18(−5)	4.47(−1)	1.93	2.94	1.38	1.61	1.04	1.70	1.56	7.97(−6)	1.69(−2)
$\sigma_{O_2,0}$	−8.35(−4)	1.00	1.02	1.02	9.75(−1)	1.92	1.01	1.04	9.31(−1)	2.05	3.68(−6)	1.26(−1)
	−8.35(−4)	1.00	1.02	1.02	9.75(−1)	1.92	1.01	1.04	9.31(−1)	2.05	3.68(−6)	1.26(−1)
$\sigma_{O,0}$	−7.79(−3)	−4.20(−4)	5.34	1.18(2)	2.81(2)	9.74(1)	4.33	1.21(1)	8.35	1.93(1)	2.55(−4)	3.46(−4)
	−7.79(−3)	−4.20(−4)	5.34	1.18(2)	2.81(2)	9.74(1)	4.33	1.21(1)	8.35	1.93(1)	2.55(−4)	3.46(−4)
$\sigma_{OH,0}$	−5.42(−3)	−1.67(−4)	5.20	2.25(1)	3.28(1)	2.56(1)	1.79(1)	1.74	2.88(1)	1.03(1)	1.48(−4)	2.47(−4)
	−5.42(−3)	−1.67(−4)	5.20	2.25(1)	3.28(1)	2.56(1)	1.79(1)	1.74	2.88(1)	1.03(1)	1.48(−4)	2.47(−4)
$\sigma_{H,0}$	−6.48(−3)	−7.74(−4)	7.69	1.19(2)	5.03(2)	8.59(1)	9.70	4.22	1.83(1)	1.33(1)	1.32(−4)	2.17(−4)
	−6.48(−3)	−7.74(−4)	7.69	1.19(2)	5.03(2)	8.59(1)	9.70	4.22	1.83(1)	1.33(1)	1.32(−4)	2.17(−4)
$\sigma_{H_2,0}$	2.06(−7)	−9.60(−8)	−2.35(−3)	5.82(−2)	3.07(3)	1.37(−2)	5.69(−3)	5.77(−5)	−1.07(−3)	−2.03(−3)	7.67(−8)	1.00(−4)
	2.06(−7)	−9.60(−8)	−2.35(−3)	5.82(−2)	3.07(3)	1.37(−2)	5.69(−3)	5.77(−5)	−1.07(−3)	−2.03(−3)	7.67(−8)	1.00(−4)

$\sigma_{C_2H_2,0}$	7.12(−9)	−6.03(−8)	−1.27(−4)	1.02(−2)	9.09(−3)	8.55(−5)	5.15(−4)	3.21(−2)	3.00(5)	3.82(2)	8.52(−8)	1.00(−4)
	7.12(−9)	−6.03(−8)	−1.27(−4)	1.02(−2)	9.09(−3)	8.55(−5)	5.15(−4)	3.21(−2)	3.00(5)	3.82(2)	8.52(−8)	1.00(−4)
$\sigma_{CO,0}$	9.91(−9)	−5.26(−9)	−1.38(−4)	3.07(−3)	3.81(−3)	8.12(−4)	−1.10(−4)	5.76(2)	−5.66(−5)	1.28(3)	6.17(−9)	1.00(−4)
	9.91(−9)	−5.26(−9)	−1.38(−4)	3.07(−3)	3.81(−3)	8.12(−4)	−1.10(−4)	5.76(2)	−5.66(−5)	1.28(3)	6.17(−9)	1.00(−4)
$\sigma_{CO_2,0}$	8.43(−11)	−4.35(−11)	−3.19(−8)	−2.48(−5)	−2.00(−5)	−5.03(−6)	2.58(−8)	1.82(−5)	2.27(−7)	7.15(7)	−8.12(−10)	1.00(−4)
	8.43(−11)	−4.35(−11)	−3.19(−8)	−2.48(−5)	−2.00(−5)	−5.03(−6)	2.58(−8)	1.82(−5)	2.27(−7)	7.15(7)	−8.12(−10)	1.00(−4)
$\sigma_{H_2O,0}$	1.38(−9)	−7.65(−11)	1.65(−5)	−1.23(−4)	7.17(−4)	−6.75(−5)	2.38(1)	−8.47(−7)	−2.88(−6)	1.02(−5)	−6.69(−10)	1.00(−4)
	1.38(−9)	−7.65(−11)	1.65(−5)	−1.23(−4)	7.17(−4)	−6.75(−5)	2.38(1)	−8.47(−7)	−2.88(−6)	1.02(−5)	−6.69(−10)	1.00(−4)
$\sigma_{Ar,0}$	1.31(−7)	−6.15(−8)	−4.67(−4)	−2.27(−2)	−1.82(−2)	−4.69(−3)	−1.71(−4)	2.94(−6)	4.41(−4)	5.08(−3)	−1.80(−6)	8.57(−1)
	1.31(−7)	−6.15(−8)	−4.67(−4)	−2.27(−2)	−1.82(−2)	−4.69(−3)	−1.71(−4)	2.94(−6)	4.41(−4)	5.08(−3)	−1.80(−6)	8.57(−1)
T_0	−1.04(−2)	−9.70(−4)	1.13(1)	1.39(1)	2.01(1)	1.62(1)	1.32(1)	2.79(1)	3.91(1)	3.98(1)	1.00	1.00
	−1.04(−2)	−9.70(−4)	1.13(1)	1.39(1)	2.01(1)	1.62(1)	1.32(1)	2.79(1)	3.91(1)	3.98(1)	1.00	1.00
p_0	−1.03(−3)	−8.71(−5)	4.69(−1)	1.93	2.89	2.30	1.62	1.08	1.63	2.61	9.85(−6)	1.00
	−1.03(−3)	−8.71(−5)	4.69(−1)	1.93	2.89	2.30	1.62	1.08	1.63	2.61	9.85(−6)	1.00

[a]For each sensitivity parameter the top row gives the BFM results and the bottom row gives the LSENS results; numbers in parentheses are powers of 10.

TABLE 4.81.—NORMALIZED SENSITIVITY COEFFICIENTS WITH RESPECT TO INITIAL CONDITION VALUES FOR TEST PROBLEM 9 AT $t = 10^{-5}$ s

Sensitivity parameter	Normalized sensitivity coefficients at $t = 10^{-5}$ s of[a]											
	$\sigma_{C_6H_6}$	σ_{O_2}	σ_{OH}	σ_{H}	σ_{H_2}	σ_{O}	σ_{H_2O}	σ_{CO}	$\sigma_{C_2H_2}$	σ_{CO_2}	T	p
$\sigma_{C_6H_6,0}$	1.00	−1.46(−3)	−2.82(−1)	−7.23(−2)	1.51	−4.41(−1)	9.65(−1)	1.00	1.18	8.72(−1)	1.23(−3)	1.81(−2)
	1.00	−1.46(−3)	−2.82(−1)	−7.23(−2)	1.51	−4.41(−1)	9.65(−1)	1.00	1.18	8.72(−1)	1.23(−3)	1.81(−2)
$\sigma_{O_2,0}$	−2.16(−2)	1.00	9.91(−1)	−3.85(−2)	3.99(−1)	1.17	1.11	1.31	2.29	2.52	1.58(−3)	1.27(−1)
	−2.16(−2)	1.00	9.91(−1)	−3.85(−2)	3.99(−1)	1.17	1.11	1.31	2.29	2.52	1.58(−3)	1.27(−1)
$\sigma_{O,0}$	−3.44(−2)	−2.43(−3)	−2.82(−1)	−1.20	4.69	−9.74(−2)	1.34	2.89	5.55	4.44	3.88(−3)	3.83(−3)
	−3.44(−2)	−2.43(−3)	−2.82(−1)	−1.20	4.69	−9.74(−2)	1.34	2.89	5.55	4.44	3.88(−3)	3.83(−3)
$\sigma_{OH,0}$	−2.29(−2)	−1.65(−3)	−1.57(−1)	−6.65(−1)	1.95	5.44(−2)	1.44	1.65	3.04	2.46	2.61(−3)	2.61(−3)
	−2.29(−2)	−1.65(−3)	−1.57(−1)	−6.65(−1)	1.95	5.44(−2)	1.44	1.65	3.04	2.46	2.61(−3)	2.61(−3)
$\sigma_{H,0}$	−3.96(−2)	−3.38(−3)	−2.37(−1)	−1.13	6.60	9.31(−2)	1.87	2.88	6.26	4.48	4.55(−3)	4.45(−3)
	−3.96(−2)	−3.38(−3)	−2.37(−1)	−1.13	6.60	9.30(−2)	1.87	2.88	6.26	4.48	4.55(−3)	4.45(−3)
$\sigma_{H_2,0}$	−1.23(−5)	−4.45(−6)	1.52(−4)	1.04(−2)	1.57(1)	−1.03(−3)	7.95(−3)	−1.56(−3)	4.75(−3)	1.22(−4)	1.20(−5)	1.11(−4)
	−1.23(−5)	−4.45(−6)	1.52(−4)	1.04(−2)	1.57(1)	−1.03(−3)	7.95(−3)	−1.56(−3)	4.75(−3)	1.22(−4)	1.20(−5)	1.11(−4)

$\sigma_{C_2H_2,0}$	−7.97(−5)	−2.56(−5)	1.89(−2)	2.58(−2)	1.97(−2)	2.04(−3)	1.28(−2)	8.99(−2)	2.98(2)	9.42(1)	5.24(−5)	1.53(−4)
	−7.97(−5)	−2.56(−5)	1.89(−2)	2.58(−2)	1.97(−2)	2.04(−3)	1.28(−2)	8.99(−2)	2.98(2)	9.42(1)	5.24(−5)	1.53(−4)
$\sigma_{CO,0}$	8.83(−7)	−8.13(−8)	−3.09(−4)	2.53(−4)	5.82(−4)	−1.41(−4)	−1.99(−4)	3.36	1.32(−4)	8.66	3.33(−7)	1.00(−4)
	8.83(−7)	−8.13(−8)	−3.09(−4)	2.53(−4)	5.82(−4)	−1.41(−4)	−1.99(−4)	3.36	1.32(−4)	8.66	3.33(−7)	1.00(−4)
$\sigma_{CO_2,0}$	1.46(−7)	1.75(−9)	9.24(−7)	−2.60(−5)	−3.71(−5)	−1.17(−5)	−4.31(−6)	2.04(−5)	1.07(−4)	1.80(4)	−3.53(−7)	9.97(−5)
	1.46(−7)	1.75(−9)	9.24(−7)	−2.60(−5)	−3.71(−5)	−1.17(−5)	−4.31(−6)	2.04(−5)	1.07(−4)	1.80(4)	−3.53(−7)	9.97(−5)
$\sigma_{H_2O,0}$	−7.54(−7)	−6.93(−8)	3.98(−4)	−4.16(−5)	6.46(−4)	3.58(−5)	9.43(−1)	2.66(−5)	3.27(−4)	3.15(−4)	−3.41(−7)	9.97(−5)
	−7.54(−7)	−6.93(−8)	3.98(−4)	−4.16(−5)	6.46(−4)	3.58(−5)	9.43(−1)	2.66(−5)	3.27(−4)	3.15(−4)	−3.41(−7)	9.97(−5)
$\sigma_{Ar,0}$	2.11(−4)	2.83(−6)	−4.50(−3)	−2.73(−2)	−3.70(−2)	−1.71(−2)	−9.57(−3)	−5.04(−3)	1.59(−1)	7.16(−2)	−7.36(−4)	8.57(−1)
	2.11(−4)	2.83(−6)	−4.50(−3)	−2.73(−2)	−3.70(−2)	−1.71(−2)	−9.57(−3)	−5.04(−3)	1.59(−1)	7.16(−2)	−7.36(−4)	8.57(−1)
T_0	−2.23(−1)	−1.88(−2)	8.88	1.28	9.94	8.48	1.17(1)	2.65(1)	3.47(1)	3.80(1)	1.01	1.01
	−2.23(−1)	−1.88(−2)	8.88	1.28	9.94	8.48	1.17(1)	2.65(1)	3.47(1)	3.80(1)	1.01	1.01
p_0	−2.15(−2)	−1.84(−3)	−2.95(−1)	−1.14	8.71(−1)	−2.86(−1)	1.07	1.31	2.63	2.46	2.07(−3)	1.00
	−2.15(−2)	−1.84(−3)	−2.95(−1)	−1.14	8.71(−1)	−2.86(−1)	1.07	1.31	2.63	2.46	2.07(−3)	1.00

[a]For each sensitivity parameter the top row gives the BFM results and the bottom row gives the LSENS results; numbers in parentheses are powers of 10.

TABLE 4.82.—NORMALIZED SENSITIVITY COEFFICIENTS WITH RESPECT TO INITIAL CONDITION VALUES FOR TEST PROBLEM 9 AT $t = 6\times10^{-5}$ s

Sensitivity parameter	Normalized sensitivity coefficients at $t = 6\times10^{-5}$ s of[a]											
	$\sigma_{C_6H_6}$	σ_{O_2}	σ_{OH}	σ_{H}	σ_{H_2}	σ_{O}	σ_{H_2O}	σ_{CO}	$\sigma_{C_2H_2}$	σ_{CO_2}	T	p
$\sigma_{C_6H_6,0}$	1.01 1.01	−8.40(−3) −8.40(−3)	−3.23(−2) −3.23(−2)	1.24(−1) 1.24(−1)	1.21 1.21	−1.91(−1) −1.91(−1)	9.14(−1) 9.14(−1)	8.58(−1) 8.58(−1)	7.64(−1) 7.64(−1)	7.01(−1) 7.01(−1)	5.83(−3) 5.83(−3)	2.29(−2) 2.29(−2)
$\sigma_{O_2,0}$	−1.08(−1) −1.08(−1)	9.99(−1) 9.99(−1)	9.47(−1) 9.47(−1)	2.23(−1) 2.23(−1)	7.58(−2) 7.58(−2)	9.45(−1) 9.45(−1)	1.03 1.03	1.21 1.21	1.89 1.89	2.39 2.39	7.48(−3) 7.48(−3)	1.34(−1) 1.34(−1)
$\sigma_{O,0}$	−2.92(−2) −2.92(−2)	−2.23(−3) −2.23(−3)	−6.90(−3) −6.90(−3)	1.28(−2) 1.28(−2)	1.19 1.19	−3.93(−2) −3.93(−2)	2.25(−1) 2.25(−1)	4.11(−1) 4.11(−1)	6.83(−1) 6.83(−1)	7.70(−1) 7.70(−1)	3.19(−3) 3.19(−3)	3.42(−3) 3.42(−3)
$\sigma_{OH,0}$	−1.93(−2) −1.93(−2)	−1.49(−3) −1.49(−3)	−7.30(−3) −7.30(−3)	2.17(−3) 2.17(−3)	4.25(−1) 4.25(−1)	−2.78(−2) −2.78(−2)	2.39(−1) 2.39(−1)	2.53(−1) 2.53(−1)	3.78(−1) 3.78(−1)	4.34(−1) 4.34(−1)	2.09(−3) 2.09(−3)	2.27(−3) 2.27(−3)
$\sigma_{H,0}$	−3.48(−2) −3.48(−2)	−3.24(−3) −3.24(−3)	−1.41(−2) −1.41(−2)	6.82(−3) 6.82(−3)	1.77 1.77	−5.10(−2) −5.10(−2)	3.31(−1) 3.31(−1)	4.63(−1) 4.63(−1)	7.81(−1) 7.81(−1)	8.71(−1) 8.71(−1)	3.93(−3) 3.93(−3)	4.16(−3) 4.16(−3)
$\sigma_{H_2,0}$	1.36(−4) 1.36(−4)	−7.57(−6) −7.57(−6)	−1.57(−3) −1.57(−3)	9.02(−3) 9.02(−3)	4.94 4.94	−4.00(−3) −4.00(−3)	6.61(−3) 6.61(−3)	−3.53(−3) −3.53(−3)	−3.69(−4) −3.69(−4)	−4.51(−3) −4.51(−3)	6.12(−5) 6.12(−5)	1.55(−4) 1.55(−4)

$\sigma_{C_2H_2,0}$	−6.09(−4)	−1.72(−4)	1.14(−2)	2.10(−2)	2.28(−2)	−1.86(−3)	1.57(−2)	2.23(−2)	2.17	2.86	3.74(−4)	4.74(−4)
	−6.09(−4)	−1.72(−4)	1.14(−2)	2.10(−2)	2.28(−2)	−1.86(−3)	1.57(−2)	2.23(−2)	2.17	2.86	3.74(−4)	4.74(−4)
$\sigma_{CO,0}$	1.74(−5)	7.17(−7)	−2.85(−4)	2.61(−4)	3.78(−4)	−2.23(−4)	−2.75(−4)	1.21(−1)	−1.98(−4)	2.30(−1)	4.56(−7)	1.00(−4)
	1.74(−5)	7.17(−7)	−2.85(−4)	2.61(−4)	3.78(−4)	−2.23(−4)	−2.75(−4)	1.21(−1)	−1.98(−4)	2.30(−1)	4.56(−7)	1.00(−4)
$\sigma_{CO_2,0}$	7.78(−7)	3.75(−8)	−1.44(−5)	−2.91(−5)	−2.27(−5)	−1.58(−5)	−1.96(−6)	−5.81(−6)	5.13(−5)	8.75(1)	−2.29(−6)	9.77(−5)
	7.78(−7)	3.75(−8)	−1.44(−5)	−2.91(−5)	−2.27(−5)	−1.58(−5)	−1.96(−6)	−5.81(−6)	5.13(−5)	8.75(1)	−2.29(−6)	9.77(−5)
$\sigma_{H_2O,0}$	−1.34(−5)	−1.16(−6)	3.03(−4)	3.41(−5)	7.93(−4)	6.97(−5)	1.65(−1)	1.32(−4)	3.31(−4)	4.82(−4)	−6.52(−7)	9.94(−5)
	−1.34(−5)	−1.16(−6)	3.03(−4)	3.41(−5)	7.93(−4)	6.97(−5)	1.65(−1)	1.32(−4)	3.31(−4)	4.82(−4)	−6.52(−7)	9.94(−5)
$\sigma_{Ar,0}$	2.47(−3)	2.16(−4)	−4.87(−2)	−7.20(−2)	−3.68(−2)	−4.89(−2)	−1.84(−2)	−4.00(−2)	2.62(−2)	2.45(−2)	−5.07(−3)	8.52(−1)
	2.47(−3)	2.16(−4)	−4.87(−2)	−7.20(−2)	−3.68(−2)	−4.89(−2)	−1.84(−2)	−4.00(−2)	2.62(−2)	2.45(−2)	−5.07(−3)	8.52(−1)
T_0	−1.27	−1.18(−1)	1.08(1)	1.51(1)	1.14(1)	1.03(1)	1.19(1)	2.00(1)	2.76(1)	3.46(1)	1.08	1.09
	−1.27	−1.18(−1)	1.08(1)	1.51(1)	1.14(1)	1.03(1)	1.19(1)	2.00(1)	2.76(1)	3.46(1)	1.08	1.09
p_0	−9.69(−2)	−8.83(−3)	−1.34(−1)	−7.25(−1)	2.44(−1)	−2.95(−1)	9.24(−1)	1.03	1.68	2.12	8.24(−3)	1.01
	−9.69(−2)	−8.83(−3)	−1.34(−1)	−7.25(−1)	2.44(−1)	−2.95(−1)	9.24(−1)	1.03	1.68	2.12	8.24(−3)	1.01

[a]For each sensitivity parameter the top row gives the BFM results and the bottom row gives the LSENS results; numbers in parentheses are powers of 10.

TABLE 4.83.—NORMALIZED SENSITIVITY COEFFICIENTS WITH RESPECT TO INITIAL CONDITION VALUES FOR TEST PROBLEM 9 AT $t = 2.8\times10^{-4}$ s

Sensitivity parameter	Normalized sensitivity coefficients at $t = 2.8\times10^{-4}$ s of[a]											
	$\sigma_{C_6H_6}$	σ_{O_2}	σ_{OH}	σ_{H}	σ_{H_2}	σ_{O}	σ_{H_2O}	σ_{CO}	$\sigma_{C_2H_2}$	σ_{CO_2}	T	p
$\sigma_{C_6H_6,0}$	1.36(−1)	−2.80(−1)	3.36	4.65	3.23	3.37	1.99	1.90	1.19	3.03	2.58(−1)	2.98(−1)
	1.36(−1)	−2.80(−1)	3.36	4.65	3.23	3.37	1.99	1.90	1.19	3.03	2.58(−1)	2.98(−1)
$\sigma_{O_2,0}$	−3.81	5.17(−1)	1.14(1)	1.23(1)	5.70	1.18(1)	4.77	4.35	1.10	9.14	6.83(−1)	8.61(−1)
	−3.81	5.17(−1)	1.14(1)	1.23(1)	5.70	1.18(1)	4.77	4.35	1.10	9.14	6.83(−1)	8.61(−1)
$\sigma_{O,0}$	−3.12(−1)	−5.12(−2)	8.99(−1)	1.07	5.76(−1)	9.33(−1)	3.87(−1)	3.56(−1)	9.74(−2)	7.60(−1)	5.85(−2)	6.30(−2)
	−3.12(−1)	−5.12(−2)	8.99(−1)	1.07	5.76(−1)	9.33(−1)	3.87(−1)	3.56(−1)	9.74(−2)	7.60(−1)	5.85(−2)	6.30(−2)
$\sigma_{OH,0}$	−1.98(−1)	−3.24(−2)	5.69(−1)	6.73(−1)	3.55(−1)	5.90(−1)	2.51(−1)	2.25(−1)	6.14(−2)	4.80(−1)	3.70(−2)	3.98(−2)
	−1.98(−1)	−3.24(−2)	5.69(−1)	6.73(−1)	3.55(−1)	5.90(−1)	2.51(−1)	2.25(−1)	6.14(−2)	4.80(−1)	3.70(−2)	3.98(−2)
$\sigma_{H,0}$	−3.59(−1)	−5.95(−2)	1.04	1.23	6.73(−1)	1.07	4.50(−1)	4.09(−1)	1.12(−1)	8.73(−1)	6.74(−2)	7.25(−2)
	−3.59(−1)	−5.95(−2)	1.04	1.23	6.73(−1)	1.07	4.50(−1)	4.09(−1)	1.12(−1)	8.73(−1)	6.74(−2)	7.25(−2)
$\sigma_{H_2,0}$	−2.85(−3)	−6.38(−4)	1.19(−2)	1.74(−2)	1.38(−1)	1.29(−2)	8.55(−3)	2.54(−3)	−6.73(−5)	7.14(−3)	8.76(−4)	9.77(−4)
	−2.85(−3)	−6.38(−4)	1.19(−2)	1.74(−2)	1.38(−1)	1.29(−2)	8.55(−3)	2.54(−3)	−6.74(−5)	7.14(−3)	8.76(−4)	9.78(−4)

$\sigma_{C_2H_2,0}$	−3.97(−2)	−7.16(−3)	1.30(−1)	1.54(−1)	7.82(−2)	1.32(−1)	5.34(−2)	4.81(−2)	2.26(−2)	1.26(−1)	8.47(−3)	9.12(−3)
	−3.97(−2)	−7.16(−3)	1.30(−1)	1.54(−1)	7.82(−2)	1.32(−1)	5.34(−2)	4.81(−2)	2.26(−2)	1.26(−1)	8.47(−3)	9.12(−3)
$\sigma_{CO,0}$	3.33(−4)	4.30(−5)	−1.06(−3)	−8.87(−4)	−2.36(−4)	−8.81(−4)	−4.37(−4)	4.76(−3)	−1.13(−4)	3.02(−3)	−5.70(−5)	3.56(−5)
	3.33(−4)	4.30(−5)	−1.06(−3)	−8.87(−4)	−2.36(−4)	−8.81(−4)	−4.37(−4)	4.76(−3)	−1.13(−4)	3.02(−3)	−5.70(−5)	3.56(−5)
$\sigma_{CO_2,0}$	5.98(−4)	9.48(−5)	−2.19(−3)	−2.61(−3)	−1.16(−3)	−2.38(−3)	−7.10(−4)	−6.46(−4)	−7.19(−5)	1.49(−1)	−1.46(−4)	−5.53(−5)
	5.98(−4)	9.48(−5)	−2.19(−3)	−2.61(−3)	−1.16(−3)	−2.38(−3)	−7.10(−4)	−6.46(−4)	−7.19(−5)	1.49(−1)	−1.46(−4)	−5.53(−5)
$\sigma_{H_2O,0}$	3.21(−4)	5.28(−5)	−1.15(−3)	−1.85(−3)	1.16(−4)	−1.87(−3)	1.07(−2)	−3.37(−4)	7.12(−5)	−8.59(−4)	−9.54(−5)	−2.01(−7)
	3.21(−4)	5.28(−5)	−1.15(−3)	−1.85(−3)	1.16(−4)	−1.87(−3)	1.07(−2)	−3.37(−4)	7.12(−5)	−8.59(−4)	−9.54(−5)	−2.07(−7)
$\sigma_{Ar,0}$	1.42	2.27(−1)	−5.14	−6.04	−2.72	−5.53	−1.70	−1.56	−1.37(−1)	−3.45	−3.40(−1)	4.88(−1)
	1.42	2.27(−1)	−5.14	−6.04	−2.72	−5.53	−1.70	−1.56	−1.37(−1)	−3.45	−3.40(−1)	4.88(−1)
T_0	−5.61(1)	−9.15	1.69(2)	2.00(2)	1.01(2)	1.77(2)	6.88(1)	6.31(1)	1.53(1)	1.37(2)	1.10(1)	1.18(1)
	−5.61(1)	−9.15	1.69(2)	2.00(2)	1.01(2)	1.77(2)	6.88(1)	6.31(1)	1.53(1)	1.37(2)	1.10(1)	1.18(1)
p_0	−3.26	−5.36(−1)	8.59	9.92	5.20	8.68	4.06	3.68	1.15	7.72	6.01(−1)	1.65
	−3.26	−5.36(−1)	8.59	9.92	5.20	8.68	4.06	3.68	1.15	7.72	6.01(−1)	1.65

[a]For each sensitivity parameter the top row gives the BFM results and the bottom row gives the LSENS results; numbers in parentheses are powers of 10.

TABLE 4.84.—NORMALIZED SENSITIVITY COEFFICIENTS WITH RESPECT TO INITIAL CONDITION VALUES FOR TEST PROBLEM 9 AT $t = 3\times10^{-4}$ s

Sensitivity parameter	Normalized sensitivity coefficients at $t = 3\times10^{-4}$ s of[a]											
	$\sigma_{C_6H_6}$	σ_{O_2}	σ_{OH}	σ_{H}	σ_{H_2}	σ_{O}	σ_{H_2O}	σ_{CO}	$\sigma_{C_2H_2}$	σ_{CO_2}	T	p
$\sigma_{C_6H_6,0}$	−1.26(1)	−2.47	2.83(1)	2.73(1)	7.74	2.89(1)	6.58	6.43	−7.87	1.40(1)	1.69	1.88
	−1.26(1)	−2.48	2.83(1)	2.73(1)	7.74	2.89(1)	6.59	6.43	−7.87	1.40(1)	1.69	1.88
$\sigma_{O_2,0}$	−4.22(1)	−5.35	8.24(1)	7.56(1)	1.66(1)	8.52(1)	1.78(1)	1.71(1)	−2.72(1)	3.99(1)	4.72	5.32
	−4.22(1)	−5.35	8.24(1)	7.57(1)	1.66(1)	8.52(1)	1.78(1)	1.71(1)	−2.72(1)	4.00(1)	4.72	5.32
$\sigma_{O,0}$	−3.33	−5.28(−1)	6.51	6.06	1.40	6.72	1.40	1.35	−2.15	3.17	3.77(−1)	4.14(−1)
	−3.33	−5.28(−1)	6.52	6.06	1.40	6.72	1.40	1.35	−2.15	3.17	3.77(−1)	4.15(−1)
$\sigma_{OH,0}$	−2.11	−3.34(−1)	4.11	3.83	8.82(−1)	4.24	8.87(−1)	8.53(−1)	−1.36	2.00	2.38(−1)	2.62(−1)
	−2.11	−3.34(−1)	4.12	3.83	8.82(−1)	4.24	8.87(−1)	8.54(−1)	−1.36	2.00	2.38(−1)	2.62(−1)
$\sigma_{H,0}$	−3.83	−6.08(−1)	7.49	6.97	1.61	7.73	1.61	1.55	−2.47	3.65	4.33(−1)	4.77(−1)
	−3.83	−6.08(−1)	7.50	6.98	1.61	7.73	1.61	1.56	−2.47	3.65	4.33(−1)	4.77(−1)
$\sigma_{H_2,0}$	−4.72(−2)	−7.85(−3)	9.76(−2)	9.21(−2)	3.85(−2)	9.99(−2)	2.38(−2)	1.87(−2)	−3.14(−2)	4.52(−2)	5.69(−3)	6.28(−3)
	−4.73(−2)	−7.85(−3)	9.76(−2)	9.21(−2)	3.85(−2)	9.99(−2)	2.38(−2)	1.87(−2)	−3.14(−2)	4.52(−2)	5.69(−3)	6.28(−3)

$\sigma_{C_2H_2,0}$	−4.79(−1)	−7.71(−2)	9.51(−1)	8.87(−1)	2.07(−1)	9.79(−1)	2.04(−1)	1.96(−1)	−3.08(−1)	4.67(−1)	5.51(−2)	6.07(−2)
	−4.79(−1)	−7.71(−2)	9.51(−1)	8.87(−1)	2.07(−1)	9.79(−1)	2.04(−1)	1.96(−1)	−3.08(−1)	4.67(−1)	5.52(−2)	6.07(−2)
$\sigma_{CO,0}$	3.46(−3)	5.14(−4)	−6.76(−3)	−5.97(−3)	−1.17(−3)	−6.72(−3)	−1.46(−3)	1.19(−3)	2.14(−3)	−1.37(−3)	−3.81(−4)	−3.26(−4)
	3.46(−3)	5.14(−4)	−6.76(−3)	−5.97(−3)	−1.17(−3)	−6.72(−3)	−1.46(−3)	1.19(−3)	2.14(−3)	−1.37(−3)	−3.81(−4)	−3.26(−4)
$\sigma_{CO_2,0}$	8.72(−3)	1.38(−3)	−1.77(−2)	−1.66(−2)	−3.79(−3)	−1.83(−2)	−3.60(−3)	−3.49(−3)	5.79(−3)	2.66(−2)	−1.04(−3)	−1.04(−3)
	8.73(−3)	1.38(−3)	−1.77(−2)	−1.66(−2)	−3.79(−3)	−1.83(−2)	−3.60(−3)	−3.49(−3)	5.79(−3)	2.66(−2)	−1.04(−3)	−1.04(−3)
$\sigma_{H_2O,0}$	6.12(−3)	9.83(−4)	−1.22(−2)	−1.22(−2)	−1.40(−3)	−1.38(−2)	2.85(−3)	−2.47(−3)	4.41(−3)	−5.83(−3)	−7.52(−4)	−7.23(−4)
	6.12(−3)	9.83(−4)	−1.22(−2)	−1.22(−2)	−1.40(−3)	−1.38(−2)	2.85(−3)	−2.47(−3)	4.42(−3)	−5.84(−3)	−7.52(−4)	−7.23(−4)
$\sigma_{Ar,0}$	2.02(1)	3.18	−4.08(1)	−3.81(1)	−8.71	−4.21(1)	−8.36	−8.11	1.34(1)	−1.91(1)	−2.38	−1.77
	2.02(1)	3.18	−4.08(1)	−3.81(1)	−8.71	−4.22(1)	−8.36	−8.11	1.34(1)	−1.91(1)	−2.38	−1.77
T_0	−6.25(2)	−9.89(1)	1.23(3)	1.14(3)	2.62(2)	1.26(3)	2.62(2)	2.53(2)	−4.03(2)	5.95(2)	7.09(1)	7.80(1)
	−6.25(2)	−9.89(1)	1.23(3)	1.14(3)	2.62(2)	1.26(3)	2.62(2)	2.53(2)	−4.04(2)	5.95(2)	7.09(1)	7.80(1)
p_0	−3.56(1)	−5.64	6.89(1)	6.39(1)	1.46(1)	7.09(1)	1.50(1)	1.44(1)	−2.27(1)	3.38(1)	4.03	5.43
	−3.56(1)	−5.64	6.89(1)	6.39(1)	1.46(1)	7.09(1)	1.50(1)	1.44(1)	−2.27(1)	3.38(1)	4.03	5.43

[a]For each sensitivity parameter the top row gives the BFM results and the bottom row gives the LSENS results; numbers in parentheses are powers of 10.

and the previous one.) Tables 4.80 to 4.84 show that LSENS agreed excellently well with the BFM at all reaction times.

The normalized sensitivity coefficients with respect to the preexponential factors at the same five output stations are given in tables 4.85 to 4.89. The SENKIN calculation used the tolerances RTLS = 10^{-5} and ATLS = 10^{-5}, and the BFM used EMAX = 10^{-12} and ATOLSP = 10^{-21}. For each dependent variable tables 4.85 to 4.89 list, up to a maximum of 10 reactions, the reaction numbers in order of decreasing importance. To minimize computational work required by the BFM, only reactions for which the normalized sensitivity coefficients were 0.1 or greater in magnitude were considered. For certain dependent variables at certain reaction times no reaction number is given because all $\{|\langle S_{ij}\rangle|\}$ were less than 0.1. Again, for succinct presentation of results, only one reaction importance list is given for each dependent variable. All methods gave the same reaction importance lists for all dependent variables at all reaction times, except at $t = 2.8\times10^{-4}$ s, when SENKIN predicted A_6 to be more important than A_{21} for $\sigma_{C_2H_2}$, whereas the BFM (and LSENS) results showed the opposite order (table 4.88). However, the differences in the normalized sensitivity coefficients were minimal, and reactions 21 and 6 were only the eighth and ninth most important. Therefore, this discrepancy is not particularly noteworthy.

Tables 4.85 to 4.89 show that the agreement between the BFM and LSENS was excellent at all reaction times. SENKIN and LSENS produced essentially the same results at all times, except $t = 3\times10^{-4}$ s. The differences at this time did not merit further study because of the reservations previously observed in the reaction mechanism. The kinetics-plus-preexponential-factor sensitivity calculation with SENKIN required 243 steps, 742 derivative evaluations, 244 Jacobian matrix evaluations, and 217 s of CPU time on the VAX 9410 computer, whereas the cost of LSENS was 49 s. The execution time needed by LSENS to solve for the dependent variables and sensitivity coefficients with respect to all 42 initial condition values and all 360 rate coefficient parameters was 137 s. Again LSENS was significantly more efficient than SENKIN. When RTLS and ATLS were set equal to EMAX and ATOLSP, respectively, SENKIN required excessive computational work and an error exit occurred at $t \approx 7.4\times10^{-8}$ s; to advance the solution to this reaction time required 5000 integration steps and over 4000 s of CPU time on the VAX 9410 computer. The run with RTLS = 10^{-2} and ATLS = 10^{-2} produced the same results at all times and cost the same as the RTLS = 10^{-5} and ATLS = 10^{-5} run. This result is additional confirmation of the adequacy of fairly loose error tolerances for the sensitivity coefficients.

Sensitivity coefficients with respect to the temperature exponents and activation energies of the five most important reactions (1, 6, 8, 12, and 22) were also computed. The solutions produced by LSENS and the BFM, which used EMAX = 10^{-12} and ATOLSP = 10^{-21}, are listed in tables 4.90 to 4.94. For all reaction conditions LSENS was very accurate. Note again that at early times $\langle \partial Y_i/\partial A_j\rangle = \langle \partial Y_i/\partial n_j\rangle = \langle \partial Y_i/\partial E_j\rangle$ for all i and all j; however, in the postinduction regimes the three quantities were, in general, different from one another.

TABLE 4.85.—REACTION IMPORTANCE LISTS AND NORMALIZED SENSITIVITY COEFFICIENTS WITH RESPECT TO PREEXPONENTIAL FACTORS FOR TEST PROBLEM 9 AT $t = 10^{-6}$ s

Dependent variable	Method or code	Reaction numbers in order of decreasing importance and normalized sensitivity coefficients at $t = 10^{-6}$ s[a]					
σ_{OH}		1	6				
	BFM	0.998	–0.536				
	LSENS	0.998	–0.536				
	SENKIN	0.998	–0.536				
σ_{H}		1	13	5	9	104	6
	BFM	0.938	0.515	0.338	0.330	–0.209	0.118
	LSENS	0.938	0.515	0.338	0.330	–0.209	0.118
	SENKIN	0.938	0.515	0.338	0.330	–0.209	0.118
σ_{H_2}		1	4	13	5	9	104
	BFM	0.957	0.947	0.639	0.249	0.235	–0.184
	LSENS	0.957	0.947	0.639	0.249	0.235	–0.184
	SENKIN	0.957	0.947	0.639	0.249	0.235	–0.184
σ_{O}		1	9	6	5	104	13
	BFM	0.989	0.748	0.538	–0.285	0.194	0.134
	LSENS	0.989	0.748	0.538	–0.285	0.194	0.134
	SENKIN	0.989	0.748	0.538	–0.285	0.194	0.134
σ_{H_2O}		1	6				
	BFM	0.999	0.630				
	LSENS	0.999	0.630				
	SENKIN	0.999	0.630				
σ_{CO}		1	8				
	BFM	0.999	0.988				
	LSENS	0.999	0.988				
	SENKIN	0.999	0.988				
$\sigma_{C_2H_2}$		1	11	6			
	BFM	1.01	0.990	0.701			
	LSENS	1.01	0.990	0.701			
	SENKIN	1.01	0.990	0.701			
σ_{CO_2}		1	8	101	6		
	BFM	2.00	0.990	0.983	–0.414		
	LSENS	1.99	0.990	0.983	–0.414		
	SENKIN	1.99	0.990	0.983	–0.414		

[a]For each dependent variable the top row lists the reaction numbers. The next three rows give the normalized sensitivity coefficients produced by BFM, LSENS, and SENKIN, respectively. For each dependent variable and method or code the $\{\langle S_{ij} \rangle\}$ are those of that variable with respect to the preexponential factors of the reactions corresponding to the numbers listed in the first row.

TABLE 4.86.—REACTION IMPORTANCE LISTS AND NORMALIZED SENSITIVITY COEFFICIENTS WITH RESPECT TO PREEXPONENTIAL FACTORS FOR TEST PROBLEM 9 AT $t = 10^{-5}$ s

Dependent variable	Method or code	Reaction numbers in order of decreasing importance and normalized sensitivity coefficients at $t = 10^{-5}$ s[a]					
σ_{OH}		6	1	104	12		
	BFM	–0.936	0.712	0.281	–0.262		
	LSENS	–0.936	0.712	0.281	–0.262		
	SENKIN	–0.936	0.712	0.281	–0.262		
σ_{H}		12	8				
	BFM	–0.958	0.126				
	LSENS	–0.958	0.126				
	SENKIN	–0.958	0.126				
σ_{H_2}		4	12	9	1	5	13
	BFM	0.916	–0.724	0.240	0.225	0.173	0.103
	LSENS	0.916	–0.724	0.240	0.225	0.173	0.103
	SENKIN	0.916	–0.724	0.240	0.226	0.173	0.103
σ_{O}		5	1	104	12	9	
	BFM	–0.980	0.528	0.466	–0.426	0.200	
	LSENS	–0.980	0.528	0.466	–0.426	0.200	
	SENKIN	–0.980	0.527	0.467	–0.427	0.200	

σ_{H_2O}		1	104	12	6						
	BFM	0.808	0.250	–0.181	0.138						
	LSENS	0.808	0.250	–0.181	0.138						
	SENKIN	0.808	0.250	–0.181	0.138						
σ_{CO}		8	1	9	104	12	6				
	BFM	0.908	0.838	0.273	0.190	–0.185	0.105				
	LSENS	0.908	0.838	0.273	0.190	–0.185	0.105				
	SENKIN	0.908	0.838	0.273	0.190	–0.185	0.105				
$\sigma_{C_2H_2}$		1	8	12	21	9	104	5	24	116	6
	BFM	1.19	0.827	–0.570	0.457	0.397	0.362	–0.260	0.244	0.208	0.174
	LSENS	1.19	0.827	–0.570	0.457	0.397	0.362	–0.260	0.244	0.208	0.174
	SENKIN	1.19	0.827	–0.570	0.457	0.397	0.363	–0.260	0.244	0.208	0.174
σ_{CO_2}		1	8	101	6	104	12	9			
	BFM	1.60	0.934	0.813	–0.611	0.493	–0.451	0.370			
	LSENS	1.60	0.934	0.813	–0.611	0.493	–0.451	0.370			
	SENKIN	1.60	0.934	0.813	–0.611	0.493	–0.451	0.371			

[a]For each dependent variable the top row lists the reaction numbers. The next three rows give the normalized sensitivity coefficients produced by BFM, LSENS, and SENKIN, respectively. For each dependent variable and method or code the $\{\langle S_{ij}\rangle\}$ are those of that variable with respect to the preexponential factors of the reactions corresponding to the numbers listed in the first row.

TABLE 4.87.—REACTION IMPORTANCE LISTS AND NORMALIZED SENSITIVITY COEFFICIENTS WITH RESPECT TO PREEXPONENTIAL FACTORS FOR TEST PROBLEM 9 AT $t = 6\times10^{-5}$ s

Dependent variable	Method or code	Reaction numbers in order of decreasing importance and normalized sensitivity coefficients at $t = 6\times10^{-5}$ s[a]						
σ_{OH}		1	6	18	12	8		
	BFM	0.763	–0.709	–0.173	–0.152	0.138		
	LSENS	0.763	–0.709	–0.173	–0.152	0.138		
	SENKIN	0.763	–0.709	–0.173	–0.152	0.138		
σ_{H}		12	8	18	22	17	16	1
	BFM	–0.847	0.760	–0.166	0.137	0.116	–0.111	0.106
	LSENS	–0.847	0.760	–0.166	0.137	0.116	–0.111	0.106
	SENKIN	–0.847	0.760	–0.166	0.136	0.116	–0.111	0.106
σ_{H_2}		4	12	8				
	BFM	0.924	–0.820	0.307				
	LSENS	0.924	–0.820	0.307				
	SENKIN	0.923	–0.820	0.307				
σ_{O}		5	1	6	12	104	8	18
	BFM	–0.938	0.612	0.231	–0.225	0.175	0.169	–0.166
	LSENS	–0.938	0.612	0.231	–0.225	0.175	0.169	–0.166
	SENKIN	–0.938	0.612	0.231	–0.226	0.176	0.169	–0.166

σ_{H_2O}		1	12	104							
	BFM	0.828	–0.159	0.145							
	LSENS	0.828	–0.159	0.145							
	SENKIN	0.828	–0.159	0.145							
σ_{CO}		1	8	12	104	9					
	BFM	0.857	0.544	–0.254	0.170	0.104					
	LSENS	0.857	0.544	–0.254	0.170	0.104					
	SENKIN	0.857	0.544	–0.254	0.171	0.104					
$\sigma_{C_2H_2}$		1	8	12	21	5	17	16	104	116	6
	BFM	0.992	0.843	–0.671	0.414	–0.361	0.353	0.292	0.231	0.156	0.140
	LSENS	0.992	0.843	–0.671	0.414	–0.361	0.353	0.292	0.231	0.156	0.140
	SENKIN	0.992	0.843	–0.672	0.414	–0.361	0.352	0.291	0.231	0.157	0.140
σ_{CO_2}		1	8	101	12	5	104	49	6	17	18
	BFM	1.60	0.803	0.605	–0.575	–0.495	0.335	0.327	–0.312	0.157	–0.157
	LSENS	1.60	0.803	0.605	–0.575	–0.495	0.335	0.327	–0.312	0.157	–0.157
	SENKIN	1.60	0.804	0.605	–0.576	–0.495	0.336	0.327	–0.312	0.157	–0.157

[a]For each dependent variable the top row lists the reaction numbers. The next three rows give the normalized sensitivity coefficients produced by BFM, LSENS, and SENKIN, respectively. For each dependent variable and method or code the $\{\langle S_{ij}\rangle\}$ are those of that variable with respect to the preexponential factors of the reactions corresponding to the numbers listed in the first row.

TABLE 4.88.—REACTION IMPORTANCE LISTS AND NORMALIZED SENSITIVITY COEFFICIENTS WITH RESPECT TO PREEXPONENTIAL FACTORS FOR TEST PROBLEM 9 AT $t = 2.8\times10^{-4}$ s

Dependent variable	Method or code	Reaction numbers in order of decreasing importance and normalized sensitivity coefficients at $t = 2.8\times10^{-4}$ s[a]									
$\sigma_{C_6H_6}$		1	8	12	17	6	104	18	16	92	5
	BFM	−1.75	−1.53	1.11	−0.844	−0.715	−0.652	0.625	−0.513	−0.455	0.244
	LSENS	−1.75	−1.54	1.11	−0.844	−0.715	−0.652	0.625	−0.513	−0.455	0.244
	SENKIN	−1.74	−1.52	1.11	−0.838	−0.711	−0.647	0.621	−0.509	−0.452	0.242
σ_{O_2}		1	8	12	17	104					
	BFM	−0.272	−0.264	0.188	−0.155	−0.102					
	LSENS	−0.272	−0.264	0.188	−0.155	−0.102					
	SENKIN	−0.270	−0.262	0.187	−0.154	−0.102					
σ_{OH}		8	1	12	17	104	18	16	6	92	5
	BFM	5.06	4.71	−3.51	2.77	2.15	−1.85	1.66	1.43	1.41	−1.16
	LSENS	5.06	4.71	−3.51	2.77	2.15	−1.85	1.66	1.43	1.41	−1.16
	SENKIN	5.02	4.68	−3.49	2.75	2.13	−1.84	1.64	1.41	1.40	−1.15
σ_H		8	1	12	17	6	104	18	16	92	5
	BFM	6.02	5.48	−4.18	3.15	1.97	1.97	−1.90	1.86	1.54	−1.32
	LSENS	6.02	5.48	−4.18	3.15	1.97	1.97	−1.90	1.86	1.54	−1.32
	SENKIN	5.98	5.44	−4.16	3.13	1.96	1.95	−1.89	1.85	1.53	−1.31

σ_{H_2}		8	1	12	17	6	18	16	92	104	5
	BFM	3.07	2.59	−2.22	1.61	0.926	−0.914	0.848	0.699	0.698	−0.608
	LSENS	3.07	2.59	−2.22	1.61	0.926	−0.914	0.848	0.700	0.698	−0.608
	SENKIN	3.06	2.58	−2.21	1.60	0.922	−0.911	0.844	0.697	0.695	−0.606
σ_O		8	1	12	17	104	6	18	16	5	92
	BFM	5.30	4.74	−3.69	2.75	2.56	1.91	−1.90	1.65	−1.62	1.42
	LSENS	5.30	4.74	−3.69	2.75	2.56	1.91	−1.90	1.65	−1.62	1.42
	SENKIN	5.26	4.70	−3.66	2.72	2.54	1.90	−1.89	1.64	−1.62	1.41
σ_{H_2O}		1	8	12	17	104	16	6	92	18	5
	BFM	2.03	1.97	−1.41	1.17	0.774	0.690	0.685	0.597	−0.549	−0.450
	LSENS	2.03	1.97	−1.41	1.17	0.774	0.691	0.685	0.597	−0.549	−0.450
	SENKIN	2.02	1.96	−1.40	1.17	0.771	0.688	0.682	0.595	−0.547	−0.449
σ_{CO}		1	8	12	17	104	16	6	92	18	5
	BFM	1.88	1.84	−1.30	1.05	0.685	0.634	0.632	0.522	−0.486	−0.388
	LSENS	1.88	1.84	−1.30	1.05	0.685	0.634	0.632	0.522	−0.486	−0.388
	SENKIN	1.87	1.84	−1.30	1.05	0.683	0.632	0.629	0.520	−0.484	−0.387

[a]For each dependent variable the top row lists the reaction numbers. The next three rows give the normalized sensitivity coefficients produced by BFM, LSENS, and SENKIN, respectively. For each dependent variable and method or code the $\{\langle S_{ij} \rangle\}$ are those of that variable with respect to the preexponential factors of the reactions corresponding to the numbers listed in the first row.

TABLE 4.88.—Concluded.

Dependent variable	Method or code	Reaction numbers in order of decreasing importance and normalized sensitivity coefficients at $t = 2.8\times10^{-4}$ s[a]									
$\sigma_{C_2H_2}$[b]		1	8	17	12	16	50	22	21	6	5
	BFM	0.618	0.434	0.416	–0.298	0.226	–0.215	–0.174	0.163	0.163	0.159
	LSENS	0.618	0.434	0.416	–0.298	0.226	–0.215	–0.174	0.163	0.163	0.159
	SENKIN	0.624	0.441	0.419	–0.303	0.228	–0.214	–0.174	0.164	0.165	0.157
σ_{CO_2}		8	1	12	17	104	16	18	6	92	5
	BFM	4.00	3.81	–2.84	2.25	1.61	1.37	–1.33	1.29	1.14	–1.14
	LSENS	4.00	3.81	–2.84	2.25	1.61	1.37	–1.33	1.29	1.14	–1.14
	SENKIN	3.99	3.80	–2.84	2.24	1.60	1.36	–1.33	1.29	1.14	–1.13
T		1	8	12	17	104	6	16			
	BFM	0.298	0.297	–0.212	0.176	0.115	0.107	0.105			
	LSENS	0.298	0.297	–0.212	0.176	0.115	0.107	0.105			
	SENKIN	0.296	0.295	–0.210	0.175	0.114	0.106	0.104			
p[c]		1	8	12	17	104	6	16			
	BFM	0.321	0.320	–0.228	0.189	0.123	0.114	0.113			
	LSENS	0.321	0.320	–0.228	0.189	0.123	0.114	0.113			

[a]For each dependent variable the top row lists the reaction numbers. The next three rows give the normalized sensitivity coefficients produced by BFM, LSENS, and SENKIN, respectively. For each dependent variable and method or code the $\{\langle S_{ij}\rangle\}$ are those of that variable with respect to the preexponential factors of the reactions corresponding to the numbers listed in the first row.

[b]Reaction importance list for $\sigma_{C_2H_2}$ produced by SENKIN was different from that obtained with the BFM (and LSENS): see text for details.

[c]Sensitivity coefficients of pressure are not calculated by SENKIN.

TABLE 4.89.—REACTION IMPORTANCE LISTS AND NORMALIZED SENSITIVITY COEFFICIENTS WITH RESPECT TO PREEXPONENTIAL FACTORS FOR TEST PROBLEM 9 AT $t = 3\times10^{-4}$ s

Dependent variable	Method or code	Reaction numbers in order of decreasing importance and normalized sensitivity coefficients at $t = 3\times10^{-4}$ s[a]									
$\sigma_{C_6H_6}$		8	1	12	17	104	6	18	16	92	5
	BFM	−18.3	−17.5	12.6	−10.1	−8.25	−6.81	6.00	−5.96	−4.97	3.79
	LSENS	−18.3	−17.5	12.6	−10.1	−8.25	−6.81	6.00	−5.96	−4.97	3.79
	SENKIN	−17.5	−16.7	12.0	−9.59	−7.86	−6.50	5.72	−5.68	−4.74	3.61
σ_{O_2}		8	1	12	17	104	6	16	18	92	5
	BFM	−2.92	−2.76	2.01	−1.63	−1.29	−1.03	−0.954	0.902	−0.788	0.655
	LSENS	−2.92	−2.76	2.01	−1.63	−1.29	−1.03	−0.954	0.902	−0.788	0.655
	SENKIN	−2.79	−2.63	1.92	−1.55	−1.23	−0.983	−0.909	0.859	−0.752	0.624
σ_{OH}		8	1	12	17	104	6	16	18	92	5
	BFM	36.3	33.9	−24.8	20.0	16.2	12.6	11.8	−11.5	9.72	−8.13
	LSENS	36.3	33.9	−24.8	20.0	16.2	12.6	11.8	−11.5	9.72	−8.13
	SENKIN	35.4	33.0	−24.2	19.5	15.8	12.2	11.5	−11.2	9.47	−7.93
σ_H		8	1	12	17	104	6	16	18	92	5
	BFM	33.9	31.6	−23.1	18.6	14.4	11.8	10.9	−10.6	9.02	−7.50
	LSENS	33.9	31.6	−23.1	18.6	14.4	11.8	10.9	−10.6	9.02	−7.50
	SENKIN	33.0	30.8	−22.5	18.1	14.0	11.5	10.7	−10.3	8.79	−7.31

[a]For each dependent variable the top row lists the reaction numbers. The next three rows give the normalized sensitivity coefficients produced by BFM, LSENS, and SENKIN, respectively. For each dependent variable and method or code the $\{\langle S_{ij}\rangle\}$ are those of that variable with respect to the preexponential factors of the reactions corresponding to the numbers listed in the first row.

TABLE 4.89.—Concluded.

Dependent variable	Method or code	Reaction numbers in order of decreasing importance and normalized sensitivity coefficients at $t = 3\times10^{-4}$ s[a]									
σ_{H_2}		8	1	12	17	6	104	16	18	92	5
	BFM	7.83	7.22	−5.34	4.31	2.74	2.72	2.51	−2.37	2.02	−1.66
	LSENS	7.83	7.22	−5.34	4.31	2.74	2.73	2.51	−2.37	2.02	−1.66
	SENKIN	7.64	7.04	−5.22	4.21	2.67	2.64	2.44	−2.31	1.96	−1.62
σ_O		8	1	12	17	104	6	16	18	92	5
	BFM	37.4	34.9	−25.6	20.5	17.0	13.1	12.1	−11.9	10.0	−8.59
	LSENS	37.5	34.9	−25.6	20.5	17.0	13.1	12.1	−11.9	10.0	−8.59
	SENKIN	36.4	33.9	−24.9	19.9	16.5	12.7	11.8	−11.6	9.72	−8.36
σ_{H_2O}		8	1	12	17	104	6	16	18	92	5
	BFM	7.71	7.30	−5.31	4.32	3.42	2.74	2.53	−2.34	2.09	−1.74
	LSENS	7.72	7.30	−5.31	4.32	3.42	2.74	2.53	−2.34	2.09	−1.74
	SENKIN	7.55	7.14	−5.20	4.22	3.34	2.68	2.47	−2.29	2.05	−1.70
σ_{CO}		8	1	12	17	104	6	16	18	92	5
	BFM	7.48	7.06	−5.13	4.16	3.27	2.64	2.44	−2.26	2.01	−1.66
	LSENS	7.48	7.06	−5.13	4.16	3.27	2.64	2.44	−2.26	2.01	−1.66
	SENKIN	7.29	6.87	−5.01	4.05	3.18	2.58	2.38	−2.20	1.96	−1.62

$\sigma_{C_2H_2}$		8	1	12	17	104	18	6	16	92	5
	BFM	−11.9	−11.1	8.19	−6.40	−5.55	4.04	−4.02	−3.85	−3.18	2.98
	LSENS	−11.9	−11.1	8.19	−6.40	−5.55	4.04	−4.03	−3.85	−3.18	2.98
	SENKIN	−11.3	−10.5	7.78	−6.06	−5.29	3.85	−3.82	−3.65	−3.02	2.85
σ_{CO_2}		8	1	12	17	104	6	16	18	92	5
	BFM	17.6	16.5	−12.1	9.74	7.71	6.09	5.73	−5.53	4.74	−4.03
	LSENS	17.6	16.5	−12.1	9.74	7.71	6.09	5.73	−5.53	4.74	−4.03
	SENKIN	17.1	16.0	−11.7	9.46	7.49	5.91	5.57	−5.37	4.61	−3.93
T		8	1	12	17	104	6	16	18	92	5
	BFM	2.07	1.96	−1.43	1.16	0.912	0.733	0.680	−0.639	0.561	−0.470
	LSENS	2.07	1.96	−1.43	1.16	0.912	0.733	0.680	−0.639	0.561	−0.470
	SENKIN	2.01	1.90	−1.39	1.12	0.883	0.710	0.659	−0.619	0.544	−0.456
p[b]		8	1	12	17	104	6	16	18	92	5
	BFM	2.28	2.16	−1.57	1.28	1.00	0.806	0.748	−0.702	0.617	−0.517
	LSENS	2.28	2.16	−1.57	1.28	1.00	0.807	0.748	−0.702	0.617	−0.517

[a]For each dependent variable the top row lists the reaction numbers. The next three rows give the normalized sensitivity coefficients produced by BFM, LSENS, and SENKIN, respectively. For each dependent variable and method or code the $\{\langle S_{ij}\rangle\}$ are those of that variable with respect to the preexponential factors of the reactions corresponding to the numbers listed in the first row.

[b]Sensitivity coefficients of pressure are not calculated by SENKIN.

TABLE 4.90.—NORMALIZED SENSITIVITY COEFFICIENTS WITH RESPECT TO TEMPERATURE EXPONENTS AND ACTIVATION ENERGIES OF SELECTED REACTIONS FOR TEST PROBLEM 9 AT $t = 10^{-6}$ s

Dependent variable	Normalized sensitivity coefficients at $t = 10^{-6}$ s with respect to[a]									
	n_1	n_6	n_8	n_{12}	n_{22}	E_1	E_6	E_8	E_{12}	E_{22}
$\sigma_{C_6H_6}$	-8.20(-4)	-1.60(-4)	-6.19(-11)	2.12(-7)	-2.39(-11)	-8.20(-4)	-1.60(-4)	-6.19(-11)	2.12(-7)	-2.39(-11)
	-8.20(-4)	-1.60(-4)	-6.21(-11)	2.12(-7)	-2.39(-11)	-8.20(-4)	-1.60(-4)	-6.21(-11)	2.12(-7)	-2.39(-11)
σ_{O_2}	-7.75(-5)	-3.04(-6)	-5.03(-10)	4.90(-8)	-1.77(-10)	-7.75(-5)	-3.04(-6)	-5.03(-10)	4.90(-8)	-1.77(-10)
	-7.75(-5)	-3.04(-6)	-5.03(-10)	4.90(-8)	-1.77(-10)	-7.75(-5)	-3.04(-6)	-5.03(-10)	4.90(-8)	-1.77(-10)
σ_{OH}	9.98(-1)	-5.36(-1)	2.15(-6)	-9.03(-4)	-4.24(-6)	9.98(-1)	-5.36(-1)	2.15(-6)	-9.03(-4)	-4.24(-6)
	9.98(-1)	-5.36(-1)	2.15(-6)	-9.03(-4)	-4.24(-6)	9.98(-1)	-5.36(-1)	2.15(-6)	-9.03(-4)	-4.24(-6)
σ_H	9.38(-1)	1.18(-1)	8.73(-4)	-5.55(-2)	1.84(-4)	9.38(-1)	1.18(-1)	8.73(-4)	-5.55(-2)	1.84(-4)
	9.38(-1)	1.18(-1)	8.73(-4)	-5.55(-2)	1.84(-4)	9.38(-1)	1.18(-1)	8.73(-4)	-5.55(-2)	1.84(-4)
σ_{H_2}	9.57(-1)	6.21(-2)	4.71(-4)	-3.43(-2)	1.21(-4)	9.57(-1)	6.21(-2)	4.71(-4)	-3.43(-2)	1.21(-4)
	9.57(-1)	6.21(-2)	4.71(-4)	-3.43(-2)	1.21(-4)	9.57(-1)	6.21(-2)	4.71(-4)	-3.43(-2)	1.21(-4)
σ_O	9.89(-1)	5.38(-1)	1.22(-4)	-9.25(-3)	3.11(-5)	9.89(-1)	5.38(-1)	1.22(-4)	-9.25(-3)	3.11(-5)
	9.89(-1)	5.38(-1)	1.22(-4)	-9.25(-3)	3.11(-5)	9.89(-1)	5.38(-1)	1.22(-4)	-9.25(-3)	3.11(-5)

σ_{H_2O}	9.99(−1)	6.30(−1)	−1.31(−6)	−2.61(−4)	−1.77(−6)	9.99(−1)	6.30(−1)	−1.31(−6)	−2.61(−4)	−1.77(−6)
	9.99(−1)	6.30(−1)	−1.31(−6)	−2.61(−4)	−1.77(−6)	9.99(−1)	6.30(−1)	−1.31(−6)	−2.61(−4)	−1.77(−6)
σ_{CO}	9.99(−1)	2.97(−2)	9.88(−1)	−1.10(−3)	2.35(−4)	9.99(−1)	2.97(−2)	9.88(−1)	−1.10(−3)	2.35(−4)
	9.99(−1)	2.97(−2)	9.88(−1)	−1.10(−3)	2.35(−4)	9.99(−1)	2.97(−2)	9.88(−1)	−1.10(−3)	2.35(−4)
$\sigma_{C_2H_2}$	1.01	7.01(−1)	1.00(−2)	−3.33(−4)	−2.24(−6)	1.01	7.01(−1)	1.00(−2)	−3.33(−4)	−2.24(−6)
	1.01	7.01(−1)	1.00(−2)	−3.33(−4)	−2.24(−6)	1.01	7.01(−1)	1.00(−2)	−3.33(−4)	−2.24(−6)
σ_{CO_2}	1.99	−4.14(−1)	9.90(−1)	−1.08(−3)	1.56(−4)	1.99	−4.14(−1)	9.90(−1)	−1.08(−3)	1.56(−4)
	1.99	−4.14(−1)	9.90(−1)	−1.08(−3)	1.56(−4)	1.99	−4.14(−1)	9.90(−1)	−1.08(−3)	1.56(−4)
T	3.61(−6)	4.83(−6)	−6.35(−7)	3.52(−7)	−5.51(−10)	3.61(−6)	4.83(−6)	−6.35(−7)	3.52(−7)	−5.51(−10)
	3.61(−6)	4.83(−6)	−6.35(−7)	3.52(−7)	−5.51(−10)	3.61(−6)	4.83(−6)	−6.35(−7)	3.52(−7)	−5.51(−10)
p	3.71(−6)	4.83(−6)	−4.63(−7)	3.28(−7)	−4.70(−10)	3.71(−6)	4.83(−6)	−4.63(−7)	3.28(−7)	−4.70(−10)
	3.71(−6)	4.83(−6)	−4.63(−7)	3.28(−7)	−4.70(−10)	3.71(−6)	4.83(−6)	−4.63(−7)	3.28(−7)	−4.70(−10)

[a]For each dependent variable the top row gives the BFM results and the bottom row gives the LSENS results; numbers in parentheses denote powers of 10.

TABLE 4.91.—NORMALIZED SENSITIVITY COEFFICIENTS WITH RESPECT TO TEMPERATURE EXPONENTS AND ACTIVATION ENERGIES OF SELECTED REACTIONS FOR TEST PROBLEM 9 AT $t = 10^{-5}$ s

Dependent variable	Normalized sensitivity coefficients at $t = 10^{-5}$ s with respect to[a]									
	n_1	n_6	n_8	n_{12}	n_{22}	E_1	E_6	E_8	E_{12}	E_{22}
$\sigma_{C_6H_6}$	−1.48(−2)	−1.40(−3)	−2.41(−4)	3.39(−3)	−2.23(−6)	−1.48(−2)	−1.40(−3)	−2.41(−4)	3.39(−3)	−2.23(−6)
	−1.48(−2)	−1.40(−3)	−2.41(−4)	3.39(−3)	−2.23(−6)	−1.48(−2)	−1.40(−3)	−2.41(−4)	3.39(−3)	−2.23(−6)
σ_{O_2}	−1.24(−3)	−1.05(−4)	−2.48(−5)	3.00(−4)	−7.19(−7)	−1.24(−3)	−1.05(−4)	−2.48(−5)	3.00(−4)	−7.19(−7)
	−1.24(−3)	−1.05(−4)	−2.48(−5)	3.00(−4)	−7.19(−7)	−1.24(−3)	−1.05(−4)	−2.48(−5)	3.00(−4)	−7.19(−7)
σ_{OH}	7.12(−1)	−9.36(−1)	3.09(−2)	−2.62(−1)	−1.62(−3)	7.11(−1)	−9.35(−1)	3.09(−2)	−2.61(−1)	−1.62(−3)
	7.12(−1)	−9.36(−1)	3.09(−2)	−2.62(−1)	−1.62(−3)	7.11(−1)	−9.35(−1)	3.09(−2)	−2.61(−1)	−1.62(−3)
σ_H	−3.22(−2)	−7.29(−2)	1.26(−1)	−9.58(−1)	6.80(−3)	−3.24(−2)	−7.29(−2)	1.26(−1)	−9.57(−1)	6.79(−3)
	−3.22(−2)	−7.29(−2)	1.26(−1)	−9.58(−1)	6.80(−3)	−3.24(−2)	−7.29(−2)	1.26(−1)	−9.57(−1)	6.79(−3)
σ_{H_2}	2.25(−1)	2.18(−2)	5.86(−2)	−7.24(−1)	2.85(−3)	2.25(−1)	2.18(−2)	5.86(−2)	−7.23(−1)	2.85(−3)
	2.25(−1)	2.18(−2)	5.86(−2)	−7.24(−1)	2.85(−3)	2.25(−1)	2.18(−2)	5.86(−2)	−7.23(−1)	2.85(−3)
σ_O	5.28(−1)	4.75(−2)	4.14(−2)	−4.26(−1)	1.04(−3)	5.28(−1)	4.73(−2)	4.14(−2)	−4.26(−1)	1.04(−3)
	5.28(−1)	4.75(−2)	4.14(−2)	−4.26(−1)	1.04(−3)	5.28(−1)	4.73(−2)	4.14(−2)	−4.26(−1)	1.04(−3)

σ_{H_2O}	8.08(−1)	1.38(−1)	1.35(−2)	−1.81(−1)	−3.80(−4)	8.08(−1)	1.38(−1)	1.35(−2)	−1.81(−1)	−3.79(−4)
	8.08(−1)	1.38(−1)	1.35(−2)	−1.81(−1)	−3.80(−4)	8.08(−1)	1.38(−1)	1.35(−2)	−1.81(−1)	−3.79(−4)
σ_{CO}	8.38(−1)	1.05(−1)	9.08(−1)	−1.85(−1)	4.44(−3)	8.38(−1)	1.05(−1)	9.07(−1)	−1.85(−1)	4.43(−3)
	8.38(−1)	1.05(−1)	9.08(−1)	−1.85(−1)	4.44(−3)	8.38(−1)	1.05(−1)	9.07(−1)	−1.85(−1)	4.43(−3)
$\sigma_{C_2H_2}$	1.19	1.74(−1)	8.27(−1)	−5.70(−1)	−2.01(−3)	1.19	1.74(−1)	8.27(−1)	−5.70(−1)	−2.00(−3)
	1.19	1.74(−1)	8.27(−1)	−5.70(−1)	−2.01(−3)	1.19	1.74(−1)	8.27(−1)	−5.70(−1)	−2.00(−3)
σ_{CO_2}	1.60	−6.11(−1)	9.34(−1)	−4.51(−1)	2.61(−3)	1.60	−6.11(−1)	9.33(−1)	−4.50(−1)	2.61(−3)
	1.60	−6.11(−1)	9.34(−1)	−4.51(−1)	2.61(−3)	1.60	−6.11(−1)	9.33(−1)	−4.50(−1)	2.61(−3)
T	1.09(−3)	1.42(−4)	−8.83(−5)	−9.86(−5)	1.29(−6)	1.09(−3)	1.42(−4)	−8.82(−5)	−9.86(−5)	1.29(−6)
	1.09(−3)	1.42(−4)	−8.83(−5)	−9.86(−5)	1.29(−6)	1.09(−3)	1.42(−4)	−8.82(−5)	−9.86(−5)	1.29(−6)
p	1.05(−3)	1.39(−4)	−6.14(−5)	−9.90(−5)	1.33(−6)	1.05(−3)	1.39(−4)	−6.13(−5)	−9.90(−5)	1.33(−6)
	1.05(−3)	1.39(−4)	−6.14(−5)	−9.90(−5)	1.33(−6)	1.05(−3)	1.39(−4)	−6.13(−5)	−9.90(−5)	1.33(−6)

[a]For each dependent variable the top row gives the BFM results and the bottom row gives the LSENS results; numbers in parentheses denote powers of 10.

TABLE 4.92.—NORMALIZED SENSITIVITY COEFFICIENTS WITH RESPECT TO TEMPERATURE EXPONENTS AND ACTIVATION ENERGIES OF SELECTED REACTIONS FOR TEST PROBLEM 9 AT $t = 6\times10^{-5}$ s

Dependent variable	Normalized sensitivity coefficients at $t = 6\times10^{-5}$ s with respect to[a]									
	n_1	n_6	n_8	n_{12}	n_{22}	E_1	E_6	E_8	E_{12}	E_{22}
$\sigma_{C_6H_6}$	-8.79(-2)	-9.64(-3)	-5.33(-3)	1.68(-2)	9.40(-4)	-8.75(-2)	-9.58(-3)	-5.31(-3)	1.68(-2)	9.33(-4)
	-8.79(-2)	-9.64(-3)	-5.33(-3)	1.68(-2)	9.40(-4)	-8.75(-2)	-9.58(-3)	-5.31(-3)	1.68(-2)	9.33(-4)
σ_{O_2}	-7.69(-3)	-7.08(-4)	-9.08(-4)	1.70(-3)	1.96(-5)	-7.66(-3)	-7.04(-4)	-9.04(-4)	1.70(-3)	1.95(-5)
	-7.69(-3)	-7.08(-4)	-9.08(-4)	1.70(-3)	1.96(-5)	-7.66(-3)	-7.04(-4)	-9.04(-4)	1.70(-3)	1.95(-5)
σ_{OH}	7.64(-1)	-7.10(-1)	1.39(-1)	-1.52(-1)	-4.98(-2)	7.56(-1)	-7.03(-1)	1.38(-1)	-1.51(-1)	-4.94(-2)
	7.64(-1)	-7.10(-1)	1.39(-1)	-1.52(-1)	-4.98(-2)	7.56(-1)	-7.03(-1)	1.38(-1)	-1.51(-1)	-4.94(-2)
σ_H	1.06(-1)	-9.28(-3)	7.61(-1)	-8.48(-1)	1.37(-1)	1.04(-1)	-9.30(-3)	7.56(-1)	-8.40(-1)	1.35(-1)
	1.06(-1)	-9.28(-3)	7.61(-1)	-8.48(-1)	1.37(-1)	1.04(-1)	-9.30(-3)	7.56(-1)	-8.40(-1)	1.35(-1)
σ_{H_2}	6.79(-2)	2.29(-3)	3.08(-1)	-8.20(-1)	4.15(-2)	6.71(-2)	2.16(-3)	3.06(-1)	-8.17(-1)	4.12(-2)
	6.79(-2)	2.29(-3)	3.08(-1)	-8.20(-1)	4.15(-2)	6.71(-2)	2.16(-3)	3.06(-1)	-8.17(-1)	4.12(-2)
σ_O	6.13(-1)	2.32(-1)	1.69(-1)	-2.26(-1)	-1.81(-2)	6.07(-1)	2.29(-1)	1.68(-1)	-2.24(-1)	-1.80(-2)
	6.13(-1)	2.32(-1)	1.69(-1)	-2.26(-1)	-1.81(-2)	6.07(-1)	2.29(-1)	1.68(-1)	-2.24(-1)	-1.80(-2)

σ_{H_2O}	8.29(−1)	8.24(−2)	6.04(−2)	−1.59(−1)	−1.79(−2)	8.25(−1)	8.19(−2)	6.02(−2)	−1.58(−1)	−1.77(−2)
	8.29(−1)	8.24(−2)	6.04(−2)	−1.59(−1)	−1.79(−2)	8.25(−1)	8.19(−2)	6.02(−2)	−1.58(−1)	−1.77(−2)
σ_{CO}	8.58(−1)	6.37(−2)	5.44(−1)	−2.54(−1)	3.80(−3)	8.54(−1)	6.35(−2)	5.41(−1)	−2.53(−1)	3.76(−3)
	8.58(−1)	6.37(−2)	5.44(−1)	−2.54(−1)	3.80(−3)	8.54(−1)	6.35(−2)	5.41(−1)	−2.53(−1)	3.76(−3)
$\sigma_{C_2H_2}$	9.93(−1)	1.40(−1)	8.44(−1)	−6.72(−1)	2.55(−3)	9.89(−1)	1.39(−1)	8.40(−1)	−6.69(−1)	2.51(−3)
	9.93(−1)	1.40(−1)	8.44(−1)	−6.72(−1)	2.55(−3)	9.89(−1)	1.39(−1)	8.40(−1)	−6.69(−1)	2.51(−3)
σ_{CO_2}	1.60	−3.12(−1)	8.04(−1)	−5.75(−1)	−2.11(−2)	1.59	−3.10(−1)	8.00(−1)	−5.73(−1)	−2.10(−2)
	1.60	−3.12(−1)	8.04(−1)	−5.75(−1)	−2.11(−2)	1.59	−3.10(−1)	8.00(−1)	−5.73(−1)	−2.10(−2)
T	6.75(−3)	6.31(−4)	−9.53(−5)	−1.42(−3)	1.33(−4)	6.72(−3)	6.28(−4)	−9.11(−5)	−1.41(−3)	1.32(−4)
	6.75(−3)	6.31(−4)	−9.53(−5)	−1.42(−3)	1.33(−4)	6.72(−3)	6.28(−4)	−9.11(−5)	−1.41(−3)	1.32(−4)
p	7.01(−3)	6.41(−4)	3.13(−4)	−1.55(−3)	1.29(−4)	6.98(−3)	6.37(−4)	3.15(−4)	−1.54(−3)	1.28(−4)
	7.01(−3)	6.41(−4)	3.13(−4)	−1.55(−3)	1.29(−4)	6.98(−3)	6.37(−4)	3.15(−4)	−1.54(−3)	1.28(−4)

[a]For each dependent variable the top row gives the BFM results and the bottom row gives the LSENS results; numbers in parentheses denote powers of 10.

TABLE 4.93.—NORMALIZED SENSITIVITY COEFFICIENTS WITH RESPECT TO TEMPERATURE EXPONENTS AND ACTIVATION ENERGIES OF SELECTED REACTIONS FOR TEST PROBLEM 9 AT $t = 2.8\times10^{-4}$ s

Dependent variable	Normalized sensitivity coefficients at $t = 2.8\times10^{-4}$ s with respect to[a]									
	n_1	n_6	n_8	n_{12}	n_{22}	E_1	E_6	E_8	E_{12}	E_{22}
$\sigma_{C_6H_6}$	−1.76	−7.21(−1)	−1.54	1.12	4.06(−3)	−1.72	−6.77(−1)	−1.48	1.07	1.03(−2)
	−1.76	−7.21(−1)	−1.54	1.12	4.06(−3)	−1.72	−6.77(−1)	−1.48	1.07	1.03(−2)
σ_{O_2}	−2.72(−1)	−9.59(−2)	−2.65(−1)	1.89(−1)	3.64(−3)	−2.67(−1)	−9.13(−2)	−2.55(−1)	1.82(−1)	4.62(−3)
	−2.72(−1)	−9.59(−2)	−2.65(−1)	1.89(−1)	3.64(−3)	−2.67(−1)	−9.13(−2)	−2.55(−1)	1.82(−1)	4.62(−3)
σ_{OH}	4.72	1.43	5.09	−3.54	−1.80(−1)	4.64	1.39	4.83	−3.36	−1.92(−1)
	4.72	1.43	5.09	−3.54	−1.80(−1)	4.64	1.39	4.83	−3.36	−1.92(−1)
σ_H	5.49	1.98	6.06	−4.21	2.19(−2)	5.40	1.89	5.74	−4.00	−2.90(−2)
	5.49	1.98	6.06	−4.21	2.19(−2)	5.40	1.89	5.74	−4.00	−2.90(−2)
σ_{H_2}	2.60	9.31(−1)	3.09	−2.23	1.44(−1)	2.57	8.92(−1)	2.95	−2.13	1.13(−1)
	2.60	9.31(−1)	3.09	−2.23	1.44(−1)	2.57	8.92(−1)	2.95	−2.13	1.13(−1)
σ_O	4.75	1.93	5.33	−3.71	7.02(−2)	4.68	1.81	5.05	−3.52	2.21(−2)
	4.75	1.93	5.33	−3.71	7.02(−2)	4.68	1.81	5.05	−3.52	2.21(−2)

σ_{H_2O}	2.03	6.89(−1)	1.98	−1.41	−3.18(−2)	2.00	6.57(−1)	1.90	−1.36	−3.78(−2)
	2.03	6.89(−1)	1.98	−1.41	−3.18(−2)	2.00	6.57(−1)	1.90	−1.36	−3.78(−2)
σ_{CO}	1.88	6.35(−1)	1.85	−1.31	−3.50(−2)	1.85	6.07(−1)	1.77	−1.26	−4.03(−2)
	1.88	6.35(−1)	1.85	−1.31	−3.50(−2)	1.85	6.07(−1)	1.77	−1.26	−4.03(−2)
$\sigma_{C_2H_2}$	6.20(−1)	1.63(−1)	4.36(−1)	−2.99(−1)	−1.76(−1)	6.05(−1)	1.61(−1)	4.20(−1)	−2.91(−1)	−1.61(−1)
	6.20(−1)	1.63(−1)	4.36(−1)	−2.99(−1)	−1.76(−1)	6.05(−1)	1.61(−1)	4.19(−1)	−2.91(−1)	−1.61(−1)
σ_{CO_2}	3.82	1.30	4.03	−2.86	−3.87(−2)	3.76	1.24	3.86	−2.74	−5.59(−2)
	3.82	1.30	4.03	−2.86	−3.87(−2)	3.76	1.24	3.86	−2.74	−5.59(−2)
T	2.98(−1)	1.08(−1)	2.98(−1)	−2.13(−1)	−3.75(−3)	2.93(−1)	1.02(−1)	2.86(−1)	−2.04(−1)	−5.05(−3)
	2.98(−1)	1.08(−1)	2.98(−1)	−2.13(−1)	−3.75(−3)	2.93(−1)	1.02(−1)	2.86(−1)	−2.04(−1)	−5.05(−3)
p	3.22(−1)	1.15(−1)	3.21(−1)	−2.29(−1)	−4.42(−3)	3.16(−1)	1.09(−1)	3.08(−1)	−2.20(−1)	−5.75(−3)
	3.22(−1)	1.15(−1)	3.21(−1)	−2.29(−1)	−4.42(−3)	3.16(−1)	1.09(−1)	3.08(−1)	−2.20(−1)	−5.75(−3)

[a]For each dependent variable the top row gives the BFM results and the bottom row gives the LSENS results; numbers in parentheses denote powers of 10.

TABLE 4.94.—NORMALIZED SENSITIVITY COEFFICIENTS WITH RESPECT TO TEMPERATURE EXPONENTS AND ACTIVATION ENERGIES OF SELECTED REACTIONS FOR TEST PROBLEM 9 AT $t = 3\times10^{-4}$ s

Dependent variable	Normalized sensitivity coefficients at $t = 3\times10^{-4}$ s with respect to[a]									
	n_1	n_6	n_8	n_{12}	n_{22}	E_1	E_6	E_8	E_{12}	E_{22}
$\sigma_{C_6H_6}$	−1.76(1)	−6.87	−1.84(1)	1.27(1)	2.37(−1)	−1.72(1)	−6.44	−1.75(1)	1.21(1)	3.49(−1)
	−1.76(1)	−6.87	−1.84(1)	1.27(1)	2.37(−1)	−1.72(1)	−6.44	−1.75(1)	1.21(1)	3.49(−1)
σ_{O_2}	−2.76	−1.04	−2.94	2.02	4.89(−2)	−2.71	−9.83(−1)	−2.78	1.92	6.63(−2)
	−2.76	−1.04	−2.94	2.02	4.89(−2)	−2.71	−9.83(−1)	−2.79	1.92	6.63(−2)
σ_{OH}	3.40(1)	1.26(1)	3.66(1)	−2.50(1)	−6.85(−1)	3.34(1)	1.20(1)	3.45(1)	−2.37(1)	−8.84(−1)
	3.40(1)	1.27(1)	3.66(1)	−2.50(1)	−6.85(−1)	3.34(1)	1.20(1)	3.45(1)	−2.38(1)	−8.84(−1)
σ_H	3.16(1)	1.19(1)	3.41(1)	−2.32(1)	−4.99(−1)	3.11(1)	1.13(1)	3.22(1)	−2.21(1)	−7.35(−1)
	3.17(1)	1.19(1)	3.41(1)	−2.33(1)	−5.00(−1)	3.11(1)	1.13(1)	3.22(1)	−2.21(1)	−7.35(−1)
σ_{H_2}	7.24	2.76	7.88	−5.38	−6.10(−2)	7.11	2.61	7.44	−5.11	−1.32(−1)
	7.24	2.76	7.89	−5.38	−6.10(−2)	7.11	2.61	7.44	−5.12	−1.32(−1)
σ_O	3.50(1)	1.31(1)	3.77(1)	−2.57(1)	−3.53(−1)	3.44(1)	1.24(1)	3.56(1)	−2.45(1)	−6.49(−1)
	3.50(1)	1.31(1)	3.77(1)	−2.58(1)	−3.53(−1)	3.44(1)	1.24(1)	3.56(1)	−2.45(1)	−6.50(−1)

σ_{H_2O}	7.32	2.75	7.77	−5.34	−1.34(−1)	7.19	2.60	7.35	−5.09	−1.78(−1)
	7.32	2.75	7.77	−5.35	−1.34(−1)	7.19	2.60	7.36	−5.09	−1.78(−1)
σ_{CO}	7.07	2.66	7.53	−5.16	−1.31(−1)	6.94	2.52	7.12	−4.92	−1.74(−1)
	7.07	2.66	7.53	−5.17	−1.31(−1)	6.94	2.52	7.12	−4.92	−1.74(−1)
$\sigma_{C_2H_2}$	−1.11(1)	−4.05	−1.20(1)	8.24	−2.13(−1)	−1.09(1)	−3.85	−1.14(1)	7.84	−5.51(−2)
	−1.11(1)	−4.05	−1.20(1)	8.24	−2.12(−1)	−1.09(1)	−3.85	−1.14(1)	7.84	−5.50(−2)
σ_{CO_2}	1.65(1)	6.13	1.77(1)	−1.22(1)	−3.09(−1)	1.62(1)	5.81	1.67(1)	−1.16(1)	−4.09(−1)
	1.65(1)	6.13	1.77(1)	−1.22(1)	−3.09(−1)	1.62(1)	5.81	1.68(1)	−1.16(1)	−4.09(−1)
T	1.96	7.38(−1)	2.09	−1.44	−3.81(−2)	1.93	6.98(−1)	1.98	−1.37	−5.01(−2)
	1.96	7.38(−1)	2.09	−1.44	−3.81(−2)	1.93	6.98(−1)	1.98	−1.37	−5.02(−2)
p	2.16	8.12(−1)	2.30	−1.58	−4.19(−2)	2.12	7.68(−1)	2.18	−1.51	−5.51(−2)
	2.16	8.12(−1)	2.30	−1.58	−4.20(−2)	2.12	7.69(−1)	2.18	−1.51	−5.51(−2)

[a]For each dependent variable the top row gives the BFM results and the bottom row gives the LSENS results; numbers in parentheses denote powers of 10.

On the Amdahl 5870 computer LSENS required 391 steps, 560 functional evaluations, 47 Jacobian matrix evaluations and LU-decompositions, and 6.3 s of execution time to solve for the dependent variables (40 species mole numbers, temperature, and density) in the interval $[0,3\times10^{-4}]$ s. (The cost of the kinetics-only solution with the unmodified LSENS was 468 steps, 681 derivative evaluations, 70 Jacobian matrix evaluations and LU-decompositions, and 7.8 s of execution time.) The CPU times for computing the dependent variables and sensitivity coefficients with respect to one initial condition value and one preexponential factor were, respectively, 19.3 and 19.4 s. For all 42 initial condition values, all 120 preexponential factors, and all 360 rate coefficient parameters the execution times were 42, 87, and 223 s, respectively. Finally to solve for the dependent variables and sensitivity coefficients with respect to all 42 initial conditions and all 360 rate coefficient parameters required 246 s. Thus, as discussed in section 4.3, although the cost (~13 s) of the first sensitivity parameter is considerable, subsequent parameters are significantly less expensive: approximately 0.55 s for each initial condition and approximately 0.57 s for each rate coefficient parameter. Both times are much less than the at least 6.3 s required by the BFM. In particular, the DDM is more efficient than the BFM by over a factor of 10. Note also that the cost associated with using the BFM for all initial conditions and all rate coefficient parameters would be over 2500 s. Of course, the trial-and-error nature of these calculations and the need to use very small EMAX would result in even larger execution times if accurate results are desired. An even more important consideration than the increased computational cost incurred by using the BFM is that, unless automated, this method would need at least 403 separate runs of the simulation program and 16 482 evaluations of sensitivity coefficients per output station.

On the NASA Lewis Research Center's IBM 370/3033 computer an earlier version of LSENS (ref. 22) required 8.3 s to solve for the composition and temperature in the interval $[0,2.16\times10^{-4}]$ s with a previous mechanism, which involved 115 reactions among the 40 species listed above. The local error tolerance parameters used for this calculation were EMAX = 10^{-4} and ATOLSP = 10^{-13}. The execution time for the dependent variables and sensitivities with respect to the initial values of all species mole numbers and temperature and all 345 rate coefficient parameters was approximately 265 s, in contrast to the more than 3200 s that the BFM would require. Thus for nonisothermal combustion kinetics problems the decoupled direct method is significantly more efficient than the brute force method of varying one parameter at a time.

The final study to assess the accuracy of the DDM for nonisothermal problems examined the sensitivities with respect to the rate coefficient parameters of the special rate coefficient expression, equation (2.5). In particular, after Baulch and Drysdale (ref. 25) the rate coefficient expression given in table 4.79 for reaction 101 was replaced with

$$k_{101} = 8.15\times10^{10}\exp(9.07\times10^{-4}T) \tag{4.102}$$

where n_{101} (= 0.0) and c_{101} (= 9.07×10^{-4}) were taken from reference 25. The A_{101} given in this reference was, however, adjusted to give the same rate constant at the initial temperature (i.e., 1405 K) as the expression in table 4.79. The new mechanism gave essentially the same temperature-time profile in the interval $[0,3\times10^{-4}]$ s as the previous one. The normalized sensitivity coefficients with respect to the three parameters A_{101}, n_{101}, and c_{101} are listed in tables 4.95 to 4.97, along with the BFM results produced with EMAX = 10^{-12} and ATOLSP = 10^{-21}. The finite-difference increment Δc_j was set equal to $5\times10^{-n}/T_0$ and $10^{-n}/T_0$ (n = 2,3,...,6), and $\delta(c_j)$ defined as

$$\delta(c_j) = T_0\ \Delta c_j \tag{4.103}$$

Tables 4.95 to 4.97 show that LSENS accurately computed the sensitivity coefficients with respect to the parameters of this rate coefficient expression also at all reaction conditions examined.

Although for reasons given previously attention was restricted to the interval $[0,3\times10^{-4}]$ s, the solutions at t = 3.1×10^{-4} s (T = 2445 K) and 3.4×10^{-4} s (T = 2858 K) were examined. The LSENS results and all BFM solutions at the former reaction time and those that converged at the latter time displayed the same level of agreement as that obtained in the earlier reaction regimes (tables 4.80 to 4.97). (Of course, these solutions may not be meaningful because the validity of the reaction mechanism at such high temperatures is in question.) Thus for this problem also the decoupled direct method was accurate in all regimes of a nonisothermal combustion kinetics problem.

4.6.8 Summary

The decoupled direct method of sensitivity analysis was illustrated by application to nine test problems, of which the first six described constant-temperature, constant-density chemical reaction. In the last three problems, however, the temperature was allowed to vary. In addition, the density varied in two cases. Comparisons of the sensitivity coefficients with either exact solutions or results obtained with the brute force method showed that the DDM was very accurate for all problem types examined. Importantly the DDM has for the first time been demonstrated to be accurate in all regimes of a nonisothermal combustion kinetics problem. The method was also shown to be significantly more efficient, as measured by the execution time, than the BFM. In particular, the DDM was more efficient than the BFM by as much as a factor of over 10 for a realistic combustion kinetics problem involving 40 species and 120 reactions.

The DDM was successfully applied to problems on which other versions of the DM had failed. The DDM was more stable, accurate, and efficient than the DM. The DDM solves two separate systems—one nonlinear and the other linear—of N equations each. It is therefore more efficient than the coupled version of the DM,

TABLE 4.95.—NORMALIZED SENSITIVITY COEFFICIENTS WITH RESPECT TO RATE COEFFICIENT PARAMETER A_{101} OF SPECIAL RATE COEFFICIENT EXPRESSION, EQUATION (2.5), FOR TEST PROBLEM 9

Dependent variable	Normalized sensitivity coefficients with respect to A_{101} at[a]				
	10^{-6} s	10^{-5} s	6×10^{-5} s	2.8×10^{-4} s	3×10^{-4} s
$\sigma_{C_6H_6}$	9.22(–12) 9.22(–12)	1.36(–7) 1.36(–7)	5.30(–5) 5.30(–5)	–1.22(–2) –1.22(–2)	–4.14(–1) –4.14(–1)
σ_{O_2}	–2.60(–12) –2.60(–12)	–2.67(–9) –2.67(–9)	2.56(–6) 2.56(–6)	–3.01(–3) –3.01(–3)	–7.55(–2) –7.55(–2)
σ_{OH}	–1.66(–7) –1.66(–7)	–8.02(–5) –8.02(–5)	–2.41(–3) –2.41(–3)	4.67(–2) 4.67(–2)	8.45(–1) 8.45(–1)
σ_{H}	2.88(–6) 2.88(–6)	8.71(–5) 8.71(–5)	1.74(–3) 1.74(–3)	1.30(–1) 1.30(–1)	9.58(–1) 9.58(–1)
σ_{H_2}	1.93(–6) 1.93(–6)	3.84(–5) 3.84(–5)	5.32(–4) 5.32(–4)	6.88(–2) 6.88(–2)	2.77(–1) 2.77(–1)
σ_{O}	4.77(–7) 4.77(–7)	–7.95(–6) –7.95(–6)	–1.65(–3) –1.65(–3)	1.06(–1) 1.06(–1)	1.03 1.03
σ_{H_2O}	–6.40(–8) –6.40(–8)	–2.35(–5) –2.35(–5)	–8.91(–4) –8.91(–4)	1.04(–2) 1.04(–2)	1.55(–1) 1.55(–1)
σ_{CO}	–7.92(–6) –7.92(–6)	–1.59(–4) –1.59(–4)	–1.38(–3) –1.38(–3)	–2.55(–4) –2.54(–4)	1.21(–1) 1.21(–1)
$\sigma_{C_2H_2}$	–2.09(–8) –2.09(–8)	7.41(–6) 7.41(–6)	–3.23(–4) –3.23(–4)	–6.48(–3) –6.48(–3)	–3.40(–1) –3.40(–1)
σ_{CO_2}	9.83(–1) 9.83(–1)	8.13(–1) 8.13(–1)	6.06(–1) 6.06(–1)	3.65(–1) 3.65(–1)	8.13(–1) 8.13(–1)
T	5.05(–12) 5.05(–12)	5.02(–8) 5.02(–8)	4.24(–6) 4.24(–6)	4.78(–3) 4.78(–3)	5.54(–2) 5.54(–2)
p	4.96(–12) 4.96(–12)	4.71(–8) 4.71(–8)	3.59(–6) 3.59(–6)	4.77(–3) 4.77(–3)	5.94(–2) 5.95(–2)

[a]For each dependent variable the top row gives the BFM results and the bottom row gives the LSENS results. Numbers in parentheses denote powers of 10.

TABLE 4.96.—NORMALIZED SENSITIVITY COEFFICIENTS WITH RESPECT TO RATE COEFFICIENT PARAMETER n_{101} OF SPECIAL RATE COEFFICIENT EXPRESSION, EQUATION (2.5), FOR TEST PROBLEM 9

Dependent variable	Normalized sensitivity coefficients with respect to n_{101} at[a]				
	10^{-6} s	10^{-5} s	6×10^{-5} s	2.8×10^{-4} s	3×10^{-4} s
$\sigma_{C_6H_6}$	9.22(–12)	1.36(–7)	5.30(–5)	–1.23(–2)	–4.22(–1)
	9.22(–12)	1.36(–7)	5.30(–5)	–1.23(–2)	–4.22(–1)
σ_{O_2}	–2.60(–12)	–2.67(–9)	2.56(–6)	–3.05(–3)	–7.71(–2)
	–2.60(–12)	–2.67(–9)	2.56(–6)	–3.05(–3)	–7.71(–2)
σ_{OH}	–1.66(–7)	–8.02(–5)	–2.41(–3)	4.72(–2)	8.62(–1)
	–1.66(–7)	–8.02(–5)	–2.41(–3)	4.73(–2)	8.62(–1)
σ_{H}	2.88(–6)	8.71(–5)	1.74(–3)	1.33(–1)	9.81(–1)
	2.88(–6)	8.71(–5)	1.74(–3)	1.33(–1)	9.81(–1)
σ_{H_2}	1.93(–6)	3.84(–5)	5.32(–4)	6.98(–2)	2.83(–1)
	1.93(–6)	3.84(–5)	5.32(–4)	6.98(–2)	2.84(–1)
σ_{O}	4.77(–7)	–7.95(–6)	–1.65(–3)	1.08(–1)	1.05
	4.77(–7)	–7.95(–6)	–1.65(–3)	1.08(–1)	1.05
σ_{H_2O}	–6.40(–8)	–2.35(–5)	–8.91(–4)	1.05(–2)	1.57(–1)
	–6.40(–8)	–2.35(–5)	–8.91(–4)	1.05(–2)	1.58(–1)
σ_{CO}	–7.92(–6)	–1.59(–4)	–1.38(–3)	–2.98(–4)	1.23(–1)
	–7.92(–6)	–1.59(–4)	–1.38(–3)	–2.97(–4)	1.23(–1)
$\sigma_{C_2H_2}$	–2.09(–8)	7.41(–6)	–3.23(–4)	–6.59(–3)	–3.48(–1)
	–2.09(–8)	7.41(–6)	–3.23(–4)	–6.59(–3)	–3.48(–1)
σ_{CO_2}	9.83(–1)	8.13(–1)	6.07(–1)	3.71(–1)	8.35(–1)
	9.83(–1)	8.13(–1)	6.07(–1)	3.71(–1)	8.35(–1)
T	5.05(–12)	5.02(–8)	4.24(–6)	4.85(–3)	5.66(–2)
	5.05(–12)	5.02(–8)	4.24(–6)	4.85(–3)	5.67(–2)
p	4.96(–12)	4.71(–8)	3.60(–6)	4.84(–3)	6.07(–2)
	4.96(–12)	4.71(–8)	3.60(–6)	4.84(–3)	6.07(–2)

[a]For each dependent variable the top row gives the BFM results and the bottom row gives the LSENS results. Numbers in parentheses denote powers of 10.

TABLE 4.97.—NORMALIZED SENSITIVITY COEFFICIENTS WITH RESPECT TO RATE COEFFICIENT PARAMETER c_{101} OF SPECIAL RATE COEFFICIENT EXPRESSION, EQUATION (2.5), FOR TEST PROBLEM 9

Dependent variable	Normalized sensitivity coefficients with respect to c_{101} at[a]				
	10^{-6} s	10^{-5} s	6×10^{-5} s	2.8×10^{-4} s	3×10^{-4} s
$\sigma_{C_6H_6}$	9.22(–12) 9.22(–12)	1.36(–7) 1.36(–7)	5.33(–5) 5.33(–5)	–1.33(–2) –1.33(–2)	–4.78(–1) –4.79(–1)
σ_{O_2}	–2.60(–12) –2.60(–12)	–2.67(–9) –2.67(–9)	2.58(–6) 2.58(–6)	–3.31(–3) –3.31(–3)	–8.83(–2) –8.84(–2)
σ_{OH}	–1.66(–7) –1.66(–7)	–8.03(–5) –8.03(–5)	–2.43(–3) –2.43(–3)	5.07(–2) 5.07(–2)	9.82(–1) 9.82(–1)
σ_H	2.88(–6) 2.88(–6)	8.72(–5) 8.72(–5)	1.75(–3) 1.75(–3)	1.48(–1) 1.48(–1)	1.14 1.14
σ_{H_2}	1.93(–6) 1.93(–6)	3.84(–5) 3.84(–5)	5.35(–4) 5.35(–4)	7.66(–2) 7.66(–2)	3.33(–1) 3.33(–1)
σ_O	4.77(–7) 4.77(–7)	–7.95(–6) –7.95(–6)	–1.66(–3) –1.66(–3)	1.20(–1) 1.20(–1)	1.22 1.22
σ_{H_2O}	–6.40(–8) –6.40(–8)	–2.35(–5) –2.35(–5)	–8.96(–4) –8.96(–4)	1.11(–2) 1.12(–2)	1.78(–1) 1.78(–1)
σ_{CO}	–7.92(–6) –7.92(–6)	–1.59(–4) –1.59(–4)	–1.39(–3) –1.39(–3)	–6.02(–4) –6.01(–4)	1.36(–1) 1.36(–1)
$\sigma_{C_2H_2}$	–2.09(–8) –2.09(–8)	7.42(–6) 7.42(–6)	–3.25(–4) –3.25(–4)	–7.29(–3) –7.29(–3)	–4.02(–1) –4.02(–1)
σ_{CO_2}	9.83(–1) 9.83(–1)	8.14(–1) 8.14(–1)	6.10(–1) 6.10(–1)	4.07(–1) 4.07(–1)	9.86(–1) 9.86(–1)
T	5.05(–12) 5.05(–12)	5.03(–8) 5.03(–8)	4.27(–6) 4.27(–6)	5.29(–3) 5.29(–3)	6.52(–2) 6.52(–2)
p	4.96(–12) 4.96(–12)	4.72(–8) 4.72(–8)	3.62(–6) 3.62(–6)	5.27(–3) 5.27(–3)	6.98(–2) 6.98(–2)

[a]For each dependent variable the top row gives the BFM results and the bottom row gives the LSENS results. Numbers in parentheses denote powers of 10.

which solves a nonlinear system of $2N$ equations. The DDM maintains accuracy and stability of the solution by using exactly the same step lengths and numerical approximations as those used for the model problem. It is therefore more accurate and efficient than the decoupled version of the DM, which computes the sensitivity coefficients after the model problem has been solved over the entire integration interval. The decoupling procedure used in the decoupled version of the DM can result in interpolation errors with attendant accuracy and stability problems and increased computational cost.

The DDM was also more stable, accurate, and efficient than the Green's function methods. The accuracy and efficiency of the GFM and GFM/AIM can be adversely affected by the choice of output stations. The computational cost may rise significantly as the number of output stations is increased. In contrast, the computational cost of the DDM is essentially independent of the number of output stations. Another advantage of the present version of the DDM is that, unlike the GFM/AIM, it requires no additional local error tolerances beyond those required for the model problem. The accuracy and efficiency of the GFM/AIM can be adversely affected by poor choices for the error tolerances. Hence the DDM is easier to use because it does not require separate trial-and-error optimizations of the error tolerances for the kinetics solution and the sensitivity coefficients. If, as is usually the case when developing a reaction mechanism, only rate coefficient parameter sensitivities are required, the DDM is even more efficient than the GFM and GFM/AIM, because the DDM does not then have to solve for the initial condition sensitivities. In contrast, the GFM and GFM/AIM must still calculate the Green's function matrix (which is related to the initial condition sensitivities) before the rate coefficient parameter sensitivities can be evaluated.

The effects of including local error tests and control for the sensitivity coefficients were explored by comparing the results for test problems 4 and 7 to 9 with other versions of the DDM that perform these operations. The present version of the DDM was shown to be both more accurate and more efficient. Thus the need for local error control during the sensitivity analysis computations is not clear. These studies also showed the importance of ensuring relative error control for the kinetics calculation. That is, the local absolute error tolerance, ATOLSP, must be sufficiently small to guarantee this result for all variables with magnitude larger than a minimum value. Even an ATOLSP that achieved this result for only mole fractions ≥ 0.1 ppm produced significantly more accurate sensitivity coefficients for all EMAX values studied than ATOLSP = 10^{-2}EMAX. For test problem 6 the smaller ATOLSP produced the correct reaction importance lists (and accurate sensitivity coefficients) with EMAX = 10^{-3}, whereas EMAX = 10^{-6} and ATOLSP = 10^{-8} did not, despite using a much smaller EMAX. These observations also support the argument that the error control in the solution of the sensitivity equations is determined by the error control in the solution of the kinetics equations. It would therefore appear to be more efficient to produce a more accurate kinetics solution than to measure and control the local errors incurred by the sensitivity coefficients.

This hypothesis was tested by performing several experiments with the code SENKIN (ref. 102) on test problems 7 to 9. It was found that decreasing the local error tolerances for the sensitivity coefficients did not necessarily improve accuracy, but the computational cost could become prohibitive. The general conclusion was that, to improve accuracy, it is preferable to increase the accuracy of the kinetics solution than to use small RTLS and ATLS. For sufficiently small EMAX and ATOLSP the sensitivity coefficients were insensitive to RTLS and ATLS during induction and heat release, but larger tolerances produced more accurate solutions during equilibration. The latter observation was tentatively attributed to the finite-difference approximations used for the partial derivatives $\{\partial f_i/\partial \eta_j\}$ in SENKIN. Nonetheless the need for error control during sensitivity analysis was not established, because LSENS produced more accurate results than SENKIN. The results for the varying-temperature problems reiterated the efficiency gains that can be achieved for chemical kinetics calculations by supplying an analytical Jacobian matrix, instead of using finite-difference approximations for the elements of this matrix.

LSENS was shown to be more efficient than the other techniques and codes examined. For test problems 4 and 6 execution times for several types of calculation—kinetics only, kinetics plus initial condition sensitivities, etc.—were much less for LSENS than for the other methods and codes. More specifically LSENS was as much as a factor of 2.5 more efficient than CHEMDDM and shown to be as much as a factor of almost 17 more efficient than a recent version of the GFM/AIM. Comparison of relative execution times for a problem describing the constant-density, constant-temperature oxidation of CO in the presence of H_2O confirmed the superior efficiency of LSENS. The results for test problems 7 to 9 showed that LSENS was a factor of approximately 4 faster than SENKIN. LSENS has several additional advantages over CHEMDDM and SENKIN. If sensitivities with respect to all parameters are not needed, LSENS is much more efficient than the other two codes because LSENS computes only the required sensitivities, whereas CHEMDDM solves for all initial condition and/or all rate constant sensitivities and SENKIN solves for all preexponential factor sensitivities. More significantly LSENS can be used for constant- and varying-temperature problems and for constant- and varying-density problems, whereas CHEMDDM is restricted to constant-temperature, constant-density problems. Similarly effects of uncertainties in initial condition values and all rate coefficient parameters can be studied with LSENS, but only the preexponential factor sensitivities can be computed with SENKIN.

This work has demonstrated the difficulty of producing reliable sensitivity coefficients with the brute force method. The solutions were strongly dependent on the finite-difference increments, which had to be selected with care. The importance of generating very accurate kinetics solutions by using very small local error tolerances was also illustrated. The need to control roundoff errors by increasing the precision of the arithmetic was found to be just as critical as the use of small EMAX and the "correct" finite-difference increment. These factors and the trial-and-error procedures required to determine both the finite-difference increment and the

EMAX that must be used make the BFM prohibitively expensive and time consuming if accurate sensitivity coefficients are desired.

For nonisothermal problems the DDM needed a rather small local relative error tolerance to track accurately the sensitivity coefficients during equilibration. The required EMAX was much smaller than that needed during heat release or for constant-temperature problems. This finding is surprising and requires further study to explain its cause.

Chapter 5
Chemical Equilibrium

The computation of the chemical equilibrium state, that is, the final state reached by a chemical reaction, is an important problem with many practical applications. For example, for combustion reactions one is often interested in how fast and how closely the kinetic process approaches the equilibrium state. Applications of chemical equilibrium calculations are discussed by van Zeggeren and Storey (ref. 112) and Gordon and McBride (ref. 113).

The problem of computing the chemical equilibrium state has been studied extensively and, as discussed in references 112 and 114 to 116, a number of solution procedures and computer codes have been developed. In the present work the solution method developed by Gordon and McBride (ref. 113) and the most recent version of their computer code, CET (ref. 117), were adapted. This code has been tested on a variety of problems and is widely accepted. However, here attention is restricted to ideal-gas mixtures and, unlike CET, condensed species are not considered.

The chemical equilibrium state for a given initial mixture composition can be obtained when any two independent thermodynamic state functions are assigned fixed values. The present work considers equilibrium calculations for four sets of assigned functions (abbreviations used in the discussion are given in parentheses):

(1) Temperature and pressure (TP)
(2) Specific enthalpy and pressure (HP)
(3) Temperature and specific volume or density (TV)
(4) Specific internal energy and specific volume or density (UV)

The chemical equilibrium state is computed for TP and HP problems by minimizing the Gibbs function and for TV and UV problems by minimizing the Helmholtz function. The advantages of minimization over other methods of computing the chemical equilibrium state are discussed in references 112, 113, and 115.

This chapter presents the equations and solution procedure used to compute the chemical equilibrium state. The accuracy of the LSENS code is illustrated by comparisons with CET for several example problems.

5.1 Equations Describing Chemical Equilibrium

For assigned-temperature problems the chemical equilibrium composition, that is, $\sigma_{j,eq}$ (j = 1,...,NS), is solved for. Here $\sigma_{j,eq}$ is the mole number of the jth species—number of moles of species j per unit mass of mixture—at chemical equilibrium, and NS is the total number of chemical species. For HP and UV problems the equilibrium temperature T_{eq} must also be computed; therefore an additional equation is required. The governing equations for the different problem types are derived in the following subsections.

5.1.1 Assigned-Pressure Problems

For an assigned-pressure and assigned-temperature (i.e., TP) problem the chemical equilibrium composition is obtained by minimizing the mixture mass-specific Gibbs function g given by (e.g., refs. 118 and 119)

$$g = \sum_{j=1}^{NS} \mu_j \sigma_j \tag{5.1}$$

In this equation μ_j is the chemical potential of the jth species and is defined by

$$\mu_j = \left(\frac{\partial g}{\partial \sigma_j} \right)_{p,T,\text{ all other } \sigma_k} \tag{5.2}$$

where p is the pressure and T the temperature. For ideal gases

$$\mu_j = g_j \tag{5.3}$$

where g_j is the molar-specific Gibbs function of the jth species. At pressure p and temperature T, $g_j(p,T)$ is given by (e.g., ref. 119)

$$g_j(p,T) = g_j^\circ(T) + RT \ln \frac{\sigma_j}{\sigma_m} + RT \ln \frac{p}{p_{st}}, \qquad j = 1,\ldots,NS \tag{5.4}$$

Here $g_j^\circ(T)$ is the molar-specific Gibbs function of the jth species at a standard pressure p_{st} (e.g., 1 atm) and temperature T, R the universal gas constant, and σ_m the sum of the species mole numbers:

$$\sigma_m = \sum_{j=1}^{NS} \sigma_j \tag{5.5}$$

For TP problems the criterion for chemical equilibrium is given by (refs. 118 and 119)

$$(dg)_{p,T} = \sum_{j=1}^{NS} \mu_j d\sigma_j = 0 \tag{5.6}$$

which upon using equation (5.3) can be rewritten as

$$\sum_{j=1}^{NS} g_j d\sigma_j = 0 \tag{5.7}$$

for ideal-gas mixtures.

Conservation of atomic species provides the following constraints on the minimization:

$$b_i = b_{i,0}, \quad i = 1, ..., \text{NLM} \tag{5.8}$$

In this equation b_i is the total number of atoms of element i per unit mass of mixture, $b_{i,0}$ the value of b_i for the initial mixture, and NLM the total number of elements. If charged or ionic species are present in the gas mixture, the element list includes the electron in addition to the atomic species. For a gas mixture

$$b_i = \sum_{j=1}^{NS} a_{ij} \sigma_j, \quad i = 1, ..., \text{NLM} \tag{5.9}$$

where a_{ij} is the number of atoms of element i in one molecule of species j. If charged species are included in the mixture, some a_{ij} have negative values; otherwise, all a_{ij} are positive. By substituting equation (5.9) into equation (5.8) the NLM atom and charge balance constraints can be expressed as

$$\sum_{j=1}^{NS} a_{ij} \sigma_j = b_{i,0}, \quad i = 1, ..., \text{NLM} \tag{5.10}$$

The problem of minimization subject to several constraints is solved by using Lagrange's method (e.g., refs. 120 and 121) as follows: First, note that the total differential dg of the Gibbs function must vanish at its minimum point (ref. 121), as already observed (see eqs. (5.6) and (5.7)). Next, because each b_i ($i = 1,...,$NLM) is equal to a constant ($b_{i,0}$, see eq. (5.8)), its total differential db_i is also equal to zero. Hence from equation (5.9)

$$db_i = \sum_{j=1}^{NS} a_{ij} d\sigma_j = 0, \qquad i = 1,..., \text{NLM} \tag{5.11}$$

Multiplying equation (5.11) by some parameter λ_i, summing over all i, and then adding the resulting equation to equation (5.7) give

$$\sum_{j=1}^{NS} g_j d\sigma_j + \sum_{i=1}^{NLM} \lambda_i \sum_{j=1}^{NS} a_{ij} d\sigma_j = 0 \tag{5.12}$$

where the as yet unknown $\{\lambda_i\}$ are called Lagrange multipliers. Equation (5.12) can be rewritten as

$$\sum_{j=1}^{NS} \left(g_j + \sum_{i=1}^{NLM} \lambda_i a_{ij} \right) d\sigma_j = 0 \tag{5.13}$$

Finally, by regarding the increments $\{d\sigma_j\}$ as independent of one another, the following conditions are obtained:

$$g_j + \sum_{i=1}^{NLM} \lambda_i a_{ij} = 0, \qquad j = 1,..., \text{NS} \tag{5.14}$$

The equations used in the present work for the thermodynamic properties produce the nondimensional quantities $\{g_j^\circ/(RT)\}$ (see chapter 8 of part II). Repeated multiplications by RT to give the $\{g_j^\circ\}$ are avoided by dividing equation (5.14) by RT to get

$$\frac{g_j}{RT} - \sum_{i=1}^{NLM} a_{ij} \pi_i = 0, \qquad j = 1,..., \text{NS} \tag{5.15}$$

where

$$\pi_i = -\frac{\lambda_i}{RT}, \quad i = 1,\ldots,\mathrm{NLM} \tag{5.16}$$

Finally the expression for $g_j/(RT)$ obtained from equation (5.4) is substituted into equation (5.15) to get

$$\frac{g_j^\circ}{RT} + \ln\frac{\sigma_j}{\sigma_m} + \ln\frac{p}{p_{\mathrm{st}}} - \sum_{i=1}^{\mathrm{NLM}} a_{ij}\pi_i = 0, \quad j = 1,\ldots,\mathrm{NS} \tag{5.17}$$

Equations (5.10) and (5.17) together form a set of NLM + NS equations, and so the π_i (i = 1,...,NLM) and σ_j (j = 1,...,NS) can be computed for assigned p and T. Now the sum σ_m of species mole numbers appears explicitly as a variable in equation (5.17). For computational convenience σ_m is therefore treated as an unknown and is determined by solving equation (5.5).

For HP problems the additional equation required to evaluate the temperature is given by

$$h = h_0 \tag{5.18}$$

where h is the mixture mass-specific enthalpy and h_0 the assigned (e.g., initial) mixture mass-specific enthalpy. For a mixture of gases

$$h = \sum_{j=1}^{\mathrm{NS}} \sigma_j h_j \tag{5.19}$$

where h_j is the molar-specific enthalpy of the jth species. Hence equation (5.18) becomes

$$\sum_{j=1}^{\mathrm{NS}} \sigma_j h_j = h_0 \tag{5.20}$$

5.1.2 Assigned-Specific-Volume Problems

For an assigned-specific-volume and assigned-temperature (i.e., TV) problem the equilibrium composition is obtained by minimizing the mixture mass-specific Helmholtz function a, and the criterion for chemical equilibrium is given by (refs. 118 and 119)

$$(da)_{v,T} = \sum_{j=1}^{NS} \mu_j d\sigma_j = 0 \tag{5.21}$$

where v is the specific volume. Examination of equations (5.6) and (5.21) shows that the chemical equilibrium criteria for TP and TV problems are identical. Indeed the criterion

$$\sum_{j=1}^{NS} \mu_j d\sigma_j = 0$$

must be satisfied by any closed system in chemical equilibrium (ref. 119).

This minimization problem is also subject to the NLM atom and charge balance constraints, equation (5.10). Hence for this problem also the NS conditions given by equation (5.14) are obtained for ideal-gas mixtures by using Lagrange's method. However, because the natural variables for a are v, T, and $\{\sigma_j\}$ (ref. 122), the expression for g_j given by equation (5.4), in which the variables are p, T, and $\{\sigma_j\}$, is not used. Instead by using the ideal-gas equation of state

$$pv = RT\sigma_m \tag{5.22}$$

equation (5.4) is rewritten as

$$g_j = g_j^\circ + RT \ln \frac{\sigma_j RT}{v p_{st}}, \qquad j = 1,\ldots,NS \tag{5.23}$$

which is substituted into equation (5.14); for reasons given in section 5.1.1, the resulting equation is then made dimensionless by dividing it by RT. These operations give the following conditions for TV problems:

$$\frac{g_j^\circ}{RT} + \ln \frac{\sigma_j RT}{v p_{st}} - \sum_{i=1}^{NLM} a_{ij}\pi_i = 0, \qquad j = 1,\ldots,NS \tag{5.24}$$

where π_i is given by equation (5.16).

Equations (5.10) and (5.24) together form a set of NLM + NS equations, and so the π_i (i = 1,...,NLM) and σ_j (j = 1,...,NS) can be computed for assigned values of v (or density ρ) and T. For this problem type, σ_m is not treated as an unknown because it does not appear explicitly in equation (5.24). Instead σ_m is assumed to be defined by equation (5.5).

For UV problems the additional equation required to evaluate the temperature is given by

$$u = u_0 \tag{5.25}$$

where u is the mixture mass-specific internal energy and u_0 the assigned (e.g., initial) mixture mass-specific internal energy. For a gas mixture

$$u = \sum_{j=1}^{NS} \sigma_j u_j \tag{5.26}$$

where u_j is the molar-specific internal energy of the jth species. Substituting equation (5.26) into equation (5.25) gives

$$\sum_{j=1}^{NS} \sigma_j u_j = u_0 \tag{5.27}$$

5.2 Solution Method

The algebraic equations given in section 5.1 are solved by using a descent Newton-Raphson (NR) iteration method (refs. 113 and 115). However, because the $\{\pi_i\}$ appear linearly in equations (5.17) and (5.24), at each iteration these variables, rather than their corrections, are solved for directly. Also, in order to avoid negative species concentrations and temperature, $\{\ln \sigma_j\}$, $\ln \sigma_m$, and $\ln T$ are solved for. Of course, for assigned-specific-volume problems σ_m is not a dependent variable. Similarly for assigned-temperature problems T is not an unknown quantity. Nevertheless for the sake of generality the two variables are included in this discussion.

Starting with initial estimates, denoted by $\{\sigma_j^{[0]}\}$, $\sigma_m^{[0]}$, and $T^{[0]}$, the NR iteration procedure generates successive approximations $\{\pi_i^{[m]}\}$, $\{\sigma_j^{[m]}\}$, $\sigma_m^{[m]}$, and $T^{[m]}$ ($m = 1,...,M$) until the iteration converges; that is, the magnitude of the difference in two successive approximations approaches zero within a specified accuracy. Here $[m]$ denotes the iteration number and M is the number of iterations required for convergence. The converged solution gives the chemical equilibrium composition and temperature:

$$\sigma_{j,\mathrm{eq}} = \sigma_j^{[M]}, \quad j = 1,...,\mathrm{NS} \tag{5.28a}$$

$$\sigma_{m,\mathrm{eq}} = \sigma_m^{[M]} \tag{5.28b}$$

$$T_{\mathrm{eq}} = T^{[M]} \tag{5.28c}$$

The procedure used to produce the $(m + 1)$th approximations ($m = 0,1,...,M-1$) from the mth estimates and the algebraic equations given in section 5.1 is as follows: The mth estimates ($m = 0,1,...,M$) for the logarithmic variables are denoted by $\ln \sigma_j^{[m]}$ ($j = 1,...,\mathrm{NS}$), $\ln \sigma_m^{[m]}$, and $\ln T^{[m]}$, and the corrections generated on the $(m + 1)$th iteration ($m = 0,1,...,M-1$) by $\Delta\ln \sigma_j^{[m]}$ ($j = 1,...,\mathrm{NS}$), $\Delta\ln \sigma_m^{[m]}$, and $\Delta\ln T^{[m]}$. The iteration procedure for assigned-pressure problems is discussed first, and then assigned-specific-volume problems are considered.

5.2.1 Assigned-Pressure Problems

For assigned-pressure problems, equations (5.5), (5.10), and (5.17) and, for HP problems, (5.20) have to be solved. The NR iteration equations for $\{\pi_i^{[m+1]}\}$ and the corrections $\{\Delta\ln \sigma_j^{[m]}\}$, $\Delta\ln \sigma_m^{[m]}$, and $\Delta\ln T^{[m]}$ on the $(m + 1)$th iteration, obtained from these four equations, are as follows:

$$\sum_{k=1}^{\mathrm{NS}} a_{ik}\sigma_k^{[m]}\,\Delta\ln \sigma_k^{[m]} = b_{i,0} - b_i^{[m]}, \quad i = 1,...,\mathrm{NLM} \tag{5.29}$$

$$-\sum_{k=1}^{\mathrm{NLM}} a_{kj}\pi_k^{[m+1]} + \Delta\ln \sigma_j^{[m]} - \Delta\ln \sigma_m^{[m]} - \frac{h_j^{[m]}}{RT^{[m]}}\Delta\ln T^{[m]} = -\frac{g_j^{[m]}}{RT^{[m]}},$$

$$j = 1,...,\mathrm{NS} \tag{5.30}$$

$$-\sum_{k=1}^{\mathrm{NS}} \sigma_k^{[m]}\,\Delta\ln \sigma_k^{[m]} + \sigma_m^{[m]}\,\Delta\ln \sigma_m^{[m]} = \sum_{k=1}^{\mathrm{NS}} \sigma_k^{[m]} - \sigma_m^{[m]} \tag{5.31}$$

$$\sum_{k=1}^{\mathrm{NS}} \sigma_k^{[m]} h_k^{[m]}\,\Delta\ln \sigma_k^{[m]} + \sum_{k=1}^{\mathrm{NS}} \sigma_k^{[m]} c_{p,k}^{[m]} T^{[m]}\,\Delta\ln T^{[m]} = h_0 - h^{[m]} \tag{5.32}$$

In equations (5.29) to (5.32), $h_j^{[m]}$ is the molar-specific enthalpy of the jth species at temperature $T^{[m]}$, $c_{p,k}^{[m]}$ is the constant-pressure, molar-specific heat of the kth species at temperature $T^{[m]}$,

$$b_i^{[m]} = \sum_{j=1}^{NS} a_{ij}\sigma_j^{[m]}, \quad i = 1,...,NLM \tag{5.33}$$

$$g_j^{[m]} = g_j^{\circ}\left(T^{[m]}\right) + RT^{[m]} \ln\frac{\sigma_j^{[m]}}{\sigma_m^{[m]}} + RT^{[m]} \ln\frac{p}{p_{st}}, \quad j = 1,...,NS \tag{5.34}$$

and

$$h^{[m]} = \sum_{j=1}^{NS} \sigma_j^{[m]} h_j^{[m]} \tag{5.35}$$

Also the facts that for any variables y and ζ

$$\frac{\partial y}{\partial \ln \zeta} = \zeta \frac{\partial y}{\partial \zeta} \tag{5.36}$$

and (e.g., ref. 119)

$$\frac{\partial}{\partial T}\left(\frac{g_j^{\circ}}{RT}\right) = -\frac{h_j}{RT^2}, \quad j = 1,...,NS \tag{5.37}$$

have been used. For computational convenience equation (5.32) is divided by $RT^{[m]}$:

$$\sum_{k=1}^{NS} \sigma_k^{[m]} \frac{h_k^{[m]}}{RT^{[m]}} \Delta \ln \sigma_k^{[m]} + \sum_{k=1}^{NS} \sigma_k^{[m]} \frac{c_{p,k}^{[m]}}{R} \Delta \ln T^{[m]} = \frac{h_0 - h^{[m]}}{RT^{[m]}} \tag{5.38}$$

Equations (5.29) to (5.31) and (5.38) together form a set of NLM + NS + 2 linear equations. Of course, for a TP problem, $\Delta \ln T^{[m]} = 0$ and equation (5.38) is not needed. Therefore NLM + NS + 1 equations have to be solved for $\pi_i^{[m+1]}$ ($i = 1,...,NLM$), $\Delta \ln \sigma_j^{[m]}$ ($j = 1,...,NS$), and $\Delta \ln \sigma_m^{[m]}$. The solution for the correction variables requires inversion of a matrix of size (NLM + NS + 2)×(NLM + NS + 2) for HP problems and (NLM + NS + 1)×(NLM + NS + 1) for TP problems. The computational cost associated with the matrix inversion can be considerable, especially when the number of species is large.

The computational work is reduced quite simply by reducing the number of equations (ref. 113). Equation (5.30) gives the following solution for the correction $\Delta\ln \sigma_j^{[m]}$:

$$\Delta\ln \sigma_j^{[m]} = \sum_{k=1}^{\mathrm{NLM}} a_{kj}\pi_k^{[m+1]} + \Delta\ln \sigma_m^{[m]} + \frac{h_j^{[m]}}{RT^{[m]}}\Delta\ln T^{[m]} - \frac{g_j^{[m]}}{RT^{[m]}} \tag{5.39}$$

This expression is substituted into equations (5.29), (5.31), and (5.38). After rearrangement the resulting reduced equation set can be expressed compactly as

$$\mathcal{J}\underline{Y}_p = \underline{\mathcal{E}}_p \tag{5.40}$$

where the various terms are defined below and the subscript p is used to indicate an assigned-pressure problem. The (NLM + 2)-dimensional column vector $\underline{Y}_p$ is given by

$$\underline{Y}_p = \left(\pi_1^{[m+1]}, \ldots, \pi_{\mathrm{NLM}}^{[m+1]}, \Delta\ln \sigma_m^{[m]}, \Delta\ln T^{[m]}\right)^T \tag{5.41}$$

where the superscript T indicates transpose. The elements $\mathcal{E}_{p,i}$ (i = 1,...,NLM+2) of the column vector $\underline{\mathcal{E}}_p$ are defined as

$$\mathcal{E}_{p,i} = b_{i,0} - b_i^{[m]} + \sum_{j=1}^{\mathrm{NS}} a_{ij}\sigma_j^{[m]}\frac{g_j^{[m]}}{RT^{[m]}}, \qquad i = 1, \ldots, \mathrm{NLM} \tag{5.42a}$$

$$\mathcal{E}_{p,\mathrm{NLM+1}} = \sigma_m^{[m]} - \sum_{j=1}^{\mathrm{NS}} \sigma_j^{[m]} + \sum_{j=1}^{\mathrm{NS}} \sigma_j^{[m]}\frac{g_j^{[m]}}{RT^{[m]}} \tag{5.42b}$$

$$\mathcal{E}_{p,\mathrm{NLM+2}} = \frac{h_0 - h^{[m]}}{RT^{[m]}} + \sum_{j=1}^{\mathrm{NS}} \sigma_j^{[m]}\frac{h_j^{[m]}}{RT^{[m]}}\frac{g_j^{[m]}}{RT^{[m]}} \tag{5.42c}$$

The (NLM + 2)×(NLM + 2) matrix $\mathcal{J}$ is given by

$$\mathcal{G} = \begin{pmatrix} \sum a_{1j}a_{1j}\sigma_j & \sum a_{1j}a_{2j}\sigma_j & \cdots & \sum a_{1j}a_{Lj}\sigma_j & \sum a_{1j}\sigma_j & \sum a_{1j}\sigma_j \frac{h_j}{RT} \\ \sum a_{2j}a_{1j}\sigma_j & \sum a_{2j}a_{2j}\sigma_j & \cdots & \sum a_{2j}a_{Lj}\sigma_j & \sum a_{2j}\sigma_j & \sum a_{2j}\sigma_j \frac{h_j}{RT} \\ \vdots & \vdots & & \vdots & \vdots & \vdots \\ \sum a_{Lj}a_{1j}\sigma_j & \sum a_{Lj}a_{2j}\sigma_j & \cdots & \sum a_{Lj}a_{Lj}\sigma_j & \sum a_{Lj}\sigma_j & \sum a_{Lj}\sigma_j \frac{h_j}{RT} \\ \sum a_{1j}\sigma_j & \sum a_{2j}\sigma_j & \cdots & \sum a_{Lj}\sigma_j & \sum \sigma_j - \sigma_m & \sum \sigma_j \frac{h_j}{RT} \\ \sum a_{1j}\sigma_j \frac{h_j}{RT} & \sum a_{2j}\sigma_j \frac{h_j}{RT} & \cdots & \sum a_{Lj}\sigma_j \frac{h_j}{RT} & \sum \sigma_j \frac{h_j}{RT} & \sum \sigma_j \left[\frac{c_{p,j}}{R} + \left(\frac{h_j}{RT} \right)^2 \right] \end{pmatrix} \tag{5.43}$$

where for clarity in presentation the summation limits (j = 1 to NS) and the iteration number have been suppressed and the new variable L (= NLM) has been introduced.

For TP problems the appropriate $\underline{Y}_p$ and $\underline{\mathcal{E}}_p$ vectors and the $\mathcal{G}$ matrix are obtained by deleting (1) $Y_{p,\mathrm{NLM+2}}$ and $\mathcal{E}_{p,\mathrm{NLM+2}}$, (2) the last term from the expression for $\mathcal{E}_{p,i}$ (i = 1,...,NLM+1), and (3) the last row and last column from the matrix given by equation (5.43).

Note that the number of equations has been reduced from NLM + NS + 2 to NLM + 2 for HP problems and from NLM + NS + 1 to NLM + 1 for TP problems. Because, in general, NS >> NLM, this reduction is significant and should result in substantially smaller CPU times. In addition, the symmetry of the iteration matrix $\mathcal{G}$ (i.e., $\mathcal{G}_{ik} = \mathcal{G}_{ki}$, i,k = 1,...,NLM+2, see eq. (5.43)) can be exploited to reduce significantly the computational cost of forming the matrix.

5.2.2 Assigned-Specific-Volume Problems

For assigned-specific-volume problems equations (5.10) and (5.24) and, for UV problems, (5.27) have to be solved. The NR iteration equations for the $(m + 1)$th iteration $(m = 0,1,...,M-1)$ obtained from these equations can be written as

$$\sum_{k=1}^{NS} a_{ik}\sigma_k^{[m]}\,\Delta\ln\sigma_k^{[m]} = b_{i,0} - b_i^{[m]}, \qquad i = 1,...,\mathrm{NLM} \tag{5.44}$$

$$-\sum_{k=1}^{NLM} a_{kj}\pi_k^{[m+1]} + \Delta\ln\sigma_j^{[m]} - \frac{u_j^{[m]}}{RT^{[m]}}\Delta\ln T^{[m]} = -\frac{g_j^{[m]}}{RT^{[m]}}, \qquad j = 1,...,\mathrm{NS} \tag{5.45}$$

$$\sum_{k=1}^{NS}\sigma_k^{[m]}\,u_k^{[m]}\,\Delta\ln\sigma_k^{[m]} + \sum_{k=1}^{NS}\sigma_k^{[m]}\,c_{V,k}^{[m]}\,T^{[m]}\,\Delta\ln T^{[m]} = u_0 - u^{[m]} \tag{5.46}$$

In equations (5.44) to (5.46), $u_j^{[m]}$ is the molar-specific internal energy of the jth species at temperature $T^{[m]}$, $c_{V,k}^{[m]}$ is the constant-volume, molar-specific heat of the kth species at temperature $T^{[m]}$, $b_i^{[m]}$ is given by equation (5.33),

$$g_j^{[m]} = g_j^{\circ}\left(T^{[m]}\right) + RT^{[m]}\ln\frac{\sigma_j^{[m]}RT^{[m]}}{Vp_{st}}, \qquad j = 1,...,\mathrm{NS} \tag{5.47}$$

and

$$u^{[m]} = \sum_{j=1}^{NS}\sigma_j^{[m]}u_j^{[m]} \tag{5.48}$$

Also equations (5.36) and (5.37) have been used. For computational convenience equation (5.46) is divided by $RT^{[m]}$:

$$\sum_{k=1}^{NS}\sigma_k^{[m]}\frac{u_k^{[m]}}{RT^{[m]}}\Delta\ln\sigma_k^{[m]} + \sum_{k=1}^{NS}\sigma_k^{[m]}\frac{c_{V,k}^{[m]}}{R}\Delta\ln T^{[m]} = \frac{u_0 - u^{[m]}}{RT^{[m]}} \tag{5.49}$$

Equations (5.44), (5.45), and (5.49) together form a set of NLM + NS + 1 linear equations. For a TV problem $\Delta \ln T^{[m]} = 0$ and equation (5.49) is not needed. By using the same procedure utilized for assigned-pressure problems, a considerably reduced set of equations is derived. Equation (5.45) is solved for the correction variable $\Delta \ln \sigma_j^{[m]}$:

$$\Delta \ln \sigma_j^{[m]} = \sum_{k=1}^{\mathrm{NLM}} a_{kj} \pi_k^{[m+1]} + \frac{u_j^{[m]}}{RT^{[m]}} \Delta \ln T^{[m]} - \frac{g_j^{[m]}}{RT^{[m]}} \tag{5.50}$$

Equation (5.50) is then substituted into equations (5.44) and (5.49), and terms are rearranged to obtain the following reduced system of equations:

$$\mathcal{A} \underline{Y}_v = \underline{\mathcal{E}}_v \tag{5.51}$$

where the subscript v denotes an assigned-specific-volume problem. The (NLM + 1)-dimensional column vector $\underline{Y}_v$ is given by

$$\underline{Y}_v = \left(\pi_1^{[m+1]}, \ldots, \pi_{\mathrm{NLM}}^{[m+1]}, \Delta \ln T^{[m]} \right)^T \tag{5.52}$$

The elements $\mathcal{E}_{v,i}$ (i = 1,...,NLM+1) of the column vector $\underline{\mathcal{E}}_v$ are defined as

$$\mathcal{E}_{v,i} = b_{i,0} - b_i^{[m]} + \sum_{j=1}^{\mathrm{NS}} a_{ij} \sigma_j^{[m]} \frac{g_j^{[m]}}{RT^{[m]}}, \qquad i = 1, \ldots, \mathrm{NLM} \tag{5.53a}$$

and

$$\mathcal{E}_{v,\mathrm{NLM+1}} = \frac{u_0 - u^{[m]}}{RT^{[m]}} + \sum_{j=1}^{\mathrm{NS}} \sigma_j^{[m]} \frac{u_j^{[m]}}{RT^{[m]}} \frac{g_j^{[m]}}{RT^{[m]}} \tag{5.53b}$$

The (NLM + 1)×(NLM +1) matrix $\mathcal{A}$ is given by

$$\mathcal{A} = \begin{pmatrix} \sum a_{1j}a_{1j}\sigma_j & \sum a_{1j}a_{2j}\sigma_j & \cdots & \sum a_{1j}a_{Lj}\sigma_j & \sum a_{1j}\sigma_j \frac{u_j}{RT} \\ \sum a_{2j}a_{1j}\sigma_j & \sum a_{2j}a_{2j}\sigma_j & \cdots & \sum a_{2j}a_{Lj}\sigma_j & \sum a_{2j}\sigma_j \frac{u_j}{RT} \\ \vdots & \vdots & & \vdots & \vdots \\ \sum a_{Lj}a_{1j}\sigma_j & \sum a_{Lj}a_{2j}\sigma_j & \cdots & \sum a_{Lj}a_{Lj}\sigma_j & \sum a_{Lj}\sigma_j \frac{u_j}{RT} \\ \sum a_{1j}\sigma_j \frac{u_j}{RT} & \sum a_{2j}\sigma_j \frac{u_j}{RT} & \cdots & \sum a_{Lj}\sigma_j \frac{u_j}{RT} & \sum \sigma_j \left[\frac{c_{v,j}}{R} + \left(\frac{u_j}{RT} \right)^2 \right] \end{pmatrix} \tag{5.54}$$

where for purposes of clarity the summation limits (j = 1 to NS) and the iteration number have been suppressed, and NLM has been replaced by L. The number of equations has been reduced to NLM + 1 for UV problems and NLM for TV problems. Equation (5.54) shows that for this problem type also the iteration matrix is symmetric. For TV problems the appropriate $\underline{Y}_V$ and $\underline{\mathcal{E}}_V$ vectors and the $\mathcal{A}$ matrix are obtained by deleting (1) $Y_{V,\mathrm{NLM+1}}$ and $\mathcal{E}_{V,\mathrm{NLM+1}}$, (2) the last term from the expression for $\mathcal{E}_{V,i}$ (i = 1,...,NLM), and (3) the last row and the last column from the matrix given by equation (5.54).

5.2.3 Initial Estimates

The initial estimates $\{\sigma_j^{[0]}\}$, $\sigma_m^{[0]}$, and $T^{[0]}$ required to start the iteration procedure are given quite simply by (ref. 113)

$$\sigma_j^{[0]} = \frac{0.1}{NS}, \quad j = 1,...,NS \tag{5.55a}$$

$$\sigma_m^{[0]} = 0.1 \tag{5.55b}$$

$$T^{[0]} = 3800\ K \tag{5.55c}$$

These estimates may be very poor approximations to the equilibrium solutions. Nevertheless, they are used because of the simplicity of the calculation procedure, equations (5.55a) to (5.55c). Also use of these estimates has always resulted in convergence, with a typical number of iterations being of order O(10) (ref. 113).

5.2.4 Corrections Control

At each iteration the variables $\{Y_{p,i}\}$ or $\{Y_{v,i}\}$ are obtained by solving the appropriate equation, (5.40) or (5.51). The system of linear equations is solved by the Gaussian elimination method (ref. 35). The corrections $\{\Delta \ln \sigma_j^{[m]}\}$ for the species mole numbers are then given by equation (5.39) or (5.50). Corrections that are too large can lead to convergence difficulties if used unchanged to compute the new estimates (refs. 113, 117, and 123). Large corrections can arise for one of two reasons: (1) in the early stages of the iteration procedure because of poor initial estimates or (2) in later stages because of large increases in the concentration of trace species (refs. 113 and 115). An underrelaxation or control factor Λ is used to restrict the magnitude of the corrections to the variables. Gordon and McBride (ref. 117) have developed two empirical rules for computing Λ. The first is applied (1) to species k that satisfy the requirements $\Delta \ln \sigma_k^{[m]} > 0$ and $\sigma_k^{[m]} > 10^{-8}\ \sigma_m^{[m]}$, (2) to the sum of the mole numbers, and (3) to the temperature. It produces the parameter Λ_1, defined for the $(m + 1)$th iteration $(m = 0,1,...,M-1)$ by

$$\Lambda_1 = \frac{2}{\max\left(\left|5\ \Delta \ln T^{[m]}\right|, \left|5\ \Delta \ln \sigma_m^{[m]}\right|, \left|\Delta \ln \sigma_k^{[m]}\right|\right)} \tag{5.56}$$

$$\text{for } \Delta \ln \sigma_k^{[m]} > 0;\ \sigma_k^{[m]} > 10^{-8}\ \sigma_m^{[m]}$$

This equation limits the change in any variable to a factor $e^{0.4}$ (= 1.4918) or e^2 (= 7.3891).

The second rule is applied to every trace species k (defined here as species k for which $\sigma_k^{[m]} \le 10^{-8}\sigma_m^{[m]}$) that satisfies the requirement $\Delta\ln\sigma_k^{[m]} > 0$ and gives the parameter Λ_2, defined for the $(m+1)$th iteration ($m = 0,1,...,M-1$) as

$$\Lambda_2 = \min\left|\frac{\ln\left(10^{-4}\sigma_m^{[m]}/\sigma_k^{[m]}\right)}{\Delta\ln\sigma_k^{[m]} - \Delta\ln\sigma_m^{[m]}}\right| \quad \text{for} \quad \Delta\ln\sigma_k^{[m]} > 0;\ \sigma_k^{[m]} \le 10^{-8}\sigma_m^{[m]} \tag{5.57}$$

This parameter prevents a mole fraction ($= \sigma_k^{[m]}/\sigma_m^{[m]}$) that is less than or equal to 10^{-8} from increasing to more than 10^{-4}.

The control factor Λ is then given by

$$\Lambda = \min\left(1, \Lambda_1, \Lambda_2\right) \tag{5.58}$$

The new estimates $\{\ln\sigma_j^{[m+1]}\}$, $\ln\sigma_m^{[m+1]}$ and $\ln T^{[m+1]}$ are computed as

$$\ln\sigma_j^{[m+1]} = \ln\sigma_j^{[m]} + \Lambda\,\Delta\ln\sigma_j^{[m]}, \qquad j = 1,...,\mathrm{NS} \tag{5.59a}$$

$$\ln\sigma_m^{[m+1]} = \ln\sigma_m^{[m]} + \Lambda\,\Delta\ln\sigma_m^{[m]} \tag{5.59b}$$

$$\ln T^{[m+1]} = \ln T^{[m]} + \Lambda\,\Delta\ln T^{[m]} \tag{5.59c}$$

Finally the new estimates $\{\sigma_j^{[m+1]}\}$, $\sigma_m^{[m+1]}$ and $T^{[m+1]}$ are obtained by exponentiating the values given by equations (5.59a) to (5.59c). For trace species j, that is, species that satisfy the relation

$$\ln\sigma_j^{[m+1]} - \ln\sigma_m^{[m]} \le \ln 10^{-8} \tag{5.60}$$

the exponentiation is not performed, and $\sigma_j^{[m+1]}$ is set equal to zero.

5.2.5 Convergence Criteria

After each iteration several tests are made to ascertain convergence. First, the value of Λ is examined. When the variables are close to the correct values, Λ will be equal to unity; when they are far from the correct values, Λ will be less than unity (ref. 113). Therefore, if Λ is not equal to unity, a new iteration is performed.

If Λ is equal to unity, the mole number sum $\sigma_m^{[m+1]}$ is checked to ensure that it satisfies equation (5.5) for assigned-pressure problems. If the test

$$\left| \frac{\sigma_m^{[m+1]} - \sum_{j=1}^{NS} \sigma_j^{[m+1]}}{\sigma_m^{[m+1]}} \right| \overset{?}{\leq} 5 \times 10^{-6} \tag{5.61}$$

is not passed, a new iteration is performed. Next, the magnitude of $\Delta \ln T^{[m]}$ must satisfy

$$\left| \Delta \ln T^{[m]} \right| \overset{?}{\leq} 10^{-4} \tag{5.62}$$

The last test involves the magnitudes of the $\{\Delta \ln \sigma_j^{[m]}\}$, which must all satisfy the criterion

$$\left| \frac{\sigma_j^{[m+1]} \, \Delta \ln \sigma_j^{[m]}}{\sum_{k=1}^{NS} \sigma_k^{[m+1]}} \right| \overset{?}{\leq} 5 \times 10^{-6}, \quad j = 1, \ldots, NS \tag{5.63}$$

The iteration process is continued until either the estimates converge or 50 iterations have been performed without success when an error exit is taken. After successful convergence several thermodynamic properties are computed, as described in section 5.3. Also the mole numbers of trace species are set equal to 10^{-11}.

5.2.6 Singular Matrix

As discussed by Gordon and McBride (ref. 113) some situations can result in a singular $\mathcal{G}$ or $\mathcal{A}$ and cause the iteration method to fail. The singularity arises when one row of the iteration matrix is a multiple of another. This situation occurs because the iteration procedure assigns zero values for the concentrations of trace species.

When a singular matrix occurs, the mole numbers of trace species are set equal to 10^{-6} and the iteration process is continued. If, after this corrective action is taken, a singular matrix is again encountered, the iteration procedure is abandoned and an error exit taken.

5.3 Equilibrium Thermodynamic Properties

After the iteration converges, several thermodynamic properties are evaluated. For an assigned-pressure problem the density is obtained by using the ideal-gas equation of state, equation (5.22). This equation gives the pressure for an assigned-specific-volume problem. For an assigned-temperature problem the mixture mass-specific enthalpy h is given by equation (5.19) and the mixture mass-specific internal energy u by

$$u = h - RT\sigma_m \tag{5.64}$$

This equation is also used to compute u for an HP problem and h for a UV problem.

The mixture mass-specific entropy s is given by

$$s = \sum_{j=1}^{NS} \sigma_j \mathfrak{s}_j = \sum_{j=1}^{NS} \left(\sigma_j \mathfrak{s}_j^\circ(T) - RT \ln \frac{\sigma_j p}{\sigma_m p_{st}} \right) \tag{5.65}$$

where $\mathfrak{s}_j$ is the molar-specific entropy of the jth species and $\mathfrak{s}_j^\circ(T)$ the molar-specific entropy of the jth species at temperature T and pressure p_{st}. Finally the mean molar mass of the mixture M_w is obtained trivially as

$$M_w = 1/\sigma_m \tag{5.66}$$

In addition to the above thermodynamic properties several thermodynamic first derivatives are calculated. Now, among all possible first derivatives that can be constructed, only three are independent and any first derivative can be expressed in terms of the chosen set of three independent derivatives (ref. 122). The derivatives $(\partial v/\partial T)_p$, $(\partial v/\partial p)_T$, and $(\partial h/\partial T)_p$ are all measurable quantities and usually used as the three independent derivatives (e.g., refs. 26 and 119). However, Gordon and McBride (ref. 113) use the logarithmic form of the volume derivatives, $(\partial \ln v/\partial \ln T)_p$ and $(\partial \ln v/\partial \ln p)_T$. Equation (5.22) gives the following expressions for these two derivatives:

$$\left(\frac{\partial \ln v}{\partial \ln T} \right)_p = 1 + \left(\frac{\partial \ln \sigma_m}{\partial \ln T} \right)_p \tag{5.67}$$

and

$$\left(\frac{\partial \ln v}{\partial \ln p} \right)_T = -1 + \left(\frac{\partial \ln \sigma_m}{\partial \ln p} \right)_T \tag{5.68}$$

The derivative $(\partial h/\partial T)_p$ (= equilibrium constant-pressure, mass-specific heat) is obtained by differentiating equation (5.19) with respect to T:

$$\left(\frac{\partial h}{\partial T}\right)_p = \sum_{j=1}^{NS} \sigma_j c_{p,j} + \sum_{j=1}^{NS} h_j \left(\frac{\partial \sigma_j}{\partial T}\right)_p = \sum_{j=1}^{NS} \sigma_j c_{p,j} + \sum_{j=1}^{NS} \sigma_j \frac{h_j}{T}\left(\frac{\partial \ln \sigma_j}{\partial \ln T}\right)_p \tag{5.69}$$

It is clear from equations (5.67) to (5.69) that the derivatives $(\partial \ln \sigma_m/\partial \ln T)_p$, $(\partial \ln \sigma_m/\partial \ln p)_T$, and $(\partial \ln \sigma_j/\partial \ln T)_p$ ($j = 1,...,NS$) are needed to evaluate the three independent first derivatives.

The derivatives $(\partial \ln \sigma_j/\partial \ln T)_p$ and $(\partial \ln \sigma_m/\partial \ln T)_p$ are obtained by solving the system of equations generated by differentiating equations (5.5), (5.10), and (5.17) with respect to $\ln T$

$$\sigma_m \left(\frac{\partial \ln \sigma_m}{\partial \ln T}\right)_p - \sum_{k=1}^{NS} \sigma_k \left(\frac{\partial \ln \sigma_k}{\partial \ln T}\right)_p = 0 \tag{5.70}$$

$$\sum_{k=1}^{NS} a_{ik} \sigma_k \left(\frac{\partial \ln \sigma_k}{\partial \ln T}\right)_p = 0, \quad i = 1,..., NLM \tag{5.71}$$

$$-\sum_{k=1}^{NLM} a_{kj} \left(\frac{\partial \pi_k}{\partial \ln T}\right)_p + \left(\frac{\partial \ln \sigma_j}{\partial \ln T}\right)_p - \left(\frac{\partial \ln \sigma_m}{\partial \ln T}\right)_p = \frac{h_j}{RT}, \quad j = 1,..., NS \tag{5.72}$$

where equations (5.36) and (5.37) have been used, as well as the fact that for any variables y and ζ

$$\frac{\partial y}{\partial \ln \zeta} = y \frac{\partial \ln y}{\partial \ln \zeta} \tag{5.73}$$

Equations (5.70) to (5.72) form a set of NLM + NS + 1 linear equations; therefore the NLM + NS + 1 derivatives $(\partial \pi_i/\partial \ln T)_p$ ($i = 1,...,NLM$), $(\partial \ln \sigma_j/\partial \ln T)_p$ ($j = 1,...,NS$), and $(\partial \ln \sigma_m/\partial \ln T)_p$ can be computed. By using the procedure outlined in section 5.2.1 for the corrector iteration equations, the number of equations can be reduced significantly. Equation (5.72) gives the solution for $(\partial \ln \sigma_j/\partial \ln T)_p$ as

$$\left(\frac{\partial \ln \sigma_j}{\partial \ln T}\right)_p = \sum_{k=1}^{NLM} a_{kj} \left(\frac{\partial \pi_k}{\partial \ln T}\right)_p + \left(\frac{\partial \ln \sigma_m}{\partial \ln T}\right)_p + \frac{h_j}{RT} \tag{5.74}$$

which is substituted into equations (5.70) and (5.71). After rearrangement the resulting reduced equation set can be expressed compactly as

$$\mathcal{G}^* \underline{Y}_p^* = \underline{\mathcal{E}}_p^* \tag{5.75}$$

where the subscript p indicates that the partial derivatives are evaluated at constant pressure. The (NLM + 1)-dimensional column vector $\underline{Y}_p^*$ is given by

$$\underline{Y}_p^* = \left[\left(\frac{\partial \pi_1}{\partial \ln T} \right)_p, \ldots, \left(\frac{\partial \pi_{NLM}}{\partial \ln T} \right)_p, \left(\frac{\partial \ln \sigma_m}{\partial \ln T} \right)_p \right]^T \tag{5.76}$$

The elements $\mathcal{E}_{p,i}^*$ ($i = 1,\ldots,NLM+1$) of the column vector $\underline{\mathcal{E}}_p^*$ are defined as

$$\mathcal{E}_{p,i}^* = -\sum_{j=1}^{NS} a_{ij} \sigma_j \frac{h_j}{RT}, \quad i = 1,\ldots,NLM \tag{5.77a}$$

$$\mathcal{E}_{p,NLM+1}^* = -\sum_{j=1}^{NS} \sigma_j \frac{h_j}{RT} \tag{5.77b}$$

The (NLM + 1)×(NLM + 1) matrix $\mathcal{G}^*$, a submatrix of the (NLM + 2)×(NLM + 2) matrix $\mathcal{G}$, is obtained by deleting the last row and the last column of $\mathcal{G}$, equation (5.43), and is symmetric. Because $\mathcal{G}^*$ is a submatrix of $\mathcal{G}$, no additional programming is needed to evaluate $\mathcal{G}^*$.

Equation (5.75) is solved for the $\{(\partial \pi_i / \partial \ln T)_p\}$ and $(\partial \ln \sigma_m / \partial \ln T)_p$ by the Gaussian elimination method. The derivatives $\{(\partial \ln \sigma_j / \partial \ln T)_p\}$ are then computed by using equation (5.74). Substituting the solution for $(\partial \ln \sigma_j / \partial \ln T)_p$ ($j = 1,\ldots,NS$) into equation (5.69) gives $(\partial h / \partial T)_p$. However, $(\partial h / \partial T)_p$ can be evaluated by a simpler procedure (ref. 113): Substituting equation (5.74) into equation (5.69) and dividing both sides of the resulting equation by R give the following expression for the dimensionless equilibrium mixture constant-pressure specific heat:

$$\frac{1}{R}\left(\frac{\partial h}{\partial T}\right)_p = \sum_{i=1}^{NLM}\sum_{j=1}^{NS} a_{ij}\sigma_j \frac{h_j}{RT}\left(\frac{\partial \pi_i}{\partial \ln T}\right)_p + \sum_{j=1}^{NS}\sigma_j \frac{h_j}{RT}\left(\frac{\partial \ln \sigma_m}{\partial \ln T}\right)_p$$

$$+\sum_{j=1}^{NS}\sigma_j\left[\frac{c_{p,j}}{R}+\left(\frac{h_j}{RT}\right)^2\right] \qquad (5.78)$$

which can be expressed compactly as

$$\frac{1}{R}\left(\frac{\partial h}{\partial T}\right)_p = \sum_{i=1}^{NLM+1} \mathcal{G}_{NLM+2,i} Y^*_{p,i} + \mathcal{G}_{NLM+2,NLM+2} \qquad (5.79)$$

where $\mathcal{G}_{NLM+2,i}$ ($i = 1,...,NLM+2$) is the ith element of the (NLM + 2)th row of $\mathcal{G}$, equation (5.43). Note that equation (5.78) requires only the temperature derivatives obtained by solving equation (5.75). Hence using equation (5.79) to compute the specific heat avoids the computational work associated with evaluating the $\{(\partial \ln \sigma_j/\partial \ln T)_p\}$ required by equation (5.69). Also, because the coefficients in equation (5.78) are the elements of the (NLM + 2)th row of $\mathcal{G}$, use of equation (5.79) requires little additional programming.

To solve for $(\partial \ln \sigma_m/\partial \ln p)_T$, equations (5.5), (5.10), and (5.17) are differentiated with respect to $\ln p$:

$$\sigma_m\left(\frac{\partial \ln \sigma_m}{\partial \ln p}\right)_T - \sum_{k=1}^{NS}\sigma_k\left(\frac{\partial \ln \sigma_k}{\partial \ln p}\right)_T = 0 \qquad (5.80)$$

$$\sum_{k=1}^{NS} a_{ik}\sigma_k\left(\frac{\partial \ln \sigma_k}{\partial \ln p}\right)_T = 0, \qquad i = 1,...,NLM \qquad (5.81)$$

$$-\sum_{k=1}^{NLM} a_{kj}\left(\frac{\partial \pi_k}{\partial \ln p}\right)_T + \left(\frac{\partial \ln \sigma_j}{\partial \ln p}\right)_T - \left(\frac{\partial \ln \sigma_m}{\partial \ln p}\right)_T = -1, \qquad j = 1,...,NS \qquad (5.82)$$

where equation (5.73) has been used.

Equations (5.80) to (5.82) form a set of NS + NLM + 1 linear equations. By using the same procedure as for the temperature derivatives, the number of equations is reduced to NLM + 1. Solving equation (5.82) for $(\partial \ln \sigma_j/\partial \ln p)_T$ gives

$$\left(\frac{\partial \ln \sigma_j}{\partial \ln p}\right)_T = \sum_{k=1}^{\mathrm{NLM}} a_{kj}\left(\frac{\partial \pi_k}{\partial \ln p}\right)_T + \left(\frac{\partial \ln \sigma_m}{\partial \ln p}\right)_T - 1 \tag{5.83}$$

which is substituted into equations (5.80) and (5.81) and terms rearranged to give the reduced system of equations

$$\mathcal{G}^* \underline{Y}_T^* = \underline{\mathcal{E}}_T^* \tag{5.84}$$

where the (NLM + 1)×(NLM + 1) matrix $\mathcal{G}^*$ has been defined previously and the subscript T indicates that the partial derivatives are evaluated at constant temperature. The (NLM + 1)-dimensional column vector $\underline{Y}_T^*$ is given by

$$\underline{Y}_T^* = \left[\left(\frac{\partial \pi_1}{\partial \ln p}\right)_T, \ldots, \left(\frac{\partial \pi_{\mathrm{NLM}}}{\partial \ln p}\right)_T, \left(\frac{\partial \ln \sigma_m}{\partial \ln p}\right)_T\right]^T \tag{5.85}$$

The elements $\mathcal{E}_{T,i}^*$ $(i = 1,\ldots,\mathrm{NLM+1})$ of the column vector $\underline{\mathcal{E}}_T^*$ are defined as

$$\mathcal{E}_{T,i}^* = \sum_{j=1}^{\mathrm{NS}} a_{ij}\sigma_j, \quad i = 1,\ldots,\mathrm{NLM} \tag{5.86a}$$

$$\mathcal{E}_{T,\mathrm{NLM+1}}^* = \sum_{j=1}^{\mathrm{NS}} \sigma_j \tag{5.86b}$$

Equation (5.84) is solved for the $\{(\partial \pi_i/\partial \ln p)_T\}$ and $(\partial \ln \sigma_m/\partial \ln p)_T$ by the Gaussian elimination method. However, note that the only pressure derivative that is needed is $(\partial \ln \sigma_m/\partial \ln p)_T$ (see eq. (5.68)).

The final thermodynamic quantity that is computed is the sonic velocity c defined as (e.g., ref. 26)

$$c = \sqrt{\left(\partial p/\partial \rho\right)_s} \tag{5.87}$$

which can be rewritten as

$$c = \sqrt{-\frac{1}{\rho^2}\left(\frac{\partial p}{\partial v}\right)_s} \tag{5.88}$$

because $v = 1/\rho$. The partial derivative $(\partial p/\partial v)_s$ is given by (ref. 26)

$$\left(\frac{\partial p}{\partial v}\right)_s = \frac{\left(\frac{\partial h}{\partial T}\right)_p}{\left(\frac{\partial h}{\partial T}\right)_p \left(\frac{\partial v}{\partial p}\right)_T + T\left(\frac{\partial v}{\partial T}\right)_p^2} \tag{5.89}$$

Equation (5.89) is rewritten by using the logarithmic form of the volume derivatives. The resulting equation is substituted into equation (5.88), and then the ideal-gas equation of state, equation (5.22), is used. After some rearrangement the resulting expression for c is

$$c = \sqrt{\frac{-RT}{\frac{1}{\sigma_m}\left(\frac{\partial \ln v}{\partial \ln p}\right)_T + \left(\frac{\partial \ln v}{\partial \ln T}\right)_p^2 \Big/ \frac{1}{R}\left(\frac{\partial h}{\partial T}\right)_p}} \tag{5.90}$$

5.4 Test Problems

To verify the accuracy of the chemical equilibrium calculation procedures built into LSENS, its predictions have been compared with the results produced by CET (ref. 117) for many problems. This section presents results for four problems representing the different problem types (i.e., HP, TP, UV, and TV) considered in this chapter. All four problems involved the computation of the equilibrium state for a stoichiometric hydrogen-oxygen-nitrogen mixture at an initial pressure of 2 atm. The nitrogen-to-oxygen ratio was the standard value (= 3.727375) built into the code (see chapter 8 of part II). The following 13 species were considered in all calculations: H_2, O_2, N_2, O, H, OH, HO_2, H_2O_2, N, NO, NO_2, N_2O, and H_2O. For the HP and UV problems the initial temperature was 1500 K. For the TP and TV problems, however, the temperature was increased to 2500 K, for reasons discussed here.

TABLE 5.1.—CHEMICAL EQUILIBRIUM PROPERTIES FOR STOICHIOMETRIC
INITIAL PRESSURE OF
[Initial temperature, 1500 K for HP and UV problems and

Variable	HP problem		TP problem	
	CET	LSENS	CET	LSENS
x_O	6.904×10^{-3}	6.903×10^{-3}	7.517×10^{-4}	7.517×10^{-4}
x_{H_2O}	0.2564	0.2564	0.3206	0.3206
x_{OH}	3.032×10^{-2}	3.032×10^{-2}	8.890×10^{-3}	8.890×10^{-3}
x_H	1.886×10^{-2}	1.886×10^{-2}	2.387×10^{-3}	2.387×10^{-3}
x_{O_2}	1.407×10^{-2}	1.407×10^{-2}	5.447×10^{-3}	5.447×10^{-3}
x_{H_2}	5.057×10^{-2}	5.057×10^{-2}	1.825×10^{-2}	1.825×10^{-2}
x_{HO_2}	1.402×10^{-5}	1.401×10^{-5}	3.294×10^{-6}	3.294×10^{-6}
$x_{H_2O_2}$	6.225×10^{-7}	6.224×10^{-7}	2.298×10^{-7}	2.298×10^{-7}
x_{NO}	9.766×10^{-3}	9.766×10^{-3}	3.341×10^{-3}	3.341×10^{-3}
x_{NO_2}	2.240×10^{-6}	2.239×10^{-6}	6.868×10^{-7}	6.868×10^{-7}
x_N	4.245×10^{-6}	4.244×10^{-6}	1.640×10^{-7}	1.640×10^{-7}
x_{N_2}	0.6131	0.6131	0.6403	0.6403
x_{N_2O}	6.923×10^{-7}	6.923×10^{-7}	2.386×10^{-7}	2.386×10^{-7}
M_w, g/mole	23.29	23.28	24.19	24.19
p, atm	2.000	2.000	2.000	2.000
T, K	2911.4	2911.4	2500.0	2500.0
ρ, g/cm^3	1.949×10^{-4}	1.949×10^{-4}	2.358×10^{-4}	2.358×10^{-4}
h, cal/g	436.2	436.2	58.60	58.61
u, cal/g	187.7	187.7	−146.8	−146.8
s, cal/g-K	2.758	2.758	2.619	2.619
$(\partial h/\partial T)_p$, cal/g-K	1.218	1.218	0.6849	0.6849
$(\partial \ln v/\partial \ln T)_p$	1.429	1.429	1.126	1.126
$(\partial \ln v/\partial \ln p)_T$	−1.020	−1.020	−1.005	−1.005
c, m/s	1088.7	1088.7	1003.7	1003.7
NITER	11	10	12	11

HYDROGEN-OXYGEN-NITROGEN MIXTURE AT
2 atm
2500 K for TP and TV problems.]

UV problem		TV problem	
CET	LSENS	CET	LSENS
8.958×10^{-3}	8.957×10^{-3}	8.294×10^{-4}	8.294×10^{-4}
0.2411	0.2411	0.3192	0.3192
3.590×10^{-2}	3.590×10^{-2}	9.318×10^{-3}	9.317×10^{-3}
2.381×10^{-2}	2.381×10^{-2}	2.626×10^{-3}	2.626×10^{-3}
1.505×10^{-2}	1.505×10^{-2}	5.728×10^{-3}	5.728×10^{-3}
5.727×10^{-2}	5.727×10^{-2}	1.906×10^{-2}	1.906×10^{-2}
2.164×10^{-5}	2.163×10^{-5}	3.290×10^{-6}	3.290×10^{-6}
1.035×10^{-6}	1.035×10^{-6}	2.180×10^{-7}	2.180×10^{-7}
1.213×10^{-2}	1.213×10^{-2}	3.425×10^{-3}	3.425×10^{-3}
3.506×10^{-6}	3.506×10^{-6}	6.708×10^{-7}	6.708×10^{-7}
8.475×10^{-6}	8.474×10^{-6}	1.764×10^{-7}	1.764×10^{-7}
0.6057	0.6057	0.6398	0.6398
1.173×10^{-6}	1.173×10^{-6}	2.272×10^{-7}	2.272×10^{-7}
23.05	23.05	24.17	24.17
3.702	3.702	1.727	1.727
3066.0	3066.0	2500.0	2500.0
3.392×10^{-4}	3.392×10^{-4}	2.035×10^{-4}	2.035×10^{-4}
557.7	557.7	62.48	62.49
293.4	293.4	−143.0	−143.0
2.746	2.746	2.633	2.633
1.283	1.283	0.7001	0.7001
1.483	1.483	1.133	1.133
−1.024	−1.024	−1.005	−1.005
1123.5	1123.5	1003.1	1003.1
10	9	12	11

The chemical equilibrium composition and thermodynamic properties generated by LSENS are given in table 5.1, together with the results obtained with CET. In this table x_i is the mole fraction of species i, NITER is the total number of iterations required for convergence of the solution, and the other variables have been defined previously. The calculations with both codes were performed on the NASA Lewis Research Center's Amdahl 5870 computer using the UTS operating system, the Fujitsu 77 compiler (optimization level, 3), and double precision.

To be consistent with LSENS, which classifies species with mole fraction $\leq 10^{-8}$ as trace species (see section 5.2.4), CET was run with a value of 10^{-8} for the variable TRACE, which is a cutoff level, and mole fractions less than TRACE are not listed. This condition resulted for the species HO_2, H_2O_2, N, NO_2, and N_2O for the TP and TV calculations at 1500 K. The temperature was therefore increased to 2500 K for the two problems. Thermodynamic data for all 13 species listed in table 5.1 were included in the input data file required by CET to ensure that only these 13 species were considered by the code and that the same thermodynamic data were used by both LSENS and CET.

The results given in table 5.1 show the excellent agreement between LSENS and CET for all four problem types, thereby validating the accuracy of LSENS for chemical equilibrium state computations. In addition, the table shows that in terms of computational work requirement LSENS compares well with CET. (CET consistently required one iteration more than LSENS because of additional convergence tests associated with the variable TRACE.) Finally for each problem the execution time needed by LSENS was only a few milliseconds, reinforcing its computational efficiency for equilibrium problems.

Chapter 6
Incident Shock

The shock tube has been used for many years to generate a high-temperature environment for the study of chemical reactions (e.g., refs. 124 and 125). It consists essentially of a long, straight tube of constant cross-sectional area. A thin diaphragm divides the tube into two sections, which contain either the same or different gases. The two sections are initially at different pressures. Hence, when the diaphragm is ruptured, a shock wave (the "incident" shock) travels into the low-pressure gas, and a rarefaction wave travels in the opposite direction to equalize the pressures in the two sections.

The passage of the shock wave creates a high-pressure, high-temperature flowing system without changing the gas composition. The new conditions behind the shock wave start a chemical reaction that proceeds toward the equilibrium state. To study the chemical reactions behind the shock, the thermodynamic state of the gas immediately after shock passage when the composition has not changed (i.e., the "frozen" shock conditions) is required. In the present work this state is solved for under idealized conditions—steady, one-dimensional, inviscid, adiabatic flow of an ideal-gas mixture with no diffusion of matter or energy. The thermodynamic state after the chemical reactions initiated by shock passage have reached equilibrium (i.e., the "equilibrium" shock conditions) is also computed.

This chapter presents the governing equations for the two idealized shock problems and describes the solution procedures, which were adapted from Gordon and McBride (refs. 113 and 117). A test problem, which illustrates the accuracy and efficiency of the LSENS code for incident shock computations, concludes the chapter.

6.1 Governing Equations

Steady, one-dimensional, inviscid flow of an ideal-gas mixture is considered, and a coordinate system attached to the shock is used, figure 6.1. The unshocked gas at known conditions p_1, T_1, and ρ_1 flows into the shock at a given constant velocity V_1. Here p, T, and ρ are the pressure, temperature, and density, respectively. The shocked gas at conditions p_2, T_2, and ρ_2 flows away from the shock at velocity V_2.

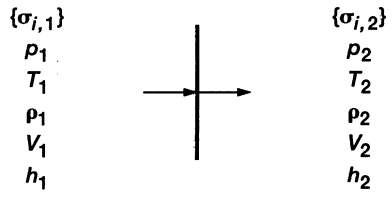

Figure 6.1.—Schematic representation of stationary incident shock wave.

For the assumptions given previously the conservation equations required to compute the thermodynamic state and gas velocity after shock passage take the form (e.g., ref. 126)

Mass conservation

$$\rho_1 V_1 = \rho_2 V_2 \tag{6.1}$$

Momentum conservation

$$p_1 + \rho_1 V_1^2 = p_2 + \rho_2 V_2^2 \tag{6.2}$$

Energy conservation

$$h_1 + \frac{1}{2} V_1^2 = h_2 + \frac{1}{2} V_2^2 \tag{6.3}$$

In equation (6.3), h is the mixture mass-specific enthalpy

$$h = \sum_{i=1}^{NS} \sigma_i h_i \tag{6.4}$$

where NS is the total number of species; σ_i the mole number of species i, that is, the number of moles of species i per unit mass of mixture; and h_i the molar-specific enthalpy of the ith species.

Because attention is restricted to ideal-gas mixtures, the density can be expressed in terms of the pressure and temperature by using the equation of state

$$\rho = p \frac{M_w}{RT} \tag{6.5}$$

where M_w is the mean molar mass of the gas mixture and R the universal gas constant. Equation (6.5) provides the following expression for the density ratio across the shock:

$$\frac{\rho_2}{\rho_1} = \frac{p_2}{p_1}\frac{T_1}{T_2}\frac{M_{w,2}}{M_{w,1}} \tag{6.6}$$

Therefore the system of equations (6.1) to (6.3) is closed, provided that the new mixture composition is known.

The problem is further simplified by solving equation (6.1) for V_2 in terms of ρ_1, V_1, and ρ_2 and then using the result

$$V_2 = \frac{\rho_1 V_1}{\rho_2} \tag{6.7}$$

to eliminate V_2 from equations (6.2) and (6.3). Substituting equation (6.7) into equations (6.2) and (6.3), rearranging terms, and then using equation (6.6) provide the following equations that can be solved for T_2 and p_2:

$$\frac{p_2}{p_1} = 1 + \frac{\rho_1 V_1^2}{p_1}\left[1 - \left(\frac{p_1}{p_2}\frac{T_2}{T_1}\frac{M_{w,1}}{M_{w,2}}\right)\right] \tag{6.8}$$

$$h_2 = h_1 + \frac{1}{2}V_1^2\left[1 - \left(\frac{p_1}{p_2}\frac{T_2}{T_1}\frac{M_{w,1}}{M_{w,2}}\right)^2\right] \tag{6.9}$$

Once these equations are solved for p_2 and T_2, ρ_2 is obtained from equation (6.5) and then V_2 from equation (6.7).

The system of equations (6.1) to (6.3) and (6.5) is incomplete for the equilibrium problem because the postshock composition is not known. As discussed in section 6.2 the solution procedure used for this problem requires the equilibrium composition for assigned temperature and pressure. The governing equations for such a calculation are given in chapter 5.

6.2 Solution Method

If the postshock mixture composition (i.e., the $\{\sigma_{i,2}\}$) is known, the system of equations (6.1) to (6.3) and (6.5) is complete and the four unknowns p_2, T_2, ρ_2, and V_2 can be solved for. The frozen shock problem, for which $\sigma_{i,2} = \sigma_{i,1}$

($i = 1,...,NS$), satisfies this condition, and equations (6.8) and (6.9) are solved for p_2 and T_2 by using an iterative technique. Starting with an initial guess for the solution, equations (6.4), (6.8), and (6.9) are used to generate successive approximations until the iteration converges, that is, until additional iteration produces little change in the solution.

For the equilibrium shock problem, however, the new composition is not known and has to be computed along with the other four quantities. The solution procedure used for this problem also involves the solution of equations (6.8) and (6.9) for p_2 and T_2 by using an iterative technique. However, before each iteration the equilibrium composition corresponding to the current estimates for T_2 and p_2 is generated by using the procedure described in chapter 5. The "new" chemical composition is then "known"; therefore equations (6.4), (6.8), and (6.9) can be used to produce improved estimates for p_2 and T_2. The cycle of computing the equilibrium composition corresponding to the current estimates for T_2 and p_2 and then using this composition together with equations (6.4), (6.8), and (6.9) to generate improved estimates for p_2 and T_2 is continued until the changes in both p_2 and T_2 are smaller than a specified amount.

Equations (6.8) and (6.9) are solved by the Newton-Raphson (NR) iteration procedure, as implemented by Gordon and McBride (refs. 113 and 117). For computational convenience the quantities that are actually solved for are the pressure and temperature ratios, p_2/p_1 and T_2/T_1, respectively, across the shock. Also, because the equations used for the thermodynamic properties produce the nondimensional quantities $h_i/(RT)$ ($i = 1,...,NS$) (see chapter 8 of part II), both sides of equation (6.9) are divided by R

$$\frac{h_2}{R} = \frac{h_1}{R} + \frac{1}{2}\frac{V_1^2}{R}\left[1 - \left(\frac{p_1}{p_2}\frac{T_2}{T_1}\frac{M_{w,1}}{M_{w,2}}\right)^2\right] \tag{6.10}$$

to avoid repeated multiplication by R.

For clarity in presentation of the solution procedure the two-dimensional column vector $\underline{y}$ with components

$$y_1 = \frac{p_2}{p_1} \tag{6.11a}$$

and

$$y_2 = \frac{T_2}{T_1} \tag{6.11b}$$

is introduced. Equations (6.8) and (6.10) are rewritten as

$$\mathcal{F}_1(\underline{y}) = 1 + \frac{\rho_1 V_1^2}{p_1}\left[1 - \left(\frac{y_2}{y_1}\frac{M_{w,1}}{M_{w,2}}\right)\right] - y_1 = 0 \tag{6.12a}$$

and

$$\mathcal{F}_2(\underline{y}) = \frac{h_1}{R} + \frac{1}{2}\frac{V_1^2}{R}\left[1 - \left(\frac{y_2}{y_1}\frac{M_{w,1}}{M_{w,2}}\right)^2\right] - \frac{h_2}{R} = 0 \tag{6.12b}$$

Expressed in this form, solving equations (6.8) and (6.10) is equivalent to finding the zero of $\underline{\mathcal{F}}$ where the column vector $\underline{\mathcal{F}}$ contains the two components $\mathcal{F}_1$ and $\mathcal{F}_2$.

The physically impossible situation of variables having negative values during the iteration procedure is avoided by solving for $\{\ln y_i\}$ rather than $\{y_i\}$. If the mth estimates are denoted by $\ln y_i^{[m]}$ (i = 1,2), the NR iteration procedure for the corrections, $\Delta \ln y_i^{[m]}$ (i = 1,2), on the (m + 1)th iteration is

$$\sum_{k=1}^{2} \left.\frac{\partial \mathcal{F}_i}{\partial \ln y_k}\right|_{\underline{y}=\underline{y}^{[m]}} \Delta \ln y_k^{[m]} = -\mathcal{F}_i\left(\underline{y}^{[m]}\right), \quad i = 1,2 \tag{6.13}$$

The (m + 1)th estimates, $\ln y_i^{[m+1]}$ (i = 1,2), are given by

$$\ln y_i^{[m+1]} = \ln y_i^{[m]} + \Delta \ln y_i^{[m]}, \quad i = 1,2 \tag{6.14}$$

If the two-dimensional column vector $\underline{Y}$ is defined as

$$\underline{Y} = \left(\ln y_1, \ln y_2\right)^T \tag{6.15}$$

where the superscript T indicates transpose, equation (6.13) can be expressed compactly as

$$\mathbf{J}^{[m]} \Delta \underline{Y}^{[m]} = -\underline{\mathcal{F}}\left(\underline{y}^{[m]}\right) \tag{6.16}$$

In this equation $\Delta \underline{Y}^{[m]}$ is the correction obtained for $\underline{Y}$ on the (m + 1)th iteration

$$\Delta \underline{Y}^{[m]} = \underline{Y}^{[m+1]} - \underline{Y}^{[m]} \tag{6.17}$$

and $\mathbf{J}^{[m]}$ is the 2×2 Jacobian matrix, with element $J_{ik}^{[m]}$ given by

$$J_{ik}^{[m]} = \left.\frac{\partial \mathcal{F}_i}{\partial Y_k}\right|_{\underline{Y}=\underline{Y}^{[m]}} = \left.\frac{\partial \mathcal{F}_i}{\partial \ln y_k}\right|_{\underline{y}=\underline{y}^{[m]}} = y_k^{[m]} \left.\frac{\partial \mathcal{F}_i}{\partial y_k}\right|_{\underline{y}=\underline{y}^{[m]}} \qquad i,k = 1,2 \tag{6.18}$$

where the partial derivatives are obtained from equations (6.12a) and (6.12b) as shown here. Equations (6.12a) and (6.12b) are first rewritten by using equations (6.6), (6.11a), and (6.11b) as follows:

$$\mathcal{F}_1 = 1 + \frac{\rho_1 V_1^2}{p_1}\left[1 - \left(\frac{\rho_1}{\rho_2}\right)\right] - y_1 = 1 + \frac{\rho_1 V_1^2}{p_1}\left[1 - \left(\frac{v_2}{v_1}\right)\right] - y_1 \tag{6.19a}$$

$$\mathcal{F}_2 = \frac{h_1}{R} + \frac{1}{2}\frac{V_1^2}{R}\left[1 - \left(\frac{\rho_1}{\rho_2}\right)^2\right] - \frac{h_2}{R} = \frac{h_1}{R} + \frac{1}{2}\frac{V_1^2}{R}\left[1 - \left(\frac{v_2}{v_1}\right)^2\right] - \frac{h_2}{R} \tag{6.19b}$$

In these equations v (= $1/\rho$) is the specific volume of the mixture. The elements $J_{ik}^{[m]}$ (i,k = 1,2) of the Jacobian matrix, equation (6.18), are then obtained from equations (6.19a) and (6.19b) and are given by

$$J_{11}^{[m]} = -\frac{\rho_1 V_1^2}{p_1}\left(\frac{\rho_1}{\rho_2^{[m]}}\right)\left(\frac{\partial \ln v}{\partial \ln p}\right)_T \Bigg|_{\underline{y}=\underline{y}^{[m]}} - y_1^{[m]} \tag{6.20a}$$

$$J_{12}^{[m]} = -\frac{\rho_1 V_1^2}{p_1}\left(\frac{\rho_1}{\rho_2^{[m]}}\right)\left(\frac{\partial \ln v}{\partial \ln T}\right)_p \Bigg|_{\underline{y}=\underline{y}^{[m]}} \tag{6.20b}$$

$$J_{21}^{[m]} = -\frac{V_1^2}{R}\left(\frac{\rho_1}{\rho_2^{[m]}}\right)^2 \left(\frac{\partial \ln v}{\partial \ln p}\right)_T \Bigg|_{\underline{y}=\underline{y}^{[m]}} - \frac{p_2^{[m]}}{R}\left(\frac{\partial h}{\partial p}\right)_T \Bigg|_{\underline{y}=\underline{y}^{[m]}} \tag{6.20c}$$

$$J_{22}^{[m]} = -\frac{V_1^2}{R}\left(\frac{\rho_1}{\rho_2^{[m]}}\right)^2 \left(\frac{\partial \ln v}{\partial \ln T}\right)_p \Bigg|_{\underline{y}=\underline{y}^{[m]}} - \frac{T_2^{[m]}}{R}\left(\frac{\partial h}{\partial T}\right)_p \Bigg|_{\underline{y}=\underline{y}^{[m]}} \tag{6.20d}$$

In equations (6.20a) to (6.20d) the partial derivatives $(\partial \ln v/\partial \ln p)_T$, $(\partial \ln v/\partial \ln T)_p$, $(\partial h/\partial p)_T$, and $(\partial h/\partial T)_p$ depend on the problem type. For the frozen case

$$\left(\frac{\partial \ln v}{\partial \ln p}\right)_T = -1 \tag{6.21a}$$

$$\left(\frac{\partial \ln v}{\partial \ln T}\right)_p = 1 \tag{6.21b}$$

$$\left(\frac{\partial h}{\partial p}\right)_T = 0 \tag{6.21c}$$

$$\left(\frac{\partial h}{\partial T}\right)_p = c_p \tag{6.21d}$$

where c_p is the constant-pressure, mass-specific heat of the frozen mixture

$$c_p = \sum_{i=1}^{NS} \sigma_i c_{p,i} \tag{6.22}$$

and $c_{p,i}$ ($\equiv dh_i/dT$) is the constant-pressure, molar-specific heat of the ith species. For the equilibrium problem

$$\left(\frac{\partial h}{\partial p}\right)_T = v - T\left(\frac{\partial v}{\partial T}\right)_p = v\left[1 - \left(\frac{\partial \ln v}{\partial \ln T}\right)_p\right] \tag{6.23}$$

and the other derivatives are given in chapter 5.

Equation (6.16) is solved for $\Delta\underline{Y}^{[m]}$ by directly inverting $\mathbf{J}^{[m]}$—because $\mathbf{J}^{[m]}$ is a 2×2 matrix, its inverse is easily obtained. The $(m + 1)$th estimate $\underline{Y}^{[m+1]}$ is then given by

$$\underline{Y}^{[m+1]} = \underline{Y}^{[m]} + \Delta\underline{Y}^{[m]} \tag{6.24}$$

Starting with an initial guess, denoted by $\underline{y}^{[0]}$, successive corrections $\Delta\underline{Y}^{[m]}$ (m = 0,1,...,M–1) and approximations $\underline{y}^{[m]}$ (m = 1,...,M–1) ($y_i^{[m]} = \exp Y_i^{[m]}$, i = 1,2) are generated until the iteration converges. The integer M is the number of iterations required for convergence, and $\underline{y}$ is taken as $\underline{y}^{[M-1]}$.

6.2.1 Initial Estimates

The initial estimates $y_i^{[0]}$ (i = 1,2) used to start the iteration process are obtained by assuming frozen composition and constant mixture mass-specific heat c_p. Equations (6.8) and (6.10) can then be solved exactly, and the (nontrivial) solution is (ref. 113)

$$y_1^{[0]} \equiv \frac{p_2^{[0]}}{p_1} = \frac{2\gamma_1 \mathcal{M}_1^2 - \gamma_1 + 1}{\gamma_1 + 1} \tag{6.25a}$$

$$y_2^{[0]} \equiv \frac{T_2^{[0]}}{T_1} = y_1^{[0]} \left(\frac{\frac{2}{\mathcal{M}_1^2} + \gamma_1 - 1}{\gamma_1 + 1} \right) \tag{6.25b}$$

In these equations γ_1 [$= c_{p,1}/(c_{p,1} - R/M_{w,1})$] is the specific-heat ratio of the unshocked gas mixture, and $\mathcal{M}_1 \left(= V_1 / \sqrt{\gamma_1 R T_1 / M_{w,1}} \right)$ its Mach number.

For the frozen shock problem the initial estimates given by equations (6.25a) and (6.25b) are in general excellent (refs. 113 and 117). However, for the equilibrium shock problem the initial temperature ratio estimate given by equation (6.25b) can be very high. A more reliable estimate is given by the equilibrium temperature obtained under conditions of constant pressure $p_2^{[0]} (= y_1^{[0]} p_1)$ and constant mixture mass-specific stagnation or total enthalpy $h_{o,2}^{[0]} (= h_{o,1} = h_1 + V_1^2/2)$ (ref. 117). Hence the initial temperature ratio estimate used for the equilibrium shock problem is

$$y_2^{[0]} = \frac{T_2^{[0]}\Big|_{eq}}{T_1} \tag{6.26}$$

where $T_2^{[0]}\Big|_{eq}$ is the equilibrium temperature at $p_2^{[0]}$ and $h_{o,2}^{[0]}$.

6.2.2 Convergence Tests and Corrections Control

The convergence criteria are based on the magnitudes of the $\{\Delta Y_i^{[m]}\}$ and are

$$\left|\Delta Y_i^{[m]}\right| \overset{?}{<} 5\times 10^{-5}, \qquad i=1,2 \tag{6.27}$$

If this equation is satisfied, the results of the mth iteration are accepted.

If either of the two variables fails to satisfy equation (6.27), the iteration process is continued. However, to avoid convergence difficulties caused by large corrections, equation (6.24) is not used to update $\underline{Y}^{[m+1]}$. Instead an arbitrary underrelaxation or control factor Λ is applied to the $\{\Delta Y_i^{[m]}\}$ given by equation (6.16) before the improved estimates $\{Y_i^{[m+1]}\}$ are computed. The control factor is defined as (ref. 117)

$$\Lambda = \min\left(1, \frac{\ln c_\Lambda}{\left|\Delta Y_1^{[m]}\right|}, \frac{\ln c_\Lambda}{\left|\Delta Y_2^{[m]}\right|}\right) \tag{6.28}$$

where the empirical constant c_Λ depends on the number of iterations:

$$c_\Lambda = \begin{cases} 1.5, & 0 \le m < 4 \\ 1.25, & 4 \le m < 12 \\ 1.1, & 12 \le m < 20 \\ 1.05, & 20 \le m \end{cases} \tag{6.29}$$

Equation (6.28) restricts the magnitudes of the corrections to be no greater than $\ln c_\Lambda$. The new estimate $\underline{Y}^{[m+1]}$ is given by

$$\underline{Y}^{[m+1]} = \underline{Y}^{[m]} + \Lambda\, \Delta\underline{Y}^{[m]}, \qquad m = 0,1\ldots, M-1 \tag{6.30}$$

The iteration process is continued until either the solution converges or 30 iterations have been performed without success when an error exit is taken.

6.3 Test Problem

The accuracy of LSENS for incident shock calculations has been examined by comparing its results with the solutions produced by CET (ref. 117) for many problems. In this section both codes are applied to a simple problem, which involves the passage of an incident shock wave at a Mach number (i.e., $\mathcal{M}_1$) of 3.3 into a stoichiometric hydrogen-oxygen-argon mixture with 94 percent argon. The unshocked gas is at pressure and temperature of 0.1 atm and 298.15 K, respectively. The equilibrium mixture was assumed to consist of the following nine species: H_2, O_2, Ar, O, H, OH, HO_2, H_2O_2, and H_2O.

The equilibrium and frozen shock conditions obtained with the two codes are given in table 6.1. In this table x_i is the mole fraction of species i and the other quantities have been defined previously. All results were generated on the NASA Lewis Research Center's Amdahl 5870 computer using the UTS operating system, the Fujitsu 77 compiler (optimization level, 3), and double precision.

As discussed in chapter 5, during the iteration procedure for the chemical equilibrium state LSENS classifies species with mole fractions $\leq 10^{-8}$ as trace species. After the iteration successfully converges, each trace species is assigned a mole number of 10^{-11}. For consistency, CET was run with a value of 10^{-8} for the variable TRACE, which is a cutoff level, and mole fractions less than TRACE are not listed. This condition was obtained for the species HO_2 and H_2O_2. Thermodynamic data for all nine species listed in table 6.1 were included in the input data file required by CET to ensure that only these nine species were considered by the code and that the same thermodynamic data were used by both LSENS and CET.

Table 6.1 shows the excellent agreement between LSENS and CET for both equilibrium and frozen shock computations, verifying the accuracy of LSENS. To solve for the equilibrium conditions, LSENS required one iteration and an execution time of approximately 0.01 s. The frozen shock solution required two iterations and less than 1 millisecond of execution time. Thus the code is efficient for incident shock computations.

TABLE 6.1.—POSTINCIDENT SHOCK CONDITIONS FOR STOICHIOMETRIC HYDROGEN-OXYGEN-ARGON MIXTURE (94% Ar) AT INITIAL PRESSURE OF 0.1 atm AND INITIAL TEMPERATURE OF 298.15 K

[Shock velocity, 1076 m/s.]

Variable	Equilibrium shock		Frozen shock	
	CET	LSENS	CET	LSENS
x_O	1.797×10^{-8}	1.796×10^{-8}	----------	----------
x_{H_2O}	4.079×10^{-2}	4.079×10^{-2}	----------	----------
x_{OH}	5.209×10^{-6}	5.209×10^{-6}	----------	----------
x_H	1.131×10^{-7}	1.131×10^{-7}	----------	----------
x_{O_2}	1.242×10^{-5}	1.241×10^{-5}	0.02	0.02
x_{H_2}	2.740×10^{-5}	2.740×10^{-5}	0.04	0.04
x_{HO_2}	(a)	(a)	----------	----------
$x_{H_2O_2}$	(a)	(a)	----------	----------
x_{Ar}	0.9592	0.9592	0.94	0.94
M_w, g/mol	39.05	39.05	38.27	38.27
p, atm	0.9515	0.9515	1.332	1.332
T, K	1515.7	1515.7	1233.8	1233.8
ρ, g/cm^3	2.988×10^{-4}	2.988×10^{-4}	5.036×10^{-4}	5.036×10^{-4}
V, m/s	563.4	563.4	334.3	334.3
h, cal/g	100.4	100.4	125.0	125.0
u, cal/g	23.30	23.30	60.93	60.93
s, cal/g-K	1.181	1.181	1.155	1.155
$(\partial h/\partial T)_p$, cal/g-K	0.1343	0.1343	0.1343	0.1343
$(\partial \ln v/\partial \ln T)_p$	1.0002	1.0002	1.0	1.0
$(\partial \ln v/\partial \ln p)_T$	−1.0000	−1.0000	−1.0	−1.0
c, m/s	721.0	721.0	661.1	661.1

[a]Less than 10^{-8}.

Chapter 7
Perfectly Stirred Reactor

The one-dimensional flow problem described in chapter 2 assumes no backmixing of reaction products with the unreacted gas mixture. In most practical combustion systems backmixing does, of course, occur. The simplest case that can be considered is instantaneous complete mixing of the reaction products and the unreacted mixture—the perfectly stirred (i.e., highly backmixed) reactor (PSR) (e.g., refs. 127 to 129). Although this model is a great simplification of highly turbulent reacting flow, it is a good first-order approximation to some practical systems, such as the primary zone of a gas turbine combustor. This chapter presents the algebraic equations describing steady-flow chemical reaction of an ideal-gas mixture in a PSR and describes their solution procedure. The chapter concludes with several illustrative examples.

A PSR consists of a reaction vessel of fixed volume $\mathcal{V}$ into which the reactant mixture enters at a constant mass flow rate $\dot{m}$, as illustrated schematically in figure 7.1. Chemical reactions occur within the reactor at constant pressure, and at steady-state operation the reaction products leave the reactor at the same mass flow rate as the reactant inflow; therefore the mass inside the reactor is constant. The entering reactant stream is assumed to mix instantaneously with the reactor contents at constant pressure. The gases in the reactor are assumed to be perfectly mixed and therefore homogeneous, with the same thermodynamic state as that of the exit stream. For the same reason the reaction rates are the same everywhere within the reactor. The reaction duration in the PSR is equal to the reactor average residence time τ_r given by

$$\tau_r = \rho\mathcal{V}/\dot{m} \tag{7.1}$$

where ρ is the mass density within the reactor.

Steady-state operation of the reactor is assumed and two types of problem are considered. In the first the mass flow rate is assigned and the composition (i.e., σ_i, $i = 1,...,NRS$), the temperature T, and the density ρ are solved for. Here σ_i is the mole number of species i, that is, number of moles of species i per unit mass of mixture, and NRS is the number of reacting species. In the second type of problem the reactor

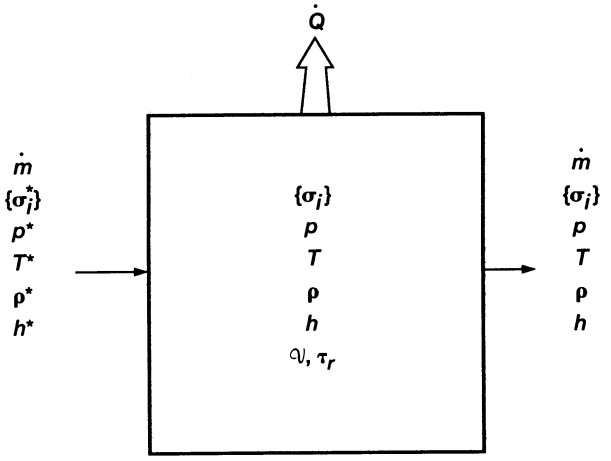

Figure 7.1.—Schematic illustration of perfectly stirred reactor.

temperature is assigned and the composition, density, and mass flow rate are solved for. For both problem types the inlet state, reactor volume, and pressure are assumed to be known, as are the chemical reaction mechanism and rate coefficient parameters. In addition, only ideal-gas mixtures are considered, and either the reactor is adiabatic or the heat transfer rate from the reactor contents is assumed to be given.

7.1 Governing Equations

For both problem types outlined previously the number of unknowns is equal to NRS + 2—the $\{\sigma_i\}$, T or $\dot{m}$, and ρ. However, because attention is restricted to ideal gases, the density can be expressed in terms of the other quantities by using the ideal-gas equation of state

$$\rho = \frac{p}{RT\sigma_m} \tag{7.2}$$

where p is the reactor pressure, R is the universal gas constant, and

$$\sigma_m = \sum_{i=1}^{NS} \sigma_i \tag{7.3}$$

where NS is the total number of (reacting and inert) species. Hence only NRS + 1 independent equations are required. For steady-state operation of the reactor NRS

equations are obtained from the molar conservation equations for the reacting species:

$$\begin{bmatrix}\text{Molar flow rate}\\ \text{of species i}\\ \text{into reactor}\end{bmatrix} - \begin{bmatrix}\text{Molar flow rate}\\ \text{of species i}\\ \text{out of reactor}\end{bmatrix} = \begin{bmatrix}\text{Net molar rate}\\ \text{of destruction}\\ \text{of species i}\end{bmatrix}, \quad i = 1,\ldots,\text{NRS} \tag{7.4}$$

This equation can be written as

$$\dot{m}\sigma_i^* - \dot{m}\sigma_i = -\rho\mathcal{V} f_i = -W_i\mathcal{V}, \qquad i = 1,\ldots,\text{NRS} \tag{7.5}$$

where the asterisk denotes reactor inlet conditions, figure 7.1. In equation (7.5), $f_i = d\sigma_i/dt$, where t is time; and $W_i\,(= \rho f_i)$, the molar formation rate of species i per unit volume, is obtained from equation (2.33) as

$$W_i = \rho f_i = \sum_{j=1}^{\text{NR}} \left(\nu_{ij}'' - \nu_{ij}'\right) r_j \tag{7.6}$$

Here r_j is the net molar rate of reaction j per unit volume

$$r_j = R_j - R_{-j}, \qquad j = 1,\ldots,\text{NR} \tag{7.7}$$

NR is the total number of reactions, ν_{ij}' and ν_{ij}'' are the stoichiometric coefficients of reactant species i and product species i in reaction j, and R_j and R_{-j} are the molar forward and reverse rates of reaction j per unit volume. The species continuity equation, equation (7.5), can then be rewritten as

$$\frac{\dot{m}}{\mathcal{V}}\left(\sigma_i^* - \sigma_i\right) = -\sum_{j=1}^{\text{NR}} \left(\nu_{ij}'' - \nu_{ij}'\right) r_j$$

or, rearranging terms, as

$$\sum_{j=1}^{\text{NR}} \left(\nu_{ij}'' - \nu_{ij}'\right) r_j + \frac{\dot{m}}{\mathcal{V}}\left(\sigma_i^* - \sigma_i\right) = 0, \qquad i = 1,\ldots,\text{NRS} \tag{7.8}$$

The (NRS + 1)th equation, needed for closure, is obtained from the energy conservation equation

$$\begin{bmatrix}\text{Enthalpy flow}\\ \text{rate into}\\ \text{reactor}\end{bmatrix} - \begin{bmatrix}\text{Enthalpy flow}\\ \text{rate out of}\\ \text{reactor}\end{bmatrix} = \begin{bmatrix}\text{Heat transfer}\\ \text{rate from}\\ \text{reactor}\end{bmatrix} \tag{7.9}$$

which can be written as

$$\dot{m}h^* - \dot{m}h = \dot{Q} \tag{7.10}$$

where h^* is the mass-specific enthalpy at the reactor inlet, h the mass-specific enthalpy both within the reactor and at the reactor outlet, and $\dot{Q}$ the heat transfer rate from the reactor, figure 7.1. For an adiabatic problem $\dot{Q} = 0$; otherwise the heat transfer rate is assumed to be assigned as a polynomial function of temperature, as discussed in chapter 11 of part II.

For a mixture of ideal gases

$$h = \sum_{i=1}^{NS} \sigma_i h_i \tag{7.11}$$

where h_i is the molar-specific enthalpy of the ith species.Therefore equation (7.10) can be rewritten as

$$\sum_{i=1}^{NS} \sigma_i h_i - \sum_{i=1}^{NS} \sigma_i^* h_i^* + \frac{\dot{Q}}{\dot{m}} = 0 \tag{7.12}$$

7.2 Solution Method

Equations (7.8) and (7.12) together form a set of NRS + 1 nonlinear algebraic equations in NRS + 1 unknowns. These equations are solved by using the Newton-Raphson (NR) iteration technique (e.g., refs. 43 and 128). For clarity in presentation the N-dimensional (N = NRS + 1) column vector $\underline{y}$, which contains the NRS + 1 unknowns, is defined as

$$y_i = \sigma_i, \qquad i = 1, \ldots, \text{NRS} \tag{7.13a}$$

$$y_N = T \text{ or } \dot{m}, \qquad N = \text{NRS} + 1 \tag{7.13b}$$

Equations (7.8) and (7.12) are written in the form

$$\phi_i(\underline{y}) = \sum_{j=1}^{NR}\left(\nu''_{ij} - \nu'_{ij}\right) r_j + \frac{\dot{m}}{\rho V}\left(\sigma_i^* - y_i\right) = 0, \qquad i = 1,\ldots,\text{NRS} \tag{7.14a}$$

$$\phi_N(\underline{y}) = \sum_{i=1}^{NS}\left(\sigma_i h_i - \sigma_i^* h_i^*\right) + \frac{\dot{Q}}{\dot{m}} = 0 \tag{7.14b}$$

Solving equations (7.8) and (7.12) is then equivalent to finding the zero of $\underline{\phi}$ where

$$\underline{\phi} = \left(\phi_1,\ldots,\phi_N\right)^T \tag{7.15}$$

and the superscript T indicates transpose.

In applying the NR iteration method $\{\ln y_i\}$ is solved for rather than $\{y_i\}$ to avoid negative $\{y_i\}$. If the mth estimates are denoted by $\ln y_i^{[m]}$ (i = 1,...,N), the NR iteration procedure for the corrections, $\Delta\ln y_i^{[m]}$ (i = 1,...,N), on the (m + 1)th iteration is

$$\sum_{k=1}^{NS} \left.\frac{\partial \phi_i}{\partial \ln y_k}\right|_{\underline{y}=\underline{y}^{[m]}} \Delta\ln y_k^{[m]} = -\phi_i\left(\underline{y}^{[m]}\right), \qquad i = 1,\ldots,N \tag{7.16}$$

The (m + 1)th approximations, $\ln y_i^{[m+1]}$ (i = 1,...,N), are given by

$$\ln y_i^{[m+1]} = \ln y_i^{[m]} + \Delta\ln y_i^{[m]}, \qquad i = 1,\ldots,N \tag{7.17}$$

The N-dimensional column vector $\underline{Y}$ is now defined as

$$\underline{Y} = \left(\ln y_1,\ldots,\ln y_N\right)^T \tag{7.18}$$

that is, the element Y_k is given by

$$Y_k = \ln y_k, \qquad k = 1,\ldots,N \tag{7.19}$$

Then equation (7.16) can be expressed compactly as

$$\mathbf{J}^{[m]}\,\Delta\underline{Y}^{[m]} = -\underline{\mathbb{f}}\left(\underline{y}^{[m]}\right) \tag{7.20}$$

where $\mathbf{J}^{[m]}$ is the $N\times N$ Jacobian matrix, with element $J_{ik}^{[m]}$ given by

$$J_{ik}^{[m]} = \left.\frac{\partial \mathbb{f}_i}{\partial Y_k}\right|_{\underline{Y}=\underline{Y}^{[m]}} = \left.\frac{\partial \mathbb{f}_i}{\partial \ln y_k}\right|_{\underline{y}=\underline{y}^{[m]}} = y_k^{[m]}\left.\frac{\partial \mathbb{f}_i}{\partial y_k}\right|_{\underline{y}=\underline{y}^{[m]}} \qquad i,k = 1,\ldots,N \tag{7.21}$$

The required partial derivatives, $\partial \mathbb{f}_i/\partial y_k$ (i,k = 1,...,N), are obtained from equations (7.14a) and (7.14b) and are derived in appendix A of part II. In evaluating $\partial \mathbb{f}_i/\partial y_k$ all other variables are, by definition, constant. In the present formulation the density is not treated as an unknown quantity although it varies with each iteration and has an effect on $\Delta\underline{Y}^{[m]}$ through $\underline{\mathbb{f}}$. This effect is taken into account by writing $\partial \mathbb{f}_i/\partial y_k$ as

$$\left(\frac{\partial \mathbb{f}_i}{\partial y_k}\right)_{\substack{\text{all other}\\ y_j}} = \left(\frac{\partial \mathbb{f}_i}{\partial y_k}\right)_{\substack{\text{all other}\\ y_j,\rho}} + \left(\frac{\partial \mathbb{f}_i}{\partial \rho}\right)_{\text{all } y_j}\left(\frac{\partial \rho}{\partial y_k}\right)_{\substack{\text{all other}\\ y_j}}, \qquad i,k = 1,\ldots,N \tag{7.22}$$

where $\partial\rho/\partial y_k$ is obtained from equation (7.2).

Starting with an initial guess, denoted by $\underline{y}^{[0]}$, successive approximations $\underline{y}^{[m]}$ (m = 1,...,M) ($y_i^{[m]} = \exp Y_i^{[m]}$, i= 1,...,N) are generated until the iteration converges, that is, the corrections $\{\Delta Y_i\}$ approach zero within a specified accuracy. The integer M is the number of iterations required for convergence, and $\underline{y}$ is taken to equal $\underline{y}^{[M]}$.

7.2.1 Initial Estimates

The initial estimates are determined from the chemical equilibrium solution generated under conditions of assigned pressure (= p^*) and mixture mass-specific enthalpy (= h^*). The computational procedure used for the equilibrium state is discussed in chapter 5. Now, for the desired mass flow rate (denoted by $\dot{m}_{\max}$) or reactor temperature (denoted by $T_{\min}$), the state in the PSR may be far from equilibrium. In such a situation the NR iteration procedure may either experience convergence difficulties or converge to a "false" solution—one that is mathematically correct but physically not realizable. To minimize these difficulties, the calculation is started with conditions (a small assigned mass flow rate or an assigned temperature close to the equilibrium temperature T_{eq}) that produce a solution close to the

equilibrium state. Because at the outset T_{eq} is not usually known, LSENS allows for the specification of the decrement ΔT in temperature for assigned-temperature problems.

Starting with initial estimates $\{\sigma_i^{[0]}\}$ and $T^{[0]}$ or $\dot{m}^{[0]}$ the governing equations are solved for the $\{\sigma_i\}$ and T or $\dot{m}$ to produce a solution close to the equilibrium state. The assigned variable $\dot{m}$ or T is then changed by the user-specified amount $\Delta\dot{m}$ or ΔT, and a second PSR solution is generated. The results given by the first PSR solution are used as initial estimates for the second solution. The process of changing the assigned variable by the user-specified amount and iterating for a new solution, starting with the previous solution as the initial estimate, is continued until the desired mass flow rate $\dot{m}_{max}$ or temperature T_{min} is obtained.

As discussed in section 7.3 it is necessary to generate at least one intermediate solution before the validity of the solution at the desired condition can be tested. To accomplish this objective, the value is restricted for the user-supplied mass flow rate $\dot{m}_1$ or temperature T_1 $(= T_{eq} - \Delta T)$ for the first PSR solution. In addition, for an assigned-mass-flow-rate problem at least two restarts of the first PSR solution are provided for in the event of a false first or second PSR solution. Finally because $\{\ln \sigma_i\}$ are solved for, it is necessary to set a minimum value for the species mole numbers $\{\sigma_i^{[0]}\}$. A minimum value of $\sigma_i = 10^{-10}$ mole/g is used in the code. Hence the initial estimates and assigned value $\dot{m}_1$ or T_1 for the first solution are

$$\sigma_i^{[0]} = \max\left(\sigma_{i,eq}, 10^{-10}\right), \qquad i = 1, \ldots, NS \tag{7.23a}$$

Assigned mass flow rate

$$\dot{m}_1 \leftarrow \min\left(\dot{m}_1, \frac{\dot{m}_{max}}{4}\right), \qquad T^{[0]} = T_{eq} \tag{7.23b}$$

Assigned temperature

$$\dot{m}^{[0]} = \dot{m}_0, \qquad T_1 = \max\left(T_{eq} - \Delta T, \frac{T_{eq} + T_{min}}{2}\right) \tag{7.23c}$$

In these equations the arrow "$\leftarrow$" denotes the replacement operator and $\dot{m}_0$ is the user-supplied mass flow rate to start the iteration for the first solution of an assigned-temperature problem.

7.2.2 Control of Corrections

At each iteration the corrections $\{\Delta Y_i^{[m]}\}$ ($m = 0,1,...,M-1$) are generated by solving equation (7.20) by the Gaussian elimination method (ref. 35). If these corrections are too large, they can lead to convergence difficulties if used unchanged in equation (7.17) to compute the new estimates (refs. 113, 117, and 123). Large corrections can arise for one of two reasons: in the early stages of the iteration procedure because of a poor initial estimate, or in later stages because of large increases in the concentration of trace species (refs. 113 and 115). In order to restrict the magnitude of the corrections to the variables, the underrelaxation or control factor Λ, developed by Gordon and McBride (ref. 117) for chemical equilibrium state calculations, is used. Their scheme for computing Λ is based on two empirical rules. The first rule is applied (1) to species k that satisfy the requirements $\Delta Y_k^{[m]} > 0$ and $\sigma_k^{[m]} > 10^{-8}\,\sigma_m^{[m]}$ and (2) to the temperature or mass flow rate. It produces the parameter Λ_1, which is defined for the $(m + 1)$th iteration $(m = 0,1,...,M-1)$ as

$$\Lambda_1 = \frac{2}{\max\left(\left|5\,\Delta Y_N^{[m]}\right|,\ \left|\Delta Y_k^{[m]}\right|\right)} \qquad \text{for } \Delta Y_k^{[m]} > 0;\ \ \sigma_k^{[m]} > 10^{-8}\sigma_m^{[m]} \tag{7.24}$$

This equation limits the change in any variable to a factor $e^{0.4}$ (= 1.4918) or e^2 (= 7.3891).

The second rule is applied to trace species k (defined here as a species with mole fraction $\sigma_k^{[m]}/\sigma_m^{[m]}$ less than or equal to 10^{-8}) for which $\Delta Y_k^{[m]} > 0$. It gives the parameter Λ_2, which is defined for the $(m + 1)$th iteration $(m = 0,1,...,M-1)$ by

$$\Lambda_2 = \min\left|\frac{\ln\left(10^{-4}\sigma_m^{[m]}\right) - Y_k^{[m]}}{\Delta Y_k^{[m]}}\right| \qquad \text{for } \Delta Y_k^{[m]} > 0;\ \ \sigma_k^{[m]} \le 10^{-8}\sigma_m^{[m]} \tag{7.25}$$

Equation (7.25) prevents a mole fraction that is less than or equal to 10^{-8} from increasing to more than 10^{-4}.

The control factor Λ is then given by

$$\Lambda = \min\left(1, \Lambda_1, \Lambda_2\right) \tag{7.26}$$

The new estimate $\underline{Y}^{[m+1]}$ is calculated as

$$\underline{Y}^{[m+1]} = \underline{Y}^{[m]} + \Lambda\,\Delta\underline{Y}^{[m]}, \qquad m = 0,\ldots,M-1 \tag{7.27}$$

Finally at each iteration it was found necessary to set a minimum value for the species mole number. A value of $\sigma_i^{[m+1]} = 10^{-10}$ is used for all trace species.

7.2.3 Convergence Criteria

After each iteration several tests are used to ascertain convergence of the solution. First, mass conservation is checked by examining the sum S_m of mass fractions

$$S_m = \sum_{i=1}^{NS} \sigma_i M_{w,i} \tag{7.28}$$

where $M_{w,i}$ is the molar mass of the ith species. If S_m is different from unity, the composition is clearly incorrect. Experience suggests that mass is conserved to sufficient accuracy if the following criterion is satisfied:

$$\left|S_m - 1\right| \overset{?}{\leq} 3\times10^{-5} \tag{7.29}$$

If S_m is significantly different from unity, continued iteration produces little improvement in the situation—the estimates remain physically unrealistic. Hence, if S_m is different from unity by more than 0.2, the iteration is abandoned and the corrective actions described in section 7.3 are taken. If S_m is not different from unity by more than 0.2 but fails to satisfy equation (7.29), the next iteration is performed.

If equation (7.29) is satisfied, the remaining convergence tests, which were all adapted from Gordon and McBride (ref . 117), are as follows: The control factor Λ is examined because it is equal to unity when the variables are close to the correct values; when they are far from the correct values, Λ will be less than unity (ref. 113). Therefore, if Λ is not equal to unity, a new iteration is performed.

Next the magnitude of $\Delta Y_N^{[m]}$ (= $\Delta \ln T^{[m]}$ for an assigned-mass-flow-rate problem or $\Delta \ln \dot{m}^{[m]}$ for an assigned-temperature problem) must satisfy

$$\left|\Delta Y_N^{[m]}\right| \overset{?}{\leq} 10^{-4} \tag{7.30}$$

The last test involves the magnitudes of $\Delta \ln \sigma_i^{[m]}$ (= $\Delta Y_i^{[m]}$, i = 1,...,NRS), which must all satisfy the criterion

$$\left|\frac{\sigma_i^{[m+1]}\ \Delta Y_i^{[m]}}{\sigma_m^{[m+1]}}\right| \overset{?}{\leq} \text{EPS}, \qquad i = 1,\ldots,\text{NRS} \tag{7.31}$$

Gordon and McBride (ref. 113) recommend a value of EPS = 5×10^{-6} for chemical equilibrium computations. However, for the PSR problem a value of 5×10^{-5} was found to be adequate.

The iteration procedure is continued until either the estimates converge or the number of iterations exceeds the maximum allowable, when an error exit is taken. The maximum number of iterations is set equal to 75, as a compromise between allowing enough iterations to obtain convergence and preventing excessive computational work with no convergence.

7.3 Converged Solution Tests

The equations describing the PSR problem are nonlinear and may therefore possess multiple solutions, only one of which represents the desired state. Of course, the nonlinearity of the equations precludes any guarantee of solution existence. Also, because a Newton-Raphson iteration technique is used, poor initial estimates may produce a false solution—one that is mathematically correct but physically unrealizable. In order to ensure that the solution is not unrealistic, several tests and corrective actions are built into the code.

As discussed in section 7.2.1, the solution at the desired condition ($\dot{m}_{\max}$ or $T_{\min}$) is obtained by solving a series of PSR problems (i.e., by generating a sequence of converged solutions). For clarity the results produced on the nth convergence ($n = 1,2,...$) are denoted by $\sigma_{i,n}$ ($i = 1,...,$NRS), $\dot{m}_n$, and T_n. For an assigned-mass-flow-rate problem $\dot{m}_n$ is prescribed and $\{\sigma_{i,n}\}$ and T_n are solved for. Similarly, for an assigned-temperature problem T_n is fixed and $\{\sigma_{i,n}\}$ and $\dot{m}_n$ are solved for. The initial estimates used to start the nth solution are denoted by $\{\sigma_{i,n}^{[0]}\}$ and $T_n^{[0]}$ or $\dot{m}_n^{[0]}$. For the first solution the initial estimates are given by equations (7.23a) to (7.23c). For subsequent solutions the previously converged solution gives the initial estimates. Hence for $n = 2,3,...$

$$\sigma_{i,n}^{[0]} = \sigma_{i,n-1}, \qquad i = 1,..., \text{NRS} \tag{7.32a}$$

Assigned mass flow rate

$$\dot{m}_n = \min(\dot{m}_{n-1} + \Delta\dot{m}, \dot{m}_{\max}), \qquad T_n^{[0]} = T_{n-1} \tag{7.32b}$$

Assigned temperature

$$\dot{m}_n^{[0]} = \dot{m}_{n-1}, \qquad T_n = \max(T_{n-1} - \Delta T, T_{\min}) \tag{7.32c}$$

The converged solution tests and corrective actions used are now described. Assigned-mass-flow-rate problems are discussed first; then assigned-temperature problems are considered.

7.3.1 Assigned-Mass-Flow-Rate Problem

For an assigned-mass-flow-rate problem each PSR solution is attempted with a larger $\dot{m}$ than the previous solution, as described above (see eq. (7.32b)). Hence each converged temperature must be less than the temperature obtained on the previous convergence. It is physically impossible for both the mass flow rate and the temperature to increase (e.g., ref. 130). Hence a simple test for solution validity is that T_n must be less than T_{n-1} ($n = 2,3,...$). For the first convergence T_1 must be less than T_{eq} because $\dot{m}_1$ is finite. Experience has shown that a failed second solution (i.e., $T_2 \geq T_1$) is usually due to poor initial estimates—a poor first convergence even though $T_1 < T_{eq}$. For this reason $\dot{m}_1$ is restricted such that at least two converged solutions have to be generated before $\dot{m}_{max}$ is reached. This precaution increases the reliability of the solution, if any, obtained for $\dot{m}_{max}$. Because a failed second solution is due to a poor first convergence, both the first and second converged solutions are rejected. A new first solution is then attempted with the same initial estimates $\{\sigma_{i,1}^{[0]}\}$ and $T_1^{[0]}$ as before (see eqs. (7.23a) and (7.23b)); however, the assigned mass flow rate $\dot{m}_1$ is increased as follows:

$$\dot{m}_1 \leftarrow \min\left(2\dot{m}_1, 0.75\dot{m}_{max}\right) \tag{7.33}$$

Now equation (7.23b) shows that the maximum mass flow rate assigned for the first attempt at producing the first converged solution is restricted to $0.25\dot{m}_{max}$. Therefore equation (7.33) allows for at least three attempts to produce a first solution and, for reasons given previously, the generation of at least one additional converged solution. These corrective actions are also taken in the event of a failed first solution (i.e., $T_1 \geq T_{eq}$). If the use of $\dot{m}_1 = 0.75\dot{m}_{max}$ does not produce a satisfactory first or second converged solution, an error exit is taken.

If the solution obtained on the third or subsequent convergence is unsatisfactory because $T_n \geq T_{n-1}$ ($n = 3,4,...$), only the latest (i.e., the nth) solution is rejected. A new nth solution is then attempted with the same initial estimates for $\{\sigma_{i,n}^{[0]}\}$ and $T_n^{[0]}$ as before (see eqs. (7.32a) and (7.32b)), but $\dot{m}_n$ is increased as follows:

$$\dot{m}_n \leftarrow \min\left(2\dot{m}_n, \dot{m}_{max}\right) \tag{7.34}$$

If the use of $\dot{m}_n = \dot{m}_{max}$ results in an invalid solution, an error exit is taken.

This procedure is repeated until either (1) a satisfactory solution is obtained at the desired mass flow rate $\dot{m}_{max}$ or (2) an error exit is taken for one of the two reasons just given or because either an invalid solution is obtained after three restarts or a converged temperature is not significantly greater than the inlet temperature. The

last condition indicates that the specified mass flow rate is too large to sustain the reaction and so "blowout" (refs. 129 and 130) occurs . It is arbitrarily required that the difference between the converged temperature and the inlet temperature must be greater than 10 K for the solution to be satisfactory.

7.3.2 Assigned-Temperature Problem

For this problem type the converged mass flow rate must clearly be greater than zero. However, because logarithmic variables are used, the converged solution will always be positive. Hence the converged mass flow rate being greater than zero is not a sufficient condition for solution validity. Now because each PSR solution is attempted with a smaller temperature than the previous solution (see eq. (7.32c)), the converged mass flow rate must increase, as observed in section 7.3.1. Thus for a solution to be accepted as satisfactory the converged mass flow rate must be greater than the $\dot{m}$ obtained on the previous convergence. Of course, in order to apply this test, at least two converged solutions must be generated. As discussed in section 7.2.1, the value assigned for T_1 (the temperature for the first convergence) guarantees that at least two solutions have to be generated before the desired temperature $T_{\min}$ is reached (see eq. (7.23c)).

If the mass flow rate $\dot{m}_2$ produced on the second convergence is not greater than $\dot{m}_1$, the following actions are taken: A poor second convergence is invariably due to a poor first convergence, which cannot of course be tested. Hence the first and second converged solutions are both rejected, and a new first solution is attempted with the same initial estimates for $\{\sigma_{i,1}^{[0]}\}$ as before (see eq. (7.23a)) but with a larger $\dot{m}_1^{[0]}$. Experience has shown that it is best to increase the initial estimate significantly, and the following empirical rule is used:

$$\dot{m}_1^{[0]} \leftarrow 10\,\dot{m}_1^{[0]} \tag{7.35}$$

If an invalid solution is obtained on the third or subsequent convergence (i.e., $\dot{m}_n \leq \dot{m}_{n-1}$, $n = 3,4,...$), only the results of the latest (i.e., the nth) convergence are rejected. A new nth solution is then attempted with the same initial estimates for the $\{\sigma_{i,n}^{[0]}\}$ as before (see eq. (7.32a)), but the initial mass flow rate estimate $\dot{m}_n^{[0]}$ is increased tenfold. This procedure is repeated until either a satisfactory solution is obtained at the desired temperature $T_{\min}$ or the converged solution is still unsatisfactory after three restarts, in which case an error exit is taken. One possible reason for the failure is that the assigned temperature is too low to sustain the reaction and so blowout occurs.

7.4 Test Problems

This section examines the accuracy and efficiency of LSENS for PSR computations. In particular, it is applied to a simple problem, which was taken from

reference 131 and describes the adiabatic combustion of a stoichiometric fuel-air mixture in a PSR. The fuel consisted of a mixture of 80 percent hydrogen and 20 percent nitrogen. The air was a mixture of 21 percent oxygen and 79 percent nitrogen. The fuel and air compositions and fuel-air stoichiometry correspond to the following reactor inlet composition: 27.54 percent hydrogen, 13.77 percent oxygen, and 58.69 percent nitrogen. (All results presented herein were obtained with this inlet mixture composition.) The remaining input data for the problem were reactor volume, 67.4 cm^3; pressure, 1 atm; inlet temperature, 298 K; and mass flow rate, 450 g/s.

The hydrogen-oxygen-nitrogen reaction mechanism consisted of 18 reversible elementary chemical reactions among 8 reacting species (H_2, O_2, O, H, OH, HO_2, H_2O_2, and H_2O) and the inert species N_2. The reaction mechanism and forward rate coefficient parameters are given in table 7.1. For each reaction the backward rate coefficient was computed by using the law of microscopic reversibility, equation (2.6), and the concentration equilibrium constant. Glarborg et al. (ref. 131) write reaction (9) as three reactions

$$H + O_2 + M \rightleftharpoons HO_2 + M \tag{7.36}$$

$$H + O_2 + O_2 \rightleftharpoons HO_2 + O_2 \tag{7.37}$$

and

$$H + O_2 + N_2 \rightleftharpoons HO_2 + N_2 \tag{7.38}$$

and assign a zero third-body collisional efficiency for O_2 and N_2 in reaction (9). Therefore the mechanism given in this reference consists of 19 reversible reactions. As described in chapters 8 and 11 of part II the present version of LSENS is restricted to two different reactant species and two different product species. Hence the reaction given by equation (7.37) could be used (see reaction (10) in table 7.1) but not that given by equation (7.38). The latter reaction was included by specifying a nonzero third-body collisional efficiency for N_2 in reaction (9). The efficiency listed in table 7.1 for N_2 was obtained by comparing the following two rate constants at the reactor exit temperature (1396.54 K) given in reference 131: The first value was computed by using Glarborg et al.'s (ref. 131) rate coefficient expression for the reaction given by equation (7.38). The second value was obtained from the rate coefficient expression given in table 7.1 for reaction (9).

Solution to this assigned-mass-flow-rate problem was attempted with LSENS, using the parameter values $\dot{m}_1$ (assigned mass flow rate for first convergence) = 10g/s, $\Delta\dot{m}$ (mass flow rate increment after each successful convergence, see eq. (7.32b)) = 100 g/s, and $\dot{m}_{max}$ (desired mass flow rate) = 450 g/s. No difficulty was encountered and the solution at the desired mass flow rate was produced after six successful convergences. The composition and thermodynamic properties at the

TABLE 7.1.—REACTION MECHANISM AND FORWARD RATE COEFFICIENT PARAMETERS FOR TEST PROBLEM

Reaction number, j	Reaction	Forward rate coefficient parameters[a,b]		
		A_j	n_j	E_j
1	$H + O_2 \rightleftharpoons O + OH$	5.1×10^{16}	−0.82	16 510
2	$H_2 + O \rightleftharpoons H + OH$	1.8×10^{10}	1.0	8 830
3	$H_2 + OH \rightleftharpoons H_2O + H$	1.2×10^{9}	1.3	3 630
4	$OH + OH \rightleftharpoons H_2O + O$	6.0×10^{8}	1.3	0
[c]5	$H + OH + M \rightleftharpoons H_2O + M$	7.5×10^{23}	−2.6	0
6	$O_2 + M \rightleftharpoons O + O + M$	1.9×10^{11}	0.5	95 560
[c]7	$H_2 + M \rightleftharpoons H + H + M$	2.2×10^{12}	0.5	92 600
8	$H_2 + O_2 \rightleftharpoons OH + OH$	1.7×10^{13}	0.0	47 780
[c]9	$H + O_2 + M \rightleftharpoons HO_2 + M$	2.1×10^{18}	−1.0	0
10	$H + O_2 + O_2 \rightleftharpoons HO_2 + O_2$	6.7×10^{19}	−1.42	0
11	$HO_2 + H \rightleftharpoons H_2 + O_2$	2.5×10^{13}	0.0	700
12	$HO_2 + H \rightleftharpoons OH + OH$	2.5×10^{14}	0.0	1 900
13	$HO_2 + O \rightleftharpoons OH + O_2$	4.8×10^{13}	0.0	1 000
14	$HO_2 + OH \rightleftharpoons H_2O + O_2$	5.0×10^{13}	0.0	1 000
15	$HO_2 + HO_2 \rightleftharpoons H_2O_2 + O_2$	2.0×10^{12}	0.0	0
16	$H_2O_2 + M \rightleftharpoons OH + OH + M$	1.2×10^{17}	0.0	45 500
17	$H_2O_2 + H \rightleftharpoons HO_2 + H_2$	1.7×10^{12}	0.0	3 750
18	$H_2O_2 + OH \rightleftharpoons H_2O + HO_2$	1.0×10^{13}	0.0	1 800

[a]Rate coefficient $k_j = A_j T^{n_j} \exp(-E_j/RT)$; units are moles, centimeters, seconds, and calories.

[b]From reference 131.

[c]Third-body collisional efficiencies:

Reaction 5: $H_2O = 20.0$

Reaction 7: $H_2O = 6.0$, $H = 2.0$, $H_2 = 3.0$

Reaction 9: $H_2O = 21.0$, $H_2 = 3.3$, $O_2 = 0.0$, $N_2 = 1.5$.

reactor exit and the average residence time are given in table 7.2. Here x_i is the mole fraction of species i and the other quantities have been defined previously. This solution and, unless otherwise indicated, all results presented in this section were generated on the NASA Lewis Research Center's Amdahl 5870 computer using the UTS operating system, the Fujitsu 77 compiler (optimization level, 3), and double precision. The computational work required for the problem was 24 iterations and approximately 0.1 s of execution time.

The solution obtained by Glarborg et al. (ref. 131) on a VAX 11/780 computer with their code PSR is also listed in table 7.2. The agreement between PSR and

TABLE 7.2.—REACTOR EXIT PROPERTIES FOR TEST PROBLEM
[Pressure, 1 atm; inlet temperature, 298 K; mass flow rate, 450 g/s.]

Variable	PSR[a]	LSENS	PSR[b]
x_H	5.02×10^{-2}	5.03×10^{-2}	5.03×10^{-2}
x_{O_2}	3.96×10^{-2}	3.92×10^{-2}	3.92×10^{-2}
x_O	7.94×10^{-3}	7.95×10^{-3}	7.95×10^{-3}
x_{OH}	5.71×10^{-3}	6.03×10^{-3}	6.03×10^{-3}
x_{H_2}	6.50×10^{-2}	6.43×10^{-2}	6.43×10^{-2}
x_{H_2O}	0.202	0.203	0.203
x_{HO_2}	1.88×10^{-5}	1.85×10^{-5}	1.85×10^{-5}
$x_{H_2O_2}$	2.70×10^{-5}	2.71×10^{-5}	2.71×10^{-5}
x_{N_2}	0.629	0.629	0.629
T, K	1396.54	1398.81	1398.72
ρ, g/cm^3	2.00×10^{-4}	2.00×10^{-4}	2.00×10^{-4}
τ_r, s	3.00×10^{-5}	2.99×10^{-5}	3.00×10^{-5}

[a]From reference 131.
[b]This work.

LSENS was, in general, excellent. In order to examine if the discrepancies in the results, especially x_{OH}, produced by the two codes were due to the different reaction mechanisms and thermodynamic data used, solution to the problem was attempted with PSR (version 2.3, dated April 1992) on the Amdahl 5870 computer using the UTS operating system, the Fujitsu 77 compiler (optimization level, 3), and double precision. However, the code could not be compiled, and therefore solution was attempted on the NASA Lewis Research Center's VAX 8800 computer using the VAX/VMS operating system (version 5.5–1), the VAX FORTRAN compiler (version 5.9), double precision, and VAX G_floating data type (i.e., the code was compiled with the G_FLOATING option). No difficulty was encountered on this system and the solution is given in table 7.2. This solution was obtained with the same reaction mechanism (i.e., table 7.1) and thermodynamic data as those used with LSENS and a value of 1398.81 K (= reactor exit temperature obtained with LSENS) for the variable TEMP, which is the user-supplied initial estimate of the reactor temperature for an assigned-mass-flow-rate problem (ref. 131). Also, to minimize execution time, a value of zero was assigned for the variable PRNT, which controls the amount of information generated by the code. Table 7.2 shows that the PSR and LSENS results were virtually identical. (LSENS produced exactly the same results on both the Amdahl 5870 and VAX 8800 computers.)

On the VAX 8800 computer LSENS required 26 iterations and 0.33 s of execution time, whereas PSR required 6.2 s. The computational cost of PSR depended on the value specified for TEMP. This quantity was varied from the reactor exit temperature to the equilibrium temperature T_{eq} for the inlet state. The effect of TEMP on the execution time is shown in table 7.3. For several values of TEMP, PSR could not

TABLE 7.3.—EFFECT OF USER-SUPPLIED ESTIMATE OF REACTOR TEMPERATURE ON EXECUTION TIME REQUIRED BY PSR ON VAX 8800 COMPUTER
[Pressure, 1 atm; inlet temperature, 298 K; mass flow rate, 450 g/s.]

Reactor temperature estimate, TEMP, K	Execution time, s
[a]1398.81	6.2
1500	5.9
1750	0.74
2000	4.6
[b]2293.56	0.80

[a]Reactor temperature produced by LSENS (see table 7.2).
[b]Equilibrium temperature computed by LSENS on VAX 8800 computer.

produce a successful first solution and so had to take relatively expensive corrective actions. Hence the runs with TEMP = 1750 K and T_{eq} were substantially faster than the others (see table 7.3), showing that the computational cost can be decreased significantly by a judicious choice of TEMP. Note, however, that in all cases the execution times were much longer than that required by LSENS. In particular, LSENS was faster than PSR by a factor of between 2.2 and approximately 19.

The same problem was reformulated as an assigned-temperature problem by using the reactor exit temperature computed with LSENS to check its accuracy for assigned-temperature problems. The parameter values were ΔT (temperature decrement for each solution, see eqs. (7.23c) and (7.32c)) = 100 K, $\dot{m}_0$ ($= \dot{m}_1^{[0]}$, the mass flow rate to start iteration for the first converged solution) = 10 g/s, and T_{min} (desired temperature at reactor exit) = 1398.81 K. No difficulty was encountered and the solution at the desired exit temperature was produced after 9 successful convergences, 46 iterations, and 0.13 s of execution time. The reactor exit properties and residence time were exactly the same as the values given in table 7.2 for the assigned-mass-flow-rate problem. Finally for the specified reactor exit temperature the converged mass flow rate was 450 g/s. Thus the accuracy of LSENS for assigned-temperature problems was verified.

The assigned-temperature problem was solved with PSR on the VAX 8800 computer. Now, unlike LSENS, which solves for $\dot{m}$ and $\{\sigma_i\}$ at the reactor exit for such a problem, PSR requires a user-supplied value for either $\dot{m}$ or τ_r and solves for the mixture composition at the reactor exit. A value of $\dot{m} = 450$ g/s was therefore assigned. The composition, residence time, and density were exactly the same as the values obtained with LSENS (table 7.2). PSR could not, however, produce a successful first solution and the execution time was 6.0 s. In contrast, LSENS

required 46 iterations and 0.42 s of execution time on the VAX 8800 computer. Thus for this problem LSENS was faster than PSR by a factor of 14.

The effects of $\dot{m}_1$ and $\Delta\dot{m}$ on LSENS accuracy and efficiency for assigned-mass-flow-rate problems were studied by varying $\dot{m}_1$ from 10^{-3} to the maximum value, 112.5 g/s (= 450/4, see eq. (7.23b)), allowed by the code. For each $\dot{m}_1$, $\Delta\dot{m}$ was varied from max($\dot{m}_1$,1) to 450 g/s. The total number of iterations and the execution time required to solve the problem are given in table 7.4 for various combinations of $\dot{m}_1$ and $\Delta\dot{m}$. The execution time includes the computational cost associated with the equilibrium state calculation and output of all results. Also listed in table 7.4 are the temperature T_1 obtained on the first convergence (i.e., for $\dot{m} = \dot{m}_1$) and the number of iterations required for this solution. The reactor exit properties and residence time for all $\dot{m}_1$ and $\Delta\dot{m}$ considered in table 7.4 were exactly the same as the results given in table 7.2. The insensitivity of the solution to $\dot{m}_1$ and $\Delta\dot{m}$ illustrates the accuracy and robustness of the code: note that $\dot{m}_1$ was varied by five orders of magnitude and $\Delta\dot{m}$ by two orders of magnitude. Table 7.4 shows that for all $\dot{m}_1$ the execution time decreased with increasing $\Delta\dot{m}$ but was relatively insensitive to $\dot{m}_1$ for a given $\Delta\dot{m}$.

The effects of ΔT and $\dot{m}_0$ on the computational work required by LSENS for assigned-temperature problems are illustrated in table 7.5. The temperature decrement was varied from 1 K to the maximum value allowed by the code. Now on the Amdahl 5870 computer T_{eq} was 2293.55 K, and because T_{min} = 1398.81 K, the smallest value that could be specified for T_1 (the temperature for the first convergence) was 1846.18 K (= ($T_{eq} + T_{min}$)/2, see eq. (7.23c)). Hence the maximum ΔT that could be assigned was 447.37 K. For each ΔT, $\dot{m}_0$ was varied from 10^{-3} to 450 g/s. The mass flow rate $\dot{m}_1$ obtained on the first convergence (i.e., with $T = T_1$) and the number of iterations required for this solution are also given in table 7.5. As expected, for each ΔT the computational work was minimum for the $\dot{m}_0$ that was closest to $\dot{m}_1$. The total number of iterations increased as $\dot{m}_0$ moved away from $\dot{m}_1$, but the execution time was relatively insensitive to $\dot{m}_0$ for a given ΔT. The computational cost, however, varied significantly with ΔT. For this problem use of a large ΔT is indicated. For all ΔT and $\dot{m}_0$ values the reactor exit properties and residence time were identical to the results given in table 7.2, and the mass flow rate was 450 g/s for T = 1398.81 K. The robustness of the code was further verified by generating results with ΔT = 100 K and various $\dot{m}_0$ values in the range [500,10^9] g/s. In each case the results given in table 7.2 were reproduced and $\dot{m}$ = 450 g/s. This observation further illustrates the insensitivity of the solution to ΔT and $\dot{m}_0$: note that $\dot{m}_0$ was varied by 12 orders of magnitude.

The following additional experiments were performed for assigned-temperature problems: Glarborg et al. (ref. 131) report that for T_1 = 1700 K and $\dot{m}_0$ = 400 g/s their code PSR could not produce a successful first solution; that is, it failed to converge. The same problem was attempted with LSENS. Now, for T_1 = 1700 K, ΔT (= 593.55 K) exceeds the maximum value (447.37 K) allowed by the code. LSENS was therefore modified so that the problem could be attempted with this ΔT. No difficulty was encountered and the solution at T = 1398.81 K was produced after two successful convergences. The computational work requirement

TABLE 7.4.—EFFECTS OF MASS FLOW RATE ASSIGNED FOR FIRST CONVERGENCE AND MASS FLOW RATE INCREMENT ON TEMPERATURE OBTAINED AFTER FIRST CONVERGENCE AND COMPUTATIONAL WORK FOR PROBLEM

Mass flow rate assigned for first convergence, $\dot{m}_1$, g/s	Mass flow rate increment, $\Delta\dot{m}$, g/s	Temperature after first convergence, T_1, K	Number of iterations for first convergence	Total number of iterations for problem	Execution time, s
10^{-3}	1	2293.54	1	923	2.3
	5	2293.54	1	204	0.54
	10	2293.54	1	115	0.32
	50	2293.54	1	35	0.12
	100	2293.54	1	23	0.093
	250	2293.54	1	14	0.073
	450	2293.54	1	10	0.065
10^{-2}	1	2293.39	1	923	2.3
	5	2293.39	1	204	0.54
	10	2293.39	1	115	0.32
	50	2293.39	1	35	0.12
	100	2293.39	1	23	0.093
	250	2293.39	1	14	0.073
	450	2293.39	1	10	0.065
0.1	1	2273.85	7	928	2.3
	5	2273.85	7	207	0.55
	10	2273.85	7	119	0.33
	50	2273.85	7	39	0.13
	100	2273.85	7	27	0.11
	250	2273.85	7	18	0.081
	450	2273.85	7	15	0.077
1	1	2192.85	7	922	2.3
	5	2192.85	7	209	0.55
	10	2192.85	7	118	0.33
	50	2192.85	7	38	0.13
	100	2192.85	7	26	0.10
	250	2192.85	7	17	0.081
	450	2192.85	7	14	0.073
5	5	2071.12	7	203	0.54
	10	2071.12	7	118	0.32
	50	2071.12	7	38	0.13
	100	2071.12	7	25	0.11
	250	2071.12	7	16	0.077
	450	2071.12	7	13	0.069
10	10	1998.93	7	114	0.31
	50	1998.93	7	37	0.13
	100	1998.93	7	24	0.097
	250	1998.93	7	16	0.077
	450	1998.93	7	13	0.069

TABLE 7.4.—Concluded.

Mass flow rate assigned for first convergence, $\dot{m}_1$, g/s	Mass flow rate increment, $\Delta\dot{m}$, g/s	Temperature after first convergence, T_1, K	Number of iterations for first convergence	Total number of iterations for problem	Execution time, s
50	50	1784.67	8	34	0.12
	100	1784.67	8	23	0.093
	250	1784.67	8	17	0.081
	450	1784.67	8	13	0.069
100	100	1674.90	8	22	0.093
	250	1674.90	8	16	0.077
	450	1674.90	8	13	0.069
[a]112.5	112.5	1655.37	8	19	0.089
	250	1655.37	8	16	0.077
	450	1655.37	8	13	0.069

[a]Maximum value allowed by code for problem.

TABLE 7.5.—EFFECTS OF TEMPERATURE DECREMENT AND MASS FLOW RATE TO START ITERATION ON MASS FLOW RATE OBTAINED AFTER FIRST CONVERGENCE AND COMPUTATIONAL WORK FOR PROBLEM

Temperature decrement, ΔT, K	Mass flow rate to start iteration, $\dot{m}_0$, g/s	Mass flow rate after first convergence, $\dot{m}_1$, g/s	Number of iterations for first convergence	Total number of iterations for problem	Execution time, s
1	10^{-3}	4.278×10^{-3}	7	1895	4.4
	5×10^{-3}	4.278×10^{-3}	3	1891	4.4
	10^{-2}	4.278×10^{-3}	5	1893	4.4
	0.1	4.278×10^{-3}	11	1899	4.4
	1	4.278×10^{-3}	17	1905	4.4
	10	4.278×10^{-3}	22	1910	4.4
	100	4.278×10^{-3}	28	1916	4.4
	450	4.278×10^{-3}	32	1920	4.5
5	10^{-3}	2.218×10^{-2}	11	552	1.2
	10^{-2}	2.218×10^{-2}	5	546	1.2
	5×10^{-2}	2.218×10^{-2}	5	546	1.2
	0.1	2.218×10^{-2}	7	548	1.2
	1	2.218×10^{-2}	13	554	1.2
	10	2.218×10^{-2}	18	559	1.2
	100	2.218×10^{-2}	24	565	1.2
	450	2.218×10^{-2}	28	569	1.3

TABLE 7.5.—Concluded.

Temperature decrement, ΔT, K	Mass flow rate to start iteration, $\dot{m}_0$, g/s	Mass flow rate after first convergence, $\dot{m}_1$, g/s	Number of iterations for first convergence	Total number of iterations for problem	Execution time, s
10	10^{-3}	4.645×10^{-2}	13	287	0.64
	10^{-2}	4.645×10^{-2}	7	281	0.64
	5×10^{-2}	4.645×10^{-2}	3	277	0.63
	0.1	4.645×10^{-2}	5	279	0.64
	1	4.645×10^{-2}	11	285	0.64
	10	4.645×10^{-2}	17	291	0.65
	100	4.645×10^{-2}	22	296	0.66
	450	4.645×10^{-2}	26	300	0.67
50	10^{-3}	0.3309	17	88	0.21
	10^{-2}	0.3309	12	83	0.20
	0.1	0.3309	5	76	0.19
	0.5	0.3309	4	75	0.19
	1	0.3309	6	77	0.20
	10	0.3309	12	83	0.20
	100	0.3309	17	88	0.21
	450	0.3309	21	92	0.22
100	10^{-3}	0.9878	20	57	0.15
	10^{-2}	0.9878	14	51	0.14
	0.1	0.9878	9	46	0.13
	0.5	0.9878	6	43	0.13
	1	0.9878	5	42	0.12
	5	0.9878	7	44	0.13
	10	0.9878	9	46	0.13
	100	0.9878	15	52	0.14
	450	0.9878	18	55	0.15
250	10^{-3}	6.609	24	44	0.12
	10^{-2}	6.609	19	39	0.11
	0.1	6.609	13	33	0.10
	1	6.609	8	28	0.092
	5	6.609	6	26	0.089
	10	6.609	6	26	0.089
	100	6.609	11	31	0.097
	450	6.609	15	35	0.11
[a]447.37	10^{-3}	32.92	28	38	0.11
	10^{-2}	32.92	23	33	0.10
	0.1	32.92	17	27	0.089
	1	32.92	12	22	0.081
	10	32.92	7	17	0.073
	50	32.92	8	18	0.073
	100	32.92	8	18	0.073
	450	32.92	11	21	0.079

[a]Maximum value allowed by code for problem.

was 17 iterations and 0.073 s. The reactor exit properties, mass flow rate, and residence time agreed with the values given in table 7.2. The same results were obtained for $\dot{m}_0$ in the range $[10^{-3},10^{9}]$ g/s.

As final tests of LSENS, solutions were attempted (1) with $\dot{m}_1$ increased to the desired mass flow rate and (2) with T_1 decreased to the desired reactor exit temperature. Thus for both problem types the code's ability to produce the desired solution after only one convergence was examined. Note that the reactor exit conditions are significantly different from the equilibrium state, which is used to start the iteration. Therefore the two problems represent the most difficult tests of the code.

The assigned-mass-flow-rate problem was attempted with $\dot{m}_1 = 450$ g/s and $\dot{m}_{max} = 2000$ g/s. No difficulty was encountered with the first convergence, and the correct reactor exit properties and residence time were obtained. Nine iterations were required for this solution.

The assigned-temperature problem was attempted with $\Delta T = 894.74$ K and $T_{min} = 310$ K, and $\dot{m}_0$ was varied from 10^{-3} to 10^{9} g/s. No difficulty was experienced with any $\dot{m}_0$; in all cases the correct reactor exit properties, mass flow rate, and residence time were generated on the first convergence. As expected, the number of iterations depended on $\dot{m}_0$ and had a minimum value of 7 for $\dot{m}_0 = 450$ g/s. The extreme conditions $\dot{m}_0 = 10^{-3}$ and 10^{9} g/s required 36 and 41 iterations, respectively. The last two examples provide additional confirmation of the efficiency, accuracy, and robustness of LSENS for PSR problems.

References

1. Gardiner, W.C., Jr., ed.: Combustion Chemistry. Springer-Verlag, New York, 1984, pp. 1–19.
2. Basevich, V.Y.: Chemical Kinetics in the Combustion Processes: A Detailed Kinetics Mechanism and Its Implementation. Prog. Energy Combust. Sci., vol. 13, no. 3, 1987, pp. 199–248.
3. Edelson, D.: Computer Simulation in Chemical Kinetics. Science, vol. 214, no. 4524, Nov. 27, 1981, pp. 981–986.
4. Westbrook, C.K.; and Dryer, F.L.: Chemical Kinetic Modeling of Hydrocarbon Combustion. Prog. Energy Combust. Sci., vol. 10, no. 1, 1984, pp. 1–57.
5. Edelson, D.: The New Look in Chemical Kinetics. J. Chem. Ed., vol. 52, no. 10, 1975, pp. 642–644.
6. Edelson, D.: Introductory Remarks. Symposium on Reaction Mechanisms, Models, and Computers. J. Phys. Chem., vol. 81, no. 25, Dec. 15, 1977, pp. 2309–2311.
7. Ebert, K.H; Deuflhard, P.; and Jager, W., eds.: Modelling of Chemical Reaction Systems. Springer Verlag, Berlin, 1981.
8. Côme, G.M.: The Use of Computers in the Analysis and Simulation of Complex Reactions. Chemical Kinetics, vol. 24, Modern Methods in Kinetics, C.H. Bamford and C.F.H. Tipper, eds., Elsevier Scientific Pub. Co., Amsterdam, 1983, pp. 249–332.
9. Cukier, R.I.; Levine, H.B.; and Shuler, K.E.: Nonlinear Sensitivity Analysis of Multi-Parameter Model Systems. J. Comput. Phys., vol. 26, no. 1, Jan. 1978, pp. 1–42.
10. Rabitz, H.; Kramer, M.; and Dacol, D.: Sensitivily Analysis in Chemical Kinetics, Ann. Rev. Phys. Chem., vol. 34, 1983, pp. 419–461.
11. Bittker, D.A.; and Scullin, V.J.: General Chemical Kinetics Computer Program for Static and Flow Reactions, With Application to Combustion and Shock-Tube Kinetics. NASA TN D–6586, 1972.
12. Bittker, D.A.; and Scullin, V.J.: GCKP84—General Chemical Kinetics Code for Gas-Phase Flow and Batch Processes Including Heat Transfer Effects. NASA TP–2320, 1984.
13. Hindmarsh, A.C.: LSODE and LSODI, Two New Initital Value Ordinary Differential Equation Solvers. ACM SIGNUM Newsletter, vol. 15, no. 4, 1980, pp. 10–11.
14. Hindmarsh, A.C.: ODEPACK: A Systematized Collection of ODE Solvers. Scientific Computing, R.S. Stepleman, et al., eds., North Holland Publishing Co., Amsterdam, 1983, pp. 55–64. (Also UCRL–88007, Lawrence Livermore Laboratory, Livermore, CA, 1982).
15. Radhakrishnan, K.; and Hindmarsh, A.C.: Description and Use of LSODE, the Livermore Solver for Ordinary Differential Equations. NASA RP–1327, 1993. (Also UCRL–ID–113855, Lawrence Livermore Laboratory, Livermore, CA, 1993.)
16. Radhakrishnan, K: Comparison of Numerical Techniques for Integration of Stiff Ordinary Differential Equations Arising in Combustion Chemistry. NASA TP–2372, 1984.
17. Radhakrishnan, K.: New Integration Techniques for Chemical Kinetic Rate Equations. I. Efficiency Comparison. Combust. Sci. and Tech., vol. 46, no. 1–2, 1986, pp. 59–81.
18. Radhakrishnan, K.: New Integration Techniques for Chemical Kinetic Rate Equations: Part II—Accuracy Comparison. J. Eng. for Gas Turbines and Power, vol. 108, Apr. 1986, pp. 348–353. (Also ASME Paper 85–GT–30, 1985, and NASA TM–86893, 1985.)

References

19. Radhakrishnan, K.: A Critical Analysis of the Accuracy of Several Numerical Techniques for Combustion Kinetic Rate Equations. NASA TP–3315, 1993.
20. Radhakrishnan, K.: Combustion Kinetics and Sensitivity Analysis Computations. Numerical Approaches to Combustion Modeling, E.S. Oran and J.P. Boris, eds., AIAA, Washington, DC, 1991, pp. 83–128.
21. Dunker, A.M.: The Decoupled Direct Method for Calculating Sensitivity Coefficients in Chemical Kinetics. J. Chem. Phys., vol. 81, no. 5, Sept. 1, 1984, pp. 2385–2393.
22. Radhakrishnan, K.: Decoupled Direct Method for Sensitivity Analysis in Combustion Kinetics. Advances in Computer Methods for Partial Differential Equations–VI, R. Vichnevetsky and R.S. Stepleman, eds., IMACS, New Brunswick, NJ, 1987, pp. 479–486, (Also NASA CR–179636, 1987.)
23. Dunker, A.M.: A Computer Program for Calculating Sensitivity Coefficients in Chemical Kinetics and Other Stiff Problems by the Decoupled Direct Method. GMR–4831, Env. 192, General Motors Research Laboratories, Warren, MI, 1985.
24. Pratt, G.L.: Gas Kinetics. Wiley, London, 1969.
25. Baulch, D.L.; and Drysdale, D.D.: An Evaluation of the Rate Data for the Reaction CO + OH → CO_2 + H. Combust. Flame, vol. 23, 1974, pp. 215–225.
26. Penner, S.S.: Chemistry Problems in Jet Propulsion. Pergamon, New York, 1957.
27. Sánchez, D.A.: Ordinary Differential Equations and Stability Theory; An Introduction. W.H. Freeman and Co., San Francisco, CA, 1968.
28. Shampine, L.F.; and Gordon, M.K.: Computer Solution of Ordinary Differential Equations; The Initial Value Problem. W.H. Freeman and Co., San Francisco, CA, 1975.
29. Pratt, D.T.; and Radhakrishnan, K.: CREK1D: A Computer Code for Transient, Gas-Phase Combustion Kinetics. NASA TM–83806, 1984.
30. Shampine, L.F.: What is Stiffness? Stiff Computation, R.C. Aiken, ed., Oxford University Press, New York, 1985, pp. 1–16.
31. Shampine, L.F.; and Gear, C.W.: A User's View of Solving Stiff Ordinary Differential Equations. SIAM Rev., vol. 21, 1979, pp. 1–17.
32. Pratt, D.T.; and Radhakrishnan, K.: Physical and Numerical Sources of Computational Inefficiency in Integration of Chemical Kinetic Rate Equations: Etiology, Treatment, and Prognosis. NASA TP–2590, 1986.
33. Radhakrishnan, K.; and Pratt, D.T.: Fast Algorithm for Calculating Chemical Kinetics in Turbulent Reactive Flow. Combust. Sci. and Tech., vol. 58, no. 1–3, 1988, pp. 155–176.
34. Henrici, P.: Discrete Variable Methods in Ordinary Differential Equations. Wiley, New York, 1962.
35. Stoer, J.; and Bulirsch, R. (R. Bartels, W. Gautschi, and C. Witzgall, transl.): Introduction to Numerical Analysis. Second ed., Springer-Verlag, New York, 1992.
36. Radhakrishnan, K.: A Comparison of the Efficiency of Numerical Methods for Integrating Chemical Kinetic Rate Equations. Computational Methods, 1984 JPM Specialist Session, K.L. Strange, ed., Chemical Propulsion Information Agency Publication 401, Johns Hopkins Applied Physics Laboratory, Laurel, MD, 1984, pp. 69–82. (Also NASA TM–83590, 1984.)
37. Gelinas, R.J.: Stiff Systems of Kinetics Equations—A Practicioner's View. J. Comput. Phys., vol. 9, 1972, pp. 222–236.
38. Shampine, L.F.: Stiffness and the Automatic Selection of ODE Codes. J. Comput. Phys., vol. 54, no. 1, Apr. 1984, pp. 74–86.
39. Byrne, G.D.; and Hindmarsh, A.C..: Stiff ODE Solvers: A Review of Current and Coming Attractions. J. Comput. Phys., vol. 70, no. 1, 1987, pp. 1–62.
40. May, R.; and Noye, J.: The Numerical Solution of Ordinary Differential Equations: Initial Value Problems. Computational Techniques for Differential Equations, J. Noye, ed., North-Holland, New York, 1984, pp. 1–94.
41. Lambert, J.D.: Computational Methods in Ordinary Differential Equations. Wiley, Chichester, U.K., 1973.
42. Gear, C.W.: Numerical Initial Value Problems in Ordinary Differential Equations, Prentice-Hall. Englewood Cliffs, NJ, 1971..

43. Forsythe, G.E.; Malcolm, M.A.; and Moler, C.B.: Computer Methods for Mathematical Computations. Prentice-Hall, Englewood Cliffs, NJ, 1977.
44. Curtiss, C.F.; and Hirschfelder, J.O.: Integration of Stiff Equations. Proc. Natl. Acad. Sci., U.S.A., vol. 38, 1952, pp. 235–243.
45. Seinfeld, J.H.; Lapidus, L.; and Hwang, M.: Review of Numerical Integration Techniques for Stiff Ordinary Differential Equations. Ind. Eng. Chem. Fundam., vol. 9, 1970, pp. 266–275.
46. Lapidus, L.; and Seinfeld, J.H.: Numerical Solution of Ordinary Differential Equations. Academic Press, New York, 1971.
47. Willoughby, R.A., ed.: Stiff Differential Systems. Plenum Press, New York, 1974.
48. Hall, G.; and Watt, J.M., eds.: Modern Numerical Methods for Ordinary Differential Equations. Clarendon Press, Oxford, U.K., 1976.
49. Lapidus, L.; and Schiesser, W.E., eds.: Numerical Methods for Differential Systems. Recent Developments in Algorithms, Software, and Applications. Academic Press, New York, 1976.
50. Finlayson, B.A.: Nonlinear Analysis in Chemical Engineering. McGraw-Hill, New York, 1980.
51. Miranker, W.L.: Numerical Methods for Stiff Equations and Singular Perturbation Problems. D. Reidel Publishing Co., Dordrecht, Holland, 1981.
52. Aiken, R.C., ed.: Stiff Computation. Oxford University Press, New York, 1985.
53. Tyson, T.J.: An Implicit Integration Method for Chemical Kinetics, TRW–9840–6002–RU–000, TRW Space Technology Laboratory, Redondo Beach, CA, 1964.
54. Lomax, H.; and Bailey, H.E.: A Critical Analysis of Various Numerical Integration Methods for Computing the Flow of a Gas in Chemical Nonequilibrium. NASA TN D–4109, 1967.
55. Symposium on Reaction Mechanisms, Models, and Computers. J. Phys. Chem., vol. 81, no. 25, Dec. 15, 1977, pp. 2309–2586.
56. Oran, E.S.; and Boris, J.P.: Numerical Simulation of Reactive Flow. Elsevier, New York, 1987.
57. Hindmarsh, A.C.: GEAR: Ordinary Differential Equation System Solver. UCID–30001, Rev. 3, Lawrence Livermore Laboratory, Livermore, CA, 1974.
58. Hindmarsh, A.C.; and Byrne, G.D.: EPISODE: An Effective Package for the Integration of Systems of Ordinary Differential Equations. UCID–30112, Rev. 1, Lawrence Livermore Laboratory, Livermore, CA, 1977.
59. Byrne, G.D.; and Hindmarsh, A.C.: A Polyalgorithm for the Numerical Solution of Ordinary Differential Equations. ACM Trans. Math. Software, vol. 1, no. 1, 1975, pp. 71–96.
60. Gear, C.W.: The Numerical Integration of Ordinary Differential Equations. Math. Comp., vol. 21, 1967, pp. 146–156.
61. Gear, C.W.: The Automatic Integration of Ordinary Differential Equations. Comm. ACM, vol. 14, no. 3, Mar. 1971, pp. 176–179.
62. Shampine, L.F.: Type-Insensitive ODE Codes Based on Implicit A-Stable Formulas. Math. Comp., vol. 36, no. 154, 1981, pp. 499–510.
63. Hindmarsh, A.C.: Linear Multistep Methods for Ordinary Differential Equations: Method Formulations, Stability, and the Methods of Nordsieck and Gear. UCRL–51186, Rev. 1, Lawrence Livermore Laboratory, Livermore, CA, 1972.
64. Forsythe, G.E.; and Moler, C.B.: Computer Solution of Lienar Algebraic Systems. Prentice-Hall, Englewood Cliffs, NJ, 1967.
65. Strang, G.: Linear Algebra and Its Applications. Second ed., Academic Press, New York, 1980.
66. Ortega, J.; and Rheinboldt, W.C.: Iterative Solution of Nonlinear Equations in Several Variables. Academic Press, New York, 1970.
67. Shampine, L.F.: Type-Insenitive ODE Codes Based on Implicit A(α)-Stable Formulas. Math. Comp., vol. 39, no. 159, 1982, pp. 109–123.
68. Nordsieck, A.: On Numerical Integration of Ordinary Differential Equations. Math. Comp., vol. 16, 1962, pp. 22–49.
69. Hindmarsh, A.C.: Construction of Mathematical Software. Part III: The Control of Error in the GEAR Package for Ordinary Differential Equations. UCID–30050, Part 3, Lawrence Livermore Laboratory, Livermore, CA, 1972.
70. Radhakrishnan, K.; and Bittker, D.A.: GCKP86—An Efficient Code for General Chemical Kinetics and Senitivity Analysis Computations. Proceedings of the 1986 Fall Technical Meeting

of the Eastern Section of the Combustion Institute, The Combustion Institute, Pittsburgh, PA, 1986, pp. 46–1 to 46–4.

71. Shampine, L.F.: Implementation of Implicit Formulas for the Solution of ODEs. SIAM J. Sci. Stat. Comput., vol. 1, no. 1, Mar. 1980, pp. 103–118.
72. Byrne, G.D.; Hindmarsh, A.C.; Jackson, K.R.; and Brown, H.G.: A Comparison of Two ODE Codes: GEAR and EPISODE. Comp. Chem. Eng., vol. 1, no. 2, 1977, pp. 133–147.
73. Radhakrishnan, K.: Integrating Combustion Kinetics Rate Equations by Selective Use of Stiff and Nonstiff Methods. AIAA J., vol. 25, no. 11, Nov. 1987, pp. 1449–1455. (Also AIAA Paper 85–0237, 1985, and NASA TM–86923, 1985.)
74. Zeleznik, F.J.; and McBride, B.J.: Modeling the Internal Combustion Engine. NASA RP–1094, 1984.
75. McBride, B.J.; Gordon, S.; and Reno, M.A.: Coefficients for Calculating Thermodynamic and Transport Properties of Individual Species. NASA TM–4513, 1993.
76. Engleman, V.S.: Detailed Approach to Kinetic Mechanisms in Complex Systems. Symposium on Reaction Mechanisms, Models, and Computers. J. Phys. Chem., vol. 81, no. 25, Dec. 15, 1977, pp. 2320–2322.
77. Frank, P.M.: Introduction to System Sensitivity Theory. Academic Press, New York, 1978.
78. Teets, R.E., and Bechtel, J.H.: Sensitivity Analysis of a Model for the Radical Recombination Region of Hydrocarbon-Air Flames. Eighteenth Symposium (International) on Combustion, The Combustion Institute, Pittsburgh, PA, 1981, pp. 425–432.
79. Edelson, D.; Kaufman, L.C.; and Warner, D.D.; The Use of a High-Speed Vector Processor Machine for Chemical Kinetic Sensitivity Analysis. Supercomputers in Chemistry. P. Lykos and I. Shavitt, eds., ACS Symp. Ser., no. 173, 1981, pp. 79–88.
80. Coffee, T.P.; and Heimerl, J.M.: Sensitivity Analysis for Premixed, Laminar, Steady State Flames. Combust. Flame, vol. 50, 1983, pp. 323–340.
81. Kramer, M.A.; Rabitz, H.; Calo, J.M.; and Kee, R.J.: Sensitivity Analysis in Chemical Kinetics: Recent Developments and Computational Comparisons. Int. J. Chem. Kin., vol. 16, 1984, pp. 559–578.
82. Tilden, J.W.; Constanza, V.; McRae, G.J.; and Seinfeld, J.H.: Sensitivity Analysis of Chemically Reacting Systems. Modelling of Chemical Reaction Systems, K.H., Ebert, P. Deuflhard, and W. Jager, eds., Springer-Verlag, Berlin, 1981, pp. 69–91.
83. Burcat, A.; and Radhakrishnan, K.: The High Temperature Oxidation of Propene. Combust. Flame, vol. 60, no. 2, May 1985, pp. 157–169.
84. Radhakrishnan, K.; and Burcat, A.: Kinetics of the Ignition of Fuels in Artificial Air Mixtures. II: Oxidation of Propyne. Combust. Sci. and Tech., vol. 54, 1987, pp. 85–101.
85. Dagaut, P.; Cathonnet, M.; Boettner, J.C.; and Gaillard, F.: Kinetic Modeling of Propane Oxidation. Combust Sci. and Tech., vol. 56, 1987, pp. 23–63.
86. Atherton, R.W.; Schainker, R.B.; and Ducot, E.R.: On the Statistical Sensitivity Analysis of Models for Chemical Kinetics. AIChE J., vol. 21, no. 3, 1975, pp. 441–448.
87. Dickinson, R.P.; and Gelinas, R.J.: Sensitivity Analysis of Ordinary Differential Equation Systems—A Direct Method. J. Comput. Phys., vol. 21, no. 2, June 1976, pp. 123–143.
88. Gelinas, R.J.; and Skewes-Cox, P.D.: Tropospheric Photochemical Mechanisms. J. Phys. Chem., vol. 81, no. 25, Dec. 15, 1977, pp. 2468–2479.
89. Hwang, J-T.; Dougherty, E.P.; Rabitz, S.; and Rabitz, H.: The Green's Function Method of Sensitivity Analysis in Chemical Kinetics. J. Chem. Phys., vol. 69, no. 11, Dec. 1, 1978, pp. 5180–5191
90. Dougherty, E.P.; Hwang, J-T.; and Rabitz, H.: Further Developments and Applications of the Green's Function Method of Sensitivity Analysis in Chemical Kinetics. J. Chem. Phys., vol. 71, no. 4, Aug. 15, 1979, pp. 1794–1808.
91. Kramer, M.A.; Calo, J.M.; and Rabitz, H.: An Improved Computational Method for Sensitivity Analysis: Green's Function Method With 'AIM,' Appl. Math. Modelling, vol. 5, no. 6, Dec. 1981, pp. 432–441.

92. Kramer, M.A.; Calo, J.M.; Rabitz, H.; and Kee, R.J.: AIM: The Analytically Integrated Magnus Method for Linear and Second-Order Sensitivity Coefficients. SAND82–8231, Sandia National Laboratories, Albuquerque, NM, 1982.
93. Hwang, J-T.: The Scaled Green's Function Method of Sensitivity Analysis and Its Application to Chemical Reaction Systems. Proc. Nat. Sci. Council Rep. China, pt. B, vol. 6, no. 1, 1982, pp. 37–44.
94. Hwang, J-T.; and Chang, Y-S.: The Scaled Green's Function Method of Sensitivity Analysis. II. Further Developments and Application. Proc. Nat. Sci. Council Rep. China, pt. B, vol. 6, no. 3, 1982, pp. 308–318.
95. Koda, M.; Dogru, A.H.; and Seinfeld, J.H.: Sensitivity Analysis of Partial Differential Equations With Application to Reaction and Diffusion Processes. J. Comput. Phys., vol. 30, no. 2, Feb. 1979, pp. 259–282.
96. Seigneur, C.; Stephanopoulos, G.; and Carr, R.W., Jr.: Dynamic Sensitivity Analysis of Chemical Reaction Systems. A Variational Method. Chem. Eng. Sci., vol. 37, no. 6, 1982, pp. 845–853.
97. Grouset,D.; Plion, P.; Znaty, E; and Galant, S.: Development of a Variational Method for Chemical Kinetic Sensitivity Analysis. Twenty-first Symposium (International) on Combustion, The Combustion Institute, Pittsburgh, PA, 1986, pp. 795–807.
98. Leis, J.R.; and Kramer, M.A.: Sensitivity Analysis of Systems of Differential and Algebraic Equations. Comp. Chem. Eng., vol. 9, no. 1, 1985, pp. 93–96.
99. Caracotsios, M.; and Stewart, W.E.: Sensitivity Analysis of Initial Value Problems With Mixed ODEs and Algebraic Equations. Comp. Chem. Eng., vol. 9, no. 4, 1985, pp. 359–365.
100. Leis, J.R.; and Kramer, M.A.: The Simultaneous Solution and Sensitivity Analysis of Systems Described by Ordinary Differential Equations. ACM Trans. Math. Software, vol. 14, no. 1, 1988, pp. 45–60.
101. Leis, J.R.; and Kramer, M.A.: Algorithm 658, ODESSA—An Ordinary Differential Equation Solver With Explicit Simultaneous Sensitivity Analysis. ACM Trans. Math. Software, vol. 14, no. 1, 1988, pp. 61–67.
102. Lutz, A.E.; Kee, R.J.; and Miller, J.A.: SENKIN: A Fortran Program for Predicting Homogeneous Gas Phase Chemical Kinetics With Sensitivity Analysis. SAND87–8248 UC–4, Sandia National Laboratories, Albuquerque, NM, 1988.
103. Seinfeld, J.H.; and Lapidus, L.: Process Modeling, Estimation, and Identification, Mathematical Methods in Chemical Engineering, Vol. 3, Prentice-Hall, Englewood Cliffs, NJ, 1974.
104. Dougherty, E.P.; and Rabitz, H.: Computational Kinetics and Sensitivity Analysis of Hydrogen-Oxygen Combustion. J. Chem. Phys., vol. 72, no. 12, June 15, 1980, pp. 6571–6586.
105. Reuven, Y.; Smooke, M.D.; and Rabitz, H.: Sensitivity Analysis of Boundary Value Problems: Application to Nonlinear Reaction-Diffusion Systems. J. Comput. Phys., vol. 64, May 1986, pp. 27–55.
106. Boni, A.A.; and Penner, R.C.: Sensitivity Analysis of a Mechanism for Methane Oxidation Kinetics. Combust. Sci. and Tech., vol. 15, Mar. 1977, pp. 99–106.
107. Petzold, L.R.: A Description of DASSL: A Differential/Algebraic System Solver. SAND82–8637, Sandia National Laboratories, Albuquerque, NM, 1982.
108. Kee, R.J.; Rupley, F.M.; and Miller, J.A.: CHEMKIN–II: A Fortran Chemical Kinetics Package for the Analysis of Gas Phase Chemical Kinetics. SAND89–8009B UC–706, Sandia National Laboratories, Albuquerque, NM, 1992.
109. Brabbs, T.A.; and Musiak, J.D.: Ignition Delay Time Measurements and Proposed Kinetic Model for Hydrogen-Oxygen. NASP CR–1030, 1988.
110. Bittker, D.A.: Detailed Mechanism for Oxidation of Benzene. Combust. Sci. and Tech., vol. 79, 1991, pp. 49–72.
111. Brabbs, T.A.; Lezberg, E.A.; Bittker, D.A.; and Robertson, T. F.: Hydrogen Oxidation Mechanism With Applications to (l) the Chaperon Efficiency of Carbon Dioxide and (2) Vitiated Air Testing. NASA TM–100186, 1987.
112. van Zeggeren, F.; and Storey, S.H.: The Computation of Chemical Equilibria, Cambridge Univ. Press, London, 1970.

References

113. Gordon, S.; and McBride, B.J.: Computer Program for Calculation of Complex Chemical Equilibrium Compositions, Rocket Performance, Incident and Reflected Shocks, and Chapman-Jouguet Detonations. NASA SP–273, 1971. (Interim Revision, 1976.)
114. Zeleznik, F.J.; and Gordon, S.: An Analytical Investigation of Three General Methods of Calculating Chemical Equilibrium Compositions. NASA TN D–473, 1960.
115. Zeleznik, F.J.; and Gordon, S.: Calculation of Complex Chemical Equilibria. Ind. Eng. Chem., vol. 60, no. 6, 1968, pp. 27–57.
116. Meintjes, K.; and Morgan, A.P.: Performance of Algorithms for Calculating the Equilibrium Composition of a Mixture of Gases. J. Comput. Phys., vol. 60, Sept. 15, 1985, pp. 219–234.
117. Gordon, S.; and McBride, B.J.: Computer Program for Calculation of Complex Chemical Equilibrium Compositions and Applications. Part I–Analysis, NASA RP–1311, 1994.
118. Kirkwood, J.G.; and Oppenheim, I.: Chemical Thermodynamics, McGraw-Hill, New York, 1961.
119. Denbigh, K.G.: The Principles of Chemical Equilibrium, Fourth Ed., Cambridge Univ. Press, London, 1981.
120. Taylor, A.E.: Advanced Calculus, Ginn, Boston, MA, 1955.
121. Sokolnikoff, I.S.; and Redheffer, R.M.: Mathematics of Physics and Modern Engineering. Second Ed., McGraw-Hill, New York, 1966.
122. Callen, H.B.: Thermodynamics and an Introduction to Thermostatistics. Second Ed., Wiley, New York, 1985.
123. Zeleznik, F.J.; and Gordon, S. : A General IBM 704 or 7090 Computer Program for Computation of Chemical Equilibrium Compositions, Rocket Performance, and Chapman-Jouguet Detonations. NASA TN D–1454, 1962.
124. Wright, J.K.: Shock Tubes. Metheun, London, 1961.
125. Resler, E.L., Jr.: The Shock Tube and Chemical Kinetics. Fluid Dynamics and Applied Mathematics. J.B. Diaz and S.I. Pai, eds., Gordon and Breach Science Publishers, New York, 1962, pp. 125–145.
126. Liepmann, H.W.; and Roshko, A.: Elements of Gasdynamics. Wiley, New York, 1957.
127. Longwell, J.P.; and Weiss, M.A.: High Temperature Reaction Rates in Hydrocarbon Combustion. Ind. Eng. Chem., vol. 47, no. 8, Aug. 1955, pp. 1634–1643.
128. Jones, A.; and Prothero, A.: The Solution of the Steady-State Equations for an Adiabatic Stirred Reactor. Combust. Flame, vol. 12, 1968, pp. 457–464.
129. Denbigh, K.G.: Chemical Reactor Theory: An Introduction. Cambridge Univ. Press, London, 1966.
130. Glassman, I.: Combustion. Academic Press, New York, 1977.
131. Glarborg, P.; Kee, R.J.; Grcar, J.F.; and Miller, J.A.: PSR: A Fortran Program of Modeling Well-Stirred Reactors. SAND86–8209 UC–4, Sandia National Laboratories, Albuquerque, NM, 1986.

☆U.S. GOVERNMENT PRINTING OFFICE: 1997 - 549-007/60350

REPORT DOCUMENTATION PAGE

Form Approved
OMB No. 0704-0188

1. AGENCY USE ONLY (*Leave blank*)	2. REPORT DATE	3. REPORT TYPE AND DATES COVERED
	January 1994	Reference Publication

4. TITLE AND SUBTITLE

LSENS—A General Chemical Kinetics and Sensitivity Analysis Code for Homogeneous Gas-Phase Reactions

I. Theory and Numerical Solution Procedures

5. FUNDING NUMBERS

WU–505–62–52

6. AUTHOR(S)

Krishnan Radhakrishnan

7. PERFORMING ORGANIZATION NAME(S) AND ADDRESS(ES)

National Aeronautics and Space Administration
Lewis Research Center
Cleveland, Ohio 44135–3191

8. PERFORMING ORGANIZATION REPORT NUMBER

E–5140-1

9. SPONSORING/MONITORING AGENCY NAME(S) AND ADDRESS(ES)

National Aeronautics and Space Administration
Washington, D.C. 20546–0001

10. SPONSORING/MONITORING AGENCY REPORT NUMBER

NASA RP–1328

11. SUPPLEMENTARY NOTES

Krishnan Radhakrishnan, NYMA, Inc., Lewis Research Center Group, 2001 Aerospace Parkway, Brook Park, Ohio 44142. Responsible person, Edward J. Mularz, organization code 2650, (216) 433–5850.

12a. DISTRIBUTION/AVAILABILITY STATEMENT

Unclassified - Unlimited
Subject Categories 25, 61, and 64

12b. DISTRIBUTION CODE

13. ABSTRACT ***(Maximum 200 words)***

LSENS, the Lewis General Chemical Kinetics and Sensitivity Analysis Code, has been developed for solving complex, homogeneous, gas-phase chemical kinetics problems and contains sensitivity analysis for a variety of problems, including nonisothermal situations. This report is part I of a series of three reference publications that describe LSENS, provide a detailed guide to its usage, and present many example problems. Part I derives the governing equations and describes the numerical solution procedures for the types of problems that can be solved. The accuracy and efficiency of LSENS are examined by means of various test problems, and comparisons with other methods and codes presented.

LSENS is a flexible, convenient, accurate, and efficient solver for chemical reaction problems such as static system; steady, one-dimensional, inviscid flow; reaction behind incident shock wave, including boundary layer correction; and perfectly stirred (highly backmixed) reactor. In addition, the chemical equilibrium state can be computed for the following assigned states: temperature and pressure, enthalpy and pressure, temperature and volume, and internal energy and volume. For static problems the code computes the sensitivity coefficients of the dependent variables and their temporal derivatives with respect to the initial values of the dependent variables and/or the three rate coefficient parameters of the chemical reactions.

Part II (NASA RP–1329) describes LSENS, its usage, illustrated by example problems, and how to modify it. Part III (NASA RP–1330) explains the kinetics and kinetics-plus-sensitivity-analysis problems supplied with LSENS and presents sample results.

14. SUBJECT TERMS

Chemical kinetics; Combustion; First-order ODE's; Stiff ODE's; Numerical methods; Backward differentiation formula method; Sensitivity analysis; Local methods; Decoupled direct method; Comparison of methods; Chemical equilibrium; Incident shock; Perfectly stirred reactor

15. NUMBER OF PAGES

376

16. PRICE CODE

A17

17. SECURITY CLASSIFICATION OF REPORT	18. SECURITY CLASSIFICATION OF THIS PAGE	19. SECURITY CLASSIFICATION OF ABSTRACT	20. LIMITATION OF ABSTRACT
Unclassified	Unclassified	Unclassified	